A sexual misconduct case rocks anthropology *p. 652*

Long life in the valley *p. 688*

Hybrid autoantigens drive type 1 diabetes *p. 711*

Science

$15
12 FEBRUARY 2016
sciencemag.org

AAAS

Gordon Research Conferences

Topics include behavior of thin films *p. 742*

CONTENTS

12 FEBRUARY 2016 • VOLUME 351 • ISSUE 6274

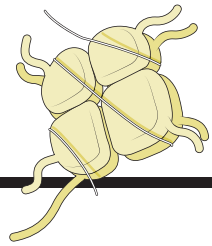

667 & 725
Modular cooperation controls transcription

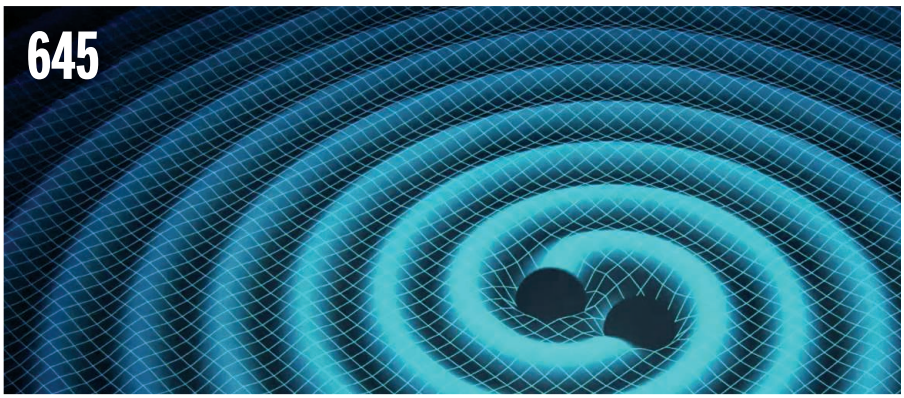

NEWS

IN BRIEF

642 News at a glance

IN DEPTH

645 **TRIUMPH FOR GRAVITATIONAL WAVE HUNT**
Observation made with newly detectable radiation clinches case for black holes *By A. Cho*

647 **BENDY BUGS INSPIRE ROBOTICISTS**
Bees, wasps, and cockroaches are built to survive bashing and squeezing *By E. Pennisi*

648 **NEANDERTAL GENES LINKED TO MODERN DISEASES**
DNA inherited from our extinct cousins boosts risk of depression, other disorders *By A. Gibbons*
▸ REPORT P. 737

649 **RESEARCH CHIEF CUTS CLIMATE STUDIES, SETS NEW PRIORITIES**
CSIRO to trim staff as it seeks closer alignment with industry *By L. Dayton*

650 **RECORD OZONE HOLE MAY OPEN OVER ARCTIC IN THE SPRING**
Unusual polar cold produces clouds that could help push ozone losses beyond 2011 mark, releasing extra UV radiation *By E. Hand*

651 **A CRYSTAL BALL FOR CHEMICAL SAFETY**
By comparing new chemicals to known compounds, toxicologists seek early hazard warning *By T. Rabesandratana*

FEATURE

652 **AFTER THE ACCUSATION**
A complex case of alleged sexual misconduct rattles a field and signals a cultural shift
By M. Balter

INSIGHTS

PERSPECTIVES

658 **A NEW DIET FOR METHANE OXIDIZERS**
Archaea that normally depend on sulfate-reducing bacteria can also grow alone *By A.-E. Rotaru and B. Thamdrup*
▸ REPORT P. 703

659 **PATHOGEN TO POWERHOUSE**
How did the precursors to the mitochondrion and the plastid evade host defense?
By S. G. Ball et al.

661 **A UNIFYING MODEL OF EPIGENETIC REGULATION**
Single-cell tracking reveals a common "algorithm" of operation used by chromatin regulators *By A. J. Keung and A. S. Khalil*
▸ REPORT P. 720

662 **MODULATING PULMONARY INFLAMMATION**
Neuroepithelial cells suppress pulmonary inflammation and alveolar remodeling
By J. A. Whitsett and E. E. Morrisey
▸ REPORT P. 707

664 **CLIMATE CONFUSION AMONG U.S. TEACHERS**
Teachers' knowledge and values can hinder climate education
By E. Plutzer et al.

666 **COPPER CATALYSIS IN A BLUE LIGHT**
Visible light, copper, and a phosphine ligand combine for C-N bond formation at fully substituted chiral centers
By M. F. Greaney
▸ REPORT P. 681

667 **IT TAKES TEAMWORK TO MODIFY CHROMATIN**
The organization of constituents in a large chromatin-modifying complex reveals specific roles *By J. L. Workman*
▸ REPORT P. 725

668 **FINDING AN ETHICAL PATH FORWARD FOR MITOCHONDRIAL REPLACEMENT**
It is ethically permissible to initiate clinical investigations of mitochondrial replacement techniques in humans so long as significant conditions and restrictions are in place
By A. B. Claiborne et al.

670 **(TORC)ING UP PURINE BIOSYNTHESIS**
An enzyme complex coordinates metabolism and nucleotide production to fuel cell growth *By E. H. Ma and R. G. Jones*
▸ REPORTS PP. 728 & 733

BOOKS *ET AL.*

672 **THE SECRET WORLD INSIDE YOU**
R. DeSalle and S. Perkins, curators, reviewed by V. Thompson

673 **UNINFORMED**
By A. Lupia, reviewed by J. Junn

673 **THE HUMAN FACE OF BIG DATA**
S. Smolan, director

LETTERS

674 **THE CRUSHING WEIGHT OF URBAN WASTE**
By H. Yang et al.

674 **CHINA'S PARTIAL EMISSION CONTROL**
By A. Lin et al.

675 **MISGUIDED STRATEGY FOR MOSQUITO CONTROL**
By V. M. Azevedo-Santos et al.

Downloaded from on February 11, 2016

Published by AAAS

CONTENTS

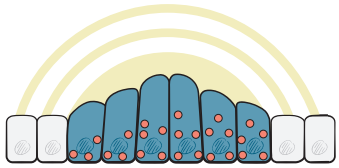

662 & 707
Suppressing pulmonary inflammation

12 FEBRUARY 2016 • VOLUME 351 • ISSUE 6274

RESEARCH

IN BRIEF

676 From *Science* and other journals

REVIEW

679 **GENE REGULATION**
Retrotransposons as regulators of gene expression *R. A. Elbarbary* et al.
REVIEW SUMMARY; FOR FULL TEXT: dx.doi.org/10.1126/science.aac7247

RESEARCH ARTICLE

680 **GENE REGULATION**
Lineage-specific enhancers activate self-renewal genes in macrophages and embryonic stem cells *E. L. Soucie* et al.
RESEARCH ARTICLE SUMMARY; FOR FULL TEXT: dx.doi.org/10.1126/science.aad5510

REPORTS

681 **PHOTOCATALYSIS**
Asymmetric copper-catalyzed C-N cross-couplings induced by visible light *Q. M. Kainz* et al.
▸ PERSPECTIVE P. 666

684 **PLANT IMMUNITY**
Using decoys to expand the recognition specificity of a plant disease resistance protein *S. H. Kim* et al.

688 **VALLEYTRONICS**
Valley-polarized exciton dynamics in a 2D semiconductor heterostructure *P. Rivera* et al.

691 **MATERIALS SCIENCE**
On-chip and freestanding elastic carbon films for micro-supercapacitors *P. Huang* et al.

696 **CARBON CYCLE**
Enhanced seasonal CO_2 exchange caused by amplified plant productivity in northern ecosystems *M. Forkel* et al.

699 **GLOBAL WATER CYCLE**
A decade of sea level rise slowed by climate-driven hydrology *J. T. Reager* et al.

703 **MICROBIAL PHYSIOLOGY**
Artificial electron acceptors decouple archaeal methane oxidation from sulfate reduction *S. Scheller* et al.
▸ PERSPECTIVE P. 658

707 **LUNG PHYSIOLOGY**
Pulmonary neuroendocrine cells function as airway sensors to control lung immune response *K. Branchfield* et al.
▸ PERSPECTIVE P. 662

711 **AUTOIMMUNITY**
Pathogenic CD4 T cells in type 1 diabetes recognize epitopes formed by peptide fusion *T. Delong* et al.

714 **IMMUNOLOGY**
Broadly targeted $CD8^+$ T cell responses restricted by major histocompatibility complex E *S. G. Hansen* et al.

720 **EPIGENETICS**
Dynamics of epigenetic regulation at the single-cell level *L. Bintu* et al.
▸ PERSPECTIVE P. 661

725 **TRANSCRIPTION**
Structural basis for histone H2B deubiquitination by the SAGA DUB module *M. T. Morgan* et al.
▸ PERSPECTIVE P. 667

728 **METABOLISM**
mTORC1 induces purine synthesis through control of the mitochondrial tetrahydrofolate cycle *I. Ben-Sahra* et al.
▸ PERSPECTIVE P. 670; REPORT P. 733

733 **BIOCHEMISTRY**
Spatial colocalization and functional link of purinosomes with mitochondria *J. B. French* et al.
▸ PERSPECTIVE P. 670; REPORT P. 728

737 **HUMAN GENOMICS**
The phenotype legacy of admixture between modern humans and Neandertals *C. N. Simonti* et al.
▸ NEWS STORY P. 648; PODCAST

DEPARTMENTS

641 **EDITORIAL**
Economics of public safety
By Marcia McNutt

782 **WORKING LIFE**
Science in the shadows
By Andrew Scott

ON THE COVER

Bubbles floating on top of a foaming solution, showing the formation of thin films, which give rise to interference effects. Analysis of thin-film drainage and stability is an active research area with many open questions. The Gordon Research Conference on Granular Matter will be held 24 to 29 July 2016 in Easton, Massachusetts. See page 742 for the Gordon Research Conference schedule and preliminary programs. *Photo: Wiebke Drenckhan, Université Paris-Sud, CNRS, France*

Science Staff 640
Gordon Research Conferences 742
New Products 775
Science Careers 776

SCIENCE (ISSN 0036-8075) is published weekly on Friday, except the last week in December, by the American Association for the Advancement of Science, 1200 New York Avenue, NW, Washington, DC 20005. Periodicals mail postage (publication No. 484460) paid at Washington, DC, and additional mailing offices. Copyright © 2016 by the American Association for the Advancement of Science. The title SCIENCE is a registered trademark of the AAAS. Domestic individual membership and subscription (51 issues): $165 ($74 allocated to subscription). Domestic institutional subscription (51 issues): $1522; Foreign postage extra: Mexico, Caribbean (surface mail) $55; other countries (air assist delivery) $89. First class, airmail, student, and emeritus rates on request. Canadian rates with GST available upon request, GST #1254 88122. Publications Mail Agreement Number 1069624. **Printed in the U.S.A.**
Change of address: Allow 4 weeks, giving old and new addresses and 8-digit account number. **Postmaster:** Send change of address to AAAS, P.O. Box 96178, Washington, DC 20090–6178. **Single-copy sales:** $15.00 current issue, $20.00 back issue prepaid includes surface postage; bulk rates on request. **Authorization to photocopy** material for internal or personal use under circumstances not falling within the fair use provisions of the Copyright Act is granted by AAAS to libraries and other users registered with the Copyright Clearance Center (CCC) Transactional Reporting Service, provided that $35.00 per article is paid directly to CCC, 222 Rosewood Drive, Danvers, MA 01923. The identification code for *Science* is 0036-8075. *Science* is indexed in the *Reader's Guide to Periodical Literature* and in several specialized indexes.

Published by AAAS

Science
AAAS
1200 New York Avenue, NW, Washington, DC 20005
Bateman House, 82-88 Hills Road, Cambridge, UK CB2 1LQ

Editor-in-Chief Marcia McNutt
Executive Editor Monica M. Bradford News Editor Tim Appenzeller
Managing Editor, Research Journals Katrina L. Kelner
Deputy Editors Barbara R. Jasny, Andrew M. Sugden(UK), Valda J. Vinson, Jake S. Yeston

Research and Insights

SR. EDITORS Caroline Ash(UK), Gilbert J. Chin, Lisa D. Chong, Julia Fahrenkamp-Uppenbrink(UK), Pamela J. Hines, Stella M. Hurtley(UK), Paula A. Kiberstis, Marc S. Lavine(Canada), Kristen L. Mueller, Ian S. Osborne(UK), Beverly A. Purnell, L. Bryan Ray, Guy Riddihough, H. Jesse Smith, Jelena Stajic, Peter Stern(UK), Phillip D. Szuromi, Sacha Vignieri, Brad Wible, Nicholas S. Wigginton, Laura M. Zahn **ASSOCIATE EDITORS** Brent Grocholski, Keith T. Smith **ASSOCIATE BOOK REVIEW EDITOR** Valerie B. Thompson **ASSOCIATE LETTERS EDITOR** Jennifer Sills **CHIEF CONTENT PRODUCTION EDITOR** Cara Tate **SR. CONTENT PRODUCTION EDITORS** Harry Jach, Lauren Kmec **CONTENT PRODUCTION EDITORS** Jeffrey E. Cook, Chris Filiatreau, Cynthia Howe, Barbara P. Ordway, Catherine Wolner **SR. EDITORIAL COORDINATORS** Carolyn Kyle, Beverly Shields **EDITORIAL COORDINATORS** Joi S. Granger, Lisa Johnson, Anita Wynn **PUBLICATIONS ASSISTANTS** Aneera Dobbins, Jeffrey Hearn, Dona Mathieu, Le-Toya Mayne Flood, Shannon McMahon, Scott Miller, Caitlyn Phillips, Jerry Richardson, Rachel Roberts(UK), Alice Whaley(UK), Brian White **EXECUTIVE ASSISTANT** Anna Bashkirova **ADMINISTRATIVE SUPPORT** Janet Clements(UK), Lizanne Newton(UK), Maryrose Madrid, John Wood(UK)

News

NEWS MANAGING EDITOR John Travis **INTERNATIONAL EDITOR** Richard Stone **DEPUTY NEWS EDITORS** Daniel Clery(UK), Robert Coontz, Elizabeth Culotta, David Grimm, David Malakoff, Leslie Roberts **CONTRIBUING EDITOR** Martin Enserink(Europe) **SR. CORRESPONDENTS** Jeffrey Mervis, Elizabeth Pennisi **NEWS WRITERS** Adrian Cho, Jon Cohen, Jennifer Couzin-Frankel, Carolyn Gramling, Eric Hand, Jocelyn Kaiser, Catherine Matacic, Kelly Servick, Robert F. Service, Erik Stokstad(Cambridge, UK), Emily Underwood **INTERNS** Hanae Armitage, Nala Rogers **CONTRIBUTING CORRESPONDENTS** Michael Balter(Paris), John Bohannon, Ann Gibbons, Mara Hvistendahl, Sam Kean, Eli Kintisch, Kai Kupferschmidt(Berlin), Andrew Lawler, Christina Larson(Beijing), Mitch Leslie, Charles C. Mann, Eliot Marshall, Virginia Morell, Dennis Normile(Shanghai), Heather Pringle, Tania Rabesandratana(London), Gretchen Vogel(Berlin), Lizzie Wade(Mexico City) **CAREERS** Donisha Adams, Rachel Bernstein(Editor) **COPY EDITORS** Julia Cole, Dorie Chevlen, Jennifer Levin (Chief) **ADMINISTRATIVE SUPPORT** Jessica Williams

Executive Publisher Rush D. Holt
Interim Publisher Bill Moran Chief Digital Media Officer Rob Covey

BUSINESS OPERATIONS AND PORTFOLIO MANAGEMENT DIRECTOR Sarah Whalen **PRODUCT DEVELOPMENT DIRECTOR** Will Schweitzer **PRODUCT DEVELOPMENT ASSOCIATE** Hal Moore **BUSINESS SYSTEMS AND FINANCIAL ANALYSIS DIRECTOR** Randy Yi **MANAGER OF FULFILLMENT SYSTEMS** Neal Hawkins **SYSTEMS ANALYST** Nicole Mehmedovich **ASSISTANT DIRECTOR, BUSINESS OPERATIONS** Eric Knott **MANAGER, BUSINESS OPERATIONS** Jessica Tierney **BUSINESS ANALYST** Cory Lipman **FINANCIAL ANALYST** Robert Clark **RIGHTS AND PERMISSIONS ASSISTANT DIRECTOR** Emilie David **PERMISSIONS ASSOCIATE** Elizabeth Sandler **RIGHTS, CONTRACTS, AND LICENSING ASSOCIATE** Lili Kiser

MARKETING DIRECTOR Elise Swinehart **ASSOCIATE DIRECTOR OF ACQUISITION AND RETENTION** Julianne Wielga **MARKETING ASSOCIATE** Elizabeth Sattler **SR. MARKETING EXECUTIVE** Jennifer Reeves **ASSOCIATE DIRECTOR, CREATIVE SERVICES** Tzeitel Sorrosa **ART ASSOCIATE** Seil Lee **JR. ART ASSOCIATE** Kim Huynh **ASSISTANT COMMERCIAL EDITOR** Selby Frame **MARKETING PROJECT MANAGER** Angelissa McArthur **PROGRAM DIRECTOR, AAAS MEMBER CENTRAL** Peggy Mihelich **FULFILLMENT SYSTEMS AND OPERATIONS** membership@aaas.org **MANAGER, MEMBER SERVICES** Pat Butler **SPECIALISTS** Terrance Morrison, Latasha Russell **MANAGER, DATA ENTRY** Mickie Napoleoni **DATA ENTRY SPECIALISTS** Brenden Aquilino, Fiona Giblin

INTERIM DIRECTOR, SITE LICENSING Will Schweitzer **PUBLISHER RELATIONS MANAGER** Catherine Holland **PUBLISHER RELATIONS, EASTERN REGION** Keith Layson **PUBLISHER RELATIONS, WESTERN REGION** Ryan Rexroth **SALES RESEARCH COORDINATOR** Aiesha Marshall **MANAGER, SITE LICENSE OPERATIONS** Iquo Edim **SENIOR PRODUCTION SPECIALIST** Robert Koepke **SENIOR OPERATIONS ANALYST** Lana Guz **FULFILLMENT ANALYST** Judy Lillibridge **ASSOCIATE DIRECTOR, MARKETING** Christina Schlecht **MARKETING ASSOCIATES** Thomas Landreth, Isa Sesay-Bah

WEB TECHNOLOGIES SR. DEVELOPER Chris Coleman **DEVELOPERS** Dan Berger, Jimmy Marks, Ryan Jensen **SR. PROJECT MANAGER** Trista Smith **PROJECT MANAGER** Nick Fletcher

DIGITAL MEDIA DIRECTOR OF ANALYTICS Enrique Gonzales **DIGITAL REPORTING ANALYST** Eric Hossinger **SR. WEB PRODUCER** Sarah Crespi **WEB PRODUCER** Alison Crawford **VIDEO PRODUCER** Nguyen Nguyen **SOCIAL MEDIA PRODUCER** Brice Russ

DIRECTOR OF OPERATIONS PRINT AND ONLINE Lizabeth Harman **DIGITAL/PRINT STRATEGY MANAGER** Jason Hillman **QUALITY TECHNICAL MANAGER** Marcus Spiegler **PROJECT ACCOUNT MANAGER** Tara Kelly **DIGITAL PRODUCTION MANAGER** Lisa Stanford **ASSISTANT MANAGER DIGITAL/PRINT** Rebecca Doshi **SENIOR CONTENT SPECIALISTS** Steve Forrester, Antoinette Hodal, Lori Murphy, Anthony Rosen **CONTENT SPECIALISTS** Jacob Hedrick, Kimberley Oster

DESIGN DIRECTOR Beth Rakouskas **DESIGN EDITOR** Marcy Atarod **SENIOR DESIGNER** Garvin Grullón **DESIGNER** Chrystal Smith **GRAPHICS MANAGING EDITOR** Alberto Cuadra **SENIOR SCIENTIFIC ILLUSTRATORS** Chris Bickel, Katharine Sutliff **SCIENTIFIC ILLUSTRATOR** Valerie Altounian **SENIOR ART ASSOCIATES** Holly Bishop, Nathalie Cary, Preston Huey **PHOTOGRAPHY MANAGING EDITOR** William Douthitt **PHOTO EDITORS** Leslie Blizard, Christy Steele

DIRECTOR, GLOBAL COLLABORATION, CUSTOM PUBLICATIONS, ADVERTISING Bill Moran **EDITOR, CUSTOM PUBLISHING** Sean Sanders: 202-326-6430 **ASSISTANT EDITOR, CUSTOM PUBLISHING** Tianna Hicklin: 202-326-6463 **ADVERTISING MARKETING MANAGER** Justin Sawyers: 202-326-7061 science_advertising@aaas.org **ADVERTISING SUPPORT MANAGER** Karen Foote: 202-326-6740 **ADVERTISING PRODUCTION OPERATIONS MANAGER** Deborah Tompkins **SR. PRODUCTION SPECIALIST/GRAPHIC DESIGNER** Amy Hardcastle **SR. TRAFFIC ASSOCIATE** Christine Hall **SALES COORDINATOR** Shirley Young **ASSOCIATE DIRECTOR, COLLABORATION, CUSTOM PUBLICATIONS/CHINA/TAIWAN/KOREA/SINGAPORE** Ruolei Wu: +86-186 0082 9345, rwu@aaas.org **COLLABORATION/CUSTOM PUBLICATIONS/JAPAN** Adarsh Sandhu + 81532-81-5142 asandhu@aaas.org **EAST COAST/E. CANADA** Laurie Faraday: 508-747-9395, FAX 617-507-8189 **WEST COAST/W. CANADA** Lynne Stickrod: 415-931-9782, FAX 415-520-6940 **MIDWEST** Jeffrey Dembski: 847-498-4520 x3005, Steven Loerch: 847-498-4520 x3006 **UK EUROPE/ASIA** Roger Goncalves: TEL/FAX +41 43 243 1358 **JAPAN** Katsuyoshi Fukamizu(Tokyo): +81-3-3219-5777 kfukamizu@aaas.org **CHINA/TAIWAN** Ruolei Wu: +86-186 0082 9345, rwu@aaas.org

WORLDWIDE ASSOCIATE DIRECTOR OF SCIENCE CAREERS Tracy Holmes: +44 (0) 1223 326525, FAX +44 (0) 1223 326532 tholmes@science-int.co.uk **CLASSIFIED** advertise@sciencecareers.org **U.S. SALES** Tina Burks: 202-326-6577, Nancy Toema: 202-326-6578 **EUROPE/ROW SALES** Sarah Lelarge **SALES ASSISTANT** Kelly Grace **JAPAN** Hiroyuki Mashiki(Kyoto): +81-75-823-1109 hmashiki@aaas.org **CHINA/TAIWAN** Ruolei Wu: +86-186 0082 9345 rwu@aaas.org **MARKETING MANAGER** Allison Pritchard **MARKETING ASSOCIATE** Aimee Aponte

AAAS BOARD OF DIRECTORS RETIRING PRESIDENT, CHAIR Gerald R. Fink **PRESIDENT** Geraldine (Geri) Richmond **PRESIDENT-ELECT** Barbara A. Schaal **TREASURER** David Evans Shaw **CHIEF EXECUTIVE OFFICER** Rush D. Holt **BOARD** Bonnie L. Bassler, May R. Berenbaum, Carlos J. Bustamante, Stephen P.A. Fodor, Claire M. Fraser, Michael S. Gazzaniga, Laura H. Greene, Elizabeth Loftus, Mercedes Pascual

SUBSCRIPTION SERVICES For change of address, missing issues, new orders and renewals, and payment questions: 866-434-AAAS (2227) or 202-326-6417, FAX 202-842-1065. Mailing addresses: AAAS, P.O. Box 96178, Washington, DC 20090-6178 or AAAS Member Services, 1200 New York Avenue, NW, Washington, DC 20005

INSTITUTIONAL SITE LICENSES 202-326-6730 **REPRINTS:** Author Inquiries 800-635-7181 **COMMERCIAL INQUIRIES** 803-359-4578 **PERMISSIONS** 202-326-6765, permissions@aaas.org **AAAS Member Services** 202-326-6417 or http://membercentral.aaas.org/discounts

Science serves as a forum for discussion of important issues related to the advancement of science by publishing material on which a consensus has been reached as well as including the presentation of minority of conflicting points of view. Accordingly, all articles published in *Science*—including editorials, news and comment, and books reviews—are signed and reflect the individual views of the authors and not official points of view adopted by AAAS or the institutions with which the authors are affiliated.

INFORMATION FOR AUTHORS See pages 678 and 679 of the 6 February 2015 issue or access www.sciencemag.org/about/authors

SENIOR EDITORIAL BOARD
Gary King, Harvard University, **Susan M. Rosenberg**, Baylor College of Medicine, **Ali Shilatifard**, Northwestern University Feinberg School of Medicine

BOARD OF REVIEWING EDITORS (Statistics board members indicated with **($)**)
Adriano Aguzzi, U. Hospital Zürich
Takuzo Aida, U. of Tokyo
Leslie Aiello, Wenner-Gren Foundation
Judith Allen, U. of Edinburgh
Sonia Altizer, U. of Georgia
Sebastian Amigorena, Institut Curie
Kathryn Anderson, Memorial Sloan-Kettering Cancer Center
Meinrat O. Andreae, Max-Planck Inst. Mainz
Paola Arlotta, Harvard U.
Johan Auwerx, EPFL
David Awschalom, U. of Chicago
Clare Baker, University of Cambridge
Jordi Bascompte, University of Zurich
Facundo Batista, London Research Inst.
Ray H. Baughman, U. of Texas, Dallas
David Baum, U. of Wisconsin
Carlo Beenakker, Leiden U.
Kamran Behnia, ESPCI-ParisTech
Yasmine Belkaid, NIAID, NIH
Philip Benfey, Duke U.
May Berenbaum, U. of Illinois
Gabriele Bergers, U. of California, San Francisco
Bradley Bernstein, Massachusetts General Hospital
Peer Bork, EMBL
Bernard Bourdon, Ecole Normale Supérieure de Lyon
Chris Bowler, École Normale Supérieure
Ian Boyd, U. of St. Andrews
Emily Brodsky, U. of California, Santa Cruz
Ron Brookmeyer, U. of California Los Angeles **($)**
Christian Büchel, U. Hamburg-Eppendorf
Joseph A. Burns, Cornell U.
Carter Tribley Butts, U. of California, Irvine
Gyorgy Buzsaki, New York U. School of Medicine
Blanche Capel, Duke U.
Mats Carlsson, U. of Oslo
Ib Chorkendorff, U. of Denmark
David Clapham, Children's Hospital Boston
Joel Cohen, Rockefeller U., Columbia U.
James J. Collins, MIT
Robert Cook-Deegan, Duke U.
Lisa Coussens, Oregon Health & Science U.
Alan Cowman, Walter & Eliza Hall Inst.
Robert H. Crabtree, Yale U.
Roberta Croce, Vrije Universiteit
Janet Currie, Princeton U.
Jeff L. Dangl, U. of North Carolina
Tom Daniel, U. of Washington
Frans de Waal, Emory U.
Stanislas Dehaene, Collège de France
Robert Desimone, MIT
Claude Desplan, New York U.
Dennis Discher, U. of Pennsylvania
Gerald W. Dorn II, Washington U. School of Medicine
Jennifer A. Doudna, U. of California, Berkeley
Bruce Dunn, U. of California, Los Angeles
William Dunphy, Caltech
Christopher Dye, WHO
Todd Ehlers, U. of Tuebingen
David Ehrhardt, Carnegie Inst. of Washington
Tim Elston, U. of North Carolina at Chapel Hill
Gerhard Ertl, Fritz-Haber-Institut, Berlin
Barry Everitt, U. of Cambridge
Ernst Fehr, U. of Zurich
Anne C. Ferguson-Smith, U. of Cambridge
Michael Feuer, The George Washington U.
Toren Finkel, NHLBI, NIH
Kate Fitzgerald, U. of Massachusetts
Peter Fratzl, Max-Planck Inst.
Elaine Fuchs, Rockefeller U.
Daniel Geschwind, UCLA
Karl-Heinz Glassmeier, TU Braunschweig
Ramon Gonzalez, Rice U.
Julia R. Greer, Caltech
Elizabeth Grove, U. of Chicago
Nicolas Gruber, ETH Zurich
Kip Guy, St. Jude's Children's Research Hospital
Taekjip Ha, U. of Illinois at Urbana-Champaign
Christian Haass, Ludwig Maximilians U.
Michael Hasselmo, Boston U.
Martin Heimann, Max-Planck Inst. Jena
Yka Helariutta, U. of Cambridge
James A. Hendler, Rensselaer Polytechnic Inst.
Janet G. Hering, Swiss Fed. Inst. of Aquatic Science & Technology
Kai-Uwe Hinrichs, U. of Bremen
David Hodell, U. of Cambridge
David Holden, Imperial College
Lora Hooper, UT Southwestern Medical Ctr. at Dallas
Tamas Horvath, Yale University
Raymond Huey, U. of Washington
Fred Hughson, Princeton U.
Auke Ijspeert, EPFL Lausanne
Stephen Jackson, U. of Arizona, USGS
Steven Jacobsen, U. of California, Los Angeles
Stephen Jackson, U. of Arizona
Kai Johnsson, EPFL Lausanne
Peter Jonas, Inst. of Science & Technology (IST) Austria
Matt Kaeberlein, U. of Washington
William Kaelin Jr., Dana-Farber Cancer Inst.
Daniel Kahne, Harvard U.
Daniel Kammen, U. of California, Berkeley
Abby Kavner, U. of California, Los Angeles
Masashi Kawasaki, U. of Tokyo
V. Narry Kim, Seoul National U.
Joel Kingsolver, U. of North Carolina at Chapel Hill
Robert Kingston, Harvard Medical School
Etienne Koechlin, Ecole Normale Supérieure
Alexander Kolodkin, Johns Hopkins U.
Thomas Langer, U. of Cologne
Mitchell A. Lazar, U. of Pennsylvania
David Lazer, Harvard U.
Thomas Lecuit, IBDM
Virginia Lee, U. of Pennsylvania
Stanley Lemon, U. of North Carolina at Chapel Hill
Ottoline Leyser, Cambridge U.
Wendell Lim, U.C. San Francisco
Marcia C. Linn, U. of California, Berkeley
Jianguo Liu, Michigan State U.
Luis Liz-Marzan, CIC biomaGUNE
Jonathan Losos, Harvard U.
Ke Lu, Chinese Acad. of Sciences
Christian Lüscher, U. of Geneva
Laura Machesky, CRUK Beatson Inst. for Cancer Research
Anne Magurran, U. of St. Andrews
Oscar Marin, CSIC & U. Miguel Hernández
Charles Marshall, U. of California, Berkeley
C. Robertson McClung, Dartmouth College
Graham Medley, U. of Warwick
Tom Misteli, NCI
Yasushi Miyashita, U. of Tokyo
Mary Ann Moran, U. of Georgia
Richard Morris, U. of Edinburgh
Alison Motsinger-Reif, NC State U. **($)**
Thomas Murray, The Hastings Center
Daniel Neumark, U. of California, Berkeley
Kitty Nijmeijer, U. of Twente
Pär Nordlund, Karolinska Inst.
Helga Nowotny, European Research Advisory Board
Ben Olken, MIT
Joe Orenstein, U. of California Berkeley & Lawrence Berkeley National Lab
Harry Orr, U. of Minnesota
Pilar Ossorio, U. of Wisconsin
Andrew Oswald, U. of Warwick
Steve Palumbi, Stanford U.
Jane Parker, Max-Planck Inst. of Plant Breeding Research
Giovanni Parmigiani, Dana-Farber Cancer Inst. **($)**
John H. J. Petrini, Memorial Sloan-Kettering Cancer Center
Samuel Pfaff, Salk Institute for Biological Studies
Joshua Plotkin, U. of Pennsylvania
Albert Polman, FOM Institute AMOLF
Philippe Poulin, CNRS
Jonathan Pritchard, Stanford U.
David Randall, Colorado State U.
Felix Rey, Institut Pasteur
Trevor Robbins, U. of Cambridge
Jim Roberts, Fred Hutchinson Cancer Research Ctr.
Barbara A. Romanowicz, U. of California, Berkeley
Amy Rosenzweig, Northwestern University
Mike Ryan, U. of Texas, Austin
Mitinori Saitou, Kyoto U.
Shimon Sakaguchi, Kyoto U.
Miquel Salmeron, Lawrence Berkeley National Lab
Jürgen Sandkühler, Medical U. of Vienna
Alexander Schier, Harvard U.
Vladimir Shalaev, Purdue U.
Robert Siliciano, Johns Hopkins School of Medicine
Denis Simon, Arizona State U.
Uri Simonsohn, U. of Pennsylvania
Alison Smith, John Innes Centre
Richard Smith, U. of North Carolina **($)**
John Speakman, U. of Aberdeen
Allan C. Spradling, Carnegie Institution of Washington
Jonathan Sprent, Garvan Inst. of Medical Research
Eric Steig, U. of Washington
Paula Stephan, Georgia State U. and National Bureau of Economic Research
Molly Stevens, Imperial College London
V. S. Subrahmanian, U. of Maryland
Ira Tabas, Columbia U.
Sarah Teichmann, Cambridge U.
John Thomas, North Carolina State U.
Shubha Tole, Tata Institute of Fundamental Research
Christopher Tyler-Smith, The Wellcome Trust Sanger Inst.
Herbert Virgin, Washington U.
Bert Vogelstein, Johns Hopkins U.
Cynthia Volkert, U. of Göttingen
David Wallach, Weizmann Inst. of Science
Ian Walmsley, U. of Oxford
Jane-Ling Wang, U. of California, Davis **($)**
David A. Wardle, Swedish U. of Agric. Sciences
David Waxman, Fudan U.
Jonathan Weissman, U. of California, San Francisco
Chris Wikle, U. of Missouri **($)**
Ian A. Wilson, The Scripps Res. Inst. **($)**
Timothy D. Wilson, U. of Virginia
Rosemary Wyse, Johns Hopkins U.
Jan Zaanen, Leiden U.
Kenneth Zaret, U. of Pennsylvania School of Medicine
Jonathan Zehr, U. of California, Santa Cruz
Len Zon, Children's Hospital Boston
Maria Zuber, MIT

BOOK REVIEW BOARD
David Bloom, Harvard U., **Samuel Bowring**, MIT, **Angela Creager**, Princeton U., **Richard Shweder**, U. of Chicago, **Ed Wasserman**, DuPont

Published by AAAS

EDITORIAL

Economics of public safety

Marcia McNutt
Editor-in-Chief
Science *Journals*

By now, the tragic saga of the lead-contaminated drinking water in Flint, Michigan, is well known. Unlike some disasters, this one was not inevitable, and there were many warning signs that could have halted it much sooner. In the developed world, citizens have come to trust that basic public services such as water, power, and sanitation will be provided, for a fee, safely and reliably. Therefore, Flint is not just a nightmare for its 100,000 residents, because it causes all citizens to question whether public officials, who are entrusted with providing essential services, have health and welfare in mind. With criminal investigation of the Flint crisis now under way, my focus is not on assigning blame but on how to prevent a tragedy like this from happening again.

One strong recommendation is to involve scientists early on in major decisions that affect public health or safety. The city of Flint faced a $15 million budget shortfall, so it examined options for saving money by disconnecting from the Detroit municipal water system. The interim solution, while waiting for a pipeline to be built to a new water source, Lake Huron, was to use water from the Flint River. The plan should have factored in costs to limit the corrosion of lead from the aging pipe system. The water that Flint received from Detroit had been treated to prevent chloride from leaching lead from the pipes; Flint River water has eight times as much chloride, but was not treated as such.

Just as important, public safety needs to be put into perspective with other costs. What is inexcusable in the Flint case is the apparent failure by the Michigan Department of Environmental Quality to weigh the costs of corrosion control against the harm to public health, despite informing the U.S. Environmental Protection Agency (EPA) of their intent to control corrosion. For the 2 years that the Flint River water would be temporarily used, the total cost of corrosion control would have been about $1 per resident of Flint, so about $100,000. Surely residents have spent many times that on bottled water. By comparison, Governor Snyder of Michigan sought $28 million to fix the problem that his office created.

In cases of major issues affecting public health and safety, U.S. federal agencies should consider having policies that involve mandatory reporting to regional or national headquarters, if they do not already. Many federal agencies benefit greatly from local presence and good relations with their counterpart state agencies, but it can create too cozy a relationship that prevents confrontation. When EPA water-quality experts detected lead in the Flint River water up to 1000 times in excess of the federally accepted level, the agency apparently tried to work with the state privately to address the problem. But the state tried to undermine the EPA science, delaying any further action on the problem by many months.

"Has trust in science has been poisoned, along with the water?"

The Flint situation offered many opportunities for the research community. Within months of switching to the Flint River in the spring of 2014, local doctors reported signs of adverse reactions such as rashes and hair loss, all coincident with the tap water looking and smelling strange. By fall, General Motors publicly announced that it would stop using the water because it corroded engine parts at its Flint plant. A year later, the first academic reports of water-quality and human health impacts became public and were probably instrumental in prompting the switch back to Detroit municipal water. Researchers could rebuild public trust if scientists identify issues affecting public safety early, complete good-quality research quickly, and publicly release their findings.

Flint is a disaster of many proportions, from the illnesses of its victims to the questions it raises about the integrity of government officials and science agencies. Has trust in science been poisoned, along with the water? I can no longer drink a glass of tap water without thinking about either.

– Marcia McNutt

10.1126/science.aaf4014

PHOTOS: (INSET) ASSOCIATED PRESS; (TOP) STACEY PENTLAND PHOTOGRAPHY

Downloaded from on February 11, 2016

Published by AAAS

NEWS

"From ... the moon, international politics look so petty. You want to grab a politician ... and drag him a quarter of a million miles out and say, 'Look at that, you son of a bitch.'"

Apollo 14 astronaut Edgar Mitchell to *People* magazine in 1974. Mitchell died last week at the age of 85.

IN BRIEF

Obama makes last budget request

The president met with his national security team to discuss new cybersecurity measures in the request.

President Barack Obama's final budget request to Congress, released 9 February, calls for boosting federal research spending in 2017 by 4%, or $6 billion, to $152 billion. But about two-thirds of the new money would come from so-called mandatory funding mechanisms, which aren't popular with Congress. Mandatory spending dedicates revenue from a specific source, such as the sale of communications spectrum, to specific programs, which gives lawmakers less control over the annual budget. The request calls for the National Institutes of Health to get about an $800 million increase to $33.1 billion. The National Science Foundation would get a 6.7% increase to about $8 billion. The Department of Energy's Office of Science would get $5.7 billion, a 6.6% boost. NASA's science office would remain flat at $5.6 billion. Basic science spending at the Department of Defense would drop 9%, to $2.1 billion. The Defense Advanced Research Projects Agency would get about a 4% bump to $3 billion. Competitive grants for agricultural science would double, to $700 million. The White House also wants $1.8 billion in emergency spending to address the Zika virus. http://scim.ag/Budget2017

AROUND THE WORLD

Response to trial crisis faulted

PARIS | Why one man died and four others fell ill during a drug safety study in France last month is still unclear (*Science*, 22 January, p. 320). But a preliminary report by France's General Inspectorate of Social Affairs (IGAS) lashes out at Biotrial, the company that conducted the tests of a compound called BIA 10-2474, developed by Portuguese pharma company Bial as a candidate drug for a range of diseases. The study had proceeded without incident since July 2015, but on 6 January, a group of eight people entered the study, six of whom received multiple high doses of the drug. One subject complained of headaches and blurry vision and was hospitalized on 10 January; he was declared brain-dead the following day. The IGAS report, released 4 February, cites three major errors that put other volunteers at risk: Biotrial gave the five remaining volunteers their daily dose on 11 January without checking on the first subject's status; it did not inform the volunteers about his status, robbing them of a chance to reconsider their participation; and it did not report the disaster to health authorites until 14 January, 3 days after the study was halted. http://scim.ag/IGASBiotrial

Chinese firm bids for GM giant

BEIJING | In a move that could change how China regulates genetically modified (GM) crops, the country's biggest state-owned chemicals company last week offered $43.8 billion for Swiss-owned seed and agrichemicals giant Syngenta AG. If the deal goes through, China National Chemical Corporation would control one of the world's largest GM seed portfolios. Currently, China does not allow the domestic cultivation of most GM crops, though it allows some—such as those used in animal feed—to be imported. The move comes at a time when China's top policymakers are pushing against strong public opposition to GM foods. Syngenta's board of directors, which has pledged to keep the company's current management in place, has voiced support for the buyout. But any

PHOTO: REUTERS/KEVIN LAMARQUE

Downloaded from on February 11, 2016

Published by AAAS

Rusingoryx atopocranion may have used the bony tube in its skull to communicate at low frequencies (artist's conception).

Odd wildebeest cousin had 'vuvuzela' in its head

In 1983, paleontologists gave a now-extinct cousin of the wildebeest the name *Rusingoryx atopocranion*, noting its oddly shaped head. That cranium, researchers reported last week in *Current Biology*, housed an S-shaped tube that may have allowed the creature to bellow at very low frequencies. The team performed CT scans on several skulls of the species unearthed on Kenya's Rusinga Island; the fossils were entombed in floodplain sediments between 40,000 and 285,000 years ago. Using computer analyses, researchers suggest that airflow through the bony tube would have generated sound at frequencies between 248 and 746 cycles per second—a range that encompasses the drone of the South African vuvuzela (which achieved fame during the 2010 FIFA World Cup). When further modulated by the soft tissues of the throat and windpipe, the frequency could have dropped below 20 cycles per second, below the hearing threshold for most humans—and most predators on the African savanna. Although absent in all living animals, similar tubes have been found inside the skull crests of certain dinosaurs.

deal would still have to clear regulatory hurdles in Europe and the United States.

Scandal engulfs Nobel official

STOCKHOLM | The widening scandal surrounding surgeon Paolo Macchiarini and his employment at the Karolinska Insitute (KI) in Stockholm has prompted Urban Lendahl, secretary general of the Nobel Assembly, to resign. Lendahl, a developmental geneticist at KI, was involved in hiring Macchiarini in 2010. Last summer, KI cleared Macchiarini of charges that he had overstated the success of his pioneering artificial trachea implants in a series of scientific papers. But in January, a Swedish documentary suggested that Macchiarini didn't properly inform his patients about the operation's risks (six of his eight patients have died), and questioned KI's handling of the scandal. KI announced last month that it had "lost confidence" in Macchiarini and has said it will launch an external investigation into the university's interactions with him. A statement from the Nobel Committee this week said that Lendahl expected to be involved in the investigation and was giving up his work on the committee "out of respect for the integrity of the Nobel Prize work." **http://scim.ag/Lendahlresig**

FINDINGS

A 6th century 'Little Ice Age'

Historians have long identified a "Little Ice Age" period of modest cooling in the Northern Hemisphere that lasted roughly from the 16th to the 19th centuries. But a thousand years earlier, another cold spell even more profoundly chilled the Northern Hemisphere for more than a century, researchers reported this week in *Nature Geoscience*. Analyses of tree rings from more than 150 living trees and 500 fallen trees in the Russian Altai-Sayan Mountains provide a chronicle of climate from 359 B.C.E. to 2011 C.E. The tree rings show that 13 of the 20 coldest summers in the record occurred in the 6th

BY THE NUMBERS

42

Wind speed, in meters per second, at which trees tend to break, regardless of their diameter, height, or elastic properties (*Physical Review E*). **http://scim.ag/treebreak**

13%

Fraction, on average, of Antarctica's floating ice shelves that could be lost with little impact on the ice sheet upstream. Some areas are even more susceptible to ice loss, such as the Amundsen and Bellingshausen seas (*Nature*).

ILLUSTRATION: TODD S. MARSHALL. HTTP://WWW.MARSHALLS-ART.COM

Published by AAAS

A 6th century cold spell may have helped spread the Plague of Justinian (shown in a 15th century painting).

century, after the year 536, when a huge volcanic eruption dimmed the Northern Hemisphere. Two additional eruptions, in 540 and 547, helped render that decade the coldest in 2300 years, the team reports. They dubbed the 120-year cold spell the Late Antique Little Ice Age, noting that it may have helped trigger societal upheaval by leading to widespread crop failures, migrations, and the spread of plague.

Sleep loss and false confessions

Sleep deprivation can make false confessions easy to extract, a new study shows, putting hard numbers to a problem criminal law reformers have worried about for decades. Researchers at Michigan State University in East Lansing recruited 88 students to solve problems at computers and instructed them not to press the escape key for fear of erasing study data. Half of the subjects were then forced to stay awake all night, while the rest got a full night's sleep. The next morning, the subjects each received a statement accusing them of hitting the key, although none had. They were asked to sign the statement; if they refused, they were asked to sign a second time. Lack of sleep took a toll: Twenty-two of the 44 sleep-deprived subjects signed the false confession the first time, and 30 confessed when asked again (compared with eight and 16 of the 44 well-rested subjects, respectively), the team reported this week in the *Proceedings of the National Academy of Sciences*. http://scim.ag/sleepdepconfess

Indigenous groups to share malaria drug profits

A French government research agency has agreed to share revenues from a potential malaria drug with the people who helped discover it after a human rights organization accused the institute of biopiracy. Scientists at the Institute of Development Research (IRD) isolated the candidate drug from *Quassia amara* (shown), a small red-flowered tree native to Central and South America, after collecting knowledge about medicinal plants from indigenous and local communities in French Guiana. They reported its antimalarial activity in 2009 and obtained a patent in March 2015. In a 25 January letter, the Fondation Danielle Mitterrand France Libertés along with legal scholar Thomas Burelli of the University of Ottawa called IRD's actions "immoral" and announced they had challenged the patent. IRD initially mounted a vigorous defense, but on 5 February agreed to share any proceeds if the drug makes it to the market. Details of the deal still need to be worked out. **http://scim.ag/IRDmalaria**

NEWSMAKERS

New HHMI president

The Howard Hughes Medical Institute (HHMI) has chosen as its next president **Erin O'Shea**, a biochemist who is now chief scientific officer of the giant medical research philanthropy in Chevy Chase, Maryland. On 1 September O'Shea will become the first woman to head HHMI. HHMI has an $18.2 billion endowment and spent $666 million on research last year, mostly by supporting about 330 investigators at universities. O'Shea, 50, is a long-time HHMI investigator who studies gene regulation and signal transduction; she left Harvard University for HHMI in 2013 but maintains a lab there. She is a former postdoc of current HHMI President Robert Tjian, who has led the organization since 2009. O'Shea expects to expand HHMI's partnerships with other philanthropies and launch a major new program to promote diversity in biomedical research. **http://scim.ag/OSheaHHMI**

Brain scientist to head Stanford

Neuroscientist **Marc Tessier-Lavigne**, who has strong ties to both academia and the biotech industry, has been tapped to be the new head of Stanford University in Palo Alto, California. Tessier-Lavigne, 56, is now the president of The Rockefeller University in New York City, where he directs a lab specializing in brain development and neurodegenerative brain disease. Previously, he was chief scientific officer and executive vice president for research at biotech giant Genentech. He has also been involved in several start-ups, helping to found San Francisco, California–based Denali Therapeutics, which focuses on Alzheimer's and neurodegenerative diseases, and serving on the board of Seattle, Washington–based Juno Therapeutics, which investigates cancer immunotherapy drugs. Tessier-Lavigne will replace outgoing Stanford President John Hennessy, who has been president of the university for 16 years, on 1 September.

IMAGES: (TOP TO BOTTOM) JOSSE LIEFERINXE. FROM "ST. SEBASTIAN BETET FÜR DIE PESTOPFER" (1497–1499); © BLICKWINKEL/ALAMY STOCK PHOTO

Published by AAAS

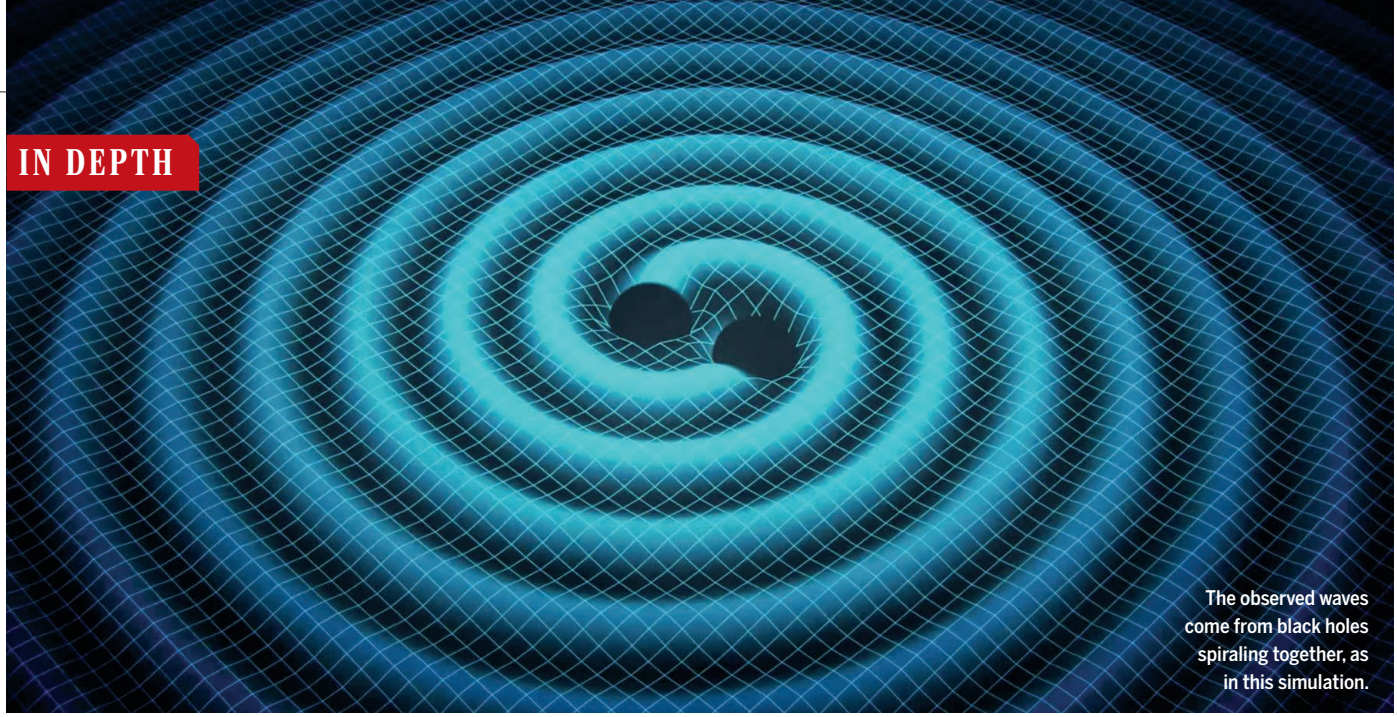

The observed waves come from black holes spiraling together, as in this simulation.

ILLUSTRATION: SWINBURNE ASTRONOMY PRODUCTIONS

PHYSICS

Triumph for gravitational wave hunt

Observation made with newly detectable radiation clinches case for black holes

By **Adrian Cho**

Long ago, deep in space, two massive black holes—the ultrastrong gravitational fields left behind by gigantic stars that collapsed to infinitesimal points—slowly drew together. The stellar ghosts spiraled ever closer, until, about 1.3 billion years ago, they whirled about each other at half the speed of light and finally merged. The collision sent a shudder through the universe: ripples in the fabric of space and time called gravitational waves. Five months ago, they washed past Earth. And, for the first time, physicists detected the waves, fulfilling a 4-decade quest and opening new eyes on the heavens.

The discovery marks a triumph for the 1000 physicists with the Laser Interferometer Gravitational-Wave Observatory (LIGO), a pair of gigantic instruments in Hanford, Washington, and Livingston, Louisiana. Rumors of the detection had circulated for months. But as *Science* went to press, the LIGO team planned to make it official on 11 February in a press conference in Washington, D.C. "We did it!" says David Reitze, a physicist and LIGO executive director at the California Institute of Technology (Caltech) in Pasadena. "All the rumors swirling around out there got most of it right."

Albert Einstein predicted the existence of gravitational waves 100 years ago, but directly detecting them required mind-boggling technological prowess. LIGO researchers sensed a wave that stretched space by one part in 10^{21}, making the entire Earth expand and contract by 1/100,000 of a nanometer, about the width of an atomic nucleus. The observation tests Einstein's theory of gravity, the general theory of relativity, with unprecedented rigor and provides proof positive that black holes exist. "It will win a Nobel Prize," says Marc Kamionkowski, a theorist at Johns Hopkins University in Baltimore, Maryland.

LIGO watches for a minuscule stretching of space with what amounts to ultraprecise rulers: two L-shaped contraptions called interferometers with arms 4 kilometers long. Mirrors at the ends of each arm form a long "resonant cavity," in which laser light of a precise wavelength bounces back and forth, resonating just as sound of a specific pitch rings in an organ pipe. Where the arms meet, the two beams can overlap. If they have traveled different distances along the arms, their waves will wind up out of step and interfere with each other. That will cause some of the light to warble out through an exit called a dark port in synchrony with undulations of the wave.

From the interference, researchers can compare the relative lengths of the two arms to within 1/10,000 the width of a proton—enough sensitivity to see a passing gravitational wave as it stretches the arms by different amounts. To spot such tiny displacements, however, scientists must damp out vibrations such as the rumble of seismic waves, the thrum of traffic, and the crashing of waves on distant coastlines.

On 14 September 2015, at 9:50:45 universal time—4:50 a.m. in Louisiana and 2:50 a.m. in Washington—LIGO's automated systems detected just such a signal. The oscillation emerged at a frequency of 35 cycles per second, or Hertz, and sped up to 250 Hz before disappearing 0.25 seconds later. The increasing frequency, or chirp, jibes with two massive bodies spiraling into each other. The 0.007-second delay between the signals in Louisiana and Wash-

Signals in synchrony

When shifted by 0.007 seconds, the signal from LIGO's observatory in Washington (red) neatly matches the signal from the one in Louisiana (blue).

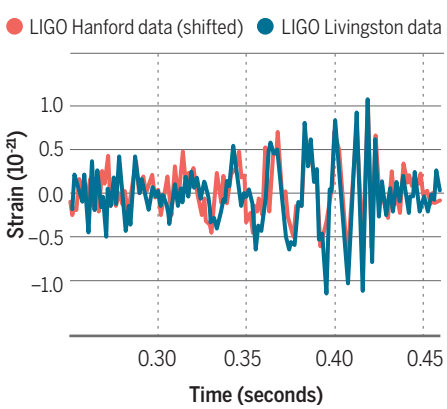

Downloaded from on February 11, 2016

Published by AAAS

ington is the right timing for a light-speed wave zipping across both detectors.

The signal exceeds the "five-sigma" standard of statistical significance that physicists use to claim a discovery, LIGO researchers report in a paper scheduled to be published in *Physical Review Letters* to coincide with the press conference. It's so strong it can be seen in the raw data, says Gabriela González, a physicist at Louisiana State University, Baton Rouge, and spokesperson for the LIGO scientific collaboration. "If you filter the data, the signal is obvious to the eye," she says.

Comparison with computer simulations reveals that the wave came from two objects 29 and 36 times as massive as the sun spiraling to within 210 kilometers of each other before merging. Only a black hole—which is made of pure gravitational energy and gets its mass through Einstein's famous equation $E=mc^2$—can pack so much mass into so little space, says Bruce Allen, a LIGO member at the Max Planck Institute for Gravitational Physics in Hanover, Germany. The observation provides the first evidence for black holes that does not depend on watching hot gas or stars swirl around them at far greater distances. "Before, you could argue in principle whether or not black holes exist," Allen says. "Now you can't."

The collision produced an astounding, invisible explosion. Modeling shows that the final black hole totals 62 solar masses—3 solar masses less than the sum of the initial black holes. The missing mass vanished in gravitational radiation—a conversion of mass to energy that makes an atomic bomb look like a spark. "For a tenth of a second [the collision] shines brighter than all of the stars in all the galaxies," Allen says. "But only in gravitational waves."

For 5 months, LIGO physicists struggled to keep a lid on their pupating discovery. Ordinarily, most team members would not have known whether the signal was real. LIGO regularly salts its data readings with secret false signals called "blind injections" to test the equipment and keep researchers on their toes. But on 14 September 2015, that blind injection system was not running. Physicists had only recently completed a 5-year, $205 million upgrade of the machines, and several systems—including the injection system—were still offline as the team wound up a preliminary "engineering run." As a result, the whole collaboration knew that the observation was likely real. "I was convinced that day," González says.

Still, LIGO physicists had to rule out every alternative, including the possibility that the reading was a malicious hoax. "We spent about a month looking at the ways that somebody could spoof a signal," Reitze says, before deciding it was impossible. For González, making the checks "was a heavy responsibility," she says. "This was the first detection of gravitational waves, so there was no room for a mistake."

Proving that gravitational waves exist may not be LIGO's most important legacy, as there has been compelling indirect evidence for them. In 1974, U.S. astronomers Russell Hulse and Joseph Taylor discovered a pair of radio-emitting neutron stars called pulsars orbiting each other. By timing the pulsars, Taylor and colleague Joel Weisberg demonstrated that they are very slowly spiraling toward each other—as they should if they're radiating gravitational waves.

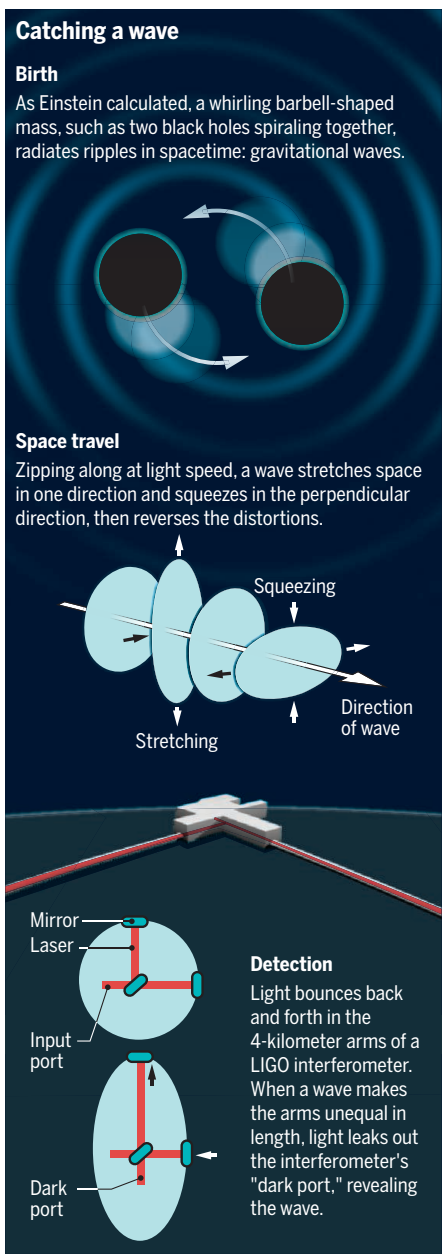

It is the prospect of the science that might be done with gravitational waves that really excites physicists. For example, says Kamionkowski, the theorist at Johns Hopkins, the first LIGO result shows the power of such radiation to reveal unseen astrophysical objects like the two ill-fated black holes. "This opens a new window on this vast population of stellar remnants that we know are out there but of which we have seen only a tiny fraction," he says.

The observation also paves the way for testing general relativity as never before, Kamionkowski says. Until now, physicists have studied gravity only in conditions where the force is relatively weak. By studying gravitational waves, they can now explore extreme conditions in which the energy in an object's gravitational field accounts for most or all of its mass—the realm of strong gravity so far explored by theorists alone.

With the black hole merger, general relativity has passed the first such test, says Rainer Weiss, a physicist at the Massachusetts Institute of Technology (MIT) in Cambridge, who came up with the original idea for LIGO. "The things you calculate from Einstein's theory look exactly like the signal," he says. "To me, that's a miracle."

The detection of gravitational waves marks the culmination of a decades-long quest that began in 1972, when Weiss wrote a paper outlining the basic design of LIGO. In 1979, the National Science Foundation funded research and development work at both MIT and Caltech, and LIGO construction began in 1994. The $272 million instruments started taking data in 2001, although it was not until the upgrade that physicists expected a signal.

If LIGO's discovery merits a Nobel Prize, who should receive it? Scientists say Weiss is a shoo-in, but he demurs. "I don't like to think of it," he says. "If it wins a Nobel Prize, it shouldn't be for the detection of gravitational waves. Hulse and Taylor did that." Many researchers say other worthy recipients would include Ronald Drever, the first director of the project at Caltech who made key contributions to LIGO's design, and Kip Thorne, the Caltech theorist who championed the project. Thorne also objects. "The people who really deserve the credit are the experimenters who pulled this off, starting with Rai and Ron," he says.

Meanwhile, other detections may come quickly. LIGO researchers are still analyzing data from their first observing run with their upgraded detectors, which ended 12 January, and they plan to start taking data again in July. A team in Italy hopes to turn on its rebuilt VIRGO detector—an interferometer with 3-kilometer arms—later this year. Physicists eagerly await the next wave. ■

ILLUSTRATION: V. ALTOUNIAN/*SCIENCE*

Published by AAAS

Cockroaches squeezing through tight crevices are leading to robust robots.

PHOTO: POLYPEDAL LAB UC BERKELEY

BIOMECHANICS

Bendy bugs inspire roboticists

Bees, wasps, and cockroaches are built to survive bashing and squeezing

By **Elizabeth Pennisi**

Insects, whether they creep or fly, live in a world of hard knocks. Who has not stepped on a cockroach, then raised her shoe to watch the creature get up and scoot under a door? Bees and wasps, for their part, face a never-ending obstacle course of leaves, stems, and petals—bumblebees crash their wings into obstacles as often as once a second. Now, researchers are learning how these creatures bend but don't break.

The results do more than explain why cockroaches are so hard to kill. By mimicking the combination of rigid and flexible parts that gives insect exoskeletons and wings their resilience, biomechanicists are making robots tougher. "Bend but not break is a lot of what happens in these insects," says Harvard University roboticist Robert Wood. "We're trying the same thing to see if we can have similar robustness in our robots."

Until recently, most engineers designed for a tough-and-tumble world by making machines stiff and sturdy or agile enough to avoid danger. Modern cars incorporate a third approach: They absorb impacts by crumpling, sacrificing the structure to protect the occupants. "Nature has come up with a tactic that we don't have," says David Hu, a mechanical engineer at Georgia Institute of Technology in Atlanta. "Crumple … and then keep on going."

To see how cockroaches do it, integrative biologist Robert Full at the University of California (UC), Berkeley, and Ph.D. student Kaushik Jayaram coaxed the insects through ever smaller slits or tighter tunnels while filming them with a high-speed video camera. They also lowered weights of up to 100 grams onto different parts of the insects' bodies and watched how the creatures collapsed.

Full and Jayaram found that when the 9-millimeter-tall *Periplaneta americana* approaches a slit no more than 3 millimeters high, the roach first inspects the opening with its antennae. Then it jams its head through, follows with its front legs, and begins pulling the rest of its body into the breach. The back legs splay but continue to push. In about 1 second, it emerges on the far side unscathed. That ability to squeeze through a tight spot "goes far beyond any other animals that we have measured, except maybe the octopus," says Stacey Combes, a biologist at UC Davis. But an octopus—a model for the "soft" robots some designers are pursuing—can't match the speed of a cockroach or other arthropods. "Not only insects, but crabs, spiders, and scorpions are pretty good at going anywhere and are pretty indestructible," Full says.

Jayaram and Full's study, published this week in the *Proceedings of the National Academy of Sciences*, showed that the cockroach's secret lies in the design of its exoskeleton. It consists of hard yet bendable plates—capable of efficiently transmitting energy to its legs—connected by elastic membranes that allow the plates to overlap as the insect compresses. Thanks to spines that give traction when its legs are splayed, a cockroach can scuttle even at maximum scrunch.

At a meeting of the Society for Integrative and Comparative Biology last month in Portland, Oregon, Harvard postdoc Andrew Mountcastle reported that a similar blending of hard and soft parts enables bees and wasps to survive their aerial obstacle courses. Using high-speed video, he found that wasp wings actually buckle during collisions and then snap back into place. He also noticed that the wings have a small patch of an elastic protein called resilin about two-thirds of the way down the wing. He and Combes hypothesized that the patch serves as a hinge.

To test the idea, Mountcastle mounted a wasp on a rotational motor and hit the wing over and over. "He showed the wing can pop out many, many times," Hu says. When Mountcastle splinted the hinge so the wing couldn't buckle, the wing quickly wore down. He and Combes also found that many insects have a similar hinge, but that bumblebee wings incorporate a different design principle. The veins that support the bee wing are concentrated close to the body, resulting in a flexible wingtip that can bounce off obstacles with less wear and tear. "It's different means to the same ends," Mountcastle says.

Both the roach exoskeleton and the insect wings are inspiring robot design. Jayaram has built a 75-millimeter-tall robot, with a roach-like collapsible exoskeleton and legs with "spines" that work both in the uncompressed and compressed positions. It can squeeze to one-half its height and still move five to 10 times faster than soft robots, Jayaram says. "What is exciting is that this gives us an order of magnitude reduction in voids where we can deploy robots," says Robin Murphy of Texas A&M University, College Station, who specializes in robots for use in disasters.

Mountcastle has joined forces with Jayaram—now also a Harvard postdoc—and Wood to refit hinged wings to an insect-sized flying robot called Robobee. "Designing [it] was not trivial; they are not simple, linear hinges," Mountcastle said at the Portland meeting. The group hopes begin testing the new design in the real world by spring.

Hu applauds the insect-inspired designs: "It would be great to see more robots built with potential damage in mind." As for killing cockroaches—Jarayam suggests simply slamming the shoe down as hard as you can. ■

Downloaded from on February 11, 2016

Published by AAAS

HUMAN EVOLUTION

Neandertal genes linked to modern diseases

DNA inherited from our extinct cousins boosts risk of depression and other disorders

By **Ann Gibbons**

Depressed? Your inner Neandertal may be to blame. Modern humans met and mated with these archaic people in Europe or Asia about 50,000 years ago, and researchers have long suspected that genes picked up in these trysts might be shaping health and well-being today. Now, a study on p. 737 details their impact. It uses a powerful new method for scanning the electronic health records of 28,000 Americans to show that some Neandertal gene variants today can raise the risk of depression, skin lesions, blood clots, and other disorders.

Neandertal genes aren't all bad. "These variants sometimes protect against a disease, sometimes make people more susceptible to disease," says paleogeneticist Svante Pääbo of the Max Planck Institute for Evolutionary Anthropology in Leipzig, Germany. Two other new studies identified three archaic genes that boost immune response. And most archaic genes that persist in humans were likely beneficial in prehistoric times. But some now cause disease because modern lifestyles and environments are so different.

Living people carry only trace amounts of Neandertal DNA, which makes its impact on health more striking. "The Neandertal genetic contribution to present-day people seems to have larger physiological effects than I would have naïvely thought," says Pääbo, who helped launch this avenue of research by sequencing the first ancient genomes but was not involved in these studies. On average, Europeans and Asians have inherited about 1.5% of their genomes from Neandertals. Island Melanesians carry an additional 2% to 3% of DNA inherited from another extinct group, the Denisovans. Most Africans lack this archaic DNA because the interbreeding happened after modern humans left Africa.

By comparing the genomes of a few Neandertals and one Denisovan with people in the 1000 Genomes database, computational biologists have recently uncovered about 12,000 Neandertal gene versions, or haplotypes, in living Europeans and Asians (*Science*, 28 February 2014, p. 1017). Researchers had clues to the function of a handful of these haplotypes—some were thought to be involved in the immune system, or the development of skin or hair, for example. But nailing down their precise function has required costly gene expression studies in tissue or animal models (*Science*, 3 July 2015, p. 21).

A breakthrough came when population geneticist Joshua Akey of the University of Washington, Seattle, and evolutionary genomicist Tony Capra of Vanderbilt University in Nashville independently realized that they could fish for Neandertal gene variants in a medical database, the Electronic Medical Records and Genomics (eMERGE) Network. This consortium in nine U.S. cities links patients' genetic data with their medical data, in the form of specific billing codes that record diagnoses for illnesses and other conditions. Thus eMERGE allows researchers to track correlations between genes and symptoms in tens of thousands of people.

Akey and Capra joined forces and searched for more than 6000 Neandertal haplotypes in genetic data from 28,416 adults of European ancestry. After pinpointing chunks of DNA inherited from Neandertals, the team used statistical analysis to link possession of these archaic variants to a higher risk of the diseases or other traits captured in the billing data, Capra says.

The search netted a dozen Neandertal genes likely to cause significant risk of disease today. For example, one gene variant apparently makes blood more sticky and prone to coagulate. This fast clotting may have spelled the difference between life and death when Neandertals hunted dangerous animals or hemorrhaged after birthing big-brained babies. But it can also increase the risk of blood clots and strokes, which would have been much less common in prehistoric times when most people died young.

The researchers also found a number of Neandertal genes associated with neurological conditions, including depression, which can be triggered by disturbed circadian rhythms. Other variants were linked to precancerous skin lesions called actinic keratoses. Capra speculates that Neandertal brain chemistry and their skin responses to sunlight may both have been attuned to the light conditions and lifestyles of prehistoric Europe. The gene variants responsible may be maladaptive now that most people live by artificial light.

Other Neandertal alleles regulate the transport of thiamine, or vitamin B1, which metabolizes carbohydrates in cells of the gut. Neandertal diets, rich in meat and nuts, may have provided ample thiamine, but people munching processed foods today may not get enough, and having the Neandertal vari-

Neandertals' hidden legacy

In many people today, genes inherited from Neandertals affect systems all over the body, raising the risk of certain diseases. But some Neandertal genes have beneficial effects, for example boosting the immune system.

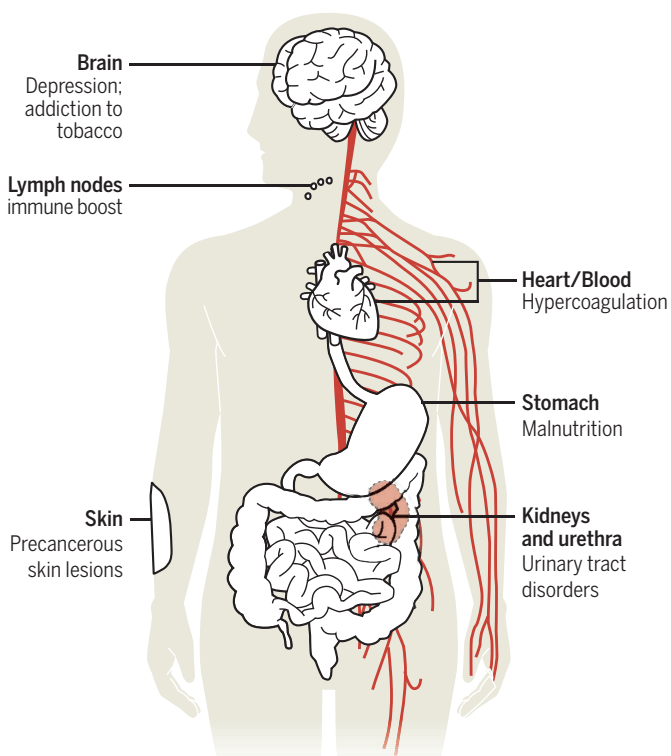

DIAGRAM: ADAPTED FROM DEBORAH BREWINGTON/VANDERBILT UNIVERSITY

Downloaded from on February 11, 2016

Published by AAAS

ant may predispose them to malnutrition, Capra speculates.

The study also revealed Neandertal genes associated with incontinence, bladder pain, and urinary tract disorders. And a single base change was associated with nicotine addiction, making it the second Neandertal allele found so far to boost the risk of tobacco addiction.

The Neandertal health legacy isn't entirely negative. Two studies published in *The American Journal of Human Genetics* last month identified three archaic genes that boost the innate immune response, which helps defend against fungi and parasites as well as bacteria. All three have been strongly selected for in Europeans and Asians, says computational biologist Janet Kelso of Max Planck, lead author of one study. The three genes work together in subtle ways to regulate the expression of toll-like receptors on the surface of white blood cells, presumably boosting the innate response, says Lluis Quintana-Murci, a population geneticist at the Pasteur Institute and the French National Center for Scientific Research in Paris, lead author of the other study.

Such examples suggest that as modern humans entered new environments that harbored new pathogens, they took an evolutionary shortcut by picking up beneficial genes from other hominins (*Science*, 24 July 2015, p. 362). "You just borrow diversity from another species or population that had lived there longer," Quintana-Murci says. Neandertals had at least 200,000 years to adapt to life in the Middle East and Europe before moderns got there.

But however beneficial in the Pleistocene and to people living in poor conditions today, even immune-boosting genes may have deleterious effects in the United States and Europe, where people face fewer parasites: Kelso found that the archaic receptor genes were strongly linked to allergies. "The price to pay today is that when you boost the immune response, it can be bad for us in terms of autoimmunity, inflammation, and allergies," Quintana-Murci says.

Exactly how these genes affected Neandertals themselves is not always clear. "This doesn't mean that Neandertals were depressed," or had more skin cancer, cautions computational geneticist Sriram Sankararaman of the University of California, Los Angeles.

These studies are just the beginning, as researchers search for more Neandertal variants passed on in those ancient encounters, and broaden their databases of modern genomes to the hundreds of thousands. "We suspect there are many more Neandertal alleles floating out there," Capra says. ■

AUSTRALIA

Research chief cuts climate studies, sets new priorities

CSIRO to trim staff as it seeks closer alignment with industry

By **Leigh Dayton**, *in Sydney, Australia*

Australia's premier research agency has long been at the vanguard of climate science. "Our climate models are among the best in the world and our measurements honed those models to prove global climate change," Larry Marshall, chief executive of the Commonwealth Scientific and Industrial Research Organisation (CSIRO) in Canberra, gushed in an email to his staff last week. But Marshall says that job is finished now, and it's time for his organization to move on.

For scores of climate scientists at CSIRO, Marshall's email amounts to a eulogy. To "realign and restore our business for growth," the former Silicon Valley, California, venture capitalist stated that up to 350 jobs could be eliminated over the next 2 years, including 110 positions in the Oceans and Atmosphere division, the bulwark of CSIRO's climate research. The job losses, Marshall wrote, are "something that we must do to renew our business."

5200
Total CSIRO positions

350
Job losses over the next 2 years

110
Climate researchers will be let go

Outsiders warn that the cuts will gut CSIRO's vaunted work on climate science in the Southern Hemisphere. "I am stunned by reports that CSIRO management no longer thinks measuring and understanding climate change is important, innovative, or impactful," says former Australian chief scientist Penny Sackett, now at the Australian National University in Canberra. "This is a flawed strategy," adds John Church, who leads CSIRO's Sea Level Rise program, which he says is on the chopping block. The cuts, he argues, will prevent Australia from gathering data necessary to meet its obligations under the 2015 climate accord to slash greenhouse gas emissions by 26% to 28% from 2005 levels by 2030.

In his email, Marshall cited a number of priorities that he would like to boost instead, to more closely align CSIRO with industry. For instance, he espouses research to make titanium ink for 3D printing from Australia's mineral sands, produce cleaner diesel fuel from coal, and breed "new strains of food and agricultural products that are healthier, more sustainable and highly differentiated." Marshall is confident that CSIRO scientists will get with the program: "Our people are innovative and many can reinvent themselves to learn these new areas," he wrote.

CSIRO's realignment comes on the heels of more than $15 million in cuts to climate and environmental science in the 2014–15 federal budget. In light of both developments, Andrew Holmes, president of the Australian Academy of Science in Canberra, urges the government "to quickly make alternative arrangements" to continue a national program of climate research.

Marshall did not respond to requests for comment. But in an 8 February statement posted to CSIRO's website, he stated that the cuts will not affect the Cape Grim air pollution monitoring station, jointly managed by CSIRO and the Bureau of Meteorology, which is the source of much of Australia's greenhouse gas data. Other climate science assets, including CSIRO's *Investigator* research vessel, will be protected, he noted. Fears that CSIRO is turning its back on climate research are misplaced, a spokesperson for science minister Christopher Pyne told *Science*. "CSIRO will continue to invest heavily in climate research," he said.

Much of the angst appears to be a reaction to Marshall's management style. "Turnover is essential for a healthy business," he wrote in his email. Marshall's use of phrases such as "reductions in headcount," "renew our business," and "business units," says Ian Lowe, an expert in science and society with Griffith University, Brisbane, in Australia, "reveals that the government is trying to sabotage our public science body and turn it into a consulting business." Nadine Flood, national secretary of the union in Haymarket that represents CSIRO employees, charges that Marshall is modeling CSIRO on Netflix and Silicon Valley. "IT startups might be agile," she says, "but deep science cannot be simply switched on and off again." ■

DATA: CSIRO

Published by AAAS

Rare nacreous clouds, such as these over Belfast, Ireland, form in extreme stratospheric cold and can destroy ozone.

PHOTO: ESKLING/FLICKR

ATMOSPHERIC SCIENCE

Record ozone hole may open over Arctic in the spring

Unusual polar cold produces clouds that could help push ozone losses beyond 2011 mark, releasing extra UV radiation

By **Eric Hand**

Lingering atmospheric pollutants and a blast of frigid air have carved an unusually deep hole in Earth's protective ozone layer over the Arctic, and it threatens to get deeper. Atmospheric scientists are analyzing data from weather balloons and satellites for clues to how the ozone will fare when sunlight—a third factor in ozone loss—returns to the Arctic in the spring. But they are already worrying about how extra ultraviolet light might affect humans and ecosystems below and wondering whether climate change will make such Arctic holes more common or severe.

Record cold temperatures in the Arctic stratospheric ozone layer, 15 to 35 kilometers up, are the proximate cause for this year's losses, because they help to unleash ozone-destroying chemicals. "This winter has been stunning," says Markus Rex, an atmospheric chemist at the Alfred Wegener Institute in Potsdam, Germany. By next week, about 25% of the Arctic's ozone will be destroyed, he says.

This time of year, the stratosphere tends to warm up with the breakdown of the polar vortex, a cyclone that traps cold air. But if a strong vortex persists another month as light returns to the Arctic after the dark winter, ozone losses will get much bigger, Rex says. Conditions are ripe for losses to surpass a record Arctic ozone hole observed in the spring of 2011, he adds.

At Earth's surface, ozone is a caustic chemical and a health hazard. But in the stratosphere, it shields the planet from UV light. Scientists noticed in the 1980s that chlorine-containing chemicals commonly used in refrigerants were reacting to form compounds that ate away stratospheric ozone, especially over the poles. The 1989 Montreal Protocol led to the phaseout of those chemicals, but their long atmospheric lifetime means that seasonal ozone losses will persist well into this century. Every year, a major ozone hole opens up over Antarctica, where winters are colder and polar vortices are stronger and more stable than over the Arctic.

But this year, the Arctic could be the poster child. Cold temperatures have allowed nitric acid, mostly from natural sources, to condense and form the peculiar, iridescent clouds that have been spotted all over northern latitudes this winter. "They're beautiful, but once I see them, I'm concerned—they're dangerous," Rex says. That's because the clouds catalyze the reactions that mobilize chlorine into active chemicals that can react in the presence of sunlight to destroy ozone.

An instrument on the NASA AURA satellite has detected record lows of the inert forms of chlorine and rising amounts of the active ones, notes Gloria Manney, an atmospheric scientist at NorthWest Research Associates in Socorro, New Mexico. "Conditions are primed," she says. "The last ingredient we need is sunlight." Weather models are predicting some warming of the stratosphere this week, she adds, but probably not enough to halt the ozone-destroying brew.

The Arctic vortex tends to behave erratically, with blobs of cold air often dipping into more heavily populated northern latitudes. The influx of ozone-poor air could cause problems for people there, who are unused to wearing sunscreen in March, Rex says. "If we get such a deep minimum, then people need to be informed," he says. The extra radiation could even adversely affect phytoplankton, which typically bloom in the Arctic Ocean each spring, Rex suggests.

Ross Salawitch, an atmospheric chemist at the University of Maryland, College Park, says the health hazards shouldn't be sensationalized. "The worst-case scenario would be folks in high northern latitudes being in a type of ultraviolet environment that people are exposed to all the time in San Diego."

For Salawitch, the bigger question is what role climate change might be playing. The notoriously mercurial polar weather is the main factor determining how much ozone is destroyed each spring, he says. But climate change is also expected to cool the stratosphere over the long run. The same greenhouse gases that trap heat in the lower atmosphere allow the stratosphere to more effectively radiate energy into space.

On its own, the stratospheric cooling could make bad ozone years in the Arctic more common. It should also make polar vortices stronger, and more stable. But there is evidence that storminess at lower latitudes—another thing that is expected to increase in a warming world—will make stable polar vortices less common.

Which effects will win out? Salawitch offers a parallel to hurricanes. Climate change is expected to make tropical hurricanes less frequent but more intense. Persistent Arctic vortices, too, could become scarcer but stronger. "When you have cold winters, they tend to be whoppers." And that could mean that Arctic holes like this year's could get deeper in the future. ■

Downloaded from on February 11, 2016

Published by AAAS

TOXICOLOGY

A crystal ball for chemical safety

By comparing new chemicals to known compounds, toxicologists seek early hazard warnings

By **Tania Rabesandratana**

Every year, chemists invent thousands of new chemicals, and many ultimately find their way into global use. Predicting which ones will pose health or environmental hazards, however, has proven difficult. This week, a group of researchers unveiled a tool that could help streamline the process: a vast database of safety information that will allow users to compare new chemicals to existing compounds with similar structures, and flag potential risks.

"You could imagine that, before even synthesizing [a chemical], a chemist puts the structure into the [tool] to ask if it's safe," says toxicologist Thomas Hartung of the Johns Hopkins Bloomberg School of Public Health in Baltimore, Maryland, who led the effort.

Such predictive screening could help companies and government regulators reduce the need for lengthy, expensive animal testing, observers say, and identify safer alternatives to existing compounds. "We are very enthusiastic about what [Hartung's team] has done," says Tina Bahadori of the U.S. Environmental Protection Agency (EPA) in Washington, D.C., which has been expanding its own computational toxicology efforts. But Bahadori cautions that structural similarities, although promising, are just "one piece of the puzzle" in assessing a compound's safety.

To create the screening tool, which Hartung's team describes this week in *Alternatives to Animal Experiments*, the researchers dug deep into what he calls a "gold mine" of data collected by the European Chemicals Agency (ECHA). Under a 2007 law known as REACH (Registration, Evaluation, Authorisation and Restriction of Chemicals), the agency requires companies that produce or import at least 1 ton of a chemical per year to submit detailed safety information on that substance. Those ECHA submissions are chunks of text, which are difficult to analyze on a large scale.

To solve that problem, the researchers used software to extract text from 816,000 ECHA documents, which refer to some 9800 chemicals. Next, they analyzed the safety findings and organized compounds by their effects. They found that about 20% were labeled as skin sensitizers, for instance, and 17% irritate eyes. Finally, they created a visualization that displays the toxicological properties of the chemicals, and clusters them by their structural similarities (see image, above). It shows, for example, that some clusters are "full of problematic substances," Hartung says.

Such maps could ultimately help researchers evaluate the risks posed by new chemicals without testing them in vitro or in vivo, Hartung says, saving time, money, and possibly the lives of millions of lab animals. That hope has driven other predictive efforts, but they have generally lacked the extensive data underlying the new effort. Bahadori applauds the team for "unearthing and making the [ECHA] data accessible." And she predicts that "these tools will really show their promise … as more decision-making bodies invest in generating data that are comparable and can interact with each other."

But the approach has limits. In some cases, what really matters is not only a chemical's structure, Bahadori says, but also how organisms are exposed and respond to it. "The idea that we're going to do this based on similarity of structure is overly simplistic," warns biomedical researcher Andre Nel, who studies the safety of nanomaterials at the University of California, Los Angeles. Still, Nel says "starting with pockets of knowledge," such as the eye irritation data, "is a useful, practical way to begin."

Legal obstacles could also hamper use of the screening method. Although ECHA's safety reports are public, the companies that registered the chemicals own the data in the reports. That could complicate Hartung's plans to share his database with other researchers and create a spinoff company that would help clients screen new chemicals. He is currently negotiating with the agency over the use of the data; an ECHA spokesperson says "we are keen to see data on chemicals being made use of to enhance their safe use, promote innovation, and avoid unnecessary testing on animals … [but] we need to be sure that the appropriate rights have been respected."

In the meantime, Hartung says that "the fact that we got this public data is fantastic." But he says ECHA and other regulators could do more to make it usable by requiring companies to submit standardized, organized data instead of just text. His team is also meeting with experts in the United States and Europe to share practical read-across guidance, which he hopes will help the method catch on more quickly among regulators, academics, and industrial users.

Nel says that's a "sensible and laudatory goal" but predicts it will take years for such methods to be accepted internationally. Until then, Bahadori says, "we can make the chemistry of the future much smarter by making data available." ■

Troubling resemblances

A study of thousands of industrial chemicals registered in the European Union suggests that those with similar molecular structures can have similar health effects, such as causing skin sensitivity (dark blue). Also shown are nonsensitizing chemicals (light blue) and those with unknown effects (yellow).

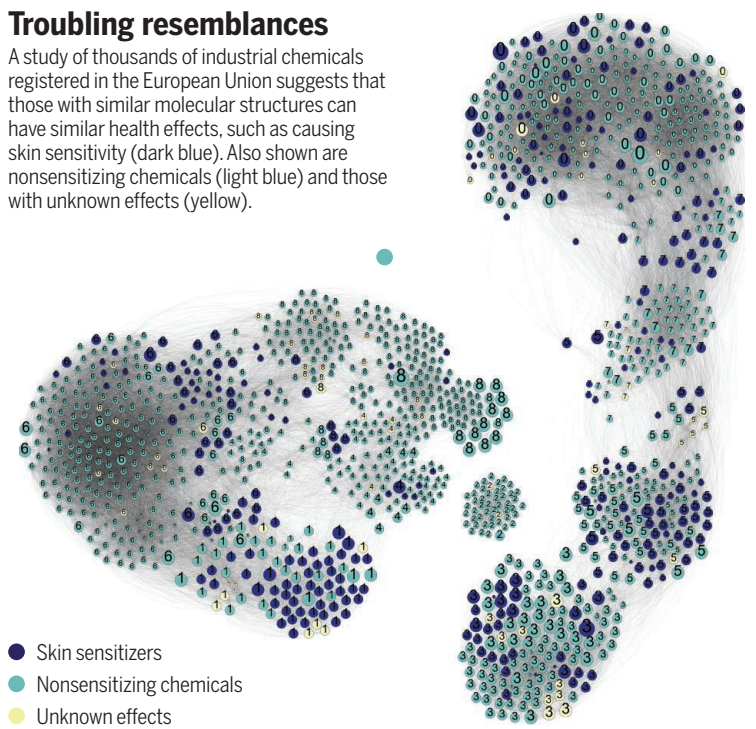

DIAGRAM: LUECHTEFELD *ET AL.*, *ALTEX*. (2016)

Downloaded from on February 11, 2016

Published by AAAS

Allegations of sexual misconduct have roiled the American Museum of Natural History in New York City.

PHOTO: VIEW PRESS/CORBIS

Downloaded from on February 11, 2016

AFTER THE ACCUSATION

A complex case of alleged sexual misconduct rattles a field and signals a cultural shift

By **Michael Balter**, *in New York City*

On a cold evening last March, as researchers descended upon St. Louis, Missouri, for the annual meeting of the American Association of Physical Anthropologists (AAPA), a dramatic scene unfolded at the rooftop bar of the St. Louis Hilton at the Ballpark, the conference hotel. From here, attendees had spectacular views of the city, including Busch Stadium and the Gateway Arch, but many were riveted by an animated discussion at one table.

Loudly, and apparently without caring who heard her, a research assistant at the American Museum of Natural History (AMNH) charged that her boss—noted paleoanthropologist Brian Richmond, the museum's curator of human origins—had "sexually assaulted" her in his hotel room after a meeting the previous September in Florence, Italy. (She requested that her name not appear in this story to protect her privacy.) Over the next several days, as the 1700 conference attendees presented and discussed the latest research, word of the allegations raced through the meeting.

Richmond, who was also at the meeting, has vigorously denied the accusations in a statement to *Science* and in email responses. (He declined to be interviewed in person or by telephone.) The encounter in the hotel room, he wrote, was "consensual and reciprocal," adding that "I never sexually assaulted anyone."

Although the most recent high-profile cases of sexual harassment in science have arisen in astronomy and biology, many researchers say paleoanthropology also has been rife with sexual misconduct for decades. Fieldwork, often in remote places, can throw senior male

Published by AAAS

faculty and young female students together in situations where the rules about appropriate behavior can be stretched to the breaking point. Senior women report years of unwanted sexual attention in the field, at meetings, and on campus. A widely cited anonymous survey of anthropologists and other field scientists, called the SAFE study and published in July 2014 in *PLOS ONE*, reported that 64% of the 666 respondents had experienced some sort of sexual harassment, from comments to physical contact, while doing fieldwork (*Science*, 19 April 2013, p. 265).

Even a few years ago, the research assistant might not even have aired her complaint, as few women—or men—felt emboldened to speak out about harassment. Of the 139 respondents in the SAFE study who said they experienced unwanted physical contact, only 37 had reported it (see graphic, p. 654). Those who remained silent may have feared retaliation. Senior paleoanthropologists control access to field sites and fossils, write letters of recommendation, and might end up as reviewers on papers or grant proposals. "The potential for [senior scientists] to make a phone call and kill a careermaking paper feels very real," says Leslea Hlusko, a paleontologist at the University of California (UC), Berkeley.

Now, however, the SAFE study, along with a few high-profile cases has spurred a major shift in how some academic communities deal with sexual misconduct, says anthropologist Katie Hinde of Arizona State University, Tempe, who co-authored the study. What was once tolerated, overlooked, or kept quiet now may be publicly censured, and institutions are increasingly sensitive to how faculty can—sometimes unwittingly—abuse their power over students and employees. Last month, the California Institute of Technology in Pasadena suspended astronomer Christian Ott for a year for allegedly harassing graduate students (*Science*, 15 January, p. 216). Astronomer Geoff Marcy at UC Berkeley was found to have sexually harassed women students for a decade, and when Berkeley did not fire him, the outrage among astronomers forced him to resign late last year (*Science*, 23 October 2015, p. 364). "How the astronomy community responded to [the Marcy case] is a model for every other field," Hinde says.

"I never sexually assaulted anyone."
Brian Richmond

Now, paleoanthropology is responding to its own complex case. Outsiders may never know for sure what happened in that Florence hotel room. But the incident ultimately triggered a cascade of other allegations against Richmond and a resolve by some senior paleoanthropologists to do battle against sexual misconduct, hoping to change the climate of their field. The charges and the community's response also roiled two leading institutions, which struggled with shifting cultural expectations, inadequate reporting and disciplinary tools, and the challenge of treating all parties fairly.

The research assistant, who still feels that she did not get justice, continues to tell her story. Richmond, who says the museum has asked him to resign and who is the subject of a new investigation, continues to protest his innocence. She no longer reports to him, but until recently they passed each other almost daily in the halls of AMNH. Other paleoanthropologists are working to limit Richmond's contact with students, and find the current situation distressing for all parties. "This is a tragedy of many dimensions, and contemplating it makes me infinitely sad," says Ian Tattersall, the former curator of human origins at the museum.

IN 2010, Tattersall, who had led human origins research at AMNH for more than 30 years, retired, and the search was on for his replacement. It would not be easy, because the personable Tattersall had become a leading voice of paleoanthropology, writing numerous books and making endless public appearances. "He was the spokesperson for our profession," Hlusko says.

In 2014, after a long search, Richmond, then at George Washington University (GWU) in Washington, D.C., was chosen. He began work at the museum in August of that year.

Described as charming and sociable, Richmond, 47, is best known for the co-discovery of 1.5-million-year-old hominin footprints at the site of Ileret, in Kenya (*Science*, 27 February 2009, p. 1197, and 26 April 2013, p. 426). He has co-authored at least 170 publications and served as principal adviser for several grad students and postdocs. Researchers who know Richmond well say that he was a good mentor and worked hard to give his students both field and laboratory experience.

Richmond also supervised the research assistant, who has a key job in AMNH's anthropology division. She received a master's degree in anthropology from New York University (NYU) here, began working at AMNH about a decade ago, and is widely described as hard-working and well-liked.

In late September 2014, less than 2 months after Richmond had begun at AMNH, he and the research assistant attended a meeting of the European Society for the study of Human Evolution (ESHE) in Florence. The research assistant says that on the last night of the meeting, she, Richmond, and several young European researchers were out on the town, visiting bars and drinking red wine and shots of limoncello, an Italian liqueur. She recalls "walking around Florence and realizing that I was way too drunk." The next thing she remembers, she says, is waking up on the bed in Richmond's hotel room in the wee hours of the morning with him on top of her, kissing her and groping under her skirt.

The research assistant says that she immediately told Richmond to stop, and left the room. Because she was not a guest at the hotel, the reception desk in the lobby, perhaps concerned that she was not supposed to be there, would not let her leave without authorization. She had to call up to Richmond and get him to vouch for her. Still in shock, she says, she allowed Richmond to accompany her to her Airbnb nearby. With just a couple of hours before her flight back to New York, she quickly packed and made her way to the airport.

Shortly after her return to New York, the research assistant told her story to at least three friends, all of whom report hearing essentially the same version of events that she later told to *Science*. But she says she delayed officially reporting the incident until sometime in November 2014, fearing that she would not be believed or would be fired. She says she considered making a police report, but doubted that the Italian authorities, who have jurisdiction, would prosecute now that she and Richmond were back in the United States. Finally, after telling her husband, she went to AMNH's human resources (HR) department.

Richmond tells a different story of that night. Although he confirmed in an email to *Science* that he made his room "available" to the research assistant when she could not find her Airbnb, in his written statement Richmond says that the encounter was consensual. It "did not progress beyond kissing and embracing," he wrote, and "ceased the instant my colleague said, 'This isn't a good idea.'" Richmond also says that "while we were both drinking, neither of us was incapacitated."

Back in New York in the late fall, the museum's human resources staff spoke to both Richmond and the research assistant. An email

Published by AAAS

Breaking the silence on sexual harassment

The 2014 SAFE study of fieldwork experiences in anthropology and other fields found confusion about how to report sexual harassment, and many incidents went unreported. Yet some of the 666 survey respondents felt compelled to tell their stories.

Out of the 139 surveyed who experienced unwanted physical contact,

Out of those who reported, seven were satisfied by the outcome.

to her from AMNH's vice president for HR, Daniel Scheiner, dated 22 July 2015, describes the results of that late 2014 investigation—the first of three initiated by the museum. Scheiner wrote: "We had determined that Brian violated the Museum's policy prohibiting inappropriate relationships between supervisors" and their subordinates. Scheiner added that "Brian would be held accountable for the violation of the policy" and that the research assistant would report to a different supervisor.

Anne Canty, AMNH's senior vice president for communications and marketing, clarified that decision in a statement to *Science*, writing that "a zero tolerance warning was issued to Dr. Richmond." According to Canty, from then on the only contact allowed between the two was by email.

In his statement, Richmond confirms that AMNH "disciplined me for violating Museum policy against personal activity between supervisors and those who report to them," and says that he "sincerely apologized to my colleague and the Museum for the breach of that policy." Richmond adds that during the HR investigation, "I was advised that … my colleague recalled virtually nothing" of the incident. He says that he has "since been informed that my colleague's stance has changed over time from simply not remembering what took place after a night in which we had both been drinking with other people, to accusing me of taking advantage of her when she was incapable of consent."

The research assistant vigorously rejects the assertion that she changed her story. She has "no memory of going to Brian's hotel," she says, but does recall waking up in his room. "My clearest memory of that night is waking up to being touched below the waist and how shocking and distressing that was."

STILL UPSET AND ANGRY in March 2015, the research assistant headed for the St. Louis meeting. She felt that the museum should have fired Richmond, and she decided to tell her story to everyone who would listen, especially female colleagues.

At the meeting, one person who heard the allegations was Bernard Wood, 70, a senior paleoanthropologist originally from the United Kingdom. Wood is now at GWU, where Richmond was on the faculty for 12 years before moving to AMNH. Widely regarded as one of Richmond's key mentors, Wood was stunned by the allegations. He says he had no way to know whether they were true. But he was mindful that his recommendations had bolstered Richmond's career for years, and he wanted to be sure that Richmond's behavior while on the GWU faculty had been professional. Also, Richmond continued to teach at the Koobi Fora Field School in Kenya, a summer institute that is now co-run by GWU and the National Museums of Kenya and is mainly attended by undergraduates.

In St. Louis, Wood canvassed younger researchers about their experiences with Richmond. He asked everyone the same question: "Does this alleged behavior come as any surprise to you?" But he didn't get the "yes" he was expecting. Nearly all said that they were not surprised, and two individuals told Wood that they had been the direct subjects of unwanted sexual advances by Richmond. "It was clear that there was a pattern of behavior," Wood says. He continued his efforts once he returned to GWU, speaking to present and former members of the multidisciplinary program he leads, the Center for Advanced Study of Human Paleobiology (CASHP). "As I talked to more and more current and former students at GWU, I became more concerned and alarmed about what I heard," he says.

In important ways, the ground had been prepared at GWU to deal with such allegations. Hinde had spoken to CASHP members about the SAFE study in March 2014, and GWU archaeologist David Braun, co-director of the Koobi Fora Field School, had asked her to help create a policy document about sexual harassment for field school staff to sign. "I have been doing fieldwork in Kenya, Ethiopia, and South Africa for the past 20 years and I have definitely observed these kinds of problems," Braun wrote Hinde, adding that he wanted there to be "no question about our policy."

Now, CASHP responded quickly to the allegations concerning Richmond. Just a few days after the St. Louis meeting ended, program members contacted GWU's coordinator for enforcement of Title IX, a 1972 education law that prohibits discrimination based on sex in educational institutions that receive federal funds. (Most early claims of Title IX violations focused on discrimination in athletics, but today sexual harassment and misconduct are the No. 2 cause of claims.) On 3 April 2015, the coordinator wrote to all members of GWU's anthropology department, soliciting "any knowledge about specific incidents" of sexual harassment.

GRAPHIC: V. ALTOUNIAN/*SCIENCE*

Published by AAAS

Despite his association with Koobi Fora, Richmond was no longer a GWU employee, so the university could not launch a formal investigation, Wood says. So, according to Wood and three others in the meetings, the CASHP faculty decided in early April 2015 to use their discretion to remove Richmond from teaching at the field school.

Braun then communicated this decision to Richmond, according to sources at the meetings. On 6 April 2015, Richmond responded to Braun in an email saying that he was "writing to indicate my willingness to resign my role in the Koobi Fora Field School." On 13 April 2015, CASHP faculty removed Richmond's name and photo from the faculty list on the field school's website. The CASHP faculty also asked the university administration to send Richmond a letter formally confirming that his ties to the field school had been severed. "I urged the university to make it clear that Brian Richmond was no longer welcome at the Koobi Fora Field School and was no longer part of it," Wood says. The university reportedly did so about a month later.

Wood also signaled his growing vigilance about harassment in other ways. He called for zero tolerance for sexual misconduct in two blog posts on the CASHP website, on 21 April 2015 and 9 September 2015, and in a *Science* editorial in October 2015 (*Science*, 30 October 2015, p. 487). He timed his 9 September blog, posted the day before the 2015 ESHE meeting opened in London, to head off Richmond's candidacy for a seat on the organization's governing council. (Richmond did not receive enough votes to be elected.) At the meeting, Wood also resigned as chair of a session just before Richmond spoke in it.

Richmond notes in his statement to *Science* that before the incident in Italy, "there had never been a complaint or report against me throughout my career," including from students at the field school. He stresses that he "voluntarily resigned my affiliation" with the field school, and explained in an email that he hoped his resignation "would help address the anger Wood reported to me" from those accusing him of inappropriate behavior.

Richmond also says that his relationships with female researchers were consensual. Nevertheless, he says in his statement, "I take full responsibility for exercising poor judgment in the past by mixing my professional and personal lives, including having consensual affairs, and I have changed my thinking and my behavior. I am deeply distressed to learn that I have upset the women involved and colleagues in my field. I regret that I was not sensitive to how my academic position could impact the dynamics of consensual relationships."

"As I talked to more and more current and former students at GWU, I became more concerned and alarmed about what I heard."
Bernard Wood

WORD QUICKLY REACHED AMNH OFFICIALS about the events in St. Louis. Although HR chief Scheiner, who is also the museum's Title IX coordinator, had completed his investigation, the museum soon assigned in-house attorney Rhea Gordon to conduct a second investigation. The research assistant gave Gordon several people to talk to about Richmond's alleged past actions, including Rebecca Ackermann, 46, a U.S. physical anthropologist at the University of Cape Town in South Africa.

On 14 April 2015, Gordon emailed Ackermann to ask for her help with investigating "instances of misconduct in the field in connection with Brian Richmond." Gordon told Ackermann that she was "particularly interested in hearing from any individuals who can speak first-hand about their experiences."

Ackermann agreed to help. She says she had been the object of sexual harassment from high school through graduate school but always felt she had limited power to do anything about it. For her, the Richmond allegations set off alarm bells, because some of her own students had reported that he had made sexual advances to them at Koobi Fora.

Back home in Cape Town, she spoke with two former undergraduates at the field school who had previously told her that Richmond had engaged in inappropriate behavior with them, as well as a third person whose experiences she had heard about. All three agreed to provide written testimony that Ackermann could transmit to Gordon. They asked not to be named but said they were willing to provide their names in case of formal proceedings at the museum.

On 30 April 2015, Ackermann began to send the written accounts and vouched for the former students' identities. *Science* interviewed the three women, two by phone and one by email.

One account, written together by two former students who identify themselves as P1 and P2, describes events that allegedly took place late in the evening of 4 July 2007 at the field school, which at that time was run jointly by Rutgers University, New Brunswick, in New Jersey, and the National Museums of Kenya. During a celebration of U.S. Independence Day, the pair related that people were dancing and socializing. P1 was dancing when she "felt someone come up behind her, startling her," according to the account. She turned around and saw that it was Richmond. "Dr. Richmond smiled and grabbed P1['s] breast," the account relates. "P1 removed herself from the situation as soon as she could." P1 told P2 what had happened.

Later that night, the testimonial relates, while P1 and P2 were sitting together around the fire, Richmond sat down next to P2, "and subtly moved his hand to P2['s] leg" while continuing to converse with someone else. The testimonial concludes that "Neither P1 nor P2 reported these incidents to senior members of the staff of the Koobi Fora Field School as it was generally accepted that this was part of the field school experience." P1, interviewed by email, elaborated: "There was an atmosphere of tolerance or at least a 'what happens in the field stays in the field' mentality."

In the third account provided to Gordon, a former Koobi Fora undergraduate related that one evening in July 2012 she and Richmond were part of a group standing around a bonfire. "Brian put his arm around me, and plunged his hand down the back of my skirt all the way to my thighs, and forcefully grabbed my posterior," she wrote. This witness, who admits that she was "properly drunk," wrote that she put her hand around Richmond's waist while he "continued to fondle my bottom." Shortly afterwards, she related, Richmond "pulled me away from the circle" and "kissed me quite passionately," asking her to go to a more remote spot and have sex with him. But she was not interested and declined, slipping away to her friends.

Richmond in an email declined to make a "point-by-point response" to these incidents, "except to say that I strongly disagree with the central salacious details." He added that it is "unfair" for *Science* to "publish and confront me with anonymous complaints." Richmond noted that the incidents "would have occurred before the Koobi Fora Field School became affiliated with GWU" and did not involve GWU students or students whom he graded or supervised.

Ackermann argues that all three accounts represent examples of an abuse of power. "With undergraduates especially, there can be no

PHOTO: SERGIO ALMÉCIJA

Published by AAAS

consensual acts on the part of the women, who have no power." For a young student approached by a senior figure, as that third undergraduate explained to *Science*, "it is so hard to understand what is appropriate or not appropriate."

A growing number of university campuses in the United States now acknowledge that the power imbalance between professors and students makes sexual relationships problematic. In February 2015, for example, Harvard University's Faculty of Arts and Sciences (FAS) formally banned sexual relationships between professors and undergraduates, and Yale University and the University of Connecticut have adopted similar policies in recent years. "We were trying to avoid situations where one party might think a relationship was consensual and another party might not feel safe expressing that it wasn't," explains Alison Johnson, a historian at Harvard who chaired the panel that wrote the new policy.

Harvard allows relationships between faculty and graduate students only if the student is not under the professor's supervision or otherwise linked to them. GWU's current guidelines do not go as far, but consider it "inappropriate" for a faculty member to have such a relationship with a student in their class or whose work they are currently evaluating. They also proscribe "unwelcome sexual advances" and "unwelcome physical contact of a sexual nature."

All three of the Koobi Fora incidents were part of Gordon's broader investigation, which she finished by June 2015. Gordon wrote to sources to thank them for their help, but according to both Canty and Richmond, the museum took no further action against him at the time. Richmond says that sometime after this second investigation he received a raise and a positive job evaluation. (Canty declined to comment on this.)

Ackermann, for one, says she "was shocked and deeply disappointed" that the museum apparently did nothing further. "This is the classic thing that happens when women report" sexual misconduct, she says. "They go through the trauma of doing it and then nothing happens."

According to sources at the museum, the ultimate decision about disciplining Richmond was made by paleontologist Michael Novacek, AMNH's provost of science, who also convened the lengthy search for Richmond's position. (Canty, citing "the confidentiality of the information involved," declined *Science*'s request for an interview with Novacek.) But Canty's statement helps explain the museum's response: "Those reporting misconduct requested anonymity and none had filed complaints at the institutions where this occurred, thus inhibiting further action."

Richmond argues that the museum's protracted investigation process has been unfair to him. He wrote in an email that "on or about the first days of December 2015, I was informed by the Museum that if I did not voluntarily resign, [it] would launch a new investigation." (Canty declined to confirm or deny this, again citing confidentiality.) Richmond says that the new investigation constitutes double jeopardy and that its timing, after he was asked to resign and shortly after *Science* began investigating the case, "would seem to speak for itself."

As they pay more attention to allegations of sexual misconduct, institutions around the United States are struggling to balance the rights of victims and accused. Unlike in a criminal trial, which requires certainty beyond a reasonable doubt to convict, current Title IX guidelines require only a "preponderance of the evidence" for faculty or students to be found guilty of misconduct. "Universities have to be the prosecutor and the defense attorney and the judge and the jury," says Billie Dziech, a professor of English at the University of Cincinnati in Ohio known for her work on sexual harassment in academia. "It's a very difficult position to be in." Some, for example, have criticized Harvard's new FAS guidelines for insufficient due process to the accused, and Harvard Law School has adopted different procedures.

AS *SCIENCE* GOES TO PRESS, AMNH has launched its third investigation, which deals with "all allegations" concerning Richmond, Canty says, and is conducted by an outside firm, T&M Protection Resources in New York. Richmond is still employed by AMNH although working offsite during this investigation, Canty says. There are signs that the museum is taking the episode as a broader wakeup call. On 22 December 2015, Scheiner sent a memo to all staff announcing that the museum had asked T&M to review its sexual harassment policies and to institute training.

"This is the classic thing that happens when women report [sexual misconduct] ... They go through the trauma of doing it and then nothing happens."
Rebecca Ackermann

For many researchers and activists, the growing institutional sensitivity to alleged sexual misconduct has been a long time coming, and reflects changing societal views. Evolving interpretations of Title IX have also played a part, in particular a 2011 letter released by the Office for Civil Rights reminding educational institutions of their obligations to both prevent and respond to sexual misconduct, including sexual violence. "Title IX makes it very clear that a beautiful 19-year-old female wearing a halter top and a miniskirt can go check on her fruit flies at night without being touched or made uncomfortable by her professor," Harvard's Johnson says.

Last November AAPA released a new nine-page statement on sexual harassment and assault. AAPA President Susan Antón of NYU says that for years the organization has had a code of ethics that prohibits sexual harassment, but that after the SAFE study, she and other AAPA leaders realized that it needed a separate, more detailed statement focusing specifically on this issue. The new guidelines do not have a provision for investigating complaints, unlike guidelines adopted by the American Astronomical Society. But Antón agrees with other advocates that going beyond rules on paper and changing the culture of the field is the only real way to stop sexual misconduct. "Changing each individual institutional environment is the only answer to that," she says.

One way to go about it, Ackermann suggests, is to create a network of mentors, senior scientists "who have the power to do something about it. ... If you have a famous field school, you could have people outside the field school who could be reported to, a formal structure with real people attached to it rather than just a document."

Others insist that science needs policies to encourage witnesses to speak out. "By turning a blind eye, senior colleagues are accessories to what is happening," Hinde says. "We need to hold colleagues accountable who violate professionally accepted norms of sexual conduct." She praises the examples set by Wood and Ackermann, who used their power and experience to act and speak on behalf of younger and vulnerable researchers. "Leaders in my field are saying we won't accept this anymore," Hinde says. "I am incredibly hopeful. We are seeing the culture change in real ways in real time. We are seeing it now." ■

PHOTO: K. WARREN

Published by AAAS

Catalysis in a softer light p. 666

Origins of mitochondria p. 659 ▸

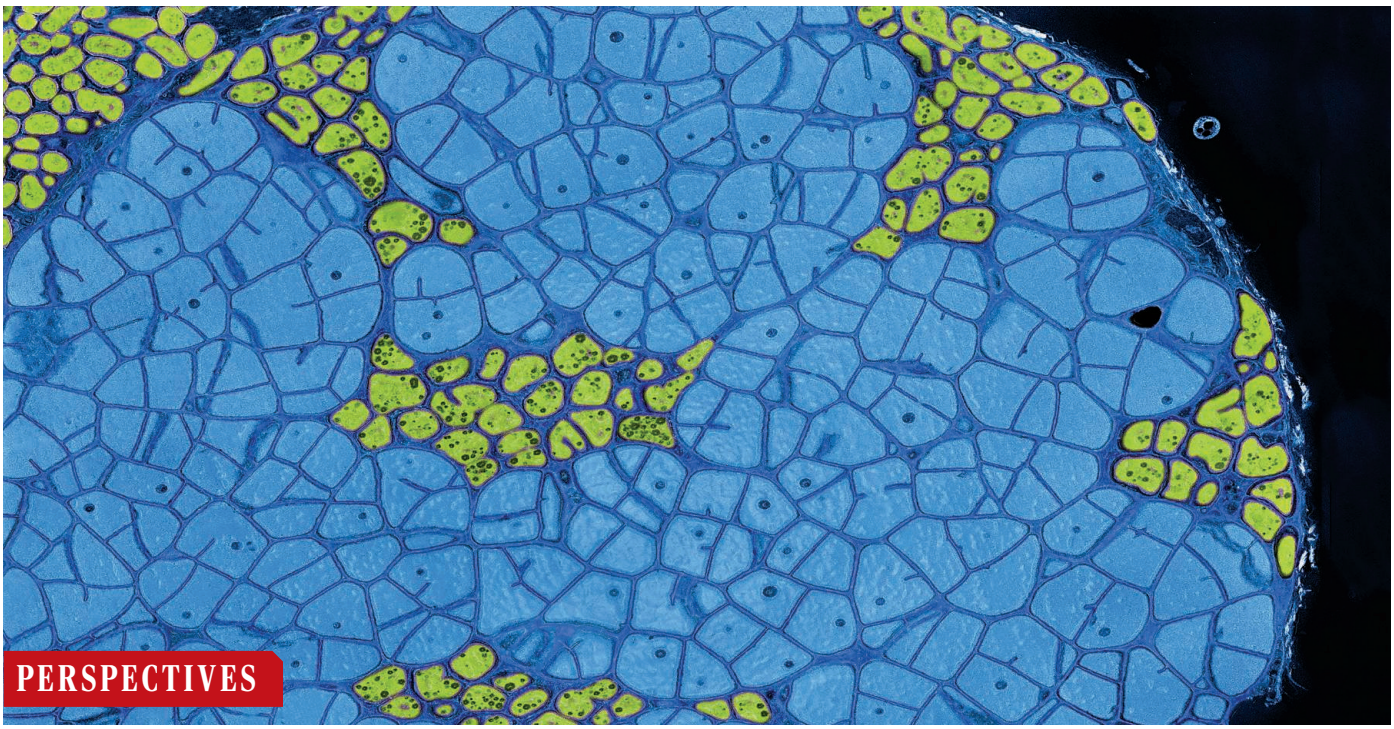

PERSPECTIVES

Working together. This false-color transmission electron micrograph shows a consortium of methane-oxidizing ANME-2 (blue) and sulfate-reducing deltaproteobacteria (green).

BIOGEOCHEMISTRY

A new diet for methane oxidizers

Archaea that normally depend on sulfate-reducing bacteria can also grow alone

By **Amelia-Elena Rotaru** *and* **Bo Thamdrup**

In anoxic marine sediments, consortia of methane-consuming archaea and sulfate-reducing bacteria oxidize methane. Together, they thereby control methane discharge in a metabolism of global importance. During this cooperative interspecies interaction, known as syntrophy, the excess reducing equivalents released by one species feed the second species (see the first figure). The two species only gain energy when they work together. On page 703 of this issue, Scheller *et al.* (*1*) show that these partners can be decoupled in the laboratory. The results help to elucidate the molecular mechanisms that control methane discharge in marine systems.

Department of Biology, University of Southern Denmark, 5230 Odense, Denmark. E-mail: arotaru@biology.sdu.dk

Cooperative metabolic interactions between different species are generally based on the transfer of reducing equivalents via diffusible chemicals like H_2 or formate. However, a few species cooperate by transferring reducing equivalents directly as electrons through conductive structures on the cell surface (*2*–*4*). This process is called direct interspecies electron transfer (DIET). The nature of the cooperative interaction between archaea and bacteria in consortia performing anaerobic oxidation of methane (AOM) coupled with sulfate reduction has long remained elusive. Milucka *et al.* have suggested that anaerobic methanotrophic archaea (ANME) in AOM consortia do not need a sulfate-reducing partner and can perform AOM and sulfate reduction on their own (*5*). However, the latest evidence points toward a cooperative interaction between ANME and sulfate reducers via direct electron transfer (see the second figure, panel A) (*6*, *7*).

The main barrier to understanding the metabolism of the AOM partners was the inability to decouple the two species and study their physiology separately. Scheller *et al.* now show that syntrophic ANME archaea can be decoupled from their bacterial partners by providing exogenous electron acceptors. The work complements previous studies in which the bacterial partners from different AOM consortia were decoupled from ANME archaea by adding colloidal sulfur (*5*) or H_2 (*7*).

Specifically, Scheller *et al.* show that one type of consortium-building ANME archaea known as ANME-2 can also live nonsyntrophically, in a different way than previously suggested (*5*). To disconnect ANME-2 from their bacterial partners, Scheller *et al.* used soluble electron acceptors, including

PHOTO: TOM DEERINCK AND MARK ELLISMAN/NATIONAL CENTER FOR MICROSCOPY AND IMAGING RESEARCH, SHAWN MCGLYNN/CALTECH

Downloaded from on February 11, 2016

Published by AAAS

ferric iron (Fe^{3+}) complexes and humic analogs. They noticed exclusively an increase in the cellular activity of ANME, not of their SRB partners. This is the first direct evidence for a respiratory metabolism in normally syntrophic ANME-2 archaea (see the second figure, panel B).

A respiratory ANME metabolism would explain the frequent occurrence of solitary ANME in environments such as microbial mats from the Black Sea, seep sediments, and mud volcano sediments (*8*). The soluble electron acceptors used by Scheller *et al.* are not abundant in marine sediments, where Fe^{3+} is mainly available as insoluble Fe^{3+} oxides (*9*). However, Scheller *et al.* suggest that insoluble Fe^{3+} oxides could also be used by solitary ANME as electron acceptors for methane oxidation (see the second figure, panel C).

How could ANME release electrons to minerals outside of the cells? Based on syntrophy. Previously, consortium-building ANME-2 could not be decoupled from their bacterial partner. In contrast, some freshwater ANME don't need a partner at all; for example, type 2d can oxidize methane alone using nitrate (*11*). Together, these findings extend the possible niches occupied by ANME archaea. This greater diversity of niches complicates the elucidation of what controls anaerobic methane sinks in marine environments.

Forty years after the discovery of AOM, the physiology of the microbes involved is still mysterious. To understand their physiology, scientists must now investigate whether ANME can indeed grow on insoluble electron acceptors and, if so, which genes are uniquely overexpressed in this process compared to ANME grown with soluble electron acceptors. Validation of the role of these genes will require

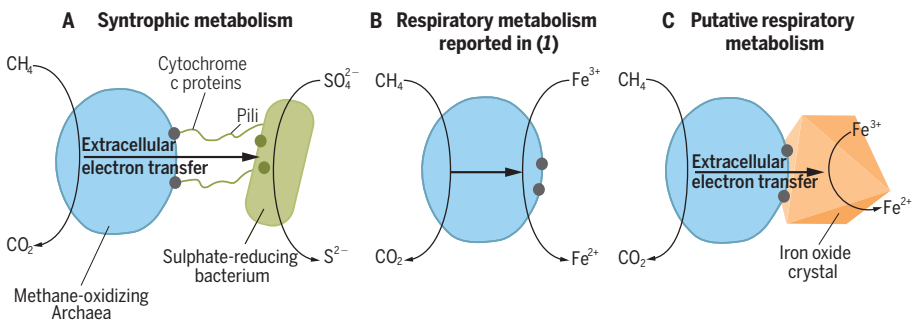

Diversity of ANME-2 metabolisms. (**A**) During syntrophic metabolism, ANME-2 archaea are thought to transfer electrons directly to a sulfate reducing partner (*5*). (**B**) Scheller *et al.* now report that ANME-2 are also capable of a respiratory metabolism, in which soluble metal complexes are the electron acceptors. (**C**) It remains to be shown whether ANME-2 can use insoluble metal oxides, such as iron oxides found in marine sediments, as electron acceptors.

what we know about extracellular electron transfer in bacteria (*9*), this is likely to take place either indirectly through mediation by soluble electron shuttles (*10*) or directly via an extracellular network of conductive pili and/or cytochromes (*9*). McGlynn *et al.* recently proposed that during DIET syntrophy, ANME-2 archaea release electrons via cytochrome c proteins (see the second figure, panel A) (*6*). ANME-2 archaea genomes encode more cytochrome c proteins (*6*, *10*) than do, for example, *Geobacter*, which require cytochromes in addition to pili for electron transfer to metal oxides (*9*) and for DIET during microbe-microbe interactions (*2*, *4*). Cytochrome c proteins and pili are also involved in extracellular electron transfer between the cells of other consortia carrying out thermophilic AOM (*7*). However, the role of cytochromes in the metabolism of ANME is yet to be uncovered. To do so, ANME must be grown solitarily.

By uncoupling ANME-2 from their bacterial partner, Scheller *et al.* reveal a flexible ANME metabolism that is not restricted to gene-deletion studies and therefore pure cultures. As Scheller *et al.* show that ANME can live alone and can therefore be purified, it should be only a matter of time until the AOM puzzle is resolved. ■

REFERENCES AND NOTES

1. S. Scheller, H. Yu, G. L. Chadwick, S. E. McGlynn, V. J. Orphan, *Science* **351**, 703 (2016).
2. A.-E. Rotaru *et al.*, *Appl. Environ. Microbiol.* **80**, 4599 (2014).
3. A.-E. Rotaru *et al.*, *Energy Environ. Sci.* **7**, 408 (2014).
4. Z. M. Summers *et al.*, *Science* **330**, 1413 (2010).
5. J. Milucka *et al.*, *Nature* **491**, 541 (2012).
6. S. E. McGlynn, G. L. Chadwick, C. P. Kempes, V. J. Orphan, *Nature* **526**, 531 (2015).
7. G. Wegener, V. Krukenberg, D. Riedel, H. E. Tegetmeyer, A. Boetius, *Nature* **526**, 587 (2015).
8. K. Knittel, A. Boetius, *Annu. Rev. Microbiol.* **63**, 311 (2009).
9. D. R. Lovley *et al.*, *Adv. Microbial Physiol.* **59**, 1 (2010).
10. D. R. Lovley *et al.*, *Acta Hydrochim. Hydrobiol.* **26**, 152 (1998).
11. M. F. Haroon *et al.*, *Nature* **500**, 567 (2013).

ACKNOWLEDGMENTS

A.E.R. is funded by two Danish Research council grants (FNU1325-00022A and FNU4181-00203) and the Novo Nordisk Foundation.

10.1126/science.aaf0741

CREDIT: N. CARY/*SCIENCE*

EVOLUTION

Pathogen to powerhouse

How did the precursors to the mitochondrion and the plastid evade host defense?

By **Steven G. Ball,[1] Debashish Bhattacharya,[2] Andreas P. M. Weber[3]**

Mitochondria and plastids are essential for harnessing energy in eukaryotic cells. They are believed to have formed through primary endosymbioses, in which bacterial symbionts were converted into energy-producing organelles. Primary endosymbiosis is extremely rare: Only one other case is known, in the amoeba *Paulinella* (*1*). This rarity is usually attributed to the many innovations that are required for organelles to be integrated into the cellular machinery (*2*). However, the first challenges for an endosymbiont are to avoid being digested by the host and to replicate in its novel environment. Recent studies provide clues to how the precursors to mitochondria and the plastid overcame these challenges.

Molecular phylogenies of mitochondrial genes suggest that the ancestor of the mitochondrion may have been a member of the Rickettsiales, an order of small Alphaproteobacteria (see the figure) (*3*). These intracellular organisms are often referred to as energy parasites because they encode a protein responsible for the unidirectional import of adenosine 5′-triphosphate from the host cytosol. Specialized Rickettsiales pathogens transmitted by arthropods have a highly reduced gene inventory (*4*). However, other *Rickettsia* pathogens have relatively large genomes and appear to infect various protists (*5*). Unlike the animal pathogens, these intracellular Rickettsiales are deeply rooted within Alphaproteobacteria (*3*) and are therefore more likely to resemble the mitochondrial ancestor.

Research also provides clues to a possible host for the mitochondrial endosymbiosis. A recently discovered archaeal lineage, the

[1]*Université de Lille CNRS, UMR 8576–UGSF–Unité de Glycobiologie Structurale et Fonctionnelle, F 59000 Lille, France.* [2]*Department of Ecology, Evolution and Natural Resources, Rutgers University, New Brunswick, NJ 08901, USA.* [3]*Institute for Plant Biochemistry, Center of Excellence on Plant Sciences, Heinrich-Heine-University, Universitätsstrasse 1, D-40225 Düsseldorf, Germany. E-mail: debash.bhattacharya@gmail.com*

Downloaded from on February 11, 2016

Published by AAAS

Lokiarchaeota (see the figure), is unique among Archaea in that it shares an array of signature eukaryotic genes thought to be critical for enabling endosymbiosis. These genes are involved in membrane remodeling, vesicular trafficking, and endocytosis. The latter would have allowed the capture of the mitochondrial precursor (*6*). The discovery of the Lokiarchaeota thus provides a potential missing link in the story of eukaryote evolution: membrane trafficking, mitochondrion-lacking cells that could have hosted the mitochondrial endosymbiosis.

It is likely that endocytosis in Archaea originally evolved to facilitate the harvesting of macromolecules in nutrient-rich external media. This process may have opened the door to incidental capture of harmful bacteria. The resulting intimate contact between the host and foreign cells likely precipitated an evolutionary arms race: The host evolved mechanisms such as autophagy, production of antimicrobial peptides, and reactive oxygen species induction to protect itself (*7*), whereas foreign cells evolved virulence effector molecules to evade host defense mechanisms. Over time, some foreign cells became obligate intracellular pathogens suited to life in the cytosol of the cell lineage that was to become the eukaryotic ancestor. Many effectors evolved to interact specifically with host proteins to allow replication of the intracellular pathogen, thereby preadapting them to symbiosis.

If we assume that this series of events is reasonably accurate, then free-living bacteria lacking the toolkit for intracellular life would not have survived long enough in the well-protected host cell cytosol to give rise to the mitochondrion. It is thus significant that *Rickettsia* is among the few pathogens that can multiply directly in the host cytosol (rather than in membrane-bound vacuoles termed inclusion vesicles). It thereby meets a key requirement for endosymbiosis: the ability to withstand host defenses.

These results also help explain why ancestrally mitochondrion-lacking eukaryotes (so-called archezoans) have never been found: They likely do not exist. The mitochondrion was already present in the Lokiarchaeota ancestor of eukaryotes and powered the transition from endocytosis of nutrients to a full-fledged phagocytic lifestyle (*8*). And finally, the Lokiarchaeota discovery has shifted focus away from metabolic symbiosis models for eukaryote origin (the hydrogen hypothesis) (*9*, *10*) that rely on cell fusion. The mitochondrion appears to have originated via classical endosymbiosis, whereby a host cell engulfs and maintains a foreign cell.

When we turn our attention to primary plastid origin, the story becomes more complex. The host of this endosymbiosis was a mitochondrion-containing unicellular eukaryote, but the cyanobacterial endosymbiont was likely not a pathogen. Living cyanobacteria neither possess the genetic toolkit to evade host defenses, nor do they encode effector proteins to interact with the host cellular machinery. So, how did the unprotected photosynthetic cell survive the early phases of the endosymbiosis? A potential solution to this conundrum was provided by the discovery of several dozen genes of chlamydial origin in the nuclear genome of algae and plants (*11*). These results suggest that a chlamydial bacterium entered the host cell together with a cyanobacterium (see the figure). This allowed the cyanobacterium to escape host defenses and establish a tripartite symbiosis through the help of chlamydial-encoded effector proteins and transporters (*12*, *13*). However, the details of this complex process remain incompletely understood.

As the recent studies discussed here show, we are in an exciting phase of endosymbiosis research. However, we still lack some crucial information. The Lokiarchaeota were identified from assembly of metagenomic data (*6*); no living cells have yet been isolated to validate the genome assembly or test their actual physiological capabilities. Protist-infecting chlamydial cells with large genomes are continuously being isolated, but only a handful have been studied in detail and are represented in genome databases. Therefore, more data are needed to test the proposed role of pathogens in organelle origin.

But perhaps what we need most are attempts at experimental primary endosymbiosis in the lab to learn the rules underlying this remarkable process. These data can be used to test the pathogen-centered view of primary endosymbiosis presented here and may help us get beyond phylogenies and simple diagrams. Ultimately, these advances will help us address the most vexing question about primary endosymbiosis: Why is it so rare? ■

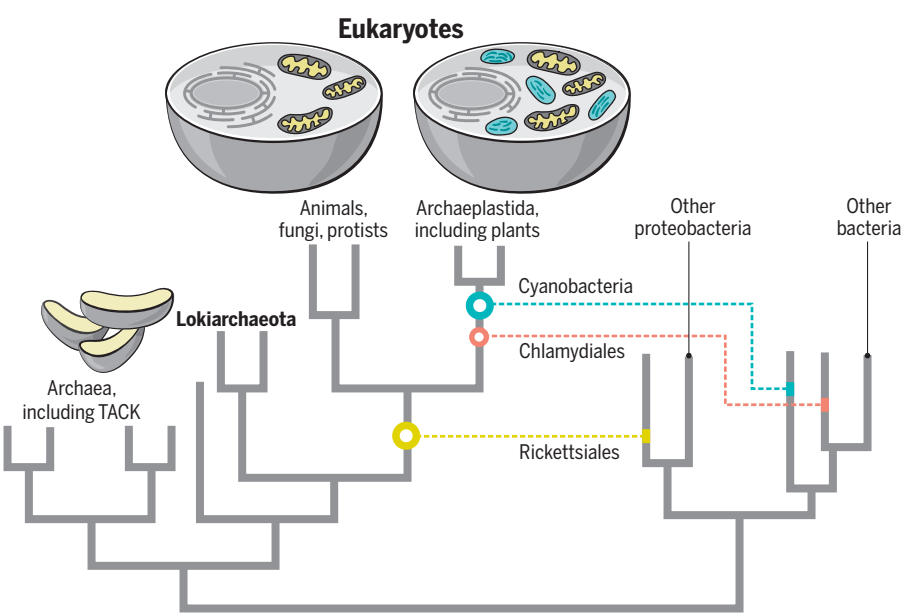

Pathogen roots of eukaryotic organelles. The original archaeal host cell was a member of the Lokiarchaeota that underwent primary endosymbiosis (yellow circle) with a Rickettsiales-like obligate intracellular bacterium, giving rise to the mitochondrion (*6*). Thereafter, the Archaeplastida ancestor underwent primary endosymbiosis (blue circle) with a cyanobacterium, putatively aided by a chlamydial infection (red circle) (*12*, *13*).

REFERENCES AND NOTES

1. E. C. Nowack, M. Melkonian, G. Glockner, *Curr. Biol.* **18**, 410 (2008).
2. T. Cavalier-Smith, *Int. J. Syst. Evol. Microbiol.* **52**, 297 (2002).
3. Z. Wang, M. Wu, *Sci. Rep.* **5**, 7949 (2015).
4. M. W. Gray, *Nature* **396**, 109 (1998).
5. J. Martijn *et al.*, *ISME J.* **46**, 1 (2015).
6. A. Spang *et al.*, *Nature* **521**, 173 (2015).
7. L. C. Gomes, I. Dikic, *Mol. Cell* **54**, 224 (2014).
8. N. Lane, W. Martin, *Nature* **467**, 929 (2010).
9. W. Martin, M. Müller, *Nature* **392**, 37 (1998).
10. A. Poole, D. Penny, *Nature* **447**, 913 (2007).
11. J. Huang, J. P. Gogarten, *Genome Biol.* **8**, R99 (2007).
12. S. G. Ball *et al.*, *Plant Cell* **25**, 7 (2013).
13. F. Facchinelli *et al.*, *Trends Plant Sci.* **18**, 673 (2013).

ACKNOWLEDGMENTS

S.G.B. was supported by the CNRS, the Université des Sciences et technologies de Lille, and the ANR grants "expendo" and "ménage à trois." D.B. was supported by NSF grants MGSP 0625440 and MCB 0946528, and A.P.M.W. was supported by German Research Foundation grants CRC-TR1, CRC 1208, and EXC 1028. All authors contributed equally to this work. We thank G. Greub, Ch. Colleoni, S. Aebi, M. Ducatez, B. Bouchet, H. Qiu, and D. C. Price for helpful comments on the manuscript. In memory of Fabrice Rappaport, a distinguished student of organelle powerhouses.

10.1126/science.aad8864

ILLUSTRATION: K. SUTLIFF/*SCIENCE*

Published by AAAS

A unifying model of epigenetic regulation

Single-cell tracking reveals a common "algorithm" of operation used by chromatin regulators

By **Albert J. Keung**[1] *and* **Ahmad S. Khalil**[2,3]

Expression of the genome is controlled by an intricate "web" of proteins, chemical modifications, and RNA that together organize genomic DNA into chromatin. Molecular studies of the various forms and levels of chromatin organization are advancing rapidly, revealing an increasing number of connections between chromatin and cellular and disease processes, as well as a fast-expanding web of known chromatin factors (*1*). On page 720, Bintu *et al.* take a radically different approach to dissecting chromatin, focusing not on molecular but on "algorithmic" chromatin biology (*2*). By studying how individual chromatin regulators (CRs) operate to produce distinct gene expression outputs within individual cells, they find that chromatin's complexity can be reduced into an elegant and unifying model of gene regulation.

In eukaryotic organisms, gene expression states are established in part by a system of CRs that act on chromatin in diverse ways (*3*). The principal questions posed by Bintu *et al.* concern how these CRs modulate gene expression, how permanent these expression changes are, and how the CRs' "operations" relate to one another. To study this, the authors developed a framework for quantitatively interrogating the input-output relationship between the presence (or absence) of a CR and gene expression in live mammalian cells. The framework combines artificial recruitment of CRs to a target reporter locus with precise temporal control—an increasingly popular strategy for focusing the activity of CRs (*4*–*8*)—with time-lapse microscopy to track reporter activity in individual cells.

The authors used this framework to compare four repressive CRs that use distinct chromatin modifications. The embryonic ectoderm development (EED) protein of Polycomb repressive complex 2 catalyzes histone H3 lysine 27 (H3K27) methylation. The Krüppel associated box (KRAB) protein promotes H3K9 methylation. DNA methyltransferase 3b (DNMT3B) catalyzes DNA methylation. The histone deacetylase 4 (HDAC4) enzyme directs histone deacetylation. Previous work has shown that different types of repressed chromatin are generally associated with distinct time scales of repression. For example, DNA methylation is widely associated with heritable gene repression (*9*), whereas histone acetylation is typically transient (*10*). However, by comparing these distinct CRs side by side, Bintu *et al.* were able to bring them under a unified quantitative model.

What is key to the authors' approach are the longitudinal measurements they make of single cells via time-lapse microscopy. In this way, they could track not only changes in reporter protein levels in individual cells, but also changes in protein production rate during and after recruitment of the CRs to chromatin. This approach revealed that all the CRs silence the reporter gene in all-or-none fashion, as characterized by an abrupt change in protein production rate in individual cells. Moreover, when the CRs are released from chromatin, reactivation of the reporter gene also occurs in all-or-none fashion. This leads to a general and simplified model in which cells are stochastically switching between active and silent states, rather than transitioning gradually through different activity levels.

The key distinction among the four CRs is how quickly a proportion of the cells in a population transition to the silent state. To complete the model, the authors extended their tracking of silent cells over longer times to quantify the heritable stability of the silent state. This revealed a third state, ultimately yielding a model in which cells can stochastically transition between active, reversibly silent, and irreversibly silent states. Consistent

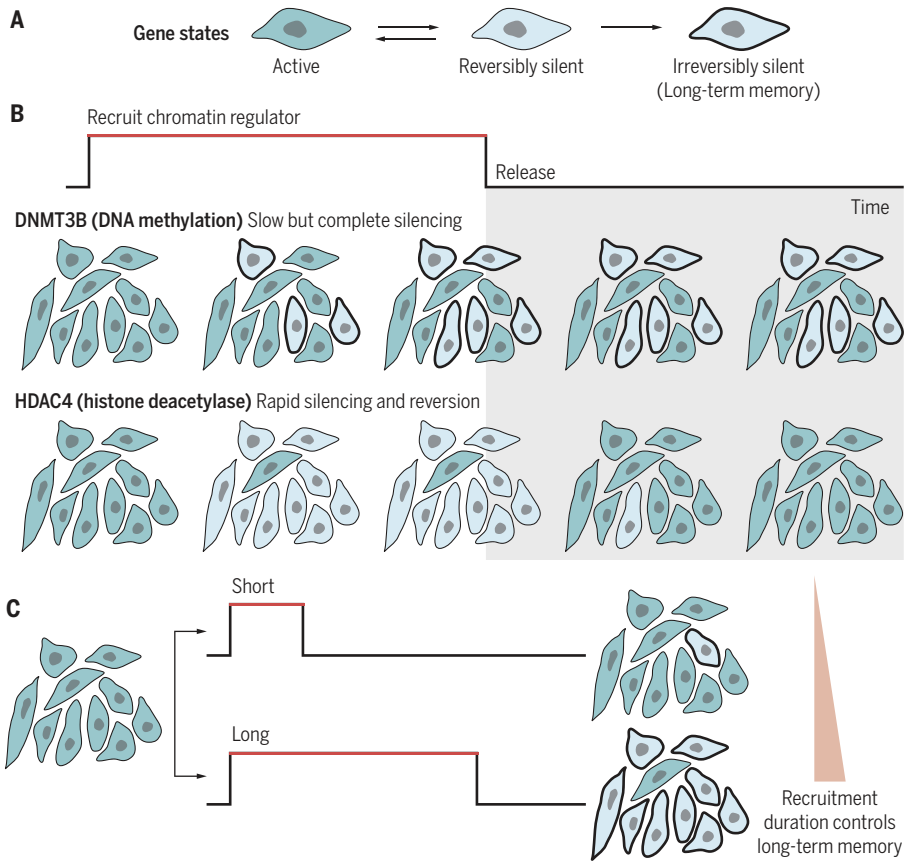

Unifying epigenetic regulation. (**A**) A proposed three-state model of gene regulation by repressive CRs, in which cells stochastically transition between active, reversibly silent, and irreversibly silent states. (**B**) The model is obtained by quantifying silencing events in individual cells during CR recruitment, and reactivation events upon release of the CR, by means of time-lapse microscopy. Filmstrips for two CRs are shown. DNMT3B induces slow but complete commitment to irreversibly silent states, whereas HDAC4 leads to rapid silencing and reactivation. (**C**) Duration-dependent fractional control of long-term (irreversible) silencing.

[1]*Department of Chemical and Biomolecular Engineering, North Carolina State University, Raleigh, NC, USA.* [2]*Department of Biomedical Engineering and Biological Design Center, Boston University, Boston, MA, USA.* [3]*Wyss Institute for Biologically Inspired Engineering, Harvard University, Boston, MA, USA.* *E-mail: akhalil@bu.edu*

ILLUSTRATION: P. HUEY/*SCIENCE*

Downloaded from on February 11, 2016

Published by AAAS

with other studies (*5*), the proportion of cells entering the final, irreversibly silent state is controlled by varying the duration of time that the CR is recruited to the gene.

From conceptually simple but technically exquisite experiments, the authors have produced an elegant model for capturing the dynamics of epigenetic regulation. What is compelling about this work is the minimalism of the three-state model, and the fact that CRs with diverse molecular identities and mechanisms can be collapsed into it. Dynamic control of fractions of a population would seem to be an effective way of transmitting and recording environmental signals, and suggests distinct advantages of CRs over canonical transcriptional networks. It is intriguing to consider how cells potentially exploit this rate control mechanism to link specific CRs and associated chromatin modifications with specific cellular processes, such as selectively turning off genes in the right cells during development. Additionally, we know that CRs and modifications rarely exist or act in isolation (*11*). Thus, it will be interesting to see how this rate control framework extends to combinatorial contexts.

The simplicity of the model is less suited for problems involving a higher level of biochemical detail, given that there is little direct connection to molecular mechanisms. Connecting aspects of the model to the wealth of existing chromatin data [derived from chromatin immunoprecipitation sequencing (ChIP-seq), biochemistry, etc.] will represent an exciting area of investigation. Yet this work is a critical step in our efforts to find logic within the regulatory complexity of chromatin. Distilling complex processes into phenomenological models has been historically central to our understanding of biology. For example, simplified descriptions such as the FitzHugh-Nagumo model have been used for decades to describe the behavior of neurons without full molecular details (*12*). Finally, this work nicely illustrates the importance of synthetic approaches for providing a functional view of biology, in this case revealing CRs as sophisticated "devices" inherently capable of controlling the time scale and epigenetic memory of gene expression. ■

REFERENCES

1. ENCODE Project Consortium, *Nature* **489**, 57 (2012).
2. L. Bintu *et al.*, *Science* **351**, 720 (2016).
3. T. Kouzarides, *Cell* **128**, 693 (2007).
4. P. N. Audergon *et al.*, *Science* **348**, 132 (2015).
5. N. A. Hathaway *et al.*, *Cell* **149**, 1447 (2012).
6. A. J. Keung *et al.*, *Cell* **158**, 110 (2014).
7. E. M. Mendenhall *et al.*, *Nat. Biotechnol.* **31**, 1133 (2013).
8. K. Ragunathan, G. Jih, D. Moazed, *Science* **348**, 1258699 (2015).
9. A. Bird, *Genes Dev.* **16**, 6 (2002).
10. Y. Katan-Khaykovich, K. Struhl, *Genes Dev.* **16**, 743 (2002).
11. B. E. Bernstein *et al.*, *Cell* **125**, 315 (2006).
12. R. FitzHugh, *Biophys. J.* **1**, 445 (1961).

10.1126/science.aaf1647

INFLAMMATION

Modulating pulmonary inflammation

Neuroepithelial cells suppress pulmonary inflammation and alveolar remodeling

By **Jeffrey A. Whitsett**[1] *and* **Edward E. Morrisey**[2]

The human respiratory tract transports millions of liters of gases throughout life. Because the conducting airways are exposed to countless microbes, particles, and toxicants, the tract has evolved an immune system that protects lung structure and function (*1*). Ventilation is primarily controlled by neuromuscular activity in the diaphragm and other muscles, and by sensory inputs from relatively rare pulmonary neuroepithelial cells. These cells cluster and form neuroepithelial bodies (NEBs) at branch points along the lung's airways. On page 707 of this issue, Branchfield *et al.* (*2*) reveal how NEBs arise during lung morphogenesis and clarify how their role in inflammation and tissue remodeling is relevant to the pathogenesis of chronic lung diseases that affect children.

The ability to sense, interpret, and integrate complex environmental stimuli debuted as individual neuroepithelial cells and evolved into the complex nervous systems typical of vertebrates. Ancient neuroepithelial sensors, such as those in mollusks and insects, are found in cellular niches that direct the homing of hemocytes and immunocytes to recognize and engulf pathogens (*3*). Phylogenetic remnants of these ancient sensors remain in vertebrates, represented by neuroepithelial plexuses in the lung. The findings of Branchfield *et al.* and of other recent studies by Kuo *et al.* (*4*) and Noguchi *et al.* (*5*) provide new insights into the mechanisms by which neuroepithelial cells migrate and cluster in the mammalian lung to form highly innervated NEB plexuses. These NEBs sense metabolic and other environmental signals, which they transmit to the central nervous system via postganglionic parasympathetic neurons and the vagus nerve (*6*).

Neuroepithelial cells constitute less than 1% of the airway epithelium. They exhibit ultrastructural and cellular characteristics of neural cells, and they release a unique set of neuroendocrine peptides and bioactive compounds, such as calcitonin gene–related peptide (CGRP), bombesin-gastrin releasing peptide, and 5-hydroxytryptamine (serotonin), with a range of functions including control of vascular tone and permeability. They are also innervated by a rich network of neural fibers (*6*). Despite their rarity, neuroepithelial cells have been implicated in several important roles in the postnatal lung. Pediatric patients with chronic lung diseases, including cystic fibrosis and bronchopulmonary dysplasia, share alterations in the number or localization of pulmonary neuroepithelial cells, along with deregulation of O_2 and CO_2 sensing and ventilation; such alterations have also been observed in cases of sudden infant death. Secretory cells that contribute to regeneration of the airway epithelium after injury reside in close proximity to NEBs (*7*). However, lineage tracing studies indicate that neuroepithelial cells do not contribute to this process (*8*). Thus, despite clinical and experimental insights, the function of neuroepithelial cells in the lung has remained a long-standing mystery.

> ***"...the function of neuroepithelial cells in the lung has remained a long-standing mystery."***

Branchfield *et al.* demonstrate that, similar to the migration of neurons in the central nervous system, the membrane protein Roundabout (Robo) and its ligands from the Slit family of secreted proteins direct the migration of pulmonary neuroepithelial cells to airway branch points. The authors found that Slit1 and Slit2 are released by a subset of neuroepithelial cells within clusters in the mouse lung; Robo expression appears restricted to rare epithelial cells in the airways that express CGRP. The authors also observed Slit3 expression in the vascular smooth muscle of pulmonary ar-

[1]*Perinatal Institute, Division of Neonatology and Pulmonary Biology, Cincinnati Children's Hospital, Cincinnati, OH 45229, USA.* [2]*Penn Center for Pulmonary Biology, University of Pennsylvania, Philadelphia, PA 19104, USA.*
E-mail: jeff.whitsett@cchmc.org; emorrise@upenn.edu

Downloaded from on February 11, 2016

Published by AAAS

teries, which lies in close apposition to the conducting airway. The authors propose that Robo-Slit interaction directs the formation of organized signaling centers at airway branch points that are highly innervated, providing a circuit that links chemosensing by the NEBs to the central nervous system.

Kuo *et al*. (*4*) and Noguchi *et al*. (*5*) demonstrate that NEBs arise from progenitor cells (endodermal epithelial cells) that migrate from peripheral regions in the mouse lung to locations that are proximal to airway branch points. Their differentiation is controlled by the membrane protein Notch. The intensity of Notch signaling directs the differentiation of progenitors to pulmonary neuroepithelial, ciliated, secretory, club, or goblet cells (*9*). Inhibition of Notch is thus required for differentiation to neuroepithelial cells. Consistent with this, Noguchi *et al*. show that deletion of Hes-1 (hairy and enhancer of split-1, a transcription factor that mediates Notch activity in airway progenitor cells, induces NEB formation. Interestingly, loss-of-function mutations in Notch are common in small cell pulmonary carcinomas (*10*). This cancer type is highly metastatic, consistent with the finding that pulmonary neuroepithelial cells are highly migratory during embryogenesis.

The role of NEBs as airway sensors may derive from their unique location at airway branch points, which are sites of relatively low gas flow. Pulmonary neuroepithelial cells respond rapidly to hypoxia through the transcription factor hypoxia-inducible factor–1α, (HIF1α) and to hypercarbia through carbonic anhydrase (*6*). Neuroepithelial cells in the carotid body play the dominant role in sensing O_2, CO_2, and pH in circulating blood to control ventilation and maintain acid-base homeostasis after birth (*11*). In the carotid body, olfactory receptor 78 senses hypoxia and is activated by lactate, a metabolite that accumulates in the blood when ventilation and blood O_2 concentration decline. Similarly, in the lung, NEBs respond to hypoxia through K^+ channels that are sensitive to the amounts of O_2 and the metabolite nicotinamide adenine dinucleotide (NAD^+). In turn, pulmonary neuroepithelial cells secrete a diversity of peptides and metabolites that influence the contractile activities of endothelial cells and myofibroblasts in the pulmonary vasculature as well as innate immune cells in the lung.

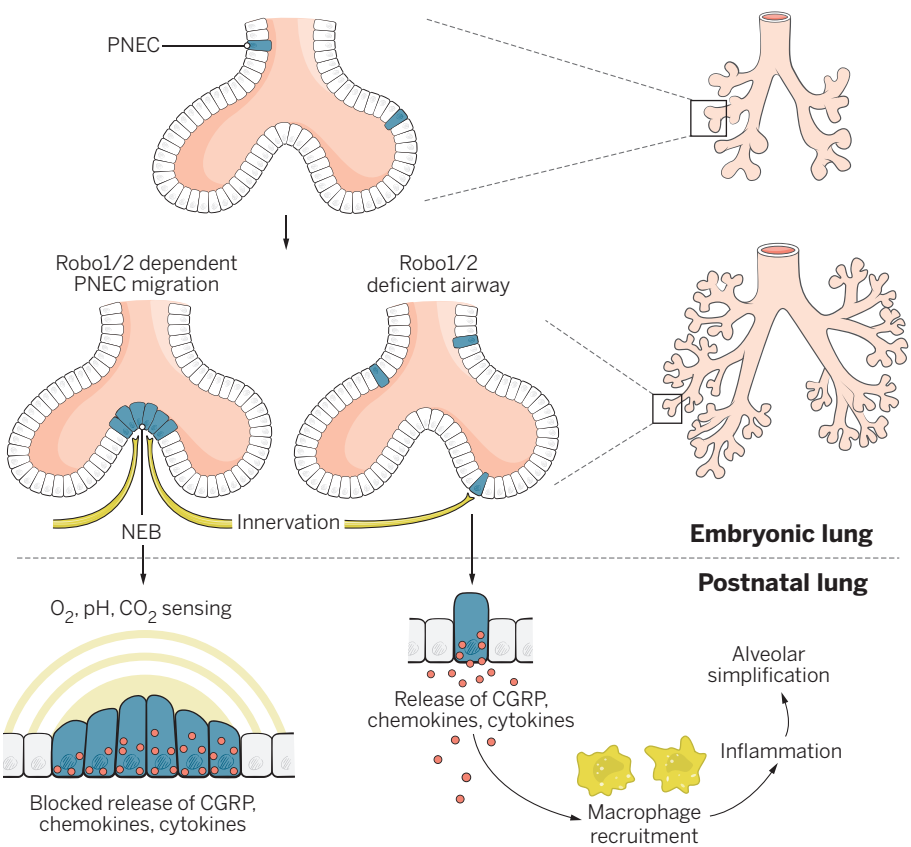

ILLUSTRATION: K. SUTLIFF/*SCIENCE*

Clustered sensors. Pulmonary neuroepithelial cells (PNECs) normally migrate and cluster into bodies NEBs at airway branch points during lung development. Loss of signaling by Robo1/2 leads to a failure to cluster. The absence of NEBs results in the increased expression of immunoregulatory proteins, increased inflammation, and disruption of lung structure (alveolar simplification).

Branchfield *et al*. found that after birth, clustering of neuroepithelial cells in the mouse lung plays a critical role in preventing pulmonary inflammatory signaling, presumably mediated in part by the exposure to O_2 after birth. The authors observed that Robo-Slit interactions are required for suppressing macrophage recruitment to the mouse lung. Clustering of neuroepithelial cells to form NEBs suppressed their release of chemokines and cytokines that recruit and activate alveolar macrophages. Clustering also blocked the release of CGRP. CGRP influences airway epithelial repair, stimulating mucus production and proliferation of airway progenitor cells located in submucosal glands (*12*). Failure to form NEBs in the mice lacking Robo1/2 activated lung inflammation and caused alveolar simplification, mediated in part by the actions of CGRP on alveolar macrophages. These findings are consistent with histologic changes seen in the lungs of premature infants who develop bronchopulmonary dysplasia.

From a clinical viewpoint, the findings of Branchfield *et al*. provide a model that better explains the development of hypercarbia, hypoxemia, inflammation, and tissue remodeling in chronic lung diseases in children. NEBs act as O_2 and chemical sensors that calibrate ventilation during infancy, when carotid body and central neurosensing are less well developed. Robo and Slit—by creating the NEB environment—suppress abnormal proinflammatory signaling by the pulmonary neuroepithelium. Thus, the lack of migration and clustering of neuroepithelial cells to form NEBs results in immune cell activation and alveolar tissue injury. Pulmonary neuroepithelial cells may exemplify archetypal neuroepithelial sensing systems that evolved to accommodate increasingly complex environmental and metabolic challenges that integrated with neural control of breathing and pulmonary innate immunity. ■

REFERENCES

1. J. A. Whitsett, T. Alenghat, *Nat. Immunol.* **16**, 27 (2015).
2. K. Branchfield *et al., Science* **351**, 707 (2016).
3. D. Malagoli, M. Mandrioli, F. Tascedda, E. Ottaviani, *Biol. Rev. Camb. Philos. Soc.* 10.1111/brv.12234 (2015).
4. C. S. Kuo, M. A. Krasnow, *Cell* **163**, 394 (2015).
5. M. Noguchi, K. Sumiyama, M. Morimoto, *Cell Rep.* **13**, 2679 (2015).
6. E. Cutz, *Semin. Diagn. Pathol.* **32**, 420 (2015).
7. S. D. Reynolds, A. Giangreco, J. H. Power, B. R. Stripp, *Am. J. Pathol.* **156**, 269 (2000).
8. H. Song *et al., Proc. Natl. Acad. Sci. U.S.A.* **109**, 17531 (2012).
9. M. Morimoto, R. Nishinakamura, Y. Saga, R. Kopan, *Development* **139**, 4365 (2012).
10. J. George *et al., Nature* **524**, 47 (2015).
11. A. J. Chang *et al., Nature* **527**, 240 (2015).
12. W. Xie *et al., J. Clin. Invest.* **121**, 3144 (2011).

10.1126/science.aaf1429

Published by AAAS

SCIENCE EDUCATION

Climate confusion among U.S. teachers

Teachers' knowledge and values can hinder climate education

By **Eric Plutzer,[1] Mark McCaffrey,[2] A. Lee Hannah,[3] Joshua Rosenau,[2] Minda Berbeco,[2] Ann H. Reid[2]**

Although more than 95% of active climate scientists attribute recent global warming to human causes (*1*, *2*) and most of the general public accepts that climate change is occurring, only about half of U.S. adults believe that human activity is the predominant cause (*3*), which is the lowest among 20 nations polled in 2014 (*4*). We examine how this societal debate affects science classrooms and find that, whereas most U.S. science teachers include climate science in their courses, their insufficient grasp of the science may hinder effective teaching. Mirroring some actors in the societal debate over climate change, many teachers repeat scientifically unsupported claims in class. Greater attention to teachers' knowledge, but also values, is critical.

EDUCATION

Prior surveys [e.g., (*5*, *6*)] suggest that many teachers devote class time to climate change. Although these surveys are suggestive, their use of nonprobability sampling undermines the validity of their results. None quantified the amount of class time or the specific topics covered in class. We undertook the first nationally representative survey of science teachers focused on climate change. Working from a commercial database of 3.9 million teachers, we drew a stratified probability sample of 5000 names and implemented a multiple-contact paper and Web survey protocol during academic year 2014–15. We collected data from 1500 public middle- and high-school science teachers from all 50 U.S. states, representative of the population of science teachers in terms of school size, student socioeconomic status, and community economic and political characteristics. See supplemental materials (SM) for details.

INTRODUCING THE BASICS. Three in four science teachers allocate at least an hour to discussing recent global warming in their formal lesson plans, including 70% of middle-school science teachers and 87% of high-school biology teachers (table S7). Because virtually all students take middle-school science and 97% enroll in a general biology class (*7*, *8*), the likelihood of any student missing instruction in climate change altogether is low—on the order of 3 to 4%. Most teachers reported covering the greenhouse effect (66%), the carbon cycle (63%), and four or more observable consequences, such as sea-level rise, or changes in seasonal patterns, like the flowering of plants and animal migrations. Teachers also discuss responses to climate change and careers addressing the challenges it poses.

Although most students will hear something about climate change in a science class, the median teacher devotes only 1 to 2 hours to the topic (table S7), inconsistent with guidance from leading science and education bodies [e.g., (*9*)]. Of course, quality of instruction is more important than quantity, so we turn to how students are introduced to climate change science.

MIXING MESSAGES. Notably, 30% of teachers emphasize that recent global warming "is likely due to natural causes," and 12% do not emphasize human causes (half of whom do not emphasize any explanation and thereby avoid the topic altogether). Of teachers who teach climate change, 31% report sending explicitly contradictory messages, emphasizing both the scientific consensus that recent global warming is due to human activity and that many scientists believe recent increases in temperature are due to natural causes (see the first chart). Why might this be the case? Some teachers may wish to teach "both sides" to accommodate values and perspectives that students bring to the classroom (*6*, *10*). Beyond that, the survey data allow us to evaluate three explanations.

First, teachers might experience overt pressure from parents, community leaders, or school administrators not to teach climate change. Only 4.4% of teachers reported such pressure (6.1% reported pressure to teach it, mostly from fellow teachers). This is less than the 15% reporting pressure in Wise's pioneering survey (*6*), and far less than biology teachers reported in a survey on teaching evolution (*10*).

Second, teachers also may not be very knowledgeable about a wide range of evidence—e.g., CO_2 measurements from ice cores and from direct measures at Mauna Loa—and how climate models work. Given the relative novelty of the topic in classrooms, instructional materials, and preservice training, this would not be surprising, and nearly 50% said that they would prioritize one or

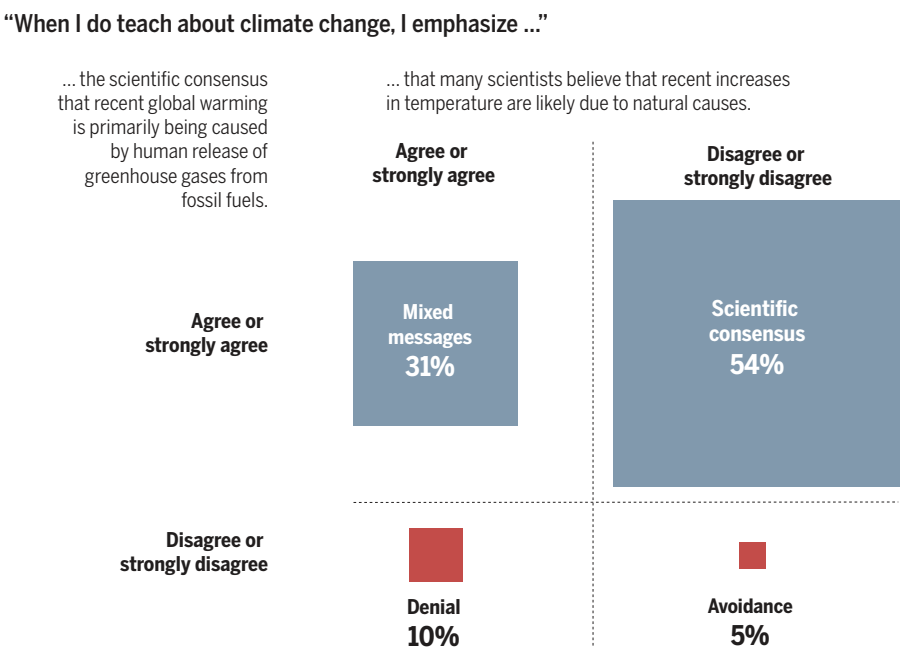

Teachers' emphasis. Teachers reported emphasis on causes of global warming, among those devoting an hour or more to the topic (see SM for details on calculation).

ILLUSTRATION: P. HUEY/*SCIENCE*

[1]*Department of Political Science, The Pennsylvania State University, University Park, PA 16802, USA.* [2]*National Center for Science Education, Oakland, CA 94609, USA.* [3]*Department of Political Science, Wright State University, Dayton, OH 45435, USA.* *Corresponding author. E-mail: plutzer@psu.edu

Downloaded from on February 11, 2016

Published by AAAS

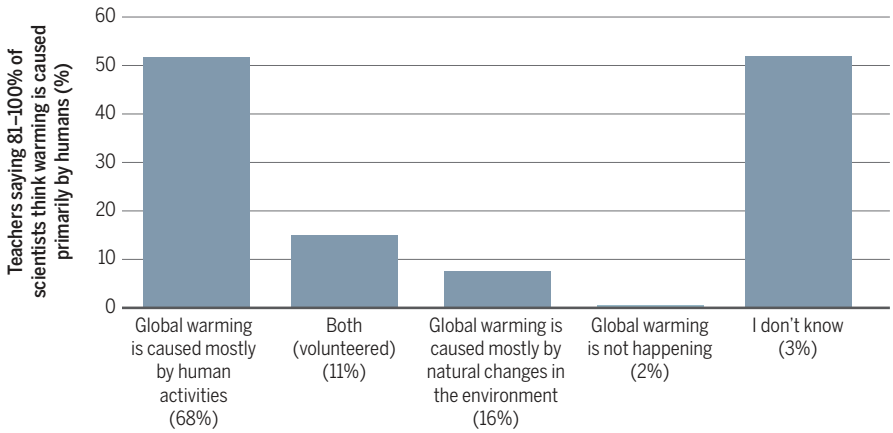

Teacher's views. Teachers' perceptions of scientific consensus, by their personal opinion about the causes of recent global warming. (Numbers in parentheses are the percentage of teachers selecting each statement as the one coming closest to their views).

more unrelated topics (e.g., pesticides, ozone layer, or impacts of rocket launches).

Third, many teachers are unaware of the extent of scientific agreement. This is critical because we might expect that, with limited technical mastery, teachers may defer to scientific expertise. Yet, when asked "what proportion of climate scientists think that global warming is caused mostly by human activities?"—only 30% of middle-school and 45% of high-school science teachers selected the correct option of "81 to 100%." Even among teachers who agree that human activities are the main cause of global warming (a large majority of all science teachers), only 52% know the percentage of scientists who share their view. If a majority of science teachers believe that more than 20% of climate scientist disagree that human activities are the primary cause, it is understandable that many would teach "both sides," by conveying to students that there is legitimate scientific debate instead of deep consensus.

The combination of limited training and uncertainty about the scientific consensus affects teachers' acceptance of anthropogenic climate change. Although only 2% of teachers personally denied that recent global warming is happening, almost one-sixth (15%) believe that it is mostly driven by natural causes, and another one-sixth thought that human and natural causes are equally important. Indeed, teachers' assessment of the scientific consensus is intertwined with their personal conclusions about global warming and its causes (see the second chart).

IMPROVING TEACHERS' KNOWLEDGE. Advances in climate science and consolidation of scientific consensus have outpaced textbooks and teachers' training. Fewer than half of the teachers report any formal instruction in climate science in college. Two-thirds of teachers (including 50% of those who believe that natural causes drive global warming) said they would be interested in continuing education "entirely focused on climate change." Provision of such continuing education (*11*) and development of networks of support to provide ongoing and connected professional education opportunities (*12*) would be helpful.

Continued development and dissemination of teacher-tested, standards-aligned educational materials that document the basis for the scientific consensus about human-caused climate change would also be valuable. High-quality, vetted, and up-to-date online instructional resources [e.g., (*13*–*15*)] provide examples for teachers and science communicators.

The aim of such efforts would be to improve teachers' knowledge of climate science, so as to distinguish what is scientifically uncertain (e.g., exactly how quickly sea levels will rise) from what is well supported (e.g., that sea levels have risen and are rising more quickly owing to human-caused climate change). Teachers must expect, and be equipped to counter, specific misinformation and misconceptions about climate change likely to be voiced by students. Teachers prepared for such challenges are more likely to have confidence to provide scientifically sound instruction.

POLITICS AND IDENTITY THREAT. Content knowledge is not the only area in need of attention. Rejection of sound scientific conclusions is often rooted in value commitments rather than ignorance (*16*), and science teachers are not immune from this tendency. A question measuring political ideology was a more powerful predictor of teachers' classroom approach than any measure of education or content knowledge, with those leaning toward "It's not the government's business to protect people from themselves" most willing to teach "both sides" (table S8).

Our data suggest that, especially for political or cultural conservatives, simply offering teachers more traditional science education may not lead to better classroom practice. Education efforts will need to draw on science communication research and acknowledge resistance to accepting the science and addressing its root causes (*17*, *18*). College and university instructors will need help reaching teachers and teachers-in-training who bring diverse political and value commitments to the classroom—particularly in avoiding "boomerang effects," in which attempts to promote a particular view can instead harden opposition. This may entail acknowledging and addressing conflicts that teachers (and their students) may feel between their values and the science. Such instruction will promote understanding of the science as well as the pedagogy that future teachers will need to promote climate science literacy. ■

REFERENCES AND NOTES

1. P. T. Doran, M. K. Zimmerman, *Eos* **90**, 22 (2009).
2. J. Cook *et al.*, *Environ. Res. Lett.* **8**, 024024 (2013).
3. C. Funk, L. Rainie, "Public and scientists' views on science and society" (Pew Research Center, Washington, DC, 29 January 2015); www.pewinternet.org/2015/01/29/public-and-scientists-views-on-science-and-society/.
4. Ipsos MORI, Global Trends Survey (Ipsos MORI, London, 2014); www.ipsosglobaltrends.com/environment.html.
5. R. Johnson, M. Holzer, *National Earth Science Teachers Association K-12 Climate Change Education Survey* (National Earth Science Teachers Association, Fort Collins, CO, 2011), Executive Summary; www.nestanet.org/cms/sites/default/files/documents/executiveSummaryClimateChangeEducationSurveyDecember2011.pdf.
6. S. Wise, *J. Geosci. Educ.* **58**, 297 (2010).
7. National Center for Education Statistics, *High School Transcript Study* (U.S. Department of Education, Washington, DC, 1990 and 2009).
8. National Center for Education Statistics, *Digest of Education Statistics 2012* (U.S. Department of Education, Washington, DC, 2013), Table 179, p. 252.
9. National Research Council, *A Framework for K–12 Science Education: Practices, Crosscutting Concepts, and Core Ideas* (Board on Science Education, National Academies Press, Washington, DC, 2012).
10. M. Berkman, E. Plutzer, *Evolution, Creationism, and the Battle to Control America's Classrooms* (Cambridge Univ. Press, Cambridge, 2010).
11. E. Hestness, R. McDonald, W. Breslyn, J. McGinnis, C. Mouza, *J. Geosci. Educ.* **62**, 319 (2014).
12. L. M. Desimone, A. C. Porter, M. S. Garet, K. S. Yoon, B. F. Birman, *Educ. Eval. Policy Anal.* **24**, 81 (2002).
13. Transition Region and Coronal Explorer (TrACE) (NASA, 2016); http://science.nasa.gov/missions/trace/.
14. NOAA, Teaching resources, Climate.gov (NOAA, 2016); https://www.climate.gov/teaching.
15. CLEAN: Climate Literacy and Energy Awareness Network (2016); http://cleanet.org.
16. D. Kahan, *Adv. Polit. Psychol.* **36**, 1 (2015).
17. T. Dietz, *Proc. Natl. Acad. Sci. U.S.A.* **110** (suppl. 3), 14081 (2013).
18. D. M. Kahan, in *Culture, Politics and Climate Change*, M. Boykoff and D. Crow, Eds. (Routledge Press, New York, 2014), pp. 203–220.

ACKNOWLEDGMENTS

Data were collected by the Penn State Survey Research Center with the support of the National Center for Science Education. The NCSE's climate change program is made possible by donations from its donors. The authors thank G. Branch for his suggestions.

SUPPLEMENTARY MATERIALS

www.sciencemag.org/content/351/6274/664/suppl/DC1

10.1126/science.aab3907

ILLUSTRATION: P. HUEY/*SCIENCE*

Published by AAAS

PHOTOCATALYSIS

Copper catalysis in a blue light

Visible light, copper, and a phosphine ligand combine for C-N bond formation at fully substituted chiral centers

By **Michael F. Greaney**

A plethora of biologically active molecules contain chiral carbon centers bearing four different functional groups. However, as more groups are added to the carbon during chemical synthesis, the more likely they are to inhibit or even block subsequent reactions on the way to full substitution. To obtain a particular enantiomer also demands a chiral catalyst that displays both high reactivity and exquisite shape selectivity in the catalyst-substrate binding event. On page 681 of this issue, Kainz *et al.* (*1*) describe a solution to this problem that focuses on nitrogen-containing carbon centers, a frequent feature of pharmaceuticals, materials, and natural products, by combining base-metal catalysis, visible-light photoredox catalysis, and asymmetric synthesis.

School of Chemistry, University of Manchester, Oxford Road, Manchester M13 9PL, UK. E-mail: michael.greaney@manchester.ac.uk

The use of visible light to effect photochemical transformations has seen unprecedented growth in recent years (*2*). In contrast to classical ultraviolet (UV) photochemistry, which requires specialized equipment, visible-light photocatalysis uses domestic light sources and standard laboratory glassware and can be applied to a multitude of reaction classes. Because most organic molecules are colorless (they do not absorb visible light), a light-sensitive catalyst must be used that can undergo electron transfer with the substrate upon photoexcitation. These electron transfer events provide alternative reaction pathways that frequently occur under milder conditions than the analogous energy-transfer mechanisms characteristic of UV photochemistry (*3*).

The visible light photocatalyst systems are often formed from noble metal complexes of ruthenium and iridium, which are well-studied materials that display long lifetimes in the photoexcited state. The use of cheaper, earth-abundant metals such as copper in these processes is appealing as a sustainable alternative (*4*). Kainz *et al.* used a simple copper salt, CuCl, in the presence of a chiral phosphine ligand and a nitrogen nucleophile to assemble a photoactive complex in situ.

Upon irradiation with blue light, this species can instigate photoreduction of a tertiary alkyl halide substrate to form a tertiary alkyl radical through electron transfer (see the figure). Formation of a C-N bond then affords the tertiary alkyl amine products with high enantioselectivity, and the copper phosphine complex is released to begin another catalytic cycle. Crucially, the pathway is enantioconvergent, in that a racemic alkyl halide substrate is transformed into a highly enantiomer-enriched alkyl amine product. Both enantiomers of the starting material produce the same radical intermediate; control experiments show that this step occurs at essentially the same rate for either enantiomer. Subsequent C-N bond formation is controlled by the environment of the catalyst. Levels of control in this key step were high, with the catalyst effectively discriminating between substituents at the incipient fully substituted carbon center to produce highly enantiomer-enriched products.

A variety of alkyl and aryl substitution can be accommodated at the newly formed chiral center for a range of amide-activating groups and indole and carbazole nucleophiles. The transformation also displays good functional group tolerance, an important feature for future synthetic applications. A variety of common functional groups (e.g., ketones, alcohols, esters, and alkenes) were tried as additives in the reaction and recovered intact, with the reaction proceeding uninterrupted with high yield and enantioselectivity.

The central role played by metal complexes in visible light photoredox catalysis suggests that enantioselective transformations should be possible, especially given the inherent chirality present in many common photocatalyst structures (*5*). In practice, it has proven difficult to merge electron-transfer chemistry and the asymmetric control elements into a single catalyst structure, and most chiral photoredox systems have used two separate catalysts (*6*). Remarkably, Kainz *et al.* show that a phosphine ligand and a base metal can assemble in situ to accomplish both redox and asymmetric bond-forming chemistry. ■

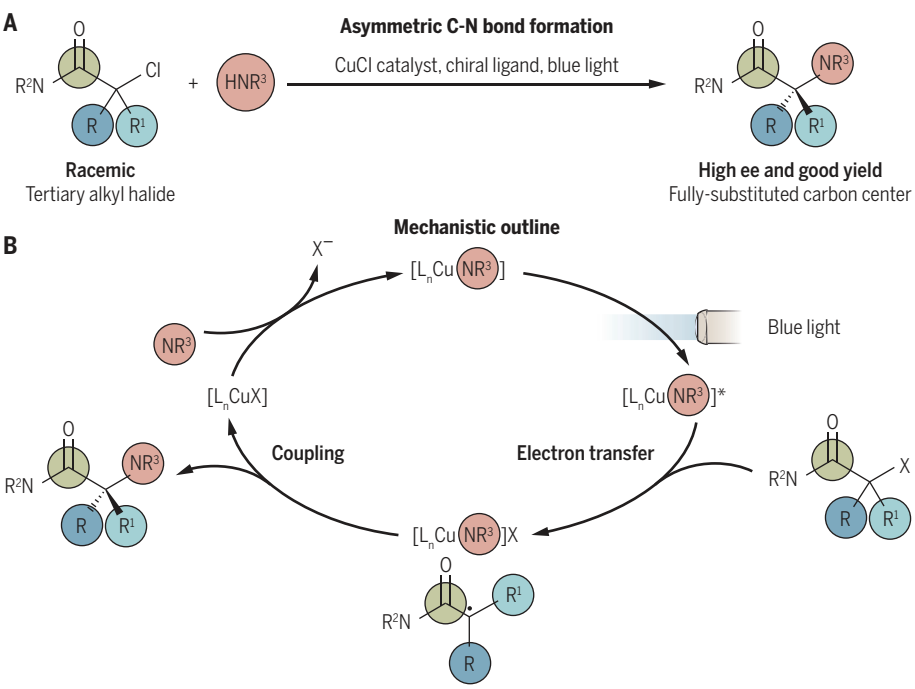

Copper photoredox catalysis. (**A**) Racemic tertiary alkyl halides and nitrogen nucleophiles are coupled under chiral copper catalysis and blue-light irradiation, forming tertiary alkyl amine products with high enantioselectivity. (**B**) Single-electron transfer reduces the substrate to form a tertiary radical, which undergoes asymmetric C-N bond formation to give the products.

REFERENCES

1. Q. M. Kainz *et al.*, *Science* **351**, 681 (2016).
2. C. K. Prier, D. A. Rankic, D. W. C. MacMillan, *Chem. Rev.* **113**, 5322 (2013).
3. M. A. Ischay *et al.*, *J. Am. Chem. Soc.* **130**, 12886 (2008).
4. S. Paria, O. Reiser, *ChemCatChem.* **6**, 2477 (2014).
5. H. Huo *et al.*, *Nature* **515**, 100 (2014).
6. D. A. Nicewicz, D. W. C. MacMillan, *Science* **322**, 77 (2008).

10.1126/science.aaf1071

ILLUSTRATION: P. HUEY/*SCIENCE*

Downloaded from on February 11, 2016

Published by AAAS

CHROMATIN

It takes teamwork to modify chromatin

The organization of constituents in a large chromatin-modifying complex reveals specific roles

By **Jerry L. Workman**

To participate in the choreography of signals that occur on the chromosome during gene activation, many multisubunit chromatin-modifying complexes contain more than one enzyme that chemically alter histones, the protein constituent of chromatin. These complexes themselves often contain modules or clusters of subunits dedicated to specific functions of the complex (*1*). The Spt-Ada-Gcn5 acetyltransferase (SAGA) complex is a good example of this organization. It is highly conserved from yeast to humans, contains up to 20 subunits, and is about 2 MDa in size. SAGA contains several functional modules, two of which have enzymatic activities and others that mediate SAGA interactions with proteins that control transcription (*2*). Hence, teamwork between these modules is crucial for the steps leading to transcription initiation and its transition to RNA elongation (*3*). Even within each module, teamwork between individual subunits is necessary to promote accurate enzymatic activity. On page 725 in this issue, Morgan *et al.* (*4*) provide structural and biochemical data that nicely illustrate cooperation between subunits within the module that contains a histone deubiquitinase, and between this module and the remainder of the SAGA complex.

Ubiquitination of histone H2B provides an important checkpoint in the transition from the early initiated form of RNA polymerase II to the full elongating form. This change is governed by the phosphorylation status of heptapeptide repeats in the carboxyl-terminal domain (CTD) of the largest subunit of RNA polymerase II. Immediately after initiation, these repeats are phosphorylated on serine 5 and serine 7, which brings cofactors to the polymerase that facilitate early elongation steps. These repeats are then phosphorylated on serine 2, which recruits cofactors that function during subsequent transcription elongation (*5*). Monoubiquitination of the carboxyl-terminal tail of H2B blocks the enzyme that phosphorylates serine 2 of the CTD repeats, thus regulating the transition to full elongation.

The Stowers Institute for Medical Research, 1000 East 50th Street, Kansas City, MO 64110, USA. E-mail: jlw@stowers.org

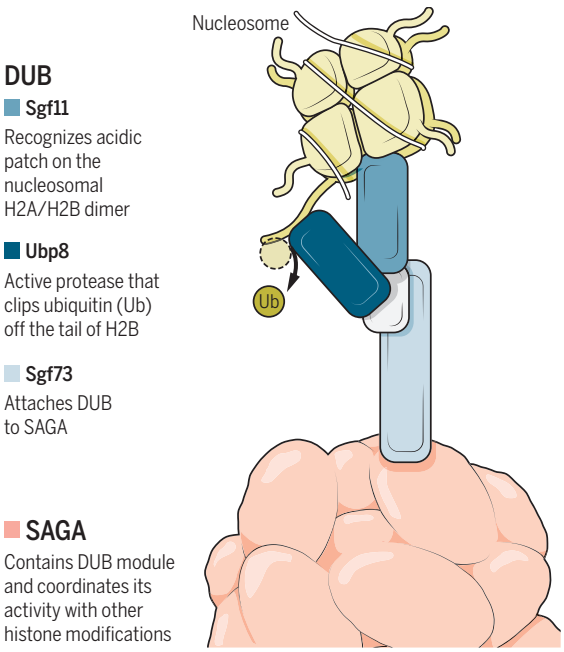

DUB module. Different subunits of the DUB module of the SAGA complex play distinct roles in regulating its ubiquitin protease activity. Sgf73 attaches the DUB module to the SAGA complex;Sgf11 provides specificity for H2B by recognizing the acidic patch on the nucleosomal H2A/H2B dimer. This and additional contacts between the DUB module and the nucleosome position Ubp8 at the carboxyl-terminal tail of H2B. Ubp8 is the ubiquitin protease that clips ubiquitin off the carboxyl-terminal tail of H2B.

Deubiquitination of H2B by the SAGA complex allows phosphorylation of serine 2 of the CTD repeats, promoting transition from the early elongation to the full elongation form of RNA polymerase II (*6*).

In addition to containing a histone acetyltransferase module that acts on histones H2B and H3, SAGA contains a deubiquitinase (DUB) module comprising the ubiquitin protease Ubp8, and the subunits Sgf11, Sgf73, and Sus1. These subunits have unique roles in H2B deubiquitination (*7*). Whereas Ubp8 removes ubiquitin from H2B, Sgf11 largely determines its specificity for H2B. By analyzing the crystal structure (at 3.8 Å resolution) of the DUB module bound to a ubiquitinated nucleosome modified on histone H2B, Morgan *et al.* show that Sgf11 uses a zinc finger domain to bind to the acidic patch on the H2A/H2B dimer. This interaction, along with additional contacts, positions Ubp8 in proximity to the ubiquitin on H2B. Interestingly, the acidic patch also binds to the H4 tail from an adjacent nucleosome (*8*), suggesting that this acidic patch plays a role in higher-order nucleosome packing. In addition, several other nucleosome-binding proteins and complexes recognize the acidic patch (*9*), suggesting that binding of these proteins or Sgf11 could also affect nucleosome packing. Sgf73 attaches the DUB module to the remainder of the SAGA complex. Morgan *et al.* also observed that the amino terminus of Sgf73 is buried within the DUB module, whereas the carboxyl terminus attaches to the SAGA complex (*4*, *10*, *11*). Attachment of the DUB module to SAGA is important for regulating its deubiquitination activity. In the absence of Sgf73, the DUB module detaches from SAGA and becomes inactive in yeast but hyperactive in flies (*10*, *12*).

The structural data provided by Morgan *et al.* provide new insights into how cooperation among the DUB module subunits enables the SAGA complex to control transcription (see the figure). It also offers a possible mechanism for how H2A phosphorylation affects deubiquitination. ■

REFERENCES AND NOTES

1. M. E. Lalonde, X. Cheng, J. Cote, *Genes Dev.* **28**, 1029 (2014).
2. E. Koutelou, C. L. Hirsch, S. Y. Dent, *Curr. Opin. Cell Biol.* **22**, 374 (2010).
3. V. M. Weake, J. L. Workman, *Trends Cell Biol.* **22**, 177 (2012).
4. M. T. Morgan *et al.*, *Science* **351**, 725 (2016).
5. S. Buratowski, *Mol. Cell* **36**, 541 (2009).
6. A. Wyce *et al.*, *Mol. Cell* **27**, 275 (2007).
7. S. Rodriguez-Navarro, *EMBO Rep.* **10**, 843 (2009).
8. K. Luger, A. W. Mader, R. K. Richmond, D. F. Sargent, T. J. Richmond, *Nature* **389**, 251 (1997).
9. R. K. McGinty, S. Tan, *Chem. Rev.* **115**, 2255 (2015).
10. K. K. Lee, S. K. Swanson, L. Florens, M. P. Washburn, J. L. Workman, *Epigenetics Chromatin* **2**, 2 (2009).
11. K. Kamata *et al.*, *Genes Cells* **18**, 823 (2013).
12. R. D. Mohan *et al.*, *Genes Dev.* **28**, 259 (2014).

ACKNOWLEDGMENTS

I thank S. M. Abmayr for help. This work was supported by National Institute of General Medical Sciences grant GM099945 and the Stowers Institute.

10.1126/science.aaf1495

ILLUSTRATION: V. ALTOUNIAN/*SCIENCE*

Downloaded from on February 11, 2016

Published by AAAS

ETHICS OF NEW TECHNOLOGIES

Finding an ethical path forward for mitochondrial replacement

It is ethically permissible to initiate clinical investigations of mitochondrial replacement techniques in humans so long as significant conditions and restrictions are in place

Anne B. Claiborne[1]*†, Rebecca A. English[1]*, Jeffrey P. Kahn[2]*†

Mitochondria are organelles found in nearly all cells in the human body and are best known for their role in regulating cellular energy balance (sometimes described as the "energy factory" of the cell). Mitochondrial DNA (mtDNA) is the only source of DNA in human cells found outside of the nucleus. The mitochondrial genome contains 37 genes (as compared with the 20,000 to 30,000 found in the nuclear genome), but pathogenic mutations in mtDNA can lead to rare, serious diseases that tend to affect organs with the highest energy demand and can be severely debilitating, progressive, and sometimes fatal in childhood (*1, 2*). mtDNA diseases involve extensive clinical and genetic heterogeneity, creating a challenge for estimates of prevalence. Estimates range from 1 in 200 (*3*) to 1 in 5000 (*4*) people harboring a pathogenic mtDNA mutation that may result in disease.

Proposed mitochondrial replacement techniques (MRTs) would potentially prevent maternal transmission of pathogenic mtDNA by removing from the intended mothers' oocytes (eggs) or zygotes (fertilized eggs) the nuclear DNA (nDNA) and transferring that genetic material into another woman's oocyte or zygote from which the nDNA has been removed (*5*). If shown to be effective, MRT could satisfy the desire of some women to have a genetically related child (by maintaining a nuclear DNA connection), while mitigating the risk of passing on pathogenic mutations in their mtDNA.

POLICY

[1]Institute of Medicine, U.S. National Academies of Sciences, Engineering, and Medicine, Washington, DC 20001, USA. [2]Johns Hopkins Berman Institute of Bioethics, Johns Hopkins University, Baltimore, MD 21205, USA. *Responsibility for the content of this article rests with the authors and does not necessarily represent the views of the Institute of Medicine (IOM), its committees, and its convening activities. †J. P. Kahn was chair of the IOM committee. ‡Corresponding author. E-mail: aclaiborne@nas.edu

In 2015, the United Kingdom approved MRT for clinical use (*6*) and remains, as of early 2016, the only country to have authorized the techniques. Remaining scientific reviews of MRT and procedures for licensing clinics and individual patients are being finalized. A U.S. Food and Drug Administration (FDA) Advisory Committee discussed MRT in 2014 and received public comments that reflected concern about certain ethical, social, and policy issues surrounding the techniques (*7*). The FDA requested that the Institute of Medicine (IOM) convene an expert committee to consider whether MRT clinical investigations could ethically be conducted. The committee's report was released on 3 February 2016, and we summarize its general findings and recommendations here (*8*).

> *"The committee's recommendations—place a high priority on a cautious approach and reduction of risk."*

DO ETHICAL, SOCIAL, OR POLICY CONSIDERATIONS PRECLUDE MRT? *Parental desire to pursue MRT.* Women at risk for transmitting mtDNA disease to their offspring but who wish to become mothers currently have reproductive options that result in varying degrees of nuclear genetic connection with the resulting child. Options range from unassisted sexual reproduction (and variable but possibly high risk of disease transmission) or preimplantation genetic diagnosis (with limited ability to identify embryos that would not carry risk of mtDNA disease), to in vitro fertilization using an egg from an unrelated female or adoption or childlessness. The latter three avoid transmission of disease but lack genetic relatedness to offspring. The committee concluded that, from an ethical perspective, the desire of some women to pursue MRT in order to maintain an nDNA connection while significantly reducing the risk of passing on pathogenic mtDNA can justify proceeding with clinical investigations, subject to limits that focus on protecting the health and well-being of children who would be born as a result of MRT.

Genetic modification of germ cells and the germ line. Over the past few decades, there has been a growing international consensus supporting prohibition of genetic modification to germ cells where such genetic changes could be inherited by subsequent generations; in addition to those countries that would prohibit such modifications, a number of countries (including the United States) have laws or policies that would restrict if not fully prohibit it (*9, 10*). There has been much controversy about whether genetic modification of humans, whether inheritable by future generations or not, is ethically acceptable or constitutes inappropriate interference with the human genome (*11*).

It is the committee's view that MRT involves genetic modification, but it is only heritable genetic modification ("germline modification") "if used to produce female offspring because mtDNA is solely maternally inherited, and therefore any changes to mtDNA in male offspring would not be inherited by their descendants" (*8*) (see the figure). The committee considered a number of ethical, social, and policy concerns that have been raised about human genetic modification, whether heritable or not, and concluded that these concerns, in the context of MRT, warrant caution and the imposition of restrictions rather than a blanket prohibition.

Unintended downstream implications of MRT. In the U.S. regulatory context, social and market forces largely drive uptake of innovative reproductive technologies. The committee noted that, if MRT is approved by the FDA, its expanded use for scientifically unproven or potential enhancement purposes would be of concern. For example, expanding the use of MRT to female idiopathic or age-related infertility would considerably enlarge the pool of possible users of the technology. The committee concluded that federal regulations would be needed, and professional society guide-

Downloaded from on February 11, 2016

Published by AAAS

lines interpreting the regulations would be helpful to limit the use of MRT and to prevent expansion into applications that raise other ethical issues. The committee recommended limiting initial clinical investigations to women at risk of transmitting a serious mtDNA disease (i.e., where "the mutation's pathogenicity is undisputed, and the clinical presentation of the disease is predicted to be characterized by early mortality or substantial impairment of basic function") (*8*).

Implications of the DNA contribution of two women. Combining mtDNA and nDNA from two women via MRT could blur traditional concepts of relatedness and undermine intergenerational connections and lineage that are traditionally measured by mtDNA. Some reviews have also suggested that introducing mtDNA from a second woman could have negative effects on the child's self-perception (*12*). In the committee's view, the contribution of genetic material from two women does not form a basis for prohibiting initial MRT investigations; rather, it is a "matter for reflection by families considering undertaking MRT and for societal discussions related to conceptions of identity, kinship, and ancestry" (*8*).

Distinguishing modification of mtDNA and nDNA. A central question for the committee was to consider whether the heritable modification of mtDNA resulting from MRT raises ethical, social, and policy issues comparable to those raised by heritable modification of the nuclear genome. Recent advances in gene-editing technologies such as CRISPR-Cas9, which has been used to modify nDNA and could also be used to modify mtDNA, have renewed international debate about the appropriate use of these technologies (*13*). The committee concluded that there are substantial and "important distinctions between modification of mtDNA and nDNA that matter for an analysis of the ethical, social, and policy issues" of MRT (*8*) and that could allow justification of MRT independent of considerations about heritable genetic modification of nDNA. MRT would involve wholesale replacement of the mtDNA genome. By design, the procedures lack precise editing capabilities that could target particular phenotypes, which helps circumscribe MRT's applications and places some natural limitations on the potential for its misuse. In addition, the committee found that traits encoded by nDNA constitute, in the public understanding, the "core of genetic relatedness" and most forms of disease and that modification of nDNA could be more susceptible to efforts to perform undesirable "genetic enhancement" than would modification of mtDNA. In the committee's judgment, the most germane ethical, social, and policy issues can be avoided through limitations on the use of MRT or are blunted by meaningful differences between the modification of mtDNA and nDNA. Therefore, the committee concluded that it is ethically permissible to conduct clinical investigations of MRT, although only under certain conditions and principles.

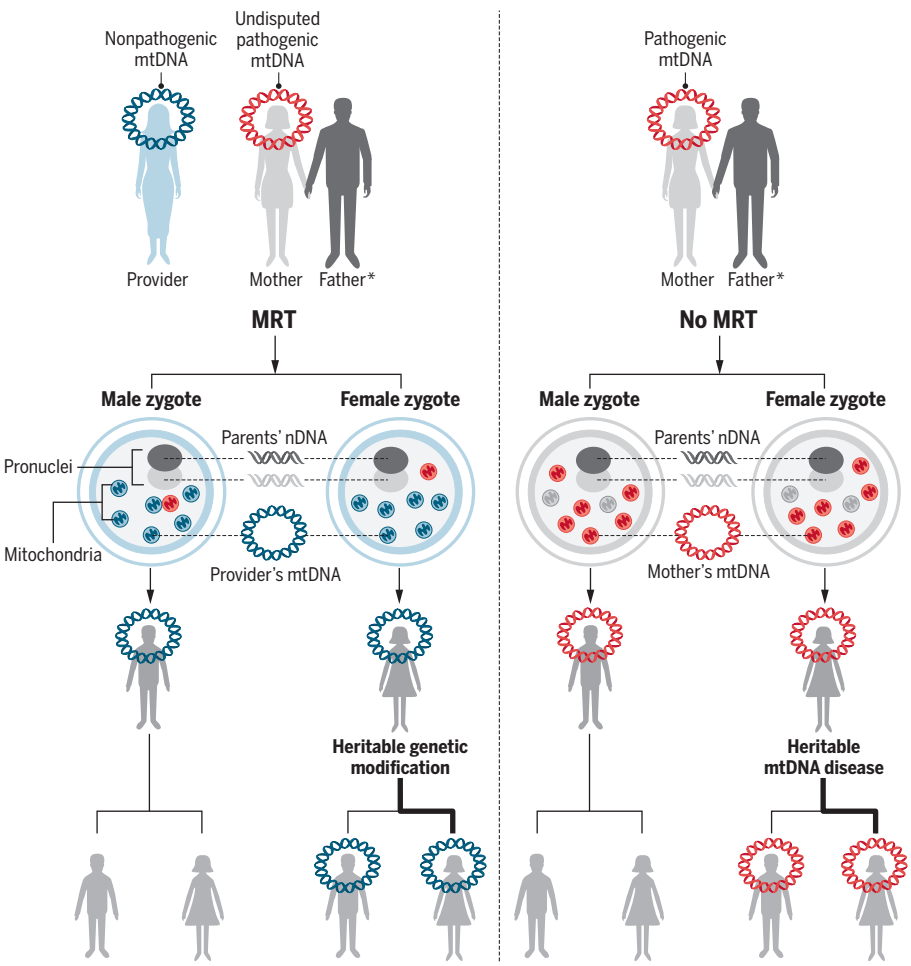

ILLUSTRATION: K. SUTLIFF/*SCIENCE*

Heritable genetic modification via MRT. MRT replaces pathogenic mtDNA from the intended mother with nonpathogenic mtDNA from an oocyte provider. For simplicity, reproductive partners are not shown and are assumed not to carry pathogenic mtDNA mutations. As shown, it is largely accepted that in transferring the nDNA there could be some carryover of pathogenic mtDNA, the level of which would be part of the evaluation of the zygotes suitable for transfer.

REGULATION AND OVERSIGHT OF MRT IN HUMANS. *Initial restriction to transfer of male embryos.* The committee's recommendations for the necessary conditions for any initial investigations of MRT place a high priority on a cautious approach and reduction of risk. The first such condition is that initial investigations be limited to transferring male embryos for gestation. Although there is ethical debate about whether sex selection is acceptable, this recommendation is not based on the preferential selection of one sex "but on the need to proceed slowly and to prevent potential adverse and uncertain consequences of MRT from being passed on to future generations" (*8*). Preclinical research to study intergenerational effects of MRT could continue while investigations proceed in which MRT is used to give some families the opportunity to have male children. Any births resulting from initial investigations would occur in an investigational context, and the initial limitation to males is a matter of responsible clinical investigation focused on minimizing risk. Although some research questions cannot be examined if initial MRT investigations are limited to male embryos, the committee believes that this is justified and necessary to effectively eliminate the risk of introducing adverse genetic modifications that are heritable by future generations. The restriction is also consistent with research staging and other design features used routinely in biomedical clinical investigations.

Before expanding MRT to include transfer of female embryos, robust evidence of

Published by AAAS

the safety and efficacy of the techniques in males—no matter how long it will take to collect it—would be needed. This evidence would come from experience with numerous male children followed at least through their early childhood years, as well as evidence from animal models that showed no adverse intergenerational effects when MRT was used to produce female offspring. This long-term follow-up is not unique to boys but, rather, is a feature of the necessity of monitoring the results of these initial investigations.

Should sufficiently compelling evidence of safety and efficacy (*8*) be obtained, expanding MRT to include transfer of female embryos would remain a controversial step as it would introduce a heritable genetic modification. A public discussion and international process is under way to create a shared framework to guide the circumstances of when, if ever, it would be acceptable to perform heritable genetic modification (*13, 14*).

Safeguards in the conduct of clinical investigations. Consideration of issues of safety and efficacy, and the ultimate determination about whether the agency should move forward with evaluating applications for MRT clinical investigations, rests with the FDA. The committee cautioned, however, that, with significant complexities and unknowns remaining regarding the field of mitochondrial genetics, it will be important for the scientific community and the agency to develop a thorough understanding of the state of the science related to mtDNA genetics and MRT to further inform, in an ongoing way, the benefit and risk assessment entailed in clinical investigations. Although providing guidance to the FDA about what preclinical research would need to be conducted was outside the scope of the committee's charge, the committee noted that the FDA's Advisory Committee had suggested a need for animal studies across a variety of species designed to evaluate safety over the long term. If MRT were ever to be extended to transfer of female embryos, the committee noted, "animal studies of second, and perhaps third, generations would need to be performed" (*8*).

"If shown to be effective, MRT could satisfy the desire of some women to have a genetically related child..."

The primary value to be considered in assessing the ethics of the balance of benefits and risks in clinical investigations of MRT is the minimization of risk of harm to the resulting child. For initial clinical investigations, the committee recommended, in addition to restricting transfer to male embryos, limiting clinical investigations to women who are otherwise at risk of transmitting a serious mtDNA disease (as defined above). Additional principles for all clinical investigations include attention to clinical issues specific to the technique, such as the health of the intended mother to carry a pregnancy, ensuring technical expertise of MRT investigators and centers, and attention to the science relating to addressing potential mtDNA–nDNA incompatibilities. The design of protocols should include mechanisms for standardization, maximizing data quality, data sharing, and collection of long-term information. The report also emphasizes the need to pay close attention to best practices for consent in research and special attention to communicating the novel aspects of MRT research to potential participants. Transparency and partnership with prospective parents and the general public are crucial, and public engagement is vital. ■

REFERENCES AND NOTES

1. S. B. Vafai, V. K. Mootha, *Nature* **491**, 374 (2012).
2. R. P. Saneto, M. M. Sedensky, *Neurotherapeutics* **10**, 199 (2013).
3. H. R. Elliott, D. C. Samuels, J. A. Eden, C. L. Relton, P. F. Chinnery, *Am. J. Hum. Genet.* **83**, 254 (2008).
4. G. S. Gorman *et al.*, *Ann. Neurol.* **77**, 753 (2015).
5. D. P. Wolf, N. Mitalipov, S. Mitalipov, *Trends Mol. Med.* **21**, 68 (2015).
6. U.K. Parliament, Lords discusses mitochondrial donation (29 October 2015); http://bit.ly/1KIxvfx.
7. FDA, 59th Meeting of the Cellular, Tissue, and Gene Therapies Advisory Committee, Gaithersburg, MD, 25 February 2014 (FDA, 2014); http://1.usa.gov/1OSXrJ8.
8. National Academies of Sciences, Engineering, and Medicine, "Mitochondrial replacement techniques: Ethical, social, and policy considerations" (National Academies Press, Washington, DC, 2016).
9. M. Araki, T. Ishii, *Reprod. Biol. Endocrinol.* **12**, 108 (2014).
10. R. Isasi, E. Kleiderman, B. M. Knoppers, *Science* **351**, 337 (2016).
11. International Bioethics Committee, "Report of the IBC on updating its reflection on the human genome and human rights" (United Nations Educational, Scientific, and Cultural Organization, Paris, 2015).
12. Nuffield Council on Bioethics, *Novel Techniques for the Prevention of Mitochondrial DNA Disorders: An Ethical Review* (Nuffield Council on Bioethics, London, 2012); http://bit.ly/NuffieldPubs.
13. National Academy of Medicine, "International Summit on Human Gene-Editing: A Global Discussion," 1 to 3 December, 2015, Washington, DC (National Academies, Washington, DC, 2015); bit.ly/209qZKZ.
14. National Academies of Sciences, Engineering, and Medicine, Human Gene-Editing Initiative (2015); http://bit.ly/20w0A75.

ACKNOWLEDGMENTS

R.E. and A.C. were supported by U.S. Department of Health and Human Services, Food and Drug Administration (contract no. 10002265). We would like to thank the members of the Committee and also M. Stathem and M. Berrios of the IOM.

Published online 3 February 2016

10.1126/science.aaf3091

CELL GROWTH

(TORC)ing up purine biosynthesis

An enzyme complex coordinates metabolism and nucleotide production to fuel cell growth

By **Eric H. Ma**[1,2] ***and*** **Russell G. Jones**[1,2]

Proliferating cells must coordinate their metabolic activities to meet the bioenergetic and biosynthetic demands of anabolic growth. Rapidly growing cells—such as cancer cells—achieve this in part by rewiring their metabolic pathways to increase flux through specific biosynthetic pathways. A more complex issue is how metabolic enzymes are organized to ensure efficient processing of metabolic intermediates. On pages 728 and 733 of this issue, Ben-Sahra *et al.* (*1*) and French *et al.* (*2*), reveal how a protein complex called mammalian/mechanistic target of rapamycin complex 1 (mTORC1) orchestrates metabolism and purine nucleotide biosynthesis to promote cell proliferation.

Purine nucleotides are important metabolic intermediates for growth as they function both as energy carriers (i.e., adenosine 5′-triphosphate and guanosine 5′-triphosphate and building blocks for RNA and DNA synthesis. Whereas purine bases can be recycled through endogenous salvage pathways, de novo purine biosynthesis is increased in proliferating cells and required for optimal cell proliferation (*3*). The construction of purine nucleotides is sourced from several nutrients: The ribose sugar is derived from carbohydrates such as glucose; the purine base is constructed from the amino acids glutamine, aspartate, and glycine; and one-carbon groups are derived from the tetrahydrofolate (THF) cycle (*4*).

mTORC1 is a protein kinase complex that integrates growth signals and environmental cues to regulate diverse metabolic and growth control programs in mammalian cells (*5*). Given previous work linking mTORC1 to de novo pyrimidine biosynthesis (*6*), Ben-Sahra *et al.* used metabolic tracing techniques to assess the impact of mTORC1 activity on the production of purine nucleotides. Using both genetic and pharmacologi-

Downloaded from on February 11, 2016

Published by AAAS

cal approaches, the authors demonstrate that mTORC1 activation enhanced de novo purine biosynthesis in human and mouse cells. mTORC1 affected purine biosynthesis at multiple levels: by regulating the expression of phosphoribosyl-pyrophosphate synthetase 2 (PRPS2), an enzyme whose function is a rate-limiting step for nucleotide biosynthesis (*7*); by enhancing nucleotide production from serine and glycine; and by increasing the expression of methylenetetrahydrofolate dehydrogenase 2 (MTHFD2), an enzyme of the mitochondrial tetrahydrofolate (mTHF) cycle. MTHFD2 was essential for generating a pool of mitochondrial-derived formate to fuel purine biosynthesis. Silencing the expression of MTHFD2 blocked both serine and glycine incorporation (for the purine bases) into growing RNA chains and arrested cell proliferation to a similar extent as either cells treated with the mTORC1 inhibitor rapamycin or cells in which expression of the essential mTORC1 component Raptor was silenced.

protein synthesis (*5*). The authors found that mTORC1 promoted increased translation of activating transcription factor 4 (ATF4), a stress-responsive transcription factor linked to metabolic control (*8*). ATF4 drove the expression of the mitochondrial enzyme MTHFD2 as well as serine biosynthesis pathway genes, thereby stimulating purine production in response to mTORC1 signals. Ben-Sahra *et al.* thus show that by mobilizing both the mitochondrial machinery of the mTHF cycle and shunting metabolic intermediates into this pathway to fuel serine-dependent one-carbon metabolism, mTORC1 can translate growth signals into cell division.

Purine biosynthesis occurs at multienzyme complexes celled purinosomes, which form transiently in response to low purine amounts to stimulate de novo biosynthesis (*9*). This raises the question of how mTORC1-stimulated metabolic products, such as formate, are shuttled from the mitochondrion to purinosomes. French *et al.* address this issue through three-dimensional stochastic optical reconstruction microscopy (3D STORM) (*10*). The authors mapped the cellular location of purinosomes upon stimulation of de novo purine biosynthesis, and found colocalization of these enzyme complexes with mitochondria. Using an RNA interference–based screening approach, the authors identified mTOR as a regulator of epinephrine-induced purinosome formation. Furthermore, culturing cells with the mTORC1 inhibitor rapamycin blocked colocalization of purinosomes with mitochondria, but did not affect the amount of purinosomes. Although the mechanism by which mTORC1 controls purinosome-mitochondrial association remains unclear, the findings of French *et al.* indicate that mTORC1 exerts spatial and temporal control over purinosome assembly.

mTORC1 is an important regulator of cellular metabolism, influencing diverse pathways from glycolysis and mitochondrial metabolism to lipid biosynthesis (*11, 12*). The studies of French *et al.* and Ben-Sahra *et al.* provide new insight into how this protein complex coordinates metabolic reprogramming to promote cell growth and proliferation. In essence, mTORC1 directs a cellular supply chain system, channeling mitochondrial-derived metabolic intermediates to the purinosome machinery for efficient nucleotide production (see the figure). Perhaps more importantly, the studies highlight how successful metabolic remodeling involves coordination of both metabolic flux and spatial organization of organelles and enzyme complexes. This coordination promotes efficient production of metabolic intermediates essential for growth.

It remains to be seen whether mTORC1 exerts similar effects on other metabolic enzyme complexes, such as those that drive glycolysis or lipid biosynthesis, and whether this is a common mechanism of other signal transduction networks. Regardless, both studies highlight how mitochondrial function and anabolic growth are orchestrated to drive cell proliferation, which has substantial implications for many diseases, including cancer. ■

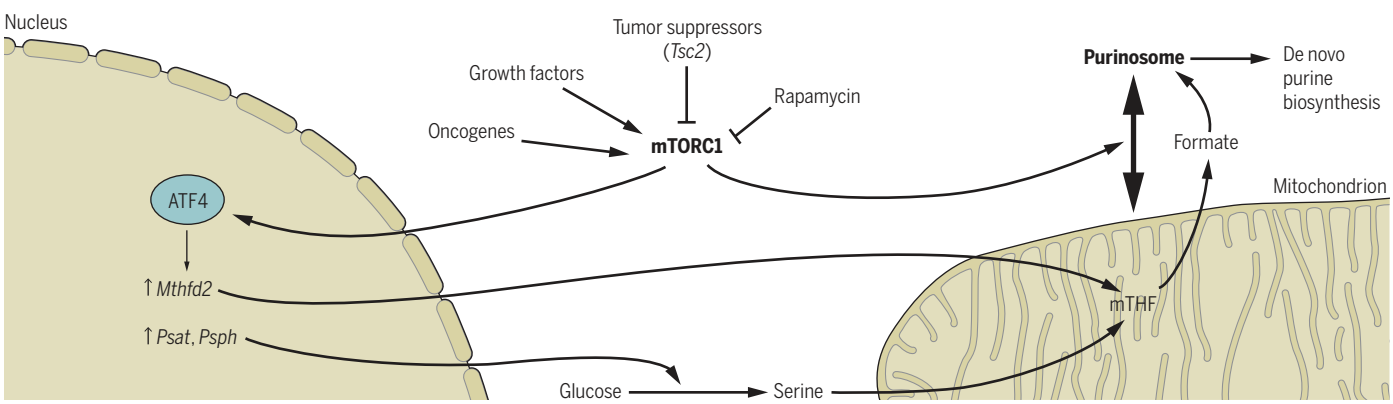

The mitochondria-purinosome shuttle. Factors that activate the mTORC1 complex lead to increased expression of the transcription factor ATF4. ATF4 promotes the expression of genes in the serine biosynthesis and mitochondrial tetrahydrofolate (mTHF) pathways that drive formate production. In parallel, mTORC1 promotes association of purinosomes with mitochondria, enabling the efficient shuttling of metabolic intermediates for de novo purine biosynthesis. *Tsc2, tuberous sclerosis complex 2*.

ILLUSTRATION: P. HUEY/*SCIENCE*

[1]*Goodman Cancer Research Centre, Department of Physiology, McGill University, Montreal, QC, H3A 1A3, Canada.* [2]*Department of Physiology, McGill University, Montreal, QC, H3G 1Y6, Canada. E-mail: russell.jones@mcgill.ca*

REFERENCES

1. I. Ben-Sahra, *Science* **351**, 728 (2016).
2. J. B. French, *Science* **351**, 733 (2016).
3. T. Yamaoka *et al.*, *J. Biol. Chem.* **272**, 17719 (1997).
4. S. Y. Lunt, M. G. Vander Heiden, *Annu. Rev. Cell Dev. Biol.* **27**, 441 (2011).
5. M. Laplante, D. M. Sabatini, *Cell* **149**, 274 (2012).
6. I. Ben-Sahra *et al.*, *Science* **339**, 1323 (2013).
7. J. T. Cunningham, M. V. Moreno, A. Lodi, S. M. Ronen, D. Ruggero, *Cell* **157**, 1088 (2014).
8. J. Seo *et al.*, *Diabetes* **58**, 2565 (2009).
9. S. An *et al.*, *Science* **320**, 103 (2008).
10. B. Huang *et al.*, *Nat. Methods* **5**, 1047 (2008).
11. M. Morita *et al.*, *Cell Metab.* **18**, 698 (2013).
12. K. Duvel *et al.*, *Mol. Cell* **39**, 171 (2010).

10.1126/science.aaf1929

Published by AAAS

BOOKS *et al.*

EXHIBITION

The hidden organ

The much-maligned microbe is recast as an essential element of human health

By **Valerie Thompson**

If you were to gather up all of the microbes that reside in and on your body, they'd tip the scale at between two and three pounds—roughly the same weight as your brain. But heft might not be the only thing the two have in common: A growing body of research suggests that the bacteria, fungi, and archaea that populate our bodies—whose genetic milieu are referred to collectively as our "microbiome"—may also be critical to human health and survival. This realization has prompted some, including microbiologist Susan Perkins, to refer to the microbiome as "the hidden organ."

Perkins is one of the curators of the American Museum of Natural History's new exhibition, *The Secret World Inside You*, which invites visitors to rethink the role of the microbe in human health. Or, as Rob DeSalle, Perkins's cocurator, puts it, "We take on the idea of microbes as 'the bad guys' head-on."

Gone are the days when microbes were considered mere disease-spreading agents that must be purged at all costs. Through a combination of videos, larger-than-life models, interactive displays, and live performance, *The Secret World* shows how microbes engage in complex, and often mutually beneficial, interactions with our skin, immune, and digestive systems.

The entrance to the exhibition features a darkened, mirror-lined hallway strung with tiny, twinkling lights that serve as a disorienting introduction to the ubiquity of microbial life. Following a brief introductory video, visitors are ushered into an area dedicated to the microbes that reside on human skin. Flippable panels on a freestanding display explore how different factors—including gender, age, and lifestyle—can alter a person's microbiome. But microbial communities don't just vary across people. "From the point of view of a microbe, your skin is like an enormous continent, with resources that vary dramatically from one region to another," reads one exhibit. Temperature, texture, and humidity, we learn, are among the factors that determine where a microbe sets up shop.

A diverse microbiome is not something that we are inherently endowed with, and many of our early experiences can have a lasting effect on it. In "Brand New Microbiome," visitors learn that bacteria that are typically found on the skin are more likely to populate the digestive tract of babies born via cesarean section, whereas babies delivered via the birth canal tend to acquire gut bacterial communities that resemble those that are found in the vagina. Several studies have suggested that individuals delivered via cesarean may be more susceptible to allergies and asthma, leading some researchers to speculate that initial differences in the seeding of the microbiome may underlie these conditions.

In the exhibition's final display space, visitors learn about the microbes that populate our digestive systems. More than a thousand different kinds of bacteria live in the human mouth, we learn—including the microscopic culprits behind tooth decay and morning breath. But the benefits of a rich microbiome in our digestive tract would seem to outweigh the negatives: Gut microbes ferment fiber, produce nutrients, and can protect the lining of the digestive system from inflammation.

A small exhibit in this section entitled "Mind-Altering Microbes" offers visitors a tantalizing glimpse into our emerging understanding of the connections between the gut microbiome and brain function. We learn, for example, that introducing *Bacteroides fragilis* can improve autism-like symptoms in mice and that humans infected with *Toxoplasma gondii* have slower reaction times than noninfected individuals and tend to get in more car accidents.

Throughout the exhibition, the organizers make an admirable effort to temper the findings of new and emerging research by emphasizing the limits of our current understanding. Referencing a map in which obesity, poverty, and antibiotic use appear to be related, for example, one display asks, "Do antibiotics cause obesity? Or do poor people get sicker and need more antibiotics? Or is the cause something else entirely? Map data alone can't provide an explanation. But they can suggest topics for future research."

Still, some of the exhibition's nuance may be lost on less attentive visitors. During my visit, I watched as a child, encouraged by his adult companion, gleefully flung broad-spectrum antibiotics at a microbial community in a computerized pinball-style game. Both celebrated when the fictional throat infection that had necessitated the antibiotics was declared "cured." Neither appeared to notice the message that popped up next, however, which cautioned visitors about the devastating consequences these drugs can have on beneficial microbial communities.

The reviewer is on staff at Science *magazine, AAAS, Washington, DC 20005, USA.*

The Secret World Inside You
Rob DeSalle and Susan Perkins, curators
American Museum of Natural History
Through 14 August 2016

10.1126/science.aad9684

PHOTOS: (LEFT TO RIGHT) © AMNH/D. FINNIN; © AMNH

Downloaded from on February 11, 2016

Published by AAAS

POLITICAL SCIENCE

The savvy citizen

A new logic-based strategy promises to help civic educators improve the public's understanding of politics

By **Jane Junn**

In 1965, the year the Voting Rights Act was signed into law, only 5% of the population held a postsecondary degree. Despite the steady rise in educational attainment (nearly one-third of Americans currently have a college degree) and voting enfranchisement over the past 50 years, American democracy continues forward with the seemingly paradoxical circumstance of relatively high levels of education and low levels of political knowledge. In an engaging new book, eminent political scientist Arthur Lupia sets out to provide answers to the question of "why people know so little about politics and what we can do about it."

Lupia begins by critiquing the conventional wisdom that we are, in fact, lacking when it comes to political knowledge. He argues that studies that draw such conclusions are often based on unrealistic expectations, poor quality of measurement, and faulty reasoning from the data.

There is far too much detailed and policy-specific political information at any given moment for any person to be considered knowledgeable about all things political, Lupia maintains. "A democracy would be a farce if nobody knew anything at all about politics or policy," he writes. "[H]owever, it requires a grand leap of logic (usually accompanied by a substantial dose of illogic) to go from this possibility to the conclusion that everyone, or even most people, ought to be able to answer a narrow and oddly selected slice of questions about the federal government that a small group of elites has privileged."

Instead, Lupia argues that "[p]olitics produces disagreements about what others should know," and therefore there can be no single set of factual questions to adequately measure either the degree of knowledge or ignorance of politics among ordinary Americans. He believes that researchers and educators alike should instead, seek to "ask better questions, produce better measures, and draw more accurate inferences about what people do and do not know."

Lupia urges educators to assess the competencies of specific audiences, then offer logic and evidence that are likely to motivate the group to learn more about the issue at hand. Employing this "logic of competence" approach, Lupia presents solutions to improve the interaction and communication strategies of those who would seek to improve citizens' political knowledge, which are summarized in a helpful table at the conclusion of chapter 18. At the heart of his recommendations is the idea that educators should make material relevant to people in order to increase their motivation to learn.

This appeal to implement a logical process for teaching political information is both good strategy and uncontroversial advice. However, political information and knowledge are, to varying degrees, subjective—a circumstance that a method rooted in positivist logic cannot escape. Consequently, a process mirroring an underlying logic of competence is but a partial solution for encouraging political knowledge. At the same time, Lupia's silence on what kind of information is necessary and desirable is less helpful in guiding educators toward a substantive program for teaching political information.

Similarly, Lupia's plan of action is focused solely on educators and learners, whereas the typical "producers" of political information—government officials, experts, and the media—are not implicated in a legitimate plan of action. He also neglects to discuss the reality that entities are sometimes motivated to spread misinformation. A logical process might indeed increase competence and enhance political knowledge and decision-making, but only if the information is sound and the source of that knowledge is reliable. Looking back to the U.S. congressional decision to approve military involvement in Iraq in 2003, for example, a plan of action cast by Lupia's guidelines would have been as misguided as any other, given the widely accepted belief at the time that Iraq possessed weapons of mass destruction.

More than a half-century ago, another famous political scientist named V. O. Key observed that the public is but an echo chamber of what political elites shout into the vortex. In *Uninformed*, Lupia provides sightlines for educators to teach and expand the chamber, which may ultimately add new voices of reason, inflections of passion, and, perhaps, murmurs of compromise to our political discourse.

10.1126/science.aad6057

The reviewer is in the Department of Political Science at the University of Southern California, Los Angeles, CA 90089, USA. E-mail: junn@usc.edu

Uninformed
Why People Know So Little About Politics and What We Can Do About It
Arthur Lupia
Oxford University Press, 2016. 357 pp.

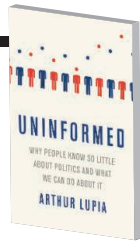

PHOTO: CATHERINE BALET; "STRANGERS IN THE LIGHT" (STEIDL), 2012/FROM *THE HUMAN FACE OF BIG DATA*)

DATA SCIENCE

The Human Face of Big Data
Sandy Smolan, director; Rick Smolan, executive producer
Premieres February 24, 2016, on PBS; check local listings

Virtually every movement, purchase, query, and comment that we make today leaves a digital trace that can be mined, mapped, and analyzed. But how do we use this information? And how might it be used against us? Combining beautifully animated data visualizations with commentary from scientists, futurists, tech creators, and other experts, this 1-hour documentary highlights how researchers are using big data to tackle everything from malaria outbreaks and traffic jams to poverty and recidivism. Although the "dark side of data" receives only perfunctory treatment, the program ultimately succeeds in humanizing an unwieldy and abstract topic.

10.1126/science.aaf3194

Downloaded from on February 11, 2016

Published by AAAS

LETTERS

Edited by **Jennifer Sills**

The crushing weight of urban waste

ON 20 DECEMBER 2015, a mountain of construction waste collapsed in Shenzhen, north of Hong Kong. The man-made landslide destroyed 33 buildings, killed 69 people, and left 8 others missing (*1*). This disaster occurred only 4 months after the chemical explosions in a hazardous material storage facility in Tianjin (*2*). These events highlight the importance of proper design and risk management during China's rapid urbanization.

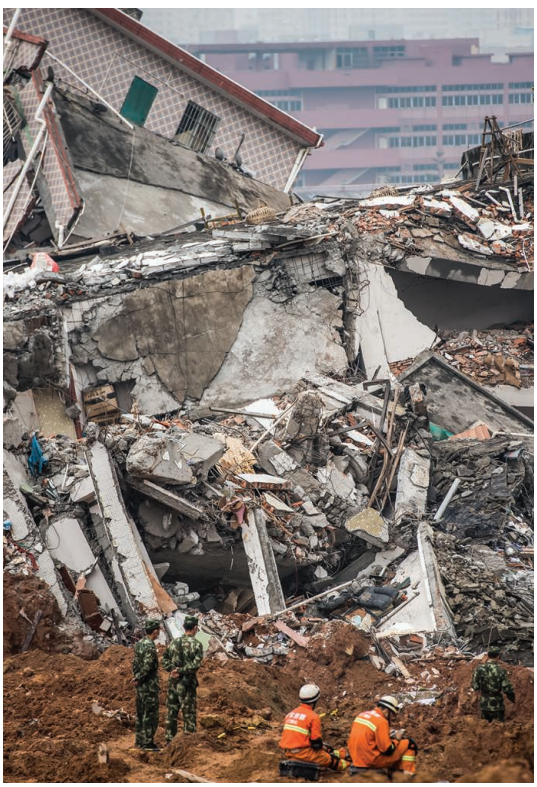

Construction waste collapse in Shenzhen, China.

Along with unparalleled urbanization, China produced approximately 30% of the world's municipal solid waste (MSW) in 2012 (*3*, *4*). Construction generates nearly 40% of China's MSW, more than 200 million tons every year. It also consumes about 40% of China's natural resources and energy. Rapid urban development is encroaching onto areas previously used for waste disposal that contain toxic substances, endangering human health (*5*). Landfill areas are filled so rapidly that many cities lack sufficient space to store the waste that is generated. Shenzhen's landfill capacity has been inadequate since early 2015 (*6*), but urbanization and the development of a network of underground railway lines continue.

The key solution is the implementation of construction waste minimization at the design stage, as described in the European Commission Waste Framework Directive (*7*). However, this concept is unknown to more than 60% of Chinese architects (*8*). Shenzhen was selected by China's Ministry of Housing and Urban-Rural Development as the pilot city for construction waste minimization and comprehensive utilization in 2012, but this did not stop the landslide tragedy (*9*). Close monitoring with GPS and other remote sensing techniques of large landfill sites and risk management are also important.

China is not alone. A similar landfill collapse happened in the Philippines' Quezon City, killing at least 278 people (*10*). These disasters should serve as a turning point for China and other countries to improve construction waste minimization and risk management.

Hong Yang,[1,2]* Xianjin Huang,[3]* Julian R. Thompson,[4] Ryan M. Bright,[1] Rasmus Astrup[1]

[1]Norwegian Institute of Bioeconomy Research (NIBIO), 1431 Ås, Norway. [2]CEES, Department of Biosciences, University of Oslo, Blindern 0316, Oslo, Norway. [3]School of Geographic and Oceanographic Science, Xianlin Campus, Nanjing University, Nanjing 210023, China. [4]Department of Geography, University College London, London WC1E 6BT, UK.

*Corresponding author. E-mail: hongyanghy@gmail.com (H.Y.); hxj369@nju.edu.cn (X.H.)

REFERENCES

1. Chinese Government, "69 people found dead in Shenzhen landslide" (2016); www.gov.cn/xinwen/2016-01/13/content_5032448.htm [in Chinese].
2. Z. W. Tang, Q. F. Huang, Y. F. Yang, *Nature* **525**, 455 (2015).
3. J. Li, X. Zhong, H. Cai, *J. Eng. Manage.* **29**, 38 (2015).
4. D. Hoornweg, P. Bhada-Tata, "What a waste: A global review of solid waste management" (World Bank, Washington, DC, 2012).
5. H. Yang, X. Huang, J. R. Thompson, R. J. Flower, *Science* **344**, 691 (2014).
6. L. Chen, "Shenzhen's 12-landfill storage capacity is full next year" (2014); http://wb.sznews.com/html/2014-10/15/content_3030704.htm [in Chinese].
7. European Commission, Construction and Demolition Waste Management Practices and Their Economic Impacts (1999); http://ec.europa.eu/environment/waste/studies/cdw_report.htm.
8. Y. Hao, J. Kang, *Building Sci.* **26**, 4 (2010).
9. J. Wang, X. Kang, V. W. Tam, *J. Eng. Des. Tech.* **6**, 227 (2008).
10. S. M. Merry, E. Kavazanjian Jr., W. U. Fritz, *J. Perform. Constr. Facil.* **19**, 100 (2005).

China's partial emission control

IN DECEMBER 2015, Beijing and other Chinese cities issued their first "red alert" for heavy air pollution, as heavy smog blanketed many parts of the country (*1*). China's red alert is the government's highest emergency response level to severe air pollution and includes school closures, suspensions of factory production, and driving restrictions (*1*, *2*). Nevertheless, Beijing's air quality index during the red alert remained hazardous, measuring 20 to 35 times above safe levels (*3*).

Over the past 35 years, China has implemented an antipollution system of total emission control (TEC) to curb increasing levels of environmental pollution (*4*). The Chinese government claims that the system has played a critical role in cutting annual emissions of targeted pollutants and improving the quality of the environment (*5*). The core of the TEC system is to set a 10% reduction for targeted pollutants and allocate total emission quotas on a year-to-year basis to provincial and regional governments.

However, the emission reduction target and quotas have been criticized for being unrealistic and lacking in scientific rationality from an environmental perspective (*4*, *6*). For instance, the TEC system is inconsistent in targeting the type and range of pollutants. From 1996 to 2000, the targeted pollutants included soot, sulfur dioxide, industrial dust, chemical oxygen demand (COD), cyanide, oil pollutants, five heavy metals (arsenic, mercury, lead, cadmium, and hexavalent chromium), and industrial solid waste. Yet, between 2001 and 2005, the list was reduced by half. From 2006 to 2010, only two pollutants were targeted (sulfur dioxide levels in air and COD levels in water) (*4*). Heavy metals were removed from the list in 2001, and the air pollutants soot and industrial dust are no longer targeted. As a result, heavy metals and air pollution have expanded across the country at an alarming rate (*7*). The increase took place despite the addition of ammonia-nitrogen and nitrogen oxides to the other two targeted pollutants (sulfur dioxide and COD) for the years 2011 to 2015 (*8*). Heavy metals comprise 82.8% of soil contaminants, and 16.1% of the country's total soil is polluted by heavy metals (*9*). Only 3 out of 74 key cities met the national standard of air quality in 2013 (*10*). The state media Xinhua News reported that Beijing's average density of fine particles (less than 2.5 mm) between 15 November and 31

PHOTO: STRINGER-IMAGINECHINA

Downloaded from on February 11, 2016

Published by AAAS

December 2015 rose by 75.9% since the previous year (*11*); in 2015, the fine-particle density averaged 80.6 mg/m^3 (*11*), compared with a safe level of 15 mg/m^3 (*12*).

China is taking steps to deal with its environmental problems by adjusting its industrial structure toward green development and environmental priority and by reviewing and strengthening its environmental policies and laws to ensure stronger enforcement, greater grass-roots accountability, system stability, and transparency and accountability of pollution data. To make these efforts meaningful, China must reinstate its original list of targeted pollutants and work to minimize them.

Aijun Lin,[1] Yuan Pu,[1] Weikang Qi,[1] Xiaoliang Li,[2] Xiujin Li,[1] Canfa Wang,[3] X. Jin Yang[1]*

[1]School of Chemical Engineering, Beijing University of Chemical Technology, Beijing 100029, China. [2]Department of Environmental Economics, Chinese Academy for Environmental Planning, Beijing 100012, China. [3]Institute of Environmental and Resources Law, China University of Political Science and Law, Beijing 100088, China.

*Corresponding author.
E-mail: yangxj@mail.buct.edu.cn

REFERENCES

1. Xinhua News, "40 cities issue alerts for pollution in N China" (2015); http://news.xinhuanet.com/english/2015-12/22/c_134941702.htm.
2. Ministry of Environmental Protection of the People's Republic of China, Guidelines for Urban Heavy Air Pollution Emergency Response (2013); www.mep.gov.cn/gkml/hbb/bgth/201305/t20130510_251978.htm [in Chinese].
3. China's Air Quality Online Monitoring and Analysis Platform (www.aqistudy.cn/) [in Chinese].
4. C. Ge, J. Chen, J. Wang, F. Long, *Chin. J. Popul. Res. Environ.* **7**, 50 (2009).
5. Ministry of Environmental Protection of the People's Republic of China, China's Environmental Status Report, 2000–2014 (http://jcs.mep.gov.cn/hjzl/zkgb/) [in Chinese].
6. Y. Geng, J. Sarkis, *Environ. Sci. Technol.* **46**, 107 (2012).
7. Q. Wang, *Nature* **497**, 159 (2013).
8. J. Wang, C. Jiang, W. Zhang, *Environ. Prot.* **43**, 21 (2015) [in Chinese].
9. Ministries of Environmental Protection and Land and Resources of the People's Republic of China, National Soil Pollution Report 2013 (2014); www.mlr.gov.cn/xwdt/jrxw/201404/t20140417_1312998.htm [in Chinese].
10. Ministry of Environmental Protection of the People's Republic of China, Air Quality in China's Key Regions and Cities in 2013 (2014); ww.zhb.gov.cn/gkml/hbb/qt/201403/t20140325_269648.htm [in Chinese].
11. Xinhua News, "Expert: Super El Nino winter superimposed emissions caused by heavy pollution Beijing" (2016); http://news.xinhuanet.com/politics/2016-01/08/c_128606630.htm [in Chinese].
12. Ministry of Environmental Protection of the People's Republic of China, Ambient Air Quality Standards (2012); http://kjs.mep.gov.cn/hjbhbz/bzwb/dqhjbh/dqhjzlbz/201203/t20120302_224165.htm [in Chinese].

Misguided strategy for mosquito control

AEDES AEGYPTI, a mosquito native to Africa, has recently transmitted zika, chikungunya, and dengue to humans in Brazil (*1*). In response, several Brazilian municipalities have encouraged the use of non-native "mosquito fish" (*Poecilia* spp.) to control *A. aegypti* by eating their larvae (*2*, *3*). This strategy is misguided.

The mosquito fish eats mosquito larvae.

PHOTO: © GARY MESZAROS/VISUALS UNLIMITED/CORBIS

Introducing non-native fishes into the aquatic environments of Brazil has been shown to negatively affect native biodiversity (*4*, *5*). The use of non-native species to manage other non-native organisms has also led to unintended consequences (*6*), and positive interactions between invasive species can make the environment more vulnerable to a secondary invasion (*7*).

If local policy-makers insist on the use of fish to cull the mosquito population, they should choose from Brazil's rich diversity of aquatic species (*8*). However, the efficacy of mosquito control by fish is questionable (*9*). Brazilian authorities should instead propose environmentally friendly strategies to control these epidemics (e.g., vaccines) and to suppress *A. aegypti* (e.g., sanitary measures), instead of encouraging the introduction of more non-native organisms.

Valter M. Azevedo-Santos,[1]* Jean R. S. Vitule,[2] Emili García-Berthou,[3] Fernando M. Pelicice,[4] Daniel Simberloff[5]

[1]Laboratório de Ictiologia, Departamento de Zoologia, Universidade Estadual Paulista "Júlio de Mesquita Filho, Campus de Botucatu," SP, 18618-970, Brazil. [2]Laboratório de Ecologia e Conservação (LEC), Universidade Federal do Paraná, Curitiba, PR, 81531-970, Brazil. [3]Institute of Aquatic Ecology, University of Girona, Catalonia, Spain. [4]Núcleo de Estudos Ambientais, Universidade Federal de Tocantins, Porto Nacional, TO, 77500-000, Brazil. [5]Department of Ecology and Evolutionary Biology, University of Tennessee, Knoxville, TN 37996, USA.

*Corresponding author.
E-mail: valter.ecologia@gmail.com

REFERENCES

1. P. F. C. Vasconcelos, *Rev. Pan-Amaz. Saude* **6**, 9 (2015).
2. "Peixe é usado como alternativa no combate à dengue em Alfenas, MG" (2015); http://g1.globo.com/mg/sul-de-minas/noticia/2015/12/peixe-e-usado-como-alternativa-no-combate-dengue-em-alfenas-mg.html [in Portuguese].
3. "Peixe que come larvas é aliado no combate à dengue em Ipameri, GO" (2015); http://g1.globo.com/goias/noticia/2015/05/peixe-que-come-larvas-e-aliado-no-combate-dengue-em-ipameri-go.html [in Portuguese].
4. J. R. S. Vitule *et al.*, *Fish Fish.* **10**, 98 (2009).
5. F. M. Pelicice *et al.*, *Conserv. Lett.* **7**, 55 (2014).
6. P. B. Moyle, H. W. Li, B. A. Barton, in *Fish Culture in Fisheries Management*, R. H. Stroud, Ed. (American Fisheries Society, Bethesda, MD, 1986), pp. 415–426.
7. D. Simberloff, *Ecol. Lett.* **9**, 912 (2006).
8. A. A. Agostinho *et al.*, *Conserv. Biol.* **19**, 646 (2005).
9. G. H. Pyke, *Annu. Rev. Ecol. Evol. Syst.* **39**, 171 (2008).

Published by AAAS

REVIEW SUMMARY

GENE REGULATION

Retrotransposons as regulators of gene expression

Reyad A. Elbarbary,* Bronwyn A. Lucas,* Lynne E. Maquat†

BACKGROUND: Genomes are subject to two types of changes: changes to the DNA sequence, and changes that are epigenetic in nature. Changes to the DNA sequence can result from errors made during DNA replication and/or repair, or from the insertion of mobile DNA. Mobile DNAs, also called transposable elements (TEs), have the potential to provide regulatory and/or protein-coding sequences at a new integration site. Depending on its nucleotide sequence and genomic insertion site, an individual TE can disrupt gene expression, directly or indirectly create an advantageous modification to gene expression, or be of no immediate consequence. Changes can be genetic, epigenetic, or both. In this way, TEs are molecular parasites and evolutionary drivers, each role originating from the ability to insert into, spread through, and restructure genomes. This review focuses on the types of TEs that transpose via RNA intermediates—retrotransposons—that are not bounded by long terminal repeats. The most abundant retrotransposons in animal genomes come in two forms: long interspersed elements (LINEs) and short interspersed elements (SINEs).

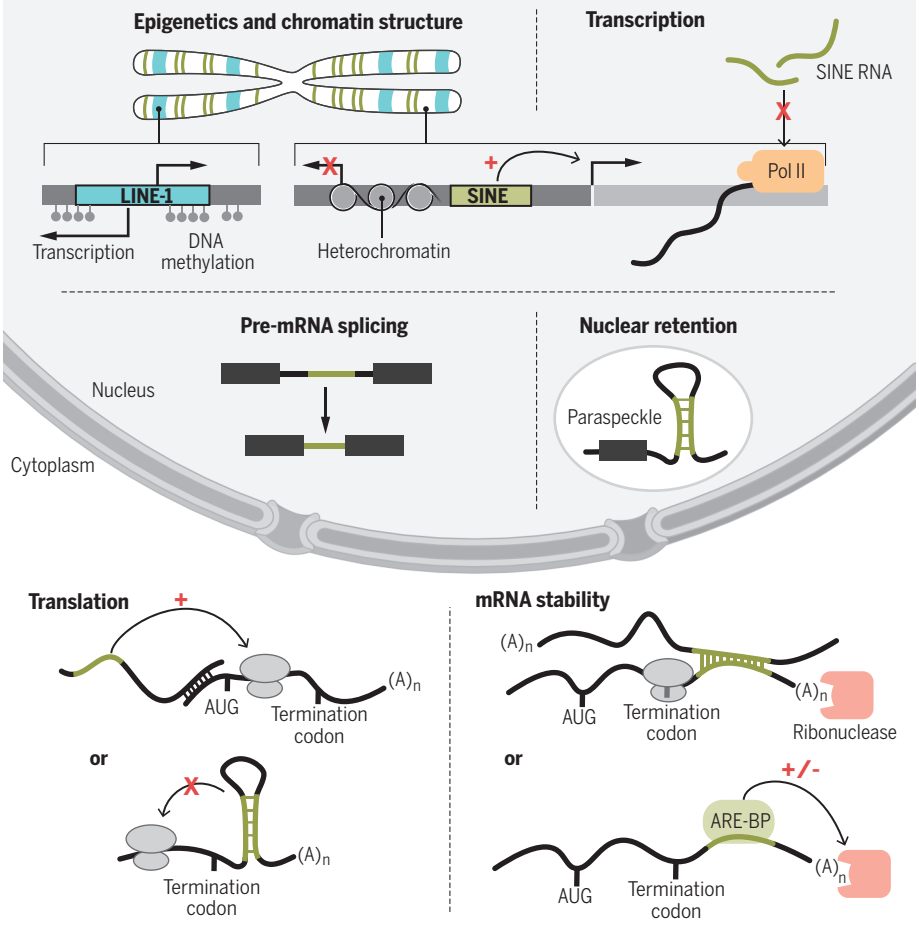

Some of the steps in the expression of mammalian genes that can be affected by cis- or trans-acting LINEs or SINEs. LINE and SINE genomic insertions can regulate gene expression by altering transcription and/or chromatin structure. When embedded in the transcripts of RNA polymerase II (Pol II)–transcribed genes, SINEs can influence nuclear pre-mRNA splicing, nuclear mRNA retention in paraspeckles, cytoplasmic mRNA stability, or cytoplasmic mRNA translation. ARE-BP, AU-rich element–binding protein.

ILLUSTRATION: K. SUTLIFF/*SCIENCE*

ADVANCES: The advent of deep genomic and transcriptomic sequencing, together with studies of individual LINE or SINE functions, has led to a greater appreciation of how the two TEs influence gene expression. Our review focuses principally on data that derive from human and mouse studies. These data demonstrate that LINEs and SINEs perform many diverse roles within cells. As DNA sequences, they can regulate gene transcription by altering chromatin structure and by functioning as enhancers or promoters. When transcribed as part of a larger transcript, they can create new transcript isoforms (by influencing alternative pre-mRNA splicing or 3′-end formation), alter mRNA localization, change mRNA stability, tune the level of mRNA translation, or encode amino acids that diversify the proteome. Further, the RNA transcripts of LINEs or SINEs may themselves function to regulate gene expression. Through their various roles, TEs influence many aspects of cellular metabolism, including the ability to divide, migrate, differentiate, and respond to stress.

ON OUR WEB SITE

Read the full article at http://dx.doi.org/10.1126/science.aac7247

OUTLOOK: TEs continue to spread throughout our genomes in both gametes and somatic tissues, introducing new gene regulatory activities or causing disease. Although deep transcriptome sequencing has identified a myriad of SINE-containing noncoding RNAs, the functional importance of most of these transcripts remains unknown. Additionally, we need to understand the consequence of the very high degree of TE transposition in our brains. We also need to uncover the determinants that influence the effect of a specific SINE on gene expression, and, given that different organisms can contain SINEs of distinct origins, the extent to which these SINEs contribute to species-specific differences. Moreover, it will be important to determine the extent to which independently evolved SINEs have been co-opted for similar functions. ■

The list of author affiliations is available in the full article online.
*These authors contributed equally to this work.
†Corresponding author. E-mail: lynne_maquat@urmc.rochester.edu
Cite this article as R. A. Elbarbary *et al.*, *Science* 351, aac7247 (2016). DOI: 10.1126/science.aac7247

Downloaded from on February 11, 2016

REVIEW

GENE REGULATION

Retrotransposons as regulators of gene expression

Reyad A. Elbarbary,[1,2]* Bronwyn A. Lucas,[1,2]* Lynne E. Maquat[1,2,3]†

Transposable elements (TEs) are both a boon and a bane to eukaryotic organisms, depending on where they integrate into the genome and how their sequences function once integrated. We focus on two types of TEs: long interspersed elements (LINEs) and short interspersed elements (SINEs). LINEs and SINEs are retrotransposons; that is, they transpose via an RNA intermediate. We discuss how LINEs and SINEs have expanded in eukaryotic genomes and contribute to genome evolution. An emerging body of evidence indicates that LINEs and SINEs function to regulate gene expression by affecting chromatin structure, gene transcription, pre-mRNA processing, or aspects of mRNA metabolism. We also describe how adenosine-to-inosine editing influences SINE function and how ongoing retrotransposition is countered by the body's defense mechanisms.

Transposable elements (TEs) are DNA sequences that have the ability to be integrated elsewhere in a genome. With few exceptions, TEs have been identified in all eukaryotic genomes sequenced to date (*1*). There are two main classes of TEs: Retrotransposons (class I) transpose via an RNA intermediate, whereas DNA transposons (class II) transpose directly without an RNA intermediate (*2*). The three major retrotransposon orders are long terminal repeat (LTR) retrotransposons, long interspersed elements (LINEs), and short interspersed elements (SINEs). Retrotransposons propagate via a copy-and-paste amplification mechanism that has allowed them to accumulate in DNA, giving rise to the bulk of repeats in eukaryotic genomes.

Mobile LINEs are RNA polymerase II (Pol II)–transcribed autonomous retrotransposons of several thousand base pairs (bp) (*3*). In the copy step, their internal Pol II promoter generates an mRNA-like capped and polyadenylated transcript (*4*). The transcript of LINE-1 (L1), which is the only active class of autonomous retrotransposons in humans, contains two open reading frames (ORFs) that are crucial for retrotransposition: ORF1 encodes an RNA-binding protein, and ORF2 encodes a protein with reverse transcriptase (RT) and endonuclease activities (Fig. 1A) (*5*). In the subsequent paste step, these proteins recognize a specific sequence in the 3′ end of the LINE transcript that encodes them, create two staggered nicks at specific sequences in the genome and, by using the genomic sequence as a primer, reverse-transcribe the LINE RNA into cDNA that is simultaneously incorporated into the genome (Fig. 1B) (*5*, *6*). Acquisition of an additional L1 ORF 5′ to ORF1 (ORF0) was recently demonstrated in the primate lineage (*7*).

Mobile SINEs are RNA polymerase III (Pol III)–transcribed nonautonomous retrotransposons that do not encode any proteins (Fig. 1C) but retrotranspose by hijacking the RT and endonuclease activities of a partner LINE-encoded protein (Fig. 1B). In most cases, LINE-encoded proteins recognize SINE RNAs with 3′ sequences that are similar to the 3′ sequence of the LINE RNA from which these proteins were synthesized; subsequently, they generate and integrate a cDNA copy of the SINE RNA into the genome (Fig. 1, B and C) (*8*).

The lengths of SINE family members generally range from 85 to 500 bp (*9*). A SINE typically has three parts: a 5′ head, a body, and a 3′ tail. Head sequences, which harbor the internal Pol III promoter, have been used to categorize SINEs into three superfamilies according to their derivation from, and thus similarity to, cellular Pol III genes encoding tRNA (such as mouse B2 or ID elements), 7SL RNA (such as mouse B1 and human *Alu* elements), or 5*S* rRNA (SINE3) (*2*, *9*, *10*). Most LINEs and SINEs in mammalian genomes have lost their functional promoters and thus lack the ability to retrotranspose (*5*).

LINEs and SINEs constitute ~30% of the human genome sequence and show a nonrandom genomic distribution (*11*). SINEs are generally localized in gene-rich regions, whereas LINEs are enriched in intergenic regions (*12*). The relative sparsity of LINEs in genic regions likely reflects negative selection against insertion of their large sequence (several thousand bp) in or near genes. In contrast, the smaller SINEs are more apt to be tolerated, and some SINEs in genic regions have assumed regulatory roles that control gene expression. The expansion of LINEs and SINEs has drastically shaped the genomes of multicellular organisms by providing regions of similarity that act as hotspots for nonallelic homologous recombination (Fig. 1, D and E) and acting as reservoirs of potential coding, regulatory, or disruptive sequences (*13*, *14*). In addition to their own retrotransposition and that of SINEs, LINEs have supported the retrotransposition of mRNAs (*15*, *16*). The resulting "retrogenes," in the presence of their functional counterpart, are free from selective pressure and thus can accumulate mutations and acquire novel functions (*16*). Thus, retrotransposition contributes to genetic diversity within a species and among different species in many ways. Additionally, retrotransposition appears to be active in some somatic tissues, including early in development (*17*), in developing neurons (*18*, *19*), and in the adult brain (*20*), leading to mosaicism whereby different cells within an individual have different genetic sequences. Most insertion events are neutral or detrimental to the host; here, we describe instances whereby inserted LINEs and SINEs have been harnessed to regulate gene expression.

Regulation of chromatin structure and transcription

Primate LINEs and SINEs have a high GC content, making them hotspots for DNA methylation, which is used by cells to suppress transcription (*21*). The methylation of LINE- and SINE-embedded CpG islands has the potential to silence the expression of nearby genes (*22*). LINEs and SINEs can demarcate the boundary between heterochromatin and euchromatin. For example, one mouse B2 element functions as a boundary element to prevent cis-residing heterochromatin from silencing developmental expression of the five genes located in the mouse growth hormone locus (Fig. 2A) (*23*). LINEs also participate in X-chromosome inactivation (XCI) via one of two mechanisms: Transcriptionally silent L1 elements contribute to the formation of a silent nuclear compartment during XCI, whereas L1 RNAs that derive from young LINE elements (which are enriched in the X chromosome) participate in inactivating X-chromosome loci that would otherwise escape XCI (*24*).

SINEs, and Alu elements in particular (*25*), can function as transcriptional enhancers, as exemplified by two members of the ancient SINE family Amniota SINE1 (AmnSINE1), which act as enhancers for the genes encoding fibroblast growth factor 8 (Fgf8) and special AT-rich sequence–binding protein 2 (Satb2) in the developing brain (Fig. 2A) (*25*, *26*). Retrotransposons located immediately upstream of protein-coding genes may function as promoters because putative binding sites for many transcription factors have been identified in SINEs (Fig. 2A) (*27*). However, it is unclear whether the majority of SINE-embedded transcription factor binding sites act to modulate gene transcription or simply act as sinks that titrate transcription factors away from their active binding sites. LINEs and SINEs can also introduce a new transcription start site (TSS); 6 to 30% of human and mouse

[1]Department of Biochemistry and Biophysics, School of Medicine and Dentistry, University of Rochester, Rochester, NY, USA. [2]Center for RNA Biology, University of Rochester, Rochester, NY, USA. [3]Department of Oncology, Wilmot Cancer Institute, School of Medicine and Dentistry, University of Rochester, Rochester, NY, USA.
*These authors contributed equally to this work. †Corresponding author. E-mail: lynne_maquat@urmc.rochester.edu

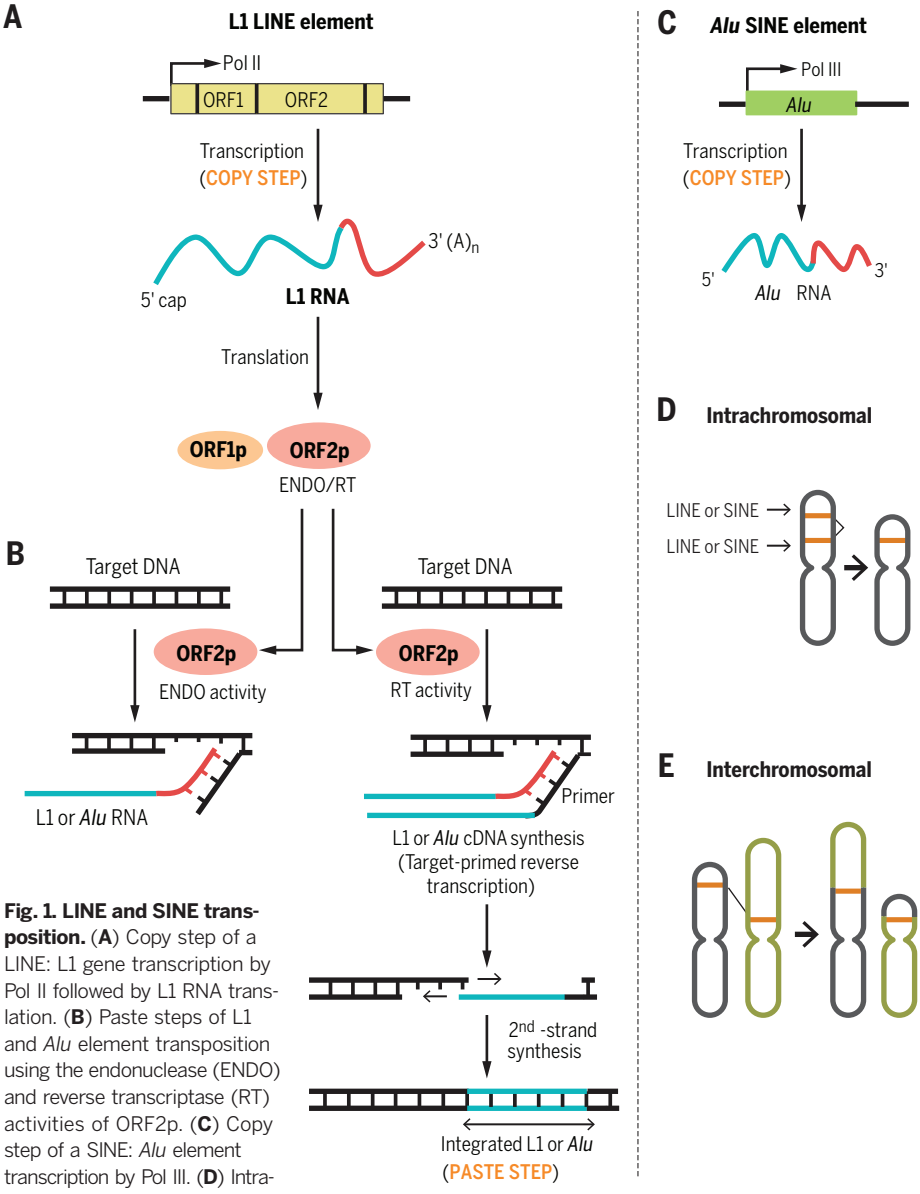

Fig. 1. LINE and SINE transposition. (**A**) Copy step of a LINE: L1 gene transcription by Pol II followed by L1 RNA translation. (**B**) Paste steps of L1 and *Alu* element transposition using the endonuclease (ENDO) and reverse transcriptase (RT) activities of ORF2p. (**C**) Copy step of a SINE: *Alu* element transcription by Pol III. (**D**) Intrachromosomal recombination between related LINEs or SINEs resulting in genomic deletion. (**E**) Interchromosomal recombination between related LINEs or SINEs resulting in genomic rearrangements.

5′-capped transcripts use repetitive sequence-associated TSSs (*27*).

The functional influences of LINEs and SINEs on transcription are mediated not only as DNA elements but also via the RNAs that they encode. SINEs normally are transcriptionally silenced in somatic tissues; however, in response to stressors such as heat shock, SINE Pol III promoters are activated and SINE RNAs are massively up-regulated. Stress-mediated up-regulation of human *Alu* and mouse B2 RNAs inhibits the transcription of most genes, excluding those up-regulated during heat shock, by binding to Pol II (Fig. 2B) (*28*, *29*).

Regulation of RNA processing

Some SINE insertions, in particular *Alu* elements, can influence gene expression by altering pre-mRNA splicing. In humans, 66% of *Alu* elements and 65% of mammalian-wide interspersed repeats (MIRs) are found in introns (*30*). In the antisense orientation, the consensus *Alu* sequence contains seven potential 5′ splice sites and 12 potential 3′ splice sites, whereas sense *Alu* elements contain three potential 5′ splice sites and one potential 3′ splice site (*31*, *32*). *Alu*-derived splice sites are usually cryptic, requiring few mutations to become functional and to promote exonization (i.e., inclusion of a intronic sequence within the resulting spliced mRNA) (Fig. 2C) (*31*). It is estimated that 5% of alternatively spliced exons in humans derive from *Alu* sequences and that most *Alu*-containing exons are alternatively spliced (*32*). Although the majority of exonized *Alu* elements form cassette exons that are included in one or more minor splice isoforms (*30*), in the human brain a substantial portion of *Alu*-containing exons reside in major splice isoforms (*33*). RNA-binding proteins are able to regulate the availability of splice signals within SINEs to associate with the splicing machinery (*34*).

When embedded within Pol II transcripts, the length of *Alu* elements (~300 bp) and their high (>70%) similarity (*14*) allow two elements that coexist in opposite orientation within the same transcript (inverted-repeat *Alu*s or IR*Alu*s) to form intramolecular imperfect duplexes of >100 bp (*35*, *36*). Recently, intronic IR*Alu*s have been shown to promote pre-mRNA "backsplicing" so as to facilitate the formation of circular noncoding RNAs (circRNAs) that may have biological functions (*37*–*39*).

The vast majority of protein-coding mRNAs, as well as many long noncoding RNAs (lncRNAs), are polyadenylated at their 3′ ends. Most polyadenylation occurs upon recognition of a polyadenylation signal (PAS) that consists of the conical AAUAAA sequence or the closely related AUUAAA sequence (*40*). Most human genes harbor more than one PAS that, when used, generate mRNA isoforms with alternative 3′ ends (Fig. 2D) (*41*). New PAS sequences are commonly created via spontaneous mutations within the A-rich tails of LINEs and SINEs (*42*–*44*). Retrotransposon-associated PASs are largely not conserved between different species, which suggests that retrotransposons have contributed to interspecies differences in transcript 3′ ends (*43*). *Alu*-derived PASs, 99% of which derive from sense *Alu* elements, are efficiently used (*43*, *44*). Some of these putative *Alu*-embedded PASs are intronic and result in shortened transcripts, presumably explaining the observed low abundance of sense *Alu* elements relative to antisense *Alu* elements in intronic regions (*44*).

When transcribed as part of mRNA 3′ untranslated regions (3′UTRs), SINEs have the potential to act in cis and/or in trans to influence mRNA turnover. The poly(T) sequence that exists in antisense *Alu* elements is the source of ~40% of identified 3′UTR AU-rich elements (AREs), which regulate mRNA half-life through the competitive binding of proteins that stabilize or destabilize the transcript (Fig. 3A) (*45*). Additionally, LINEs and SINEs can activate the function of microRNAs (miRNAs) by acting as promoters for miRNA synthesis or as miRNA-binding sites in target mRNAs (*46*, *47*) (Fig. 3B); miRNAs are ~22-nucleotide noncoding RNAs that mediate decay and/or translational repression of transcripts to which they bind.

As a consequence of their high similarity and presence in 5.7% of human mRNA 3′UTRs (*27*), *Alu* elements can also mediate intermolecular base pairing between two RNA molecules. For example, *Alu* elements in some human mRNA 3′UTRs can form base pairs with partially complementary, reverse-oriented *Alu* elements in lncRNAs (*48*) or in the 3′UTRs of other mRNAs (Fig. 3C) (*49*). The intermolecular double-stranded RNA (dsRNA) formed, if bound by the dsRNA-binding protein (dsRBP) Staufen 1 (STAU1) and/or its paralog STAU2, can result in mRNA decay in a mechanism that depends on translation (Fig. 3C) (*50*, *51*). This

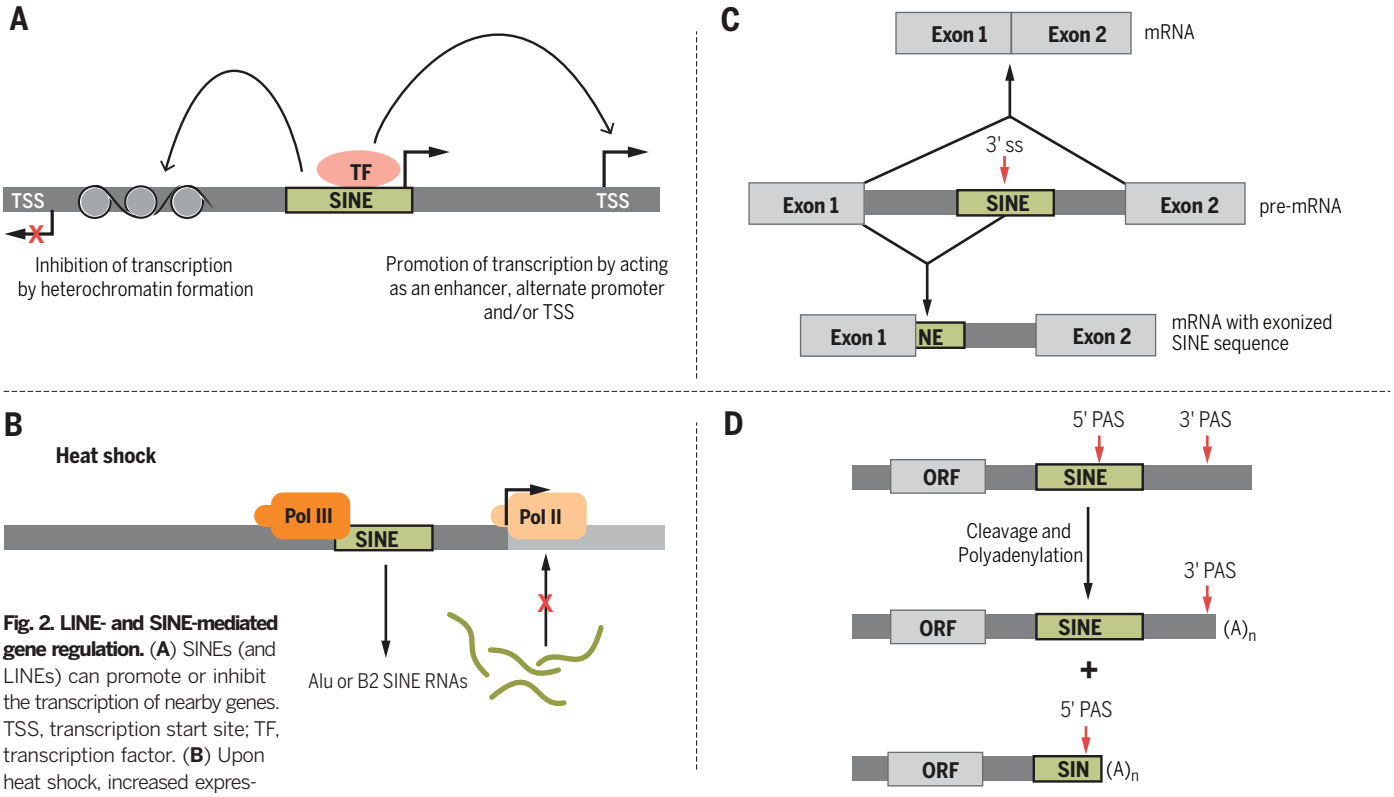

Fig. 2. LINE- and SINE-mediated gene regulation. (**A**) SINEs (and LINEs) can promote or inhibit the transcription of nearby genes. TSS, transcription start site; TF, transcription factor. (**B**) Upon heat shock, increased expression of *Alu* and B2 RNAs inhibits Pol II. (**C**) SINEs contain potential splice sites (ss) that, if used, can lead to mRNAs with intronic sequences. (**D**) SINEs (in particular, *Alu* elements) can contain a polyadenylation signal (PAS).

STAU-mediated mRNA decay (SMD) contributes to cell motility, cell invasion, and other processes (*48*, *49*, *52*). B SINEs and identifier (ID) SINEs in mouse mRNA 3′UTRs can also form duplexes with, respectively, partially complementary B and ID SINEs in lncRNAs (or, most likely, in the 3′UTRs of mRNAs) and likewise trigger SMD so as to regulate cellular processes (*53*). The presence of a 3′UTR *Alu* or B element is not always predictive of SMD (*54*). Both CUB domain–containing protein 1 (CDCP1) mRNA and BCL2-associated athanogene 5 (BAG5) mRNA have a 3′UTR *Alu* element that is predicted to bind the same lncRNA *Alu* element, but only CDCP1 mRNA is an SMD target in HeLa cells (*48*). The features that distinguish a SINE-directed SMD target remain to be determined until more is understood about transcript folding, what defines a STAU-binding site, and how other dsRNA-binding proteins compete with STAU for binding to duplexed SINEs (*48*).

Messenger RNA localization and translation

Not all mRNAs are efficiently exported from the nucleus to the cytoplasm for translation. Some nuclear-retained transcripts contain 3′UTR IR*Alus* (IR*Alus* mRNAs; Fig. 4A) (*55*–*60*) and are localized in paraspeckles (Fig. 4A), which are subnuclear bodies containing the lncRNA *NEAT1* and multiple RNA-binding proteins (*61*). Localization of IR*Alus* mRNAs can be determined by use of alternative PASs, which could exclude the 3′UTR IR*Alus* from product mRNA. STAU1 binding to the 3′UTR IR*Alus* of a subset of IR*Alus* mRNAs precludes the binding of $p54^{nrb}$ (a protein component of paraspeckles), thereby permitting their nuclear export (Fig. 4A) (*57*, *58*). Furthermore, the affinity of dsRBPs for IR*Alus* can be altered by posttranslational modifications. For example, the methylation of $p54^{nrb}$ by the coactivator-associated arginine methyltransferase 1 (CARM1) reduces the binding of $p54^{nrb}$ to the 3′UTR IR*Alus* of particular IR*Alus* mRNAs, promoting their nuclear export (Fig. 4A) (*59*, *60*). Because different mRNAs with apparently similar 3′UTR IR*Alus* manifest distinct subcellular localizations, the regulation of IR*Alus* mRNAs is substantially more complicated than depicted in current models.

In the cytoplasm, 3′UTR IR*Alus* can also repress the translation of their host mRNAs and accelerate their accumulation in stress granules (*57*, *58*, *62*–*64*). A subset of 3′UTR IR*Alus* mediate translational repression by binding and activating dsRNA-dependent protein kinase (PKR) (Fig. 4A), which is activated by autophosphorylation once dimerized on dsRNA. PKR activation results in phosphorylation of eukaryotic translation initiation factor 2α, which in turn inhibits the bulk of cellular translation (*57*, *58*, *64*). Thus, 3′UTR IR*Alus* can act as translational repressors not only in cis but also in trans. STAU1 binding to 3′UTR IR*Alus* in the cytoplasm precludes PKR binding, alleviating translational repression of STAU1-bound IR*Alus* mRNAs and, to a lesser extent, the bulk of cellular mRNAs (Fig. 4A) (*57*, *58*, *64*). During interphase, nuclear-retained IR*Alus* mRNAs are physically segregated away from cytoplasmic PKR, thereby preventing PKR activation (Fig. 4A) (*57*, *58*, *64*). However, after breakdown of the nuclear envelope during mitosis, the boundary between nuclear-retained IR*Alus* mRNAs and cytoplasmic PKR is removed, resulting in PKR activation (Fig. 4B) (*64*). Activated PKR is necessary for the regulation of mitosis because it acts as an upstream kinase for c-Jun N-terminal kinase (JNK), which controls the abundance of multiple mitotic factors (Fig. 4B) (*64*).

SINEs can also enhance mRNA translation in trans. The normally low cellular abundance of Pol III–synthesized *Alu* RNAs transiently increases under stressful conditions that include viral infection, heat shock, and the inhibition of protein synthesis (*65*). Other mammalian SINEs, such as mouse B1 and B2 elements and the rabbit C element, exhibit a similar response, suggesting a common mode of regulation during the stress response (*65*). During heat shock, *Alu* RNAs enhance translation, presumably by sequestering PKR to discrete loci so as to inhibit its activation (*66*). Additionally, transiently introduced *Alu* RNAs in human cells, and B1 and B2 RNAs in mouse cells, selectively enhance the translation of reporter mRNAs independently of PKR without affecting global cell translation (*67*). In mouse

cells, lncRNAs called SINEUPs stimulate the translation of mRNAs with which they form base pairs via 5′-end complementary sequences. Stimulation depends on a B2 element embedded within the SINEUP (*68*).

Influence of A-to-I editing on SINE function

Adenosine-to-inosine (A-to-I) RNA editing is a tissue-specific posttranscriptional process whereby adenosine residues located within dsRNAs are deaminated to inosines by the dsRNA-specific adenosine deaminase (ADAR) proteins (*69*). In primates, IR*Alu*s are the main binding site for ADARs and are subject to editing at multiple sites (Fig. 5) (*35*, *36*, *70*). More than 90% of A-to-I editing in humans occurs within *Alu* elements (*71*–*75*). Multisite A-to-I editing within exonized *Alu* elements are predicted to result in amino acid recoding, because inosines are recognized as guanosines by translating ribosomes (*55*, *76*, *77*). A-to-I editing within intronic IR*Alu*s can generate new splice sites that lead to the exonization of *Alu* elements (Fig. 5A) (*78*). For instance, exonization of the alternatively spliced exon 8 of human nuclear prelamin A recognition factor pre-mRNA results from the A-to-I editing–dependent generation of a functional 3′ splice site within an intronic *Alu* (*78*, *79*). The editing of IR*Alu*s embedded in UTRs is not site-specific and the biological significance is not known. One possible function of UTR-embedded IR*Alu*s is to act as "sponges" that titrate ADAR away from site-specific editing sites within ORFs to prevent amino acid recoding (*55*, *76*, *77*). Because inosine forms base pairs with cytosine, A-to-I editing influences the stability of the IR*Alu*s double-stranded structure by creating mismatches or, less likely, matches (Fig. 5B). Thus, A-to-I editing might change the repertoire of proteins that bind IR*Alu*s and thereby have an impact on the metabolism of transcripts within which IR*Alu*s reside.

A-to-I editing within *Alu* elements might also reprogram the interaction network between miRNAs and their *Alu*-embedded target sites via deactivating or, possibly creating miRNA-binding sites (*80*). Recent profiling of mRNAs that bind the miRNA machinery indicates that the majority of miRNA

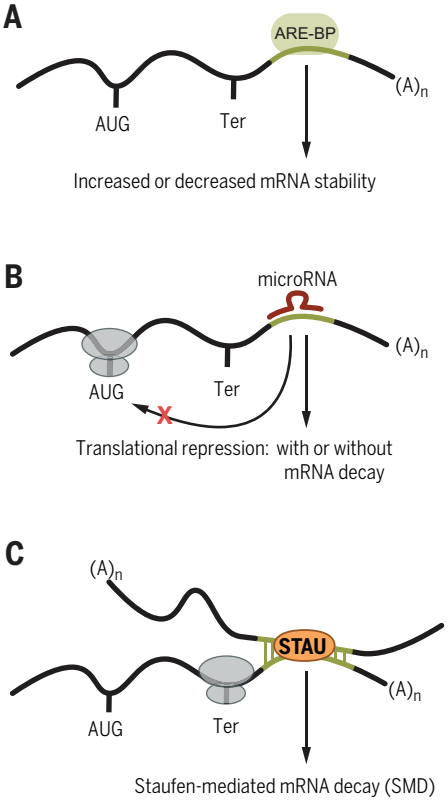

Fig. 3. Effects on mRNA stability by SINE insertions. (**A**) AU-rich element–binding proteins (ARE-BPs) may bind a 3′UTR *Alu* element–derived ARE and either stabilize or destabilize the mRNA. (**B**) *Alu* element–derived microRNA-binding sites within an mRNA can promote mRNA decay and/or inhibit mRNA translation. (**C**) Intermolecular base pairing via partially complementary SINEs can create Staufen-binding sites that trigger Staufen-mediated mRNA decay.

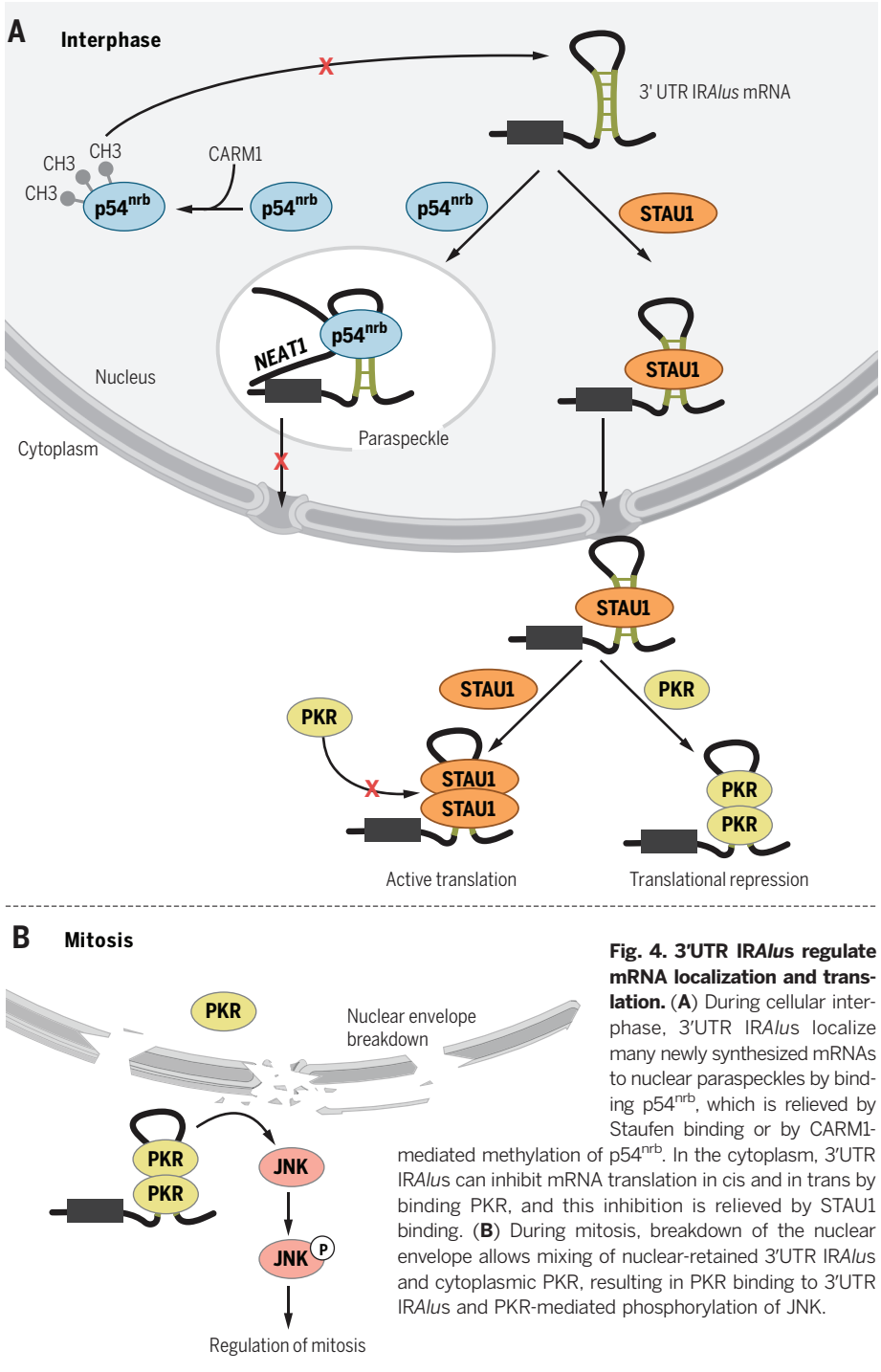

Fig. 4. 3′UTR IR*Alu*s regulate mRNA localization and translation. (**A**) During cellular interphase, 3′UTR IR*Alu*s localize many newly synthesized mRNAs to nuclear paraspeckles by binding p54^{nrb}, which is relieved by Staufen binding or by CARM1-mediated methylation of p54^{nrb}. In the cytoplasm, 3′UTR IR*Alu*s can inhibit mRNA translation in cis and in trans by binding PKR, and this inhibition is relieved by STAU1 binding. (**B**) During mitosis, breakdown of the nuclear envelope allows mixing of nuclear-retained 3′UTR IR*Alu*s and cytoplasmic PKR, resulting in PKR binding to 3′UTR IR*Alu*s and PKR-mediated phosphorylation of JNK.

targets within *Alu* elements are used less than those residing outside of *Alu* elements, presumably because *Alu*-element A-to-I editing and tight secondary structures prevent access to computationally predicted miRNA-binding sites within *Alu* elements (*81*).

Host defense against retrotransposition

Whereas some LINE and SINE insertions regulate gene expression, retrotransposition is necessarily mutagenic with the potential to cause disease. A small minority of L1, *Alu*, and SVA (SINE–variable number of tandem repeats–*Alu*) elements retain functional promoters that enable them to be transcribed and to retrotranspose. *Alu* elements are currently the most active retrotransposon in the human germ line, manifesting an estimated insertion rate of 1 in 20 live births (*82*). The estimated L1 insertion rate is 1 in 20 to 1 in 200 live births; the estimated SVA insertion rate is 1 in 900 live births (*3*). Germline insertions have been implicated in ~100 genetic diseases (Table 1) (*83*, *84*) and insertion events in somatic tissues, although not heritable, also have the potential to cause disease (*20*, *85*). Indeed, ongoing retrotransposition that results from the removal of inhibitory methylation marks on LINE and SINE promoters is a hallmark of many cancers (*86*) and also typifies neurological disorders, including schizophrenia (*87*) and Rhett syndrome (*88*).

Organisms have developed various mechanisms to protect their genomes from the deleterious effects of retrotransposon insertions [reviewed in (*89*, *90*)]. Transcriptional silencing of retrotransposons by DNA methylation has been described as a major host defense mechanism in mammals (*89*, *90*). However, recent evidence suggests that histone methylation, rather than DNA methylation, is the predominant suppressor of SINE transcription in human and mouse cells (*91*). Mammalian cells have also developed an arsenal of sequence-specific RNA degradation mechanisms to eliminate retrotransposon transcripts once produced. Endogenous small interfering RNAs (endo-siRNAs) or PIWI-interacting RNAs (piRNAs) can initiate degradation of LINE and SINE RNAs (*92*–*96*). Microprocessor, a nuclear complex of miRNA-processing enzymes, also recognizes and cleaves L1, *Alu*, and SVA transcripts, at least in vitro (*97*). The finding that L1 and *Alu* RNAs are enclosed within human cell autophagosomes has implicated autophagy (i.e., the delivery

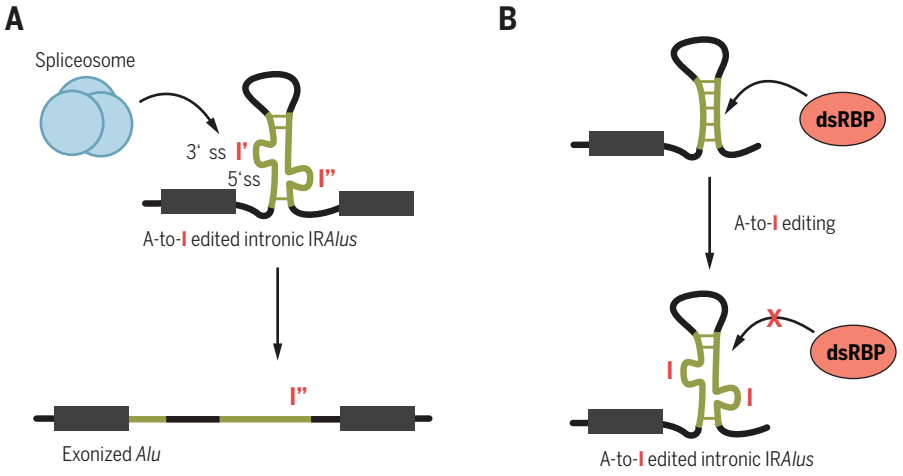

Fig. 5. The roles of A-to-I editing of IR*Alu*s. (**A**) Edited intronic IR*Alu*s can create a new splice site. (**B**) Editing in IR*Alu*s might destabilize their dsRNA structure and reduce dsRBP binding.

Table 1. Some human diseases linked to LINE and SINE insertions. The extensive role of LINEs and SINEs in the regulation of human gene expression suggests that they contribute to disease in as yet undiscovered ways.

Effect of LINE or SINE insertion	Possible mechanism(s) of pathogenesis	Examples of associated diseases	Reference
Genomic deletions and rearrangements	LINE/SINE-mediated homologous recombination: DNA sequence loss; genomic instability	Prostate cancer, pyruvate dehydrogenase complex deficiency, leukemia, Alport syndrome, breast cancer	(*83*)
		Hereditary nonpolyposis colorectal cancer, Von Hippel–Lindau disease	(*86*)
Disruption of protein-coding sequences	Aberrant protein production; nonsense-mediated mRNA decay (NMD)	Hemophilia B, breast cancer, colon cancer, neurofibromatosis type 1	(*83*)
Altered DNA methylation	Increased expression of LINE and SINE RNA	Early event in many cancers	(*86*)
Altered pre-mRNA splicing	Aberrant protein production; NMD	Fukuyama-type congenital muscular dystrophy, neurofibromatosis type 1, hemophilia A	(*83*)
		Neurofibromatosis type 1, hemophilia A, breast cancer, Coffin-Lowry syndrome	(*84*)
Altered 3′-end formation	Premature transcription termination; altered protein production; NMD; altered mRNA stability, localization, or translatability	X-linked retinitis pigmentosa	(*83*)
Altered mRNA stability	Reduced protein production; altered temporal and/or spatial gene expression	X-linked dilated cardiomyopathy	(*83*)
		Hemophilia A, hereditary nonpolyposis colorectal cancer, hyper–immunoglobulin M syndrome	(*84*)
Sites of A-to-I editing	Loss of ADAR editing of target sites, possibly at *Alu* elements	Amyotrophic lateral sclerosis (ALS), astrocytoma, metastatic melanoma, Aicardi-Goutières syndrome, hepatocellular carcinoma	(*100*)

of cytosolic constituents to the lysosome) as another host defense mechanism that degrades retrotransposon RNAs (*98*). Indeed, mice lacking the critical autophagy gene, Atg6/Beclin1, are characterized by higher levels of retrotransposon RNAs and increased rates of genomic insertions (*98*). Additionally, retrotransposition is restricted in both somatic and germ cells by members of the apolipoprotein B mRNA-editing enzyme 3 (APOBEC3) family (*89*, *99*).

Conclusions

Here we have focused on the functions of human and mouse LINEs and SINEs. However, the prevalence of LINEs and SINEs in other organisms, and known examples whereby evolutionarily unrelated human and mouse SINEs have been exapted for similar functions, leads us to propose that at least some of the LINEs and SINEs found in many organisms are likely to be used analogously as regulatory elements. In addition to their exaptation as functional sequences, the recent discovery that LINEs and SINEs are actively retrotransposing in somatic tissues (including brain) and the myriad of potential consequences of LINE and SINE insertions implicate LINEs and SINEs in the molecular pathogenesis of acquired diseases, including diseases of aging.

REFERENCES AND NOTES

1. C. R. L. Huang, K. H. Burns, J. D. Boeke, Active transposition in genomes. *Annu. Rev. Genet.* **46**, 651–675 (2012). doi: 10.1146/annurev-genet-110711-155616; pmid: 23145912
2. T. Wicker *et al*., A unified classification system for eukaryotic transposable elements. *Nat. Rev. Genet.* **8**, 973–982 (2007). doi: 10.1038/nrg2165; pmid: 17984973
3. C. R. Beck, J. L. García-Perez, R. M. Badge, J. V. Moran, LINE-1 elements in structural variation and disease. *Annu. Rev. Genomics Hum. Genet.* **12**, 187–215 (2011). doi: 10.1146/annurev-genom-082509-141802; pmid: 21801021
4. E. N. Kroutter, V. P. Belancio, B. J. Wagstaff, A. M. Roy-Engel, The RNA polymerase dictates ORF1 requirement and timing of LINE and SINE retrotransposition. *PLOS Genet.* **5**, e1000458 (2009). doi: 10.1371/journal.pgen.1000458; pmid: 19390602
5. E. M. Ostertag, H. H. Kazazian Jr., Biology of mammalian L1 retrotransposons. *Annu. Rev. Genet.* **35**, 501–538 (2001). doi: 10.1146/annurev.genet.35.102401.091032; pmid: 11700292
6. D. D. Luan, M. H. Korman, J. L. Jakubczak, T. H. Eickbush, Reverse transcription of R2Bm RNA is primed by a nick at the chromosomal target site: A mechanism for non-LTR retrotransposition. *Cell* **72**, 595–605 (1993). doi: 10.1016/0092-8674(93)90078-5; pmid: 7679954
7. A. M. Denli *et al*., Primate-specific ORF0 contributes to retrotransposon-mediated diversity. *Cell* **163**, 583–593 (2015). doi: 10.1016/j.cell.2015.09.025; pmid: 26496605
8. M. Dewannieux, C. Esnault, T. Heidmann, LINE-mediated retrotransposition of marked Alu sequences. *Nat. Genet.* **35**, 41–48 (2003). doi: 10.1038/ng1223; pmid: 12897783
9. D. A. Kramerov, N. S. Vassetzky, Origin and evolution of SINEs in eukaryotic genomes. *Heredity* **107**, 487–495 (2011). doi: 10.1038/hdy.2011.43; pmid: 21673742
10. V. V. Kapitonov, J. Jurka, A novel class of SINE elements derived from 5S rRNA. *Mol. Biol. Evol.* **20**, 694–702 (2003). doi: 10.1093/molbev/msg075; pmid: 12679554
11. E. S. Lander *et al*., Initial sequencing and analysis of the human genome. *Nature* **409**, 860–921 (2001). doi: 10.1038/35057062; pmid: 11237011
12. P. Medstrand, L. N. van de Lagemaat, D. L. Mager, Retroelement distributions in the human genome: Variations associated with age and proximity to genes. *Genome Res.* **12**, 1483–1495 (2002). doi: 10.1101/gr.388902; pmid: 12368240
13. C. Feschotte, Transposable elements and the evolution of regulatory networks. *Nat. Rev. Genet.* **9**, 397–405 (2008). doi: 10.1038/nrg2337; pmid: 18368054
14. S. K. Sen *et al*., Human genomic deletions mediated by recombination between Alu elements. *Am. J. Hum. Genet.* **79**, 41–53 (2006). doi: 10.1086/504600; pmid: 16773564
15. C. Esnault, J. Maestre, T. Heidmann, Human LINE retrotransposons generate processed pseudogenes. *Nat. Genet.* **24**, 363–367 (2000). doi: 10.1038/74184; pmid: 10742098
16. H. Kaessmann, N. Vinckenbosch, M. Long, RNA-based gene duplication: Mechanistic and evolutionary insights. *Nat. Rev. Genet.* **10**, 19–31 (2009). doi: 10.1038/nrg2487; pmid: 19030023
17. H. Kano *et al*., L1 retrotransposition occurs mainly in embryogenesis and creates somatic mosaicism. *Genes Dev.* **23**, 1303–1312 (2009). doi: 10.1101/gad.1803909; pmid: 19487571
18. A. R. Muotri *et al*., Somatic mosaicism in neuronal precursor cells mediated by L1 retrotransposition. *Nature* **435**, 903–910 (2005). doi: 10.1038/nature03663; pmid: 15959507
19. N. G. Coufal *et al*., L1 retrotransposition in human neural progenitor cells. *Nature* **460**, 1127–1131 (2009). doi: 10.1038/nature08248; pmid: 19657334
20. J. K. Baillie *et al*., Somatic retrotransposition alters the genetic landscape of the human brain. *Nature* **479**, 534–537 (2011). doi: 10.1038/nature10531; pmid: 22037309
21. K. Ichiyanagi, Epigenetic regulation of transcription and possible functions of mammalian short interspersed elements, SINEs. *Genes Genet. Syst.* **88**, 19–29 (2013). doi: 10.1266/ggs.88.19; pmid: 23676707
22. M. R. H. Estécio *et al*., SINE retrotransposons cause epigenetic reprogramming of adjacent gene promoters. *Mol. Cancer Res.* **10**, 1332–1342 (2012). doi: 10.1158/1541-7786.MCR-12-0351; pmid: 22952045
23. V. V. Lunyak *et al*., Developmentally regulated activation of a SINE B2 repeat as a domain boundary in organogenesis. *Science* **317**, 248–251 (2007). doi: 10.1126/science.1140871; pmid: 17626886
24. J. C. Chow *et al*., LINE-1 activity in facultative heterochromatin formation during X chromosome inactivation. *Cell* **141**, 956–969 (2010). doi: 10.1016/j.cell.2010.04.042; pmid: 20550932
25. T. Sasaki *et al*., Possible involvement of SINEs in mammalian-specific brain formation. *Proc. Natl. Acad. Sci. U.S.A.* **105**, 4220–4225 (2008). doi: 10.1073/pnas.0709398105; pmid: 18334644
26. K. Tashiro *et al*., A mammalian conserved element derived from SINE displays enhancer properties recapitulating Satb2 expression in early-born callosal projection neurons. *PLOS ONE* **6**, e28497 (2011). doi: 10.1371/journal.pone.0028497; pmid: 22174821
27. G. J. Faulkner *et al*., The regulated retrotransposon transcriptome of mammalian cells. *Nat. Genet.* **41**, 563–571 (2009). doi: 10.1038/ng.368; pmid: 19377475
28. P. D. Mariner *et al*., Human Alu RNA is a modular transacting repressor of mRNA transcription during heat shock. *Mol. Cell* **29**, 499–509 (2008). doi: 10.1016/j.molcel.2007.12.013; pmid: 18313387
29. T. A. Allen, S. Von Kaenel, J. A. Goodrich, J. F. Kugel, The SINE-encoded mouse B2 RNA represses mRNA transcription in response to heat shock. *Nat. Struct. Mol. Biol.* **11**, 816–821 (2004). doi: 10.1038/nsmb813; pmid: 15300240
30. N. Sela *et al*., Comparative analysis of transposed element insertion within human and mouse genomes reveals Alu's unique role in shaping the human transcriptome. *Genome Biol.* **8**, R127 (2007). doi: 10.1186/gb-2007-8-6-r127; pmid: 17594509
31. G. Lev-Maor, R. Sorek, N. Shomron, G. Ast, The birth of an alternatively spliced exon: 3′ splice-site selection in Alu exons. *Science* **300**, 1288–1291 (2003). doi: 10.1126/science.1082588; pmid: 12764196
32. R. Sorek, G. Ast, D. Graur, Alu-containing exons are alternatively spliced. *Genome Res.* **12**, 1060–1067 (2002). doi: 10.1101/gr.229302; pmid: 12097342
33. S. Shen *et al*., Widespread establishment and regulatory impact of Alu exons in human genes. *Proc. Natl. Acad. Sci. U.S.A.* **108**, 2837–2842 (2011). doi: 10.1073/pnas.1012834108; pmid: 21282640
34. K. Zarnack *et al*., Direct competition between hnRNP C and U2AF65 protects the transcriptome from the exonization of Alu elements. *Cell* **152**, 453–466 (2013). doi: 10.1016/j.cell.2012.12.023; pmid: 23374342
35. B. L. Bass, RNA editing by adenosine deaminases that act on RNA. *Annu. Rev. Biochem.* **71**, 817–846 (2002). doi: 10.1146/annurev.biochem.71.110601.135501; pmid: 12045112
36. P. Deininger, Alu elements: Know the SINEs. *Genome Biol.* **12**, 236 (2011). doi: 10.1186/gb-2011-12-12-236; pmid: 22204421
37. W. R. Jeck *et al*., Circular RNAs are abundant, conserved, and associated with ALU repeats. *RNA* **19**, 141–157 (2013). doi: 10.1261/rna.035667.112; pmid: 23249747
38. X.-O. Zhang *et al*., Complementary sequence-mediated exon circularization. *Cell* **159**, 134–147 (2014). doi: 10.1016/j.cell.2014.09.001; pmid: 25242744
39. D. Liang, J. E. Wilusz, Short intronic repeat sequences facilitate circular RNA production. *Genes Dev.* **28**, 2233–2247 (2014). doi: 10.1101/gad.251926.114; pmid: 25281217
40. E. Beaudoing, S. Freier, J. R. Wyatt, J. M. Claverie, D. Gautheret, Patterns of variant polyadenylation signal usage in human genes. *Genome Res.* **10**, 1001–1010 (2000). doi: 10.1101/gr.10.7.1001; pmid: 10899149
41. R. Elkon, A. P. Ugalde, R. Agami, Alternative cleavage and polyadenylation: Extent, regulation and function. *Nat. Rev. Genet.* **14**, 496–506 (2013). doi: 10.1038/nrg3482; pmid: 23774734
42. A. M. Roy-Engel *et al*., Human retroelements may introduce intragenic polyadenylation signals. *Cytogenet. Genome Res.* **110**, 365–371 (2005). doi: 10.1159/000084968; pmid: 16093688
43. J. Y. Lee, Z. Ji, B. Tian, Phylogenetic analysis of mRNA polyadenylation sites reveals a role of transposable elements in evolution of the 3′-end of genes. *Nucleic Acids Res.* **36**, 5581–5590 (2008). doi: 10.1093/nar/gkn540; pmid: 18757892
44. C. Chen, T. Ara, D. Gautheret, Using Alu elements as polyadenylation sites: A case of retroposon exaptation. *Mol. Biol. Evol.* **26**, 327–334 (2009). doi: 10.1093/molbev/msn249; pmid: 18984903
45. H. J. An, D. Lee, K. H. Lee, J. Bhak, The association of Alu repeats with the generation of potential AU-rich elements (ARE) at 3′ untranslated regions. *BMC Genomics* **5**, 97 (2004). doi: 10.1186/1471-2164-5-97; pmid: 15610565
46. J. Piriyapongsa, L. Mariño-Ramírez, I. K. Jordan, Origin and evolution of human microRNAs from transposable elements. *Genetics* **176**, 1323–1337 (2007). doi: 10.1534/genetics.107.072553; pmid: 17435244
47. S. Lehnert *et al*., Evidence for co-evolution between human microRNAs and Alu-repeats. *PLOS ONE* **4**, e4456 (2009). doi: 10.1371/journal.pone.0004456; pmid: 19209240
48. C. Gong, L. E. Maquat, lncRNAs transactivate STAU1-mediated mRNA decay by duplexing with 3′ UTRs via Alu elements. *Nature* **470**, 284–288 (2011). doi: 10.1038/nature09701; pmid: 21307942
49. C. Gong, Y. Tang, L. E. Maquat, mRNA-mRNA duplexes that autoelicit Staufen1-mediated mRNA decay. *Nat. Struct. Mol. Biol.* **20**, 1214–1220 (2013). doi: 10.1038/nsmb.2664; pmid: 24056942
50. M. L. Gleghorn, C. Gong, C. L. Kielkopf, L. E. Maquat, Staufen1 dimerizes through a conserved motif and a degenerate dsRNA-binding domain to promote mRNA decay. *Nat. Struct. Mol. Biol.* **20**, 515–524 (2013). doi: 10.1038/nsmb.2528; pmid: 23524536
51. E. Park, M. L. Gleghorn, L. E. Maquat, Staufen2 functions in Staufen1-mediated mRNA decay by binding to itself and its paralog and promoting UPF1 helicase but not ATPase activity. *Proc. Natl. Acad. Sci. U.S.A.* **110**, 405–412 (2013). doi: 10.1073/pnas.1213508110; pmid: 23263869
52. C. Gong, L. E. Maquat, "Alu"strious long ncRNAs and their role in shortening mRNA half-lives. *Cell Cycle* **10**, 1882–1883 (2011). doi: 10.4161/cc.10.12.15589; pmid: 21487233
53. J. Wang, C. Gong, L. E. Maquat, Control of myogenesis by rodent SINE-containing lncRNAs. *Genes Dev.* **27**, 793–804 (2013). doi: 10.1101/gad.212639.112; pmid: 23558772
54. C. Gong, M. W.-L. Popp, L. E. Maquat, Biochemical analysis of long non-coding RNA-containing ribonucleoprotein complexes. *Methods* **58**, 88–93 (2012). doi: 10.1016/j.ymeth.2012.06.020; pmid: 22789663
55. L.-L. Chen, G. G. Carmichael, Gene regulation by SINES and inosines: Biological consequences of A-to-I editing of Alu element inverted repeats. *Cell Cycle* **7**, 3294–3301 (2008). doi: 10.4161/cc.7.21.6927; pmid: 18948735
56. L.-L. Chen, J. N. DeCerbo, G. G. Carmichael, Alu element-mediated gene silencing. *EMBO J.* **27**, 1694–1705 (2008). doi: 10.1038/emboj.2008.94; pmid: 18497743
57. R. A. Elbarbary, W. Li, B. Tian, L. E. Maquat, STAU1 binding 3′ UTR IRAlus complements nuclear retention to protect cells from PKR-mediated translational shutdown. *Genes Dev.* **27**, 1495–1510 (2013). doi: 10.1101/gad.220962.113; pmid: 23824540

58. R. A. Elbarbary, L. E. Maquat, Dodging two bullets with one dsRNA-binding protein. *Cell Cycle* **13**, 345–346 (2014). doi: 10.4161/cc.27512; pmid: 24335473
59. S.-B. Hu *et al*., Protein arginine methyltransferase CARM1 attenuates the paraspeckle-mediated nuclear retention of mRNAs containing IRAlus. *Genes Dev.* **29**, 630–645 (2015). doi: 10.1101/gad.257048.114; pmid: 25792598
60. R. A. Elbarbary, L. E. Maquat, CARMing down the SINEs of anarchy: Two paths to freedom from paraspeckle detention. *Genes Dev.* **29**, 687–689 (2015). doi: 10.1101/gad.261438.115; pmid: 25838539
61. A. H. Fox *et al*., Paraspeckles: A novel nuclear domain. *Curr. Biol.* **12**, 13–25 (2002). doi: 10.1016/S0960-9822(01)00632-7; pmid: 11790299
62. C. R. Capshew, K. L. Dusenbury, H. A. Hundley, Inverted Alu dsRNA structures do not affect localization but can alter translation efficiency of human mRNAs independent of RNA editing. *Nucleic Acids Res.* **40**, 8637–8645 (2012). doi: 10.1093/nar/gks590; pmid: 22735697
63. T. Fitzpatrick, S. Huang, 3′-UTR-located inverted Alu repeats facilitate mRNA translational repression and stress granule accumulation. *Nucleus* **3**, 359–369 (2012). doi: 10.4161/nucl.20827; pmid: 22688648
64. Y. Kim *et al*., PKR is activated by cellular dsRNAs during mitosis and acts as a mitotic regulator. *Genes Dev.* **28**, 1310–1322 (2014). doi: 10.1101/gad.242644.114; pmid: 24939934
65. W. M. Liu, W. M. Chu, P. V. Choudary, C. W. Schmid, Cell stress and translational inhibitors transiently increase the abundance of mammalian SINE transcripts. *Nucleic Acids Res.* **23**, 1758–1765 (1995). doi: 10.1093/nar/23.10.1758; pmid: 7784180
66. W. M. Chu, R. Ballard, B. W. Carpick, B. R. Williams, C. W. Schmid, Potential Alu function: Regulation of the activity of double-stranded RNA-activated kinase PKR. *Mol. Cell. Biol.* **18**, 58–68 (1998). doi: 10.1128/MCB.18.1.58; pmid: 9418853
67. C. M. Rubin, R. H. Kimura, C. W. Schmid, Selective stimulation of translational expression by Alu RNA. *Nucleic Acids Res.* **30**, 3253–3261 (2002). doi: 10.1093/nar/gkf419; pmid: 12136107
68. C. Carrieri *et al*., Long non-coding antisense RNA controls Uchl1 translation through an embedded SINEB2 repeat. *Nature* **491**, 454–457 (2012). doi: 10.1038/nature11508; pmid: 23064229
69. Y. A. Savva, L. E. Rieder, R. A. Reenan, The ADAR protein family. *Genome Biol.* **13**, 252 (2012). doi: 10.1186/gb-2012-13-12-252; pmid: 23273215
70. E. Eisenberg *et al*., Is abundant A-to-I RNA editing primate-specific? *Trends Genet.* **21**, 77–81 (2005). doi: 10.1016/j.tig.2004.12.005; pmid: 15661352
71. A. Athanasiadis, A. Rich, S. Maas, Widespread A-to-I RNA editing of Alu-containing mRNAs in the human transcriptome. *PLOS Biol.* **2**, e391 (2004). doi: 10.1371/journal.pbio.0020391; pmid: 15534692
72. M. Blow, P. A. Futreal, R. Wooster, M. R. Stratton, A survey of RNA editing in human brain. *Genome Res.* **14**, 2379–2387 (2004). doi: 10.1101/gr.2951204; pmid: 15545495
73. D. D. Y. Kim *et al*., Widespread RNA editing of embedded alu elements in the human transcriptome. *Genome Res.* **14**, 1719–1725 (2004). doi: 10.1101/gr.2855504; pmid: 15342557
74. E. Y. Levanon *et al*., Systematic identification of abundant A-to-I editing sites in the human transcriptome. *Nat. Biotechnol.* **22**, 1001–1005 (2004). doi: 10.1038/nbt996; pmid: 15258596
75. D. P. Morse, P. J. Aruscavage, B. L. Bass, RNA hairpins in noncoding regions of human brain and *Caenorhabditis elegans* mRNA are edited by adenosine deaminases that act on RNA. *Proc. Natl. Acad. Sci. U.S.A.* **99**, 7906–7911 (2002). doi: 10.1038/nn.3539; pmid: 24165678
76. J. B. Li, G. M. Church, Deciphering the functions and regulation of brain-enriched A-to-I RNA editing. *Nat. Neurosci.* **16**, 1518–1522 (2013). doi: 10.1038/nn.3539; pmid: 24165678
77. A. Mallela, K. Nishikura, A-to-I editing of protein coding and noncoding RNAs. *Crit. Rev. Biochem. Mol. Biol.* **47**, 493–501 (2012). doi: 10.3109/10409238.2012.714350; pmid: 22988838
78. G. Lev-Maor *et al*., RNA-editing-mediated exon evolution. *Genome Biol.* **8**, R29 (2007). doi: 10.1186/gb-2007-8-2-r29; pmid: 17326827
79. M. Möller-Krull, A. Zemann, C. Roos, J. Brosius, J. Schmitz, Beyond DNA: RNA editing and steps toward Alu exonization in primates. *J. Mol. Biol.* **382**, 601–609 (2008). doi: 10.1016/j.jmb.2008.07.014; pmid: 18680752
80. G. M. Borchert *et al*., Adenosine deamination in human transcripts generates novel microRNA binding sites. *Hum. Mol. Genet.* **18**, 4801–4807 (2009). doi: 10.1093/hmg/ddp443; pmid: 19776031
81. Y. Hoffman, D. Dahary, D. R. Bublik, M. Oren, Y. Pilpel, The majority of endogenous microRNA targets within Alu elements avoid the microRNA machinery. *Bioinformatics* **29**, 894–902 (2013). doi: 10.1093/bioinformatics/btt044; pmid: 23361327
82. R. Cordaux, D. J. Hedges, S. W. Herke, M. A. Batzer, Estimating the retrotransposition rate of human Alu elements. *Gene* **373**, 134–137 (2006). doi: 10.1016/j.gene.2006.01.019; pmid: 16522357
83. D. C. Hancks, H. H. Kazazian Jr., Active human retrotransposons: Variation and disease. *Curr. Opin. Genet. Dev.* **22**, 191–203 (2012). doi: 10.1016/j.gde.2012.02.006; pmid: 22406018
84. K. Kaer, M. Speek, Retroelements in human disease. *Gene* **518**, 231–241 (2013). doi: 10.1016/j.gene.2013.01.008; pmid: 23333607
85. E. Helman *et al*., Somatic retrotransposition in human cancer revealed by whole-genome and exome sequencing. *Genome Res.* **24**, 1053–1063 (2014). doi: 10.1101/gr.163659.113; pmid: 24823667
86. V. P. Belancio, A. M. Roy-Engel, P. L. Deininger, All y'all need to know 'bout retroelements in cancer. *Semin. Cancer Biol.* **20**, 200–210 (2010). doi: 10.1016/j.semcancer.2010.06.001; pmid: 20600922
87. M. Bundo *et al*., Increased L1 retrotransposition in the neuronal genome in schizophrenia. *Neuron* **81**, 306–313 (2014). doi: 10.1016/j.neuron.2013.10.053; pmid: 24389010
88. A. R. Muotri *et al*., L1 retrotransposition in neurons is modulated by MeCP2. *Nature* **468**, 443–446 (2010). doi: 10.1038/nature09544; pmid: 21085180
89. H. L. Levin, J. V. Moran, Dynamic interactions between transposable elements and their hosts. *Nat. Rev. Genet.* **12**, 615–627 (2011). doi: 10.1038/nrg3030; pmid: 21850042
90. J. H. Crichton, D. S. Dunican, M. Maclennan, R. R. Meehan, I. R. Adams, Defending the genome from the enemy within: Mechanisms of retrotransposon suppression in the mouse germline. *Cell. Mol. Life Sci.* **71**, 1581–1605 (2014). doi: 10.1007/s00018-013-1468-0; pmid: 24045705
91. D. Varshney *et al*., SINE transcription by RNA polymerase III is suppressed by histone methylation but not by DNA methylation. *Nat. Commun.* **6**, 6569 (2015). doi: 10.1007/s00018-013-1468-0; pmid: 24045705
92. H. Ishizu, H. Siomi, M. C. Siomi, Biology of PIWI-interacting RNAs: New insights into biogenesis and function inside and outside of germlines. *Genes Dev.* **26**, 2361–2373 (2012). doi: 10.1101/gad.203786.112; pmid: 23124062
93. E.-M. Weick, E. A. Miska, piRNAs: From biogenesis to function. *Development* **141**, 3458–3471 (2014). doi: 10.1242/dev.094037; pmid: 25183868
94. J. M. Claycomb, Ancient endo-siRNA pathways reveal new tricks. *Curr. Biol.* **24**, R703–R715 (2014). doi: 10.1016/j.cub.2014.06.009; pmid: 25093565
95. M. J. Piatek, A. Werner, Endogenous siRNAs: Regulators of internal affairs. *Biochem. Soc. Trans.* **42**, 1174–1179 (2014). doi: 10.1042/BST20140068; pmid: 25110021
96. A. A. Aravin, G. J. Hannon, Small RNA silencing pathways in germ and stem cells. *Cold Spring Harb. Symp. Quant. Biol.* **73**, 283–290 (2008). doi: 10.1101/sqb.2008.73.058; pmid: 19270082
97. S. R. Heras *et al*., The Microprocessor controls the activity of mammalian retrotransposons. *Nat. Struct. Mol. Biol.* **20**, 1173–1181 (2013). doi: 10.1038/nsmb.2658; pmid: 23995758
98. H. Guo *et al*., Autophagy supports genomic stability by degrading retrotransposon RNA. *Nat. Commun.* **5**, 5276 (2014). doi: 10.1038/ncomms6276; pmid: 25366815
99. J. F. Arias, T. Koyama, M. Kinomoto, K. Tokunaga, Retroelements versus APOBEC3 family members: No great escape from the magnificent seven. *Front. Microbiol.* **3**, 275 (2012). doi: 10.3389/fmicb.2012.00275; pmid: 22912627
100. W. Slotkin, K. Nishikura, Adenosine-to-inosine RNA editing and human disease. *Genome Med.* **5**, 105 (2013). pmid: 24289319

ACKNOWLEDGMENTS

We thank T. Eickbush, X. Li, and M. Popp for critically reading the manuscript. We apologize to our colleagues whose work we were unable to include because of space restrictions. Research on SINEs in the Maquat lab is supported by NIH grant R37 GM074593 (L.E.M.). R.A.E. is supported by NIH Pilot Award P30 AR061307.

10.1126/science.aac7247

Science
AAAS

Retrotransposons as regulators of gene expression
Reyad A. Elbarbary *et al.*
Science **351**, (2016);
DOI: 10.1126/science.aac7247

This copy is for your personal, non-commercial use only.

If you wish to distribute this article to others, you can order high-quality copies for your colleagues, clients, or customers by clicking here.

Permission to republish or repurpose articles or portions of articles can be obtained by following the guidelines here.

The following resources related to this article are available online at www.sciencemag.org (this information is current as of February 11, 2016):

Updated information and services, including high-resolution figures, can be found in the online version of this article at:
/content/351/6274/aac7247.full.html

This article **cites 98 articles**, 34 of which can be accessed free:
/content/351/6274/aac7247.full.html#ref-list-1

This article appears in the following **subject collections:**
Molecular Biology
/cgi/collection/molec_biol

Downloaded from on February 11, 2016

Science (print ISSN 0036-8075; online ISSN 1095-9203) is published weekly, except the last week in December, by the American Association for the Advancement of Science, 1200 New York Avenue NW, Washington, DC 20005. Copyright 2016 by the American Association for the Advancement of Science; all rights reserved. The title *Science* is a registered trademark of AAAS.

RESEARCH ARTICLE SUMMARY

GENE REGULATION

Lineage-specific enhancers activate self-renewal genes in macrophages and embryonic stem cells

Erinn L. Soucie,*† Ziming Weng,† Laufey Geirsdóttir,† Kaaweh Molawi,† Julien Maurizio, Romain Fenouil, Noushine Mossadegh-Keller, Gregory Gimenez, Laurent VanHille, Meryam Beniazza, Jeremy Favret, Carole Berruyer, Pierre Perrin, Nir Hacohen, J.-C. Andrau, Pierre Ferrier, Patrice Dubreuil, Arend Sidow,* Michael H. Sieweke*

INTRODUCTION: In many organs of the body, differentiated cells are frequently lost and need to be replaced as part of normal homeostatic tissue maintenance or in response to injury. In most cases, this regeneration is assured by differentiation from tissue-specific stem cells. Together with a few other cell types, tissue macrophages represent a rare exception to this pathway, as they can be maintained independently of blood stem cells by local proliferation. Under certain conditions, mature macrophages can also be expanded and maintained long term in culture without transformation or loss of differentiation status. The gene regulatory mechanisms that allow such differentiated cells to self-renew while maintaining cell type–specific identity have so far remained unknown. Self-renewing macrophages provide a rare opportunity to study this question.

RATIONALE: Molecularly, cell identity can be defined by the genomic positions of gene regulatory enhancer elements. The cell type–specific signatures and activity status of such elements have been characterized by the analysis of specific histone modifications and the binding of regulatory proteins. To identify the regulatory mechanisms that enable macrophage self-renewal capacity to be integrated into the overall program of epigenetic macrophage identity, we have compared the enhancer repertoires of quiescent and self-renewing macrophages. Based on our previous observations that deletion of MafB and c-Maf transcription factors results in an extended self-renewal capacity of macrophages, we further investigated how the absence of Maf transcription factors affects the enhancers of specific self-renewal genes and how these mechanisms activate macrophage self-renewal under homeostatic and challenge conditions in vivo.

RESULTS: Compared to quiescent macrophages, self-renewing macrophages showed no appreciable difference with respect to genome-wide enhancer positions but displayed an increase in the activation status of many enhancers that were also bound by the lineage-specifying transcription factor PU.1 in both cell types. This finding suggests that these poised macrophage-specific enhancers became active in self-renewing macrophages. We found activated enhancers to be associated with a network of genes, centered on *Myc* and *Klf2*, that were up-regulated and functionally important for self-renewal in these cells. The same genes were also required for embryonic stem (ES) cell self-renewal but were associated with a distinct, ES cell–specific set of enhancers. We observed that activated self-renewal–associated macrophage enhancers were directly repressed by MafB binding. The loss of MafB and c-Maf expression relieved this repression and led to activation of the self-renewal gene network in MafB and cMaf knockout macrophages, as well as in alveolar macrophages that express constitutively low levels of these transcription factors. In vivo single-cell analysis further revealed that, both in the steady state and in response to immune stimulation, proliferating resident macrophages could access this network by transient down-regulation of Maf transcription factors.

ON OUR WEB SITE

Read the full article at http://dx.doi.org/10.1126/science.aad5510

CONCLUSION: Our results demonstrate that self-renewal in macrophages involves down-regulation of MafB and cMaf, as well as concomitant activation of a self-renewal gene network shared with ES cells but controlled from cell type–specific enhancers. Macrophage enhancers associated with self-renewal genes are already present in quiescent cells and can become activated when direct repression by Maf transcription factors is relieved. Our findings provide a general molecular rationale for the compatibility of self-renewal and differentiated cell functions and may also be more generally relevant for the direct activation of self-renewal activity in other differentiated cell types with therapeutic potential. ■

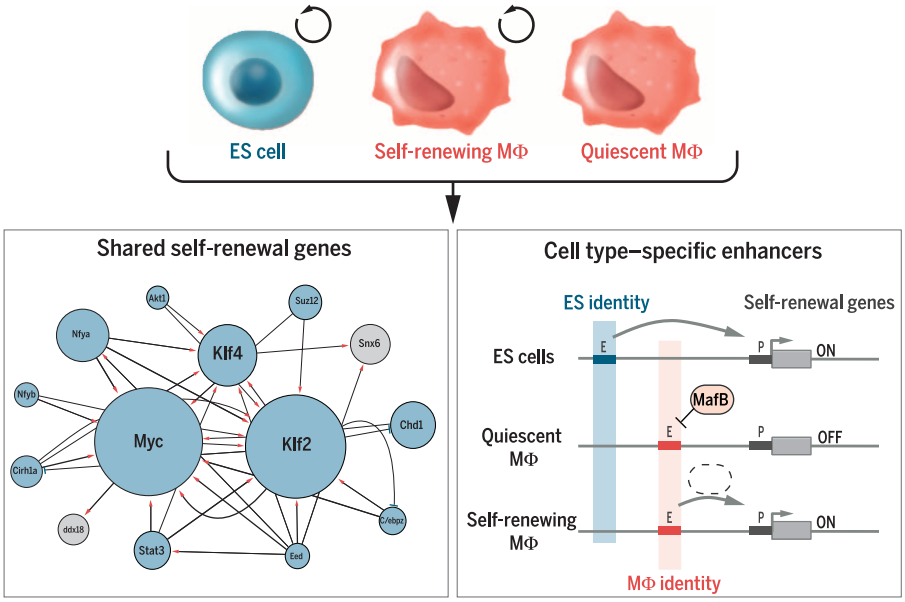

The self-renewal potential of both ES cells and differentiated macrophages is dependent on a shared network of self-renewal genes (**left**) that are controlled by distinct lineage-specific enhancers (**right**). In quiescent macrophages, the transcription factor MafB binds and represses these enhancers. The loss of MafB expression results in enhancer activation and enables macrophage self-renewal. At bottom left, red arrows indicate activation; blue bars represent inhibition. Circle size is a function of the number of times the target is affected by other regulators. MΦ, macrophage; E, enhancer; P, promoter.

The list of author affiliations is available in the full article online.
*Corresponding author. E-mail: sieweke@ciml.univ-mrs.fr (M.H.S.); erinn.soucie@inserm.fr (E.L.S.); arend@stanford.edu (A.S.)
†These authors contributed equally to this work.
Cite this article as E. L. Soucie *et al.*, *Science* **351**, aad5510 (2016). DOI: 10.1126/science.aad5510

Downloaded from on February 11, 2016

ILLUSTRATION: SERENA BIELLI

RESEARCH ARTICLE

GENE REGULATION

Lineage-specific enhancers activate self-renewal genes in macrophages and embryonic stem cells

Erinn L. Soucie,[1,2,3,4]*† Ziming Weng,[5]† Laufey Geirsdóttir,[1,2,3]† Kaaweh Molawi,[1,2,3,6]† Julien Maurizio,[1,2,3] Romain Fenouil,[1,2,3] Noushine Mossadegh-Keller,[1,2,3] Gregory Gimenez,[1,2,3] Laurent VanHille,[1,2,3] Meryam Beniazza,[1,2,3] Jeremy Favret,[1,2,3] Carole Berruyer,[1,2,3] Pierre Perrin,[1,2,3] Nir Hacohen,[7] J.-C. Andrau,[1,2,3,8] Pierre Ferrier,[1,2,3] Patrice Dubreuil,[4] Arend Sidow,[5,9]* Michael H. Sieweke[1,2,3,6]*

Differentiated macrophages can self-renew in tissues and expand long term in culture, but the gene regulatory mechanisms that accomplish self-renewal in the differentiated state have remained unknown. Here we show that in mice, the transcription factors MafB and c-Maf repress a macrophage-specific enhancer repertoire associated with a gene network that controls self-renewal. Single-cell analysis revealed that, in vivo, proliferating resident macrophages can access this network by transient down-regulation of Maf transcription factors. The network also controls embryonic stem cell self-renewal but is associated with distinct embryonic stem cell–specific enhancers. This indicates that distinct lineage-specific enhancer platforms regulate a shared network of genes that control self-renewal potential in both stem and mature cells.

In many tissues of the body, differentiated cells are frequently replaced as part of homeostatic maintenance or in response to injury. Whereas in most cases this depends on tissue-specific stem cells, tissue macrophages can be maintained by local proliferation independently of hematopoietic stem cells (*1*–*4*), possibly by self-renewal mechanisms activated in mature macrophages (*5*). Unlike the few examples of differentiated normal cells that can transiently reenter the cell cycle, such as hepatocytes, macrophages can also be expanded and maintained in long-term culture without transformation or loss of differentiation. This has been observed in macrophages with deletions of two core macrophage transcription factors (*6*)—MafB and c-Maf [Maf double-knockout (Maf-DKO) macrophages] (*7*)—or in cultures derived from fetal progenitors (*8*).

Understanding how regulatory programs are rewired to allow differentiated cells to self-renew is of considerable interest, and self-renewing macrophages present a rare opportunity to study this process. Genome-wide distribution of enhancer-associated histone modifications provides a reliable signature of cell identity (*9*–*14*) that has revealed macrophage-specific enhancer repertoires (*11*, *12*) and tissue- or activation-state–dependent modifications (*15*–*17*). To identify the regulatory mechanism that enables macrophage self-renewal capacity to be integrated into the overall program of epigenetic macrophage identity, we therefore compared the enhancer repertoires of quiescent and self-renewing macrophages.

Absence of lineage-independent self-renewal enhancers

To determine whether self-renewal in macrophages involves acquisition of dedicated, self-renewal–specific enhancers, we first compared the molecular enhancer signature defined by monomethylated histone H3 at lysine 4 (H3K4m1) (*9*, *13*, *14*) of self-renewing Maf-DKO and quiescent wild-type (WT) bone marrow macrophages (BMMs) to several other cell types with limited proliferation or extended self-renewal capacity (fig. S1). Surprisingly, our analysis revealed no common, lineage-independent repertoire of shared enhancer positions for the control of proliferation or self-renewal genes (fig. S1, A and B). We also compared genome-wide binding of the transcription factor PU.1, a key regulator of both macrophage and B cell lineage identity that defines distinct enhancer positions in the genome of these two cell types (*10*–*12*). This revealed fewer differences in the position of H3K4m1$^+$/PU.1$^+$ enhancer peaks between Maf-DKO and WT BMMs than between WT BMMs and peritoneal macrophages (PMs), as well as an equal distance of all macrophage populations to pro-B cells (fig. S1C). This indicates that Maf-DKO macrophages can activate self-renewal but retain a macrophage-specific enhancer signature similar to that of WT BMMs. Thus, macrophage self-renewal does not appear to involve the acquisition of dedicated, lineage-independent self-renewal enhancers or the loss of mature macrophage epigenetic identity.

Activation of a lineage-specific subset of enhancers in self-renewing macrophages

Because self-renewing Maf-DKO macrophages showed no appreciable difference compared to quiescent macrophages with respect to genome-wide enhancer positions, we performed chromatin immunoprecipitation sequencing (ChIP-seq) analyses for activated enhancer marks; histone acetyl transferase p300; and the histone modification mediated by this enzyme, acetylation of H3K27 (H3K27ac) (*13*, *17*–*19*), to determine whether the activation status of these enhancers differed. We found that a large number of enhancers were activated specifically in Maf-DKO macrophages only (Maf-DKO-only) (Fig. 1A, red highlight), whereas a small number of enhancers were activated specifically in WT BMMs. Specifically, we calculated 7323 enhancer regions to be enriched for p300 binding and 7489 enriched for H3K27ac in Maf-DKO macrophages compared to WT BMMs, whereas only 305 regions were enriched for p300 and 1923 for H3K27ac in WT BMMs compared with Maf-DKO macrophages (Fig. 1B and fig. S2). Further characterization of Maf-DKO-only regions revealed a typical H3K4m1$^+$/H3K4m3^{low} enhancer signature at these loci (Fig. 1, A and C), and motif search analysis of the p300- and H3K27ac-enriched Maf-DKO-only enhancer regions revealed the highest score for PU.1 binding motifs (log P = 6444) (fig. S3A). Aggregate analysis of all PU.1-bound sites in Maf-DKO and WT macrophages confirmed that the large majority of DKO-only enhancers was bound by PU.1 (Fig. 1, B and C, and fig. S3B) and that more than 60% of these positions were also bound by PU.1 in WT macrophages (Fig. 1, B and C, and fig. S3B). This PU.1 binding pattern is reminiscent of "poised" and "latent" enhancers previously described in nonstimulated and stimulated macrophages, respectively (*17*). Taken together, macrophages appear to possess a specific subset of largely poised macrophage-specific enhancers that is selectively activated in self-renewing Maf-DKO macrophages.

Self-renewing macrophages activate a gene set also required for embryonic stem cell self-renewal

Under steady-state conditions, self-renewing Maf-DKO and WT BM macrophages have highly similar global gene expression profiles (*7*). However, it is possible that the global analysis hides relevant specific mechanisms, so we specifically selected the genes associated with Maf-DKO-only–activated enhancers for further study, using the Genomic Regions Enrichment of Annotations Tool (GREAT)

[1]Centre d'Immunologie de Marseille-Luminy, Université Aix-Marseille, UM2, Campus de Luminy, Case 906, 13288 Marseille Cedex 09, France. [2]INSERM, U1104, Marseille, France. [3]CNRS, UMR 7280, Marseille, France. [4]Centre de Recherche en Cancerologie de Marseille, INSERM (U1068), CNRS (U7258), Université Aix-Marseille (UM105), Marseille, France. [5]Department of Pathology, Stanford University, Stanford, CA 94305-5324, USA. [6]Max-Delbrück-Centrum für Molekulare Medizin in der Helmholtz-Gemeinschaft, 10 Robert-Rössle-Strasse, 13125 Berlin, Germany. [7]Broad Institute of Harvard University and MIT, Cambridge, MA 02142, USA. [8]Institut de Génétique Moléculaire de Montpellier, CNRS UMR 5535, 1919 Route de Mende, 34293 Montpellier, France. [9]Department of Genetics, Stanford University, Stanford, CA 94305, USA.
***Corresponding author. E-mail: sieweke@ciml.univ-mrs.fr (M.H.S.); erinn.soucie@inserm.fr (E.L.S.); arend@stanford.edu (A.S.)** †These authors contributed equally to this work.

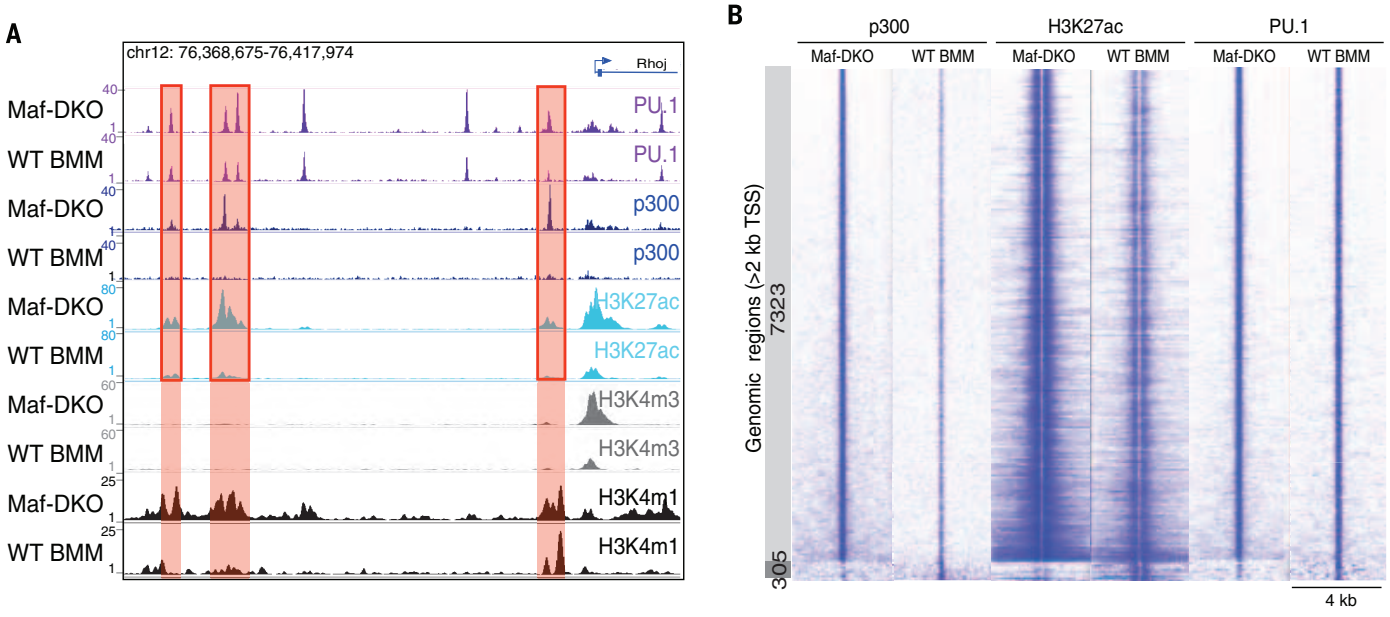

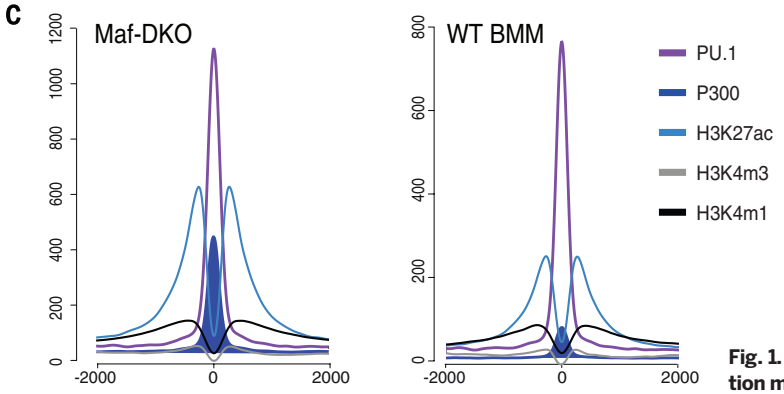

Fig. 1. A subset of lineage-specific enhancers are enriched for activation marks in self-renewing Maf-DKO macrophages. (**A**) Representative predicted enhancer regions (red shading), with greater enrichment for enhancer activation marks p300 and H3K27ac in Maf-DKO macrophages versus WT BMMs (red boxes). (**B**) Direct alignment of p300, H3K27ac, and PU.1 ChIP-seq signals for enhancer regions differentially enriched for p300 marks in Maf-DKO macrophages (7323, light gray) and WT BMMs (305, dark gray), centered and ranked on the p300 signal. (**C**) Aggregation plots showing average ChIP-seq signals for PU.1, H3K27ac, p300, H3K4m1, and H3K4m3 marks in Maf-DKO and WT BMMs for p300 regions specifically enriched in Maf-DKO macrophages [depicted in light gray in (B)]. For each protein target, results of ChIP-seq analysis were reproducible in at least two biological replicates. (**D**) Microarray gene expression ratios of Maf-DKO versus WT BMMs 2 hours after M-CSF stimulation, for total genes (white) or genes associated with Maf-DKO-only enhancers (blue). The box extends from the first to the third quartile, with the whiskers denoting 1.5 times the interquartile range. Data were derived from three biological replicates.

(*20*). We observed a specific increase in the expression of these genes after stimulation with macrophage colony-stimulating factor (M-CSF), a cytokine required to maintain self-renewal (*7*) (Fig. 1D). This indicates that Maf-DKO macrophage–activated enhancers comprise elements conferring functional responsiveness to M-CSF stimulation, potentially including those relevant to self-renewal. Gene Ontology (GO) analysis on Maf-DKO-only–associated genes revealed immune and myeloid cell functions (fig. S3C) but no groups associated with self-renewal activity. Because GO lacks self-renewal–specific categories, we performed Gene Set Enrichment Analysis (GSEA) on the Maf-DKO-only–associated genes, using both adult and embryonic stem (ES) cell–specific data modules enriched for self-renewal genes (*21*). This analysis revealed a significant enrichment of the ES cell but not the adult stem cell set in Maf-DKO over WT BM macrophage expression (Fig. 2A). On the basis of these results, we focused on functionally validated genes identified in screens for self-renewal activity in ES cells (*22*–*29*). Although the identified list of 53 genes from these screens (Fig. 2B) is not likely to be exhaustive, it constitutes the largest functionally validated gene set available that should include core elements of self-renewal activity. The genes on this list fall into two categories: those affecting self-renewal only (25 genes) and those affecting both self-renewal and pluripotency, as inferred by their influence on expression of *Oct4* or *Nanog* genes (28 genes) (Fig. 2B). Of the 25 genes in the self-renewal category, 15 (60%) were also associated with Maf-DKO-only enhancers in macrophages; of the 28 pluripotency genes, only one (4%), Chd1, also had an activated enhancer signature in Maf-DKO macrophages (Fig. 2B, red type). Similar results were obtained when the selection of self-renewal genes was based on transcription factor cross-regulatory circuits and interactome data in ES cells (*30*): None of the factors in an ES cell transcriptional cross-regulatory circuit belonging to the nanog interactome (0 of 10) and 6 of 11 (55%) genes in the network not interacting with nanog were activated in Maf-DKO macrophages (fig. S4). Our analysis revealed increased expression in Maf-DKO macrophages compared with WT BM macrophages for all 16 self-renewal genes associated with Maf-DKO-only–activated enhancers. This effect was enhanced in response to M-CSF (Fig. 2C).

Self-renewal genes are organized in a network and functionally important

To further investigate whether self-renewal genes in Maf-DKO macrophages were functionally integrated in a network of cross-regulated genes,

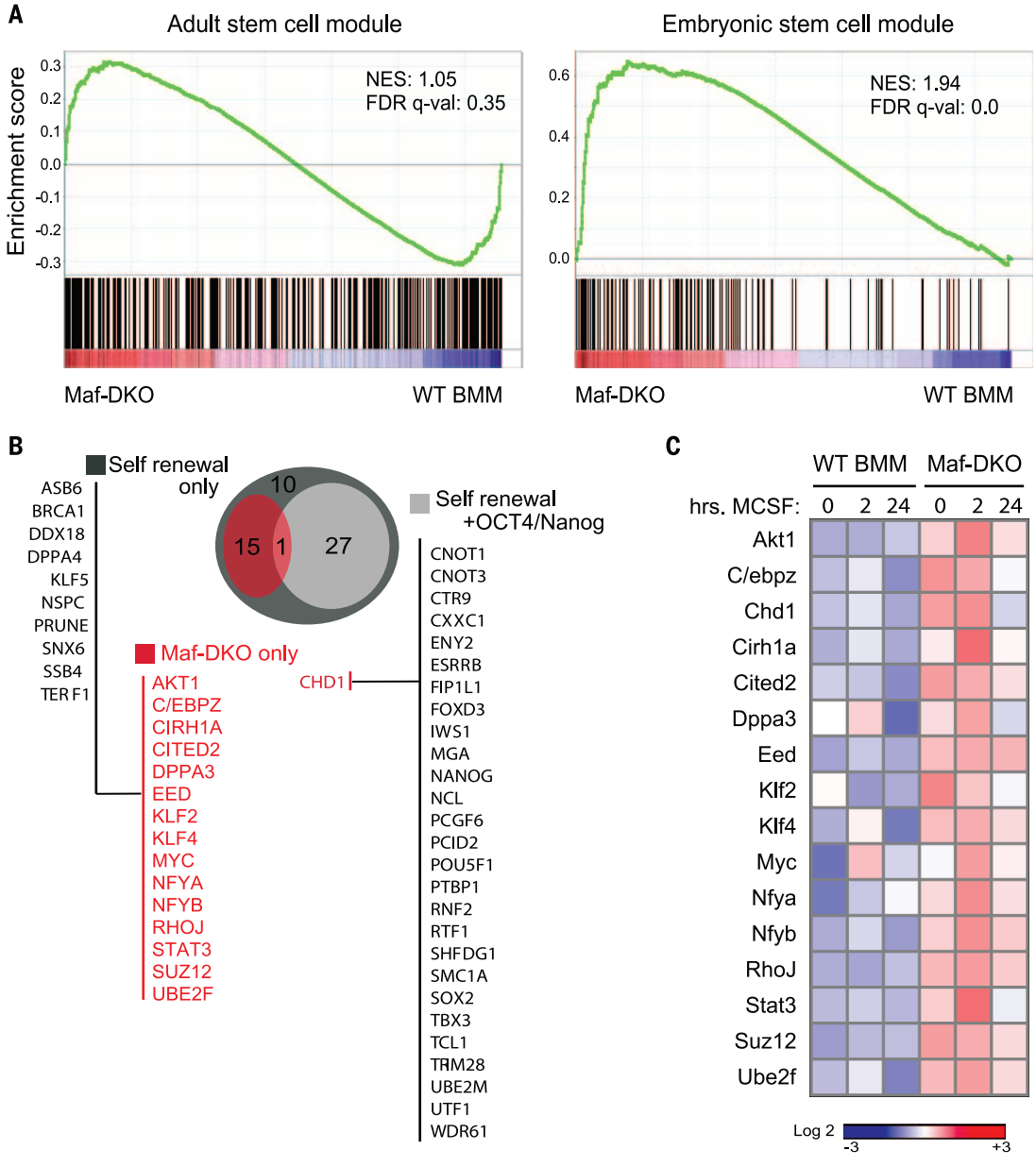

Fig. 2. Self-renewing Maf-DKO macrophages activate genes required for ES cell self-renewal. (**A**) Gene set enrichment analysis (GSEA) using gene sets defined by Wong *et al*. (*21*) for adult tissue stem cells and core ES cell modules (Broad Institute MSigDB M1999 and M7079), comparing the expression of genes associated with Maf-DKO-only–associated enhancers in Maf-DKO versus WT BMMs. NES, normalized enrichment score; FDR, false-discovery rate. (**B**) Diagram of overlapping groups of genes associated with Maf-DKO-only–activated enhancers (red) and functionally validated self-renewal (dark gray) or both self-renewal and pluripotency (self-renewal + Oct4/nanog; light gray) activity in ES cells, demonstrated by gene inactivation screens (*22*–*29*). (**C**) Gene expression by quantitative real-time PCR of self-renewal genes in Maf-DKO macrophages and WT BMMs stimulated with M-CSF for the indicated times. The heat map shows the average signal of technical replicates. Data are representative of four independent experiments.

we measured the effect of silencing individual self-renewal genes on the expression of other self-renewal genes. For 12 of the 16 identified self-renewal genes, validated short hairpin RNA (shRNA) vectors were available (*31*). In each knockdown, we measured the expression of 13 self-renewal genes associated with Maf-DKO-only macrophage enhancers and four additional self-renewal genes that might be regulated indirectly as part of a larger network. We also included probes against myeloid and housekeeping control genes (Fig. 3A). Knockdown of self-renewal genes only minimally influenced myeloid gene expression (Fig. 3A). By contrast, in all cases self-renewal–specific shRNAs substantially reduced not only the expression of their specific target but also that of other self-renewal genes. These analyses revealed a network of self-renewal gene regulation with Myc and Klf2 as the two main nodes and Klf4 as a minor node (Fig. 3B).

To determine whether the identified network of self-renewal genes was functionally important for self-renewal activity in Maf-DKO macrophages, we analyzed the effect of silencing individual self-renewal genes on colony-forming ability. We observed a significant reduction in Maf-DKO colony-forming units (CFUs) upon expression of at least one self-renewal gene–specific shRNA per gene compared with control (shLacz) for all vectors except Eed, which produced inconclusive results between different shRNA constructs and repeat experiments (Fig. 3C and fig. S5). We did not observe any significant effect of self-renewal gene silencing on apoptosis, as indicated by Annexin V and intracellular propidium iodine labeling (fig. S5B). The strongest effects on self-renewal were observed in the knockdowns of genes that occupy a central position in the network (Klf2/Myc). We observed weaker effects for several genes with peripheral positions (for example, Suz12), indicating that the knockdown of a single peripheral gene in the network might not be sufficient to compromise the activity of the entire self-renewal network.

Shared self-renewing genes have distinct enhancers in ES cells and macrophages

Our results indicated that self-renewal of Maf-DKO macrophages depends on an integrated network of cross-regulated self-renewal genes that are also employed for self-renewal in ES cells. To investigate how these very different cell types could access a similar gene network, we compared the gene regulatory mechanics

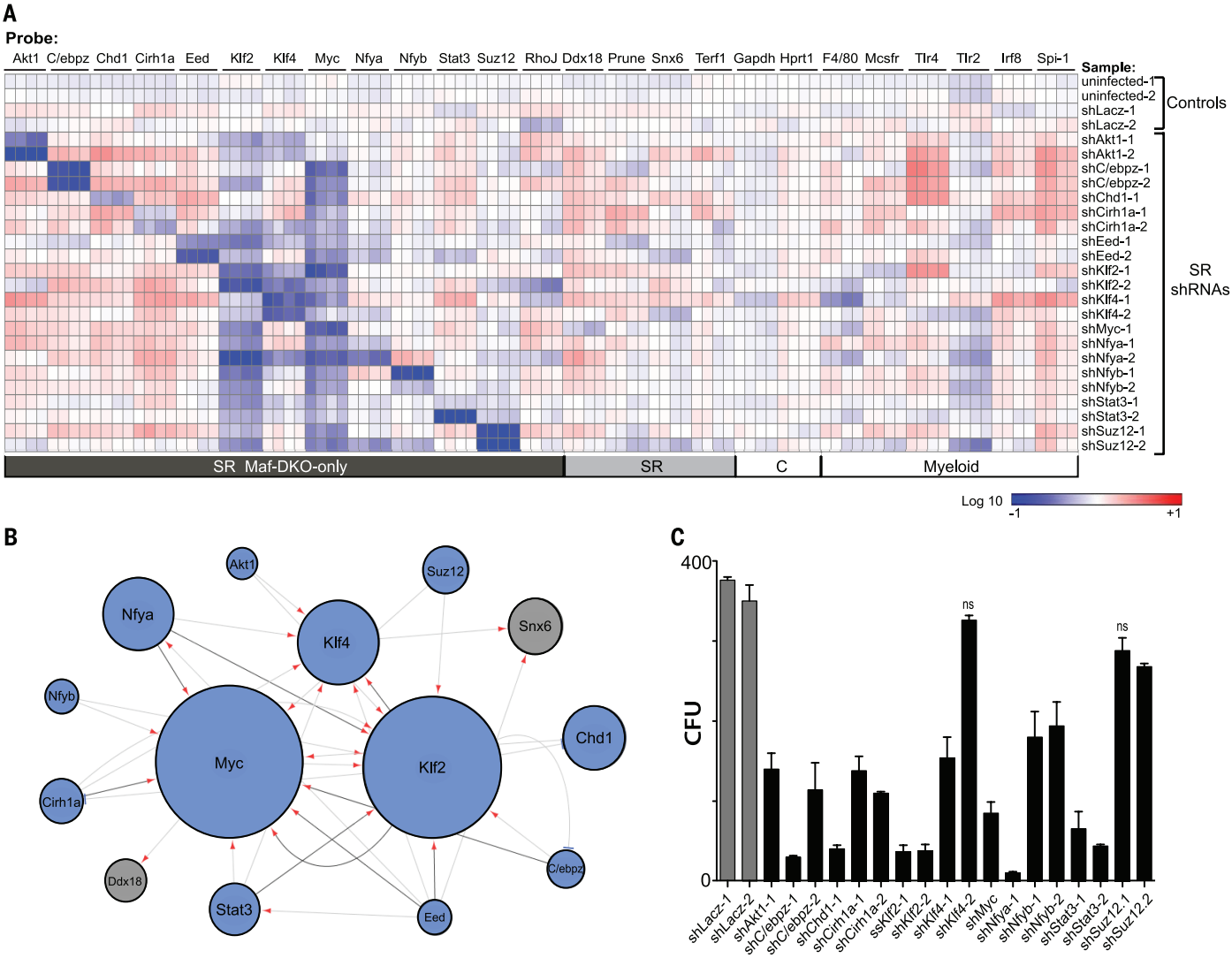

Fig. 3. Self-renewal genes are organized in a network and functionally important for Maf-DKO macrophage proliferation. (**A**) Gene expression analysis of Maf-DKO macrophages uninfected or infected with shLacZ control or shRNAs targeting self-renewal genes (rows) for self-renewal genes associated with Maf-DKO macrophage–activated enhancers, unassociated self-renewal genes (SR), housekeeping (C), and macrophage-specific (myeloid) genes (columns) using quadruplicate nanofluidic real-time PCR on Fluidigm array. For each gene, the heat map presents normalized values as percent change over average expression in noninfected and control lacZ shRNA–infected cell samples. Data are representative of three independent experiments. (**B**) Network model using an FDR approach, showing statistically significant repression of an output target gene resulting from shRNA knockdown of a regulator gene. Darker lines denote regulation in all replicates, red arrows indicate repression, and blue bars represent activation by shRNA. Circle size is a function of the number of times the target is affected by knockdown of other regulators. (**C**) Number of CFUs obtained from equal numbers of Maf-DKO macrophages infected with shRNAs against control (shLacZ) or self-renewal gene targets after 12 days of culture in MethoCult medium containing M-CSF. The mean number of CFUs for self-renewal gene shRNA–infected populations is significantly different from the mean number of CFUs for controls (one-way analysis of variance, $P < 0.05$) unless indicated (ns, not significant). Error bars represent SD of triplicate technical replicates, and data are representative of three independent experiments.

underlying activation of self-renewal genes in Maf-DKO macrophages and ES cells. As expected from the previous data and the differentiated phenotype of macrophages, genes affecting both self-renewal and pluripotency in ES cells, such as Oct4/POU5F1, showed activated enhancers in ES cells but not in macrophages (fig. S6A). By contrast, active enhancer elements were found to be associated with the genes of the identified self-renewal network both in ES cells and Maf-DKO macrophages (Fig. 4). However, the two cell types use entirely distinct sets of enhancers to activate these genes. The examples for the central factors Myc, Klf2, and Klf4 (Fig. 4A) and further network elements (fig. S6B) illustrate that ES cell–specific H3K27ac$^+$/p300$^+$ enhancers (blue in Fig. 4A and fig. S6B) and macrophage-specific H3K27ac$^+$/ p300$^+$ enhancers (red in Fig. 4A and fig. S6B) exist for each gene. To address these observations quantitatively, we identified the regulatory regions marked by H3K27ac in the three cell types (ES cells, Maf-DKO macrophages, and WT BMMs) for each of the known 16 self-renewal genes (Fig. 2B). To do this, we used a multisample-calling strategy to capture all shared regions and strong cell type–specific regions (Fig. 4B). There were 152 such regions, ranging from one region per gene (four genes) to 34 (*Cited2*), with an average of 9.5 and a median of 5. Genome browser inspection revealed almost completely nonoverlapping sets of active enhancer regions in macrophages and ES cells (Fig. 4A and fig. S6B). Consistent with these observations, we could identify two distinct enhancer clusters by *k*-means clustering ($k = 2$ clusters), where the most important characteristic separating the clusters is whether an enhancer is active in ES cells or in macrophages (Fig. 4B). The median normalized signal for enhancers in cluster one is 62 times higher in ES

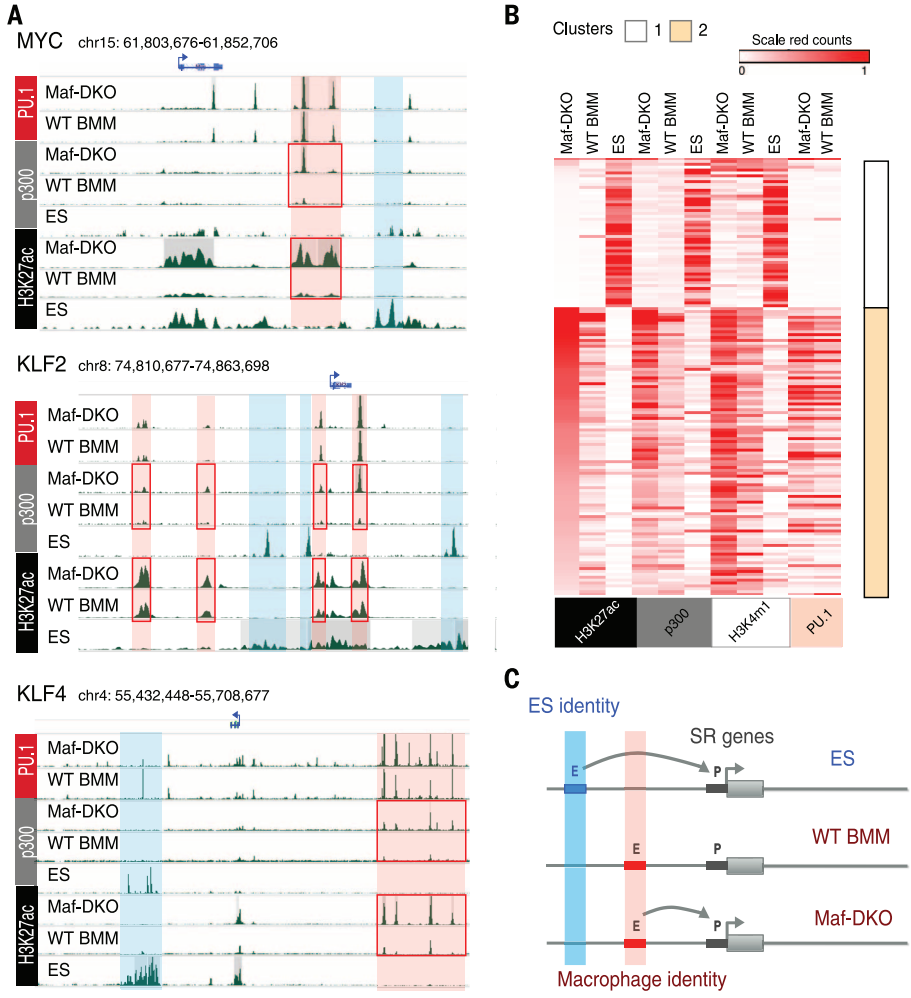

Fig. 4. Self-renewal genes are associated with distinct enhancers in ES cells and macrophages. (**A**) Genomic regions surrounding the *Myc*, *Klf2*, and *Klf4* genes, showing distinct ES cell– (blue) and macrophage- (red) specific predicted enhancer regions with differential H3K27ac and p300 enrichment in Maf-DKO over WT BMMs (red boxes). (**B**) Heat maps and *k*-means clustering ($k = 2$) of ChIP-seq signals of all H3K27ac^{+} regions associated with self-renewal genes in ES cells, Maf-DKO macrophages, and WT BMMs, including both differentially regulated Maf-DKO-only areas and nondifferentially regulated regions. Corresponding regions are shown for p300, H3K4m1, and PU.1 (ES, Maf-DKO macrophages, and WT BMMs). Read counts were individually scaled to the 95th percentile of each antibody signal. (**C**) Model to describe tissue-specific macrophage and ES cell–enhancer platforms associated with individual self-renewal genes. Color code is same as in (A). E, enhancer; P, promoter.

cells than in Maf-DKO macrophages; conversely, in cluster two the median normalized signal is 16 times higher in Maf-DKO macrophages than in ES cells. These patterns are mirrored at high statistical significance (*P* values ranging from 1.4×10^{-9} to 9.6×10^{-16}) in the ChIP-seq data from p300 and H3K4me1 (Mann-Whitney test), which had not been used in the clustering (Fig. 4B). Furthermore, enhancers associated with macrophage-specific self-renewal genes were 85 and 73% PU.1-positive in Maf-DKO and WT BM macrophages (Fig. 4B), indicating that macrophage self-renewal activates largely poised macrophage-specific enhancers. These results attest to the strong contrast among the clusters and their constituent regions and support the model that the same self-renewal genes can be accessed by distinct lineage-specific enhancer elements in two different cell types with self-renewal capacity (Fig. 4C).

MAFB directly represses self-renewal enhancers in macrophages

To better understand the mechanism leading to the activation of self-renewal enhancers in macrophages, we reexpressed MafB in Maf-DKO macrophages. MafB expression resulted in the reduction of both colony size and number in CFU assays (Fig. 5A), strongly inhibited expression of self-renewal genes (Fig. 5B), and reestablished low levels of p300 binding and H3K27ac modification, similar to WT BMMs at both Maf-DKO-only (fig. S7A) and self-renewal gene–associated enhancers (Fig. 5C). We further analyzed whether this rescue effect was due to a direct effect of MAFB on self-renewal gene–associated enhancers. Transcription factor binding sites enriched at Maf-DKO-only and, more specifically, self-renewal enhancers included Maf (MARE) and related AP-1 family binding sites (figs. S3A and S8). Furthermore, MAFB can also bind directly to PU.1 (*32*) and might thus target PU.1-positive enhancers by protein-protein interactions in the absence of consensus MARE. ChIP-seq analysis for MAFB in reconstituted Maf-DKO macrophages showed direct binding of MAFB (Fig. 5D) to 65% of PU.1-positive DKO-only enhancers and 73% of self-renewal gene–associated enhancers (Fig. 5E), as exemplified for the core factors of the network: Myc, Klf2, and Klf4 (Fig. 5F and fig. S7B). Similar binding profiles were observed for ChIP-seq analysis of endogenous MAFB in WT BMMs (fig. S9). Together, these results indicate that the activation of self-renewal is reversible and that the large majority of poised self-renewal–associated macrophage enhancers are directly repressed by MAFB binding.

Naturally low Maf levels in alveolar macrophages activate self-renewal enhancers

To further investigate whether our observations in Maf-DKO macrophages were directly relevant to the self-renewal capacity of genetically unmodified macrophages, we investigated alveolar macrophages (AMs). AMs are a population of adult resident macrophages that have the ability to autonomously self-renew (*4*) and that naturally express low levels of MafB and cMaf (*6*). Consistent with the constitutively low Maf levels compared with those of other macrophage populations (Fig. 6A and fig. S10), we could expand AMs in long-term liquid culture (Fig. 6B) and serially replate AMs, but not peritoneal macrophages (PMs), in colony-forming assays without losing replicative ability (Fig. 6C). Cultured AMs also expressed generally increased levels of self-renewal network genes (Fig. 6D). Furthermore, ChIP-seq analysis of epigenetic enhancer marks at the self-renewal gene–associated enhancer regions showed comparable binding of PU.1 between AMs, Maf-DKO macrophages, and WT BM macrophages but an enrichment of the activation mark p300 in AMs, as in Maf-DKO macrophages (Fig. 6, E and F). Statistical analysis confirmed a high correlation for PU.1 binding across all three populations and a high correlation for p300 binding between AMs and Maf-DKO macrophages but not BMMs (Fig. 6G). Thus, both experimental and natural reduction of MafB and c-Maf levels activates a set of poised macrophage-specific enhancers of the self-renewal gene network.

Low MafB levels activate self-renewal genes in resident macrophages in vivo

Many resident macrophage populations show a low level of local proliferation in vivo. Using immunofluorescence, we observed that the large majority of cycling, Ki67-positive macrophages in the peritoneum, liver, and spleen red pulp did not express MafB, whereas quiescent, Ki67-negative macrophages were nearly all MafB-positive (Fig. 7,

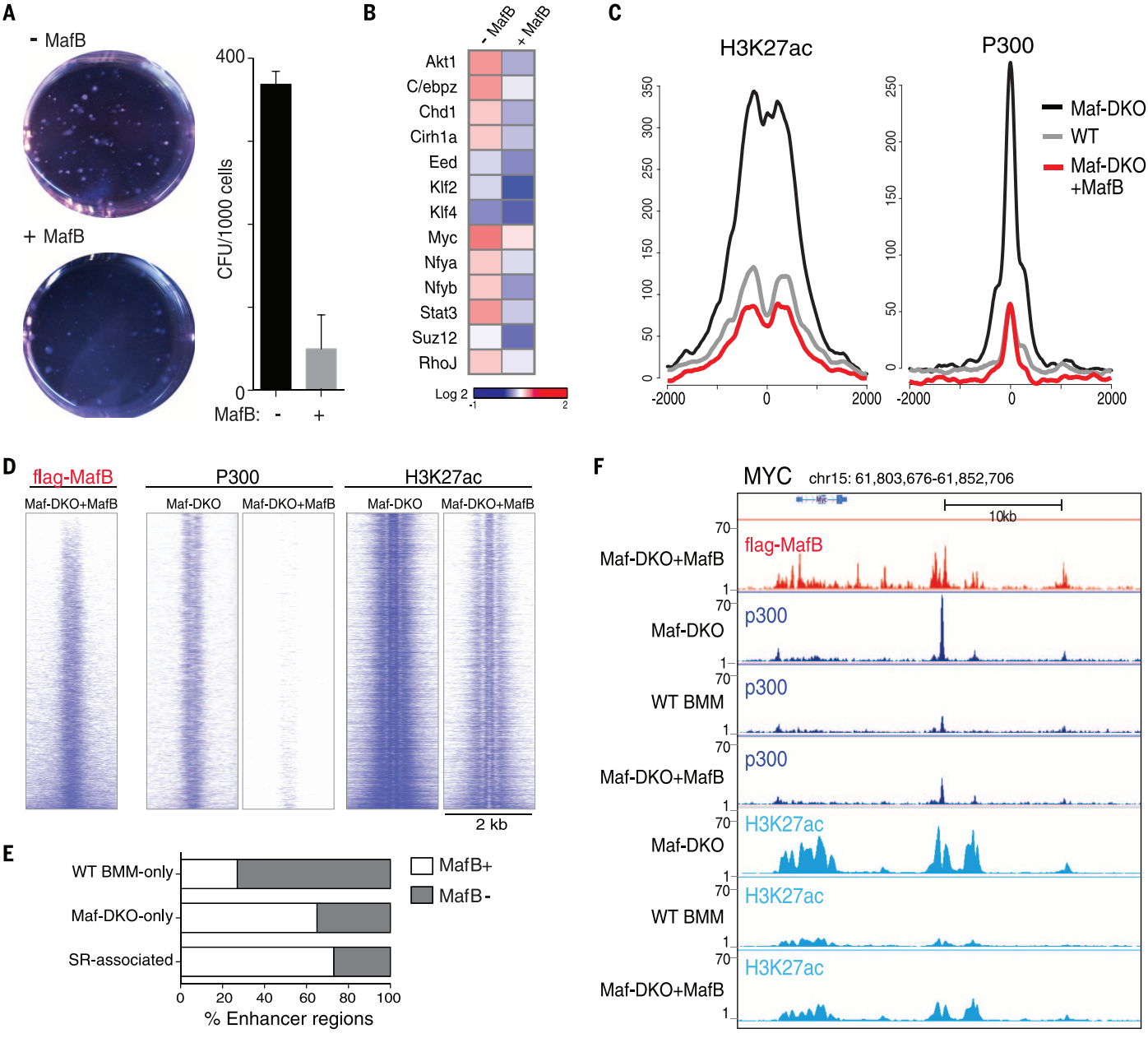

Fig. 5. MafB inhibits macrophage self-renewal by direct repression of self-renewal gene enhancers. (**A**) Colony assays for Maf-DKO macrophages expressing empty vector (−MafB) or a doxycycline-inducible Flag-tagged MafB allele (+MafB). Colonies were counted after 14 days of culture in MethoCult medium containing M-CSF and doxycycline. Culture dishes (0.63x) are shown at left, number of CFUs at right. Error bars represent SD of replicates, and data are representative of three independent experiments. $^{**}P$ = 0.004 by two-tailed, unpaired *t* test. (**B**) Expression of self-renewal genes in empty-vector Maf-DKO macrophages (−MafB) and Maf-DKO macrophages expressing a doxycycline-inducible, Flag-tagged MafB allele (+MafB), after 2 hours of stimulation with M-CSF, determined by nanofluidic real-time PCR on a Fluidigm array. Data are representative of three independent experiments. (**C**) Aggregation plots showing average ChIP-seq signals for P300 and H3K27ac in Maf-DKO macrophages expressing empty vector, WT BMMs, and Maf-DKO macrophages expressing a doxycycline-inducible, Flag-tagged MafB allele in the presence of doxycycline (Maf-DKO+MafB) for the self-renewal–associated enhancer regions (total = 88 regions). (**D**) Direct alignment of regions proximal to Maf-DKO-only enhancers for Flag-MAFB binding in Maf-DKO+MafB and corresponding regions in Maf-DKO and Maf-DKO +MafB macrophages for P300 and H3K27ac binding. (**E**) Histogram showing the percent of WT BMM-only–, Maf-DKO-only–, and self-renewal gene–associated enhancers bound by MAFB, as determined by ChIP-seq for Flag-MAFB in Maf-DKO+MafB cells. (**F**) Genomic regions surrounding the *Myc* gene with ChIP-seq tracks as labeled.

A and B; fig. S11; and table S1), indicating that macrophage proliferation in vivo also involved reduced MafB levels. Resident macrophages can further expand massively by transient local proliferation in response to specific stimuli (*5*, *33*)—for example, to M-CSF during infection of the peritoneum (*34*, *35*), which can be mimicked by direct intraperitoneal injection of the cytokine (*34*, *35*) (fig. S12). To address whether under such conditions macrophages could access the self-renewal gene network by transient repression of MafB and/or cMaf, we measured both self-renewal gene expression and MafB and cMaf expression before and at various time points after M-CSF stimulation by single-cell analysis of sorted resident peritoneal macrophages. One hour after stimulation, we observed a transient reduction of MafB (Fig. 7C) and, to a much lesser

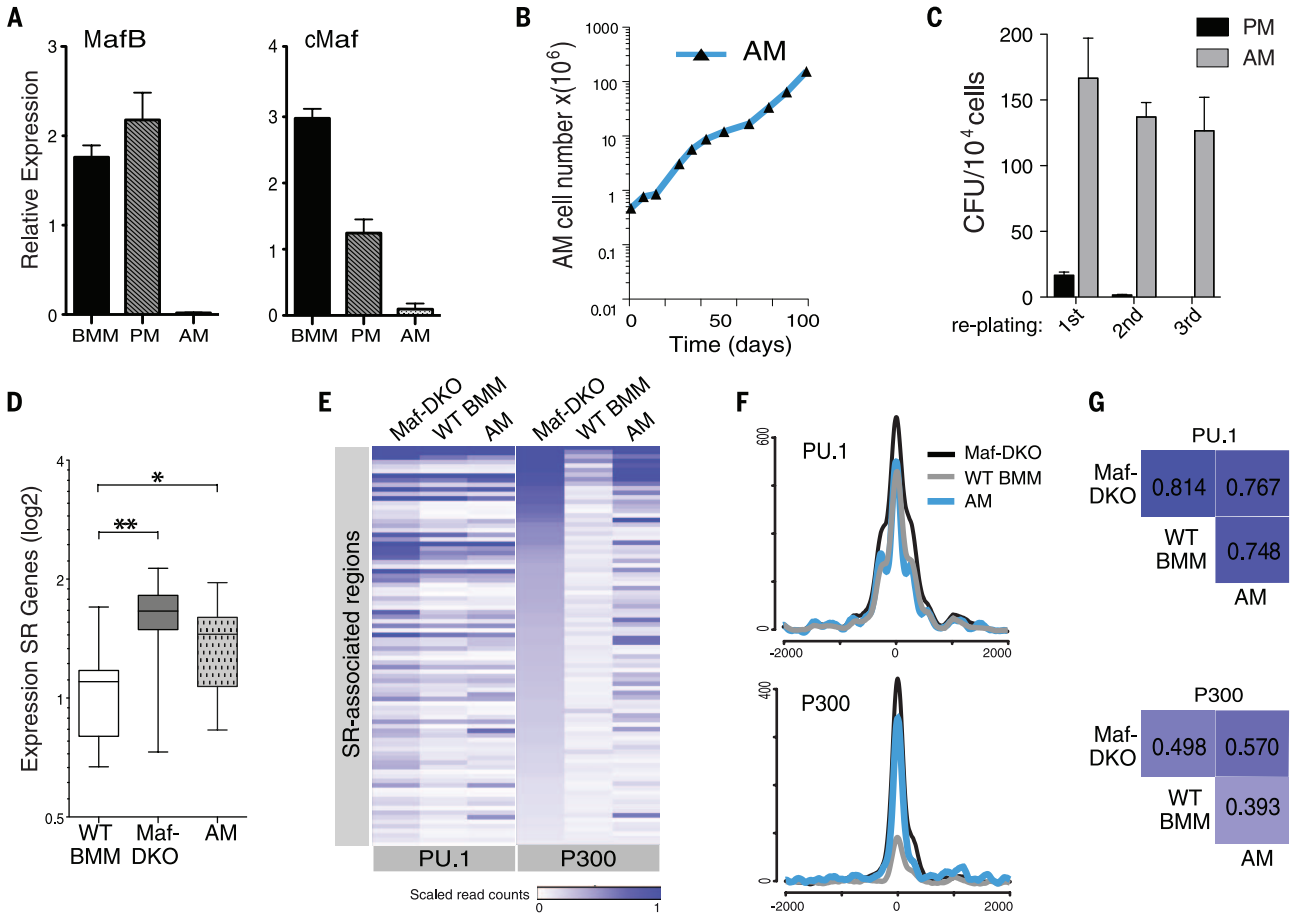

Fig. 6. The self-renewal gene network is activated in AMs expressing naturally low levels of MafB and cMaf. (**A**) Expression of MafB and cMaf relative to HPRT1, measured by RT-QPCR, in short-term cultures of BMMs, PMs, and AMs. Error bars represent SD of replicates, and data are representative of three independent experiments using biological replicates. (**B**) Growth curve showing number of AMs over time in liquid culture. Data are representative of two independent experiments. (**C**) Number of CFUs counted at day 21 per 10^4 AMs and PMs plated in MethoCult medium after the first plating, after replating 10^4 cells washed out from the first plating (2nd plating), or after the second plating (3rd plating). Error bars represent SD of replicates, and data are representative of three independent experiments. (**D**) Box plots showing average, interquartile, and 5th to 95th percentile relative expression levels of all self-renewal genes in Maf-DKO macrophages, WT BMMs, and AMs, as measured by nanofluidic real-time PCR on a Fluidigm array. *$P < 0.05$; **$P < 0.01$ (based on an unpaired t test). Data are based on the average signal from three biological replicates, each performed with technical duplicate. (**E**) Heat map of ChIP-seq signals for all regions associated with self-renewal genes (total = 88) in Maf-DKO macrophages, WT BMMs, and AMs. Corresponding regions are shown for PU.1 and P300, and read counts were individually scaled to the 95th percentile of each antibody signal. (**F**) Aggregation plots showing average ChIP-seq signals for PU.1 and P300 in Maf-DKO macrophages, WT BMMs, and AMs for the self-renewal–associated enhancer regions (total = 88 regions). (**G**) Pearson correlation matrix (PCA ranked $\log_2$ read number) for PU.1 and P300 binding to self-renewal gene–associated enhancers (total = 88 regions), based on ChIP-seq data for Maf-DKO macrophages, WT BMMs, and AMs. ChIP-seq analysis on AMs for PU.1 and p300 was performed twice.

extent, of c-Maf but not of control myeloid genes (fig. S13A). Reasoning that the behavior of resident peritoneal macrophages might be heterogeneous, we could identify three distinct groups of cells by principal component analysis (PCA) and *k*-means clustering (Fig. 7D). Whereas cells in cluster three were equally present before and after stimulation, cluster-two cells were strongly reduced and cluster-one cells strongly increased after M-CSF stimulation (Fig. 7E). Cells in cluster two expressed high levels of MafB and c-Maf but were negative for nearly all self-renewal genes. By contrast, cells in cluster one showed low MafB levels and up-regulation of the large majority of self-renewal genes (Fig. 7F). Cluster-three cells also showed high MafB levels (fig. S13B). Direct comparison of the expression of MafB and Myc in individual cells revealed a large number of cells with high MafB and low Myc levels in clusters two and three (fig. S13C). By contrast, a majority of cells in cluster one showed low or absent MafB levels and high levels of Myc (Fig. 7G). This analysis also demonstrated that a few cells with a MafB-low/Myc-high profile already existed in the steady state but their number strongly increased after M-CSF stimulation (Fig. 7G).

Overall, our results demonstrate that down-regulation of MafB and cMaf and concomitant activation of a self-renewal gene network is a hallmark of proliferating resident macrophages in culture and in vivo. Natural or experimentally induced constitutively low levels of MafB and c-Maf also enable long-term continuous self-renewal of adult macrophages in culture, as observed for AMs or Maf-DKO macrophages, respectively. Although inactivation of type I interferon signaling has also been associated with increased macrophage proliferation (*36*), we could not identify a direct link between Maf activity and this pathway. Furthermore, repression of interferon-β by MafB has been reported (*37*), which is the opposite of what would be expected if Maf transcription factors acted through interferons to limit macrophage proliferation.

We show that a network of genes that governs macrophage self-renewal overlaps substantially with that controlling self-renewal in ES cells. The regulatory mechanism by which activation of these genes is accomplished involves almost entirely separate sets of enhancers in the two cell types. The identified enhancer architecture associated with self-renewal genes in macrophages is already present in quiescent cells and can become activated when direct repression by Maf

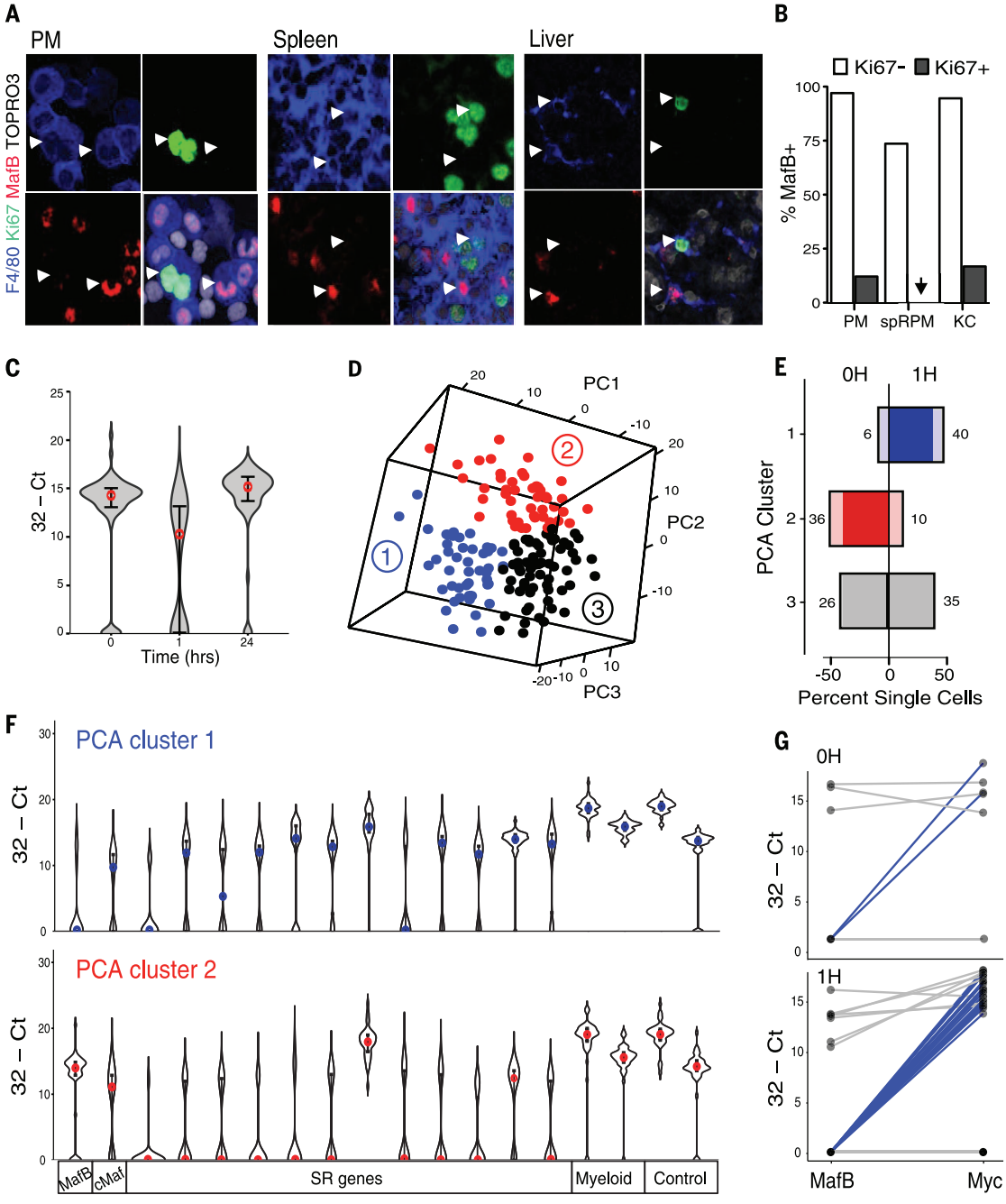

Fig. 7. Single-cell analysis of tissue macrophages in vivo reveals self-renewal gene network activation in MafB-negative macrophages. (**A**) Immunofluorescence images of MafB- and Ki67-positive peritoneal F4/80$^+$ macrophages in cytospun peritoneal macrophages (PMs) and tissue sections from spleen and liver. White arrowheads point to examples of Ki67$^-$/MafB$^+$ and Ki67$^+$/MafB$^-$ macrophages, F4/80$^+$, in each tissue. Data are representative of two independent experiments. Larger-field images are shown in fig. S11. (**B**) Quantification of percent MafB$^+$ cells in the Ki67$^-$ and Ki67$^+$ fraction of F480$^+$/SYTOX blue$^+$ resident macrophages from peritoneum (PMs; n = 969), spleen red pulp macrophages (rpSPM; n = 425), and liver Kupfer cells (KC; n = 302), corresponding to the immunofluorescence images in (A) and fig. S11. Absolute cell counts are shown in table S1. (**C**) Violin plot showing expression of MafB across single PMs isolated from a mouse at the indicated time points after intraperitoneal M-CSF injection, measured by nanofluidic real-time PCR on a Fluidigm array. Red dots mark the median value and error bars the interquartile range. (**D**) Depiction in 3D space of PCA analysis of single-cell gene expression data for a k-means = 3 of pooled data for 0 and 1 hours after M-CSF injection. Distinct PCA clusters are distinguished by colors and numbers. (**E**) Histogram showing the percentage of single cells in each cluster at the 0- and 1-hour time points [clusters as in (D)]. Absolute numbers of cells in each group are indicated, and the net change between 0 and 1 hour is shown in deeper color. (**F**) Violin plots showing expression for Maf, self-renewal (SR), myeloid, and control genes across cells in PCA cluster 1 (blue) and PCA cluster 2 (red) [clusters as in (D)]. Colored dots show the median value and error bars the interquartile range. (**G**) Line diagrams showing individual cell comparison of MafB and Myc expression for PCA cluster 1 at 0 and 1 hours. Single cells with low MafB and high Myc expression are highlighted in blue. Consistent results for (C) to (G) were obtained in a repeat experiment with cells sorted from a pool collected from five mice at each time point.

transcription factors is relieved. In summary, we have shown that self-renewal activity can be activated from an intrinsic cell type–specific enhancer repertoire in differentiated cells. Our findings provide a general molecular rationale for the compatibility of self-renewal and differentiated cell functions and may also be more generally relevant for the activation of self-renewal activity in other differentiated cell types with therapeutic potential.

Materials and methods

Cell culture

Maf-DKO macrophages were grown subconfluently in macrophage growth medium (Dulbecco's modified Eagle's medium with 20% supernatant from L929 mouse fibroblasts, 1% sodium pyruvate, and 1% L-glutamate], as described in (7). WT BMMs were differentiated from total mouse BM for 15 days in macrophage growth medium, selecting for adherent cells every 4 days. For time course analysis of self-renewal gene expression in Maf-DKO and WT BMMs, cells were seeded 18 hours before time 0 in growth medium

without supernatant from L929 mouse fibroblasts; at time 0, 100 ng/ml of recombinant murine stem cell factor (Peprotech) was added to the culture medium; and cells were harvested for RNA isolation and analysis at 0, 1, 2, and 24 hours.

For culture of AMs, alveolar lavages were pooled from 10 1-ml 37°C bronchoalveolar lavage washes [phosphate-buffered saline (PBS) without Mg^{++}/Ca^{++}, 2 mM EDTA, 2% fetal bovine serum (GE Healthcare) per mouse] and stored on ice. Red blood cell (RBC) lysis was then performed at room temperature (RT) for 3 min (RBC Lysis Buffer, Invitrogen). Cells were plated at a density of 1.1 million cells per 10-cm bacterial petri dish in complete medium [RPMI, 10% fetal calf serum (FCS), 1% Pen/Strep, 1% pyruvate, 1% glutamate] supplemented with 1% granulocyte-macrophage CSF (GM-CSF) supernatant from J558L cells transfected with murine GM-CSF cDNA.

MafB expression in Maf-DKO macrophages

The pRetroX-Tet-On Advanced (Clontech, catalog no. 632104) and pRetroX-Tight-Pur (catalog no. 632104) retroviral backbones were used for generating the Flag-tagged MafB-inducible Maf-DKO macrophages. Neo^r was replaced by $Hygro^r$ and $Puro^r$ by green fluorescent protein (GFP) in the pRetroX-Tet-On Advanced and pRetroX-Tight-Pur retroviruses, respectively. Maf-DKO macrophages were first infected with the pRetroX-Tet-On-$hygro^r$ retrovirus and selected for 2 weeks in medium containing 200 μg/ml of Hygromycin B (Life Technologies, catalog no. 10687-010). Selected Maf-DKO macrophages were next infected with the empty pRetroX-Tight-GFP or pRetroX-Tight-GFP containing the Flag-tagged MafB gene cloned downstream of the modified Tet-responsive promoter. GFP-positive Maf-DKO macrophages were then subjected to fluorescence-activated cell sorting (FACS) and cultured in the absence of doxycycline.

Stimulation and isolation of peritoneal macrophages

Either 200 μl of PBS (control) or 20 μg of recombinant M-CSF (Novartis) was injected into the peritoneums of WT C57/B6J 8- to 10-week-old mice at the indicated times before analysis. For cell cycle analysis, mice were also injected intraperitoneally with 2 mg of bromodeoxyuridine (BrdU) (BD Pharmingen) dissolved in PBS, per manufacturer's instructions, 4 hours before analysis. To harvest peritoneal cells, mice were sacrificed and subsequently injected with 10 ml of ice-cold PBS containing 2 mM EDTA (Sigma). Intraperitoneal washouts were collected in 50-ml Falcon tubes. Red cell lysis was performed on total washouts (RBC Lysis Buffer, Invitrogen) before staining for cell surface markers and cell cycle analysis or FACS. The remaining mononuclear cells were then stained using the following antibody cocktail in the presence of FcBlock (BD Biosciences)—CD11b-PE-Cy7 (BD Biosciences); MHC-II-FITC, B220-APC-Cy7, and F4/80-PE (all from eBioscience); and Fixable Aqua Dead-V500 (Life Technologies)—and either sorted for single-cell analysis or further processed for cell cycle analysis.

Cell cycle analysis

Bromodeoxyuridine analysis was performed using a BrdU Flo Kit (BD Pharmingen) according to manufacturer's instructions and with the following modifications: DNaseI digestion was performed for 90 min and intracellular staining for 60 min, and anti-BrdU-AlexaFluor 647 Ab (Invitrogen, clone MoBU-1) was substituted for anti-BrdU provided in the kit. For Ki67 staining, cells were harvested and treated as for BrdU staining but with substitution of an anti-Ki67-V450 antibody (eBiosciences, clone SolA15) for the final incubation step. Cells were analyzed using an LSRII and FlowJo software (Tree Star).

shRNA infections

Lentiviral vector particles were produced at the Centre International de Recherche en Infectiologie (INSERM, UMR 5308 Lyon, France) by tri-transfection of plasmids harboring the packaging construct, the transfer vector (*31*), and the envelope-expressing construct into producer cells using calcium chloride methodology. Virus was concentrated after transfection, and viral supernatants were harvested and used directly for infections or stored at −80°C.

Maf-DKO macrophages were seeded subconfluently in 12-well dishes, 24 hours before infection. The next day, 8 μg/ml of polybrene was incubated for 1.5 hours at 37°C and 5% CO_2 with viral supernatants, and 2 ml per well per infection was used to replace media on Maf-DKO macrophages. Spin infections were carried out at 25°C for 2 hours, with 2500 revolutions per minute (rpm). Viral supernatants were removed immediately after spin infection and replaced with macrophage growth medium. Cells were then further incubated at 37°C and 5% CO_2 for 72 hours before harvesting and divided into fractions for apoptosis, colony assay, and RNA and DNA isolation.

Apoptosis was measured using the Annexin V Apoptosis Detection Kit (eBioscience) according to the manufacturer's instructions. To control for infection, genomic DNA was isolated [using the DNeasy Blood and Tissue Kit (Qiagen)] from infected Maf-DKO cells at 72 hours postinfection. Quantitative polymerase chain reaction (QPCR) was performed to detect the quantity of puromycin cassette contained in the lentiviral vector, relative to a control genomic amplicon [actin transcription start site (TSS)], and to ensure similar infection efficiencies across all populations (fig. S5). Reactions were carried out in a 7500 Real-Time PCR System (Applied Biosystems) including dissociation curves to validate distinct amplicons. RNA was extracted from infected cells and processed for gene expression profiling.

Colony assays

For shRNA-infected cells, 5000 cells were counted from each population of infected cells and mixed with 1 ml of MethoCult medium (M3231, Stem Cell Technologies), with the addition of 100 ng/ml of recombinant M-CSF (Peprotech), plated in duplicate and grown at 37°C, 5% CO_2. For experiments using MafB-inducible Maf-DKO cells, 1000 cells were plated, and 1 μg/ml of doxycycline (Sigma) was added, in addition to M-CSF, where indicated. The number of CFUs was counted on day 12 after plating. Maf-DKO macrophages expressing empty vector (–MafB) or a doxycycline-inducible, Flag-tagged MafB allele (+MafB) were plated at 1000 cells per milliliter of MethoCult medium, as above, with the addition of 1 μg/ml of doxycycline (Sigma). AMs were plated at 10,000 cells per 1 ml of MethoCult M3231 medium (StemCell Technologies) containing 100 ng/ml of recombinant GM-CSF (Peprotech), and colonies were counted after 3 weeks. All experiments were performed with $n = 2$ replicates, and results were reproduced at least three times independently.

In situ immunofluorescent cell staining

PMs were harvested with refrigerated PBS, and 10,000 cells were loaded onto Shandon cytocentrifuge chambers and centrifuged at 1000 rpm for 3 min. Slides were air-dried, fixed with refrigerated 4% paraformaldehyde (PFA) for 10 min at RT, and washed once with PBS. Spleen and liver were harvested after perfusion with PBS and freshly embedded in TissueTeck (OCT Compound) before freezing. Serial frozen sections (8 μm) were fixed with refrigerated 4% PFA for 10 min and washed three times for 5 min with PBS at RT.

Slides were then permeabilized with Triton-X 0.05% (Sigma, catalog no. 9002-93-1) for 10 min and washed three times for 5 min with PBS. Unspecific antigens were blocked for 1 hour with PBS containing 1% FCS, 2% bovine serum albumin (BSA), and 1% goat serum before staining. After blocking, slides were incubated for 1 hour at RT with rabbit anti-mouse MafB (Bethyl, catalog no. IHC-101) diluted at 1:50 and rat anti-mouse Ki67 (eBioscience, catalog no. 14-5698-82) diluted at 1:50 in blocking solution. Slides were subsequently washed three times for 10 min with PBS at RT and incubated with the secondary antibodies donkey anti-rat A488 (Invitrogen, catalog no. A31572) diluted at 1:500 and donkey anti-rabbit A555 (Invitrogen, catalog no. A21208) diluted at 1:500 in PBS. Slides were again washed three times for 10 min with PBS at RT and, finally, incubated for 1 hour with F4/80 A647 (Serotec, catalog no. MCA497A647) diluted at 1:50. A final wash series of three times for 10 min with PBS at RT was performed before mounting with Prolong Gold (Thermo Fischer, catalog no. P36930) with SYTOX Blue diluted at 1:1000 (Thermo Fischer, catalog no. S11348) for nuclear staining. Images were analyzed on a Zeiss LSM510 confocal microscope.

ChIP-seq

Cells cultured in plates were fixed by the direct addition of 1/10 volume of freshly made cross-linking solution (11% formaldehyde, 100 mM NaCl, 1 mM EDTA, 0.5 mM EGTA, 50 mM Hepes at pH 7.8) to cell medium and incubation at RT

for 10 min. Formaldehyde was then quenched for 5 min at RT by the addition of 2.5 M glycine solution to a final concentration of 125 mM. Fixed cells were washed twice with cold PBS, scraped off the plate, counted, and transferred in 50-ml Falcon tubes. Cells were then pelleted by centrifugation at 700*g* for 5 min at 4°C, snap-frozen in liquid nitrogen, and stored at −80°C for storage or shipment on dry ice.

Each batch of 100 million cells was lysed by adding 10 ml of ChIP Lysis Buffer (Santa Cruz Biotechnology, catalog no. sc-45000) or radioimmunoprecipitation assay (RIPA) buffer (1x PBS, 1% NP-40, 0.5% sodium deoxycholate, 0.1% SDS) containing Protease Inhibitor Cocktail (PIC). One complete PIC tablet (Roche, catalog no. 11873580001) for 50 ml of buffer or one mini PIC tablet (Roche, catalog no. 11836153001) for 10 ml of buffer was used. After rotating the cell tube for 10 to 15 min at 4°C, nuclei were pelleted by centrifugation at 700*g* for 5 min at 4°C. Nuclei pellets were resuspended in 5 ml of Santa Cruz Biotechnology ChIP Lysis Buffer High Salt (catalog no. sc-45001) or RIPA buffer containing PIC. Aliquots of 1 ml containing 20 million nuclei were transferred into 1.5-ml low-bind microfuge tubes. The nuclei suspension was either sonicated immediately or snap-frozen in liquid nitrogen and stored at −80°C.

The nuclei-chromatin suspension in each milliliter was sonicated (Sonics Vibra Cell, Model CV188, with Stepped Tip 1/8"-630-0422) on ice in a cold room (4°C). Sonication was performed with nine cycles of 30 s ON at 60% intensity and 30 s OFF for chromosome modifications (H3k4me1 and H3K27ac) or with eight cycles for transcription factors (P300 and PU.1). The sheared chromatin was centrifuged at 14 thousand rpm (krpm) for 10 to 15 min and then transferred (as for the supernatant) into a new 1.5-ml tube and kept on ice for ChIP.

For ChIP, 50-μl Invitrogen Dynabeads (7×10^8 beads/ml) were used for 20 million cells, either anti-rabbit immunoglobulin G (IgG) (catalog no. 112.03D) or anti-mouse IgG (catalog no. 112.01D), depending on the source of the first antibody. The beads were first washed with PBS/BSA/PIC buffer [1x PBS, 5 mg/ml of BSA (Sigma, A3059-10G, Fraction V), Roche PIC (one mini tablet for 10 ml or one complete tablet for 50 ml, added before use)], and then the washed beads were thoroughly resuspended in 1 ml of PBS/BSA/PIC buffer in a 1.5-ml microfuge tube. The tube was placed on a magnetic rack for 1 min, after which the supernatant was removed. This wash was repeated twice by resuspending beads in 1 ml of PBS/BSA/PIC buffer, rotating for 5 min, and removing the supernatant, as described above. The beads were then coated with antibody by resuspending in 250 μl of PBS/BSA/PIC buffer in each tube, adding 5 μg of antibody, and rotating overnight at 4°C. The following antibodies were used: H3K4me1 (Abcam, catalog no. ab8895), H3K4m3 (Abcam, catalog no. ab8580), H3K27ac (Abcam, catalog no. ab4729), P300 (Santa Cruz Biotechnology, catalog no. sc-585), PU.1 (Santa Cruz Biotechnology, catalog no. sc-352), MafB (Bethyl, catalog no. IHC-101), and Flag M2 antibody (Sigma). After overnight incubation with antibody, the beads were pelleted by placing the tube on a magnetic rack for 1 min, followed by removing the supernatant. The beads were then washed three times with PBS/BSA/PIC buffer.

ChIP was carried out by adding the sheared chromatin suspension to the antibody-coated beads and rotating overnight at 4°C, followed by a series of washes. The beads were first washed once with 1 ml of a low-salt wash buffer (20 mM Tris-HCl at pH 8.0, 150 mM NaCl, 2 mM EDTA, 0.1% SDS, 1% Triton X-100), then twice with a high-salt wash buffer (20 mM Tris-HCl at pH 8.0, 500 mM NaCl, 2 mM EDTA, 0.1% SDS, 1% Triton X-100), three times with an LiCl wash buffer (10 mM Tris-HCl at pH 8.0, 250 mM LiCl, 1 mM EDTA, 1% GEPAL CA630, 1% Na-deoxyholate), and twice with TE buffer. ChIP DNA was eluted by adding 200 μl of ChIP Elution Buffer (Santa Cruz Biotechnology, catalog no. sc-45003, or 1% SDS/0.1 M $NaHCO_3$) to each bead tube, vortexing to resuspend beads, and incubating at 65°C for 1 hour with vortexing every 15 min. After beads were centrifuged for 3 min at RT and placed on a magnetic rack for 1 min, ChIP DNA in the supernatant was transferred to a new tube.

Reversal of cross-links was carried out by incubation at 65°C overnight, and DNA was extracted with an equal volume of phenol:chloroform:isoamyl alcohol (24:24:1). After centrifugation at 14 krpm for 3 min, ChIP DNA in the supernatant was transferred to a 2.0-ml low-bind tube. More DNA was extracted by adding 100 μl of water to the phenol:chloroform phase and repeating the extraction. The DNA extract was combined and mixed with five volumes of PBI buffer (5 M GuHCl, 30% isopropanol) Qiagen MinElute PCR Purification Kit, catalog no. 28004). With the use of 3 M NaAc (at pH 5.2), the pH of the mixture was adjusted to <7.5 before the mixture was applied to the column. The mixture turned back to a yellow color, which is important for DNA to bind to the Qiagen column. DNA was purified according to the manufacturer's instructions and eluted in 30 μl of buffer EB. DNA concentration was measured with Qubit (Thermo Fischer). DNA amounts ranging from 30 ng (P300, PU.1, MafB, and Flag-MafB) to 100 ng (H3K4me1 and H3K27ac) were used to make each library.

ChIP-seq libraries were generated using adaptors from Illumina (catalog no. FC102-1001) and other enzymes and reagents from New England BioLabs, following the Illumina ChIP-seq protocol with some minor modifications. ChIP DNA was end-repaired by T4 DNA polymerase (catalog no. M0203S/L), Klenow DNA polymerase (catalog no. M0210S/L), and T4 PNK (catalog no. M0201S/L) and purified with the Qiagen MinElute PCR Purification Kit. A-base was then added to the 3′ end by Klenow Fragment, 3′ to 5′ exo- (New England BioLabs, catalog no. M0212S/L), and deoxyadenosine triphosphate. The Illumina adaptors (1 μl of 1:10 dilution) were subsequently added to both ends by DNA ligase (catalog no. M2200S/L). The adaptor-ligated DNA was size-selected for 200– to 400–base pair (bp) fragments by 2% low-melting agarose gel (Lonza, catalog no. 50080) and was subsequently purified using a Qiagen MinElute Gel Extraction Kit (catalog no. 28604). Library DNA was amplified in a 100-μl reaction by Phusion PCR Master Mix (New England BioLabs, catalog no. F-531S), with primers SolexaPCR_F (5′- AAT GAT ACG GCG ACC ACC GAG ATC TAC ACT CTT TCC CTA CAC GAC GCT CTT CCG ATC T -3′) and SolexaPCR_R (5′- CAA GCA GAA GAC GGC ATA CGA GCT CTT CCG ATC T -3′). Libraries of H3K4me1 and H3K27ac were amplified by predenaturing at 98°C for 30 s; followed by 10 cycles of (i) 98°C for 10 s, (ii) 65°C for 30 s, and (iii) 72°C for 30 s; and then an extra 5 min at 72°C at the end. For the P300 and PU.1 libraries, 12 cycles of PCR were used. After library DNA was purified, library concentration was measured by Qubit, and size distribution was determined by Bioanalyzer (Agilent Technologies). Each ChIP-seq library was sequenced on one lane of Illumina GAIIx or Illumina HiSeq 2000 with 1×36–bases of read length. Biological replicates from two independently derived Maf-DKO macrophage lines (from two different mice) were sequenced, one of which was determined to be tetraploid. Comparison of ChIP-seq and gene expression data revealed no substantive differences between the two lines.

ChIP-seq analysis

Although a DNAnexus pipeline was used for peak detection algorithms (*38*) and alignments of raw data (uploaded fastq files), the aligned data (BAM files) were subsequently downloaded and processed with a custom R pipeline for bioinformatics analyses. A threshold based on the number of sequenced tags (Nseq) has been set up as Nseq/7,000,000. All regions with a number of repeated tags (with identical sequences/coordinates) above this threshold were filtered out to remove possible sequencing and/or alignment artifacts. To accurately represent and further process the ChIP-seq and input control signals, the Watson and Crick strand tags need to be merged after elongation or size extension to the gel-purified fragment size. The optimal elongation size of each ChIP-seq experiment was estimated in silico by employing a stepwise 10-bp chromosomal sequence tag shifting and score multiplication. Tag coordinates were subsequently elongated according to this estimated DNA fragment size, corresponding to the tag shift maximizing the score. Then, a nucleotide score representing the genome-wide overlap of elongated tags was computed across both strands. Wiggle (WIG) files for genome-wide scores were generated after a binning step, and the average enrichment score was calculated every 50 bp.

When input experiments were available, enrichment scores from WIG files were scaled and used as follows: Owing to the size of the genome and the relatively low frequencies of binding events, we assumed that most (>90%) of the obtained scores from the ChIP-seq experiments represent a background (BG) level. We therefore used the genome-wide average

score in each experiment to estimate the BG level. Using these average scores, it is possible to rescale the scores accordingly, acting as normalization and reducing the interexperiment differences due to effects of different sequencing depths and/or fragment sizes.

We employed an input subtraction step for each experiment, using the normalized file for the input control. This step not only allows for correction of overrepresentations of certain genomic regions due to possible (un)favorable events during sonication and/or DNA sequencing but also serves to reduce the signal-to-noise ratio, especially for experiments with low enrichment values.

H3K4me1-enriched regions were extracted from all samples (Maf-DKO, BMMs, PMs, pro-B, ES, liver, and mouse embryonic fibroblasts; annotation files available) (*12*, *13*). All regions close to annotated TSSs (<2 kb) were omitted, and the union of the resulting regions was used as a reference to extract enrichment scores of H3K4me1 derived from all samples. R scripts were developed and used for retrieving bin scores around the center of these annotations (±2 kb). These scores and their original genomic coordinates were utilized to recenter values around the H3K4me1-enriched regions, by means of linear interpolation. In total, 1000 points were interpolated for each selected region, which resulted in a 1000-column matrix. These matrices were loaded, viewed, and color-scaled according to sample read depth using Java TreeView (*39*). Finally, these matrices were assembled by sample.

A large selection of regions enriched for H3K27ac and H3K4me1 was applied to WT and DKO samples. All regions in close proximity to any annotated TSSs (<2 kb) were ignored, and the union of all regions has been defined as putative active enhancers (annotation file available). The binned enrichments of PU.1 samples in these regions were merged and compared among tissues using a nonparametric Spearman correlation method.

Heat maps were created with the same strategy as for fig. S1A (but focused on regions isolated with previously described isolated peaks). For each reference experiment (H3K27ac or P300), the regions were sorted by increasing average enrichment score, and the other heat maps were arranged with respect to this initial sorting for corresponding experiments.

For the heat map in Fig. 4B, SRA files for ES cell ChIP-seq data (*13*) were converted into FASTQ format before being uploaded and processed on the DNAnexus platform. Two replicate H3K27ac ES cell ChIP-seq BAM files were merged, and BAM files were then processed by DNAnexus, as described above. All reads from BAM files with a MAPQ (MAPping Quality) value <10 were filtered out so that only confidently mapped reads were retained. The numbers of reads in each relevant region were counted according to their start position. Each read with a start position outside the region was not taken into account, regardless of the strand considered.

The read-counts matrix was normalized by considering each mark independently of the others. For each antibody, the number of reads for each region was normalized relative to the total number of confidently mapped reads of the least-sequenced sample. Because these regions are not homogeneous in length, counts were normalized to the size of the region in kilo–base pairs. Next, considering each antibody independently, counts exceeding the 95th percentile were set to this value to avoid bias due to outliers. Values were then set to the range 0 to 1 and sorted according to the Maf-DKO region's H3K27ac level. Finally a 2-means clustering (k = 2) was performed on H3K27ac marks for the three cell types (Maf-DKO macrophages, WT BMMs, and ES cells). The analysis depicted in Fig. 6E used the same approach for PU.1 and p300 marks in Maf-DKO macrophages, WT BMMs, and AMs. All analyses were performed using Samtools, R (version 2.14), and gene-e (version 3.0.202).

Motif search at enhancer loci

Motifs analysis was performed using HOMER2 (http://homer.salk.edu/homer/) on 10,232 DKO-only peaks (the union of H3K27ac and P300 selection based on enrichment in Maf-DKO macrophages versus WT BMMs) and 88 self-renewal gene–associated peaks from within the DKO-only selection. Among other things, HOMER2 screens for enrichment of known motifs. The HOMER perl script findMotifsGenome.pl was used with the mm9 mouse genome as a background (random genomic sequences sampled according to GC content of input sequences).

GSEA analysis

Maf-DKO versus WT log2 ratios were computed for each probe set from normalized data by RMA method (robust multiarray average). H3K27ac DKO-only regions and P300 DKO-only peaks were associated with nearby genes via GREAT (http://bejerano.stanford.edu/great/public/html/index.php) (*20*).

Next, the union of DKO-only enhancer–associated genes was considered. For the purposes of GSEA (www.broad.mit.edu/gsea), 7499 Maf-DKO–versus–WT ratios of these non-unique DKO-only enhancer–associated genes (a gene can have multiple associated probe sets) were selected. Two stem cell modules were used as gene sets: (i) an adult tissue stem module regrouping genes coordinately up-regulated in a compendium of mouse adult tissue stem cells and (ii) a second module composed of genes coordinately up-regulated in mouse ES cells, as defined in (*21*). These two sets were extracted from the public Molecular Signatures Database (MSigDB) (www.broadinstitute.org/gsea/msigdb/index.jsp).

Single-cell– and bulk cell–population gene expression profiling and analysis

Single cells were sorted, using the autoclone module on an AriaIII sorter (Becton Dickinson), directly into 96-well plates in the CellsDirect Reaction Mix (Invitrogen). Individual cell lysis, cDNA synthesis, and amplification were carried out via single-cell microfluidic real-time PCR using Dynamic Array integrated fluidic circuits (IFCs) (Biomark Fluidigm), according to the Fluidigm Advanced Development Protocol. Preamplified products (20 cycles) were diluted by a factor of 5 before analysis with Universal PCR Master Mix and inventoried TaqMan gene expression assays (Applied Biosystems) in 96.96 Dynamic Arrays on a BioMark System (Fluidigm). For single-cell analysis, cycle threshold (Ct) values were calculated from the system's software (BioMark Real-time PCR Analysis, Fluidigm) and filtered according to a set of quality control rules (outlined below).

For single-cell gene expression level analysis, the raw data were preprocessed as follows: For each gene, including controls, those with a difference of duplicate Ct values ≥2.0 were considered inconsistent and removed. If the control gene (*GAPDH*) was not expressed or filtered out, the whole sample was removed. If Ct_{Call} = FAILED but the sample showed expression of at least one other gene, it was considered as "not expressed," and the Ct value was set to 31.9. The relative expression values were calculated according to the following formula: relative expression = 32 – mean (technical replicates).

R scripts with the ggplot2 package were used to construct violin plots and line plots on relative expression values. Results shown in the figures are representative of two independent experiments.

The RGL package was used for PCA to cluster relative expression values on a three-dimensional (3D) principal component space. PCA coordinates were clustered by the k-means method (*40*) using R script.

For bulk cell populations, total RNA was isolated from cells using the Quiagen RNAeasy kit and treated with RNAse-free DNAseI (Qiagen) before elution from columns. For gene expression profiling, RNA from Maf-DKO macrophages was extracted using the RNeasy Mini Kit (Qiagen) and QIAshredder columns (Qiagen) according to the manufacturer's instructions. On-column DNA digestion was performed. Total RNA (50 ng) was used for reverse transcription to cDNA using SuperScriptTM II RT (Invitrogen), Oligo(dT) primers (Invitrogen), and RNaseOUT (Invitrogen). Specific gene target amplification was performed according to Fluidigm protocols. Selected TaqMan Gene Expression assays (20x) were pooled and diluted with water by a factor of 100, so that each assay is at a final concentration of 0.2x in the pooled assay mix. For preamplification of each cDNA sample, 1.25 μl of the respective cDNA, 1.25 μl of pooled assay mix, and 2.5 μl of TaqMan PreAmp Master Mix (Applied Biosystems, catalog no. 4391128) were combined to a final volume of 5 μl in 1 well of a 96-well QPCR plate. cDNA samples were amplified using the following program: (i) 95°C for 10 min, (ii) 95°C for 15 s, and (iii) 60°C for 4 min; then repeat steps (ii) and (iii) 14 times. Amplified cDNA samples were diluted at 1:5 using 20 μl of water. For Fluidigm 96.96 Dynamic Array IFC analysis, 5 μl of each cDNA sample and 5 μl of each TaqMan probe (20x) were loaded on the chip.

Microfluidic real-time PCR using Dynamic Array IFCs (Biomark Fluidigm) was performed

with Universal PCR Master Mix and inventoried TaqMan gene expression assays (Applied Biosystems) in 96.96 Dynamic Arrays on a BioMark System (Fluidigm). Ct values were calculated from the system's software (BioMark Real-time PCR Analysis, Fluidigm) and filtered according to a set of quality control rules (outlined below).

Gene filter: (i) For each gene, including controls, data with Ct_{Call} = FAILED and $Ct_{Quality}$ < threshold were removed. (ii) For each gene, including controls, only Ct values that met the following criterion were considered: at least 2.0 below the lowest Ct value of no-RT or no-RNA controls. The purpose of this was to filter out inefficient probes and genes with very low expression. (iii) For each gene, including controls, values with a difference ≥2.0 between Ct_{max} and Ct_{min} of replicates were considered to be inconsistent and were removed. (iv) If a gene was removed [according to filters (i) to (iii)] from uninfected or control shRNA samples, it was removed from all samples. Sample filter: (i) If the control gene (*GAPDH*) was not expressed or was removed according to gene filters (i) to (iii), the whole sample was removed. (ii) If a control gene (*GAPDH*) had a Ct value with a ≥2.0 difference from the average Ct value of control genes in all samples, the whole sample was removed to eliminate nonspecific shRNA and normalization artifacts. For the heat map, each Ct value was normalized against *GAPDH* using the following formula: relative $\text{expression}_{Sample} = 2^{[\text{mean}(Ct_{GAPDH}) - Ct_{Sample}]} \times 100$. For each gene, heat maps in Fig. 2C present normalized values as percent change over average expression in noninfected and control lacZ shRNA–infected cell samples.

Furthermore, z scores were calculated for each gene of shRNA-infected cell samples based on uninfected and lacZ control shRNA–infected samples, as described in (*31*). Briefly, a statistic z was defined for each observation o_{ij} of transcript i in each shRNA experiment j

$$z_{ij} = \frac{o_{ij} - m_i}{s_i}$$

where m_i and s_i are, respectively, the mean and variance of the expression of transcript i in the control experiments (uninfected and lacZ shRNAs).

Two false discovery rate (FDR)–based approaches were used to obtain confidence estimates of the observed z scores. First, a per-gene confidence score was defined by using the variation of that gene's expression in the control shRNA experiments. Permuted scores z_k^{ij} (where k is the number of permutations) as a null distribution and the FDR for a given z score z_{ij} for gene i in experiment j are given as

$$FDR_i(z) = \frac{E_k(\#\{z_k^{ij} | z_k^{ij} \rangle z; j \in P\})}{\#\{z^{ij} > z; j = 1, \ldots, n\}}$$

where n is the number of shRNA experiments, E is the expectation, the confidence for z is $conf(z) = 1 - FDR(z)$, and $P = \{c | z^{ic} \rangle z; c = 1, \ldots, n\}$.

In the second approach, we defined a per-shRNA confidence score for each measurement of a self-renewal gene by calculating an FDR based on the variation of expression in *GAPDH* and myeloid genes. Formally, we let $z_{ij}, \ldots, z_{nj}$ be the scores for the jth experiment (shRNA) and assumed the first l transcripts were control transcripts whose expression did not change in response to any component. We defined $\tilde{z}_{ij} = \frac{z_{ij} - \tilde{m}_j}{\tilde{s}_j}$ where now $\tilde{m}_j$ and $\tilde{s}_j$ are, respectively, the mean and variance of the z scores of the control transcripts $1, \ldots, l$ in the jth shRNA experiment. We performed l permutations, as described above, by swapping each observed z score with a control transcript score and computing z, then computing an FDR as above. For the construction of the network model, we considered only values with an FDR <0.05 and where at least half of the replicates fulfilled these criteria. Circle sizes reflect the number of times the expression of a gene is affected by the perturbation of another gene, scoring each gene and shRNA replicate separately.

For time-course analysis of self-renewal gene expression in Maf-DKO macrophages and WT BMMs, values were obtained by subtracting the considered gene mean across all samples from an individual raw score and then dividing the difference by the considered gene SD across all samples. Statistical analysis was performed using R (version 2.14), heat maps were created using the software gene-e (Broad Institute), and network diagrams were generated with Cytoscape (version 3.0.2).

Construction of self-renewal gene network

To investigate the potential for cross-regulation between self-renewal genes, data from a quadruplicate nanofluidic real-time PCR on Fluidigm array, presented in Fig. 2C, were reanalyzed, and z score computations were used to decide whether a given shRNA regulated its specific target mRNA and whether this regulation affected the expression of other genes (control or self-renewal genes). Computations were performed according to per-gene and per-shRNA computation methods, as described above and with the following additional considerations: (i) With the exception of Myc and Chd1, for which only one shRNA was found to effectively knock down the expression of said target, all self-renewal genes were effectively targeted by two shRNAs. Therefore, to balance the number of replicates per sample so as not to undercount the number of regulations relative to other shRNAs, all of the regulations where shMyc and shChd1 were involved were counted twice for subsequent computations. (ii) The regulation of a gene upon expression of a given shRNA was not taken into account unless more than two replicates for gene expression were significantly regulated, regardless of the computation method considered. This concerned only 13 of 86 regulations that were subsequently filtered out for the per-gene computation and none for the per-shRNA computation. (iii) All autoregulations (shGene-x regulating Gene-x) were considered trivial and were thus removed. (iv) Baseline expression of all genes was determined according to average expression levels in control samples.

Together, these data were used to construct a gene regulation network (depicted in Fig. 3B). The size of the bubble for each gene in the network was drawn relative to the number of times the gene was regulated by an shRNA for which it was not the direct target. A line was drawn to connect genes when the shRNA regulated the expression of a nontarget RNA at least two of the four times tested for at least one of two shRNAs in both computations. Given that there are two shRNAs per gene, four gene expression replicates, and two computation methods, 16 regulations could be evaluated for a given shRNA. When all 16 regulations were significant and the same, the lines in Fig. 3B were drawn in black; otherwise, they were drawn in gray. The red end of the arrows indicates a repression of the gene by the shRNA, whereas the blue end indicates activation. Genes targeted only by shRNA with statistical significance in only one computation (single nodes) were not represented.

REFERENCES AND NOTES

1. S. J. Jenkins *et al.*, Local macrophage proliferation, rather than recruitment from the blood, is a signature of T_H2 inflammation. *Science* **332**, 1284–1288 (2011). pmid: 21566158
2. C. Schulz *et al.*, A lineage of myeloid cells independent of Myb and hematopoietic stem cells. *Science* **336**, 86–90 (2012). doi: 10.1126/science.1219179; pmid: 22442384
3. S. Yona *et al.*, Fate mapping reveals origins and dynamics of monocytes and tissue macrophages under homeostasis. *Immunity* **38**, 79–91 (2013). pmid: 23273845
4. D. Hashimoto *et al.*, Tissue-resident macrophages self-maintain locally throughout adult life with minimal contribution from circulating monocytes. *Immunity* **38**, 792–804 (2013). doi: 10.1016/j.immuni.2013.04.004; pmid: 23601688
5. M. H. Sieweke, J. E. Allen, Beyond stem cells: Self-renewal of differentiated macrophages. *Science* **342**, 1242974 (2013). doi: 10.1126/science.1242974; pmid: 24264994
6. E. L. Gautier *et al.*, Gene-expression profiles and transcriptional regulatory pathways that underlie the identity and diversity of mouse tissue macrophages. *Nat. Immunol.* **13**, 1118–1128 (2012).pmid: 23023392
7. A. Aziz, E. Soucie, S. Sarrazin, M. H. Sieweke, MafB/c-Maf deficiency enables self-renewal of differentiated functional macrophages. *Science* **326**, 867–871 (2009). doi: 10.1126/science.1176056; pmid: 19892988
8. G. Fejer *et al.*, Nontransformed, GM-CSF-dependent macrophage lines are a unique model to study tissue macrophage functions. *Proc. Natl. Acad. Sci. U.S.A.* **110**, E2191–E2198 (2013). doi: 10.1073/pnas.1302877110; pmid: 23708119
9. N. D. Heintzman *et al.*, Histone modifications at human enhancers reflect global cell-type-specific gene expression. *Nature* **459**, 108–112 (2009). doi: 10.1038/nature07829; pmid: 19295514
10. G. Natoli, Maintaining cell identity through global control of genomic organization. *Immunity* **33**, 12–24 (2010). doi: 10.1016/j.immuni.2010.07.006; pmid: 20643336
11. S. Ghisletti *et al.*, Identification and characterization of enhancers controlling the inflammatory gene expression program in macrophages. *Immunity* **32**, 317–328 (2010). doi: 10.1016/j.immuni.2010.02.008; pmid: 20206554
12. S. Heinz *et al.*, Simple combinations of lineage-determining transcription factors prime cis-regulatory elements required for macrophage and B cell identities. *Mol. Cell* **38**, 576–589 (2010). doi: 10.1016/j.molcel.2010.05.004; pmid: 20513432
13. M. P. Creyghton *et al.*, Histone H3K27ac separates active from poised enhancers and predicts developmental state. *Proc. Natl. Acad. Sci. U.S.A.* **107**, 21931–21936 (2010). doi: 10.1073/pnas.1016071107; pmid: 21106759
14. G. Natoli, J. C. Andrau, Noncoding transcription at enhancers: General principles and functional models. *Annu. Rev. Genet.* **46**, 1–19 (2012). doi: 10.1146/annurev-genet-110711-155459; pmid: 22905871

15. D. Gosselin *et al*., Environment drives selection and function of enhancers controlling tissue-specific macrophage identities. *Cell* **159**, 1327–1340 (2014). doi: 10.1016/j.cell.2014.11.023; pmid: 25480297
16. Y. Lavin *et al*., Tissue-resident macrophage enhancer landscapes are shaped by the local microenvironment. *Cell* **159**, 1312–1326 (2014). pmid: 25480296
17. R. Ostuni *et al*., Latent enhancers activated by stimulation in differentiated cells. *Cell* **152**, 157–171 (2013). doi: 10.1016/j.cell.2012.12.018; pmid: 23332752
18. A. Visel *et al*., ChIP-seq accurately predicts tissue-specific activity of enhancers. *Nature* **457**, 854–858 (2009). doi: 10.1038/nature07730; pmid: 19212405
19. A. Rada-Iglesias *et al*., A unique chromatin signature uncovers early developmental enhancers in humans. *Nature* **470**, 279–283 (2011). doi: 10.1038/nature09692; pmid: 21160473
20. C. Y. McLean *et al*., GREAT improves functional interpretation of cis-regulatory regions. *Nat. Biotechnol.* **28**, 495–501 (2010). doi: 10.1038/nbt.1630; pmid: 20436461
21. D. J. Wong *et al*., Module map of stem cell genes guides creation of epithelial cancer stem cells. *Cell Stem Cell* **2**, 333–344 (2008). doi: 10.1016/j.stem.2008.02.009; pmid: 18397753
22. N. Ivanova *et al*., Dissecting self-renewal in stem cells with RNA interference. *Nature* **442**, 533–538 (2006). doi: 10.1038/nature04915; pmid: 16767105
23. J. Z. Zhang *et al*., Screening for genes essential for mouse embryonic stem cell self-renewal using a subtractive RNA interference library. *Stem Cells* **24**, 2661–2668 (2006). doi: 10.1634/stemcells.2006-0017; pmid: 16960129
24. M. Pritsker, N. R. Ford, H. T. Jenq, I. R. Lemischka, Genomewide gain-of-function genetic screen identifies functionally active genes in mouse embryonic stem cells. *Proc. Natl. Acad. Sci. U.S.A.* **103**, 6946–6951 (2006). doi: 10.1073/pnas.0509861103; pmid: 16621925
25. J. Hall *et al*., Oct4 and LIF/Stat3 additively induce Krüppel factors to sustain embryonic stem cell self-renewal. *Cell Stem Cell* **5**, 597–609 (2009). doi: 10.1016/j.stem.2009.11.003; pmid: 19951688
26. J. Jiang *et al*., A core Klf circuitry regulates self-renewal of embryonic stem cells. *Nat. Cell Biol.* **10**, 353–360 (2008). doi: 10.1038/ncb1698; pmid: 18264089
27. A. Gaspar-Maia *et al*., Chd1 regulates open chromatin and pluripotency of embryonic stem cells. *Nature* **460**, 863–868 (2009).pmid: 19587682
28. G. Hu *et al*., A genome-wide RNAi screen identifies a new transcriptional module required for self-renewal. *Genes Dev.* **23**, 837–848 (2009). doi: 10.1101/gad.1769609; pmid: 19339689
29. L. Ding *et al*., A genome-scale RNAi screen for Oct4 modulators defines a role of the Paf1 complex for embryonic stem cell identity. *Cell Stem Cell* **4**, 403–415 (2009). doi: 10.1016/j.stem.2009.03.009; pmid: 19345177
30. B. D. Macarthur, A. Ma'ayan, I. R. Lemischka, Systems biology of stem cell fate and cellular reprogramming. *Nat. Rev. Mol. Cell Biol.* **10**, 672–681 (2009). pmid: 19738627
31. I. Amit *et al*., Unbiased reconstruction of a mammalian transcriptional network mediating pathogen responses. *Science* **326**, 257–263 (2009). doi: 10.1126/science.1179050; pmid: 19729616
32. Y. Bakri *et al*., Balance of MafB and PU.1 specifies alternative macrophage or dendritic cell fate. *Blood* **105**, 2707–2716 (2005). doi: 10.1182/blood-2004-04-1448; pmid: 15598817
33. R. Gentek, K. Molawi, M. H. Sieweke, Tissue macrophage identity and self-renewal. *Immunol. Rev.* **262**, 56–73 (2014). doi: 10.1111/imr.12224; pmid: 25319327
34. L. C. Davies *et al*., Distinct bone marrow-derived and tissue-resident macrophage lineages proliferate at key stages during inflammation. *Nat. Commun.* **4**, 1886 (2013). doi: 10.1038/ncomms2877; pmid: 23695680
35. S. J. Jenkins *et al*., IL-4 directly signals tissue-resident macrophages to proliferate beyond homeostatic levels controlled by CSF-1. *J. Exp. Med.* **210**, 2477–2491 (2013). doi: 10.1084/jem.20121999; pmid: 24101381
36. J. A. Hamilton, G. A. Whitty, I. Kola, P. J. Hertzog, Endogenous IFN-alpha beta suppresses colony-stimulating factor (CSF)-1-stimulated macrophage DNA synthesis and mediates inhibitory effects of lipopolysaccharide and TNF-alpha. *J. Immunol.* **156**, 2553–2557 (1996). pmid: 8786318
37. H. Motohashi, K. Igarashi, MafB as a type I interferon rheostat. *Nat. Immunol.* **11**, 695–696 (2010). doi: 10.1038/ni0810-695; pmid: 20644578
38. A. Valouev *et al*., Genome-wide analysis of transcription factor binding sites based on ChIP-Seq data. *Nat. Methods* **5**, 829–834 (2008). doi: 10.1038/nmeth.1246; pmid: 19160518
39. A. J. Saldanha, Java Treeview—Extensible visualization of microarray data. *Bioinformatics* **20**, 3246–3248 (2004). doi: 10.1093/bioinformatics/bth349; pmid: 15180930
40. J. A. Hartigan, M. A. Wong, A *K*-means clustering algorithm. *J. R. Stat. Soc. C Appl. Stat.* **28**, 100–108 (1979).

ACKNOWLEDGMENTS

We thank N. Spies for advice on statistical analysis, L. Chasson for immunofluorescence processing, and S. Vargas-Aguilar for reagents. The data presented in this manuscript are tabulated in the main paper and in the supplementary materials. Sequencing data can be accessed in Gene Expression Omnibus under accession number GSE75722. E.L.S. received fellowships from the European Union Marie Curie program and La Fondation de France. E.L.S. and P.D. were supported by La Ligue Nationale Contre le Cancer (Equipe Labelisée), K.M. by a Human Frontier Science Program long-term fellowship and Stiftung Charité, L.G. by the Fondation ARC pour la Recherche sur le Cancer, J.-C.A. by the Fondation pour la Recherche Médicale (grant AJE20130728183), A.S. by the NIH National Institute on Aging (grant P01AG036695), and M.H.S. by the Agence Nationale de la Recherche (grant ANR-11-BSV3-026-01) and Institut National du Cancer (grant 13-10/405/AB-LC-HS). M.H.S. is an Einstein-BIH fellow and Fondation pour la Recherche Médicale (grant DEQ20110421320) and INSERM-Helmholtz group leader.

SUPPLEMENTARY MATERIALS

www.sciencemag.org/content/351/6274/aad5510/suppl/DC1
Figs. S1 to S13
Tables S1 to S4
References

29 September 2015; accepted 22 December 2015
Published online 21 January 2016;
10.1126/science.aad5510

Science
AAAS

Lineage-specific enhancers activate self-renewal genes in macrophages and embryonic stem cells

Erinn L. Soucie *et al.*

Science **351**, (2016);
DOI: 10.1126/science.aad5510

This copy is for your personal, non-commercial use only.

If you wish to distribute this article to others, you can order high-quality copies for your colleagues, clients, or customers by clicking here.

Permission to republish or repurpose articles or portions of articles can be obtained by following the guidelines here.

The following resources related to this article are available online at www.sciencemag.org (this information is current as of February 11, 2016):

Updated information and services, including high-resolution figures, can be found in the online version of this article at:
/content/351/6274/aad5510.full.html

Supporting Online Material can be found at:
/content/suppl/2016/01/20/science.aad5510.DC1.html

This article **cites 40 articles**, 13 of which can be accessed free:
/content/351/6274/aad5510.full.html#ref-list-1

This article appears in the following **subject collections:**
Genetics
/cgi/collection/genetics
Immunology
/cgi/collection/immunology

Downloaded from on February 11, 2016

Science (print ISSN 0036-8075; online ISSN 1095-9203) is published weekly, except the last week in December, by the American Association for the Advancement of Science, 1200 New York Avenue NW, Washington, DC 20005. Copyright 2016 by the American Association for the Advancement of Science; all rights reserved. The title *Science* is a registered trademark of AAAS.

REPORTS

PHOTOCATALYSIS

Asymmetric copper-catalyzed C-N cross-couplings induced by visible light

Quirin M. Kainz, Carson D. Matier, Agnieszka Bartoszewicz, Susan L. Zultanski, Jonas C. Peters,* Gregory C. Fu*

Despite a well-developed and growing body of work in copper catalysis, the potential of copper to serve as a photocatalyst remains underexplored. Here we describe a photoinduced copper-catalyzed method for coupling readily available racemic tertiary alkyl chloride electrophiles with amines to generate fully substituted stereocenters with high enantioselectivity. The reaction proceeds at −40°C under excitation by a blue light-emitting diode and benefits from the use of a single, Earth-abundant transition metal acting as both the photocatalyst and the source of asymmetric induction. An enantioconvergent mechanism transforms the racemic starting material into a single product enantiomer.

Photochemistry can furnish reactive intermediates that would otherwise be difficult to access under synthetically useful conditions. Its application in organic synthesis has therefore expanded rapidly during the past decades (*1*), most recently in the context of enantioselective photoredox catalysis with transition metals (*2*–*4*). With several recent noteworthy exceptions, each of which involves the α-functionalization of carbonyl compounds by a chiral iridium catalyst (*5*–*7*), the metal-catalyzed methods require two catalysts, (i) a transition metal complex that undergoes photoexcitation and serves as a site for redox chemistry and (ii) a separate chiral catalyst that effects enantioselective bond formation. Transition metal–free photoredox catalysis has also been reported (*8*, *9*).

Division of Chemistry and Chemical Engineering, California Institute of Technology (Caltech), Pasadena, CA 91125, USA.
*Corresponding author. E-mail: jpeters@caltech.edu (J.C.P.); gcfu@caltech.edu (G.C.F.)

We have been interested in photocatalytic approaches to the construction of C-N bonds (*10*), given the high value of amines in fields ranging from biology to chemistry to materials science (*11*). Whereas initial efforts to develop transition metal–catalyzed C-N cross-coupling reactions focused on the use of aryl and alkenyl halides as the electrophilic coupling partner (*12*, *13*), during the past few years, alkyl halides that are not suitable substrates for classic S_N2 reactions have emerged as useful coupling partners under the combined action of light and copper catalysis (*14*, *15*). To date, progress has not yet been reported in the development of an asymmetric variant of these reactions, and the use of copper as a photoredox catalyst (*16*) is uncommon in comparison with the use of precious metals such as iridium and ruthenium. Here we describe a copper-catalyzed enantioconvergent cross-coupling of racemic tertiary alkyl halides that is induced by visible light, a process that lies at the intersection of several important dimensions of modern chemical catalysis (Fig. 1A).

Although considerable advances have recently been reported in the development of enantioconvergent cross-couplings of racemic secondary alkyl electrophiles with carbon nucleophiles to form C-C bonds (*17*–*19*), no highly effective methods have yet been described for tertiary alkyl halides, which require differentiation of three distinct carbon substituents by the catalyst in order to deliver high enantioselectivity. In the field of asymmetric synthesis as a whole, highly stereoselective reactions involving tertiary electrophiles are relatively uncommon, despite the fact that fully substituted carbons are a common motif in organic molecules (*20*). We anticipated that the radical mechanism that we have postulated for C-X bond cleavage in the presence of copper and light (vide infra) (*14*, *15*)

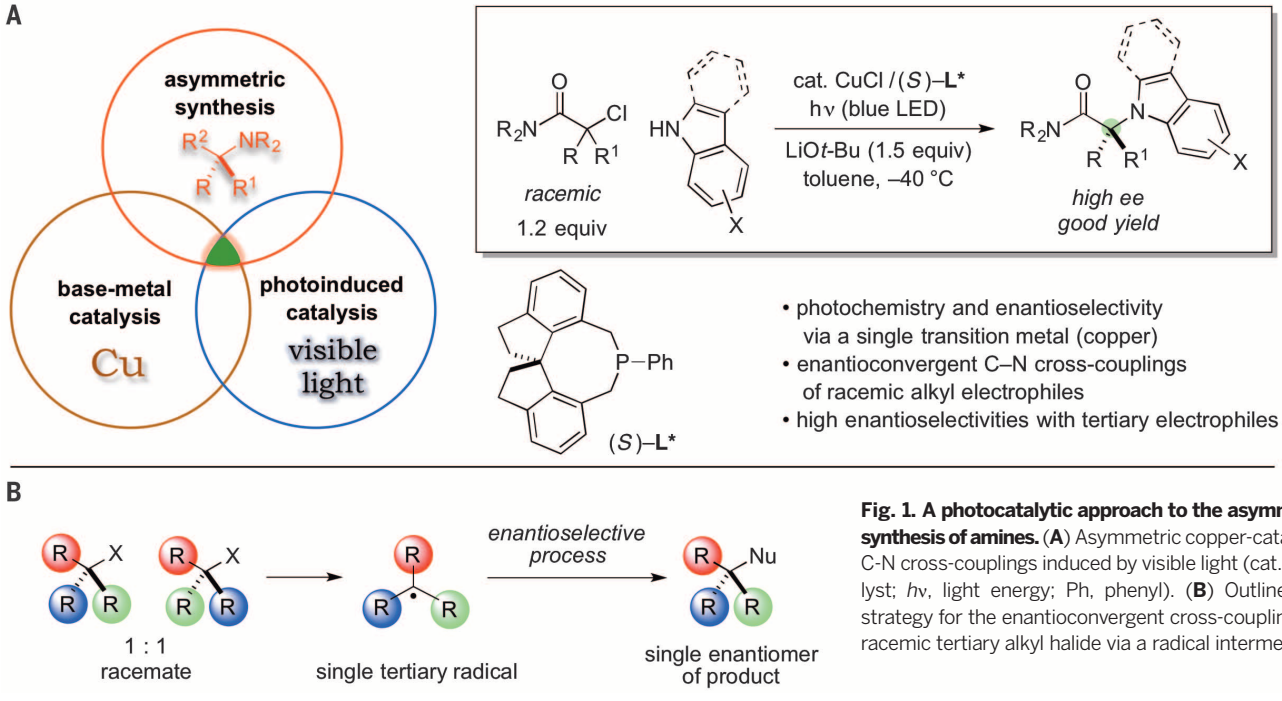

Fig. 1. A photocatalytic approach to the asymmetric synthesis of amines. (**A**) Asymmetric copper-catalyzed C-N cross-couplings induced by visible light (cat., catalyst; *hν*, light energy; Ph, phenyl). (**B**) Outline of a strategy for the enantioconvergent cross-coupling of a racemic tertiary alkyl halide via a radical intermediate.

Downloaded from on February 11, 2016

might enable us to surmount this challenge, because a single, comparatively stable tertiary radical could be formed from a racemic mixture of electrophiles (Fig. 1B).

Another issue was whether common chiral ligands such as phosphines would even bind to copper, much less induce high enantioselectivity in the C-N bond–forming process, in the presence of a much more abundant nucleophilic coupling partner. Previously described methods for photoinduced copper-catalyzed N-alkylation used CuI as a precatalyst with no added ligand (*14*, *15*).

As a model coupling process, we examined the reaction of carbazole—a heterocycle that occurs in bioactive molecules, including *N*-*tert*-alkyl–substituted compounds (*21*, *22*)—with an α-halocarbonyl compound, representing a class of electrophiles that has not previously been used in photoinduced copper-catalyzed cross-couplings. Upon investigating a range of reaction parameters, we discovered that irradiation of the cross-coupling partners at –40°C for 16 hours in the presence of CuCl, a chiral phosphine (**L***), and a Brønsted base provides the desired product in 95% yield and 95% enantiomeric excess (ee) (Fig. 2A, entry 1). In contrast to our earlier studies of photoinduced copper-catalyzed N-alkylations, this process operates under visible light from a blue light-emitting diode (rather than under an ultraviolet source) and at relatively low catalyst loading [1.0 mole percent (mol %) rather than 10 mol %]. A catalyst loading of 0.25 mol % led to only a modest loss in yield and no erosion in ee (entry 2, ~300 turnovers; previously, the highest turnover number for a photoinduced copper-catalyzed N-alkylation was about nine) (*14*, *15*).

Control experiments established that copper (Fig. 2A, entry 3; the alkyl halide is recovered quantitatively) and light (entry 4) are necessary to achieve C-N bond formation under these conditions. Furthermore, essentially no C-N coupling (<1%) occurs when the tertiary alkyl chloride, carbazole, and lithium *tert*-butoxide (Li*O*t-Bu) are heated at 80°C in toluene for 16 hours. Our concern that a phosphine (**L***) might not bind effectively to copper in the presence of a stoichiometric quantity of the nucleophile appears to be unfounded, as evidenced by our observation of high enantiomeric excess in the C-N coupling (entry 1) and of an enhanced rate in the presence of the ligand [ligand-accelerated catalysis (*23*); entry 1 versus entry 5]. From a practical point of view, it is worth noting that CuCl and the chiral phosphine are commercially available and that the process is not highly moisture-sensitive (entry 6).

We examined the scope of this photoinduced copper-catalyzed method for enantioconvergent N-alkylation by racemic tertiary alkyl halides (Fig. 2B). For couplings of carbazole with *N*-acylindoline–derived electrophiles, good to excellent

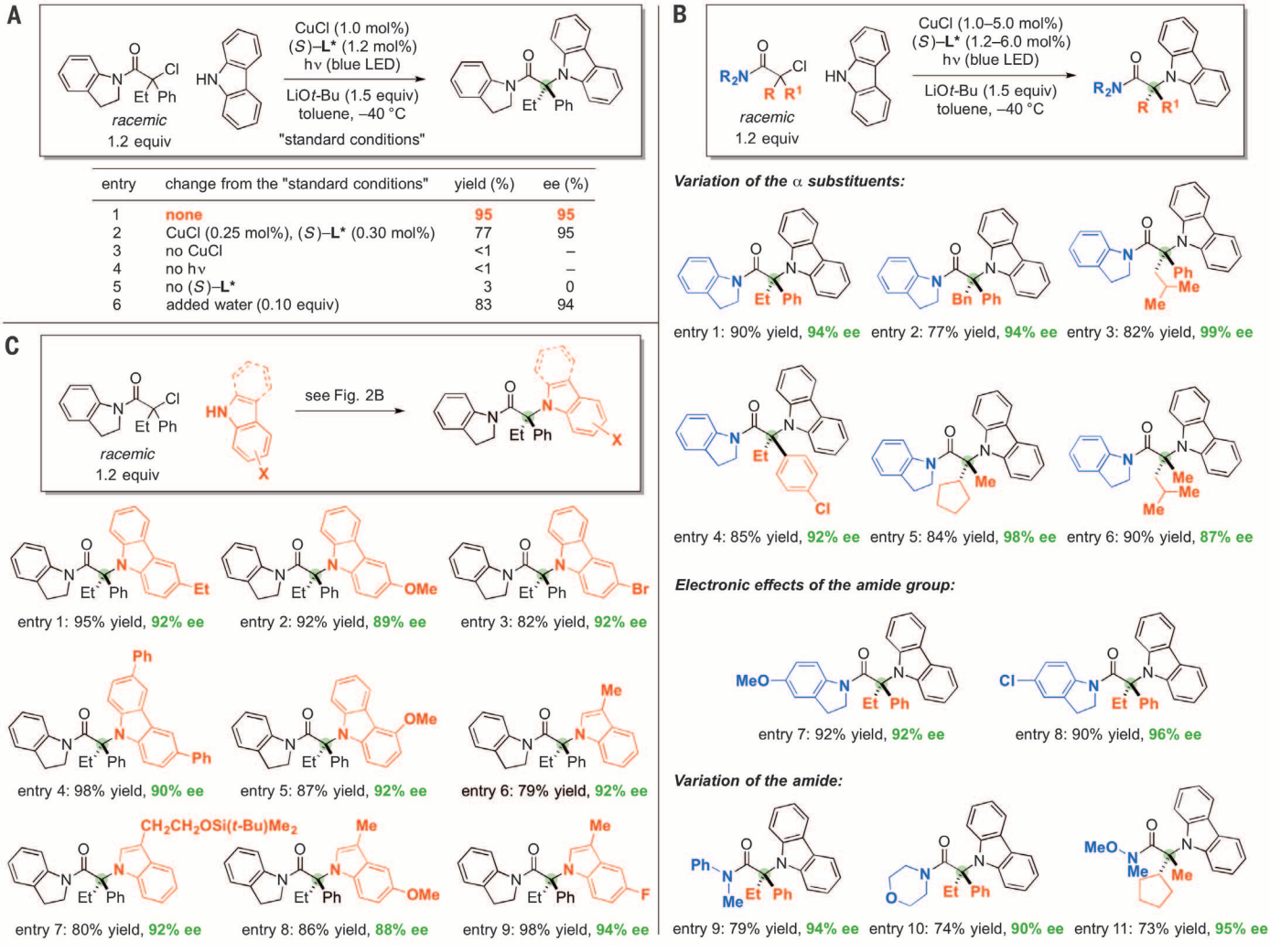

entry	change from the "standard conditions"	yield (%)	ee (%)
1	none	95	95
2	CuCl (0.25 mol%), (*S*)–**L*** (0.30 mol%)	77	95
3	no CuCl	<1	–
4	no hν	<1	–
5	no (*S*)–**L***	3	0
6	added water (0.10 equiv)	83	94

Fig. 2. Asymmetric copper-catalyzed C-N cross-couplings induced by visible light. (**A**) Effect of changes in the reaction parameters. Yields were determined through analysis by proton nuclear magnetic resonance (^{1}H NMR) spectroscopy with the aid of an internal standard. (**B**) Scope of the reaction with respect to the electrophile. Yields were determined by isolation after chromatographic purification. (**C**) Scope of the reaction with respect to the nucleophile. Yields were determined by isolation after chromatographic purification. Et, ethyl group; Bn, benzyl group; Me, methyl group; *t*-Bu, *tert*-butyl group.

yields and enantioselectivities occur with a range of substituents in the α position of the electrophile (entries 1 to 6). In the case of α,α-dialkyl–substituted electrophiles (entries 5 and 6), the catalyst selectively discriminates between two alkyl groups, including a methyl and an isobutyl group (entry 6), to furnish high ee.

The introduction of an electron-donating or an electron-withdrawing substituent onto the indoline does not compromise the efficiency of the cross-coupling (Fig. 2B, entries 7 and 8). If desired, *N*-acylindolines can be transformed into primary alcohols or carboxylic acids (*24*). A variety of other α-haloamides are also suitable electrophilic cross-coupling partners (entries 9 to 11), including a Weinreb amide (entry 11), which is important in synthesis because it serves as a useful precursor to ketones (*25*).

To gain additional insight into the compatibility of various functional groups with these conditions for enantioconvergent C-N cross-couplings of tertiary alkyl halides, we examined the impact of additives (1.0 equivalent) on the course of the coupling process shown in Fig. 2B, entry 1. We determined that adding an unactivated secondary alkyl bromide (cyclohexyl bromide), a ketone (2-nonanone), a secondary alcohol (5-nonanol), an ester (methyl octanoate), an alkene (*cis*- or *trans*-5-decene), an alkyne (5-decyne), or a nitrile (valeronitrile) has no adverse impact on the yield or enantioselectivity, and these additives can be recovered intact at the end of the cross-coupling, whereas adding a primary amine (3-phenylpropylamine) or an aldehyde (octanal) impedes N-alkylation.

With respect to the nucleophilic coupling partner, substituted carbazoles are also suitable substrates (Fig. 2C, entries 1 to 5); the enantioconvergent C-N cross-coupling can be conducted on a gram scale with a similar outcome (entry 1 resulted in 1.29 g of product, 94% yield, and 94% ee). Indoles can also be used as nucleophiles in these photoinduced copper-catalyzed couplings, delivering the desired product with good yield and enantioselectivity (entries 6 to 9). Because indoles are common subunits in bioactive compounds (*26*), and natural products with a tertiary *N*-alkyl substituent are known (*27*, *28*), these represent a useful addition to the limited families of nitrogen nucleophiles that are compatible with metal-catalyzed C-N alkylations with alkyl halides (*14*, *15*).

Because we are able to obtain the cross-coupling product in high yield and ee when using only 1.2 equivalents of a racemic electrophile, it is evident that both enantiomers of the electrophile can be transformed under the reaction conditions into a particular enantiomer of the product (enantioconvergence), although not necessarily at identical rates [kinetic resolution (*29*)]. To gain insight into whether a kinetic resolution was occurring, we measured the ee of the unreacted tertiary alkyl halide at the end of the cross-coupling shown in Fig. 2B, entry 1. Our observation that the recovered electrophile is racemic suggests either that the enantiomeric substrates are reacting at essentially identical rates (no kinetic resolution) or that in situ racemization of the electrophile is occurring. Through the use of enantiopure alkyl halides, we established that virtually no racemization takes place under the reaction conditions (Fig. 3A). These couplings with enantiopure electrophiles further establish that the chiral ligand very effectively controls the absolute configuration of the product, regardless of the stereochemistry of the starting electrophile, and that C-Cl bond cleavage is essentially irreversible.

An outline of a possible mechanism for photoinduced copper-catalyzed C-N couplings of alkyl halides is illustrated in Fig. 3B (*14*, *15*). Irradiation of a copper-nucleophile complex (**A**) could lead to an excited-state adduct (**B**) that would then engage in electron transfer with the alkyl halide (R-X) to generate an alkyl radical; next, bond formation between the nucleophile and the radical (Nu-R) could occur through an inner-sphere pathway involving a copper-nucleophile complex (**C**). In contrast to most asymmetric photoredox reactions catalyzed by transition metals (*2*–*4*), a single metal (copper) appears to be responsible for both the photochemistry and the enantioselective bond-forming process. The binding of the nucleophile to copper in situ to form a copper complex that can serve as a photoreductant is important in this outline.

We have synthesized and crystallographically characterized a copper complex that includes the chiral phosphine and the carbazolide nucleophile, (**L***)$_2$Cu(carbazolide) (**1**) (Fig. 3C). The three ligands are arranged in a trigonal planar geometry around copper. When complex **1** (1.0 mol %) is used in place of CuCl and **L*** under our standard reaction conditions, the yield and the ee of the C-N cross-coupling product are essentially unchanged [92% yield, 94% ee; compare with Fig. 2A, entry 1 (95% yield, 95% ee)]. Furthermore, irradiation of complex **1** in the presence of a stoichiometric amount of a racemic tertiary alkyl halide leads to C-N bond formation in good yield and with enantioselectivity that is comparable to the catalyzed

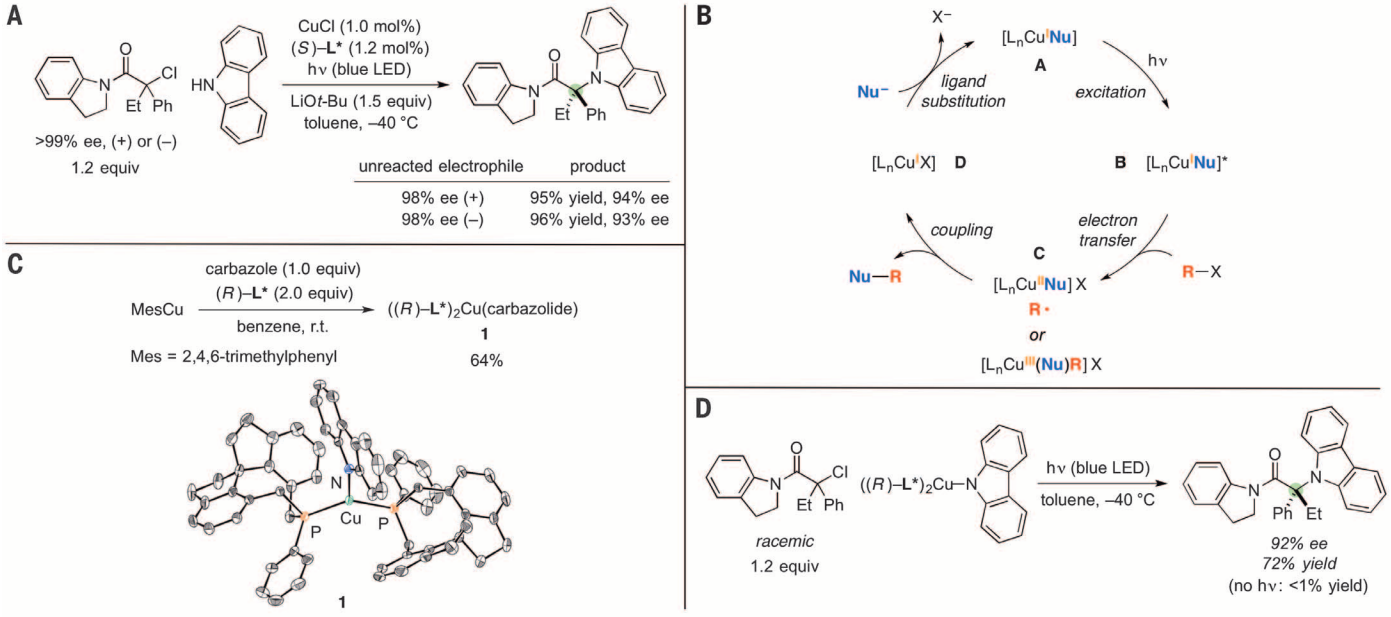

Fig. 3. Mechanistic studies. (**A**) Investigation of kinetic resolution. (**B**) Outline of a possible pathway for photoinduced copper-catalyzed C-N cross-couplings of alkyl halides. For simplicity, all copper complexes are illustrated as neutral species, and all processes are depicted as being irreversible; X may be serving as an inner- or an outer-sphere ligand [L_n denotes additional ligand(s) coordinated to copper]. (**C**) Synthesis and structural characterization of (**L***)$_2$Cu(carbazolide) (thermal ellipsoids are drawn at 50% probability, and H atoms are omitted for clarity). (**D**) Stoichiometric cross-coupling reaction with isolated (**L***)$_2$Cu(carbazolide).

process [(Fig. 3D; compare with Fig. 2A, entry 1 (95% ee)]; no coupling occurs in the absence of light. Collectively, these observations are consistent with the suggestion that complex **1**, or a copper-carbazolide-**L*** species that can be derived from complex **1**, is a plausible intermediate in the catalytic cycle.

Whereas enantioconvergent metal-catalyzed cross-couplings of racemic secondary alkyl halides have recently emerged as powerful tools for C-C bond construction, there has been little progress in corresponding C-heteroatom bond–forming processes or in the use of tertiary alkyl halides as coupling partners. We have established that, with the aid of visible light, a copper-based chiral catalyst derived from commercially available components can achieve enantioconvergent C-N cross-coupling reactions of racemic tertiary alkyl chlorides with good to excellent enantioselectivity. In contrast to nearly all metal-catalyzed asymmetric photoredox methods described to date, which use separate catalysts to effect redox chemistry and bond formation, in this method a single catalyst is responsible for the photochemistry and for the enantioselective bond construction. This work stands at a previously unexplored intersection of asymmetric synthesis, catalysis with Earth-abundant metals, photoinduced processes, and cross-coupling reactions of alkyl electrophiles, each of which represents an important current theme in chemical synthesis. We anticipate that our observations comprise the initial advances in a fertile area of asymmetric catalysis: the enantioconvergent synthesis of secondary and tertiary C-heteroatom bonds through photoinduced transition metal–catalyzed couplings of alkyl halides.

REFERENCES AND NOTES

1. A. Albini, M. Fagnoni, *Photochemically-Generated Intermediates in Synthesis* (Wiley, 2013).
2. C. K. Prier, D. A. Rankic, D. W. C. MacMillan, *Chem. Rev.* **113**, 5322–5363 (2013).
3. R. Brimioulle, D. Lenhart, M. M. Maturi, T. Bach, *Angew. Chem. Int. Ed.* **54**, 3872–3890 (2015).
4. D. M. Schultz, T. P. Yoon, *Science* **343**, 1239176 (2014).
5. H. Huo *et al.*, *Nature* **515**, 100–103 (2014).
6. H. Huo, C. Wang, K. Harms, E. Meggers, *J. Am. Chem. Soc.* **137**, 9551–9554 (2015).
7. C. Wang *et al.*, *Chemistry* **21**, 7355–7359 (2015).
8. A. Bauer, F. Westkämper, S. Grimme, T. Bach, *Nature* **436**, 1139–1140 (2005).
9. D. A. Nicewicz, T. M. Nguyen, *ACS Catal.* **4**, 355–360 (2014).
10. S. E. Creutz, K. J. Lotito, G. C. Fu, J. C. Peters, *Science* **338**, 647–651 (2012).
11. S. A. Lawrence, *Amines: Synthesis, Properties and Applications* (Cambridge Univ. Press, 2004).
12. L. Jiang, S. L. Buchwald, in *Metal-Catalyzed Cross-Coupling Reactions*, A. de Meijere, F. Diederich, Eds. (vol. 2, Wiley–VCH, 2004), pp. 699–760.
13. J. F. Hartwig, S. Shekhar, Q. Shen, F. Barrios-Landeros, in *Chemistry of Anilines*, Z. Rappoport, Ed. (vol. 1, Wiley, 2007), pp. 455–536.
14. A. C. Bissember, R. J. Lundgren, S. E. Creutz, J. C. Peters, G. C. Fu, *Angew. Chem. Int. Ed.* **52**, 5129–5133 (2013).
15. H.-Q. Do, S. Bachman, A. C. Bissember, J. C. Peters, G. C. Fu, *J. Am. Chem. Soc.* **136**, 2162–2167 (2014).
16. S. Paria, O. Reiser, *ChemCatChem* **6**, 2477–2483 (2014).
17. C. Fischer, G. C. Fu, *J. Am. Chem. Soc.* **127**, 4594–4595 (2005).
18. Y. Liang, G. C. Fu, . *J. Am. Chem. Soc.* **137**, 9523–9526 (2015).
19. M. Jin, L. Adak, M. Nakamura, *J. Am. Chem. Soc.* **137**, 7128–7134 (2015).
20. K. W. Quasdorf, L. E. Overman, *Nature* **516**, 181–191 (2014).
21. C. Schuster *et al.*, *J. Org. Chem.* **80**, 5666–5673 (2015).
22. A. W. Schmidt, K. R. Reddy, H.-J. Knölker, *Chem. Rev.* **112**, 3193–3328 (2012).
23. D. J. Berrisford, C. Bolm, K. B. Sharpless, *Angew. Chem. Int. Ed. Engl.* **34**, 1059–1070 (1995).
24. P. M. Lundin, G. C. Fu, *J. Am. Chem. Soc.* **132**, 11027–11029 (2010).
25. S. Balasubramaniam, I. S. Aidhen, *Synthesis* **2008**, 3707–3738 (2008).
26. G. W. Gribble, Ed., *Heterocyclic Scaffolds II: Reactions and Applications of Indoles* (Springer, 2010).
27. R. Vallakati, J. A. May, *J. Am. Chem. Soc.* **134**, 6936–6939 (2012).
28. E. K. Schmitt *et al.*, *Angew. Chem. Int. Ed.* **50**, 5889–5891 (2011).
29. H. Pellissier, in *Separation of Enantiomers*, M. Todd, Ed. (Wiley–VCH, 2014), pp. 75–122.

ACKNOWLEDGMENTS

Support has been provided by NIH (National Institute of General Medical Sciences, grant R01–GM109194), the Gordon and Betty Moore Foundation, the Alexander von Humboldt Foundation (fellowship for Q.M.K.), and the Bengt Lundqvist Memorial Foundation of the Swedish Chemical Society (fellowship for A.B.). We thank J. M. Ahn, L. M. Henling (Caltech X-Ray Crystallography Facility), M. W. Johnson, N. D. Schley, M. Shahgholi (Caltech Mass Spectrometry Facility), M. K. Takase (Caltech X-Ray Crystallography Facility), N. Torian (Caltech Mass Spectrometry Facility), D. G. VanderVelde (Caltech NMR Facility), and S. C. Virgil (Caltech Center for Catalysis and Chemical Synthesis) for assistance and helpful discussions. Experimental procedures and characterization data are provided in the supplementary materials. Metrical parameters for the structures of compounds **1** to **4** are available free of charge from the Cambridge Crystallographic Data Centre under accession numbers CCDC 1435979, 1435978, 1435977, and 1435980.

SUPPLEMENTARY MATERIALS

www.sciencemag.org/content/351/6274/681/suppl/DC1
Materials and Methods
Supplementary Text
Figs. S1 to S5
Tables S1 to S23
References (*30*–*37*)
Spectral Data

10 November 2015; accepted 7 January 2016
10.1126/science.aad8313

PLANT IMMUNITY

Using decoys to expand the recognition specificity of a plant disease resistance protein

Sang Hee Kim,* Dong Qi,† Tom Ashfield, Matthew Helm, Roger W. Innes‡

Maintaining high crop yields in an environmentally sustainable manner requires the development of disease-resistant crop varieties. We describe a method to engineer disease resistance in plants by means of an endogenous disease resistance gene from *Arabidopsis thaliana* named *RPS5*, which encodes a nucleotide-binding leucine-rich repeat (NLR) protein. RPS5 is normally activated when a second host protein, PBS1, is cleaved by the pathogen-secreted protease AvrPphB. We show that the AvrPphB cleavage site within PBS1 can be substituted with cleavage sites for other pathogen proteases, which then enables RPS5 to be activated by these proteases, thereby conferring resistance to new pathogens. This "decoy" approach may be applicable to other NLR proteins and should enable engineering of resistance in plants to diseases for which we currently lack robust genetic resistance.

Intracellular receptors belonging to the nucleotide-binding leucine-rich repeat (NLR) family play central roles in both the human and plant innate immune systems (*1*, *2*). In plants, their primary function is in pathogen detection, and this often involves the recognition of pathogen-derived virulence factors known as effector proteins. After detection of effector proteins, NLRs become activated, leading to the induction of numerous defense responses, including a localized cell death response termed the hypersensitive response (HR) that serves to prevent spread of infection. NLR proteins are highly specific with regard to the pathogen effectors that each can detect, with a single NLR protein capable of detecting only a limited number of effectors. Research on plant NLRs conducted over the past 20 years has focused on understanding the mechanistic basis of this specificity, with a long-term goal of being able to create new specificities. The ability to engineer novel specificities would enable the production of crop plants with genetically based resistance to diseases that currently must be controlled by environmentally damaging, and expensive, pesticides.

Department of Biology, Indiana University, Bloomington, IN 47405, USA.
*Present address: Division of Plant Sciences, University of Missouri, Columbia, MO 65211, USA. †Present address: Center for Research and Technology, Altria Group, Richmond, VA 23219, USA.
‡Corresponding author. E-mail: rinnes@indiana.edu

Downloaded from on February 11, 2016

Although substantial progress has been made toward understanding how plant NLRs detect pathogen effectors, it has not yet been possible to engineer entirely new specificities. The successes to date have resulted in only minor expansion of specificities (*3*–*5*). Because the direct modification of NLR proteins has met with limited success, we have been pursuing an alternative strategy to activate the defense pathways regulated by NLR proteins. Many NLR proteins detect pathogen effector proteins indirectly by sensing modification of other host proteins that are themselves targeted by pathogen effectors. This indirect recognition mechanism can be likened to a mousetrap in which the NLR protein is the trap, the effector is the mouse, and the effector target is the bait. When the mouse (effector) nibbles on the bait (effector target), it triggers the trap (NLR protein) to undergo a large conformational change. We hypothesized that it would be possible to alter the type of mouse caught (detected) by altering the bait rather than the trap.

To pursue this strategy, we used the *Arabidopsis* NLR protein RESISTANCE TO *PSEUDOMONAS SYRINGAE* 5 (RPS5), which mediates detection of the effector protein AvrPphB from this pathogen (*6*). AvrPphB is a protease that targets a small family of protein kinases that function in basal immune signaling (*7*, *8*). One of these kinases is PBS1. Cleavage of PBS1 by AvrPphB activates RPS5 (*9*). By analogy to the mousetrap model, PBS1 serves as the bait in this system. RPS5 and PBS1 form a preactivation complex, and when PBS1 is cleaved by AvrPphB, the resulting conformational change in PBS1 triggers RPS5 (*10*). This conformational change can be mimicked by insertion of three amino acids at the cleavage site; the kinase so altered can activate RPS5 in the absence of AvrPphB and in the absence of cleavage (*10*). Thus, activation of RPS5 does not require direct binding of RPS5 to the bacterial effector. RPS5 should be able to respond to any pathogen effector that can cause the requisite conformational change in the plant's intermediary kinase, PBS1.

We tested this hypothesis by swapping the proteolytic target site in PBS1 normally cleaved by AvrPphB (Gly-Asp-Lys-Ser-His-Val-Ser) with another proteolytic site (Val-Pro-Lys-Phe-Gly-Asp-Trp) that would be recognized by a different *P. syringae* effector, AvrRpt2 (Fig. 1A). This proteolytic site is found in a target of AvrRpt2 named RPM1 INTERACTING PROTEIN 4 (RIN4) (*11*). Cleavage of RIN4 by AvrRpt2 normally triggers immune responses through a different NLR protein, RPS2 (*12*). We refer to this modified PBS1 as PBS1^{RCS2} because this sequence corresponds to RIN4 cleavage site 2 (*11*, *12*). We transiently coexpressed PBS1^{RCS2} with RPS5 and AvrRpt2 in *Nicotiana glutinosa* and assessed RPS5 activation by monitoring tissue collapse resulting from induction of HR-associated cell death. AvrRpt2 induced a strong HR that was dependent on AvrRpt2 protease activity and on the modified PBS1 (Fig. 1B). This HR was also dependent on coexpression of RPS5, indicating that we had succeeded in switching the recognition specificity of RPS5 from AvrPphB to AvrRpt2. To quantify the HR, we measured electrolyte leakage, a proxy for cell death. Consistent with the macroscopic symptoms, PBS1^{RCS2} with AvrRpt2 induced as much electrolyte leakage as wild-type PBS1 cleaved by AvrPphB, whereas PBS1^{RCS2} with the mutation $Cys^{122} \rightarrow$ Ala (C122A) only weakly activated RPS5 (Fig. 1C). Immunoblot analysis confirmed that AvrRpt2 cleaved PBS1^{RCS2} at 4 hours after induction, whereas C122A or AvrPphB did not (Fig. 1D). Together, these data establish that PBS1^{RCS2} is a substrate for AvrRpt2 and that AvrRpt2-mediated cleavage activates RPS5, at least when transiently overexpressed in *N. glutinosa*.

Encouraged by these results, we used the native *PBS1* promoter to generate transgenic *Arabidopsis* plants expressing PBS1^{RCS2}. For this experiment, we needed to use a genotype of *Arabidopsis* that does not normally activate a HR in response to AvrRpt2. We thus used an *Arabidopsis* mutant line that lacked both RIN4 and RPS2 (*13*). We assessed four independent transgenic lines expressing PBS1^{RCS2} for HR to infection by *P. syringae* expressing AvrRpt2. At 21 hours after inoculation with *P. syringae* strain DC3000 (*avrRpt2*), two independent transgenic lines (#5 and #2) showed a visible HR, whereas the untransformed *rin4rps2* mutant did not (Fig. 2A). In planta bacterial growth assays showed that growth of DC3000(*avrRpt2*) in lines #5 and #2 was less than in the parent *rin4rps2* line by a factor of 100 to 200, whereas bacterial growth in lines #1 and #3 was reduced by a factor of 5 to 50 (Fig. 2B). However, these lines were equally susceptible to DC3000(*C122A*), indicating that AvrRpt2 protease activity is required to activate resistance. Both induction of HR and restriction of bacterial growth correlated with expression levels of PBS1^{RCS2} (Fig. 2C). At 12 hours after inoculation, we detected a cleavage product of PBS1^{RCS2} in transgenic line #5 after inoculation with DC3000(*avrRpt2*), but not with DC3000 lacking *avrRpt2* [DC3000(empty vector); Fig. 2D]. Thus, cleavage of PBS1^{RCS2} by AvrRpt2 activates RPS5 in *Arabidopsis*. These transgenic plants, which still contain a wild-type copy of *PBS1*, also displayed HR 21 hours after injection with DC3000(*avrPphB*) (Fig. 2E), demonstrating that the native recognition specificity of RPS5 was retained. Together these results suggest that RPS5-mediated disease resistance can be activated by two different protease effector proteins in the *PBS1^{RCS2}* transgenic plants, and that the recognition specificity of RPS5 can be expanded by addition of new "decoy" variations of PBS1.

To test whether this approach could be extended to recognize pathogens beyond *P. syringae*, we created a PBS1 variant that can be cleaved by the NIa protease of tobacco etch virus (TEV), which was chosen because the recognition sequence of TEV NIa protease is well characterized (*14*). We replaced the AvrPphB cleavage site in PBS1 with a TEV protease cleavage site, generating PBS1^{TCS} (Fig. 3A). TEV is a positive-stranded RNA virus that encodes a polyprotein

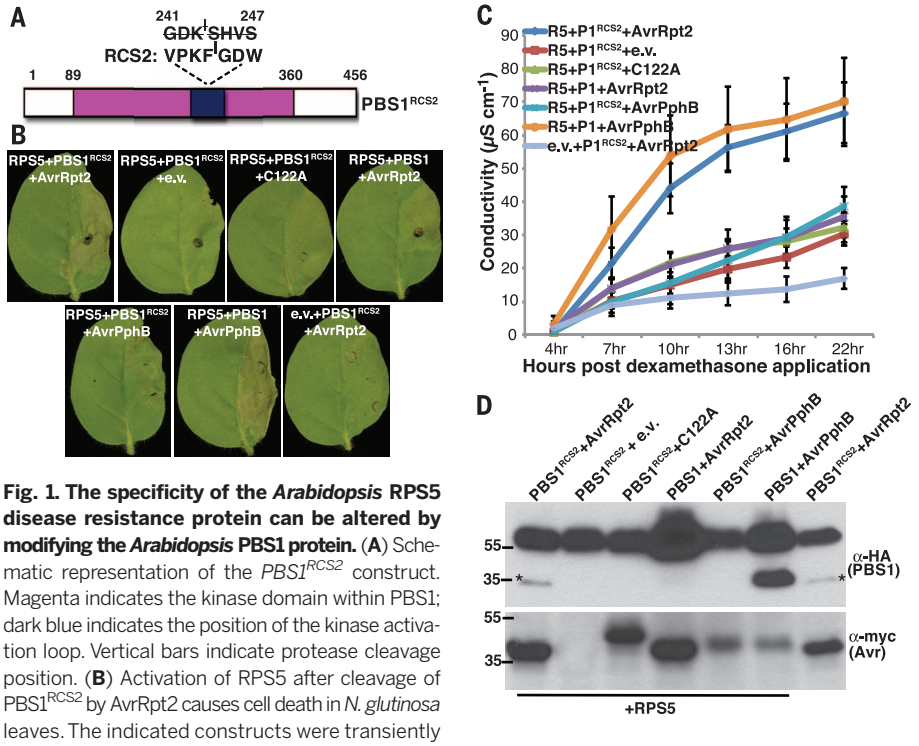

Fig. 1. The specificity of the *Arabidopsis* RPS5 disease resistance protein can be altered by modifying the *Arabidopsis* PBS1 protein. (**A**) Schematic representation of the *PBS1^{RCS2}* construct. Magenta indicates the kinase domain within PBS1; dark blue indicates the position of the kinase activation loop. Vertical bars indicate protease cleavage position. (**B**) Activation of RPS5 after cleavage of PBS1^{RCS2} by AvrRpt2 causes cell death in *N. glutinosa* leaves. The indicated constructs were transiently coexpressed in *N. glutinosa* by means of *Agrobacterium tumefaciens* infiltration. C122A indicates a protease-inactive form of AvrRpt2. (**C**) Activation of RPS5 after cleavage of PBS1^{RCS2} by AvrRpt2 causes electrolyte leakage in *N. glutinosa* leaves. Data are means ± SD (n = 4). R5 and P1 denote *RPS5* and *PBS1*. (**D**) Cleavage of PBS1^{RCS2} by AvrRpt2. Total protein was isolated from duplicates of the leaves shown in (B) and analyzed by immunoblotting with the indicated antibodies. Transient gene expression was induced using dexamethasone (DEX). Asterisk indicates position of the PBS1 C-terminal cleavage product.

that must be posttranslationally processed by its embedded NIa protease. This protease is essential for viral replication; thus, disease resistance that is triggered by its enzymatic activity should be highly durable, as it would be extremely difficult for the virus to simultaneously change the specificity of its protease and the protease cleavage sites embedded within its polyprotein. Because all potyviruses depend on endogenous proteases for replication, this general approach could enable engineering durable resistance to many different plant viruses of economic importance.

We transiently coexpressed PBS1^{TCS} with TEV NIa protease and RPS5 in *N. benthamiana*. Cell death was induced when RPS5 was coexpressed with PBS1^{TCS} and TEV protease, but was not induced when either PBS1^{TCS} or TEV protease was excluded (Fig. 3B). Quantification of cell death, assessed by electrolyte leakage, showed that PBS1^{TCS} and TEV protease induced cell death equivalent to wild-type PBS1 and AvrPphB (Fig. 3C). Immunoblot analysis confirmed that TEV protease cleaved the target PBS1^{TCS} at 6 hours after induction, whereas AvrPphB did not (Fig. 3D). Also, TEV protease did not cleave wild-type PBS1.

These results establish that PBS1 can be engineered to function as a target for proteases from two very different classes of pathogen: viruses and bacteria. To determine whether cleavage of modified PBS1 can productively activate RPS5 and initiate an effective immune response against viruses, we created a PBS1 decoy containing a consensus cleavage site for the NIa protease from turnip mosaic virus (PBS1^{TuMV}; fig. S1). This virus was selected because it is more virulent on *Arabidopsis* than is TEV, but belongs to same family of viruses (Potyviridae) (*15*). Transient expression assays in *N. benthamiana* confirmed that PBS1^{TuMV} is cleaved by TuMV NIa protease and activates RPS5 (fig. S1). We generated transgenic *Arabidopsis* plants expressing *PBS1^{TuMV}* under the native *PBS1* promoter and terminator sequences, and then infected them with a TuMV derivative that contained a fusion between the viral 6K2 protein and green fluorescent protein (GFP) (*16*). This 6K2-GFP fusion protein enabled us to visualize the spread of the virus through plants by means of ultraviolet light. At 11 days after inoculation, TuMV/6K2-GFP had spread throughout the rosette leaves and newly emerging leaves of wild-type (nontransgenic) *Arabidopsis* (Fig. 4, A and B). In three *PBS1^{TuMV}* transgenic *Arabidopsis* lines, most of the newly emerging leaves became chlorotic and died (Fig. 4, A and B, and fig. S2). This cell death correlated with reduced spread of the GFP fluorescence. To quantify whether the transgenic plants carried less virus, we collected entire rosettes, isolated total protein, and then assessed viral protein quantities by immunoblot (Fig. 4C). Consistent with the observed reduction in GFP fluorescence, we observed a sharp reduction in GFP in transgenic lines that displayed severe necrosis (Fig. 4C). We also analyzed three lines that displayed a moderate necrosis phenotype and one that displayed susceptible mosaic symptoms. The quantity of 6K2-GFP was inversely correlated with

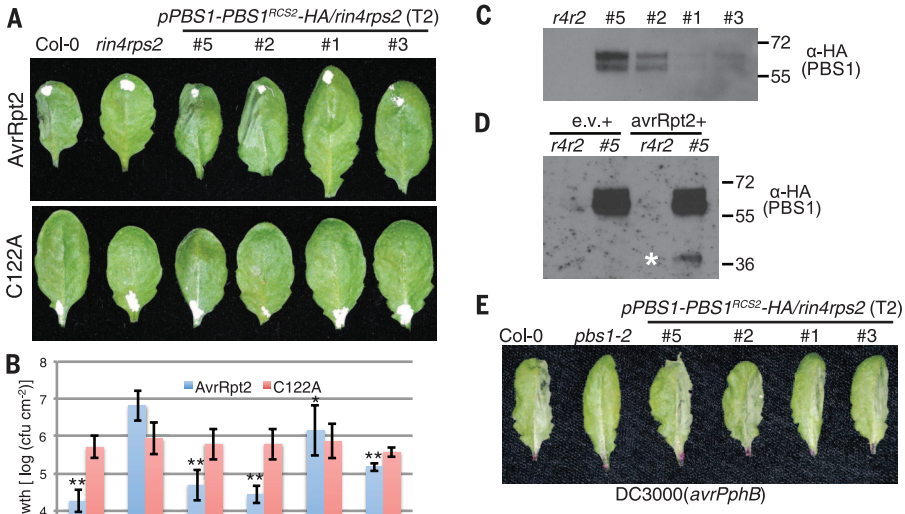

Fig. 2. Transgenic expression of *PBS1^{RCS2}* in *Arabidopsis* confers resistance to *P. syringae* expressing *avrRpt2*. (**A**) Recognition of AvrRpt2 by transgenic *Arabidopsis* plants expressing PBS1^{RCS2}. The indicated *Arabidopsis* lines were inoculated with *P. syringae* DC3000(*avrRpt2*) (top row) or DC3000(*C122A*) (bottom row) in the left half of each leaf and scored for HR. Col-0 indicates wild-type *Arabidopsis*, which recognizes AvrRpt2 using RPS2; *rin4rps2* indicates the double mutant parent used to generate the transgenic lines. (**B**) PBS1^{RCS2} confers resistance to DC3000(*avrRpt2*) in *Arabidopsis*. Bacterial growth was measured in the indicated plant lines shown in (A). Data are shown as mean colony-forming units (cfu) cm^{-2} ± SD (n = 4). Asterisks indicate statistically significant differences from growth observed in the *rin4rps2* parent for a given strain (**P < 0.01, *P < 0.05; Tukey's honest significant difference test). (**C**) Resistance to DC3000(*avrRpt2*) correlates with expression of PBS1^{RCS2}. Proteins from transgenic lines shown in (A) were immunoprecipitated with anti-HA agarose and immunoblotted. (**D**) PBS1^{RCS2} expressed in transgenic *Arabidopsis* is cleaved by AvrRpt2 delivered by DC3000. The asterisk indicates the C-terminal PBS1^{RCS2} cleavage product. (**E**) *PBS1^{RCS2}* transgenic plants, which contain a wild-type copy of *PBS1*, recognize both AvrRpt2 and AvrPphB. *PBS1^{RCS2}* transgenic plants displayed a visible HR 21 hours after injection with *P. syringae* strain DC3000(*avrPphB*).

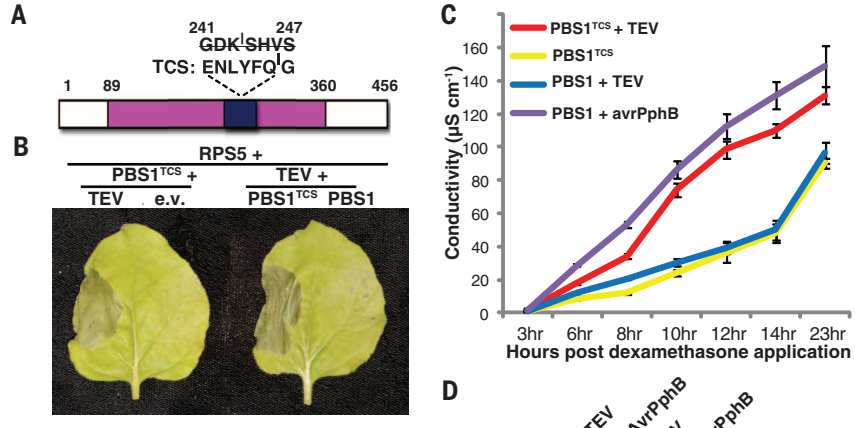

Fig. 3. Replacement of the AvrPphB cleavage site in PBS1 with a TEV NIa protease cleavage site enables HR activation by TEV protease. (**A**) Schematic representation of the *PBS1^{TCS}* construct. (**B**) Cleavage of PBS1^{TCS} by TEV protease activates HR in *N. benthamiana* leaves when coexpressed with RPS5. The indicated constructs were transiently coexpressed in *N. benthamiana*. (**C**) Electrolyte leakage analysis of *N. benthamiana* leaf disks coexpressing *RPS5*, *PBS1^{TCS}*, and *TEV protease*. Data are means ± SD (n = 4). (**D**) Cleavage of PBS1^{TCS} by TEV protease. PBS1^{TCS}-HA or PBS1-HA was transiently coexpressed with TEV protease-Myc (TEV) or AvrPphB-Myc in *N. benthamiana* and proteins analyzed by immunoblotting. Asterisk indicates position of C-terminal PBS1 cleavage product. PBS1^{TCS} is rapidly degraded after cleavage, hence the faint signal in lane 1.

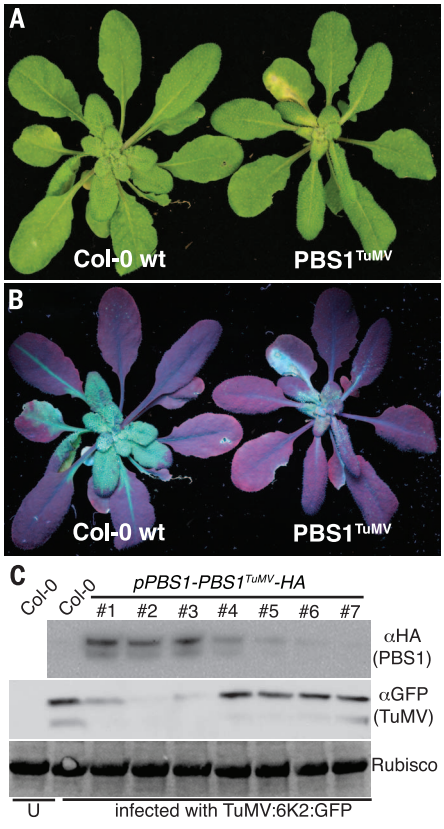

Fig. 4. Transgenic *Arabidopsis* expressing PBS1 containing a TuMV NIa protease cleavage site accumulate less virus. TuMV induces trailing necrosis in transgenic *Arabidopsis* expressing PBS1^{TuMV}. (**A**) Wild-type and transgenic plants under white light 11 days after agro-infection with TuMV/6K2:GFP. (**B**) The same plants under UV light. Note the extensive green fluorescence in the wild-type plant, indicating systemic viral infection. The transgenic plant shown is from line #1 and is representative of three independent lines showing severe necrosis. (**C**) Virus accumulation in PBS1^{TuMV} transgenic plants is inversely correlated with PBS1^{TuMV} expression. Whole rosettes of five to six plants from each line were harvested at 15 days after agro-infection, tissue combined, protein extracted, and virus content compared using an anti-GFP immunoblot. The Rubisco (ribulose-1,5-bisphosphate carboxylase-oxygenase) band is shown as a loading control. PBS1^{TuMV} levels were assessed using an anti-hemagglutinin (HA) immunoblot after anti-HA immunoprecipitation. Lines 1 to 3 were severely necrotic, lines 4 to 6 moderately necrotic, and line 7 fully susceptible.

the quantity of PBS1^{TuMV} (Fig. 4C), indicating that the level of defense activation is proportional to the level of PBS1^{TuMV} expression. These data indicate that RPS5 can be activated by cleavage of engineered PBS1 by the cognate TuMV NIa protease and that this activation limits virus accumulation, presumably through cell death.

The cell death phenotype we observed in the PBS1^{TuMV} transgenic plants is similar to a phenomenon previously described in plant-virus interactions called "trailing necrosis" or "lethal systemic necrosis" (*17*). In severe cases, trailing necrosis can lead to plant death due to destruction of the apical meristem, which is what we observed in our severely necrotic lines (fig. S2). Trailing necrosis is usually associated with partially compromised disease resistance responses, which can be caused by an imperfect match between an NLR protein and the virus being detected (*3*, *17*). We speculate that in our system, the viral protease must attain high levels before it encounters PBS1, which is tethered to the plasma membrane (*18*). Potyvirus NIa proteases accumulate in the nucleus (NIa stands for "nuclear inclusion antigen"), with only a small portion found in the cytoplasm (*19*). We thus think it is likely that RPS5 is being activated at a late stage of infection, which could account for the spread of virus to adjacent cells prior to cell death.

To be an effective virus resistance mechanism, the RPS5-PBS1 system will require modifications that enable more rapid activation of RPS5. Given the observed correlation between PBS1 protein expression and levels of resistance (Figs. 2 and 4), increasing the expression level of PBS1 may be sufficient. More likely, however, it will be necessary to relocate RPS5 and PBS1 to sites of viral replication, which would enable early encounters between the viral protease and PBS1. This could be accomplished by replacing the N-terminal acylation motifs of RPS5 and PBS1, which direct PBS1 and RPS5 to the plasma membrane (*18*, *20*), with the 6K2 domain of TuMV, which localizes to viral replication complexes (*21*).

Although further optimization is needed, the above experiments demonstrate that swapping protease cleavage sites in PBS1 can change the specificity of the RPS5 immune response pathway. This system should thus be usable to engineer resistance to any pathogen that uses a protease as part of its infection process, provided that the protease targets a defined recognition sequence of seven or fewer amino acids and localizes to the host cell cytoplasm early in the infection cycle. To assure durability, the protease should also be essential for infectivity of the pathogen. Pathogens known to secrete or express proteases during host infection include viruses, bacteria, oomycetes, fungi, and nematodes (*22*–*27*), hence this strategy may be broadly applicable.

Using such a decoy approach to engineer resistance in crop plants might not require transfer of the *Arabidopsis RPS5* gene if crop plants already possess the ability to detect AvrPphB by a similar mechanism. Indeed, we have determined that most varieties of soybean display a HR in response to *P. syringae* expressing AvrPphB (*28*), as do some varieties of barley (*22*), indicating that these crops species possess an NLR gene functionally analogous to *RPS5*. In addition, *PBS1* is highly conserved among crop plants, including soybean and barley (*29*, *30*). It may thus be possible to engineer soybean, barley, and other crop plants to detect various pathogen proteases by using genome editing techniques to modify endogenous *PBS1* genes. More generally, similar decoy approaches may be applicable to other NLR proteins that use an indirect recognition mechanism to detect pathogen effectors.

REFERENCES AND NOTES

1. J. von Moltke, J. S. Ayres, E. M. Kofoed, J. Chavarría-Smith, R. E. Vance, *Annu. Rev. Immunol.* **31**, 73–106 (2013).
2. D. Qi, R. W. Innes, *Front. Immunol.* **4**, 348 (2013).
3. C. J. Harris, E. J. Slootweg, A. Goverse, D. C. Baulcombe, *Proc. Natl. Acad. Sci. U.S.A.* **110**, 21189–21194 (2013).
4. M. E. Segretin *et al.*, *Mol. Plant Microbe Interact.* **27**, 624–637 (2014).
5. A. Giannakopoulou *et al.*, *Mol. Plant Microbe Interact.* **28**, 1316–1329 (2015).
6. M. T. Simonich, R. W. Innes, *Mol. Plant Microbe Interact.* **8**, 637–640 (1995).
7. J. Zhang *et al.*, *Cell Host Microbe* **7**, 290–301 (2010).
8. F. Shao *et al.*, *Science* **301**, 1230–1233 (2003).
9. J. Ade, B. J. DeYoung, C. Golstein, R. W. Innes, *Proc. Natl. Acad. Sci. U.S.A.* **104**, 2531–2536 (2007).
10. B. J. DeYoung, D. Qi, S. H. Kim, T. P. Burke, R. W. Innes, *Cell. Microbiol.* **14**, 1071–1084 (2012).
11. S. T. Chisholm *et al.*, *Proc. Natl. Acad. Sci. U.S.A.* **102**, 2087–2092 (2005).
12. B. Day *et al.*, *Plant Cell* **17**, 1292–1305 (2005).
13. M. J. Axtell, B. J. Staskawicz, *Cell* **112**, 369–377 (2003).
14. M. J. Adams, J. F. Antoniw, F. Beaudoin, *Mol. Plant Pathol.* **6**, 471–487 (2005).
15. A. D. Lellis, K. D. Kasschau, S. A. Whitham, J. C. Carrington, *Curr. Biol.* **12**, 1046–1051 (2002).
16. J. Wan, D. G. Cabanillas, H. Zheng, J. F. Laliberté, *Plant Physiol.* **167**, 1374–1388 (2015).
17. M. Nam *et al.*, *Mol. Cells* **32**, 421–429 (2011).
18. D. Qi *et al.*, *Plant Physiol.* **164**, 340–351 (2014).
19. M. A. Restrepo, D. D. Freed, J. C. Carrington, *Plant Cell* **2**, 987–998 (1990).
20. D. Qi, B. J. DeYoung, R. W. Innes, *Plant Physiol.* **158**, 1819–1832 (2012).
21. J. Jiang, C. Patarroyo, D. Garcia Cabanillas, H. Zheng, J. F. Laliberté, *J. Virol.* **89**, 6695–6710 (2015).
22. E. Whigham *et al.*, *Mol. Plant Microbe Interact.* **28**, 968–983 (2015).
23. J. R. Alfano, A. Collmer, *Annu. Rev. Phytopathol.* **42**, 385–414 (2004).
24. S. Hartmann, R. Lucius, *Int. J. Parasitol.* **33**, 1291–1302 (2003).
25. C. L. Casteel *et al.*, *Plant Physiol.* **169**, 209–218 (2015).
26. H. S. Lim *et al.*, *Plant Pathol. J.* **27**, 315–323 (2011).
27. S. Raffaele, J. Win, L. M. Cano, S. Kamoun, *BMC Genomics* **11**, 637 (2010).
28. A. R. Russell, T. Ashfield, R. W. Innes, *Mol. Plant Microbe Interact.* **28**, 727–735 (2015).
29. K. S. Caldwell, R. W. Michelmore, *Genetics* **181**, 671–684 (2009).
30. M. R. Swiderski, R. W. Innes, *Plant J.* **26**, 101–112 (2001).

ACKNOWLEDGMENTS

We thank S. Pottinger for assistance with statistical analyses. T-DNA insertion mutants of *Arabidopsis* were obtained from the *Arabidopsis* Biological Resource Center at Ohio State. pCambiaTuMV/6K2:GFP was kindly provided by A. Laliberte. Supported by National Institute of General Medical Sciences grant R01 GM046451, NSF Plant Genome Research Program grant IOS-1339348, and the Indiana University Office of the Vice Provost for Research Faculty Research Support Program. A patent application has been submitted covering the RPS5-PBS1 protease recognition system (U.S. Patent App. 14/427,753). Author contributions: S.H.K., D.Q., T.A., M.H., and R.W.I. designed and performed the experiments; R.W.I. and S.H.K. wrote the manuscript with editing provided by D.Q., T.A., and M.H. Supplement contains additional data.

SUPPLEMENTARY MATERIALS

www.sciencemag.org/content/351/6274/684/suppl/DC1
Materials and Methods
Figs. S1 and S2
Table S1
References (*31*–*34*)

31 August 2015; accepted 21 January 2016
10.1126/science.aad3436

VALLEYTRONICS

Valley-polarized exciton dynamics in a 2D semiconductor heterostructure

Pasqual Rivera,[1]* Kyle L. Seyler,[1]* Hongyi Yu,[2] John R. Schaibley,[1] Jiaqiang Yan,[3,4] David G. Mandrus,[3,4,5] Wang Yao,[2] Xiaodong Xu[1,6]†

Heterostructures comprising different monolayer semiconductors provide an attractive setting for fundamental science and device technologies, such as in the emerging field of valleytronics. We realized valley-specific interlayer excitons in monolayer WSe_2-$MoSe_2$ vertical heterostructures. We created interlayer exciton spin-valley polarization by means of circularly polarized optical pumping and determined a valley lifetime of 40 nanoseconds. This long-lived polarization enables the visualization of the expansion of a valley-polarized exciton cloud over several micrometers. The spatial pattern of the polarization evolves into a ring with increasing exciton density, a manifestation of valley exciton exchange interactions. Our work introduces van der Waals heterostructures as a promising platform from which to study valley exciton physics.

Van der Waals heterostructures of two-dimensional (2D) materials provide an exciting platform for engineering artificial material systems with distinct properties (*1*). A beautiful example is the demonstration of the Hofstadter butterfly physics in moiré superlattice structures composed of graphene and hexagonal boron nitride (*2*–*4*). As the library of 2D crystals is explored further, the range of possible new phenomena in condensed matter physics becomes ever more diverse. For example, heterostructures of 2D semiconductors [namely, transition metal dichalcogenide monolayers (MX_2)] have been assembled with type-II band alignment (*5*–*8*), in which electrons and holes energetically favor different layers (Fig. 1A). These heterostructures form atomically thin p-n junctions that can be used for photon-energy harvesting (*9*–*15*) and host interlayer excitons (X_I), with the Coulomb-bound electron and hole located in different monolayers (*14*–*17*). This species of exciton has a lifetime far exceeding those in monolayer MX_2, and the vertical separation of holes and electrons entails a permanent out-of-plane electric dipole moment, providing an optical means to pump interlayer electric polarization and facilitating electrical control of interlayer excitons (*17*).

The interlayer excitons in 2D heterostructures are similar to spatially indirect excitons in III-V quantum wells (*18*–*22*). In both systems, the electron-hole wave function overlap is reduced in the out-of-plane direction, suppressing the magnitude of exciton oscillator strength and the electron-hole exchange interaction. This leads to greatly enhanced population and spin lifetimes for spatially indirect excitons as compared with their direct exciton counterparts.

MX_2 heterostructures possess several features distinct from quantum well systems. First, the monolayers' band edges are at doubly degenerate corners of the hexagonal Brillouin zone, so X_I has an internal degree of freedom specified by the combination of electron and hole valley indices (*23*). Second, the twist angle between the crystal axes of constituent monolayers leads to a displacement of the conduction and valence band edges in momentum space, making the X_I dark—momentum indirect—at its minimum energy and bright only at finite center-of-mass velocities. The location of the X_I light cones depends on the twist angle between the monolayers, allowing for control over the optoelectronic properties (*24*–*26*), such as the dipole strength and interlayer exciton lifetime (*27*). Third, the constituent MX_2 monolayers exhibit valley-contrasting physical properties such as spin-valley locking, optical selection rules (*28*–*30*), and Berry curvature (*23*). The inheritance of valley physics in twisted MX_2 heterostructures is predicted to give rise to previously unknown optical and transport properties of X_I (*27*), allowing the possibility of excitonic optoelectronic circuits with valley functionalities and providing a platform for investigating excitonic superfluidity and condensation (*31*).

We observed long valley lifetime and valley drift-diffusion of X_I in $MoSe_2$-WSe_2 heterostructures with small twist angles. Our devices consist of a pair of exfoliated monolayers of WSe_2 and $MoSe_2$, which are stacked by means of dry transfer (*32*) on a 285-nm insulating layer of SiO_2 on a silicon substrate. We used standard electron beam lithography techniques to fabricate metallic contacts (V/Au) on the heterostructure, and the silicon substrate functions as a global backgate, as shown in Fig. 1A (*33*). The optical brightness of the X_I depends sensitively on the relative alignment of the two constituent monolayers. Theory shows that for twist angles near zero or 60°, there exist light cones at small kinematic momenta in which the X_I can directly interconvert with photons (*27*). In such heterostructures, the X_I can radiatively recombine after scattering into these light cones through, for example, exciton-phonon or exciton-exciton interactions (*27*). In our study, we focused on this type of heterostructure. To fabricate such samples, we identified the armchair axes of individual monolayers by means of polarization-resolved second-harmonic generation and then aligned these axes (fig. S1). This yields heterostructures with twist angles near zero or 60° (*33*). As such, the X_I can be observed in photoluminescence (PL), even at room temperature (fig. S2). All data in the main text are taken at a temperature of 30 K from the device shown in the optical microscope image in Fig. 1B, with WSe_2 stacked on $MoSe_2$, and the excitation laser energy in resonance with the A exciton of WSe_2 (1.72 eV).

We first performed polarization-resolved PL at zero gate voltage (V_g = 0 V). We applied circularly polarized continuous-wave laser excitation and separately detected the right circular (σ^+) and left circular (σ^-) PL. The σ^+ (black) and σ^- (red) components of the X_I PL under circularly polarized excitation are shown in Fig. 1C. These results show that X_I emission is strongly co-polarized with the incident light. Denoting the degree of polarization by $\rho = \frac{I_+ - I_-}{I_+ + I_-}$, where $I_\pm$ is the intensity of the $\sigma^\pm$ PL components, we observed $|\rho_{max}| > 0.3$. Similar results were obtained from several other samples (fig. S3). We also performed measurements in the linear basis, which do not show appreciable polarization (fig. S4).

The observation of circularly polarized PL demonstrates that the X_I can retain memory of the excitation light helicity, which is a consequence of the valley optical selection rules in 2D heterostructures (*27*). In the following, we discuss the generation of valley polarization in heterostructures near AA-like stacking (twist angle near 0°) (Fig. 1D), but similar conclusions can be drawn for heterostructures near AB-like stacking (twist angle near 60°) (fig. S5) (*33*). The valley configuration of X_I is specified by the valley indices of its electron and hole. With the spin-valley locking in monolayer MX_2, a universal assignment of the valley index is applicable in the twisted heterostructures, and here we denote the valley with electron spin up as $+K$ and spin down as $-K$ in both layers. First, σ^+ excitation creates valley-polarized intralayer excitons in the $+K_W$ valley in WSe_2 and $+K_M$ valley in $MoSe_2$. Next, charge carriers relax to the heterostructure band edges through interlayer charge transfer on subpicosecond time scales (*11*, *15*) to form X_I. Because of the large momentum difference, interlayer hopping between $+K_W$ and $-K_M$ valleys is strongly suppressed. Conversely, the $+K_W$ and $+K_M$ valleys have small momentum mismatch, and the spin-conserving interlayer hopping between these valleys becomes the dominant relaxation channel. Therefore, the σ^+ excitation leads to valley-polarized X_I (Fig. 1E). The situation for σ^- excitation can be

[1]Department of Physics, University of Washington, Seattle, WA 98195, USA. [2]Department of Physics and Center of Theoretical and Computational Physics, University of Hong Kong, Hong Kong, China. [3]Materials Science and Technology Division, Oak Ridge National Laboratory, Oak Ridge, TN 37831, USA. [4]Department of Materials Science and Engineering, University of Tennessee, Knoxville, TN 37996, USA. [5]Department of Physics and Astronomy, University of Tennessee, Knoxville, TN 37996, USA. [6]Department of Materials Science and Engineering, University of Washington, Seattle, WA 98195, USA.
*These authors contributed equally to the work. †Corresponding author. E-mail: xuxd@uw.edu

Downloaded from on February 11, 2016

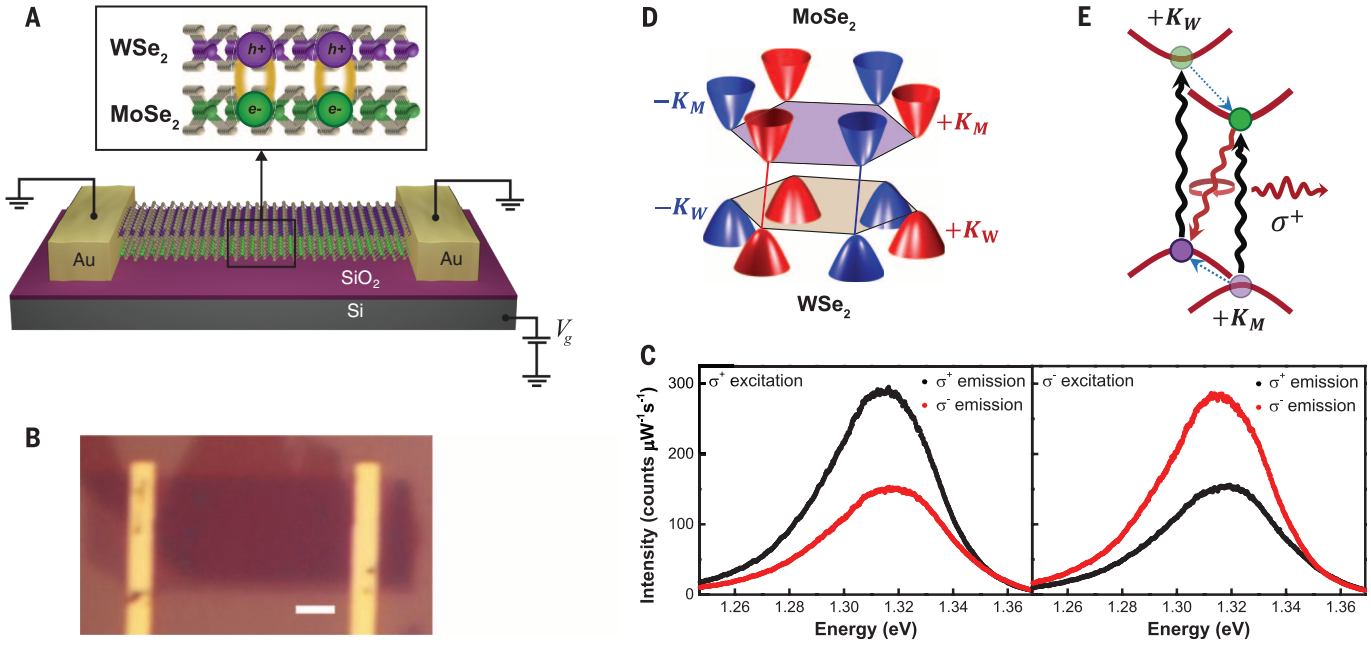

Fig. 1. Interlayer exciton spin-valley polarization in $MoSe_2$-WSe_2 heterostructures. (**A**) Side view of $MoSe_2$-WSe_2 heterostructure device. Boxed region depicts the interlayer exciton, with holes (h^+) and electrons (e^-) located in WSe_2 and $MoSe_2$, respectively. (**B**) Optical image of device, with WSe_2 on top of $MoSe_2$. Scale bar, 2 μm. (**C**) Circular polarization–resolved PL spectra of the interlayer exciton showing the generation of strong valley polarization. (**D**) Illustration of the Dirac points in the hexagonal Brillouin zone of a $MoSe_2$-WSe_2 heterobilayer, with small twisting angle. The $+K$ (red) and $-K$ (blue) valleys at the conduction band minimum (in $MoSe_2$) and valence band maximum (in WSe_2) are nearly aligned in momentum space. (**E**) Schematic of the interlayer exciton in the $+K$ valley. First, σ^+ circularly polarized light (black wavy lines) excites intralayer excitons in the $+K_M$ and $+K_W$ valleys. Fast interlayer charge hopping (blue dotted lines) forms the interlayer exciton in the $+K$ valley. The optical selection rules in the $+K_W$ and $+K_M$ valleys produce co-polarized PL.

obtained through time reversal. The radiative recombination of the valley-polarized X_I is facilitated by the interlayer coupling, which allows emission of photons that are co-polarized with the excitation source (*27*).

We found that the degree of X_I valley polarization can be electrically controlled by the gate. Shown in Fig. 2A are polarization-resolved PL spectra at selected V_g under σ^+ excitation with ~50-ps laser pulses. There is a strong gate dependence of the valley polarization, which is greatest at +60 V and highly suppressed at −60 V (the full data set is provided in fig. S6). In Fig. 2B, we show the decay of co-polarized (Fig. 2B, black) and cross-polarized (Fig. 2B, red) interlayer exciton PL, as well as the degree of polarization (Fig. 2B, blue), at the same V_g values as in Fig. 2A (the full data set is provided in fig. S7). The valley polarization lifetime increases with V_g, reaching 39 ± 2 ns at +60 V, as determined by fitting a single exponential decay. We also measured long valley lifetimes in heterostructures with the opposite stacking order ($MoSe_2$ on WSe_2) (fig. S8).

These measurements imply a strong suppression of intervalley scattering for the X_I and a valley lifetime several orders of magnitude longer than that of intralayer excitons in monolayers, in which valley depolarization occurs on picosecond time scales (*34*–*36*). Our measurement also shows that the initial PL polarization of X_I is ~40% at +60 V. The imperfect initial valley polarization of X_I is likely due to valley depolarization of intralayer excitons in the constituent

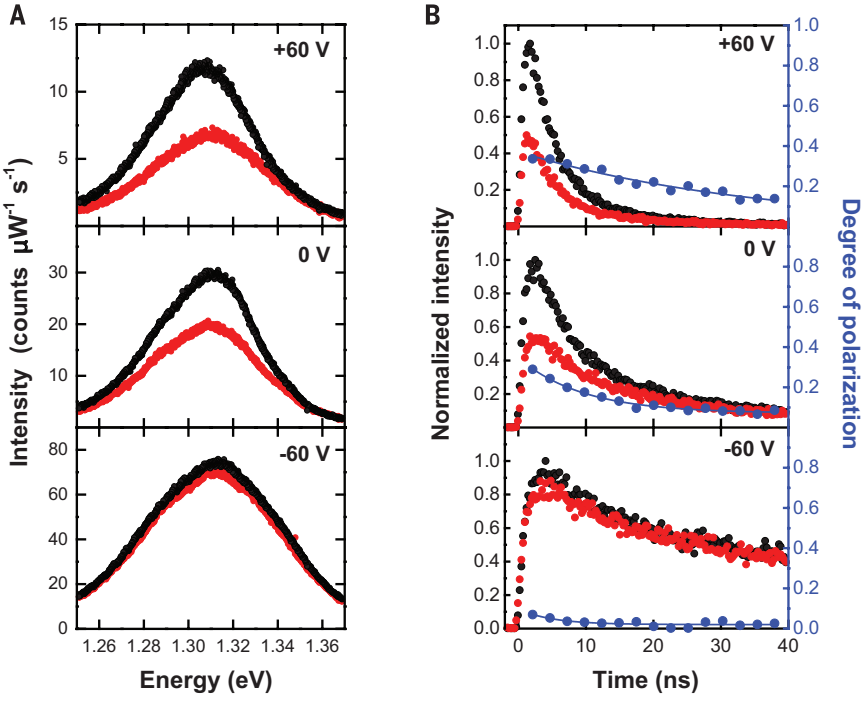

Fig. 2. Gate-tunable interlayer exciton valley polarization and lifetime. All plots are for σ^+ pulsed laser excitation with co-polarized and cross-polarized PL shown in black and red, respectively. (**A**) Polarization-resolved interlayer exciton PL at selected gate voltages. (**B**) Time-resolved interlayer exciton PL at selected gate voltages. The blue curve (right axis) shows the decay of valley polarization. Solid lines are single exponential fits to valley polarization decay, with lifetimes of 39 ± 2, 10 ± 1, and 5 ± 2 ns for gate voltages of +60, 0, and −60 V, respectively.

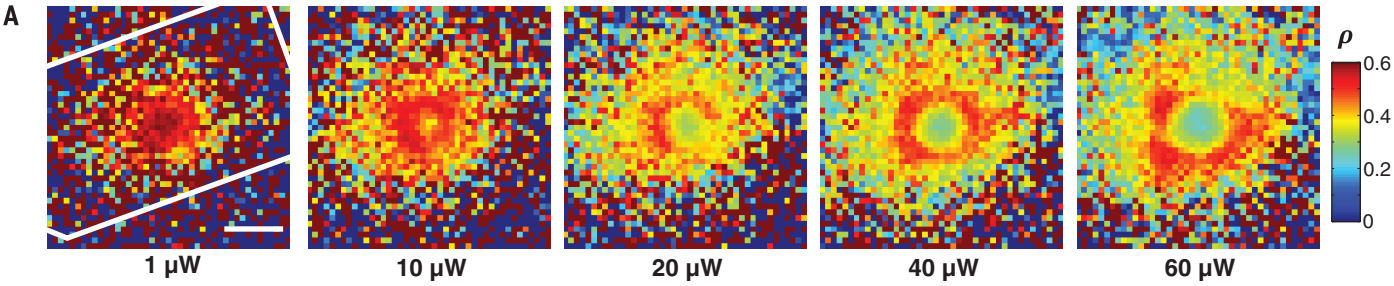

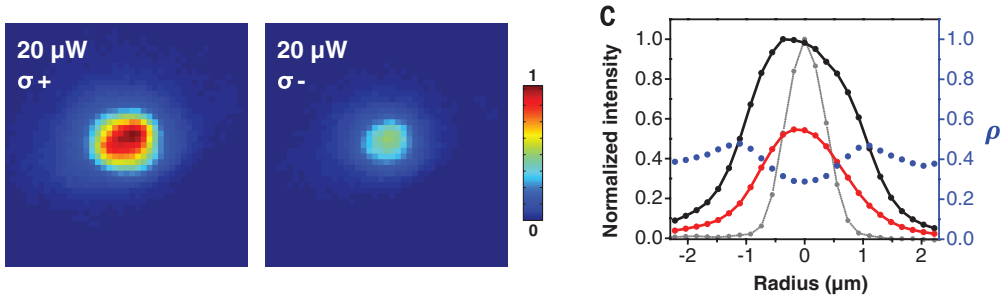

Fig. 3. Drift-diffusion of valley-polarized interlayer exciton gas. All plots are for σ^+ pulsed laser excitation. (**A**) Spatial map of valley polarization under 1 to 60 μW excitation. Sample outline is shown in white overlay. Scale bar, 2 μm. (**B**) Spatial maps of σ^+ (left) and σ^- (right) interlayer exciton PL normalized intensity under 20 μW excitation. (**C**) Polarization-resolved spatial profiles of σ^+ (black) and σ^- (red) components of interlayer exciton PL under 40 μW excitation. The spatial distribution of valley polarization is shown in blue, and the laser excitation profile is shown in gray. Line cuts are radially averaged through the excitation center, and curves are added as guides to the eye.

monolayers, which mediate the X_I formation. Because the X_I is dark at the minimum of the energy dispersion (*27*), caused by the finite twisting angle and slight lattice mismatch between the two layers, it effectively provides a reservoir from which the X_I are scattered into the light cones and luminesce. The momentum-indirect nature of X_I is supported by temperature-dependent measurements, which show enhanced lifetime at low temperature (fig. S9). This complicated exciton-light coupling is likely responsible for the subtle but intriguing features in Fig. 2B, such as the increase of PL lifetime accompanying the decrease of valley polarization lifetime. However, future studies are required to gain a clear understanding of the microscopic mechanism for the observed gate-dependent PL dynamics of the X_I.

The long valley lifetime of the X_I allows visualization of their lateral drift and diffusion. A sequence of spatial maps of the X_I PL polarization under pulsed excitation (40 MHz repetition rate) at V_g = 60 V is displayed in Fig. 3A for selected average excitation powers. The spatial pattern of ρ shows the evolution of a ring with a diameter that increases with excitation intensity (the full data set is available in fig. S10). The pattern of polarization stands in contrast to the spatial distribution of the emission. The polarization-resolved PL intensity spatial maps are shown in Fig. 3B at 20 μW, where both σ^+ and σ^- PL components display an approximately Gaussian profile centered at the excitation spot. For direct comparison of the different spatial profiles, Fig. 3C gives the average PL intensity and ρ as a function of the distance from the beam center for the 40 μW case. The data show the drift-diffusion of σ^+ (Fig. 3C, black) and σ^- (Fig. 3C, red) polarized excitons away from the laser spot (0.7 μm full-width at half maximum) (Fig. 3C, dashed line) as well as the ring of larger ρ (Fig. 3C, blue), demonstrating the striking difference between the spatial distribution of polarization and the total density of X_I.

One possible explanation for the observed polarization ring is density-dependent intervalley scattering. However, consideration of the valley polarization as a function of excitation intensity suggests otherwise (fig. S11). Rather, the observed spatial patterns in the valley polarization can be understood as manifestations of valley-dependent many-body interactions in the dense interlayer exciton gas (*33*). The spin-valley polarized X_I, which possess out-of-plane dipoles, interact through dipole-dipole and exchange interactions, both of which are repulsive. Because of the small interlayer separation of ~7 Å, we estimate that the exchange interaction is stronger than the dipole-dipole repulsion (*33*). Because the exchange interactions are appreciable only between excitons of the same valley species (*33*), in a cloud of valley-polarized interlayer excitons the majority valley excitons experience stronger mutually repulsive force (fig. S13A), leading to more rapid expansion than that of the minority valley excitons (fig. S13B). On the other hand, the density gradient of excitons will also give rise to diffusion, which is valley-independent and does not produce a ring pattern. Therefore, the relative strength of the diffusion and valley-dependent drift controls the pattern of the spatial polarization. If the interlayer exciton density is large enough that the valley-dependent repulsive interaction dominates the expansion of the exciton gas, higher valley polarization can appear away from the excitation center (fig. S15). Indeed, a pronounced ring in the polarization is generated at sufficiently high excitation intensity, as seen in Fig. 3A.

A temperature difference between the majority and minority X_I could, in principle, cause them to expand at different speeds. However, under excitation by polarized laser pulse, the minority excitons are created at the excitation spot through intervalley relaxation. Because the relaxation of this internal degree of freedom does not change the kinetic energy of the exciton, the majority and minority X_I are expected to have the same initial temperature before the expansion of the exciton cloud. This precludes valley-dependent temperature as a driving force for the ring formation.

REFERENCES AND NOTES

1. A. K. Geim, I. V. Grigorieva, *Nature* **499**, 419–425 (2013).
2. C. R. Dean *et al.*, *Nature* **497**, 598–602 (2013).
3. B. Hunt *et al.*, *Science* **340**, 1427–1430 (2013).
4. L. A. Ponomarenko *et al.*, *Nature* **497**, 594–597 (2013).
5. J. Kang, S. Tongay, J. Zhou, J. Li, J. Wu, *Appl. Phys. Lett.* **102**, 012111 (2013).
6. K. Kośmider, J. Fernández-Rossier, *Phys. Rev. B* **87**, 075451 (2013).
7. H. Terrones, F. López-Urías, M. Terrones, *Sci. Rep.* **3**, 1549 (2013).
8. M.-H. Chiu *et al.*, *Nat. Commun.* **6**, 7666 (2015).
9. R. Cheng *et al.*, *Nano Lett.* **14**, 5590–5597 (2014).
10. M. M. Furchi, A. Pospischil, F. Libisch, J. Burgdörfer, T. Mueller, *Nano Lett.* **14**, 4785–4791 (2014).
11. X. Hong *et al.*, *Nat. Nanotechnol.* **9**, 682–686 (2014).
12. C. H. Lee *et al.*, *Nat. Nanotechnol.* **9**, 676–681 (2014).
13. Y.-C. Lin *et al.*, *Nat. Commun.* **6**, 7311 (2015).
14. Y. Gong *et al.*, *Nat. Mater.* **13**, 1135–1142 (2014).
15. F. Ceballos, M. Z. Bellus, H.-Y. Chiu, H. Zhao, *ACS Nano* **8**, 12717–12724 (2014).
16. H. Fang *et al.*, *Proc. Natl. Acad. Sci. U.S.A.* **111**, 6198–6202 (2014).
17. P. Rivera *et al.*, *Nat. Commun.* **6**, 6242 (2015).
18. L. V. Butov, A. C. Gossard, D. S. Chemla, *Nature* **418**, 751–754 (2002).
19. D. Snoke, S. Denev, Y. Liu, L. Pfeiffer, K. West, *Nature* **418**, 754–757 (2002).
20. J. R. Leonard *et al.*, *Nano Lett.* **9**, 4204–4208 (2009).
21. E. Finkman, M. D. Sturge, M. C. Tamargo, *Appl. Phys. Lett.* **49**, 1299–1301 (1986).

22. G. D. Gilliland *et al.*, *Phys. Rev. Lett.* **71**, 3717–3720 (1993).
23. D. Xiao, G. B. Liu, W. Feng, X. Xu, W. Yao, *Phys. Rev. Lett.* **108**, 196802 (2012).
24. W.-T. Hsu *et al.*, *ACS Nano* **8**, 2951–2958 (2014).
25. A. M. van der Zande *et al.*, *Nano Lett.* **14**, 3869–3875 (2014).
26. K. Liu *et al.*, *Nat. Commun.* **5**, 4966 (2014).
27. H. Yu, Y. Wang, Q. Tong, X. Xu, W. Yao, *Phys. Rev. Lett.* **115**, 187002 (2015).
28. T. Cao *et al.*, *Nat. Commun.* **3**, 887 (2012).
29. K. F. Mak, K. He, J. Shan, T. F. Heinz, *Nat. Nanotechnol.* **7**, 494–498 (2012).
30. H. Zeng, J. Dai, W. Yao, D. Xiao, X. Cui, *Nat. Nanotechnol.* **7**, 490–493 (2012).
31. M. M. Fogler, L. V. Butov, K. S. Novoselov, *Nat. Commun.* **5**, 4555 (2014).
32. P. J. Zomer, M. H. D. Guimarães, J. C. Brant, N. Tombros, B. J. van Wees, *Appl. Phys. Lett.* **105**, 013101 (2014).
33. Materials and methods are available as supplementary materials on *Science* Online.
34. C. Mai *et al.*, *Nano Lett.* **14**, 202–206 (2014).
35. Q. Wang *et al.*, *ACS Nano* **7**, 11087–11093 (2013).
36. C. R. Zhu *et al.*, *Phys. Rev. B* **90**, 161302 (2014).

ACKNOWLEDGMENTS

We thank D. Cobden and F. Wang for helpful discussion. This work is mainly supported by the U.S. Department of Energy (DOE), Basic Energy Sciences (BES), Materials Sciences and Engineering Division (DE-SC0008145 and SC0012509). The spectroscopy work is partially supported by NSF-EFRI-1433496. H.Y. and W.Y. were supported by the Croucher Foundation (Croucher Innovation Award), and the Research Grants Counciland University Grants Committee of Hong Kong (HKU17305914P, HKU9/CRF/13G, AoE/P-04/08). J.Y. and D.G.M. were supported by the DOE, BES, Materials Sciences and Engineering Division. X.X. acknowledges a Cottrell Scholar Award and support from the State of Washington–funded Clean Energy Institute. Device fabrication was performed at the University of Washington Microfabrication Facility and NSF-funded Nanotech User Facility. Data described in this paper are presented in the supplementary materials and are available upon request. X.X. and W.Y. conceived and supervised the project. P.R. and K.L.S. fabricated the samples and performed the experiments, assisted by J.R.S. P.R., K.L.S., and X.X. analyzed data. H.Y. and W.Y. provided theoretical support and performed the simulation. J.Y. and D.G.M. synthesized and characterized the bulk crystal. P.R., K.L.S., X.X., W.Y., and H.Y. cowrote the paper. All authors discussed the results.

SUPPLEMENTARY MATERIALS

www.sciencemag.org/content/351/6274/688/suppl/DC1
Materials and Methods
Figs. S1 to S15
References (*37*–*45*)

11 June 2015; accepted 8 January 2016
10.1126/science.aac7820

MATERIALS SCIENCE

On-chip and freestanding elastic carbon films for micro-supercapacitors

P. Huang,[1,2] C. Lethien,[2,3] S. Pinaud,[4] K. Brousse,[1,2] R. Laloo,[1,2] V. Turq,[1,2] M. Respaud,[4,5] A. Demortière,[2,6] B. Daffos,[1,2] P. L. Taberna,[1,2] B. Chaudret,[4] Y. Gogotsi,[7] P. Simon[1,2]*

Integration of electrochemical capacitors with silicon-based electronics is a major challenge, limiting energy storage on a chip. We describe a wafer-scale process for manufacturing strongly adhering carbide-derived carbon films and interdigitated micro-supercapacitors with embedded titanium carbide current collectors, fully compatible with current microfabrication and silicon-based device technology. Capacitance of those films reaches 410 farads per cubic centimeter/200 millifarads per square centimeter in aqueous electrolyte and 170 farads per cubic centimeter/85 millifarads per square centimeter in organic electrolyte. We also demonstrate preparation of self-supported, mechanically stable, micrometer-thick porous carbon films with a Young's modulus of 14.5 gigapascals, with the possibility of further transfer onto flexible substrates. These materials are interesting for applications in structural energy storage, tribology, and gas separation.

The plethora of portable electronic devices and the continued expansion of electronics into new mobile applications highlight the need for high-performance miniaturized electrochemical storage devices able to deliver energy from their environment. Radio frequency identification (RFID) tags for the development of smart environments are another critical application that requires compact energy storage. Accordingly, designing efficient miniaturized energy storage devices for energy delivery or harvesting with high-power capabilities remains a challenge (*1*).

Electrochemical double-layer capacitors (EDLCs), also known as supercapacitors, store the charge through reversible ion adsorption at the surface of high-surface-area carbons. Aside from an outstanding cycle life, this electrostatic charge storage results in devices with medium energy density (~6 W·h kg^{-1}) and high power densities (>10 kW kg^{-1}). As a result, supercapacitors complement—or can even sometimes replace—batteries in applications from electronics to public transportation and renewable energy storage, in which high-power delivery and uptake and very long cycle life are required (*2*).

A large variety of materials such as graphene (*3*–*5*), nanotubes (*6*, *7*), carbide-derived carbons (CDC) (*8*, *9*), and pseudocapacitive materials (*1*, *10*, *11*) have been explored in micro-supercapacitors in the past 5 years. Much of the recent work focused on the use of wet processing routes (using colloidal solutions or suspensions of particles for the electrode preparation) for the development of flexible micro-devices for printable electronics (*1*, *4*, *5*, *12*). However, the wet processing methods are not fully compatible with semiconductor device manufacturing used in the electronics industry, thus hampering supercapacitor manufacturing on silicon chips. Vapor phase methods, such as atomic layer deposition, are limited to the preparation of thin layers of active materials, limiting the areal energy and power performance of the electrodes (*13*, *14*). Direct growth of graphene or carbon nanotubes on a Si wafer results in low-energy-density devices (*15*). The pioneering concept of laser scribing of graphene developed by Kaner's group for preparing flexible micro-supercapacitors has shown outstanding power performance but fails to achieve high areal capacitance (< 5 mF cm^{-2}) (*3*, *5*). Another strategy is to use pseudocapacitive materials, which have a larger capacitance, but moving from pure double-layer to pseudocapacitive charge storage comes with disadvantages, such as a decrease in power capabilities and cycle life because of the kinetic limitations of the redox reactions (*10*, *11*, *16*–*20*). Bulk CDC films (*8*, *9*, *21*) have shown high capacitance and high areal and volumetric energy density but poor integrity of the film from cracking and delamination (*9*).

To produce carbon films, TiC coatings of several micrometers in thickness were deposited by using a direct current magnetron sputtering (DC-MS) technique (supplementary materials, materials and methods). Shown in fig. S1A is a cross section of a 6.3-μm-thick TiC film deposited onto a SiO_2-coated Si wafer, by using the DC-MS technique. The resistivity, thickness, and mechanical stress of the TiC film can be fine-tuned by changing the deposition parameters (fig. S1, B and C). The film thickness changes linearly with the deposition time (fig. S1D), and films up to 20 μm thick could be prepared, with controlled roughness (fig. S1E). Samples were placed in a furnace and chlorinated at 450°C, thus transforming

[1]Université Paul Sabatier-Toulouse III, Laboratoire Centre Inter-universitaire de Recherche et d'Ingénierie des Matériaux (CIRIMAT), UMR CNRS 5085, 118 route de Narbonne, 31062 Toulouse, France. [2]Réseau sur le Stockage Electrochimique de l'Energie, FR CNRS n°3459, France. [3]Université Lille 1 Sciences et Technologies, Laboratoire Institut d'Electronique de Microélectronique et de Nanotechnologie (IEMN), UMR CNRS 8520, Cité scientifique, Avenue Henri Poincaré, CS 60069, 59652 Villeneuve d'Ascq cedex, France. [4]Laboratoire de Physique et Chimie des Nano-Objets (LPCNO), UMR 5215 Institut National des Sciences Appliquées (INSA)–Université Paul Sabatier (UPS)–CNRS, Université de Toulouse, INSA, 135 Avenue de Rangueil, 31077 Toulouse, France. [5]Atelier Interuniversitaire de Micro-nano Électronique (AIME), Université de Toulouse, INSA, UPS, INP, 135 avenue de Rangueil, 31077 Toulouse Cedex 4, France. [6]Laboratoire de Chimie et de Réactivité des Solides, UMR CNRS 7314, Université de Picardie Jules Verne, 80039 Amiens, France. [7]Department of Materials Science and Engineering, and A. J. Drexel Nanomaterials Institute, Drexel University, 3141 Chestnut Street, Philadelphia, PA 19104, USA.
***Corresponding author. E-mail: simon@chimie.ups-tlse.fr**

Downloaded from on February 11, 2016

the TiC film into CDC (*8*, *9*, *21*, *22*) with a growth rate of 1 μm/min (table S2) by the reaction

$$TiC + 2Cl_2 \rightarrow TiCl_4 + C \quad (1)$$

The chlorination time t_1 was fixed at 5 min for achieving a partial chlorination of the TiC layer, as shown in Fig. 1A, top. Shown in Fig. 1B is a cross section of the SiO_2 (Fig. 1B, bottom)/TiC (Fig. 1B, middle)/porous CDC structure. The thickness of the CDC layer was ~5 μm, so that a ~1.3-μm-thick film of metallically conducting TiC remained under the CDC layer.

Because of the partial chlorination, the transformation of TiC into porous CDC was, for the first time, achieved without any film delamination at either the CDC/TiC or TiC/SiO_2 interface. The presence of the ~1-μm-thick underlayer of TiC keeps the TiC/SiO_2 interface identical to the one observed before chlorination, with no trace of delamination or cracks.

Last, this TiC layer not only acts as a buffer and adhesion layer that accommodates the mechanical stresses between the Si wafer and the porous CDC but also can be used as a current collector because the electrical conductivity was kept above 10^3 S cm^{-1} (table S1).

Raman spectra of the TiC film before (Fig. 1C, red) and after (Fig. 1C, blue) chlorination were recorded. Peaks in the 250 to 750 nm range are shown in Fig. 1C, namely 250 cm^{-1}, 433 cm^{-1}, and 608 cm^{-1}, which are attributed to the TiC (*23*). The peaks completely disappeared after chlorination, and only the D and G bands of graphitic carbon, fairly typical for TiC-CDC (*8*, *21*), were visible, thus confirming that Ti was removed during chlorination.

We measured the pore volume and the pore size distribution (Fig. 1D) using Ar and CO_2 gas sorption. The type 1 Ar adsorption isotherm (fig. S2A) shows a microporous sample, with all adsorption occurring at low pressures. The Brunauer-Emmett-Teller (BET) surface area was calculated at 977 ± 30 m^2 g^{-1}. CO_2 gas sorption measurements (fig. S2B) gave a micropore volume of 0.47 cm^3 g^{-1} and a very narrow pore size distribution (Fig. 1D), with a mean pore size of 0.59 nm and no pores larger than 1 nm. This zeolite-like pore size distribution confirms a very uniform structure of the film.

The transmission electron microscopy (TEM) investigation (Fig. 2) of a thin cross-sectional sample prepared with the focused ion beam (FIB) technique revealed a rugged interface, with sharp needles of TiC penetrating into the carbon layer and providing excellent adhesion (Fig. 2, A to F). CDC shown in Fig. 2, G and H, was analyzed by means of high-angle annular dark-field scanning TEM (HAADF-STEM), and the estimated roughness and porosity of the surface were less than 1 nm.

The electrochemical characterization of the TiC/CDC films on Si wafers was performed in aqueous (1 M H_2SO_4) and organic (1 M EMI, BF_4 in acetonitrile) electrolytes in three-electrode cells. After chlorination, the samples were annealed under vacuum at 600°C for 2 hours so as to remove trapped chlorine and chlorides, as evidenced with Auger spectroscopy (fig. S3B). Cyclic voltammograms of a CDC sample in 1 M H_2SO_4 electrolyte, at 20 and 1 mV s^{-1} (Fig. 3A), have a rectangular shape typical for capacitive behavior. The slight current increase at negative potentials during negative sweep below −0.5 V versus Hg_2SO_4/Hg is assumed to originate from the pseudocapacitive contribution of proton reduction in confined carbon micropores, as proposed by Béguin *et al.* (*24*). The gravimetric capacitance is meaningless for microdevices (*25*); therefore, values of 410 F cm^{-3} and 205 mF cm^{-2} were calculated at 1 mV s^{-1} for the volumetric and

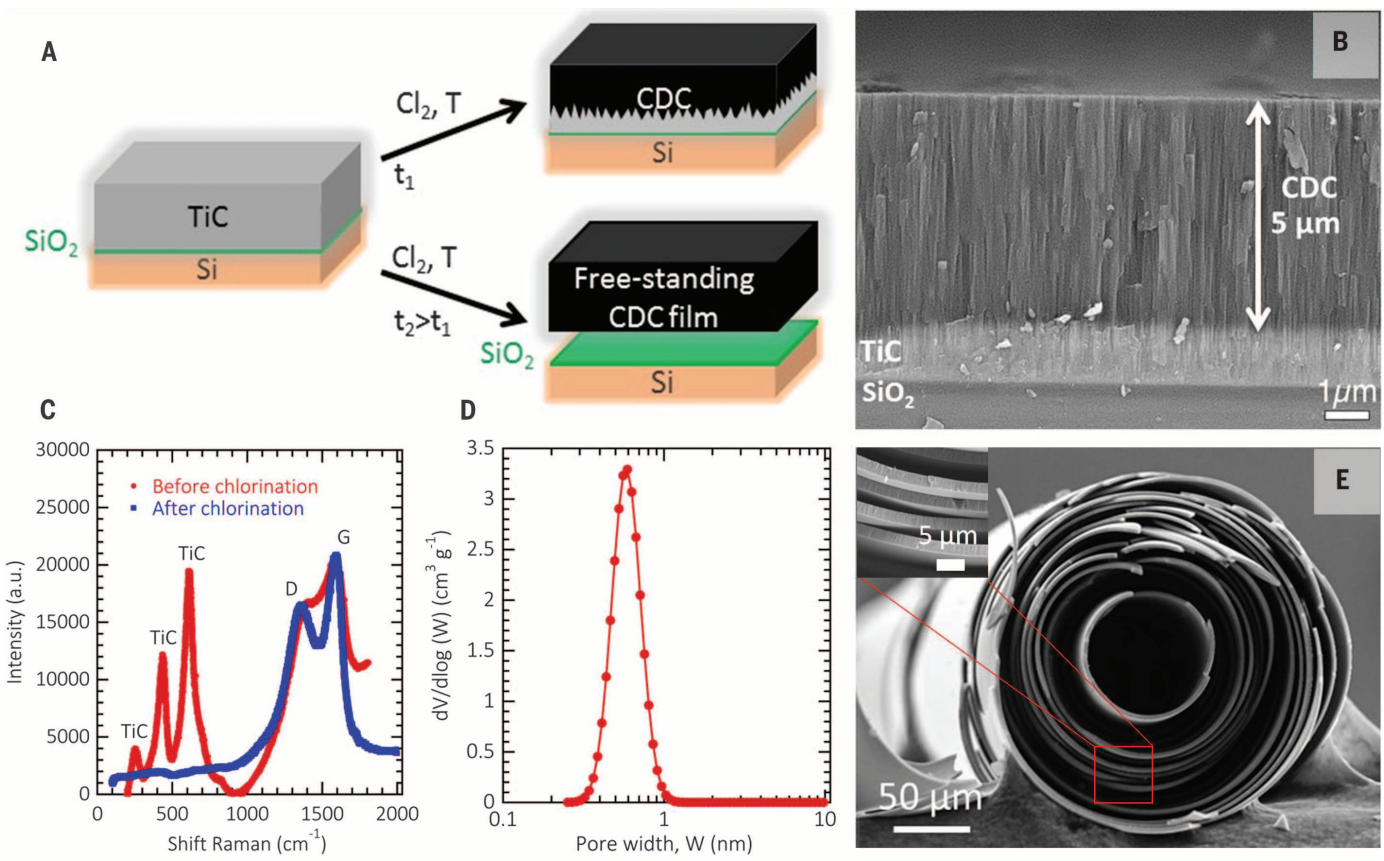

Fig. 1. Preparation of the microporous carbon films. (**A**) Scheme of the chlorination process. Starting from TiC films deposited onto a Si wafer, the partial chlorination of the films leads to SiO_2/TiC/CDC layered structures (top right). The full chlorination allows the synthesis of freestanding CDC films (bottom right). (**B**) SiO_2/TiC/CDC layered structures obtained after chlorination for 5 min at 450°C. (**C**) Raman spectra of the TiC and the CDC layers. (**D**) Pore size distribution of the porous CDC films from CO_2 gas sorption, using the Reverse Monte Carlo model. The isotherm shows a microporous sample, with an estimated average pore size of 0.59 nm. (**E**) Cross-sectional SEM images of rolled freestanding delaminated films obtained through full chlorination.

areal capacitance, respectively. Cyclic voltammetry at low scan rates provides evidence of a low-leakage current in the cell. The electrode capacitance was stable over 10,000 cycles (Fig. 3B). The change of the normalized capacitance versus the potential scan rate provides evidence for the high power capability of these films (Fig. 3B, inset) as more than 200 F cm^{-3} (100 mF cm^{-2}) were still delivered during 0.9 s discharge (1 V s^{-1}), which outperforms the current state of the art of carbon-based double-layer capacitors and micro-supercapacitors (*26*–*30*).

The cyclic voltammogram (CV) of a Si/TiC/CDC film annealed at 600°C in hydrogen and tested as a single electrode at 20 mV s^{-1} in 1 M EMI,BF_4 in acetonitrile electrolyte shows a typical capacitive behavior within a potential window limited to 2.0 V (fig. S3D). The volumetric capacitance of the sample reached 170 F cm^{-3}, which is in line with the data reported for TiC-CDC films (*8*). Annealing at 600°C under H_2 atmosphere opens carbon pores (*22*), thus improving accessibility to large EMI^+ ions compared with that of a nonannealed sample (fig. S3C) without affecting the adherence at the CDC/TiC interface. CDC pore size, which determines capacitance, can be controlled with the synthesis temperature (*8*, *21*, *22*). Shown in Fig. 3C are CVs of a 2.2-μm-thick CDC film on a Si/TiC/CDC electrode prepared through partial chlorination at 700°C for 30 s, obtained at different rates. CVs show a typical capacitive behavior within a potential window up to 3 V, resulting in an improvement of the energy and power density (Fig. 4) and the volumetric capacitance reaching 160 F cm^{-3} at 20 mV s^{-1}.

Following the electrochemical characterizations of the CDC films, two-electrode micro-supercapacitor devices were manufactured and characterized. Micro-supercapacitors containing nine fingers per polarity (2 mm long, 100 μm wide, with 15 μm separation) (Fig. 3D) were prepared according to the different steps detailed in figs. S4 and S5, A to C. A picture of a 7.62-cm Si wafer containing 40 patterned micro-supercapacitors is shown in Fig. 3E, thus confirming that the process can be easily scalable. Ti/Au film was evaporated on both sides of the large pad for ensuring electrical contact. The CVs of a micro-supercapacitor in H_2SO_4 1 M electrolyte are presented in Fig. 3F. In this example, the chlorination of a 3.5-μm-thick patterned TiC layer led to formation of a 1.4-μm-thick CDC film. The electrode volumetric capacitance reached 350 F cm^{-3}, which is in line with the electrochemical performance of three-electrode cells presented in Fig. 3A. The slight decrease of the volumetric capacitance compared with that of a single electrode (410 F cm^{-3}) may originate from very small separation (only 15 μm) between the electrode fingers. The capacitance change with the potential scan rate is shown in fig. S5D; the initial capacitance is 350 F cm^{-3}. More than 50%

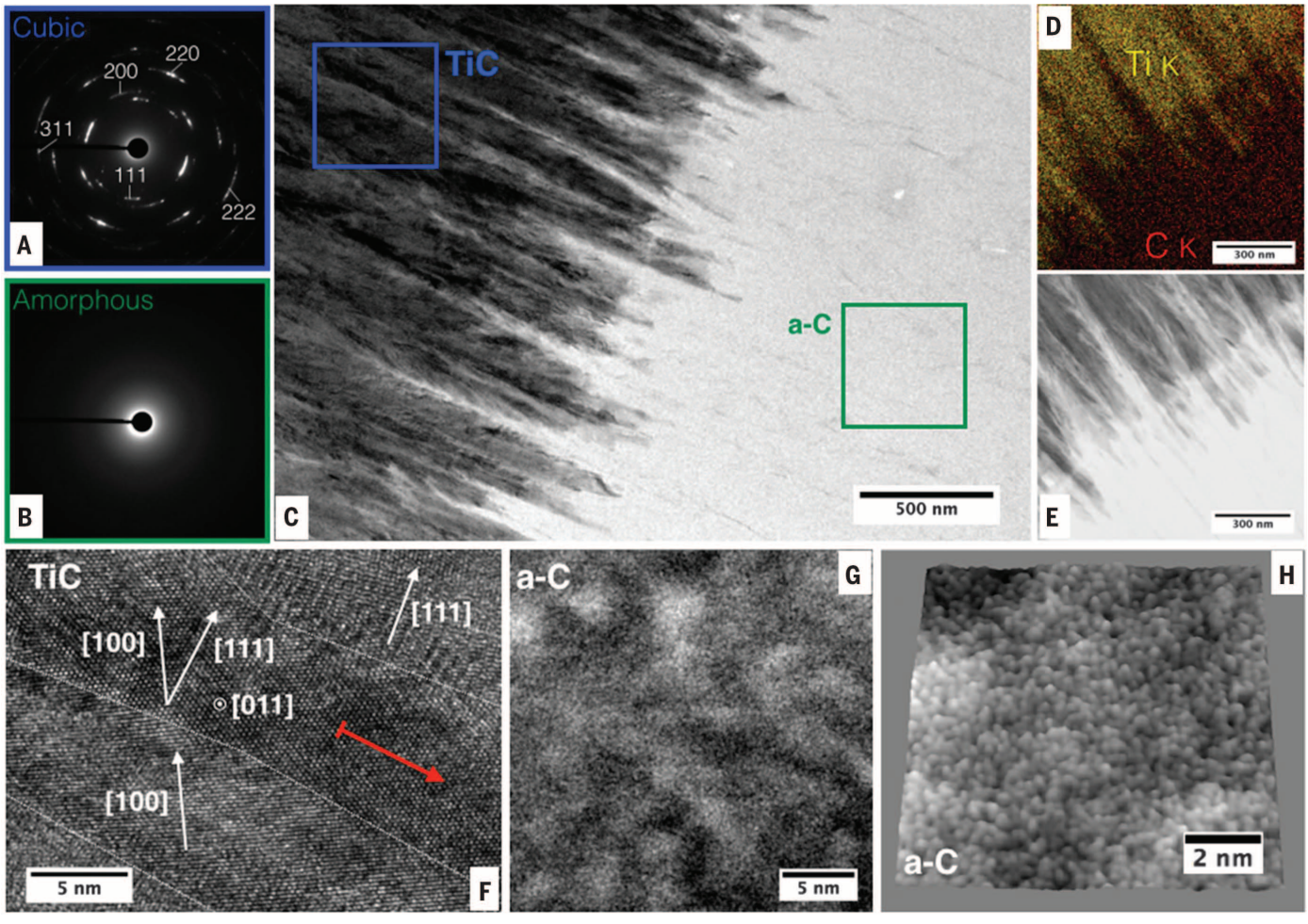

Fig. 2. Structural characterization of the SiO_2/TiC/CDC electrodes. (**A**) Selected-area electron diffraction (SAED) pattern of TiC [(C), blue square] showing the cubic structure. (**B**) SAED pattern of CDC [(C), green square], showing an amorphous structure. (**C**) TEM image of the TiC/CDC interface, with the areas for the SAED analysis [blue and green squares in (A) and (B), respectively]. (**D**) Energy-dispersive x-ray analysis showing the absence of Ti in the carbon film. (**E**) Bright-field STEM image of the interface, showing the interpenetration of TiC and carbon structures, which proves the excellent adhesion between the layers. (**F**) High-resolution TEM image showing the crystallographic orientation of the TiC cubic structure. (**G**) HAADF-STEM image of the amorphous carbon and (**H**) roughness of the CDC surface, which is estimated to be less than 1 nm (scanned area, 10 by 10 nm).

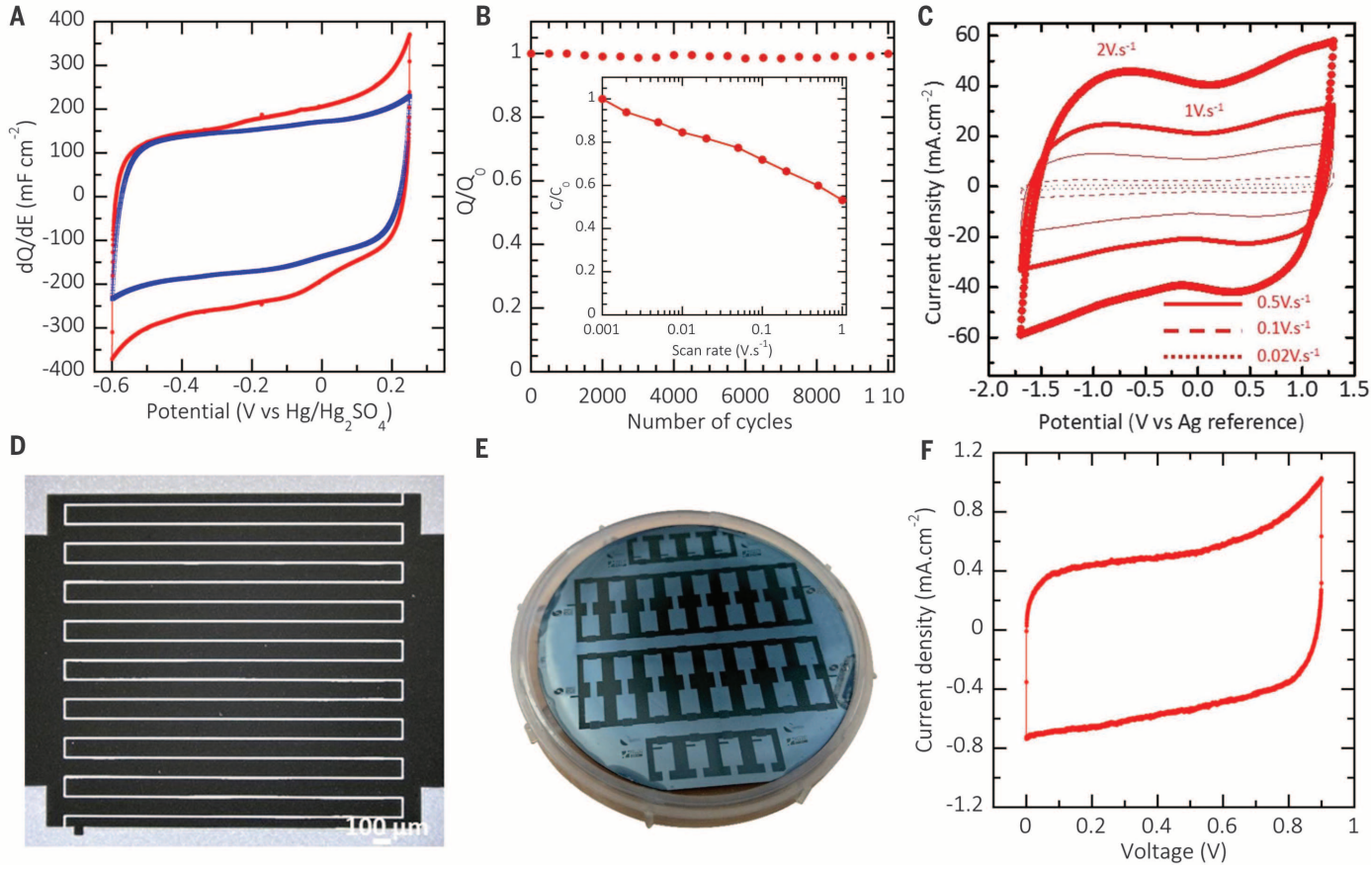

Fig. 3. Electrochemical characterizations. (**A**) CVs of a Si/TiC/CDC electrode in 1 M H_2SO_4 electrolyte at 20 mV s^{-1} (blue curve) and 1 mV s^{-1} (red curve), both after annealing 2 hours at 600°C under vacuum. The volumetric capacitance reaches 410 F cm^{-3} or 205 mF cm^{-2}. (**B**) No capacitance loss was observed up to 10,000 cycles. (Inset) Change of the normalized capacitance with the potential scan rate for a 5-µm-thick CDC sample. The initial value is 410 F cm^{-3} (205 mF cm^{-2}). (**C**) CVs of a SiO_2/TiC/CDC electrode (2.2-µm-thick CDC film), which was chlorinated at 700°C and annealed in H_2 for 1 hour at 600°C, in 2 M EMI,BF_4 in CH_3CN electrolyte at various scan rates. The volumetric capacitance reaches 160 F cm^{-3} within a 3-V potential window. (**D**) Optical picture (top view) of the micro-supercapacitor after the chlorination process. The 18 interdigitated electrodes of CDC are separated by a 15-µm distance. (**E**) A 7.62-cm Si wafer containing 40 patterned micro-supercapacitors. (**F**) CV of a micro-supercapacitor in 1 M H_2SO_4 electrolyte recorded at 10 mV s^{-1}. The volumetric capacitance reaches 350 F cm^{-3}.

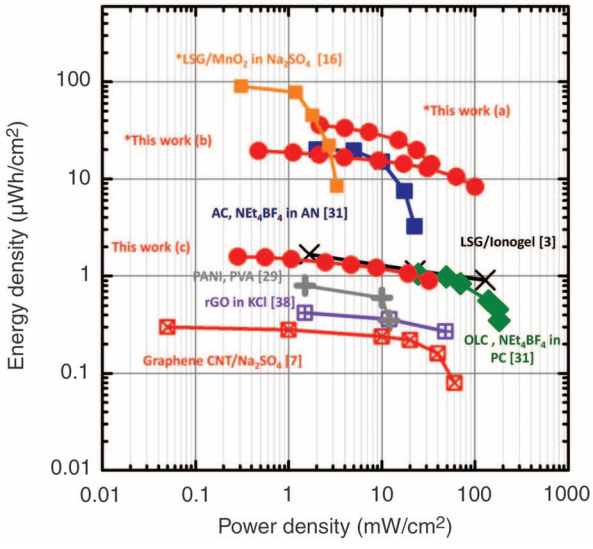

Fig. 4. Electrical performance. Areal-normalized Ragone plots showing the performance of several microsystems using carbon and pseudocapacitive materials in interdigitated or parallel-plate (noted with asterisks) configurations. AC, activated carbon; LSG, laser scribed graphene; OLC, onions like carbon; PANI, polyaniline; PVA, polyvinylic acetate; rGO, reduced graphene oxide; PC, polypropylene. "This work (a)" refers to 2 M EMI,BF_4 in AN, 4.1-µm-thick TiC film (fig. S3E), two parallel plates device. "This work (b)" refers to 2 M EMI,BF_4 in AN, 2.2-µm-thick TiC film, two parallel plates device (Fig. 3C). "This work (c)" refers to 1 M H_2SO_4, 1.4-µm-thick, interdigitated microdevice (Fig. 3F). Numbers in brackets are cited references.

of the capacitance (180 F cm^{-3}) is still retained at 10 V s^{-1}, thus outperforming the state-of-the-art micro-supercapacitors (*1*, *16*, *17*, *27*, *29*, *31*), as can be seen in the volume-normalized Ragone plot in fig. S6 showing performance of micro-supercapacitors in interdigitated and parallel-plate configurations. Because performance per device area is a key metric for the integration of electrochemical capacitors with Si-based electronics, Fig. 4 shows an area-normalized Ragone plot. Compared with other carbon-based systems, our devices show the best performance in terms of areal energy and power density in the parallel-plate configuration. Moreover, our present results obtained with carbon materials even compare favorably with thick pseudocapacitive laser-scribed graphene (LSG)/MnO_2 composite electrodes, achieving a very high areal capacitance of 800 mF cm^{-2}. Indeed, unlike in the present results, high areal capacitance is generally accompanied by a low-power performance because of the use of thick electrodes (*32*–*34*) or low areal energy and power densities because of the use

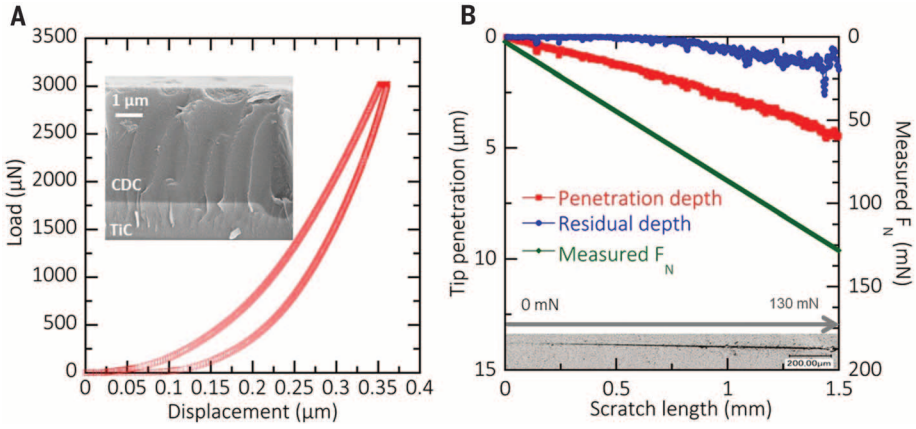

Fig. 5. Mechanical properties of the TiC/CDC layered structure. (**A**) The load versus displacement plot measured with a Berkovich nano-indenter shows more than 75% elastic recovery, with a Young's modulus of 14.5 GPa, a hardness of 1.6 GPa, and an equivalent Vickers hardness of 151 HV. (Inset) Cross section of the TiC/CDC layered structure studied. (**B**) The nano-scratch test (picture at bottom) reveals a low friction coefficient of about 0.2, which is half of that measured on TiC.

of faradic materials with a narrow operating potential window (*13*).

The mechanical properties of the films reported here differ from cracked and low-strength CDC films that frequently suffered from delamination upon cycling (*9*, *21*) or graphite, activated carbon, or nanotube films, in which particles are weakly bonded by van der Waals forces or kept together by a polymer binder (*5*–*7*, *31*, *35*). The load as a function of the displacement plot for a 5-μm-thick CDC film is shown in Fig. 5A, using a Berkovich indenter (supplementary materials, materials and methods). The CDC coating shows a hardness of 1.6 GPa and a Young's modulus of 14.5 GPa, which are in good agreement with the literature (*36*), with a large elastic contribution (>75%) to the loading. The excellent adhesion at the TiC/CDC interface is also confirmed by the propagation of the fractures from the CDC down into the TiC layer (Fig. 5A, inset), with no crack deflection at the interface, suggesting that the CDC film has mechanical properties comparable with that of TiC (*36*).

Penetration depth during a nanoscratch test and residual depth after the test are plotted versus the distance and normal force (Fig. 5B). The delamination of the coating occurred for a normal load of 130 mN, which corresponds to a work of adhesion of 18 J m^{-2}. However, the residual depth (Fig. 5B, blue plot) remains 0 during the first 0.6 mm of the scratch tests (up to a normal force of 40 mN), giving evidence to outstanding elasticity of the porous CDC film. The friction coefficient measured during the scratch test (0.2) is twice lower on the CDC surface than on the TiC surface, highlighting the lubricating effect of the coating.

Increasing the chlorination time t_2 of the TiC film (Fig. 1A, down) leads to the separation of CDC from the Si substrate and formation of self-supported CDC films of several square centimeters in area (fig. S7, A and B). The CV at 20 mV s^{-1} in a 1 M H_2SO_4 electrolyte is shown in fig. S7C. Similarly to the partially chlorinated films, a high capacitance of 180 mF cm^{-2} (300 F cm^{-3}) was obtained. By tuning the pressure in the chamber during the TiC deposition process (0.001 mbar) and the chlorination temperature (350°C), internal stress in 3-μm-thick TiC films led to CDC rolls (Fig. 1E). Such rolling has been observed for CVD semiconductor films (*37*). A TEM image of the film (fig. S7D) shows its amorphous structure. The excellent mechanical properties as well as the absence of large pores or cracks (Figs. 1B and 2C), which would act as defects that weaken the film, may be responsible for the observed film integrity after separation. X-ray photoelectron spectroscopy (XPS) analysis shows that the free-standing films have similar composition from the film surface to the bulk (Fig. S7, E and F). Another key feature is the possibility offered by these freestanding CDC films to be transferred onto flexible substrates, as shown in fig. S8, A and B. The electrochemical performance of a 8-μm-thick CDC film transferred onto a flexible polyethylene terephthalate substrate reached 240 mF cm^{-2} (300 F cm^{-3}) in the 1 M H_2SO_4 electrolyte. Additionally, freestanding patterned CDC microelectrodes could also be prepared from the full chlorination of patterned TiC (fig. S7G), which is promising for further development of high-performance stand-alone supercapacitors that could be used in flexible or wearable applications.

REFERENCES AND NOTES

1. M. Beidaghi, Y. Gogotsi, *Energy Environ. Sci.* **7**, 867–884 (2014).
2. P. Simon, Y. Gogotsi, *Nat. Mater.* **7**, 845–854 (2008).
3. M. F. El-Kady, R. B. Kaner, *Nat. Commun.* **4**, 1475 (2013).
4. Z. Peng, J. Lin, R. Ye, E. L. G. Samuel, J. M. Tour, *ACS Appl. Mater. Interfaces* **7**, 3414–3419 (2015).
5. M. F. El-Kady, V. Strong, S. Dubin, R. B. Kaner, *Science* **335**, 1326–1330 (2012).
6. B. Hsia *et al.*, *Nanotechnology* **25**, 055401 (2014).
7. J. Lin *et al.*, *Nano Lett.* **13**, 72–78 (2013).
8. J. Chmiola, C. Largeot, P. L. Taberna, P. Simon, Y. Gogotsi, *Science* **328**, 480–483 (2010).
9. P. Huang *et al.*, *J. Power Sources* **225**, 240–244 (2013).
10. E. Eustache *et al.*, *Electrochem. Commun.* **28**, 104–106 (2013).
11. X. Wang, Y. Yin, X. Li, Z. You, *J. Power Sources* **252**, 64–72 (2014).
12. M. S. Kim, B. Hsia, C. Carraro, R. Maboudian, *Carbon* **74**, 163–169 (2014).
13. C. Guan *et al.*, *Nanotechnology* **26**, 094001 (2015).
14. R. Warren, F. Sammoura, F. Tounsi, M. Sanghadasa, L. Lin, *J. Mat. Chem. A* **3**, 15568–15575 (2015).
15. J. J. Yoo *et al.*, *Nano Lett.* **11**, 1423–1427 (2011).
16. M. F. El-Kady *et al.*, *Proc. Natl. Acad. Sci. U.S.A.* **112**, 4233–4238 (2015).
17. X. Wang *et al.*, *Nanoscale* **5**, 4119–4122 (2013).
18. C. Shen *et al.*, *J. Power Sources* **234**, 302–309 (2013).
19. Z.-S. Wu *et al.*, *Adv. Mater.* **27**, 4054–4061 (2015).
20. T. M. Dinh *et al.*, *Nano Energy* **10**, 288–294 (2014).
21. M. Heon *et al.*, *Energy Environ. Sci.* **4**, 135–138 (2011).
22. J. Chmiola *et al.*, *Science* **313**, 1760–1763 (2006).
23. B. H. Lohse, A. Calka, D. Wexler, *J. Alloys Compd.* **434–435**, 405–409 (2007).
24. F. Béguin *et al.*, *Electrochim. Acta* **51**, 2161–2167 (2006).
25. Y. Gogotsi, P. Simon, *Science* **334**, 917–918 (2011).
26. C. Zhang, W. Lv, Y. Tao, Q.-H. Yang, *Energy Environ. Sci.* **8**, 1390–1403 (2015).
27. L. Wei, N. Nitta, G. Yushin, *ACS Nano* **7**, 6498–6506 (2013).
28. Y. Tao *et al.*, *Sci. Rep.* **3**, 2975 (2013).
29. C. Z. Meng, J. Maeng, S. W. M. John, P. P. Irazoqui, *Adv. Energy Mater.* **4**, 1301269 (2014).
30. S. Li, X. Wang, H. Xing, C. Shen, *J. Micromech. Microeng.* **23**, 114013 (2013).
31. D. Pech *et al.*, *Nat. Nanotechnol.* **5**, 651–654 (2010).
32. G. Xiong, C. Meng, R. G. Reifenberger, P. P. Irazoqui, T. S. Fisher, *Electroanalysis* **26**, 30–51 (2014).
33. B. Dunn, J. W. Long, *Electrochem. Soc. Interface* **17**, 49 (2008).
34. A. Ferris, S. Garbarino, D. Guay, D. Pech, *Adv. Mater.* **27**, 6625–6629 (2015).
35. M. Beidaghi, C. L. Wang, *Electrochim. Acta* **56**, 9508–9514 (2011).
36. Y. Gogotsi, S. Welz, D. A. Ersoy, M. J. McNallan, *Nature* **411**, 283–287 (2001).
37. V. Y. Prinz, *Microelectron. Eng.* **69**, 466–475 (2003).
38. M. Beidaghi, C. L. Wang, *Adv. Funct. Mater.* **22**, 4501–4510 (2012).

ACKNOWLEDGMENTS

P.H. was supported by the French Government [L'Agence Nationale de la Recherche (ANR) ASTRID program, MISE project]. K.B. was supported by the Chair of Excellence from the Airbus Group. P.S. acknowledges funding from the European Research Council (ERC Advanced Grant, "Ionaces" project). Y.G. was supported by Fluid Interface Reactions, Structures and Transport (FIRST) Center, an Energy Frontier Research Center funded by the U.S. Department of Energy, Office of Science, Office of Basic Energy Sciences. C.L was supported by the French RENATECH network. P.S., P.L.T., A.D., and C.L. thank the ANR (Labex Store-Ex and MISE project) for its support. The authors thank C. Brillard and J. P. Nys for atomic force microscopy and Auger analyses, D. Troadec for the Focus ion beam preparation, F. Guerin and R. P. Tan for microfabrication support, O. Mashtalir for XPS analyses of the TiC and CDC films, and K. Maleski for helpful comments on the manuscript.

SUPPLEMENTARY MATERIALS

www.sciencemag.org/content/351/6274/691/suppl/DC1
Materials and Methods
Supplementary Text
Figs. S1 to S8
Tables S1 and S2
References (*39*–*51*)

29 August 2015; accepted 7 January 2016
10.1126/science.aad3345

CARBON CYCLE

Enhanced seasonal CO_2 exchange caused by amplified plant productivity in northern ecosystems

Matthias Forkel,[1]*† Nuno Carvalhais,[1,2]* Christian Rödenbeck,[1] Ralph Keeling,[3] Martin Heimann,[1,4] Kirsten Thonicke,[5] Sönke Zaehle,[1] Markus Reichstein[1,6]

Atmospheric monitoring of high northern latitudes (above 40°N) has shown an enhanced seasonal cycle of carbon dioxide (CO_2) since the 1960s, but the underlying mechanisms are not yet fully understood. The much stronger increase in high latitudes relative to low ones suggests that northern ecosystems are experiencing large changes in vegetation and carbon cycle dynamics. We found that the latitudinal gradient of the increasing CO_2 amplitude is mainly driven by positive trends in photosynthetic carbon uptake caused by recent climate change and mediated by changing vegetation cover in northern ecosystems. Our results underscore the importance of climate–vegetation–carbon cycle feedbacks at high latitudes; moreover, they indicate that in recent decades, photosynthetic carbon uptake has reacted much more strongly to warming than have carbon release processes.

The seasonal cycle of atmospheric carbon dioxide (CO_2) in the Northern Hemisphere is mainly controlled by carbon uptake and release processes of the land biosphere (*1*), specifically by the difference between photosynthetic carbon uptake [gross primary production (GPP)] and ecosystem respiration (Reco) (*2*). Airborne and surface data show that the amplitude of the seasonal cycle (henceforth "CO_2 amplitude") has increased since 1960, particularly north of 45°N, where increases as large as 50% have occurred (*1*–*4*). The strong seasonality of GPP and Reco in northern land ecosystems causes a larger average CO_2 amplitude in high northern latitudes than in low ones (*2*, *5*). The larger trends in CO_2 amplitude at higher latitudes consequently imply that they are caused by changing carbon cycle dynamics in northern ecosystems (*4*).

A variety of factors may contribute to the CO_2 amplitude trend. Arctic and boreal regions have experienced strong warming in recent decades (*6*), and a "greening" trend has been detected from satellites, indicating enhanced plant growth (*7*, *8*) (Fig. 1, A and B). These satellite observations are confirmed by ground observations showing increases in shrub coverage in the tundra (*9*), tree growth along the tundra–boreal forest transition zone (*10*), and deciduous tree cover from recovery after severe boreal forest fires (*11*). Additionally, various estimates show positive trends in both annual amplitudes and annual totals of GPP (*12*, *13*) and in net biome productivity (NBP) (*14*) in northern ecosystems (Fig. 1, C and D). The intensification of agriculture in the mid-latitudes also likely contributes to the CO_2 amplitude trends (*15*, *16*). These multiple observational signals point to amplified plant productivity as a likely cause of the increase in CO_2 amplitude (*1*, *3*, *7*, *17*). Nonetheless, a quantitative explanation of the amplitude trends is still lacking. Current Earth system models consistently underestimate the CO_2 amplitude trend (*4*) and its gradient with latitude, which suggests that these models are missing or underrepresenting key processes (*18*).

Here, we examined the cause of the CO_2 amplitude increase by combining observations from long-term monitoring sites of atmospheric CO_2 concentration, satellite observation of vegetation greenness (*19*), and global observation-based data sets of GPP (*12*) and NBP (*14*) with results from the LPJmL dynamic global vegetation model (*20*, *21*) coupled with the TM3 atmospheric transport model (*22*) [hereinafter called LPJmL +TM3 (*23*)] to explain the observed latitudinal gradient of CO_2 amplitude trends. Unlike other biosphere models that were previously evaluated against CO_2 amplitude trends (*4*), LPJmL considers several processes that potentially contribute to a better explanation of these trends, including agriculture, irrigation, and land use change (*21*); vegetation dynamics; and processes that control northern vegetation dynamics, such as permafrost (*24*) and fire (*25*) driven by observed burned-area data (*26*). Moreover, LPJmL uses an improved phenology module (*26*) that has been optimized against satellite observations of FAPAR (fraction of absorbed photosynthetic active radiation), albedo, and an observation-based data set of GPP, resulting in a better representation of climate controls on vegetation dynamics as well as global carbon fluxes and stocks (*26*, *27*). Note that atmospheric CO_2 data were not used to constrain LPJmL.

We estimated CO_2 amplitude trends in observed time series at 19 monitoring sites with at least 20 years of data (table S1). We found much stronger positive CO_2 amplitude trends at high-latitude sites [e.g., 0.08 ppm $year^{-1}$ ≈ 0.53% $year^{-1}$ at Point Barrow (BRW) during 1971–2011] than at low-latitude sites [e.g., 0.005 ppm $year^{-1}$ ≈ 0.076% $year^{-1}$ at Mauna Loa (MLO) during 1970–2011] (Fig. 1E). These estimated trends were similar to those of previous studies (*2*, *4*) with small differences due to station selection, time series analysis methods, and time series length. We found weaker trends in the CO_2 amplitude, especially at MLO, because this trend originates mostly from low CO_2 amplitude values in the 1960s and weakens from 1970 onward. To account for the effect of time series length, we estimated the uncertainties in CO_2 amplitude trends by computing trends for different combinations of start and end years (fig. S1). The estimated uncertainties ($0.53^{0.64}_{0.39}$% $year^{-1}$ at BRW, $0.076^{0.19}_{-0.059}$% $year^{-1}$ at MLO, $50^{97.5}_{2.5}$percentiles of trend slope ensemble) demonstrate that only high-latitude sites have persistent long-term increases in CO_2 amplitude.

In comparison to surface-level site observations, LPJmL+TM3 had stronger CO_2 amplitude trends on average (Fig. 2A and table S2). However, LPJmL+TM3 reproduced the observed changes in CO_2 amplitude at higher atmospheric levels (fig. S2). LPJmL+TM3 simulations were well correlated with site observations regarding spatial patterns of mean CO_2 amplitude values (r = 0.84) and trends (r = 0.51, $P \leq 0.05$) (fig. S3). LPJmL+TM3 had a modest performance in representing the year-to-year variability of the CO_2 amplitude at some sites (*23*), which may indicate the importance of the effect of regional extreme events on the land carbon balances (*28*). LPJmL+TM3 reproduced the observed pattern of strong positive CO_2 amplitude trends north of 45°N, the large variability of trends in the mid-latitudes, and the small or nonsignificant trends south of 20°N. We found that simulations of CO_2 amplitudes were sensitive to the choice of the meteorological forcing data set for the TM3 transport model (fig. S4A). Therefore, we propagated the uncertainty both from time series length and meteorological forcing to the overall uncertainty of simulated CO_2 amplitude trends for a more robust model evaluation. The interannual variability of ocean CO_2 uptake had no distinct contribution to CO_2 amplitude trends in comparison to a climatology of ocean uptake (fig. S4B). LPJmL yielded positive trends in annual maximum FAPAR in northern ecosystems that are in good agreement with satellite observations (*27*) and yielded increases in annual amplitudes and totals of GPP and NBP that agree with independent observation-based GPP and NBP estimates (Fig. 1, B to D, and fig. S5). Although the model does not fully account for trends in agricultural fertilizer usage, the simulated trends in GPP of agricultural regions are comparable to an independent

[1]Max Planck Institute for Biogeochemistry, 07745 Jena, Germany. [2]CENSE, Departamento de Ciências e Engenharia do Ambiente, Faculdade de Ciências e Tecnologia, Universidade NOVA de Lisboa, Caparica, Portugal. [3]Scripps Institution of Oceanography, La Jolla, CA 92093, USA. [4]Department of Physical Sciences, University of Helsinki, Helsinki, Finland. [5]Potsdam Institute for Climate Impact Research, 14473 Potsdam, Germany. [6]Michael-Stifel-Center Jena for Data-driven and Simulation Science, 07743 Jena, Germany.
***Corresponding author. E-mail: matthias.forkel@geo.tuwien.ac.at (M.F.); ncarval@bgc-jena.mpg.de (N.C.)** †Present address: Department of Geodesy and Geoinformation, Technische Universität Wien, 1040 Vienna, Austria.

Downloaded from on February 11, 2016

estimate (fig. S7). This comparison of LPJmL simulations and independent data sets demonstrates an amplification of plant productivity in northern ecosystems.

We quantified the contribution of land NBP from different regions to CO_2 amplitude trends (table S5 and fig. S6B). NBP from boreal regions contributed 51% to the average CO_2 amplitude in the 1970s at high northern latitude sites (>45°N). In the 2000s, the contribution of boreal regions increased to 54%, corresponding to an annual increase of $0.35^{0.41}_{0.14}$% year^{-1}. The contribution of arctic NBP was 17% in the 1970s and increased by $0.18^{0.24}_{0.12}$% year^{-1}. NBP from global agricultural regions contributed 11% in the 1970s and increased by $0.14^{0.16}_{0.01}$% year^{-1}. Temperate and tropical regions made only minor contributions to the trends in CO_2 amplitude. However, only trends in the contribution of arctic and boreal NBP were significant (P = 0.03 and P = 0.01, respectively) at northern sites. At low-latitude sites (0° to 45°N), NBP from boreal regions still contributed dominantly to the increase in CO_2 amplitude with $0.46^{0.52}_{0.09}$% year^{-1} (P = 0.12), followed by NBP from agricultural regions with $0.17^{0.26}_{-0.21}$% year^{-1} (P = 0.37) and NBP from arctic regions with $0.14^{0.19}_{0.08}$% year^{-1} (P = 0.12). Therefore, boreal regions contributed approximately 57%, arctic regions 25%, and agricultural regions 17% to the overall CO_2 amplitude trend at northern-latitude sites (41%, 14%, and 20% at low-latitude sites, respectively). The agricultural contribution in LPJmL is within the ranges found in previous studies (*15*, *16*). Similar to (*4*), we found that fossil fuel emissions and ocean CO_2 exchange have little impact on the trends in CO_2 amplitude (table S5). Consistent with Graven *et al.* (*4*), LPJmL attributes a dominant role to boreal and arctic ecosystems in driving the CO_2 amplitude increase.

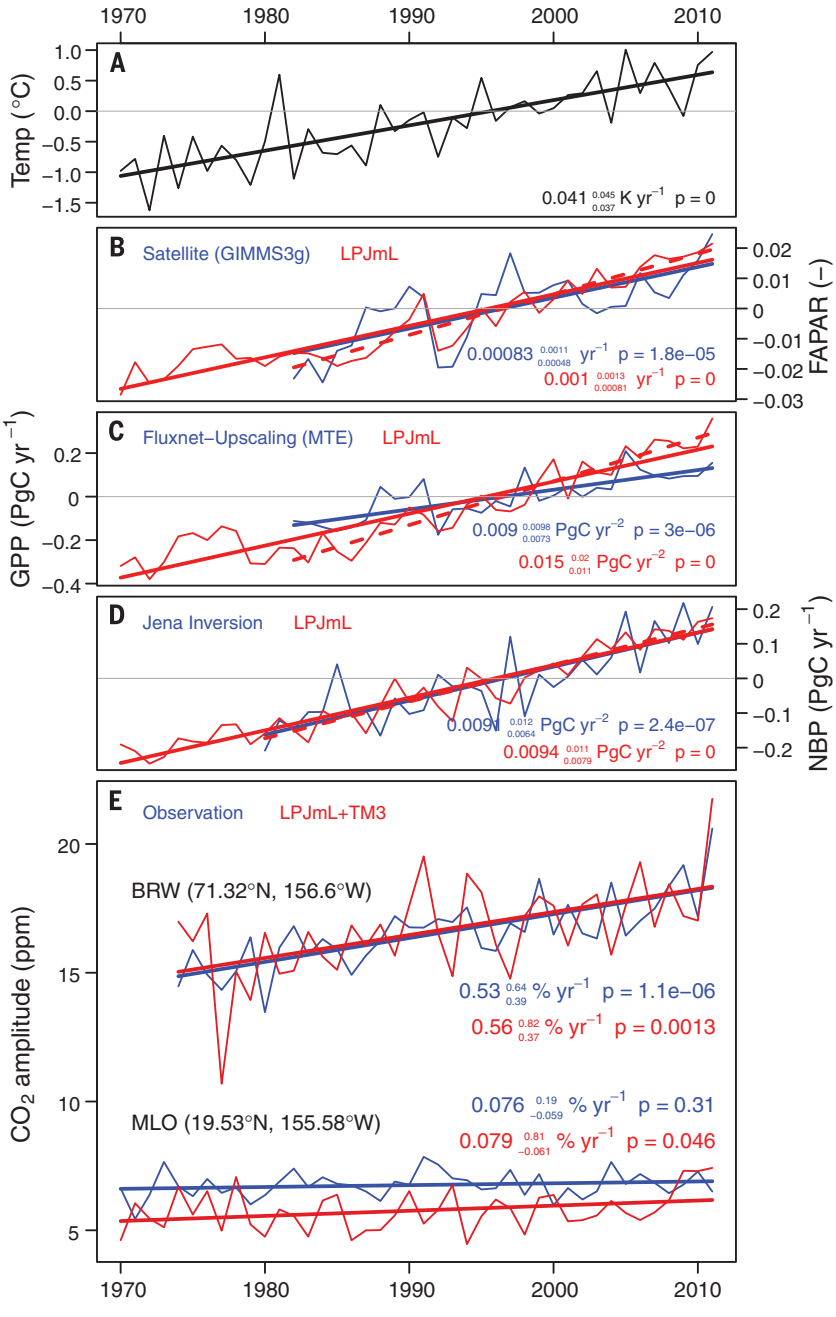

Fig. 1. Amplification of plant activity in the northern biosphere. (**A** to **E**) Annual time series and linear trends of mean annual air temperature (A), peak FAPAR (fraction of absorbed photosynthetic active radiation) (B), annual amplitude of GPP (gross primary production) (C), annual amplitude of NBP (net biome productivity) (D), and seasonal amplitude of atmospheric CO_2 (E) at Point Barrow (BRW) and Mauna Loa (MLO). Time series in (A) and (B) are spatially averaged; in (C) and (D) they are aggregated for boreal and arctic land regions north of 41°N (fig. S12), and the 1982–2011 mean has been subtracted. Dashed lines and trend values refer to the overlapping period of LPJmL simulations and observations. *P* values were calculated with the Mann-Kendall trend test.

Both GPP and Reco can potentially contribute to the increasing CO_2 amplitude. We found stronger trends in annual total GPP ($0.065^{0.083}_{0.053}$ PgC year^{-2}, LPJmL during 1970–2011) than in annual total Reco ($0.061^{0.07}_{0.051}$ PgC year^{-2}, LPJmL during 1970–2011) in northern ecosystems (fig. S8) and stronger trends in the GPP than in Reco annual amplitudes across all northern latitudes (fig. S9). The contribution of GPP to the CO_2 amplitude increased by $2.3^{3.2}_{-0.1}$% year^{-1}, whereas the increasing Reco contributed to a decrease of the seasonal amplitude of $-1.5^{0.22}_{-2.24}$% year^{-1}. Consequently, given the opposite signs of GPP and Reco fluxes, the effect of GPP on the CO_2 amplitude is attenuated but not compensated by Reco (table S5). This is consistent with earlier results (*29*) showing that the spatial variability of NEE and NBP amplitudes is strongly related to GPP. The stronger increase in GPP relative to Reco leads to a positive trend in northern ecosystem NBP of $0.011^{0.017}_{0.006}$ PgC year^{-2} (LPJmL), which is confirmed by independent estimates from the Jena CO_2 inversion scheme [$0.014^{0.02}_{0.0086}$ PgC year^{-2}, version s81_v3.6 (*14*)] (fig. S10). Trends in annual total GPP in northern ecosystems and CO_2 amplitude trends at northern-latitude sites show a strong linear relation across different LPJmL+TM3 model experiments (r^2 = 0.96; Fig. 3 and fig. S11). For example, an increase in CO_2 amplitude of 0.08 ppm year^{-1} at BRW requires an increase in boreal and arctic GPP of 0.07 PgC year^{-2}. Thus, the increase in the seasonal CO_2 amplitude can be explained by a photosynthesis-driven increase in net carbon uptake of northern ecosystems.

Several factors can contribute to the increased photosynthetic carbon uptake and hence to the latitudinal gradient of the increasing CO_2 amplitude. Rising atmospheric CO_2 and climate change directly affect physiological processes that can enhance photosynthesis (*30*). To test the relative effect of CO_2 fertilization and climate change on CO_2 amplitude trends, we performed

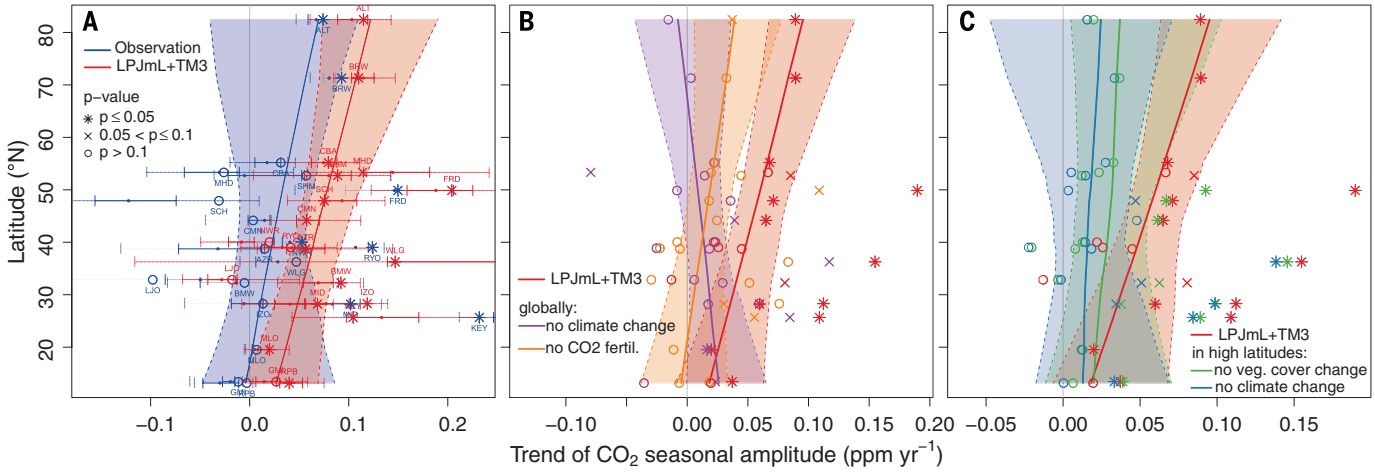

Fig. 2. Latitudinal gradients of trends in the seasonal CO_2 amplitude and its drivers. (**A**) Simulated and observed CO_2 amplitude trends with 95% confidence intervals (dashed lines) and the uncertainty distribution of site-level trend slopes (solid lines are interquartile range; dots are median values). Site-level uncertainty distributions are not shown in (B) and (C) for clarity. (**B**) Global effects of CO_2 fertilization and climate change on the latitudinal gradient. Removing the effect of CO_2 fertilization on photosynthesis reduces CO_2 amplitude trends globally but has no effect on the latitudinal gradient. The latitudinal gradient disappears with a constant climate. (**C**) Separation of the indirect effect of changing vegetation cover and the direct effect of climate change on photosynthesis in high-latitude regions on the latitudinal gradient. The latitudinal gradient disappears both without changes in vegetation cover (i.e., climate change but no vegetation cover change) and without climate change (i.e., forcing changes in vegetated area but no climate change).

two model experiments with LPJmL in which we kept temperature and precipitation at 1965–1975 levels for the period 1970–2011 (i.e., no climate change) and held CO_2 constant at 325.7 ppm after 1970 to quantify the effect of CO_2 fertilization (Fig. 2B). We found that both climate change and CO_2 fertilization affect CO_2 amplitude trends, but with regional differences: Climate change was the dominant factor on CO_2 amplitude trends north of 40°N, whereas CO_2 fertilization was the dominant factor south of 40°N. Without the effect of CO_2 fertilization, CO_2 amplitude trends were generally lower (~ −0.04 ppm year^{-1} across all latitudes) but the latitudinal gradient of stronger CO_2 amplitude trends in northern relative to southern latitudes was not affected. However, the strong CO_2 amplitude trends in northern latitudes disappeared under constant climate and reverted the latitudinal gradient toward stronger trends south of 40°N (Fig. 2B). Therefore, the stronger CO_2 amplitude trends at northern latitudes are mainly dominated by climate change–induced increases in boreal and arctic GPP (Fig. 3). Increasing GPP results in increasing plant growth, which again enhances GPP. LPJmL simulates an increasing coverage of trees across the boreal zone at the expense of tundra (*23*).

To quantify the role of this indirect vegetation cover feedback on GPP and CO_2 amplitude trends, we performed two more model experiments. In the first, we again fixed climate during the period 1970–2011 according to the climate conditions in 1965–1975 but prescribed changes in vegetated area as simulated in the standard experiment (i.e., changes in vegetation cover but no climate change). In the second, we used observed climate but fixed vegetated area after 1970 (i.e., constant vegetation cover with climate change).

Fig. 3. Trend in the CO_2 amplitude at Point Barrow against trends in northern ecosystem gross primary production across different factorial model experiments with LPJmL. Dots and error bars represent median values and 95% confidence intervals of the estimated trends. Gray horizontal solid and dashed lines show the median and 95% confidence interval for the estimated trend in the observed CO_2 amplitude time series.

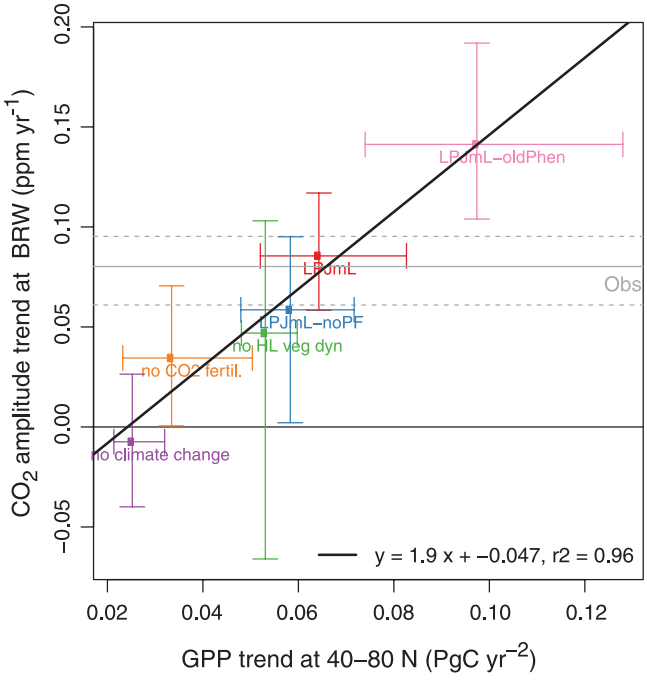

Both experiments were performed only for northern ecosystems; the rest of the world was simulated following the normal simulation protocol. The latitudinal gradient of stronger CO_2 amplitude trends in northern latitudes disappeared both without the direct effect of climate change and without the indirect effect of changing vegetation cover in northern ecosystems (Fig. 2C). Thus, the interaction between the direct climate effects on photosynthesis and the indirect effect of changing vegetation cover drives the trend in the CO_2 amplitude.

The climate effect is likely mostly exerted via temperature, given earlier results from eddy covariance sites, indicating that variability in ecosystem GPP north of 42°N is driven by temperature (*31*). Additional processes, such as increasing plant available water from enhanced seasonal thawing of permafrost soils and changes in plant phenology, contribute to plant productivity in northern ecosystems. Indeed, we found weaker GPP and CO_2 amplitude trends in a LPJmL simulation without considering permafrost dynamics (*24*) (LPJmL-noPF in Fig. 3)

and overestimated observed GPP and CO_2 amplitude trends with a too-simplistic phenology model that only accounts for temperature effects but ignores radiation and hydrological effects on seasonal leaf development (*26*) (LPJmL-oldPhen in Fig. 3). These examples demonstrate a strong but complex control of climate on plant productivity in northern ecosystems, which ultimately results in the major contribution of enhanced plant growth to the strong CO_2 amplitude trends in northern latitudes.

Our results suggest that a major driver of the large increase in CO_2 amplitude at high northern latitudes involves the interaction of recent climate change with vegetation dynamics. Climate change affects processes such as plant physiology, phenology, water availability, and vegetation dynamics, ultimately leading to increased plant productivity and vegetation cover in northern ecosystems in recent decades. Our results further highlight the gradual replacement of herbaceous vegetation with forests as a major specific factor. Lastly, we identified a dominance of changes in photosynthesis over respiration in driving the changes. Sensitivities of these processes to climate need to be carefully assessed in current ecosystem and Earth system models against observational data to accurately reproduce observed changes in CO_2 amplitude. However, the stimulation of photosynthesis and vegetation growth by climate change cannot be unlimited because of nutrient limitations, radiation, and possibly increased mortality (*32*). Thus, at some point in the future, the positive trends in plant productivity (and thus the CO_2 amplitude increase) might stall. Continued long-term observation of atmospheric CO_2, together with ground and satellite observations of vegetation productivity and dynamics, will be the key to detection, modeling, and better prediction of such changes in high-latitude carbon cycle dynamics.

REFERENCES AND NOTES

1. C. D. Keeling, J. F. S. Chin, T. P. Whorf, *Nature* **382**, 146–149 (1996).
2. J. T. Randerson, M. V. Thompson, T. J. Conway, I. Y. Fung, C. B. Field, *Global Biogeochem. Cycles* **11**, 535–560 (1997).
3. R. B. Bacastow, C. D. Keeling, T. P. Whorf, *J. Geophys. Res.* **90**, 10529–10540 (1985).
4. H. D. Graven *et al.*, *Science* **341**, 1085–1089 (2013).
5. M. Heimann, C. D. Keeling, C. J. Tucker, in *Aspects of Climate Variability in the Pacific and the Western Americas*, D. H. Peterson, Ed. (American Geophysical Union, Washington, DC, 1989), pp. 277–303.
6. IPCC, *Climate Change 2013—The Physical Science Basis: Working Group I Contribution to the Fifth Assessment Report of the Intergovernmental Panel on Climate Change* (Cambridge Univ. Press, 2014).
7. R. B. Myneni, C. D. Keeling, C. J. Tucker, G. Asrar, R. R. Nemani, *Nature* **386**, 698–702 (1997).
8. W. Lucht *et al.*, *Science* **296**, 1687–1689 (2002).
9. I. H. Myers-Smith *et al.*, *Environ. Res. Lett.* **6**, 045509 (2011).
10. L. T. Berner, P. S. A. Beck, A. G. Bunn, S. J. Goetz, *Glob. Change Biol.* **19**, 3449–3462 (2013).
11. P. S. A. Beck *et al.*, *Glob. Change Biol.* **17**, 2853–2866 (2011).
12. M. Jung *et al.*, *J. Geophys. Res.* **116**, G00J07 (2011).
13. A. Anav *et al.*, *Rev. Geophys.* **53**, 785–818 (2015).
14. C. Rödenbeck, S. Houweling, M. Gloor, M. Heimann, *Atmos. Chem. Phys.* **3**, 1919–1964 (2003).
15. J. M. Gray *et al.*, *Nature* **515**, 398–401 (2014).
16. N. Zeng *et al.*, *Nature* **515**, 394–397 (2014).
17. J. Barichivich *et al.*, *Glob. Change Biol.* **19**, 3167–3183 (2013).
18. N. MacBean, P. Peylin, *Nature* **515**, 351–352 (2014).
19. Z. Zhu *et al.*, *Remote Sens.* **5**, 927–948 (2013).
20. S. Sitch *et al.*, *Glob. Change Biol.* **9**, 161–185 (2003).
21. A. Bondeau *et al.*, *Glob. Change Biol.* **13**, 679–706 (2007).
22. M. Heimann, S. Körner, "The global atmospheric tracer model TM3," *Tech. Rep. Max Planck Inst. Biogeochem. 5* (2003), p. 131.
23. See supplementary materials on *Science* Online.
24. S. Schaphoff *et al.*, *Environ. Res. Lett.* **8**, 014026 (2013).
25. K. Thonicke *et al.*, *Biogeosciences* **7**, 1991–2011 (2010).
26. M. Forkel *et al.*, *Biogeosciences* **11**, 7025–7050 (2014).
27. M. Forkel *et al.*, *Glob. Change Biol.* **21**, 3414–3435 (2015).
28. M. Reichstein *et al.*, *Nature* **500**, 287–295 (2013).
29. C. Beer *et al.*, *Science* **329**, 834–838 (2010).
30. R. J. Norby *et al.*, *Proc. Natl. Acad. Sci. U.S.A.* **102**, 18052–18056 (2005).
31. M. Reichstein *et al.*, *Geophys. Res. Lett.* **34**, L01402 (2007).
32. S. Trumbore, P. Brando, H. Hartmann, *Science* **349**, 814–818 (2015).

ACKNOWLEDGMENTS

We thank the following institutions and scientists that acquired and provided CO_2 site data: E. Dlugokencky (NOAA), Scripps Institution of Oceanography, D. Worthy (Environment Canada), F. Meinhardt (Umweltbundesamt), R. Langenfelds and P. Krummel (CSIRO), and H. Koide (JMA). We further thank the following groups, institutions, or scientists for sharing their data sets: AFS, CRU, EC/JRC, ECMWF, GIMMS, NCEP, NRCan, L. Giglio (UMD), M. Jung (MPI-BGC), and S. E. Mikaloff Fletcher (National Institute of Water and Atmospheric Research). We thank S. Schaphoff (PIK) for comments on LPJmL and I. C. Prentice and R. Thomas for comments on the manuscript. Supported by the European Union (FP7) through the projects GEOCARBON (283080), CARBONES (242316), and EMBRACE (283201); U.S. Department of Energy grant DE-SC0012167; NSF grant 1304270; and NOVA grant UID/AMB/04085/2013. Table S7 provides an overview of used data and how it can be obtained. Results from factorial model experiments with LPJmL+TM3 are available at http://doi.pangaea.de/10.1594/PANGAEA.856722.

SUPPLEMENTARY MATERIALS

www.sciencemag.org/content/351/6274/696/suppl/DC1
Materials and Methods
Supplementary Text
Figs. S1 to S13
Tables S1 to S7
References (*33*–*69*)

4 May 2015; accepted 11 January 2016
Published online 21 January 2016
10.1126/science.aac4971

Downloaded from on February 11, 2016

GLOBAL WATER CYCLE

A decade of sea level rise slowed by climate-driven hydrology

J. T. Reager,[1]* A. S. Gardner,[1] J. S. Famiglietti,[1,2] D. N. Wiese,[1] A. Eicker,[3] M.-H. Lo[4]

Climate-driven changes in land water storage and their contributions to sea level rise have been absent from Intergovernmental Panel on Climate Change sea level budgets owing to observational challenges. Recent advances in satellite measurement of time-variable gravity combined with reconciled global glacier loss estimates enable a disaggregation of continental land mass changes and a quantification of this term. We found that between 2002 and 2014, climate variability resulted in an additional 3200 ± 900 gigatons of water being stored on land. This gain partially offset water losses from ice sheets, glaciers, and groundwater pumping, slowing the rate of sea level rise by 0.71 ± 0.20 millimeters per year. These findings highlight the importance of climate-driven changes in hydrology when assigning attribution to decadal changes in sea level.

Over the past century, sea level rose at an average rate of 1.5 ± 0.2 mm year^{-1}, increasing to 3.2 ± 0.4 mm year^{-1} during the past two decades (*1*). The increase in the rate of rise is attributed to an increase in mass loss from glaciers and ice sheets and to ocean warming. Although these contributions are fairly well constrained, trends in sea level also contain a land water storage component that is acknowledged to be among the most important yet most uncertain contributions (*1*–*3*), in which land water storage is defined by the Intergovernmental Panel on Climate Change (IPCC) (*1*) as all snow, surface water, soil moisture, and groundwater storage, excluding glaciers. Every year, land temporarily stores then releases a net 6000 ± 1400 Gt of mass through the seasonal cycling of water, which is equivalent to an oscillation in sea level of 17 ± 4 mm (*4*–*6*). Thus, natural changes in interannual to decadal cycling and storage of water from oceans to land and back can have a large effect on the rate of sea level rise (SLR) on decadal intervals (*7*, *8*). From 2003 to 2011, SLR slowed to a rate of ~2.4 mm year^{-1} (*9*) during a period of increased mass loss from glaciers (*10*) and ice sheets (*11*). Climate-driven changes in land water storage have been suggested to have contributed to this slowdown (*9*), but this assertion has not been verified with direct observations.

Until recently, little data have existed to constrain land water storage contributions to global

[1]Jet Propulsion Laboratory, California Institute of Technology, CA, USA. [2]Department of Earth System Science, Department of Civil and Environmental Engineering, University of California, Irvine, CA, USA. [3]Institute of Geodesy and Geoinformation, University of Bonn, Bonn, Germany. [4]Department of Atmospheric Sciences, National Taiwan University, Taipei, Taiwan.
*Corresponding author. E-mail: john.reager@jpl.nasa.gov

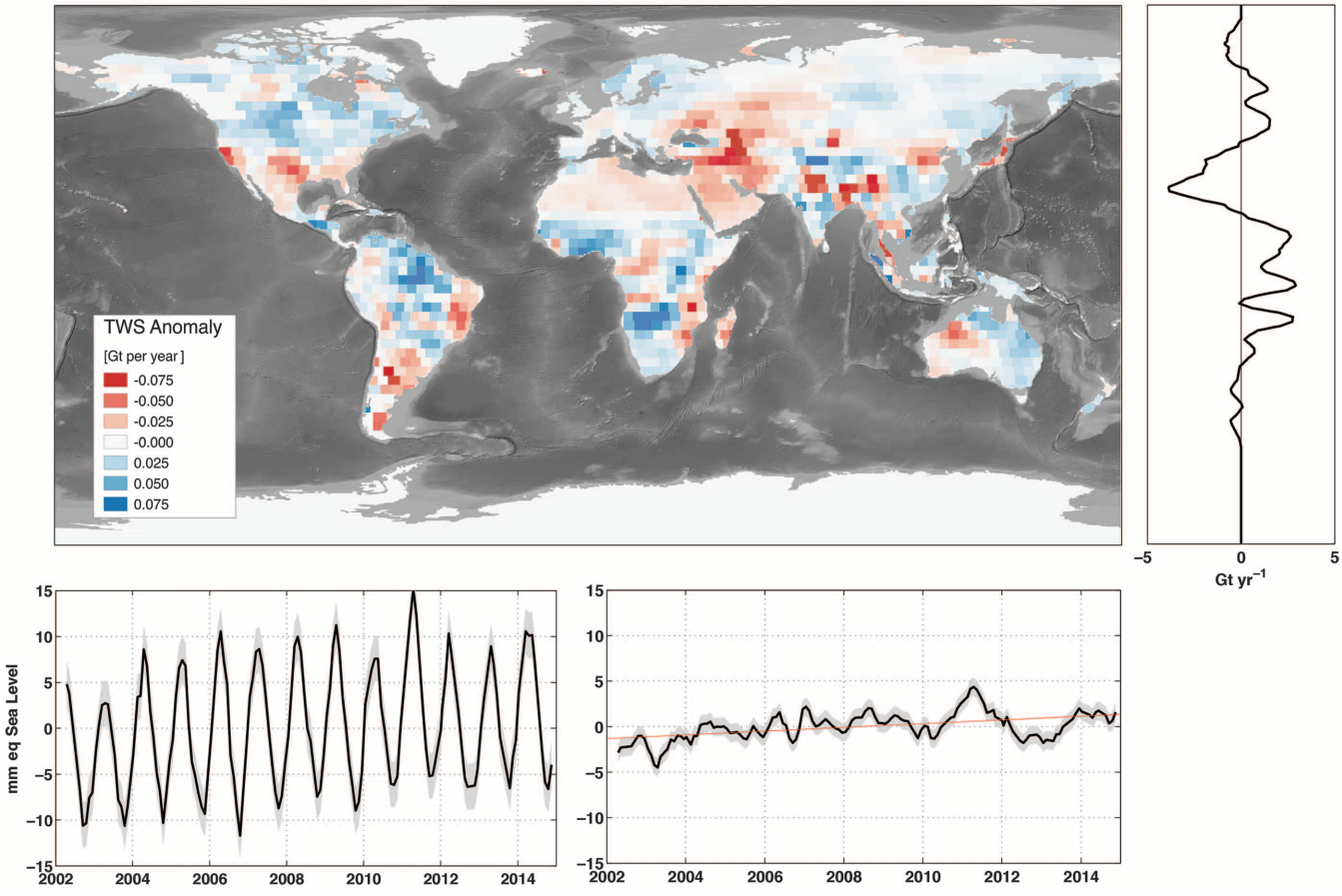

Fig. 1. Trends in land water storage from GRACE observations, April 2002 to November 2014. Glaciers and ice sheets are excluded. Shown are the global map (gigatons per year per 1/2-degree grid), zonal total trends, full time series (millimeters per year SLE), and best-fit linear regression with climatology removed (millimeters per year SLE). The strongest gains and losses are associated with climate-driven variability in precipitation.

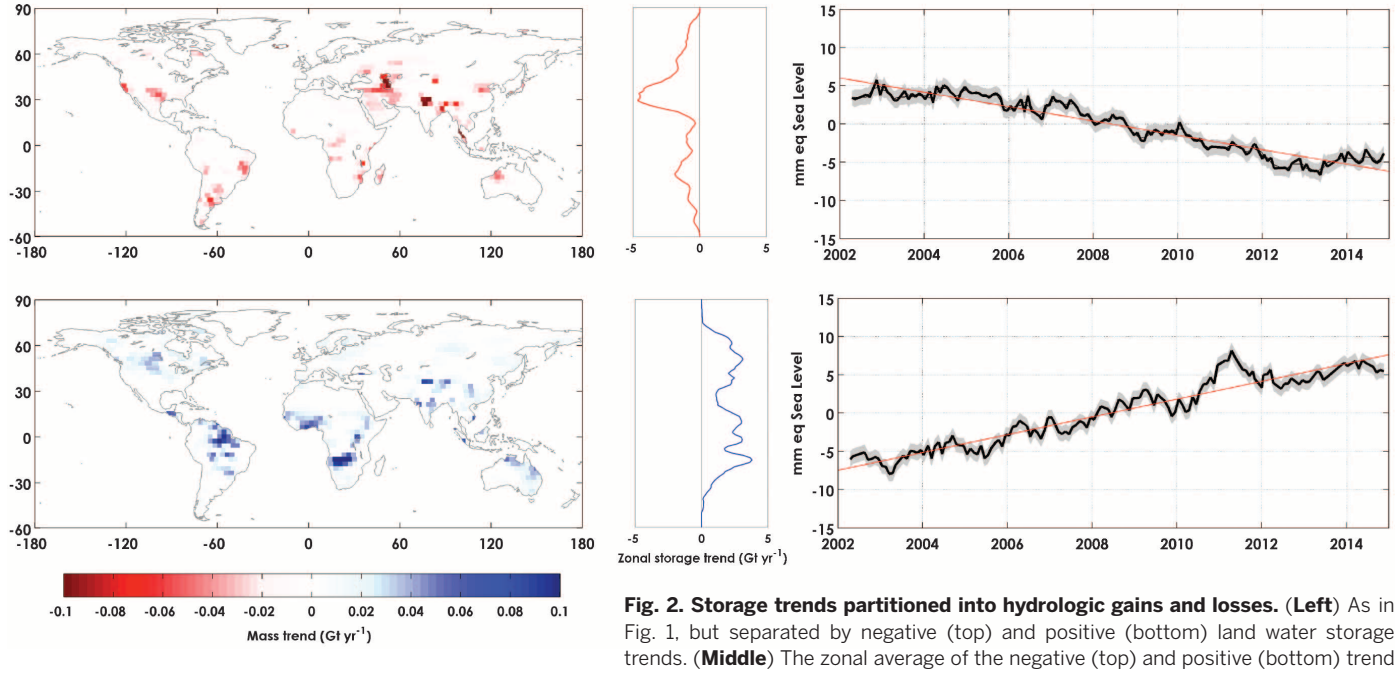

Fig. 2. Storage trends partitioned into hydrologic gains and losses. (**Left**) As in Fig. 1, but separated by negative (top) and positive (bottom) land water storage trends. (**Middle**) The zonal average of the negative (top) and positive (bottom) trend map (gigatons per year per 1/2-degree grid). (**Right**) GRACE land water storage time series averaged for the negative (top) and positive (bottom) land water storage trend map (climatology removed). Estimated glacier trends are shown in the supplementary materials (*44*).

Table 1. Estimates of net direct-human water management contributions to SLR from previous studies. The range of estimates results from different methodological approaches and assumptions, including modeling, remote sensing, and ground-based methods. To achieve a net human-driven contribution, the IPCC AR5 applied an estimate of reservoir retention to the average of the Konikow (*14*) and Wada (*13*) groundwater depletion estimates.

Previous studies	Method	Time period	Contribution (mm year^{-1} SLE)
Konikow *et al.* (2011)	Scaling of in situ measurements	2000 to 2008	0.41 ± 0.10
Wada *et al.* (2012)	PCR-GLB Model	2000	0.57 ± 0.09
Döll *et al.* (2014)	WaterGAP Model	2000 to 2009	0.31 ± 0.0
IPCC AR5 (2013)	(*13*) + (*14*) averaged (including reservoirs)	1993 to 2010	0.38 ± 0.12
Richey *et al.* (2015)	GRACE net subsurface storage	2003 to 2014	0.24 ± 0.02

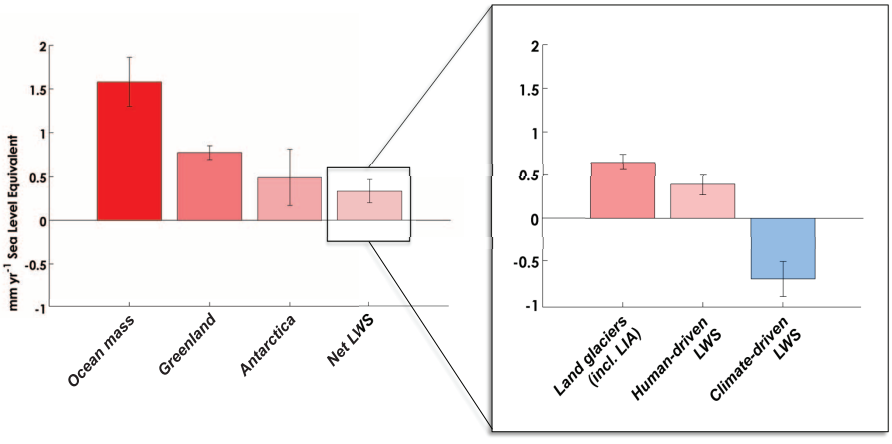

Fig. 3. Observed global mass contributions to SLR, 2002 to 2014, including the disaggregated land water storage term. (**Left**) Global mass contributions to sea level from GRACE mascons, including total ocean mass change (1.58 mm year^{-1} SLE), partitioned between contributions from Greenland (0.77 mm year^{-1} SLE), Antarctica (0.49 mm year^{-1} SLE), and net land water storage (LWS) (0.32 mm year^{-1} SLE). (**Right**) Disaggregation of net LWS contributions, including the estimate of land glacier losses (0.65 mm year^{-1}) anthropogenic hydrology (0.38 mm year^{-1}) (*1*), and climate-driven land water storage from this study (−0.71 mm year^{-1}).

Table 2. The components of total continental water storage used to calculate climate-driven land water storage change from April 2002 to November 2014. LIA, Little Ice Age correction (supplementary materials).

	Source	Contribution (mm year^{-1} SLE)	Uncertainty (mm year^{-1})
Land glaciers (including LIA)	This study	0.65	± 0.09
Human-driven land water storage	IPCC AR5 (*1*)	0.38	± 0.12
Climate-driven land water storage	This study	−0.71	± 0.20
Total continental water storage	This study	0.32	± 0.13

mean SLR. As a result, this term has either been excluded from SLR budgets (*3*) or has been approximated by using ad hoc accounting that includes modeling or scaling of a variety of ground-based observations (*1*, *2*). Human-induced changes in land water storage (hereafter referred to as "human-driven land water storage") include the direct effects of groundwater extraction, irrigation, impoundment in reservoirs, wetland drainage, and deforestation. These activities may play a major role in modulating rates of sea level change (*12*–*16*), and several studies of large aquifers suggest that trends in regional and global land water storage are now strongly influenced by the effects of groundwater withdrawal (*17*). Currently, human activity (including groundwater depletion and reservoir impoundment) is estimated to have directly resulted in a net 0.38 ± 0.12 mm year^{-1} sea level equivalent (SLE) between 1993 and 2010 (*1*) or 15 to 25% of observed barystatic SLR, but estimates are acknowledged to have large uncertainties (*18*–*20*).

Climate-driven variability in rainfall, evaporation, and runoff also contributes to decadal rates of sea level change through changes in the total amount of water held in snow, soil, surface waters, and aquifers (*8*, *21*). Climate-driven changes in land water storage have been assumed to be too small to include in sea level budgets (*1*), but there is little observational evidence to support this assumption. The vast spatial scale of climate-driven changes in land water storage has made them too difficult to observe with accuracy (*22*). As such, current IPCC sea level budgets exclude a potentially large water storage term that is required for closure of barystatic SLR on decadal time scales.

We assessed the role of land water storage in SLR over the 12-year period from 2002 to 2014. We examined global changes in surface mass derived from satellite measurements of time-variable gravity that are well-suited to constrain global changes in water storage. From this data, we extracted an observation-based estimate of the net contributions of the continents to SLR. By incorporating recently reconciled estimates of glacier losses [an update to Gardner *et al.* (*10*)] and recent estimates of global groundwater depletion (*1*, *13*–*16*), we are able to disaggregate this net mass change into the contributions of glaciers, direct human-driven land water storage, and climate-driven land water storage.

Measurements of time-variable gravity come from NASA's Gravity Recovery and Climate Experiment (GRACE) satellite mission (*23*). GRACE provides monthly observations of changes in the Earth's gravity field that, after the removal of signals owing to changes in solid earth and atmosphere, result from the movement of water and ice through the Earth system at specific temporal and spatial scales. GRACE has provided monthly gravity field solutions since April 2002 and has proved to be an effective tool with which to observe changes in the mass of ice sheets (*24*), glaciers (*10*, *25*–*27*), snow mass (*28*), regional groundwater storage (*17*, *29*, *30*), and surface water storage (*31*). Previous studies have shown that because the accuracy of GRACE measurements generally increases with the size of the domain, GRACE observations may be useful to constrain hydrology contributions to sea level change (*6*, *32*–*34*), although only Rietbroek *et al.* (*35*) have attempted to disaggregate those contributions by process. The increasing length of the GRACE record, combined with recent improvements in the processing of the intersatellite range-rate measurements (*36*) and modeling of gravity change resulting from changes in solid earth displacement (supplementary materials, materials and methods) (*37*), have now made the GRACE record more relevant to investigation of land water storage contributions to sea level.

We used 140 monthly solutions from the new Jet Propulsion Laboratory GRACE mascon solution (JPL RL05M) (*36*) for the period spanning April 2002 through November 2014. The JPL RL05M mascon solution solves for gravity anomalies in terms of globally distributed, equal-area 3° spherical cap mass concentration functions coupled with Bayesian regularization based on near-global geophysical models and altimetry observations. This approach optimally reduces correlated error in the gravity solution, resulting in less signal loss and higher spatial resolution than those of traditional methods. The solution also applies a post-processing algorithm to better partition between land and ocean mass changes, limiting "leakage" signal between oceans and land.

Several post-processing corrections are applied to the GRACE solutions in order to correct for known limitations of the GRACE measurements and to isolate the terrestrial water storage signal of interest. These include replacing the degree 2, order 0 spherical harmonic coefficients for each month with those estimated from satellite laser ranging (*38*), correcting the position of the mean pole (*39*), adding an estimate of geocenter motion (*40*), removing a Glacial Isostatic Adjustment (GIA) signal (*37*), removing a glacier change signal (*10*), and removing solid earth response to tectonic events (*41*). Because little to no trend in mass over Greenland and Antarctica is attributed to changes in land water storage, these regions are excluded from our analysis.

The resulting mass anomalies, with appropriately propagated errors, are attributable to changes in land water storage. We estimate a total continental land mass change (including glaciers) over the study period of –0.32 ± 0.13 mm year^{-1} SLE (ocean gaining). To show that our work is consistent with current knowledge, we compared trends in our mascon-based land and ocean mass change time series with mass trends reported by Riva *et al.* (*42*), Llovel *et al.* (*34*), Llovel *et al.* (*43*), and Jensen *et al.* (*6*). In all cases, we find good agreement with earlier works when time periods over which trends are calculated are properly accounted for. We then proceeded to remove glacial signals in order to isolate a hydrology-only "land water storage" signal (*44*).

Shown in Fig. 1 is a global map of the GRACE-observed trend in hydrologic land water storage only (after removing glacier signals) over the 2002–2014 period as well as the global time series; in Fig. 1, blue indicates water gains, and red indicates water losses. Globally, glacier-free land gained water at a rate of 120 ± 60 Gt year^{-1} (0.33 ± 0.16 mm year^{-1} SLE). Regionally, we find good agreement with previous hydrology studies that have applied GRACE to determine water mass trends for individual water basins and aquifers. Positive trends are generally associated with climate variations rather than human water management—such as large flooding periods in the upper Missouri River basin (*45*), recovery from drought in the Amazon (*46*) and the Zambezi and Niger basins in Africa (*47*–*49*), and weaker gains in Northern Australia associated with La Niña (*50*)—and are consistent with observed land precipitation changes during the observation period (*45*). A small portion of the gain signal can also be attributed to human activities—primarily, the filling of reservoirs. Land water storage losses are generally associated with changing precipitation patterns (*45*) and drought, and with human-driven change, primarily attributable to groundwater depletion. The negative trends in land water storage in Fig. 1 correspond well with recent studies of global groundwater stress (*17*) and with regional studies of groundwater depletion in the Middle East region (*51*, *52*), Northwestern India (*29*), California and the Southern High Plains in North America (*30*, *53*, *54*), and the North China Plain (*55*).

To highlight the spatial patterns of change, we partition the global land water storage trend map into its positive and negative components in Fig. 2, left. A spatial mask was constructed at the interface between positive and negative trend signals (along the zero-trend contour) for individual mascons. The partitioned trend maps and their zonal averages (Fig. 1, right, and Fig. 2, center) reveal a distinct pattern of mid-latitude drying, which is more pronounced in the northern hemisphere, and of high- and low-latitude wetting.

We measured a gross negative mass trend of –350 Gt year^{-1}, or –0.97 mm year^{-1} SLE (ocean gaining), for 2002–2014 land water storage losses (Fig. 2, top), which includes human-driven changes in storage, largely due to groundwater depletion as a portion of the total. Recent estimates proposed by IPCC (*1*) for the net human-driven land water storage contribution to sea level (0.38 ± 0.12 mm year^{-1}, 1993–2010) represent only a fraction (<40%) of the total losses observed here, which is expected because our results also include the previously unknown climate-driven land water storage signal. We also measured a gross positive mass trend of 470 Gt year^{-1}, or 1.3 mm year^{-1} SLE for the gaining land water storage regions (Fig. 2, bottom). The combined impacts of gaining and losing regions in land water storage result in a net sea level decrease that can be largely attributable to decadal-scale climate-driven processes.

Our analysis indicates that land water storage acted as a net sea level sink during the 2002–2014 period, resulting from a balance between human- and climate-driven changes in hydrology. Using previously published estimates of the direct anthropogenic component of this balance, we are able to isolate changes in land water storage resulting from climate variability. Recent research on direct human-driven changes in land water storage (*10*–*14*) has yielded a suite of estimates whose mean (–0.38 ± 0.11 mm year^{-1}) is not significantly different than the IPCC (*1*) 1993–2010 estimate of –0.38 ± 0.12 mm year^{-1} SLE (*45*), even though study estimates span a range of temporal intervals (Table 1). Because the net land water storage mass gain calculated here (0.33 ± 0.16 mm year^{-1}) represents the sum of both the human- and climate-driven components of land water storage change, we subtracted the IPPC estimate for human-driven changes to calculate a climate-driven land water storage uptake equivalent to –0.71 ± 0.20 mm year^{-1} SLE. This climate-driven land water storage uptake is required to close the observed land water storage balance (Fig. 3 and Table 2) (*1*). This result is consistent with the hypothesis posed by Cazenave *et al.* (*9*) that El Niño Southern Oscillation (ENSO) modulations of the global water cycle are important in sea level budgeting because they augment the delivery of water to the continents (*19*, *44*). However, we recognize that the hydrologic variability observed here could change with a longer record and may not represent a long-term offset to global SLR.

To illustrate the importance of including climate-driven changes in land water storage in decadal sea level budgets, we place our estimate of climate-driven land water storage uptake in the context of other mass contributions to sea level change as estimated by using the JPL RL05M GRACE mascon solution (*45*), the results of which are shown in Fig. 3. Over the past decade, climate-driven land water storage uptake is of opposite sign and of magnitude comparable with ice losses from glaciers and ice sheets and nearly twice as large as mass losses from direct human-driven changes in land water storage. Our results show that climate-driven changes in land water storage are now observable on a global scale and that these changes are large and necessary for closure of decadal-scale sea level budgets.

REFERENCES AND NOTES

1. J. A. Church *et al.*, in *Climate Change 2013: The Physical Science Basis. Contribution of Working Group I to the Fifth Assessment Report of the Intergovernmental Panel on Climate Change*, T. F. Stocker *et al.*, Eds. (Cambridge Univ. Press, 2013).
2. J. A. Church *et al.*, in *Climate Change 2001: The Physical Scienc Basis. Contribution of Working Group I to the Third Assessment Report of the Intergovernmental Panel on Climate Change*, B.C. Douglas, A. Ramirez, Eds. (Cambridge Univ. Press, 2001).
3. N. L. Bindoff *et al.*, in *Climate Change 2007: The Physical Science Basis. Contribution of Working Group I to the Fourth Assessment Report of the Intergovernmental Panel on Climate Change*, S. Solomon *et al.*, Eds. (Cambridge Univ. Press, 2007).
4. D. P. Chambers, J. Wahr, R. S. Nerem, *Geophys. Res. Lett.* **31**, L13310 (2004).
5. B. Wouters, R. E. M. Riva, D. A. Lavallée, J. L. Bamber, *Geophys. Res. Lett.* **38**, L03303 (2011).
6. L. Jensen, R. Rietbroek, J. Kusche, *J. Geophys. Res. Oceans* **118**, 212–226 (2013).
7. P. C. D. Milly, A. Cazenave, C. Gennero, *Proc. Natl. Acad. Sci. U.S.A.* **100**, 13158–13161 (2003).
8. T. H. Syed, J. S. Famiglietti, D. P. Chambers, J. K. Willis, K. Hilburn, *Proc. Natl. Acad. Sci. U.S.A.* **107**, 17916–17921 (2008).
9. A. Cazenave *et al.*, *Nature Climate Change* **4**, 358–361 (2014).
10. A. S. Gardner *et al.*, *Science* **340**, 852–857 (2013).
11. A. Shepherd *et al.*, *Science* **338**, 1183–1189 (2012).
12. B. F. Chao, Y. H. Wu, Y. S. Li, *Science* **320**, 212–214 (2008).
13. Y. Wada *et al.*, *Geophys. Res. Lett.* **39**, L09402 (2012).
14. L. F. Konikow, *Geophys. Res. Lett.* **38**, L17401 (2011).
15. Y. N. Pokhrel *et al.*, *Nat. Geosci.* **5**, 389–392 (2012).
16. P. Döll, H. Müller Schmied, C. Schuh, F. T. Portmann, A. Eicker, *Water Resour. Res.* **50**, 5698–5720 (2014).
17. A. S. Richey *et al.*, *Water Resour. Res.* **51**, 5217–5238 (2015).
18. J. Gonçalvès, J. Petersen, P. Deschamps, B. Hamelin, O. Baba-Sy, *Geophys. Res. Lett.* **40**, 2673–2678 (2013).
19. M.-H. Lo, J. S. Famiglietti, *Geophys. Res. Lett.* **40**, 301–306 (2013).
20. L. F. Konikow, *Nat. Geosci.* **6**, 2 (2013).
21. C. Boening, J. K. Willis, F. W. Landerer, R. S. Nerem, J. Fasullo, *Geophys. Res. Lett.* **39**, L19602 (2012).
22. D. Lettenmaier, P. Milly, *Nat. Geosci.* **2**, 452–454 (2009).

23. B. D. Tapley, S. Bettadpur, J. C. Ries, P. F. Thompson, M. M. Watkins, *Science* **305**, 503–505 (2004).
24. I. Velicogna, J. Wahr, *Science* **311**, 1754–1756 (2006).
25. S. B. Luthcke, A. A. Arendt, D. D. Rowlands, J. J. McCarthy, C. F. Larsen, *J. Glaciol.* **54**, 767–777 (2008).
26. A. S. Gardner *et al.*, *Nature* **473**, 357–360 (2011).
27. T. Jacob, J. Wahr, W. T. Pfeffer, S. Swenson, *Nature* **482**, 514–518 (2012).
28. G.-Y. Niu *et al.*, *Geophys. Res. Lett.* **34**, L15704 (2009).
29. M. Rodell, I. Velicogna, J. S. Famiglietti, *Nature* **460**, 999–1002 (2009).
30. J. S. Famiglietti *et al.*, *Geophys. Res. Lett.* **38**, L03403 (2011).
31. H. Kim, P. J.-F. Yeh, T. Oki, S. Kanae, *Geophys. Res. Lett.* **36**, L17402 (2009).
32. G. Ramillien *et al.*, *Global Planet. Change* **60**, 381–392 (2008).
33. P. C. D. Milly *et al.*, in *Understanding Sea-Level Rise and Variability*, J. A. Church, P. L. Woodworth, T. Aarup, W. S. Wilson, Eds. (Wiley-Blackwell, 2010), pp. 226–255.
34. W. Llovel, M. Becker, A. Cazenave, J.-F. Crétaux, G. Ramillien, *C. R. Geosci.* **342**, 179–188 (2010).
35. R. Rietbroek, S.-E. Brunnabend, J. Kusche, J. Schroeter, C. Dahle, *Proc. Natl. Acad. Sci. U.S.A.* 10.1073/pnas.1519132113 (2015).
36. M. M. Watkins, D. N. Wiese, D.-N. Yuan, C. Boening, F. W. Landerer, *J. Geophys. Res. Solid Earth* **120**, 2648–2671 (2015).
37. W. R. Peltier, D. F. Argus, R. Drummond, *J. Geophys. Res. Solid Earth* **120**, 450–487 (2015).
38. M. Cheng, B. D. Tapley, *J. Geophys. Res.* **109** (B9), B09402 (2004).
39. J. Wahr, R. S. Nerem, S. V. Bettadpur, *J. Geophys. Res. Solid Earth* **120**, 4597–4615 (2015).
40. S. Swenson, D. Chambers, J. Wahr, *J. Geophys. Res.* **113** (B8), B08410 (2008).
41. S.-C. Han, R. Riva, J. Sauber, E. Okal, *J. Geophys. Res. Solid Earth* **118**, 1240–1267 (2013).
42. R. Riva, J. Bamber, D. Lavallee, B. Wouters, *Geophys. Res. Lett.* **37**, L19605 (2010).
43. W. Llovel, J. K. Willis, F. W. Landerer, I. Fukumori, *Nature Climate Change* **4**, 1031–1035 (2014).
44. Materials and methods are available as supplementary materials on *Science* Online.
45. J. T. Reager, B. F. Thomas, J. S. Famiglietti, *Nat. Geosci.* **7**, 588–592 (2014).
46. J. L. Chen, C. R. Wilson, B. D. Tapley, *Water Resour. Res.* **46**, W12526 (2010).
47. G. Ramillien, F. Frappart, L. Seoane, *Remote Sens.* **6**, 7379–7405 (2014).
48. E. Forootan *et al.*, *Surv. Geophys.* **35**, 913–940 (2014).
49. J. T. Reager, J. S. Famiglietti, *Geophys. Res. Lett.* **36**, L23402 (2009).
50. J. T. Fasullo, C. Boening, F. W. Landerer, R. S. Nerem, *Geophys. Res. Lett.* **40**, 4368–4373 (2013).
51. K. A. Voss *et al.*, *Water Resour. Res.* **49**, 904–914 (2013).
52. E. Forootan *et al.*, *Remote Sens. Environ.* **140**, 580–595 (2014).
53. B. R. Scanlon, L. Longuevergne, D. Long, *Water Resour. Res.* **48**, W04520 (2012).
54. B. R. Scanlon *et al.*, *Proc. Natl. Acad. Sci. U.S.A.* **109**, 9320–9325 (2012).
55. W. Feng *et al.*, *Water Resour. Res.* **49**, 2110–2118 (2013).

ACKNOWLEDGMENTS

We thank M. Watkins, E. Ivins, D. Argus, G. Cogley, A. Richey, Y. Wada, R. Nerem, and D. Chambers for their contributions and discussion. This work was supported by funding from the NASA NEWS, Sea Level, and Cryosphere programs; the NASA GRACE Science Team; and the University of California Multicampus Research Programs and Initiatives. This multidisciplinary collaboration grew from the interactions of the NASA Sea Level Change Team. The research was conducted at the University of California, Irvine and at the Jet Propulsion Laboratory, California Institute of Technology under contract with NASA. M.-H. Lo was supported by the Ministry of Science and Technology (MOST), Taiwan, MOST 103-2111-M-002-006. GRACE RL05M data are available at podaac.jpl.nasa.gov. The authors declare no competing interests.

SUPPLEMENTARY MATERIALS

www.sciencemag.org/content/351/6274/699/suppl/DC1
Materials and Methods
Figs. S1 to S11
Tables S1 to S4
References (*56*–*69*)

9 November 2015; accepted 7 January 2016
10.1126/science.aad8386

MICROBIAL PHYSIOLOGY

Artificial electron acceptors decouple archaeal methane oxidation from sulfate reduction

Silvan Scheller,* Hang Yu, Grayson L. Chadwick, Shawn E. McGlynn,† Victoria J. Orphan*

The oxidation of methane with sulfate is an important microbial metabolism in the global carbon cycle. In marine methane seeps, this process is mediated by consortia of anaerobic methanotrophic archaea (ANME) that live in syntrophy with sulfate-reducing bacteria (SRB). The underlying interdependencies within this uncultured symbiotic partnership are poorly understood. We used a combination of rate measurements and single-cell stable isotope probing to demonstrate that ANME in deep-sea sediments can be catabolically and anabolically decoupled from their syntrophic SRB partners using soluble artificial oxidants. The ANME still sustain high rates of methane oxidation in the absence of sulfate as the terminal oxidant, lending support to the hypothesis that interspecies extracellular electron transfer is the syntrophic mechanism for the anaerobic oxidation of methane.

Biological methane oxidation in the absence of oxygen is restricted to anaerobic methanotrophic archaea (ANME) that are phylogenetically related to methanogens (*1*, *2*). These organisms evolved to metabolize methane to CO_2 near thermodynamic equilibrium ($E^{o\prime}$ = −245 mV for CH_4/CO_2) via the pathway of reverse methanogenesis (*3*), which includes the chemically challenging step of methane activation without oxygen-derived radicals (*4*). Reported terminal electron acceptors for anaerobic oxidation of methane (AOM) include sulfate (*1*, *2*), nitrate (*5*), and metal oxides (*6*). Nitrate reduction coupled to methane oxidation is directly mediated by a freshwater archaeal methanotroph "*Ca. Methanoperedens nitroreducens*" ANME-2d (*5*); however, the electron transport mechanism coupling methane oxidation with other terminal electron acceptors (such as sulfate and metal oxides) is still debated (*7*–*9*).

Sulfate-coupled methane oxidation (Eq. 1) is the dominant mechanism for methane removal within marine sediments, preventing the release of teragrams per year of this greenhouse gas from the oceans (*10*).

$$CH_4 + SO_4^{2-} = HCO_3^- + HS^- + H_2O$$
$$\text{Gibbs free energy } (\Delta G^{o\prime}) = -17 \text{ kJ mol}^{-1} \quad (1)$$

Multiple methanotrophic archaeal lineages (ANME-1; ANME-2a,b,c; and ANME-3) form syntrophic consortia with sulfate-reducing deltaproteobacteria (SRB) that drive AOM in areas of methane release at the seabed (*11*). The metabolism of AOM with sulfate appears to be partitioned between the two partners, requiring the exchange of electrons or intermediates. The mechanism underlying this syntrophic association has been studied using microcosm experiments [with AOM microorganisms exhibiting doubling times of 2 to 7 months (*12*–*17*)], as well as through the application of stable isotope analyses (*2*), radiotracer rate measurements (*18*), metagenomics (*3*, *5*, *19*, *20*), and theoretical modeling (*21*, *22*).

Attempts to metabolically decouple the syntrophic association and identify the intermediate compound passaged between ANME archaea and their SRB partners have been unsuccessful when diffusive intermediates such as hydrogen, acetate, formate, and some redox active organic electron shuttles were used (*16*, *23*). Culture-independent evidence for direct interspecies electron transfer in sulfate-coupled AOM by members of the ANME and their SRB partners (*8*, *9*) supports earlier genomic predictions of this process occurring in the methanotrophic ANME-1 (*19*).

Guided by the recent evidence of direct interspecies electron transfer from ANME-2 to SRB (*8*), we probed whether artificial electron acceptors can substitute for the role of the SRB partner as a terminal oxidant for AOM. Respiration of the artificial electron acceptor 9,10-anthraquinone-2,6-disulfonate (AQDS, $E^{o\prime}$ = −186 mV) has been previously reported in methanogens (*24*). We tested AQDS as a sink for methane-derived electrons generated by the ANME archaea in incubations with deep-sea methane seep sediment. The stoichiometry of methane oxidation coupled to AQDS predicts the reduction of four equivalents of AQDS per methane (Eq. 2).

$$CH_4 + 4\,AQDS + 3H_2O = HCO_3^- + H^+ + 4\,AQH_2DS$$
$$\Delta G^{o\prime} = -41 \text{ kJ mol}^{-1} \quad (2)$$

To quantify AOM with AQDS, we performed anaerobic microcosm experiments using methane seep sediment from the Santa Monica basin

Division of Geological and Planetary Sciences, California Institute of Technology, Pasadena, CA 91125, USA.
***Corresponding author. E-mail: vorphan@gps.caltech.edu (V.J.O.); scheller@caltech.edu (S.S.)** †Present address: Department of Biological Sciences, Tokyo Metropolitan University, Tokyo 192-0397, Japan; and Biofunctional Catalyst Research Team, RIKEN Center for Sustainable Resource Science, Saitama 351-0198, Japan.

Downloaded from on February 11, 2016

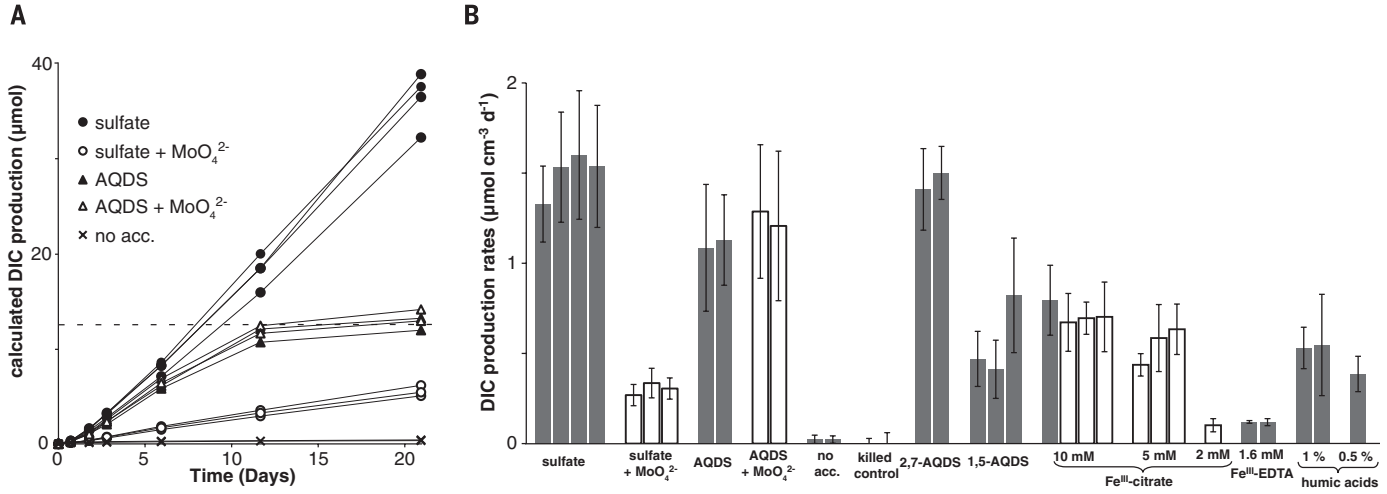

Fig. 1. DIC production per vial in incubations with 1.0 cm^3 of methane seep sediment. (**A**) Methane oxidation coupled to sulfate reduction [140 µmol of SO_4^{2-} (28 mM), methane oxidation unlimited, circles], and methane oxidation coupled to AQDS reduction [50 µmol of AQDS (10 mM) in the absence of sulfate, triangles]. Due to the 1:4 stoichiometry between CH_4 and AQDS, the produced DIC plateaued at approximately 12.5 µmol (dashed line). Open symbols depict incubations with the addition of the sulfate-reduction inhibitor sodium molybdate (25 mM). Control incubations without electron acceptors added (x symbol). (**B**) Initial rates of methane oxidation with different electron acceptors for individual incubation bottles. Values from the linear regression of time points 1 to 6 days (four points) are calculated per cubic centimeter of wet sediment; error bars represent the 95% confidence interval. White bars depict incubations with sodium molybdate (25 mM). Time course measurements for these experiments are provided in fig. S1; raw data are provided in fig. S2.

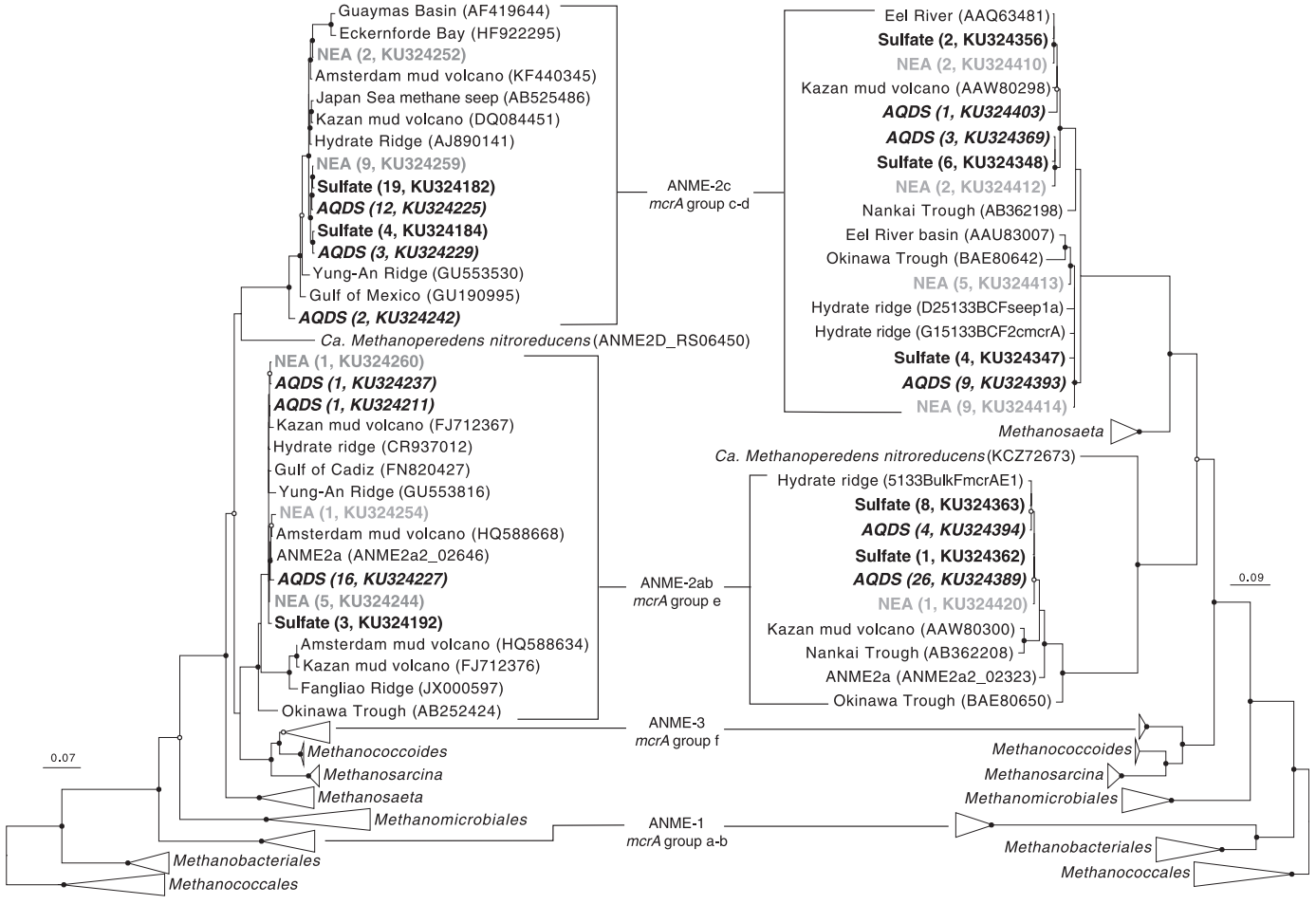

Fig. 2. Bayesian phylogeny of expressed archaeal RNA recovered from different AOM microcosms. 16S rRNA (left) and mcrA (right) transcripts obtained from AOM incubations with either sulfate or AQDS as the primary oxidant (bold text) or no electron acceptor added (NEA, gray text). Numbers in parentheses represent numbers of sequences recovered for each taxa. Bayesian likelihood values >75 and >90% are indicated by open and solid circles, respectively. Scale bars represent estimated sequence divergence or amino acid changes.

that had been rendered sulfate- and sulfide-free (*25*) and amended with 50 μmol AQDS and ^{13}C-labeled methane [0.35 MPa (*25*)]. After a 21-day incubation at 4°C, approximately 12.5 μmol of dissolved inorganic carbon (DIC) formed from the ^{13}C-methane (Fig. 1A), concomitant with the reduction of AQDS close to the predicted 1:4 stoichiometry (table S1). The initial rates of AOM with AQDS were equivalent to the rates measured with sulfate over the first 6 days (Fig. 1B) and later diverged as the AQDS was depleted from solution. At 22.5°C, where AQDS has higher solubility (table S2), the AOM rates with AQDS exceeded those with sulfate (fig. S3).

To confirm that the observed methane oxidation with AQDS was not coupled to traces of sulfate, we tracked AOM in the presence of sodium molybdate, a competitive inhibitor for sulfate reduction (*26*). With the addition of 25 mM molybdate, rates of sulfate-coupled AOM decreased by approximately fivefold relative to controls, which is consistent with previous reports (*16*). The high rates of methane oxidation in our sulfate-free incubations containing AQDS showed no inhibitory response if molybdate was included, indicating a decoupling of AOM from sulfate-reduction (Fig. 1, A and B).

Stimulation of AOM without sulfate is not restricted to AQDS. Regioisomers of AQDS (1,5-AQDS and 2,7-AQDS), humic acids, and soluble iron(III) complexes (ferric citrate and ferric-EDTA) also stimulated anaerobic oxidation of methane at rates that were at least 0.1 μmol cm^{-3} day^{-1} (Fig. 1B; a list of all oxidants tested is provided in table S3). In control incubations without an added electron acceptor, we measured a small apparent methane oxidation activity (1.5% relative to sulfate-coupled AOM, Fig. 1B) that is probably attributed to enzyme-catalyzed isotope exchange between methane and DIC without net methane oxidation (*27*, *28*). In killed control experiments (formaldehyde addition), we did not detect any conversion of ^{13}C-methane to DIC (Fig. 1B).

The archaeal 16*S* ribosomal RNA (rRNA) gene diversity of the seep sediment used in our AOM microcosm experiments was dominated by ANME-2 of the subgroups ANME-2a and ANME-2c, with a low relative abundance of ANME-1 phylotypes (fig. S4). To identify the active archaea potentially involved in methane oxidation in our experiments, after 4 weeks, we sequenced expressed archaeal 16*S* rRNA and the alpha subunit of the methyl coenzyme M reductase (mcrA) from microcosm treatments containing either sulfate, AQDS, or no added electron acceptor. The archaeal sequences recovered from the 16*S* rRNA and mcrA cDNA clone libraries were similar in the three treatments, with each containing only representatives of ANME-2a and -2c (Fig. 2). The detection of transcripts from multiple subgroups of ANME-2 in each treatment suggests that the same ANME lineages are active in AOM, independent of whether sulfate or AQDS is supplied as the oxidant. In contrast to the similar ANME composition, the relative abundance of recovered bacterial SRB clones (e.g. Desulfobacteraceae SEEP-SRB1) in the cDNA libraries decreased in treatments lacking sulfate as compared to microcosms supporting active sulfate-coupled AOM (table S4), and suggests that ANME may be capable of using AQDS directly without syntrophic interaction.

To directly test this hypothesis, we used cell-specific stable isotope analysis to quantify the anabolic activity of ANME-2 (including ANME-2c) and their co-associated syntrophic partners in consortia recovered from incubations supplied with different oxidants (including sulfate, AQDS, humic acids, and ferric iron). Using $^{15}NH_4^+$ stable isotope probing combined with fluorescence in situ hybridization and nanoscale secondary ion mass spectrometry [FISH-SIMS (*2*)], we measured the cell-specific anabolic activity (^{15}N cellular enrichment) in paired ANME and SRB populations in consortia (*8*). After 18 days of incubation with $^{15}NH_4^+$, consortia were phylogenetically identified by FISH using ANME-2c and Desulfobacteraceae-targeted oligonucleotide probes and were analyzed by nanoSIMS to quantify the assimilation of $^{15}NH_4^+$ for each paired population of ANME-2 and SRB (*25*).

In AOM microcosms containing sulfate, the $^{15}NH_4^+$ assimilation by co-associated bacteria and archaea in consortia from two sets of experiments (n = 20 and n = 19 consortia) was positively correlated at a ratio of approximately 1:1, indicating balanced syntrophic growth during AOM similar to (*8*) (Fig. 3C and Fig. 4, A and B). ANME-SRB consortia recovered from sulfate-free incubations amended with AQDS also showed high levels of $^{15}NH_4^+$ assimilation; however, in this case, anabolic activity within each of these consortia occurred only in the ANME archaea and not in their co-associated bacterial partners (Figs. 3F and 4A). This is consistent with the weak FISH signal observed for the Desulfobacteraceae. These data offer direct validation of results based on RNA analysis, demonstrating that when AQDS was supplied as the terminal electron acceptor for AOM, the ANME-2 archaea sustained active biosynthesis that was decoupled from the activity of the SRB partner. This was directly shown for ANME-2c (n = 11 consortia) and inferred for ANME-2a on the basis of nanoSIMS results from the eight non–ANME-2c aggregates that were all anabolically active. Consortia from incubations with methane and $^{15}NH_4^+$, but lacking an electron acceptor, showed no measurable anabolic activity in either partner (n = 9 ANME-SRB consortia; Fig. 4A, inset, and fig. S5).

The ANME cells paired with SRB in consortia from AQDS incubations showed similar levels of anabolic activity [3.3 months doubling time based on average ^{15}N incorporation (*25*)] as those of ANME archaea conserving energy through conventional sulfate-coupled AOM [2.9 months doubling time (*25*)] in parallel incubations, suggesting equivalent potential for growth (Fig. 4A).

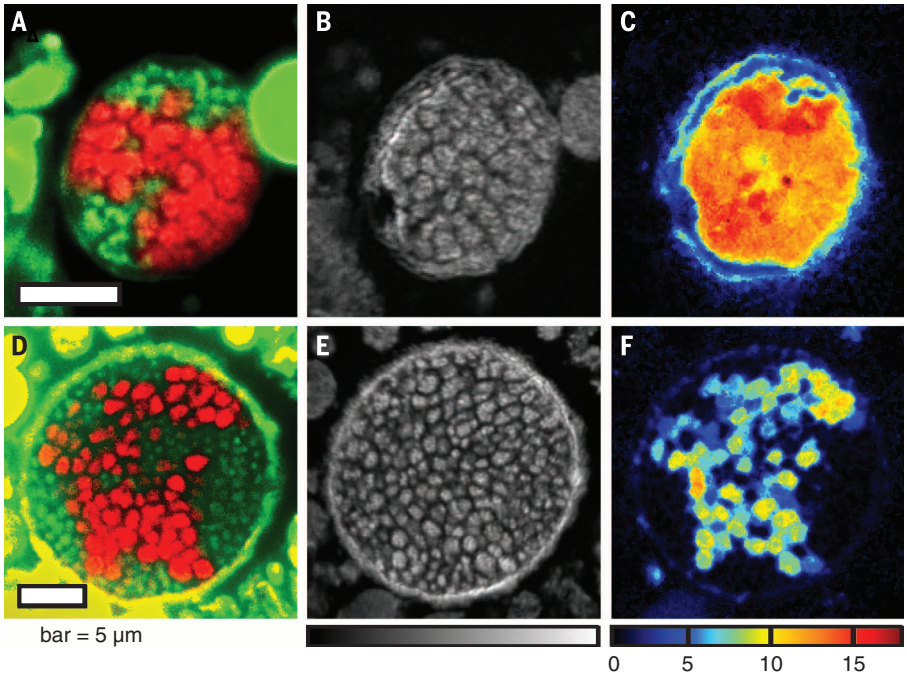

Fig. 3. Representative FISH-nanoSIMS images from sulfate and AQDS microcosms. The correlation between phylogenetic identity (FISH) and anabolic activity (^{15}N enrichment) for example consortia of ANME-2c archaea and sulfate-reducing bacteria analyzed from AOM incubations amended with sulfate or AQDS is shown. (**A** to **C**) AOM consortium from microcosm with sulfate. (**D** to **F**) Consortium from microcosm with AQDS as the sole electron acceptor. In each case, the at % of ^{15}N isotope enrichment was calculated from ratios of secondary ion images of $^{12}C^{15}N^-$ and $^{12}C^{14}N^-$. (A) and (D) FISH images, with ANME-2c in red and Desulfobacteraceae in green; the FISH signal for the bacterial cells in (D) is weak, probably due to the low abundance of cellular rRNA in SRB in the AQDS treatment without sulfate. (B) and (E) nanoSIMS ion image of $^{12}C^{14}N^-$ for cellular biomass, linear scale (0 to 4500 counts per pixel). (C) and (F) Fractional abundance of ^{15}N (in at %) as a proxy for anabolic activity.

Apparently, ANME-2 archaea are capable of conserving energy for biosynthesis independent of sulfate availability and separated from the activity of their syntrophic bacterial partners.

AOM incubations with iron(III)-citrate and humic acids as the alternative electron acceptors also demonstrated exclusive biosynthetic activity of ANME-2c and other ANME-2 cells (Fig. 4B and fig. S6). In contrast to incubations with sulfate or AQDS, only a few and mostly small AOM consortia [14 out of 31 for iron(III)-citrate and 4 out of 46 for humic acids] were anabolically active (>10% archaeal activity relative to cells in the sulfate treatments, or >0.8 atomic % (at %) of ^{15}N), despite the high rates of AOM measured with those compounds (Fig. 1B).

All compounds that were able to replace the role of the SRB partners during AOM, including AQDS isomers, humic acids, and iron(III) complexes, have the ability to accept single electrons. Mechanistically, extracellular electron transfer (*8*, *9*) from ANME-2 to single electron acceptors can account for all our findings. Large, S-layer–associated multi-heme c-type cytochromes in members of the ANME-2 archaea (*8*) could putatively conduct electrons [discussed in (*29*)] derived from reverse methanogenesis from the archaeal membrane to the outside of the cell, where they can be taken up by a suitable electron acceptor. A congruent path of extracellular electron transfer has been proposed for the bacterium *Geobacter sulfurreducens* when oxidizing acetate coupled to the reduction of AQDS or humic acids (*30*). The similar catabolic and anabolic activities observed within ANME-2 archaea, independent of whether the terminal electron acceptor is AQDS or sulfate, suggest that the biochemistry within these organisms may follow the same pathway under AQDS conditions as when syntrophically coupled to SRB. Our data therefore also lend experimental evidence in support of the hypothesis of direct interspecies electron transfer as the syntrophic coupling mechanism between methane-oxidizing ANME-2 and SRB in the environment (*8*).

The apparent ability of ANME-2 to oxidize methane via the release of single electrons constitutes a versatile half-metabolism. This physiology suggests that methanotrophic ANME-2 archaea should also be able to respire solid electron acceptors directly via extracellular metal reduction, which would explain methane oxidation coupled to insoluble iron(III) and manganese(IV) reduction reported previously (*6*). Evolutionarily, methane oxidation with metal oxides could have served as a transient life style for ANME before the establishment of a syntrophic association with SRB. According to this hypothesis, methanogenic archaea first evolved the capability to conserve energy as a methanotroph coupled with the respiration of solid metal oxides as electron acceptors. In a subsequent evolutionary step, SRB developed a symbiosis with ANME archaea, gaining a direct source of electrons for sulfate reduction and leading to the highly structured syntrophic consortia common today in seep environments. This physiology of using extracellular electron transfer to enable syntrophic interaction (*8*, *9*) has the advantage that intermediates cannot be lost via diffusion and that electrical conductance is much faster than diffusive transfer of reducing equivalents (*8*). Further, this described metabolism may have industrial utility, providing a mechanism for the conversion of methane to CO_2 plus single electrons that can be catalyzed reversibly at low temperatures, with the potential to convert methane to electricity at high overall efficiencies. Finally, these findings offer a promising path forward for isolating members of the ANME-2 in pure culture, enabling detailed characterization of the ecophysiology of these key players in the global methane cycle.

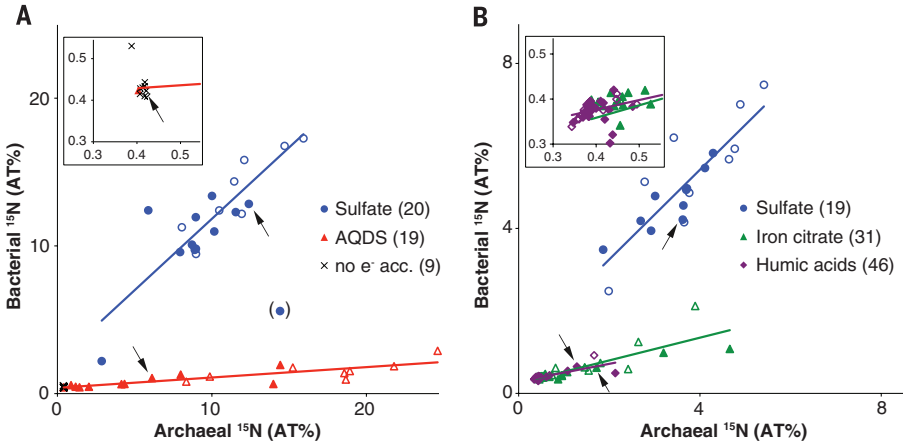

Fig. 4. Summary of FISH-nanoSIMS ^{15}N incorporation data. Average anabolic activity for paired ANME and SRB populations in each AOM consortium from incubations with different terminal electron experiments is shown. Each solid symbol represents the average ^{15}N at % for the population of paired ANME-2c cells relative to bacterial cells in a single consortium. Open symbols represent other unidentified ANME-SRB consortia (putative ANME-2a). (Insets) ^{15}N at % values close to natural abundance value (0.36 at % ^{15}N). FISH-nanoSIMS images of consortia marked with an arrow are displayed in Fig. 3 and figs. S5 and S6. (A) and (B) constitute two independent sets of experiments; experiments in (A) contained ~80% $^{15}NH_4^+$, whereas those in (B) contained ~40% (*25*). Numeric data for each aggregate are provided in table S5. The activity of bacterial cells (b) relative to the archaeal cell activity (a) was determined via linear regression as follows: (**A**) Sulfate: b = 0.97a + 2.17, R^2 = 0.75; AQDS: b = 0.070a + 0.39, R^2 = 0.69. (**B**) Sulfate: b = 1.09a + 1.07, R^2 = 0.74; iron citrate: b = 0.28a + 0.25, R^2 = 0.71; humic acids: b = 0.21a + 0.29, R^2 = 0.60. The blue data point in parentheses (A) was not included for the linear regression (see fig. S7 for single-cell analysis and further discussion). The small apparent ^{15}N enrichment in bacteria from sulfate-free incubations was found to be due to inaccuracies in pixel assignments for SRB cells during data processing, determined by manual inspection of each nanoSIMS image.

REFERENCES AND NOTES

1. A. Boetius *et al.*, *Nature* **407**, 623–626 (2000).
2. V. J. Orphan, C. H. House, K. U. Hinrichs, K. D. McKeegan, E. F. DeLong, *Science* **293**, 484–487 (2001).
3. S. J. Hallam *et al.*, *Science* **305**, 1457–1462 (2004).
4. S. Scheller, M. Goenrich, R. Boecher, R. K. Thauer, B. Jaun, *Nature* **465**, 606–608 (2010).
5. M. F. Haroon *et al.*, *Nature* **500**, 567–570 (2013).
6. E. J. Beal, C. H. House, V. J. Orphan, *Science* **325**, 184–187 (2009).
7. J. Milucka *et al.*, *Nature* **491**, 541–546 (2012).
8. S. E. McGlynn, G. L. Chadwick, C. P. Kempes, V. J. Orphan, *Nature* **526**, 531–535 (2015).
9. G. Wegener, V. Krukenberg, D. Riedel, H. E. Tegetmeyer, A. Boetius, *Nature* **526**, 587–590 (2015).
10. W. S. Reeburgh, *Chem. Rev.* **107**, 486–513 (2007).
11. K. Knittel, A. Boetius, *Annu. Rev. Microbiol.* **63**, 311–334 (2009).
12. P. R. Girguis, A. E. Cozen, E. F. DeLong, *Appl. Environ. Microbiol.* **71**, 3725–3733 (2005).
13. V. J. Orphan, K. A. Turk, A. M. Green, C. H. House, *Environ. Microbiol.* **11**, 1777–1791 (2009).
14. R. J. W. Meulepas *et al.*, *Biotechnol. Bioeng.* **104**, 458–470 (2009).
15. T. Holler *et al.*, *ISME J.* **5**, 1946–1956 (2011).
16. K. Nauhaus, T. Treude, A. Boetius, M. Krüger, *Environ. Microbiol.* **7**, 98–106 (2005).
17. K. Nauhaus, M. Albrecht, M. Elvert, A. Boetius, F. Widdel, *Environ. Microbiol.* **9**, 187–196 (2007).
18. S. B. Joye *et al.*, *Chem. Geol.* **205**, 219–238 (2004).
19. A. Meyerdierks *et al.*, *Environ. Microbiol.* **12**, 422–439 (2010).
20. F. P. Wang *et al.*, *ISME J.* **8**, 1069–1078 (2014).
21. M. J. Alperin, T. M. Hoehler, *Am. J. Sci.* **309**, 869–957 (2009).
22. B. Orcutt, C. Meile, *Biogeosciences* **5**, 1587–1599 (2008).
23. R. J. W. Meulepas, C. G. Jagersma, A. F. Khadem, A. J. M. Stams, P. N. L. Lens, *Appl. Microbiol. Biotechnol.* **87**, 1499–1506 (2010).
24. D. R. Bond, D. R. Lovley, *Environ. Microbiol.* **4**, 115–124 (2002).
25. Additional supplementary information is available on *Science* Online.
26. L. G. Wilson, R. S. Bandurski, *J. Biol. Chem.* **233**, 975–981 (1958).
27. T. Holler *et al.*, *Proc. Natl. Acad. Sci. U.S.A.* **108**, E1484–E1490 (2011).
28. M. Y. Yoshinaga *et al.*, *Nat. Geosci.* **7**, 190–194 (2014).
29. S. Pirbadian, M. Y. El-Naggar, *Phys. Chem. Chem. Phys.* **14**, 13802–13808 (2012).
30. J. W. Voordeckers, B. C. Kim, M. Izallalen, D. R. Lovley, *Appl. Environ. Microbiol.* **76**, 2371–2375 (2010).

ACKNOWLEDGMENTS

We thank Y. Guan for assistance with the nanoSIMS, the Beckman Resource Center (BRCem) for sectioning, M. Aoki for FISH analysis of ANME-2a and ANME-2c consortia, and S. Goffredi and C. Skennerton for editorial comments. We are grateful to P. Brewer from the Monterey Bay Aquarium Research Institute

for providing the opportunity to participate in the 2013 research expedition and A. Pasulka and K. Dawson for their contributions in shipboard sample processing. This work was supported by the U.S. Department of Energy Biological and Environmental Research program (grants DE-SC0010574 and DE-SC0004940) and funding by the Gordon and Betty Moore Foundation through grants GBMF3306 and GBMF3780 (to V.J.O.). S.S. was supported in part by the Swiss National Science Foundation (grant no. PBEZP2_142903). All data are available in the supplementary materials. Archaeal 16S rRNA, mcrA genes, and bacterial 16S rRNA genes were deposited with the National Center for Biotechnology Information under accession numbers KU324182 to KU324260, KU324346 to KU324428, and KU324261 to KU324345, respectively. S.S., H.Y., and V.J.O. devised the study, and S.S., H.Y., G.L.C., and S.M. conducted the experiments and analyses. S.S. and V.J.O. wrote the manuscript, with contributions from all authors to data analysis, figure generation, and the final manuscript.

SUPPLEMENTARY MATERIALS

www.sciencemag.org/content/351/6274/703/suppl/DC1
Materials and Methods
Figs. S1 to S7
Tables S1 to S5
References (*31*–*57*)

26 October 2015; accepted 20 January 2016
10.1126/science.aad7154

LUNG PHYSIOLOGY

Pulmonary neuroendocrine cells function as airway sensors to control lung immune response

Kelsey Branchfield,[1] Leah Nantie,[1] Jamie M. Verheyden,[1] Pengfei Sui,[1] Mark D. Wienhold,[2] Xin Sun[1]*

The lung is constantly exposed to environmental atmospheric cues. How it senses and responds to these cues is poorly defined. Here, we show that Roundabout receptor (*Robo*) genes are expressed in pulmonary neuroendocrine cells (PNECs), a rare, innervated epithelial population. *Robo* inactivation in mouse lung results in an inability of PNECs to cluster into sensory organoids and triggers increased neuropeptide production upon exposure to air. Excess neuropeptides lead to an increase in immune infiltrates, which in turn remodel the matrix and irreversibly simplify the alveoli. We demonstrate in vivo that PNECs act as precise airway sensors that elicit immune responses via neuropeptides. These findings suggest that the PNEC and neuropeptide abnormalities documented in a wide array of pulmonary diseases may profoundly affect symptoms and progression.

In humans, approximately 5 to 8 liters of air passes in and out of the lung per minute when resting. The air can vary in oxygen and CO_2 concentration, may carry allergens, and confers different extents of mechanical stretch of the airway and gas-exchange surfaces. These signals are sensed, relayed, and processed into physiological outputs such as the control of pulmonary blood pressure, immune responses, and breathing rhythm, but the mechanism is unclear. Pulmonary neuroendocrine cells (PNECs) are found in a wide array of organisms from fish to mammals (*1*). In the mammalian lung, PNECs are the only innervated airway epithelial cells and represent less than 1% of the total lung epithelial cell population (*2*). Although in vitro evidence has implicated PNECs in oxygen sensing, bronchial and vascular smooth muscle tonus, and immune responses (*1*, *3*), these roles have not been demonstrated in vivo. A recent study showed that genetic ablation of PNECs in the adult did not compromise homeostasis or airway repair, leaving in question the in vivo importance of these cells (*4*). PNEC pathologies, in particular an increase in PNEC number, have been documented in a large array of lung diseases, including asthma, bronchopulmonary dysplasia, cystic fibrosis, chronic obstructive pulmonary disease, congenital diaphragmatic hernia, neuroendocrine hyperplasia of infancy, sudden infant death syndrome, and pulmonary hypertension (*5*–*8*). In each case, it remains unclear whether the PNEC increase is a cause for or the consequence of symptoms.

In mouse lung, most PNECs reside in clusters of ~3 to 20 cells called neuroepithelial bodies (NEBs) (*3*, *9*). Both solitary and clustered PNECs contain dense core vesicles, filled with bioactive neuropeptides such as calcitonin gene-related peptide (CGRP) or amines such as serotonin (*1*). These are released in response to stimuli, such as changes in oxygen level. Neuropeptides and amines have been implicated in some of the same processes as PNECs (*10*–*12*), raising the possibility that they may mediate PNEC function. However, a causal link has not been demonstrated in vivo.

We initiated the current study to uncover the mechanisms underlying congenital diaphragmatic hernia (CDH), a birth defect associated with considerable lung dysfunction, including heightened immune response and pulmonary hypertension (*13*). In a genetic mouse model of CDH, we uncovered a defect of failed PNEC clustering. This is followed by a sequence of events: an increase in PNEC neuropeptides, an increase in immune infiltrates, and remodeling of lung structure. These findings offer an in vivo demonstration of PNEC function. Because changes in PNEC number and associated neuropeptides have been documented in many lung diseases, our results have wide implications beyond CDH.

In humans, mutations in roundabout receptor (*ROBO*) genes have been associated with CDH (*13*, *14*). To study the lung defects associated with CDH, we inactivated both *Robo1* and *Robo2* in endoderm-derived epithelium, including the lung, using Shh^{cre} (hereafter *Shhcre;Robo* mutant) in mice (*15*, *16*). Although these mutants survive, they exhibit reduced gas-exchange surface area starting at postnatal day (P) 15 (Fig. 1, A and B, and fig. S1). We performed microarray followed by quantitative reverse transcriptase polymerase chain reaction (qRT-PCR) at P7, before reduction of gas-exchange surface. Fifteen of the top 20 differentially expressed genes have been implicated in immune responses, and all are significantly increased, including *Ccl3*, *Cxcl2*, *Tnfa*, and *Saa3* (Fig. 1C). Consistent with this signature, we observed elevated numbers of immune cells, including neutrophils, eosinophils, macrophages, and T cells (Fig. 1, D and E, and fig. S2). Furthermore, there is an increase in the proportion of M2 and a decrease in the proportion of M1 macrophages (fig. S3). These findings indicate that *Shhcre;Robo* mutants show heightened immune sensitivity, mimicking a common CDH comorbidity (*13*).

Although *Robo* is expressed in the alveolar region of the lung mesenchyme (fig. S4), its expression in the epithelium is restricted to rare cells along the airway (Fig. 1F). Colabeling with CGRP antibody revealed that *Robo*-expressing epithelial cells are PNECs (Fig. 1G). To confirm that *Robo* genes are required within PNECs for function, we inactivated *Robo* using *Ascl1creERT2* (*17*), a knock-in cre driver that confers PNEC-specific activity in the lung epithelium (fig. S5). We found that *Ascl1creERT2;Robo* mutants exhibited both alveolar simplification and macrophage increase, recapitulating the *Shhcre;Robo* phenotypes (fig. S6). These findings together demonstrate that *Robo* is required specifically in PNECs for restricting immune cell number and preventing alveolar simplification.

At embryonic day (E) 13.5, newly specified PNECs were solitary cells in both control and *Shhcre;Robo* mutant lungs (Fig. 2, A and B). By E15.5, a majority of PNECs had aggregated into NEBs in the control. However, PNECs were not clustered in *Shhcre;Robo* mutants (Fig. 2, C and D). This highly penetrant phenotype persisted in postnatal lungs (Fig. 2, E and F, and fig. S7). Total PNEC cell number appears unaffected, as supported by normal expression of *Ascl1* and other PNEC markers (fig. S8). Unclustered cells

[1]Laboratory of Genetics, Department of Medical Genetics, University of Wisconsin-Madison, Madison, WI 53706, USA. [2]Department of Pediatrics, School of Medicine and Public Health, University of Wisconsin-Madison, Madison, WI 53706, USA.
*Corresponding author. E-mail: xsun@wisc.edu

Downloaded from on February 11, 2016

in the mutant lose their wedge shape and are more rounded (figs. S7 and S9). Furthermore, in contrast to controls, where solitary PNECs are not innervated (*9*), ~33.3% (31 of 93 cells) of unclustered PNECs are innervated in the mutant (Fig. 2F and fig. S9), suggesting that PNEC innervation is not dependent on cluster formation or on *Robo* function in PNECs.

Ascl1creERT2;Robo mutants also exhibit PNEC unclustering (fig. S10). This phenotype manifested even when *Robo* inactivation was induced postnatally, which is subsequent to NEB formation. Together, our results establish that *Robo* is required for PNEC assembly and maintenance in NEBs.

Robo can function either dependently or independently of its ligand, Slit (*18*). Analysis of *Slit* mutants show that, whereas PNEC clustering is not affected in any of the single mutants, it is reduced in *Slit1;3* mutants (fig. S11, A to D). This result suggests that *Robo* function in this process is likely ligand dependent.

Slit and Robo function primarily to mediate cellular repulsion and rarely attraction (*19*). To determine whether Slit acts as a repulsive or attractive signal for Robo-expressing PNECs, we first determined where *Slit* genes are expressed. Combined *Slit1;2*-GFP (green fluorescent protein) reporter revealed expression in only about 1 to 3 PNECs within large NEBs, raising the possibility that the Slit1/2-expressing cells may be the nucleating cells of the cluster (fig. S11E). This also indicates PNEC subspecialization within a cluster. *Slit3* expression is restricted to the vascular smooth-muscle-cell layer surrounding arteries, which runs alongside the main bronchi where most NEBs are found (fig. S11, F and G). Together, the close proximity of *Slit*-expressing cells to *Robo*-expressing PNECs raised the possibility that Slit ligands may provide an attractive cue for PNECs.

To test this, flow cytometry sorted GAD1-GFP^{+} PNECs were seeded in the top chamber of a Boyden cell migration culture insert. When Slit protein was added with the cells in the top chamber, ~52% fewer ($P = 8.5 \times 10^{-4}$) PNECs migrated to the bottom (fig. S12, J to I). Conversely, when Slit protein was added to the bottom chamber, 18% more ($P = 7.5 \times 10^{-5}$) PNECs migrated to the bottom (fig. S11, L to N). These results suggest that Slit-Robo drive PNEC clustering into NEBs, likely through cellular attraction.

To test a possible link between PNECs and immune response, we assayed the expression of neuropeptides produced by PNECs (*1*). Of the nine neuropeptide genes assayed, five were significantly up-regulated in *Shhcre;Robo* mutants (Fig. 3A). Staining with antibody against CGRP revealed that, although its expression remains in PNECs in the mutant, the staining intensity is increased and it is no longer restricted to the basal side of these cells (figs. S7 and S9). We also note that, while unclustering occurred by E15.5, neuropeptide up-regulation is only observed after birth, presumably upon exposure to air (fig. S12).

To determine whether the increase in neuropeptides contributes to the immune response, we focused on CGRP because its transcript shows the largest increase among all assayed (Fig. 3A). We countered this increase by breeding a mutant allele of *Cgrp* into the *Shhcre;Robo* background (*20*). In *Robo* controls, loss of *Cgrp* did not alter macrophage numbers (Fig. 3, B, D, and F). However, in *Shhcre;Robo* mutants, loss of *Cgrp* significantly decreased macrophage numbers in a dose-dependent manner (Fig. 3, C, E, and F). We also found that loss of *Cgrp* partially reversed the alveolar simplification phenotype (fig. S13). We note that neither macrophage increase nor alveolar simplification were entirely prevented, suggesting that the increase in other neuropeptides may add to downstream outcomes. Together, these results provide in vivo genetic demonstration that neuropeptides mediate PNEC function.

As normal alveologenesis initiates at P4 (*21*), the late appearance of alveolar simplification at P15 suggests that disruption of alveologenesis may not be a primary cause. Although no change in cell death was observed by P10, there was a clear reduction of elastin (fig. S14), which is a possible trigger of simplification (*22*). Immune cells such as macrophages express matrix metalloproteinases that degrade elastin (*23*). Furthermore, the increase in macrophages is observed before simplification (figs. S1 and S2), raising the possibility of a causal relationship. To test this, we treated *Shhcre;Robo* and control lungs with clodronate, a hydrophilic drug that depletes macrophages (*24*). Treatment starting at P5, before the immune cell increase, effectively restricted alveolar macrophage numbers to baseline level in *Shhcre;Robo* mutants (Fig. 4, A to E). This attenuated the decrease in elastin and entirely prevented simplification (Fig. 4, F to J, and fig. S15). Together these data offer in vivo demonstration that increased immune infiltrates are responsible for alveolar simplification and that both are downstream consequences of PNEC dysfunction.

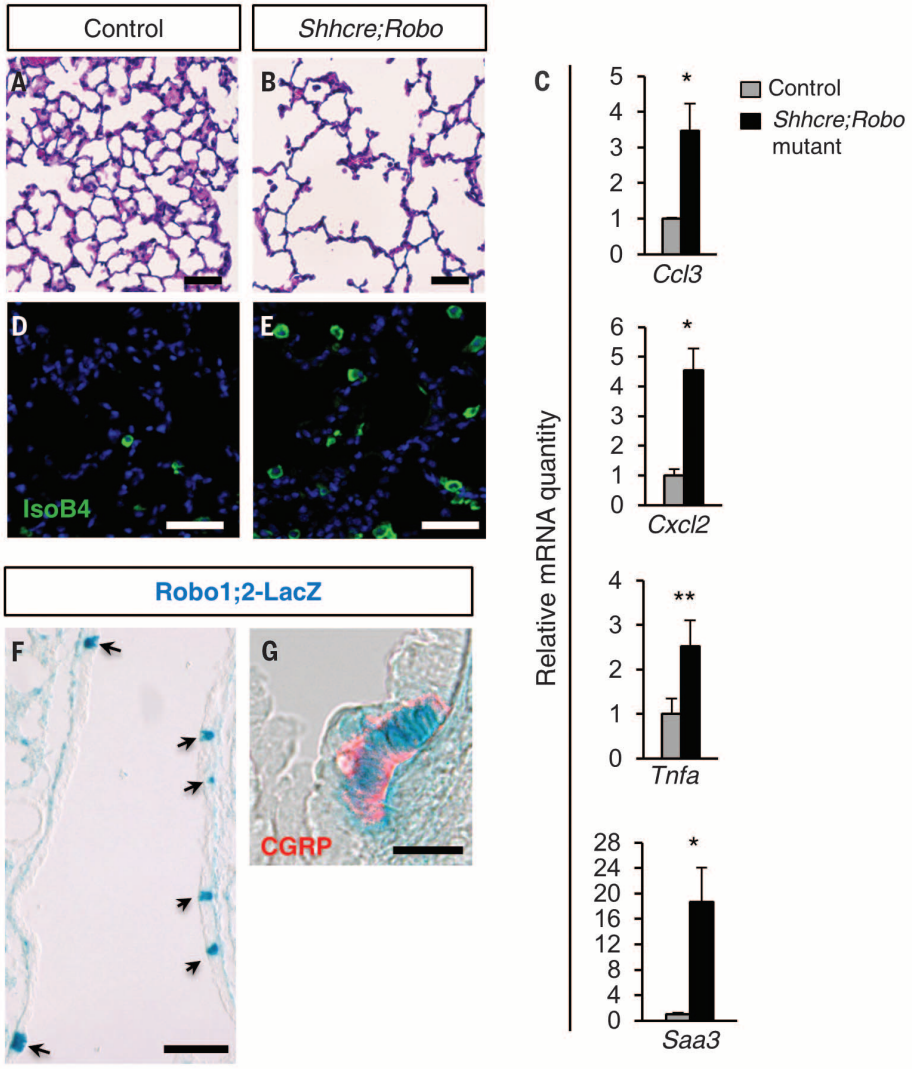

Fig. 1. *Robo* mutants exhibit alveolar simplification and heightened immune response. (**A** and **B**) Hematoxylin and eosin (H&E) staining of alveolar region at P22. (**C**) qRT-PCR of P7 lungs. (**D** and **E**) IsoB4 labeling of macrophages at P22. (**F** and **G**) X-Gal–stained heterozygous *Robo1*$^{lacZ/+}$;*Robo2*$^{lacZ/+}$ lungs. (F) P0, arrows indicate expression in PNECs. (G) E15.5, with anti-CGRP immunostaining (red). *$P <$ 0.05; **$P <$ 0.001.

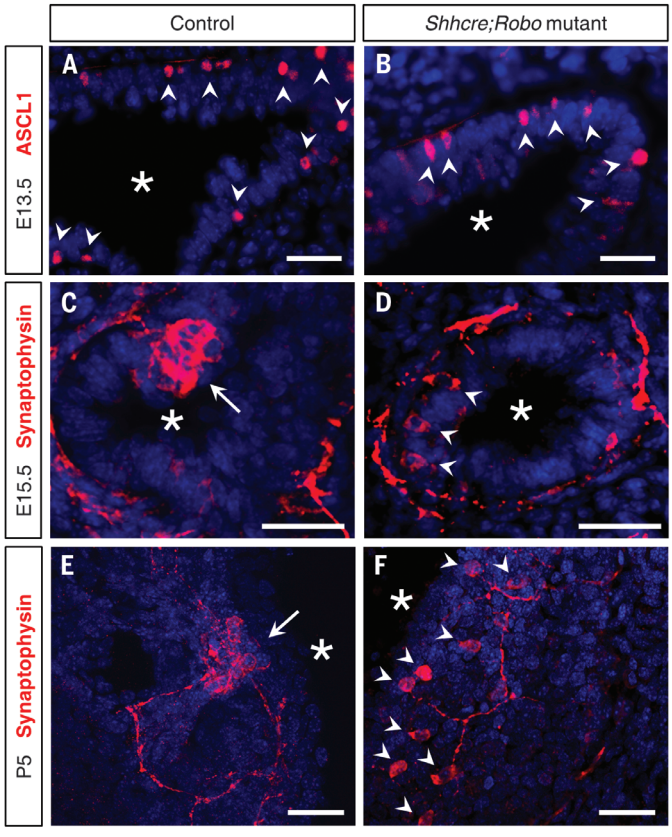

Fig. 2. *Robo1;2* are required for PNEC clustering. Immunostained vibratome lung slices. (**A** and **B**) ASCL1 immunostaining labels nascent PNECs. (**C** to **F**) Synaptophysin immunostaining labels differentiated PNECs and their associated nerves. Arrowheads indicate solitary PNECs, arrows indicate clustered PNECs in NEBs, and asterisks indicate airway lumen. Scale bars, 30 μm.

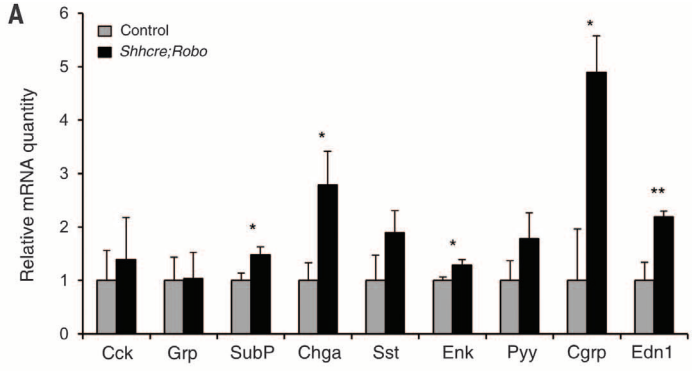

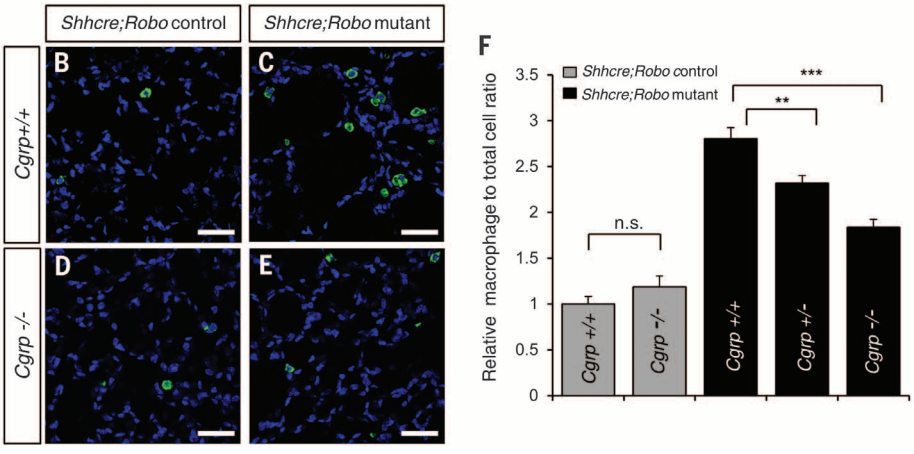

Fig. 3. Increase in neuropeptide level contributes to increased macrophage infiltration. (**A**) qRT-PCR of PNEC peptide transcript levels in P5 lungs. *$P < 0.05$, **$P < 0.001$. (**B** to **E**) IsoB4 labeling of macrophages at P22. Scale bars, 40 μm. (**F**) Quantification presented as the relative percentage of macrophage to total cell ratio normalized to *Shhcre;Robo*$^{+/-}$;*Cgrp*$^{+/+}$. **$P < 0.01$; ***$P < 0.0001$; n.s., not significantly different ($P \geq 0.05$).

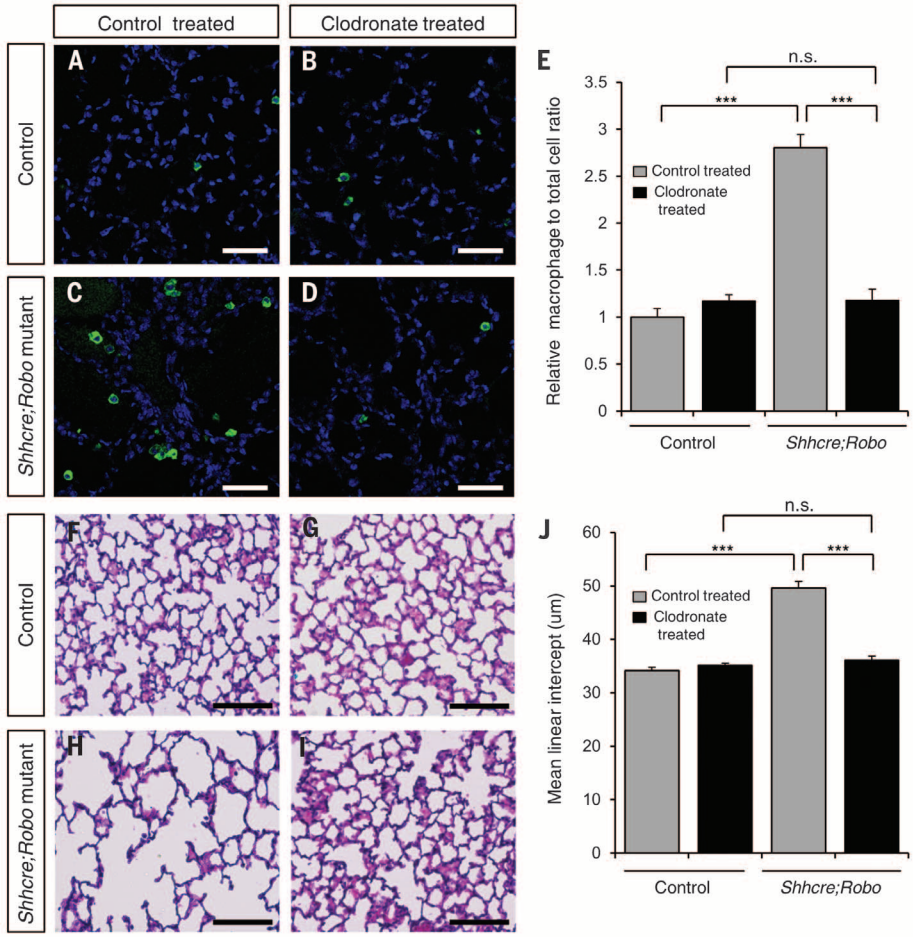

Fig. 4. Macrophage reduction by clodronate treatment attenuates alveolar simplification. (**A** to **D**) IsoB4 labeling of macrophages at P22. Scale bar, 50 μm. (**E**) Macrophage quantification as the relative percentage of macrophage to total cell ratio normalized to control mice with liposome control treatment. (**F** to **I**) H&E staining of alveolar region at P22. Scale bar, 100 μm. (**J**) Quantification of mean linear intercept (MLI). ***$P < 0.0001$; n.s., not significantly different ($P \geq 0.05$).

In this study, we present in vivo genetic evidence demonstrating that PNECs, despite their rarity, have profound impact on postnatal lung function. Although the PNEC defect is already evident at E15.5 in the *Shhcre;Robo* mutant, the physiological outcomes, beginning with up-regulation of neuropeptides, initiates after birth. This suggests that the effect of PNEC is dependent on lung exposure to air. Thus, our findings delineate a mode of signal transduction in which PNECs are sensitive rheostats on the airway wall that translate environmental cues non–cell-autonomously into immune responses.

Our results establish *Robo1,2* as a set of genes that control PNEC clustering into NEBs. It also presents *Slit* and *Robo* as players in selective cell sorting in the epithelium of a mammalian organ. Inactivation of *Robo* after NEB formation also led to unclustering, suggesting that the clusters are actively maintained. Although Slit-Robo are largely known to mediate cellular repulsion, our data indicate that they drive PNEC clustering through cellular attraction. *Robo* inactivation led to altered innervation and loss of basal-biased localization of neuropeptides. These changes may underlie the altered downstream impact of PNECs.

An increase in PNEC number has been documented in a large array of lung-associated diseases, ranging from rare disorders such as CDH to common conditions such as asthma (*5*–*8*). We note that the *Robo* mutant PNEC phenotype is distinct from increased PNEC number. However, both are associated with increased neuropeptides, which we show to be potent effectors of PNEC function. Our findings thereby predict that rather than being a passive readout of the disease, the documented PNEC pathologies and neuropeptide increases may serve as active contributors to symptoms in a large array of respiratory diseases.

REFERENCES AND NOTES

1. E. Cutz, J. Pan, H. Yeger, N. J. Domnik, J. T. Fisher, *Semin. Cell Dev. Biol.* **24**, 40–50 (2013).
2. J. E. Boers, J. L. den Brok, J. Koudstaal, J. W. Arends, F. B. Thunnissen, *Am. J. Respir. Crit. Care Med.* **154**, 758–763 (1996).
3. R. I. Linnoila, *Lab. Invest.* **86**, 425–444 (2006).
4. H. Song *et al.*, *Proc. Natl. Acad. Sci. U.S.A.* **109**, 17531–17536 (2012).
5. E. Cutz, H. Yeger, J. Pan, *Pediatr. Dev. Pathol.* **10**, 419–435 (2007).
6. D. G. Perrin, T. J. McDonald, E. Cutz, *Pediatr. Pathol.* **11**, 431–447 (1991).
7. M. E. Sunday, L. Shan, M. Subramaniam, *Endocr. Pathol.* **15**, 91–106 (2004).
8. X. Gu *et al.*, *Am. J. Respir. Cell Mol. Biol.* **50**, 637–646 (2014).
9. C. S. Kuo, M. A. Krasnow, *Cell* **163**, 394–405 (2015).
10. S. Tjen-A-Looi, R. Ekman, H. Lippton, J. Cary, I. Keith, *Am. J. Physiol.* **263**, H681–H690 (1992).
11. S. Dunzendorfer, C. Meierhofer, C. J. Wiedermann, *J. Leukoc. Biol.* **64**, 828–834 (1998).
12. B. D. Moore *et al.*, *Respiration* **83**, 529–542 (2012).
13. S. Kantarci, P. K. Donahoe, *Am. J. Med. Genet. C. Semin. Med. Genet.* **145C**, 217–226 (2007).
14. M. Longoni *et al.*, *Proc. Natl. Acad. Sci. U.S.A.* **111**, 12450–12455 (2014).
15. K. S. Harris, Z. Zhang, M. T. McManus, B. D. Harfe, X. Sun, *Proc. Natl. Acad. Sci. U.S.A.* **103**, 2208–2213 (2006).
16. E. T. Domyan *et al.*, *Dev. Cell* **24**, 52–63 (2013).
17. E. J. Kim, J. L. Ables, L. K. Dickel, A. J. Eisch, J. E. Johnson, *PLOS ONE* **6**, e18472 (2011).
18. B. Hivert, Z. Liu, C. Y. Chuang, P. Doherty, V. Sundaresan, *Mol. Cell. Neurosci.* **21**, 534–545 (2002).
19. C. Englund, P. Steneberg, L. Falileeva, N. Xylourgidis, C. Samakovlis, *Development* **129**, 4941–4951 (2002).
20. E. S. McCoy, B. Taylor-Blake, M. J. Zylka, *PLOS ONE* **7**, e36355 (2012).
21. S. I. Mund, M. Stampanoni, J. C. Schittny, *Dev. Dyn.* **237**, 2108–2116 (2008).
22. A. Shifren, A. G. Durmowicz, R. H. Knutsen, E. Hirano, R. P. Mecham, *Am. J. Physiol. Lung Cell. Mol. Physiol.* **292**, L778–L787 (2007).
23. A. M. Wallace *et al.*, *COPD* **5**, 13–23 (2008).
24. N. van Rooijen, E. Hendrikx, *Methods Mol. Biol.* **605**, 189–203 (2010).

ACKNOWLEDGMENTS

Supporting data and methods are presented in the supplementary materials. We thank X. Ai, T. Gomez, and E. Chapman for discussion; N. Hernandez-Santos for immune analysis; L. Ma, M. Tessier-Lavigne, J. Johnson, L. Wadiche, M. Zylka, and Mutant Mouse Regional Resource Center for mouse strains; and A. Lashua for technical support. This work was supported by American Heart Association predoctoral fellowship 14PRE20490146 and NIH predoctoral training grant T32 GM007133 (to K.B.), NIAID postdoctoral fellowship 5T32AI007635 (to L.N.), and NHLBI RO1 HL113870, HL097134, HL122406, University of Wisconsin Romnes Faculty Fellowship, and Wisconsin Partnership Program grant 2897 (to X.S.).

SUPPLEMENTARY MATERIALS

www.sciencemag.org/content/351/6274/707/suppl/DC1
Materials and Methods
Figs. S1 to 15
References (*25*–*28*)

5 September 2015; accepted 16 December 2015
Published online 7 January 2016
10.1126/science.aad7969

AUTOIMMUNITY

Pathogenic CD4 T cells in type 1 diabetes recognize epitopes formed by peptide fusion

Thomas Delong,[1]* Timothy A. Wiles,[1] Rocky L. Baker,[1] Brenda Bradley,[1] Gene Barbour,[1] Richard Reisdorph,[2] Michael Armstrong,[2] Roger L. Powell,[2] Nichole Reisdorph,[2] Nitesh Kumar,[3] Colleen M. Elso,[3] Megan DeNicola,[4] Rita Bottino,[5] Alvin C. Powers,[6,7] David M. Harlan,[4] Sally C. Kent,[4] Stuart I. Mannering,[3,8] Kathryn Haskins[1]*

T cell–mediated destruction of insulin-producing β cells in the pancreas causes type 1 diabetes (T1D). CD4 T cell responses play a central role in β cell destruction, but the identity of the epitopes recognized by pathogenic CD4 T cells remains unknown. We found that diabetes-inducing CD4 T cell clones isolated from nonobese diabetic mice recognize epitopes formed by covalent cross-linking of proinsulin peptides to other peptides present in β cell secretory granules. These hybrid insulin peptides (HIPs) are antigenic for CD4 T cells and can be detected by mass spectrometry in β cells. CD4 T cells from the residual pancreatic islets of two organ donors who had T1D also recognize HIPs. Autoreactive T cells targeting hybrid peptides may explain how immune tolerance is broken in T1D.

Type 1 diabetes (T1D) is an autoimmune disease mediated by T cells responding to self-antigens in the pancreatic β cell. Studies in the widely used nonobese diabetic (NOD) mouse model of T1D have shown that CD4 T cell responses to several β cell proteins, especially (pro)insulin, likely contribute to diabetes. It is, however, unclear how pathogenic T cells escape thymic deletion and how (pro)insulin becomes a target of the autoimmune T cell response. To address these questions, we have used our panel of NOD-derived, diabetogenic CD4 T cell clones (including the well-known BDC-2.5 clone) (*1*), in conjunction with proteomic analysis of β cell extracts, to identify T cell target antigens. Recently, we reported two new autoantigens for CD4 T cells in autoimmune diabetes: chromogranin A (ChgA) (*2*) and islet amyloid polypeptide (IAPP) (*3*). Like insulin, ChgA and IAPP are β cell prohormonal secretory granule proteins. WE14, a naturally occurring peptide cleavage product of ChgA, was found to be antigenic in both the NOD mouse (*2*) and in T1D patients (*4*). However, because this peptide only stimulates T cells weakly, we hypothesized that the natural ligand for pathogenic CD4 T cells may be a modified form of ChgA.

Posttranslational modification is a well-established property of antigens in many autoimmune diseases (*5*). A notable exception is T1D in which the investigation of modified peptides as antigenic epitopes has only just begun (*6*–*9*). Using mass spectrometric analysis, we verified the presence of the peptide WE14 in chromatographic fractions of mouse β cell extracts, but the peptide distribution over individual fractions did not follow the antigen distribution of the natural ligand recognized by WE14-responsive T cell clones, including BDC-2.5 (fig. S1A, top). Conversely, the propeptide region (C-peptide) from mouse proinsulin (fig. S1A, bottom) did follow the antigen distribution profile. Furthermore, a broad panel of shorter C-peptide fragments could also be identified in peak antigenic fractions (fig. S1B). The matching antigen–C-peptide distributions suggested that a C-peptide fragment is a component of the natural T cell ligand. The proposed WE14/I-Ag7 binding register (*2*), in which the peptide WE14 fills only half of the major histocompatibility complex (MHC) II binding groove (positions 5 to 9), leaves MHC II positions 1 to 4 unoccupied. The C-peptide fragments could fill these unoccupied positions, which would lead to increased peptide-MHC binding affinity and provide additional residues for improved TCR recognition. We hypothesized that C-terminal carbonyl groups of C-peptide fragments form covalent bonds with N-terminal amino groups of naturally occurring peptides, such as WE14, which results in the formation of hybrid insulin peptides (HIPs).

To investigate the possibility that BDC-2.5 and additional diabetogenic T cell clones from our panel are activated by HIPs, we used a chemical cross-linking strategy (fig. S2) to synthesize a HIP library for screening of our murine CD4 T cell clones (Fig. 1A). The peptides in the library consist of insulin sequences (left peptides) on the N-terminal side, covalently linked to peptide sequences from other secretory granule proteins (right peptides) on the C-terminal side. As left peptides, we selected C-terminal sequences derived from proinsulin C-peptide and insulin B-chain fragments that were identified through mass spectrometry in high abundance in antigenic β cell fractions (tables S1 and S2). As right peptides, we used N-terminal sequences from the ChgA peptide WE14 and the three natural cleavage products (*10*) of IAPP (amylin, IAPP1, and IAPP2). As shown in Fig. 1A, the hybrid peptide LQTLAL-WSRMD, containing the C-peptide sequence LQTLAL on the left and the WE14 sequence WSRMD on the right, activates all three WE14-reactive clones (BDC-2.5, BDC-10.1, and BDC-9.46), each of which expresses a distinct T cell receptor (TCR). To further test our hypothesis, we screened the peptide library with a second subset of T cell clones (BDC-6.9 and BDC-9.3) sharing the same TCR. We identified a single HIP sequence (LQTLAL-NAARD) recognized by both BDC-6.9 and BDC-9.3 (Fig. 1A). This peptide contains, on the left, the same C-peptide sequence LQTLAL present in the HIP recognized by the WE14-reactive T cell clones and, on the right, the IAPP propeptide 2 (IAPP2) sequence NAARD. We concluded that the endogenous ligands for the two sets of pathogenic T cell clones are HIPs containing the C-peptide sequence LQTLAL on the left side and the natural cleavage products, WE14 or IAPP2, on the right side.

To confirm the antigenicity of the peptides identified from the library, we obtained commercially synthesized preparations of 2.5 and 6.9HIPs (HIPs antigenic for BDC-2.5 and BDC-6.9) spanning the full-length insulin II (Ins2) C-peptide fragment ending in LQTLAL on the N-terminal ends and the entire WE14 or IAPP2 sequences on the C-terminal ends (see peptide section in Materials and Methods). WE14-reactive T cell clones such as BDC-2.5 recognize the 2.5HIP at low nanomolar concentrations, whereas unmodified WE14 is poorly antigenic for these clones (*2*), which mandates high peptide concentrations (>10 μM) for T cell activation (Fig. 1B); hence, the HIP was >10,000 times as potent as a stimulator for BDC-2.5 than WE14. The T cell clones BDC-6.9 and BDC-9.3 recognize the 6.9HIP, also at low nanomolar concentrations (Fig. 1, C and D). BDC-6.9 and BDC-9.3 do not react to the unmodified IAPP2 peptide, and none of the clones respond to the full-length Ins2 C-peptide or the C-peptide fragment ending with the amino acid sequence LQTLAL. T cell reactivity with WE14 or IAPP2 was not altered if these peptides were coincubated (without cross-linking) with the C-peptide fragment ending in LQTLAL, which indicated that the covalent attachment of the peptides is required to obtain full T cell activation.

To validate the in vivo presence of HIPs in β cells, we fractionated murine β cell extracts by reversed-phase high-performance liquid chromatography (RP-HPLC) and performed mass spectrometric (MS) analyses on antigenic fractions. The T cell clone BDC-2.5 responded to two chromatographic regions, which indicated that at least

[1]Department of Immunology and Microbiology, University of Colorado School of Medicine, Denver, Anschutz Medical Campus, Aurora, CO 80045, USA. [2]Pharmaceutical Sciences, University of Colorado School of Medicine, Aurora, CO 80045, USA. [3]Immunology and Diabetes Unit, St. Vincent's Institute of Medical Research, 9 Princes Street, Fitzroy, Victoria 3065, Australia. [4]Department of Medicine, Diabetes Division, Diabetes Center of Excellence, University of Massachusetts Medical School, Worcester, MA, USA. [5]Institute of Cellular Therapeutics, Allegheny-Singer Research Institute, Allegheny Health Network, Pittsburgh, PA, USA. [6]Division of Diabetes, Endocrinology, and Metabolism, Department of Medicine, and Department of Molecular Physiology and Biophysics, Vanderbilt University Medical Center, Nashville, TN, USA. [7]VA Tennessee Valley Healthcare System, Nashville, TN, USA. [8]University of Melbourne, Department of Medicine, St. Vincent's Hospital, Fitzroy, Victoria 3065, Australia.
*Corresponding author. E-mail: thomas.delong@ucdenver.edu (T.D.); katie.haskins@ucdenver.edu (K.H.)

Downloaded from on February 11, 2016

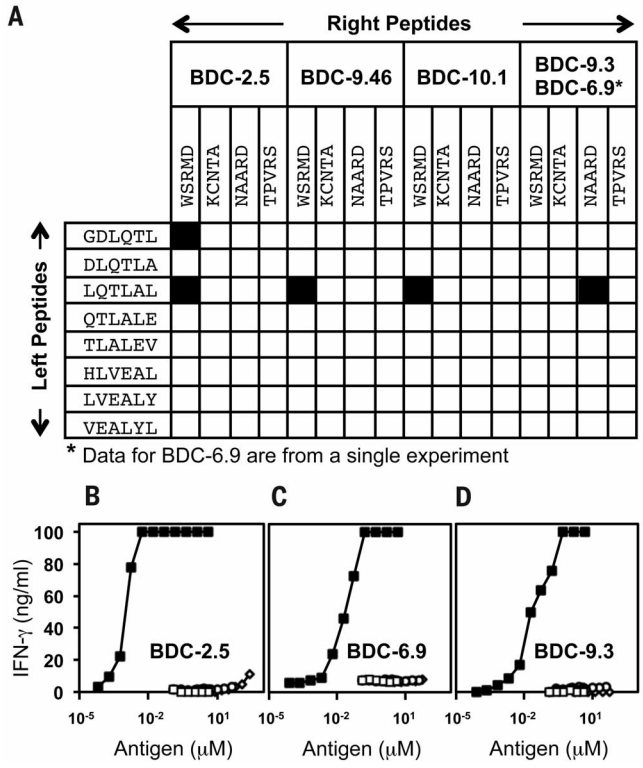

Fig. 1. Identification of HIP sequences that are recognized by pathogenic T cell clones. (**A**) A library of 32 HIPs was synthesized. Left peptides are C-terminal amino acid sequences of various mouse insulin C-peptide and B-chainfragments. Right peptides reflect the N-terminal amino acid sequences of mouse WE14 (WSRMD), IAPP1 (TPVRS), amylin (KCNTA), and IAPP2 (NAARD). T cell clones BDC-2.5, BDC-9.46, BDC-10.1, BDC-9.3, and BDC-6.9 were used to screen the peptide library. Black squares indicate positive T cell responses measured through production of interferon-γ (IFN-γ) to individual HIPs. Data shown are representative of three independently replicated experiments. (**B**) To confirm antigenicity of HIPs, pure peptides (>95%) were obtained commercially for assay with the T cell clones. Response of WE14-reactive clone BDC-2.5 to 2.5HIP (solid squares) compared with unmodified WE14 (open diamonds), Ins2 C-peptide (open circles), or the Ins2 C-peptide fragment ending with the amino acid sequence DLQTLAL (solid circles). (**C** and **D**) Response of IAPP-reactive clones, BDC-6.9 (C) and BDC-9.3 (D), to the 6.9HIP (solid squares) compared with IAPP2 alone (open diamonds), Ins2 C-peptide (open circles), or the Ins2 C-peptide fragment (solid circles). Data are representative of at least three separate experiments.

two distinct ligands (left and right peak) exist for this T cell clone (Fig. 2A). After proteolytic digestion and tandem MS (MS/MS) analysis of the left antigen peak (Fig. 2A), we identified the peptide DLQTLAL-WSRM (Fig. 2B and fig. S3). This spectrum provides physical evidence verifying the presence of the 2.5HIP in murine β cells. We have not identified a HIP in the antigen peak on the right, possibly because of limited instrumental sensitivity, poor peptide ionization, or the presence of yet another unknown HIP sequence. Purification of the endogenous ligand recognized by BDC-6.9 and BDC-9.3 (fig. S4A), followed by MS analysis, led to the identification of the corresponding 6.9HIP sequence DLQTLAL-NAAR (fig. S4, B and C). Both the 2.5HIP and the 6.9HIP contain the C-peptide fragment ending with the amino acid sequence DLQTLAL, a naturally occurring cleavage product of insulin C-peptide formed within the secretory granules of β cells (*11*). This fragment may thus provide a preferred ligation site for the formation of HIPs, but additional insulin ligation sites may also exist.

Identifying the autoreactive T cells involved in the pathogenic process is a major objective for T1D research, and achieving this goal may enable us to monitor the disease process and devise antigen-specific methods to prevent and/or reverse disease. MHC class II tetramer reagents can be used to specifically identify pathogenic T cells (*12*). To determine whether HIP-reactive T cells could be identified in diabetic NOD mice, we designed a peptide:MHC class II (I-Ag7) tetramer containing the HIP sequence antigenic for BDC-2.5; specificity of the 2.5HIP tetramer was demonstrated through staining of the three

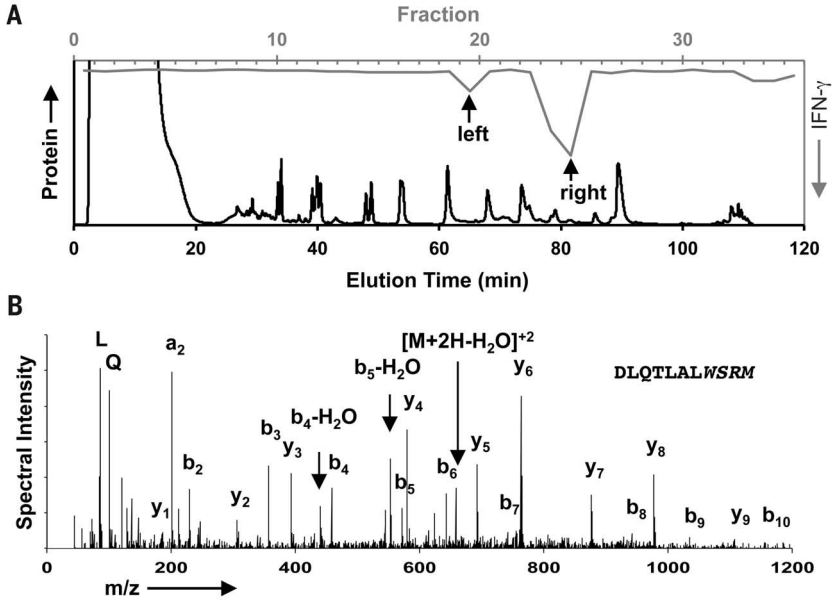

Fig. 2. Identification of HIPs in antigenic β cell fractions. (**A**) Size-exclusion chromatography fractions highly enriched for antigen were further fractionated by RP-HPLC (black line). IFN-γ production by T cells in response to individual fractions is shown for BDC-2.5 (gray line). (**B**) After proteolytic digestion with the endoproteinase AspN (which releases the core amino acid sequence of the hybrid peptide), the targeted MS/MS analysis of antigen-containing fractions reveals the spectrum of the HIP that contains the C-peptide amino acid sequence DLQTLAL and the WE14 sequence WSRM.

2.5HIP-reactive CD4 T cell clones (fig. S5A). To examine the presence of HIP-reactive T cells in NOD mice, cell suspensions from spleens, pancreatic lymph nodes (pLNs), and pancreata of diabetic NOD mice were stained with the 2.5HIP tetramer (Fig. 3 and fig. S5B). Two additional tetramers, pS3 and 2.5mi, containing peptide mimotope sequences recognized by BDC-2.5 (*2*, *13*), were used as positive controls. We found that 2.5HIP tetramer–positive cells were present in

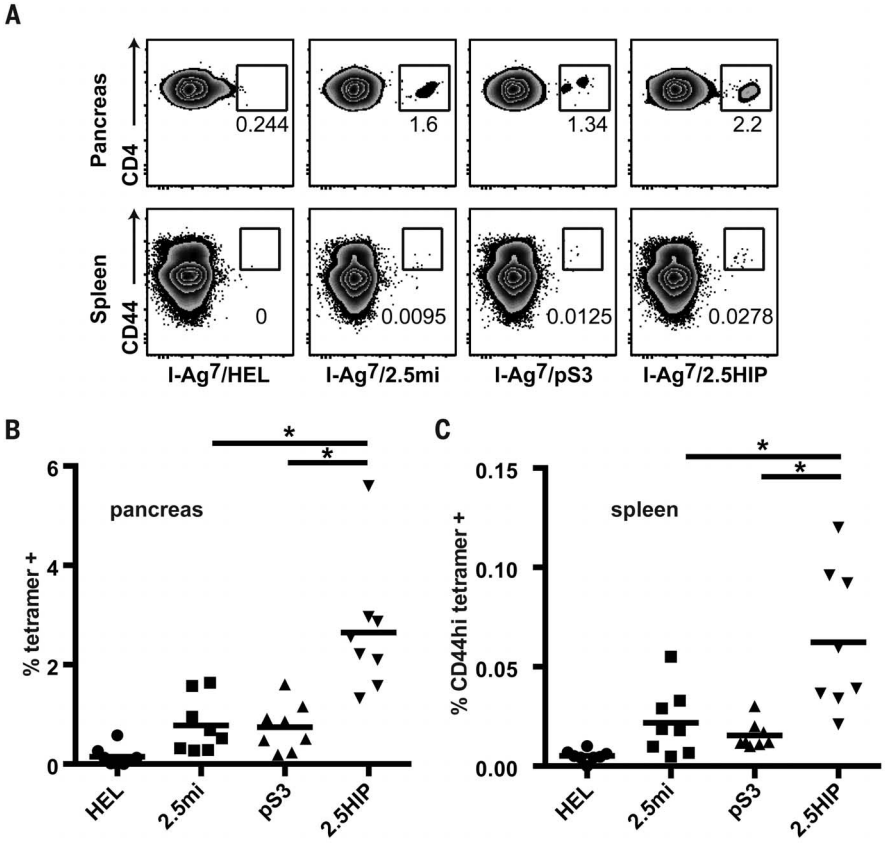

Fig. 3. Tetramer analysis of pancreas and spleen of diabetic NOD mice. Single-cell suspensions were prepared from pancreas and spleen of diabetic NOD female mice (n = 8) and stained with tetramers, antibodies, and a dead cell marker (7AAD). Gates were set on a lymphocyte gate and $CD45^+$, $CD4^+$, Lin^- cells. (**A**) Tetramer staining in the pancreas and the spleen of a representative mouse. (**B**) Summary of $CD4^+$ tetramer–positive cells present in the pancreas. (**C**) Summary of $CD4^+CD44^{hi}$ tetramer–positive cells present in the spleen. Each symbol represents a different mouse. Averages are indicated as a black horizontal bar. Data are from four independent experiments and were analyzed by two-tailed unpaired t test. Statistical significance * was defined at a $^*P < 0.05$.

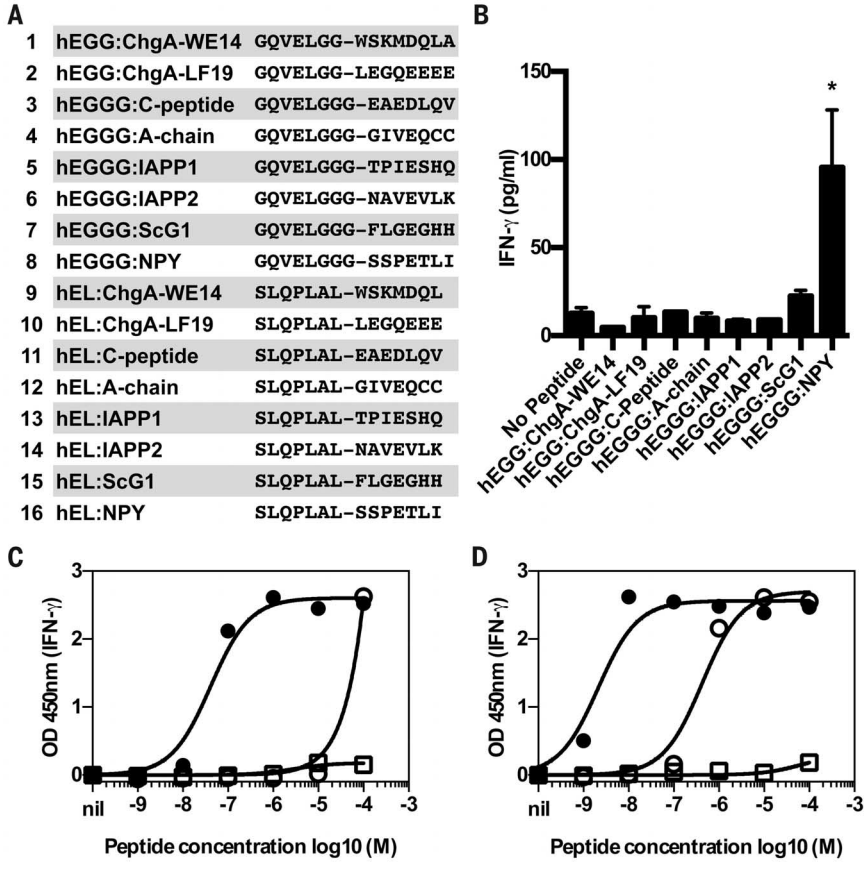

Fig. 4. Human islet-infiltrating T cells respond to HIPs. (**A**) List of HIPs (>95% purity) screened. (**B**) A CD4 T cell line grown from isolated islets of a 20-year-old male with 7 years of T1D (DR17, DR4, DQ2, and DQ8) secreted IFN-γ when a HIP, formed by the fusion of proinsulin C-peptide to the pancreatic polypeptide, neuropeptide Y (GQVELGGG-SSPETLI), was presented by Priess B cells ($DR4^{+/+}$, $DQ8^{+/+}$); all peptides at 20 μg/ml. $^*P$ = 0.0395 as compared with the media control (paired Student's t test). The mean and standard deviation of triplicates is shown. (**C** and **D**) CD4 T cell clones A3.10 (C) and A2.11 (D) were isolated from islets of a 19-year-old male with 3 years of T1D and were incubated overnight with the indicated concentration of peptide and HLA-$DQ2^+$, $DQ8^+$ Epstein-Barr virus–transformed B cell line. Responses to peptide were detected by IFN-γ secretion measured by enzyme-linked immunosorbent assay (ELISA). OD, optical density. Solid circles are the HIP (GQVELGGG-NAVEVLK), open circles are proinsulin 37 to 54 (LQVELGGG-PGAGSLQ), and open squares are another HIP incorporating the same region of IAPP2 (SLQPLAL-NAVEVLK). For (C) and (D), one representative of at least two independent experiments is shown. Clone A3.10 and A2.11 (fig. S6) recognize HIPs presented by HLA-DQ8.

both the spleen and pancreas of NOD mice. In both tissues, the 2.5HIP tetramer stained a higher percentage of CD4 T cells compared with the 2.5mi and the pS3 tetramers, a difference that was statistically significant in the pancreas and that indicated that the 2.5HIP tetramer is more efficient in the detection of 2.5HIP-reactive CD4 T cells. Our data show that most of the 2.5HIP tetramer–positive cells in the spleen were CD44 high, which indicated that a significant proportion of these cells were antigen-experienced and further substantiated their involvement in the pathogenic process.

To determine whether human CD4 T cells of individuals with T1D recognize HIPs, we screened a selection of HIPs (Fig. 4A) using CD4 T cells isolated from the residual islets of two patients. Corresponding human sequences of naturally occurring peptides found in mouse β cell extracts formed the right portion of the HIPs. The central C-peptide amino acid sequences ELGG or ELGGG, which form the left half of HIPs 1 to 8, satisfy parameters for binding to DQ8 positions 1 and 4 (*14*). Risk of developing T1D is strongly associated with human leukocyte antigen (HLA) alleles, and HLA-DQ8 confers the highest risk of developing T1D of any single HLA allele (*15*). For the left sides of HIPs 9 to 16, we used the human version (SLQPLAL) of the murine peptide sequence present in the 2.5 and 6.9HIPs. From one organ donor, 17 CD4 T cell lines were isolated from residual islets, expanded, and tested for reactivity against eight of the HIPs (Fig. 4A, peptides 1 to 8) with Priess B cells ($DR4^{+/+}$,$DQ8^{+/+}$) as presenters. The CD4 line MG1 responded to the HIP formed by fusion of proinsulin C-peptide to the pancreatic peptide, neuropeptide Y (GQVELGGG-SSPETLI) (Fig. 4B). Using CD4 T cell clones isolated from a second organ donor (*16*), we screened all 16 HIPs (Fig. 4A). Two clones responded to the same HIP that was formed by the fusion of proinsulin C-peptide to IAPP2 (GQVELGGG-NAVEVLK) (Fig. 4, C and D). Both clones responded weakly to proinsulin C-peptide (proinsulin 37–54), but the HIP was 1000 to 10,000 times as potent. Both clones recognized HIP peptides presented by HLA-DQ8 (DQA1*03:01; DQB1*03:02) (fig. S6). Although pathogenicity of human T cells cannot be directly demonstrated, the presence of HIP-specific CD4 T cells within the pancreatic islets of individuals with T1D supports the contention that these cells play a pathogenic role in human T1D.

HIPs represent not only a novel posttranslational modification in autoimmune disease, but they also constitute a new family of autoantigens in T1D. Hybrid peptides that form through protein splicing have been previously noted in tumor antigen formation, a process that occurs through the proteosomal class I pathway and yields antigens for CD8 T cells (*17*–*19*). The formation of HIPs in the secretory granules of β cells could be a side reaction of the proteolytic hydrolysis of peptide bonds in the presence of naturally occurring cleavage products (e.g., WE14), and molecular crowding of peptides in secretory granules may favor this reversed proteolytic transpeptidation (*20*). The identification of HIP-reactive CD4 T cells from the islets of individuals with T1D, together with the demonstration that several distinct pathogenic CD4 T cells from NOD mice target different HIPs in β cells, strongly suggests that HIPs play a central role in the pathogenesis of T1D. We hypothesize that HIPs are key antigens for autoreactive T cells and are responsible for the loss of self-tolerance in human T1D. We would also speculate that hybrid peptides may form in the secretory granules of other endocrine tissues and could be a source of self-antigens in other autoimmune disorders.

REFERENCES AND NOTES

1. K. Haskins, *Adv. Immunol.* **87**, 123–162 (2005).
2. B. D. Stadinski *et al.*, *Nat. Immunol.* **11**, 225–231 (2010).
3. T. Delong *et al.*, *Diabetes* **60**, 2325–2330 (2011).
4. P. A. Gottlieb *et al.*, *J. Autoimmun.* **50**, 38–41 (2014).
5. H. A. Doyle, M. J. Mamula, *Curr. Opin. Immunol.* **24**, 112–118 (2012).
6. S. I. Mannering *et al.*, *J. Exp. Med.* **202**, 1191–1197 (2005).
7. T. Delong *et al.*, *Diabetes* **61**, 3239–3246 (2012).
8. M. van Lummel *et al.*, *Diabetes* **63**, 237–247 (2014).
9. J. W. McGinty *et al.*, *Diabetes* **63**, 3033–3040 (2014).
10. C. E. Higham *et al.*, *Eur. J. Biochem.* **267**, 4998–5004 (2000).
11. C. B. Verchere *et al.*, *J. Biol. Chem.* **271**, 27475–27481 (1996).
12. G. T. Nepom, *J. Immunol.* **188**, 2477–2482 (2012).
13. T. Stratmann *et al.*, *J. Clin. Invest.* **112**, 902–914 (2003).
14. K. Y. Chang, E. R. Unanue, *Int. Immunol.* **21**, 705–713 (2009).
15. J. A. Todd, J. I. Bell, H. O. McDevitt, *Nature* **329**, 599–604 (1987).
16. V. Pathiraja *et al.*, *Diabetes* **64**, 172–182 (2015).
17. E. H. Warren *et al.*, *Science* **313**, 1444–1447 (2006).
18. K. Hanada, J. W. Yewdell, J. C. Yang, *Nature* **427**, 252–256 (2004).
19. N. Vigneron *et al.*, *Science* **304**, 587–590 (2004).
20. B. R. Somalinga, R. P. Roy, *J. Biol. Chem.* **277**, 43253–43261 (2002).

ACKNOWLEDGMENTS

The following funding sources supported this research: NIH grant 1K01DK094941 (T.D.); American Diabetes Association Pathway to Stop Diabetes Grant 1-15-ACE-14 (T.D.); American Diabetes Association grant 1-15-JF-04 (R.L.B.); NIH grant 1R01DK081166 (K.H.); the Australian National Health and Medical Research Council (NHMRC) APP1061961 (S.M.); Juvenile Diabetes Research Foundation, Career Development Award 5-CDA2014210-A-N (S.M.); Operational Infrastructure Support Program from the Victorian State Government of Australia (S.M.); Helmsley Charitable Trust 2015PG-T1D057 (S.C.K.); Juvenile Diabetes Research Foundation grant 2-SRA-2015-68-Q-R (A.C.P., D.M.H.); NIH grant 5U01DK89572 (A.C.P., D.M.H.); NIH grant DK104211 (A.C.P). We thank the NIH tetramer core for providing tetramer reagents. A patent application related to the work on the hybrid peptides has been filed (Colorado University Technology Transfer Office file no. CU3769H-PPA1, Compositions and methods for diagnosing autoimmune diseases; T.D. and K.H. as inventors). The data presented in this manuscript are tabulated in the main paper and in the supplementary materials section.

SUPPLEMENTARY MATERIALS

www.sciencemag.org/content/351/6274/711/suppl/DC1
Materials and Methods
Figs. S1 to S6
Tables S1 and S2
References (*21*–*26*)

21 August 2015; accepted 8 January 2016
10.1126/science.aad2791

Downloaded from on February 11, 2016

IMMUNOLOGY

Broadly targeted $CD8^+$ T cell responses restricted by major histocompatibility complex E

Scott G. Hansen,[1]* Helen L. Wu,[1]* Benjamin J. Burwitz,[1] Colette M. Hughes,[1] Katherine B. Hammond,[1] Abigail B. Ventura,[1] Jason S. Reed,[1] Roxanne M. Gilbride,[1] Emily Ainslie,[1] David W. Morrow,[1] Julia C. Ford,[1] Andrea N. Selseth,[1] Reesab Pathak,[1] Daniel Malouli,[1] Alfred W. Legasse,[1] Michael K. Axthelm,[1] Jay A. Nelson,[1] Geraldine M. Gillespie,[2] Lucy C. Walters,[2] Simon Brackenridge,[2] Hannah R. Sharpe,[2] César A. López,[3] Klaus Früh,[1] Bette T. Korber,[3,4] Andrew J. McMichael,[2] S. Gnanakaran,[3] Jonah B. Sacha,[1]† Louis J. Picker[1]†

Major histocompatibility complex E (MHC-E) is a highly conserved, ubiquitously expressed, nonclassical MHC class Ib molecule with limited polymorphism that is primarily involved in the regulation of natural killer (NK) cells. We found that vaccinating rhesus macaques with rhesus cytomegalovirus vectors in which genes *Rh157.5* and *Rh157.4* are deleted results in MHC-E–restricted presentation of highly varied peptide epitopes to $CD8\alpha\beta^+$ T cells, at ~4 distinct epitopes per 100 amino acids in all tested antigens. Computational structural analysis revealed that MHC-E provides heterogeneous chemical environments for diverse side-chain interactions within a stable, open binding groove. Because MHC-E is up-regulated to evade NK cell activity in cells infected with HIV, simian immunodeficiency virus, and other persistent viruses, MHC-E–restricted $CD8^+$ T cell responses have the potential to exploit pathogen immune-evasion adaptations, a capability that might endow these unconventional responses with superior efficacy.

Adaptive cellular immunity against intracellular pathogens is the primary responsibility of $CD8^+$ T cells that recognize short pathogen-derived peptide epitopes presented by highly polymorphic major histocompatibility complex class Ia (MHC-Ia) molecules on the surface of infected cells (*1*, *2*). MHC-Ia allomorphs vary considerably in their peptide-binding properties, and therefore the particular pathogen-derived peptides targeted by pathogen-

specific CD8$^+$ T cells are largely determined by the peptide-binding specificity of the limited number of MHC-Ia allomorphs expressed by the infected individual (*3*). Consequently, the epitopes recognized by CD8$^+$ T cells responding to the same pathogen are highly diverse across individuals, resulting in heterogeneity among individuals in the ability to clear or control various infections—in particular, agents such as HIV with a high intrinsic capacity for mutational immune escape (*2*, *4*). Such variation can hamper efforts to develop universally effective vaccines based on CD8$^+$ T cell responses (*4*, *5*).

We recently reported that simian immunodeficiency virus (SIV)–targeted vaccine vectors based on rhesus cytomegalovirus (RhCMV) strain 68-1 [in which genes *Rh157.5* and *Rh157.4* are deleted (ΔRh157.5/.4)] violate the rules of MHC-Ia–restricted CD8$^+$ T cell recognition (*6*) and offer a potential solution to MHC-Ia–dependent response diversity in vaccination targeted at CD8$^+$ T cells. Cellular immune responses elicited by RhCMV/SIV vectors are able to stringently control and ultimately clear a highly pathogenic SIV challenge in slightly over half of vaccinated rhesus macaques (RMs) (*7*, *8*). These vectors elicit SIV-specific CD8$^+$ T cell responses that are entirely nonoverlapping with conventional MHC-Ia–restricted CD8$^+$ T cells, despite manifesting three times the breadth of CD8$^+$ T cells elicited by conventional vaccines. Part of this lack of epitope overlap has been explained by the finding that many of the epitopes are restricted by MHC-II, rather than MHC-I, molecules (*6*). However, a 68-1 RhCMV vector expressing SIV gag protein (SIVgag) also elicited CD8$^+$ T cells that recognized MHC-I–dependent epitopes that were common to most, or even all, MHC-disparate RMs, an unprecedented degree of cross-recognition for MHC-Ia–restricted CD8$^+$ T cell responses. Two SIVgag epitopes [SIVgag$_{276–284}$(69) and SIVgag$_{482–490}$(120)] were targeted by 42 of 42 RMs immunized with the 68-1 RhCMV/SIVgag vector in our previous study (*6*), and we have since documented these "supertope" responses in 130 of 130 RMs inoculated with this vector (fig. S1).

To understand the basis of this unusual MHC-I–dependent recognition, we selected four RMs vaccinated with the 68-1 RhCMV/SIVgag vector for detailed MHC-I restriction analysis. We first sequenced the expressed MHC-I genes, including both classical MHC-Ia and nonclassical MHC-Ib (*9*), in each RM, and constructed a panel of MHC-I transfectants that individually expressed these MHC-I molecules (fig. S2). These single–MHC-I–molecule transfectants were then used in a flow-cytometric intracellular cytokine staining (ICS) assay to present 12 commonly recognized 15-mer (15–amino acid oligomer) peptides to the CD8$^+$ T cells induced by the 68-1 RhCMV/SIVgag vector in these RMs (Fig. 1, A and B, and fig. S3). Classical MHC-Ia allomorph groups were able to present only 3 of the 12 epitopic peptides to these T cells [Mamu-A1*001:01, epitopes SIVgag$_{69–83}$(18) and SIVgag$_{197–211}$(50); Mamu-A1*002:01, epitope SIVgag$_{129–143}$(33)], and expression of these allomorphs in RMs did not track with these epitope-specific CD8$^+$ T cell responses (fig. S4). However, all 12 peptides stimulated epitope-specific CD8$^+$ T cells when presented by nonclassical major histocompatibility complex E (MHC-E) molecules, and all peptides were presented by transfectants singly expressing three different RM MHC-E allomorphs (Mamu-E*02:04, -E*02:11, and -E*02:20), as well as by a transfectant expressing human MHC-E (HLA-E*01:03; HLA, human leukocyte antigen) (Fig. 1, A and B, and figs. S3 and S5).

MHC-E is known to avidly bind canonical VMAPRTL(LVI)L peptides, which are derived from positions 3 to 11 of MHC-Ia leader sequences, for presentation to NKG2A/C receptor molecules on natural killer (NK) cells (*10*–*14*). This conserved interaction predominantly inhibits NK cell activity when cells express normal levels of MHC-Ia. However, on interference with MHC-Ia biosynthesis by viral infection or neoplastic transformation, this inhibitory signal is reduced, facilitating NK cell responses to virally infected or neoplastic cells (*15*, *16*). Although a subset of CD8$^+$ T cells can express NKG2A/C (*17*), phenotypic analysis of MHC-E–dependent CD8$^+$ T cells elicited by the 68-1 RhCMV/SIVgag vector revealed that the vast majority of responding cells were CD8αβ$^+$, TCRγ/δ$^-$ T cells lacking NKG2A/C expression (fig. S6). Moreover, preincubation of MHC-E transfectants or other antigen-presenting cells with the canonical MHC-E–binding VMAPRTLLL (VL9) peptide before epitopic peptide loading specifically blocked CD8$^+$ T cell recognition of all 12 epitopic peptides (fig. S7). The epitopic SIVgag 15-mers could be truncated to optimal 9-mer peptides that were common among different 68-1 RhCMV/SIVgag vector–vaccinated RMs with MHC-E-associated CD8$^+$ T cell responses to the parent 15-mer (fig. S8) (*6*). These optimal 9-mer peptides could trigger CD8$^+$ T cells when pulsed on MHC-E transfectants (both Mamu-E and HLA-E) or autologous B cell lines at doses of ≤1 nM (Fig. 1C and fig. S9); such functional avidities are comparable to T cell recognition of classically MHC-Ia–restricted epitopes (*18*). Taken together, these data strongly suggest that the unconventional, MHC-I-dependent CD8$^+$ T cell responses elicited by the 68-1 RhCMV/SIVgag vector reflect SIVgag 9-mer epitope–specific, MHC-E–restricted CD8αβ$^+$ T cells.

MHC-E–restricted CD8$^+$ T cell responses previously have been identified in human cytomegalovirus (HCMV), hepatitis C virus, *Mycobacterium tuberculosis* (*M. tb.*), and *Salmonella enterica* infections, typically involving epitopes that are structurally related to the canonical MHC-Ia leader-sequence peptides but foreign to the host (*13*, *14*, *19*, *20*). To determine the extent to which MHC-E restricts RM CD8$^+$ T cell responses in different settings, we applied blocking with high-affinity MHC-E–binding peptide VL9 [in conjunction with blocking with the MHC-II–associated invariant chain peptide (CLIP) and the MHC-I monoclonal antibody (mAb) W6/32 (*6*)] to restriction-classify all SIVgag epitope–specific CD8$^+$ T cell responses in RMs vaccinated with the 68-1 RhCMV/SIVgag vector (ΔRh157.5/.4), a strain 68-1.2 RhCMV/SIVgag vector (*Rh157.5* and *Rh157.4* repaired), a 68-1.2 RhCMV/SIVgag vector from which the *Rh157.5* and *Rh157.4* genes were specifically reexcised (fig. S10), and a modified vaccinia Ankara (MVA)/SIVgag vector, as well as RMs infected with SIV itself (Fig. 2A and figs. S11 and S12). This analysis revealed that essentially all SIVgag epitope–specific CD8$^+$ T cells in RMs vaccinated with the 68-1 RhCMV/SIVgag or ΔRh157.5/.4 68-1.2 RhCMV/SIVgag vectors were either MHC-II– or MHC-E–restricted. In contrast, 98 to 100% of SIVgag-specific CD8$^+$ T cell responses in the RMs vaccinated with the MVA/SIVgag or 68-1.2 RhCMV/SIVgag vectors, or infected with SIV, were classically MHC-Ia–restricted. In keeping with these patterns of epitope restriction, recognition of autologous SIV-infected CD4$^+$ T cells by the SIVgag-specific CD8$^+$ T cells elicited by the 68-1 RhCMV/SIVgag vector was completely blocked by a combination of the MHC-II–blocking CLIP and the MHC-E–blocking VL9 peptides; however, SIV-infected autologous cell recognition by the SIVgag-specific CD8$^+$ T cells elicited by MVA/SIVgag vector vaccination, 68-1.2 RhCMV/SIVgag vector vaccination, or SIV infection was insensitive to the CLIP-plus-VL9 peptide combination (Fig. 2B). In addition, the VL9 peptide alone completely blocked SIV-infected cell recognition by a MHC-E–restricted SIVgag$_{482–490}$ (120)–specific CD8$^+$ T cell line (fig. S14).

Taken together, these data confirm that the 68-1 RhCMV/SIVgag vector elicits SIVgag-specific CD8$^+$ T cell responses that are either MHC-II– or MHC-E–restricted, and that this unusual immunobiology is a specific consequence of the deletion of the RhCMV *Rh157.5* and *Rh157.4* genes, which are orthologs of the HCMV *UL128* and *UL130* genes and encode two components of the pentameric receptor complex involved in CMV infection of nonfibroblasts (*21*). Moreover, these data confirm that although SIV infection does not efficiently prime MHC-E–restricted CD8$^+$ T cell responses, at least some of the SIV epitopes recognized by the CD8$^+$ T cells elicited by the 68-1 RhCMV/SIVgag vector are naturally presented by SIV-infected cells, providing for their effective recognition by these heterologous responses.

Among 42 RMs vaccinated with the 68-1 RhCMV/SIVgag vector, we identified a median of 20 distinct CD8$^+$ T cell–recognized, MHC-E–restricted SIVgag 15-mer epitopes per RM, a breadth that exceeds the median 11 and 14.5 distinct MHC-Ia–restricted SIVgag-specific epitopes identified within SIVgag-specific CD8$^+$ T cell responses elicited by conventional vaccines or SIV infection, respectively (Fig. 3A). The ability of ΔRh157.5/.4 RhCMV vectors to elicit MHC-E– and MHC-II–restricted CD8$^+$ T cells is not limited to SIVgag-specific responses (fig. S13), and the density of MHC-E–restricted epitopes (~4 independent MHC-E–restricted epitopes per 100 amino acids

[1]Vaccine and Gene Therapy Institute and Oregon National Primate Research Center, Oregon Health & Science University, Beaverton, OR 97006, USA. [2]Nuffield Department of Medicine, University of Oxford, Oxford OX37FZ, UK. [3]Theoretical Biology and Biophysics Group, Los Alamos National Laboratory, Los Alamos, NM 87545, USA. [4]The New Mexico Consortium, Los Alamos, NM 87545, USA.
*These authors contributed equally to this work. **†Corresponding author. E-mail: sacha@ohsu.edu (J.B.S.); pickerl@ohsu.edu (L.J.P.)**

of protein length) is similar among all CD8$^+$ T cell responses elicited by 68-1 RhCMV vectors, regardless of the nature of the antigen analyzed (Fig. 3B). Among the same 42 RMs vaccinated with the 68-1 RhCMV/SIVgag vector, 109 of the 125 overlapping SIVgag 15-mer peptides (87%) were recognized by MHC-E–restricted CD8$^+$ T cells in at least one RM (Fig. 3C). Although MHC-E has been shown to bind a broader array of peptides than the canonical leader-sequence peptides (*14*, *22*), the extent of this epitope diversity and breadth is unexpected, especially given the limited polymorphism of MHC-E and the observation that all tested Mamu-E and HLA-E variants present all tested MHC-E–restricted epitopes (Fig. 1, B and C, and figs. S5 and S9). In keeping with this previously unrecognized MHC-E epitope diversity, sequence analysis of 11 optimal MHC-E–restricted SIVgag 9-mer epitopes showed only one epitope, the $Gag_{273–287}$(69) supertope, with a canonical MHC-E–binding motif (methionine at position 2, leucine at position 9), whereas the other 10 optimal epitopes not only lacked this motif but manifested no statistically significant overlap with previously characterized sets of MHC-E–bound peptides (Fig. 3, D and E, and fig. S15) (*22*). Statistical analysis of a larger group of 125 SIVgag 15-mer peptides also failed to show any enrichment for previously reported MHC-E–binding motifs (figs. S16 and S17). Despite this amino acid sequence diversity, 10 of the 11 immunologically defined optimal MHC-E–restricted SIVgag 9-mer epitopes were shown to physically associate with and stabilize MHC-E, either in an ELISA (enzyme-linked immunosorbent assay)–based HLA-E–plus–peptide refolding assay or in a single-chain MHC-E–peptide expression assay, or both (figs. S18 and S19).

These data suggest that the loading and binding of epitopic peptides to MHC-E must involve novel molecular mechanisms. To explore this possibility, we performed long–time scale, all-atom molecular dynamics simulations of canonical peptide bound and unbound forms of the solved structure of HLA-E*01:03 (*23*) in comparison with simulations of the classical HLA-Ia protein HLA-A*02:01, which overlaps with HLA-E in peptide-binding specificity (*22*). This analysis revealed that HLA-E*01:03, but not HLA-A*02:01, preserves a relatively rigid peptide binding groove that remains open even in the absence of canonical peptide during the simulation time scales (Fig. 4, A and B). Docking analysis further suggests that the 11 optimal MHC-E–restricted SIVgag epitopes described above can bind to both HLA-E*01:03 and Mamu-E*02:04 by adopting a similar backbone configuration as that of the canonical peptide VL9, with diverse side-chain rotamers being accommodated in the same buried positions (Fig. 4C and fig. S20). Further characterization using all-atom molecular dynamics simulations of HLA-E–peptide complexes revealed that the SIVgag epitopic peptides bind at slightly elevated positions in the binding groove relative to VL9, which mainly uses hydrophobic amino acid side-chain interactions to stabilize its deep positioning (Fig. 4D). Consequently, in agreement with

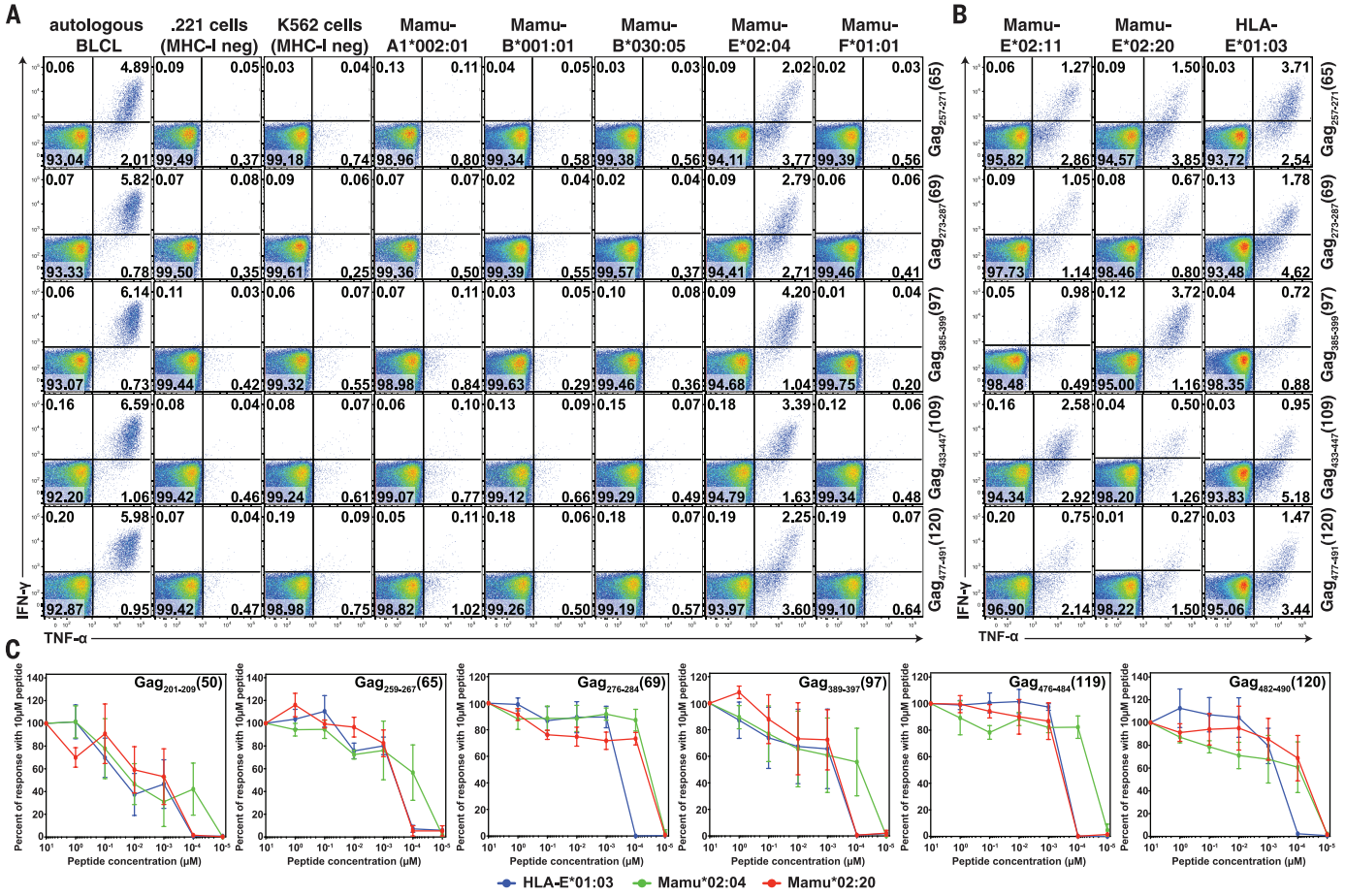

Fig. 1. MHC restriction of CD8$^+$ T cells elicited by 68-1 RhCMV/SIVgag. (**A** and **B**) Peripheral blood mononuclear cells (PBMCs) from a representative RM vaccinated with 68-1 RhCMV/SIVgag (RM Rh22034, one of four similarly analyzed; fig. S3) were stimulated with the indicated epitopic 15-mer peptides pulsed onto the surface of parental MHC-I–negative (neg) cell lines (.221 and K562 cells; negative controls), autologous B lymphoblastoid cell lines (BLCL; positive controls), or the indicated MHC-I transfectants, with CD8$^+$ T cell recognition determined by detection of interferon-γ (IFN-γ) and/or tumor necrosis factor–α (TNF-α) production by flow-cytometric ICS assay (response frequencies of gated CD8$^+$ T cells are shown in each quadrant). The MHC-I molecules tested included both those expressed by Rh22034 (A) and additional RM and human MHC-E molecules not expressed by Rh22034 (B). (**C**) Mamu-E*02:04, Mamu-E*02:20, and HLA-E*01:03 transfectants were pulsed with the serially diluted concentration of the indicated optimal SIVgag 9-mer epitopic peptides. The transfectants were combined with PBMCs from three to four 68-1 RhCMV/SIVgag–vaccinated RMs for flow-cytometric ICS determination of the frequency of responding CD8$^+$ T cells (IFN-γ– and/or TNF-α–positive). Response frequencies at each peptide dose were normalized to the response observed for the transfectant pulsed with the highest concentration (10 μM) of peptide.

direct MHC-E–peptide binding analysis (figs. S18 and S19), computationally determined binding affinities of the 11 optimal MHC-E–restricted SIVgag epitopes are lower than that of VL9 (fig. S21). However, at these elevated positions in the binding groove, epitopic peptides encounter a much more varied binding environment in terms of available polar or charged binding sites (Fig. 4E), and charged residues appear to contribute favorably to the binding of many of these peptides to MHC-E (figs. S22 and S23). Thus, in vivo conditions such as pH, ionic strength, and/or macromolecular crowding can modulate these interactions, possibly explaining some of the differences between in vitro and intracellular MHC-E–peptide binding measurements (figs. S18 and S19). There are limits to the peptide-binding breadth of MHC-E, because not all peptides can be accommodated by MHC-E in the same conformation as the canonical peptide (fig. S24). These structural analyses suggest that distinctive conformational properties of MHC-E may drive the observed epitope diversity and breadth. The open MHC-E binding groove would provide access to binding for an unusually diverse population of peptides, the side chains of which could interact with chemically varying environments at different depths within the binding groove. At the same time, the framework of the relatively rigid MHC-E binding groove would enforce a similar "canonical" backbone conformation on the

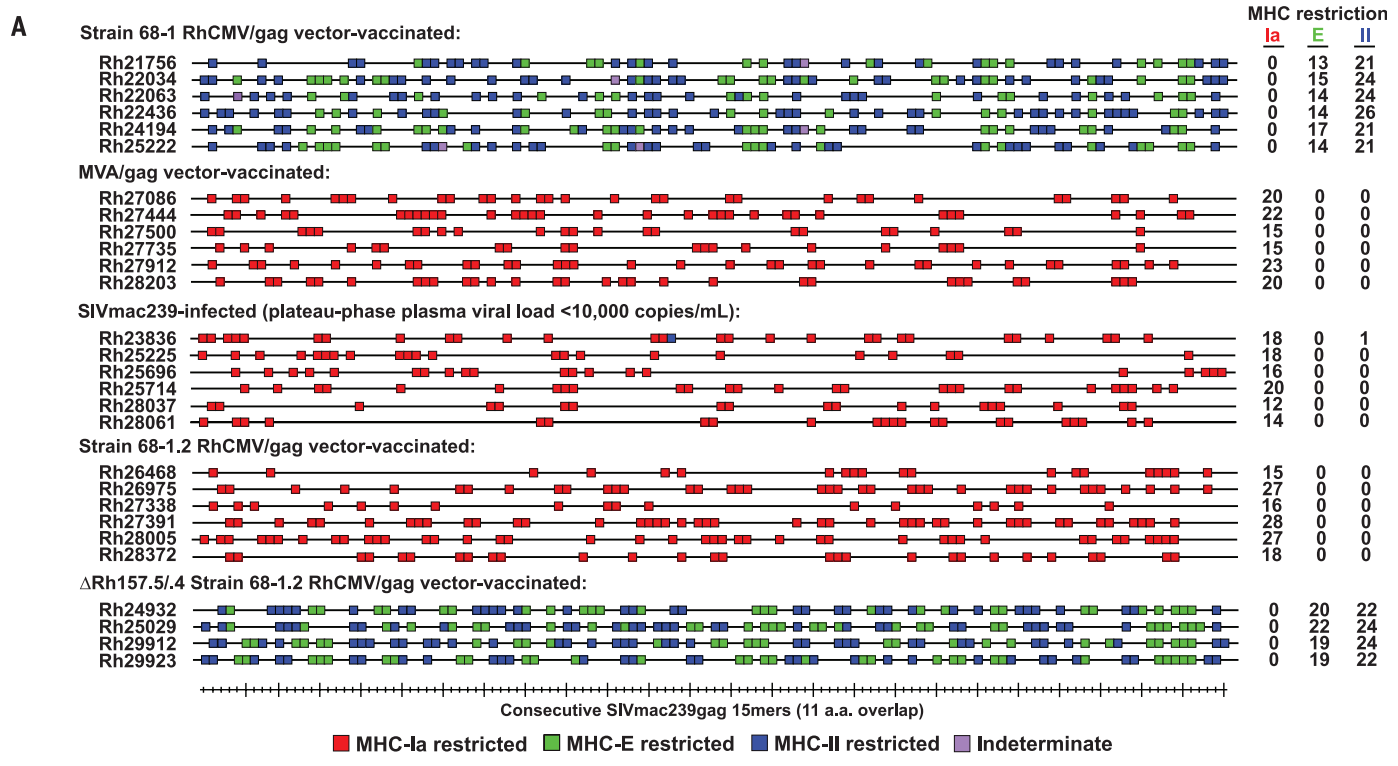

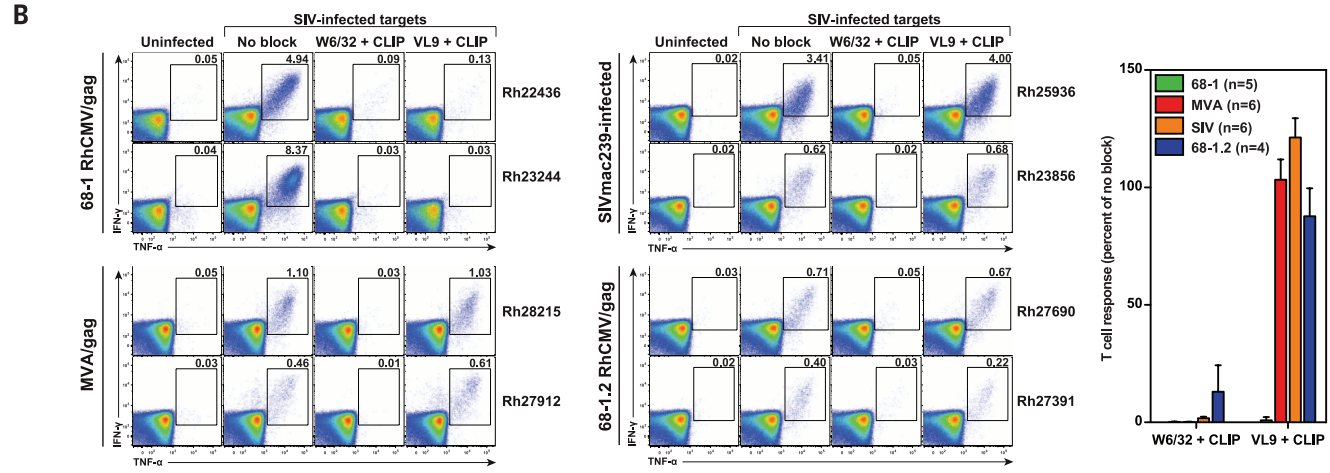

Fig. 2. MHC-E restriction is limited to CD8$^+$ T cell responses elicited by ΔRh157.5/.4 RhCMV vectors. (**A**) CD8$^+$ T cell responses to SIVgag were epitope-mapped using flow-cytometric ICS to detect recognition of 125 consecutive 15-mer SIVgag peptides [with an overlap of 11 amino acids (a.a.)] in RMs vaccinated with the indicated SIVgag-expressing viral vectors or infected with SIVmac239 (N = 4 to 6 per group shown; see fig. S12 for other studied RMs). Peptides resulting in specific CD8$^+$ T cell responses are indicated by a box, with the color of the box designating MHC restriction as determined by blocking with the pan–MHC-I–blocking mAb W6/32, the MHC-E–blocking peptide VL9, and the MHC-II–blocking peptide CLIP (see the supplementary materials). The minimal number of independent epitopes in these MHC restriction categories is shown at right for each RM. (**B**) Analysis of SIV-infected CD4$^+$ cell recognition by CD8β$^+$ cells isolated from RMs that were vaccinated with the indicated SIVgag-expressing viral vectors or infected with SIV. The flow profiles at left show IFN-γ and TNF-α production after CD8β$^+$ T cell incubation with autologous SIVmac239-infected CD4$^+$ T cells alone (no block), in the presence of mAb W6/32 plus CLIP, or in the presence of VL9 plus CLIP. All plots are gated on live CD3$^+$ CD8$^+$ cells. The bar graph at right shows the results from all studied RMs.

bound peptides, providing a stable MHC-E–peptide complex for T cell recognition.

Both HCMV and RhCMV encode proteins with a strategically embedded canonical VL9 peptide within the *UL40* and *Rh67* genes, respectively (*24*, *25*). The VL9 peptide of *UL40* has been shown to be loaded onto nascent MHC-E chains by a transporter associated with antigen processing (TAP)–independent mechanism, and it therefore functions to stabilize and up-regulate MHC-E expression in HCMV-infected cells in the face of virus-mediated TAP inhibition and the profound MHC-Ia down-regulation mediated by the HCMV *US2–11* gene products (*15*, *24*). We have demonstrated a similar function for RhCMV *Rh67* (fig. S25). MHC-E up-regulation is therefore thought to be a key viral strategy for evading the NK cell response to virally infected cells that lack MHC-Ia expression (*15*, *16*). However, this evasion strategy would have the consequence of enhancing MHC-E expression in such infected cells, increasing the opportunity for loading and presentation of novel peptides to MHC-E–restricted T cells. In this regard, the canonical MHC-E–binding VL9 peptide might act as a chaperone that facilitates stable high expression of MHC-E and delivery to an endosomal compartment (*26*) that would facilitate peptide exchange, analogous to the invariant chain–associated CLIP peptide and MHC-II (*1*). The rigid open structure of the MHC-E peptide-binding groove would be expected to facilitate peptide exchange, consistent with this putative mechanism. Also, consistent with such a peptide exchange mechanism, MHC-E peptide loading has been directly demonstrated in the *M. tb.* phagolysosome (*27*).

CMV is not the only intracellular pathogen to up-regulate MHC-E expression. Hepatitis C virus also up-regulates MHC-E expression (*28*), and both HIV and SIV up-regulate MHC-E in concert with MHC-Ia down-regulation (fig. S26) (*29*). This common adaptation suggests that for these and probably other intracellular pathogens, the evolutionary pressure to up-regulate MHC-E to counter NK cell responses outweighs the potential risk of increased susceptibility to MHC-E–restricted $CD8^+$ T cells, perhaps because MHC-E–restricted $CD8^+$ T cells are poorly primed during infection with these agents.

The reason why MHC-E–restricted $CD8^+$ T cell responses are such a minor component of the modern mammalian immune system is unclear, especially given our finding that such responses can be diverse and broad (although arguably less diverse and broad on a population level than polymorphic MHC-Ia; fig. S27). However, ΔRh157.5/.4 RhCMV vectors are able to bypass the intrinsic constraint of MHC-E–restricted $CD8^+$ T cell priming, perhaps by modulation of vector cell tropism and the priming microenvironment (*6*). The ability of these vectors to strongly elicit broad, diverse MHC-E–restricted $CD8^+$ T cell responses therefore offers the potential opportunity to develop vaccines that exploit MHC-E up-regulation, an intrinsic vulnerability in the immune-evasion strategies of many highly adapted persistent pathogens. Moreover, because of limited MHC-E polymorphism, a vaccine targeted at MHC-E–restricted $CD8^+$ T cell responses would elicit largely similar responses in all or most vaccinees, potentially providing for efficacy in all individuals regardless of MHC-I genotype. Evolution may have disfavored MHC-E as a primary restricting molecule for $CD8^+$ T cells in modern

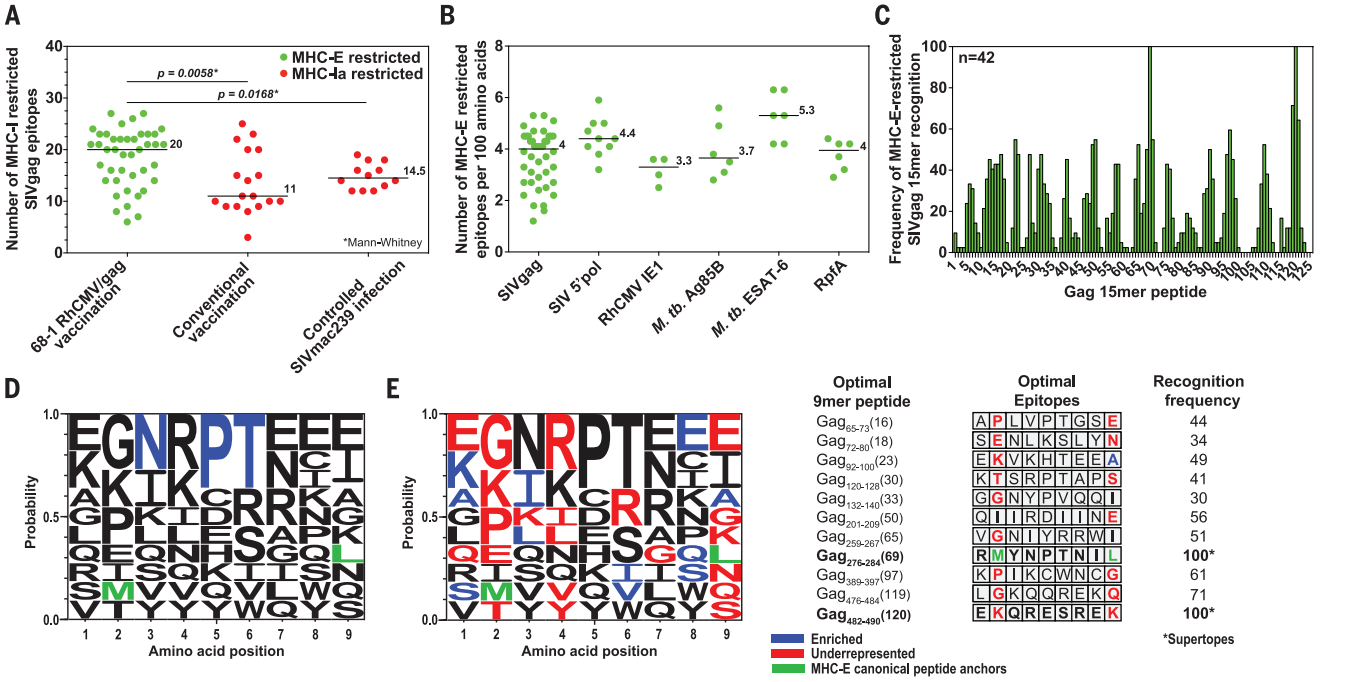

Fig. 3. Diversity of MHC-E–restricted epitopes. (**A**) Comparison of the total number of distinct MHC-E (green)– versus MHC-Ia (red)–restricted SIVgag epitopes recognized by circulating $CD8^+$ T cells in individual RMs vaccinated with 68-1 RhCMV/SIVgag or conventional viral vectors—the latter including MVA/SIVgag (N = 11), adenovirus type 5/SIVgag (N = 3), and electroporated DNA/gag plus interleukin-12 (N = 4)—or in RMs with controlled SIVmac239 infection (N = 12). The horizontal bars indicate median values (P values are from unpaired, two-tailed Mann-Whitney tests). (**B**) Comparison of the number of distinct MHC-E–restricted epitopes (per 100 amino acids of protein length) recognized by circulating $CD8^+$ T cells in individual RMs vaccinated with 68-1 RhCMV vectors expressing each of the indicated antigens (RhCMV IE1 responses were evaluated in CMV-naïve RMs that were administered 68-1 RhCMV/SIVgag). The horizontal bars indicate median values for each group. (**C**) Population-level analysis of the breadth of MHC-E–restricted SIVgag epitope–specific $CD8^+$ T cell responses across 125 consecutive 15-mer gag peptides (with an overlap of 11 amino acids) in 42 RMs vaccinated with the 68-1 RhCMV/SIVgag vector. (**D**) Sequence logo indicating the frequency of each amino acid in a given position by the height of the letter, based on 11 optimal, MHC-E–restricted SIVgag 9-mer peptide epitopes recognized by $CD8^+$ T cells in RMs vaccinated with the 68-1 RhCMV/SIVgag vector. Blue indicates significant amino acid enrichment in a given position relative to its background frequency in SIVmac239 gag (see supplementary materials). Green highlights the M2 and L9 of the canonical MHC-E–binding motif. (**E**) The same logo as in (D), colored according to enrichment (blue or green) or underrepresentation (red) among 551 peptides eluted from HLA-E*01:03 in a TAP-deficient setting by Lampen *et al.* (*22*) (fig. S15). Amino acids enriched in the second and C-terminal anchor positions among the 551 peptides from (*22*) were rare among our 11 optimal SIVgag peptides, whereas those that were significantly underrepresented in (*22*) were enriched in our SIVgag epitopic peptides, highlighted in the actual optimal epitopes listed on the right. The percentage of RMs vaccinated with 68-1 RhCMV/SIVgag (N = 42) that responded to each optimal peptide is noted as the recognition frequency.

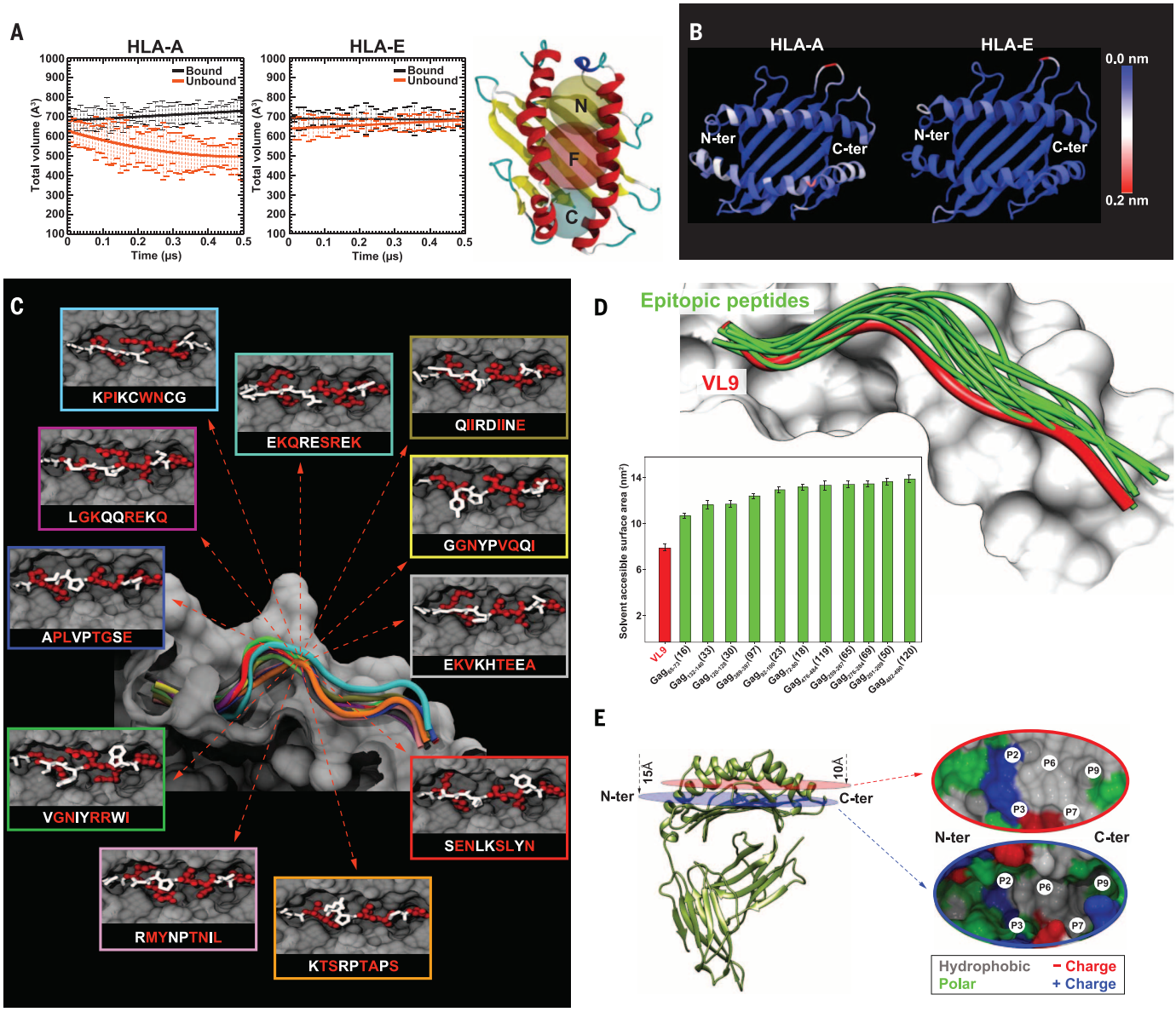

Fig. 4. Structural analysis of MHC-E–peptide binding. (**A**) Structural changes in the binding groove of canonical peptide-bound and -unbound HLA-A*02:01 and HLA-E*01:03. Calculations of changes in the volume of the binding groove indicate that, unlike in HLA-A*02:01, the HLA-E*01:03 binding groove does not collapse when the peptide is not bound during the 0.5-μs all-atom molecular dynamics simulations. Error bars indicate the 95% confidence interval, determined using standard error estimates from five independent simulations for each case. The total volume (in cubic angstroms) is calculated from the cavity volumes from the N, F, and C regions, as shown in the three-dimensional structure on the right and described in the supplementary materials. (**B**) Root-mean-square fluctuations of the backbone atoms of unbound HLA-A*02:01 and HLA-E*01:03 are mapped on the x-ray structure (-ter, terminus). Consistent with (A), the binding groove of HLA-E*01:03 is less flexible compared with that of HLA-A*02:01. The binding groove helices partially unfold in unbound HLA-A*02:01, whereas the unbound HLA-E*01:03 binding groove remains relatively stable. Increasing flexibility is captured by the change in color gradient from blue to white to red. (**C**) HLA-E*01:03 binding profile obtained from a Rosetta-based docking approach (*30*) of 11 optimal, MHC-E–restricted, SIVgag epitopic peptides. The backbones of these peptides adopt a similar conformation, as shown by the colors in front of the binding groove crosssection. The bound conformations for these 11 peptides are shown in the insets. Residues buried in HLA-E and exposed are marked in red and white, respectively. (**D**) Molecular dynamics simulations of docked complexes show that the 11 epitopic peptides are bound in a slightly elevated position relative to VL9 in the MHC-E binding groove and are more solvent-exposed (inset bar graph). (**E**) Cross sections (viewed from above) of the MHC-E binding groove at two different depths show the differences in the chemical environment recognized by the buried residues of epitopic peptides and VL9. Unlike the hydrophobic environment experienced by the buried residues of the VL9 peptide, epitopic peptides experience a chemically heterogeneous environment at their slightly elevated position in the binding groove (figs. S22 and S23).

mammals, but if HCMV vectors are able to replicate in humans the biology of ΔRh157.5/.4 RhCMV vectors in RMs (or, alternatively, if non–CMV-based strategies to elicit broadly targeted MHC-E–restricted CD8$^+$ T cell responses can be developed), vaccinologists may be able to resurrect this largely dormant MHC-E–based adaptive immune system to attack pathogens with novel immune responses that they are not adapted to effectively evade.

REFERENCES AND NOTES

1. J. Neefjes, M. L. Jongsma, P. Paul, O. Bakke, *Nat. Rev. Immunol.* **11**, 823–836 (2011).
2. J. Nikolich-Zugich, D. H. Fremont, M. J. Miley, I. Messaoudi, *Microbes Infect.* **6**, 501–512 (2004).
3. J. W. Yewdell, *Immunity* **25**, 533–543 (2006).

4. P. J. Goulder, D. I. Watkins, *Nat. Rev. Immunol.* **8**, 619–630 (2008).
5. L. J. Picker, S. G. Hansen, J. D. Lifson, *Annu. Rev. Med.* **63**, 95–111 (2012).
6. S. G. Hansen *et al.*, *Science* **340**, 1237874 (2013).
7. S. G. Hansen *et al.*, *Nature* **473**, 523–527 (2011).
8. S. G. Hansen *et al.*, *Nature* **502**, 100–104 (2013).
9. R. W. Wiseman *et al.*, *Nat. Med.* **15**, 1322–1326 (2009).
10. N. Lee, D. R. Goodlett, A. Ishitani, H. Marquardt, D. E. Geraghty, *J. Immunol.* **160**, 4951–4960 (1998).
11. N. Lee *et al.*, *Proc. Natl. Acad. Sci. U.S.A.* **95**, 5199–5204 (1998).
12. V. M. Braud *et al.*, *Nature* **391**, 795–799 (1998).
13. L. C. Sullivan, C. S. Clements, J. Rossjohn, A. G. Brooks, *Tissue Antigens* **72**, 415–424 (2008).
14. T. van Hall, C. C. Oliveira, S. A. Joosten, T. H. Ottenhoff, *Microbes Infect.* **12**, 910–918 (2010).
15. M. B. Lodoen, L. L. Lanier, *Nat. Rev. Microbiol.* **3**, 59–69 (2005).
16. L. Wieten, N. M. Mahaweni, C. E. Voorter, G. M. Bos, M. G. Tilanus, *Tissue Antigens* **84**, 523–535 (2014).
17. L. Arlettaz *et al.*, *Eur. J. Immunol.* **34**, 3456–3464 (2004).
18. D. H. O'Connor *et al.*, *Nat. Med.* **8**, 493–499 (2002).
19. G. Pietra, C. Romagnani, C. Manzini, L. Moretta, M. C. Mingari, *J. Biomed. Biotechnol.* 10.155/2010/907092 (2010).
20. N. Caccamo *et al.*, *Eur. J. Immunol.* **45**, 1069–1081 (2015).
21. A. E. Lilja, T. Shenk, *Proc. Natl. Acad. Sci. U.S.A.* **105**, 19950–19955 (2008).
22. M. H. Lampen *et al.*, *Mol. Immunol.* **53**, 126–131 (2013).
23. H. L. Hoare *et al.*, *J. Mol. Biol.* **377**, 1297–1303 (2008).
24. V. Prod'homme *et al.*, *J. Immunol.* **188**, 2794–2804 (2012).
25. R. Richards, I. Scholz, C. Powers, W. R. Skach, K. Früh, *J. Virol.* **85**, 8766–8776 (2011).
26. G. Camilli *et al.*, *J. Leukoc. Biol.* **99**, 121–130 (2016).
27. J. E. Grotzke *et al.*, *PLOS Pathog.* **5**, e1000374 (2009).
28. J. Nattermann *et al.*, *Am. J. Pathol.* **166**, 443–453 (2005).
29. J. Nattermann *et al.*, *Antivir. Ther.* **10**, 95–107 (2005).
30. T. Liu *et al.*, *J. Chem. Inf. Model.* **54**, 2233–2242 (2014).

ACKNOWLEDGMENTS

We are grateful to T. van Hall for the *HLA-E*01:03* transfectant; D. Geraghty for the 4D12 mAb; D. O'Connor and R. Wiseman for 454-based MHC typing; and Y. Guo, D. Laddy, and M. Stone (Aeras) for provision of the 68-1 RhCMV construct expressing the *M. tb.* RpFA protein. We thank A. Townsend for help with the graphics; E. McDonald, A. Klug, A. Bhusari, G. Xu, J. Bae, C. Kahl, S. Hagen, A. Sylwester, and L. Boshears for technical or administrative assistance; J. Theiler for coding assistance; and P. Borrow for helpful discussions on HLA-E biology and peptide binding. This research was supported by NIH grants P01-AI094417, R37-AI054292, R01-DE021291, R01-AI095113, R01-AI117802, R01-AI059457, U24-OD010850, P51-OD011092, and P50-GM065794 and contract HHSN272201100013C; the Center for HIV/AIDS Vaccine Immunology and Immunogen Discovery (grant UM1-AI100645-01) of the National Institute of Allergy and Infectious Diseases; the Bill and Melinda Gates Foundation (Global Health grants OPP1108533 and OPP1133649); the Aeras Global TB Vaccine Foundation; and the Center for Nonlinear Studies at the Los Alamos National Laboratory (LANL). LANL institutional computing was used for carrying out all-atom molecular dynamics simulations. The content is solely the responsibility of the authors and does not necessarily represent the official views of NIH or other funders. The Oregon Health & Science University (OHSU) has submitted a provisional patent entitled "Methods and compositions useful in generating non-canonical $CD8^+$ T cell responses" (inventors: L.J.P., K.F., J.B.S, D.M, and S.G.H.). OHSU and L.J.P., S.G.H., K.F., and J.A.N. have a substantial financial interest in TomegaVax, a company that may have a commercial interest in the results of this research and technology. L.J.P., K.F., and J.A.N. serve on the board of TomegaVax, and K.F. is also an uncompensated officer of the company. The potential individual and institutional conflicts of interest have been reviewed and managed by OHSU. Additional data used in this report are available as supplementary materials on *Science* Online.

SUPPLEMENTARY MATERIALS

www.sciencemag.org/content/351/6274/714/suppl/DC1
Materials and Methods
Figs. S1 to S27
Tables S1 and S2
References (*31*–*54*)

2 July 2015; accepted 6 January 2016
Published online 21 January 2016
10.1126/science.aac9475

EPIGENETICS

Dynamics of epigenetic regulation at the single-cell level

Lacramioara Bintu,[1]* John Yong,[1]* Yaron E. Antebi,[1] Kayla McCue,[1] Yasuhiro Kazuki,[2] Narumi Uno,[2] Mitsuo Oshimura,[2] Michael B. Elowitz[1,3]†

Chromatin regulators play a major role in establishing and maintaining gene expression states. Yet how they control gene expression in single cells, quantitatively and over time, remains unclear. We used time-lapse microscopy to analyze the dynamic effects of four silencers associated with diverse modifications: DNA methylation, histone deacetylation, and histone methylation. For all regulators, silencing and reactivation occurred in all-or-none events, enabling the regulators to modulate the fraction of cells silenced rather than the amount of gene expression. These dynamics could be described by a three-state model involving stochastic transitions between active, reversibly silent, and irreversibly silent states. Through their individual transition rates, these regulators operate over different time scales and generate distinct types of epigenetic memory. Our results provide a framework for understanding and engineering mammalian chromatin regulation and epigenetic memory.

Cells use a system of chromatin regulators (CRs) and associated histone and DNA modifications to modulate gene expression and establish long-term epigenetic memory (*1*–*4*). This system is critical in development (*5*), aging (*6*), and disease (*7*) and could provide essential capabilities for synthetic biology (*8*). In all of these contexts, the temporal dynamics and cell-to-cell variability of gene expression are critical but have been difficult to study, as current methods usually provide static correlations between chromatin modifications and gene expression or aggregate data across potentially heterogeneous cell populations. Therefore, it has remained unclear how strongly, rapidly, and uniformly each regulator can alter gene expression, and how long these effects persist (Fig. 1A).

To answer these questions, we combined targeted CR recruitment (*9*–*12*) with time-lapse microscopy (*13*) to develop a system to quantitatively track the effects of CRs on a reporter gene in individual cells. More specifically, we fused individual CRs to the reverse Tet repressor (rTetR) (*14*), which binds to DNA only in the presence of doxycycline (dox), allowing us to control the timing and duration of CR recruitment upstream of a fluorescent reporter gene expressing histone 2B (H2B)–citrine (Fig. 1B). To isolate the system from other genes, the reporter was flanked by insulators (*15*) and integrated on a human artificial chromosome (HAC) (*16*). All constructs were stably integrated in Chinese hamster ovary (CHO)–K1 cells, a major model system for synthetic mammalian biology (see supplementary materials and methods). Each cell line constitutively coexpressed H2B-mCherry, thus allowing cell tracking even when the reporter was silenced (Fig. 1, B and C). Control experiments indicated that recruitment of rTetR alone does not repress reporter expression (fig. S1) and that changes in gene regulation could be detected over time scales as short as 6 hours (fig. S2). Therefore, this system enables analysis of the effects of recruitment and release of each CR on gene expression in individual cells.

To compare the capabilities of distinct regulators, we selected four repressive CRs that span a broad range of chromatin modifications: embryonic ectoderm development (EED), Krüppel associated box (KRAB), DNA methyltransferase 3B (DNMT3B), and histone deacetylase 4 (HDAC4). EED functions as part of the Polycomb repressive complex 2 (PRC2), which methylates histone H3 at lysine 27 (H3K27me3) (*17*). KRAB functions within >400 zinc finger transcription factors (*18*), associates with other CRs that write or read H3K9me3 (*19*), and is often used in genetic engineering (*10*, *20*). DNMT3B causes de novo methylation of cytosine-guanine dinucleotides (CpGs) (*21*). HDAC4 removes acetyl groups from histones H3 and H4 (*22*). All of these CRs have been shown to silence gene expression during development, and their molecular mechanisms have been dissected in diverse studies (*19*, *23*–*25*). However, their dynamic operational behaviors have not been analyzed in single cells and compared side-by-side at the same target gene.

To analyze how recruitment of each CR alters gene expression, we used time-lapse microscopy to follow silencing in individual cells after the addition of dox (Fig. 1C, movies S1 to S8, and materials and methods). Recruitment of each CR strongly and specifically silenced H2B-citrine expression (Fig. 1D and fig. S3, B and C). Silencing occurred in an all-or-none fashion in individual cells for all four CRs (Fig. 1D) at varying times after recruitment (Fig. 1E). During the silencing

[1]Division of Biology and Biological Engineering, California Institute of Technology, Pasadena, CA 91125, USA. [2]Chromosome Engineering Research Center, Tottori University, 86 Nishicho, Yonago, Japan. [3]Howard Hughes Medical Institute (HHMI) and Department of Applied Physics, California Institute of Technology, Pasadena, CA 91125, USA. *These authors contributed equally to this work. **†Corresponding author. E-mail: melowitz@caltech.edu**

Downloaded from on February 11, 2016

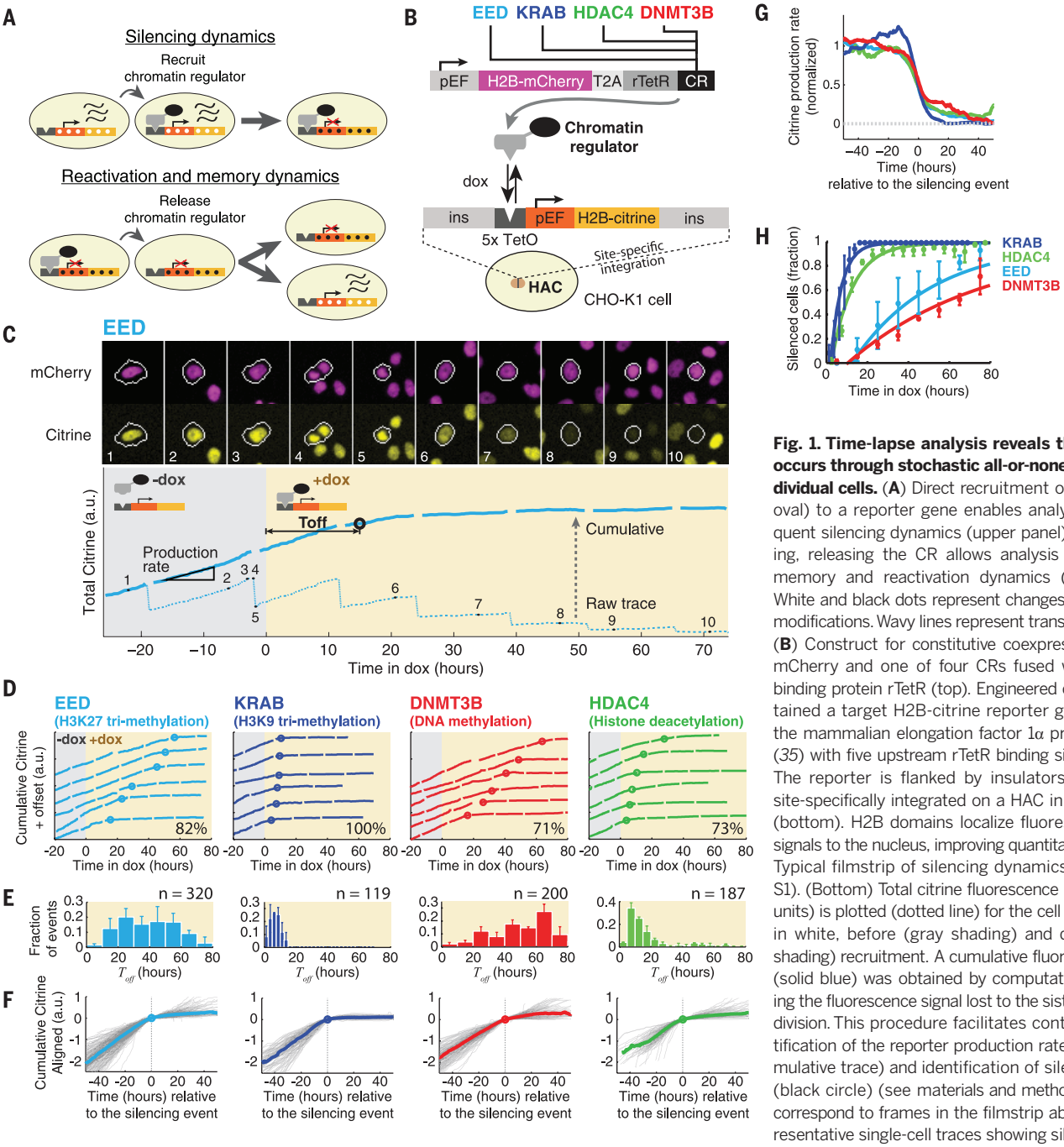

Fig. 1. Time-lapse analysis reveals that silencing occurs through stochastic all-or-none events in individual cells. (**A**) Direct recruitment of a CR (black oval) to a reporter gene enables analysis of subsequent silencing dynamics (upper panel). After silencing, releasing the CR allows analysis of epigenetic memory and reactivation dynamics (lower panel). White and black dots represent changes in chromatin modifications. Wavy lines represent transcribed mRNA. (**B**) Construct for constitutive coexpression of H2B-mCherry and one of four CRs fused with the DNA binding protein rTetR (top). Engineered cells also contained a target H2B-citrine reporter gene driven by the mammalian elongation factor 1α promoter (pEF) (*35*) with five upstream rTetR binding sites (5x TetO). The reporter is flanked by insulators (ins) and is site-specifically integrated on a HAC in CHO-K1 cells (bottom). H2B domains localize fluorescent protein signals to the nucleus, improving quantitation. (**C**) (Top) Typical filmstrip of silencing dynamics (from movie S1). (Bottom) Total citrine fluorescence (a.u., arbitrary units) is plotted (dotted line) for the cell lineage circled in white, before (gray shading) and during (yellow shading) recruitment. A cumulative fluorescence trace (solid blue) was obtained by computationally restoring the fluorescence signal lost to the sister cell at each division. This procedure facilitates continuous quantification of the reporter production rate (slope of cumulative trace) and identification of silencing events (black circle) (see materials and methods). Numbers correspond to frames in the filmstrip above. (**D**) Representative single-cell traces showing silencing events (circles) induced by recruitment of the indicated CR. Only cells silenced during the corresponding movie (see movies S1 to S4) are shown. For clarity, traces are offset by arbitrary amounts on the *y* axis. The percentage of traces that resemble those shown here is indicated on each plot (see fig. S4 for other behaviors). (**E**) Distributions of silencing times, T_{off} (mean ± SD). *n* indicates the number of events for each histogram. (**F**) Single-cell cumulative fluorescence traces (gray lines) were aligned at the silencing event (0 on the *x* axis) and superimposed. The median of all traces is plotted as a colored line. (**G**) Median reporter production rates, obtained from all slopes of the individual traces in (F), showing the all-or-none nature of silencing events. (**H**) Fraction of cells silenced as a function of time (dots, mean ± SD). Curves represent exponential fits to a single silencing rate with a time delay for each CR (materials and methods).

event, median production rates dropped below 20% of their presilencing value within ~20 hours, or about one cell cycle (Fig. 1, F and G; see also fig. S4 for deviations from this behavior). This all-or-none response is similar to that observed upon recruitment of heterochromatin protein 1 (HP1) (*9*) and is consistent with previous reports of chromatin-related gene silencing (*26*, *27*).

In contrast to the overall similarity in silencing event profiles, the timing of the silencing events we observed varied widely between cells, and the rate of silencing depended strongly on the CR used (Fig. 1, E and H). Silencing by KRAB and HDAC4 was rapid, with all cells silenced within one cell cycle (~20 hours), whereas EED and DNMT3B exhibited slower rates of silencing, with 50% of cells silenced at 35 and 62 hours, respectively. For these CRs, the broad cell-to-cell variability in T_{off} (defined as the delay between dox addition and silencing) (Fig. 1E) and the lack of a strong correlation of silencing behavior between sister cells (fig. S5) indicate that chromatin silencing is a stochastic process. In fact, after a relatively short time lag, the fraction of silenced

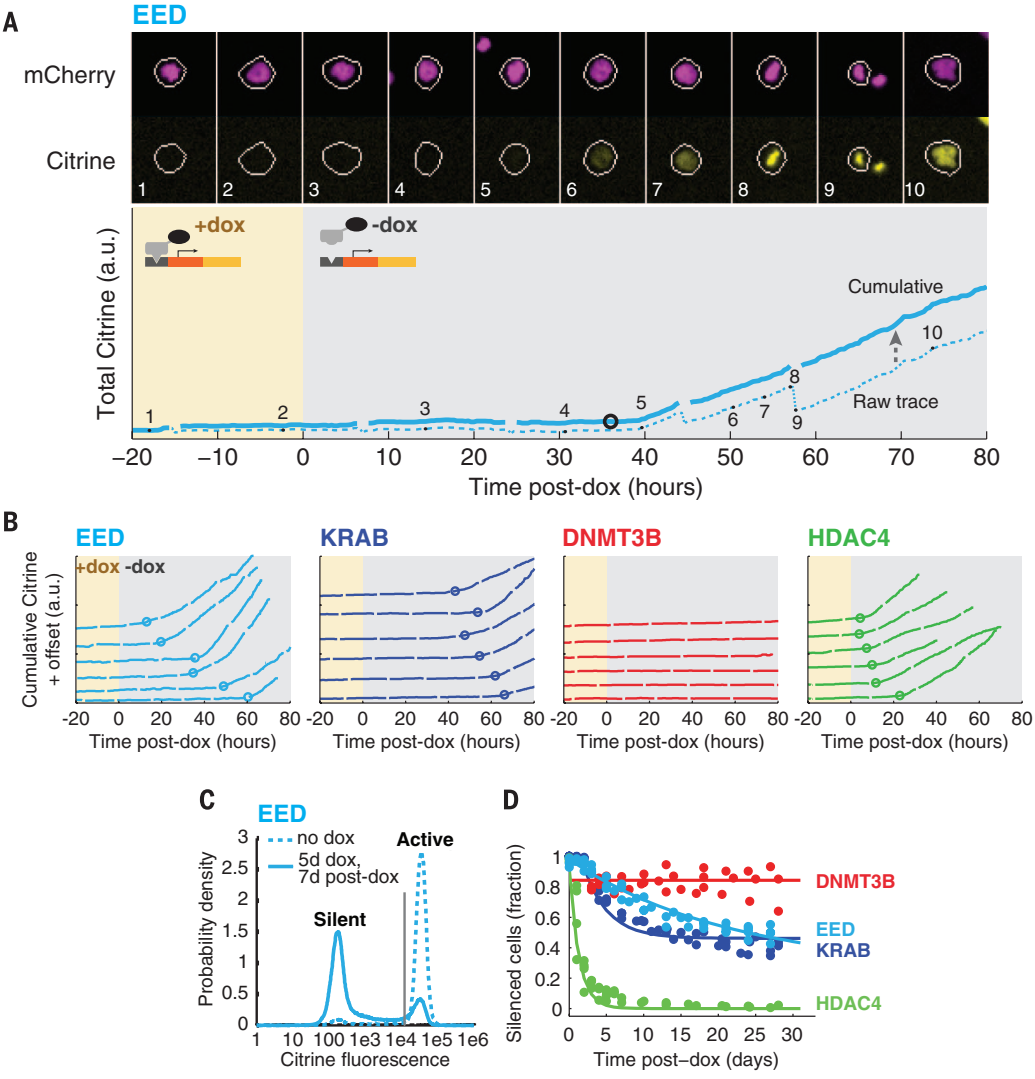

Fig. 2. Chromatin regulators produce distinct time scales of memory. (**A**) (Top) Filmstrip and (bottom) corresponding fluorescence trace before and after EED release (from movie S9). Traces, numbers, and shading are similar to those in Fig. 1C. (**B**) Representative single-cell traces showing reactivation events for EED, KRAB, and HDAC4 (circles; only reactivated cells are shown). No reactivation events were observed for DNMT3B, so only silent cells are plotted. Traces are vertically offset for clarity. (**C**) Flow cytometry enables classification of cells as silent (low-fluorescence peak) or active (high-fluorescence peak), using a threshold (gray line). (**D**) Fraction of silenced cells measured by flow cytometry at various time points after CR release. Each dot represents one flow cytometry measurement. Data from three independent experiments are shown. Spontaneous background silencing rates have been subtracted (fig. S7D and materials and methods). Solid lines are fits to the model in Fig. 3A.

cells as a function of time is well described by a single-rate process for each CR (solid lines in Fig. 1H). Together, these results strongly suggest that silencing occurs through stochastic all-or-none events at distinct rates for each CR.

We next asked how the CRs differed in terms of reactivation dynamics and epigenetic memory. After 5 days of recruitment, we washed out dox to release the CRs and tracked the resulting changes in gene expression using time-lapse movies (Fig. 2A, fig. S6, and movies S9 to S16). For EED, KRAB, and HDAC4, reactivation occurred in stochastic all-or-none events, resembling silencing events in reverse (Fig. 2B). In contrast, we observed no reactivation events in cells silenced by DNMT3B recruitment, up to 80 hours after dox removal, after which cell density became too high for tracking.

To extend these measurements to longer durations, we switched to flow cytometry analysis. As expected for all-or-none reactivation, distributions of total fluorescence were bimodal (Fig. 2C and fig. S7, A to C), allowing us to quantitatively track the fraction of silent cells as a function of time (Fig. 2D and fig. S7D). The CRs produced qualitatively different modes of epigenetic memory (Fig. 2D), associated with distinct sets of chromatin modifications, as measured by DNA and chromatin immunoprecipitation and quantitative polymerase chain reaction (fig. S8). HDAC4 imparted short-term memory: Upon its release, silencing was lost in all cells within 5 days, consistent with rapid dynamics of histone acetylation and deacetylation (*28*). In contrast, DNMT3B produced long-term memory: Cells were stably silenced for the duration of the experiment (30 days), in agreement with reports that DNA methylation is stably inherited (*4*). Finally, both EED and KRAB enabled a distinct type of hybrid memory that is not associated with DNA methylation (fig. S8B). For these CRs, a fraction of cells fully reactivated within 2 to 3 weeks, whereas the remaining fraction remained completely silenced for at least a month.

The hybrid memory could be explained by a three-state model (Fig. 3A) in which recruitment of a silencing CR causes cells to stochastically advance from an actively expressing state (A) to a reversibly silent state (R) and then to an irreversibly silent state (I). We assume that after the end of recruitment, the forward silencing rates become negligible, allowing cells in the R state to revert to the A state, reactivating gene expression, whereas cells in the I state remain silenced.

This three-state model predicts that longer durations of recruitment should increase the fraction of irreversibly silenced cells. To test this prediction, we systematically varied the duration of recruitment and analyzed the subsequent reactivation dynamics (Fig. 3B). For both EED and KRAB, the fraction of cells remaining silent 30 days after CR release increased with the duration of the initial recruitment, as predicted (Fig. 3, C and D). Similar increases in the stability of silencing with recruitment duration were also reported for HP1 (*9*). Aside from a relatively small time lag before the onset of reactivation (1 to 2 days), all data for a given CR could be fit to the three-state model with a single set of rate constants across the entire range of recruitment durations (solid lines in Fig. 3, C and D; see also materials and methods). Moreover, simplified forms of this model can also explain the behavior of HDAC4 and DNMT3B,

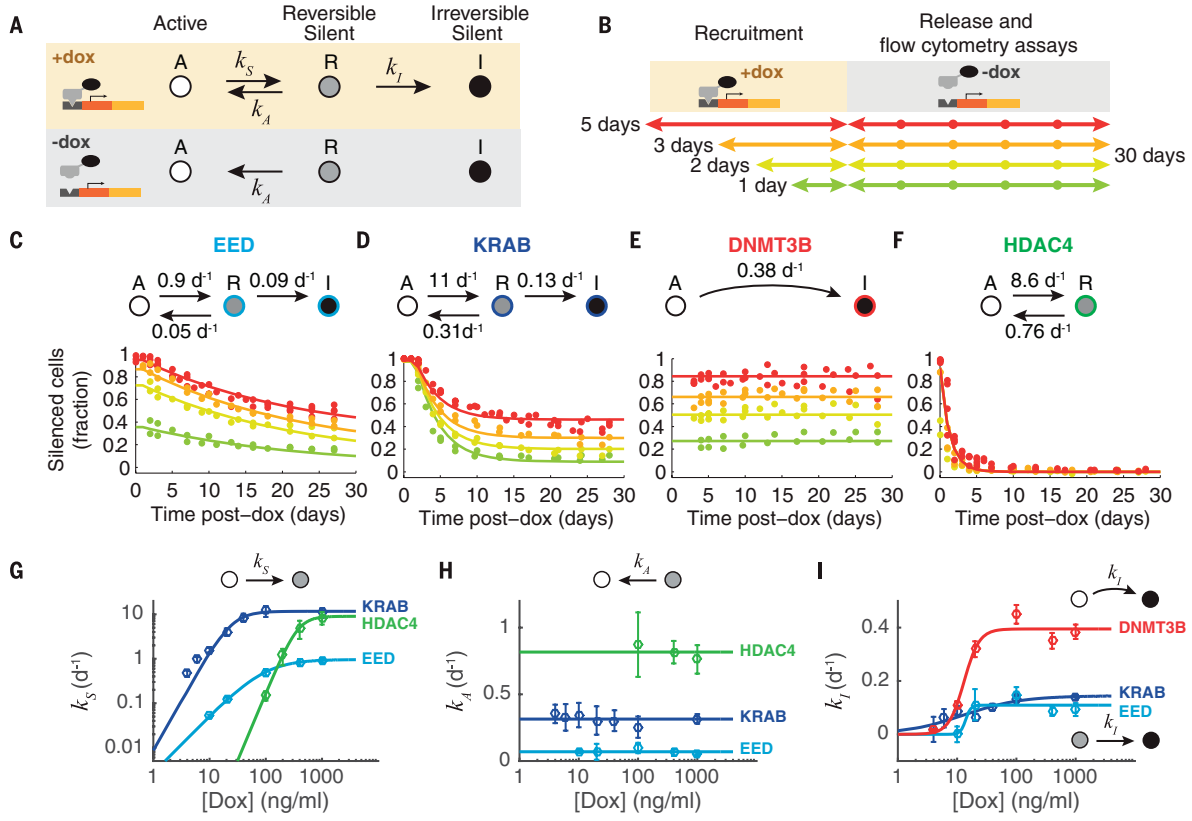

Fig. 3. A three-state model explains gene expression dynamics across different recruitment durations and strengths. (**A**) Proposed model based on stochastic transitions between actively expressing (A), reversibly silent (R), and irreversibly silent (I) states. Silencing (at rates k_S and k_I) depends on recruitment, whereas reactivation (at rate k_A) is independent of recruitment. (**B**) Experimental strategy: The duration of recruitment was varied from 1 to 5 days (colored arrows). After removal of dox, the fraction of cells remaining silenced was measured for up to 30 days. (**C** to **F**) Flow cytometry measurements show the fraction of silent cells over time after CR release. Colors indicate recruitment duration, as in (B). Data from two or more independent experiments are shown. Each set of solid lines represents a single fit of all data for that factor to the model, with rate constants indicated above each panel (see materials and methods for details of fitting). (**G** to **I**) Silencing and reactivation dynamics are measured at different dox concentrations. For each concentration, these data are fit with the corresponding model for each CR to extract the kinetic rates indicated in the diagram (dots, see materials and methods). Error bars represent the 95% confidence interval of the fit. Curves [(G) and (I)] are fits to a Michaelis-Menten–like equation. Lines in (H) are fits to a constant value.

each requiring only two of the three states (Fig. 3, E and F).

A key parameter in these experiments is the recruitment strength of the CR, which is controlled by the dox concentration. To understand how recruitment strength affects silencing and reactivation capabilities, we analyzed the effects of 5 days of CR recruitment for a range of dox concentrations. Qualitatively, each CR produced the same number and type of states across dox concentrations (compare Fig. 3, C to F, to fig. S9, B to E). Quantitatively, recruitment strength modulated the silencing rates, but not the reactivation rates, which depended only on the identity of the silencing CR (Fig. 3, G to I). Together, these data provide a comprehensive view of how the dynamic effects of each CR on gene expression depend on recruitment duration and strength.

The three-state model (Fig. 3A) provides a unifying framework for comparing the operational capabilities of different CRs. More specifically, each CR traces a distinct curve within the parameter space defined by the three rate constants of the model over a range of recruitment strengths (Fig. 4A). Going forward, it will be critical to determine how these operational parameters depend on promoter architecture, the chromatin state of the locus, and the specific set of chromatin regulatory components expressed in different cell types. Moreover, it will be important to determine how the phenomenological states and transitions associated with each CR emerge from underlying molecular states and biochemical processes. Although the stochastic nature of silencing is consistent with simple models of spreading of chromatin modifications (*9*) (supplementary text and fig. S10), other processes—such as chromatin compaction and translocation to the nuclear lamina—may be involved.

Despite their differences, the CRs analyzed here were all capable of regulating gene expression through duration-dependent fractional control. In this mode, the duration of CR recruitment controls the fraction of cells in which the target gene is silenced in all-or-none fashion. This is possible when the lifetime of the reversible silenced state is long compared with the lifetimes of mRNA and protein (supplementary text and fig. S11). Duration-dependent fractional control can be contrasted with other transcriptional regulation systems, in which more rapid dynamics enables the occupancy of a transcription factor at the promoter to control protein expression levels in a graded manner (*29*–*31*). Because of their different parameters, each CR generates a distinct control mode (Fig. 4B): DNMT3B faithfully records the duration or strength of recruitment. HDAC4 enables fast and reversible fractional control at maximum recruitment strengths but can also lead to graded changes in protein levels at lower ones (fig. S11). EED and KRAB, due to their hybrid memory, enable regulation across multiple time scales. For example, with these CRs, pulses of recruitment of different durations that both silence the entire population in the short term can establish different degrees of permanent memory in the longer term (Fig. 4C), similarly to the classical example of PRC2-mediated silencing of the flowering locus during vernalization (*32*). These types of fractional control strategies could be used to integrate signals for cellular decision-making (*33*, *34*).

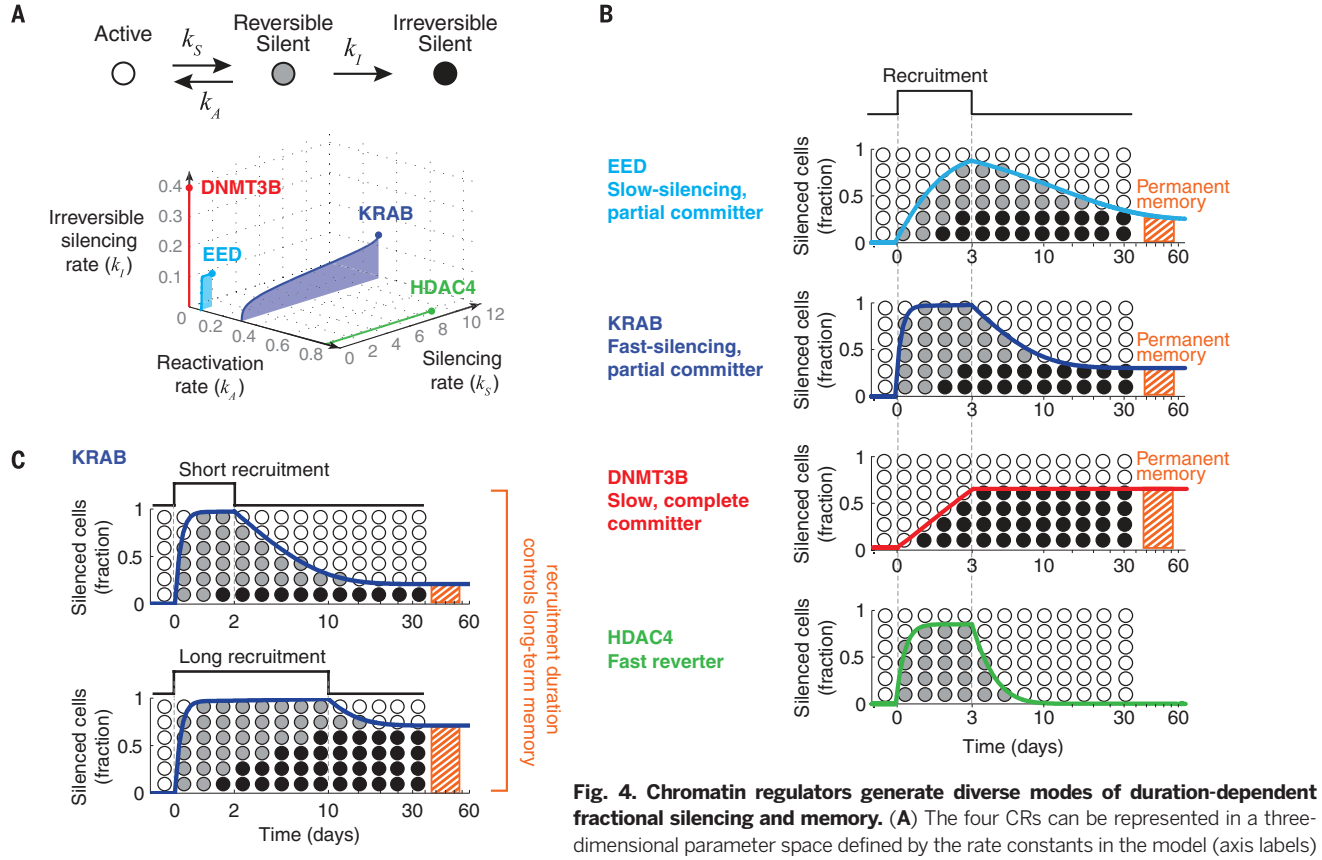

Fig. 4. Chromatin regulators generate diverse modes of duration-dependent fractional silencing and memory. (**A**) The four CRs can be represented in a three-dimensional parameter space defined by the rate constants in the model (axis labels) over a range of recruitment strengths. The curve occupied by each CR in this space encapsulates its dynamic effects on gene expression and epigenetic memory. The colored dot at the end of each curve represents rate constants at full recruitment strength (saturating dox concentration). (**B**) For each regulator, the response to a pulse of recruitment is computed and plotted using the rate constants at full recruitment strength. The total fraction of silent cells in states R and I is indicated by the solid color line; the fractions of cells in each of these states are approximately indicated by the fraction of black and gray circles. Time is indicated on the *x* axis (log scale). The final fraction of cells in the I state is indicated by the red hatched bar. (**C**) Different durations of recruitment (upper and lower panels) can similarly produce full silencing on shorter time scales but can generate different amounts of permanent memory (red hatched bars).

It is now possible to use the framework developed here to classify the operational capabilities of other CRs, as well as to determine how their behaviors depend on biological context and how they interact combinatorially to provide additional capabilities. More generally, this approach should help us to understand why specific CRs are employed in particular natural genetic circuits and to enable the design of synthetic gene circuits that take advantage of the inherent temporal control and memory capabilities of chromatin-mediated regulation.

REFERENCES AND NOTES

1. T. Kouzarides, *Cell* **128**, 693–705 (2007).
2. E. Li, Y. Zhang, *Cold Spring Harb. Perspect. Biol.* **6**, a019133 (2014).
3. V. W. Zhou, A. Goren, B. E. Bernstein, *Nat. Rev. Genet.* **12**, 7–18 (2011).
4. A. Bird, *Genes Dev.* **16**, 6–21 (2002).
5. J. Zhu *et al.*, *Cell* **152**, 642–654 (2013).
6. M. F. Fraga, M. Esteller, *Trends Genet.* **23**, 413–418 (2007).
7. G. Egger, G. Liang, A. Aparicio, P. A. Jones, *Nature* **429**, 457–463 (2004).
8. A. J. Keung, J. K. Joung, A. S. Khalil, J. J. Collins, *Nat. Rev. Genet.* **16**, 159–171 (2015).
9. N. A. Hathaway *et al.*, *Cell* **149**, 1447–1460 (2012).
10. L. A. Gilbert *et al.*, *Cell* **154**, 442–451 (2013).
11. A. J. Keung, C. J. Bashor, S. Kiriakov, J. J. Collins, A. S. Khalil, *Cell* **158**, 110–120 (2014).
12. M. L. Maeder *et al.*, *Nat. Biotechnol.* **31**, 1137–1142 (2013).
13. J. C. W. Locke, M. B. Elowitz, *Nat. Rev. Microbiol.* **7**, 383–392 (2009).
14. S. Urlinger *et al.*, *Proc. Natl. Acad. Sci. U.S.A.* **97**, 7963–7968 (2000).
15. T. M. Yusufzai, G. Felsenfeld, *Proc. Natl. Acad. Sci. U.S.A.* **101**, 8620–8624 (2004).
16. S. Yamaguchi *et al.*, *PLOS ONE* **6**, e17267 (2011).
17. R. Margueron, D. Reinberg, *Nature* **469**, 343–349 (2011).
18. R. Urrutia, *Genome Biol.* **4**, 231 (2003).
19. K. Ayyanathan *et al.*, *Genes Dev.* **17**, 1855–1869 (2003).
20. M. Fussenegger *et al.*, *Nat. Biotechnol.* **18**, 1203–1208 (2000).
21. M. Okano, D. W. Bell, D. A. Haber, E. Li, *Cell* **99**, 247–257 (1999).
22. E. A. Miska *et al.*, *EMBO J.* **18**, 5099–5107 (1999).
23. K. H. Hansen *et al.*, *Nat. Cell Biol.* **10**, 1291–1300 (2008).
24. N. P. Blackledge *et al.*, *Cell* **157**, 1445–1459 (2014).
25. J. F. Margolin *et al.*, *Proc. Natl. Acad. Sci. U.S.A.* **91**, 4509–4513 (1994).
26. H. G. E. Sutherland *et al.*, *Mamm. Genome* **11**, 347–355 (2000).
27. V. Pirrotta, D. S. Gross, *Mol. Cell* **18**, 395–398 (2005).
28. Y. Katan-Khaykovich, K. Struhl, *Genes Dev.* **16**, 743–752 (2002).
29. A. M. Kringstein, F. M. Rossi, A. Hofmann, H. M. Blau, *Proc. Natl. Acad. Sci. U.S.A.* **95**, 13670–13675 (1998).
30. S. R. Biggar, G. R. Crabtree, *EMBO J.* **20**, 3167–3176 (2001).
31. J. Stewart-Ornstein, C. Nelson, J. DeRisi, J. S. Weissman, H. El-Samad, *Curr. Biol.* **23**, 2336–2345 (2013).
32. J. Song, A. Angel, M. Howard, C. Dean, *J. Cell Sci.* **125**, 3723–3731 (2012).
33. M. Busslinger, A. Tarakhovsky, *Cold Spring Harb. Perspect. Biol.* **6**, a019307 (2014).
34. S. Tay *et al.*, *Nature* **466**, 267–271 (2010).
35. N. Wakabayashi-Ito, S. Nagata, *J. Biol. Chem.* **269**, 29831–29837 (1994).

ACKNOWLEDGMENTS

We thank G. M. Abadi, J. Cao, L. Santat, and the Caltech Flow Cytometry Facility for technical assistance and U. Alon, L. Cai, J. Garcia-Ojalvo, A. I. Geraschenko, M. Guttman, B. A. Hay, R. Kishony, A. Moses, R. Phillips, K. Plath, E. Rothenberg, M.-H. Sung, and members of the Elowitz lab for discussions and feedback. This work was supported by the NIH (grants R01 HD075335A and R01 HD075605A to M.B.E.), the Defense Advanced Research Projects Agency (grant W911NF-11-2-0055 to M.B.E.), the Human Frontier Science Program (grant RGP0020/2012 to M.B.E. and Y.E.A.), the Jane Coffin Childs Memorial Fund for Medical Research (postdoctoral fellowship to L.B.), the Beckman Institute at California Institute of Technology (equipment grant to L.B.), the Burroughs Wellcome Fund (Career at the Scientific Interface Award to L.B.), the Gordon and Betty Moore Foundation (through grant GBMF2809 to the Caltech Programmable Molecular Technology Initiative), and HHMI (M.B.E.). M.B.E., L.B., J.Y., and California Institute of Technology filed a provisional patent application (CIT-7162-P) that relates to fractional control devices based on CRs.

SUPPLEMENTARY MATERIALS

www.sciencemag.org/content/351/6274/720/suppl/DC1
Materials and Methods
Supplementary Text
Figs. S1 to S12
Table S1
References (*36*–*49*)
Movies S1 to S16

7 April 2015; accepted 1 December 2015
10.1126/science.aab2956

TRANSCRIPTION

Structural basis for histone H2B deubiquitination by the SAGA DUB module

Michael T. Morgan,[1] Mahmood Haj-Yahya,[2] Alison E. Ringel,[1] Prasanthi Bandi,[1] Ashraf Brik,[3] Cynthia Wolberger[1]*

Monoubiquitinated histone H2B plays multiple roles in transcription activation. H2B is deubiquitinated by the Spt-Ada-Gcn5 acetyltransferase (SAGA) coactivator, which contains a four-protein subcomplex known as the deubiquitinating (DUB) module. The crystal structure of the Ubp8/Sgf11/Sus1/Sgf73 DUB module bound to a ubiquitinated nucleosome reveals that the DUB module primarily contacts H2A/H2B, with an arginine cluster on the Sgf11 zinc finger domain docking on the conserved H2A/H2B acidic patch. The Ubp8 catalytic domain mediates additional contacts with H2B, as well as with the conjugated ubiquitin. We find that the DUB module deubiquitinates H2B both in the context of the nucleosome and in H2A/H2B dimers complexed with the histone chaperone, FACT, suggesting that SAGA could target H2B at multiple stages of nucleosome disassembly and reassembly during transcription.

Histone modifications such as acetylation, methylation, phosphorylation, and ubiquitination regulate chromatin structure and interactions. Histone H2B monoubiquitination (H2B-Ub) at K123 in yeast, K120 in humans, is a transient modification that is a universal feature of genes that are actively transcribed by RNA polymerase II (*1*). H2B-Ub plays a nondegradative role in transcription activation, elongation, mRNA splicing, and mRNA export, as well as in DNA replication and damage repair (*2*). Histone H2B is monoubiquitinated by Rad6/Bre1 (*3*), which is required for H3K4 and H3K79 trimethylation (*4*, *5*). H2B-Ub also enhances recruitment of FACT (facilitates chromatin transcription) (*6*), a histone chaperone that mediates H2A/H2B dimer eviction and nucleosome reassembly (*7*). H2B is deubiquitinated by the Spt-Ada-Gcn5 acetyltransferase (SAGA) coactivator complex (*8*). The minimal SAGA subcomplex with deubiquitinating (DUB) activity is called the SAGA DUB module, which in yeast contains the catalytic subunit Ubp8 as well as Sgf11, Sus1, and the Sgf73 N-terminal ~100 residues (*8*–*10*). The DUB module is an independently folding subcomplex that is connected to the remainder of the SAGA complex by the C-terminal portion of Sgf73 (*11*). The basic features of the yeast DUB module are conserved in human SAGA (*12*). The structure of the yeast DUB module in the presence and absence of bound ubiquitin (*9*, *10*) revealed a highly intertwined arrangement for the four subunits, with Sgf11, Sgf73, and Sus1 serving in part as scaffolds that help to maintain the Ubp8 catalytic domain in an active conformation (*13*, *14*).

[1]Department of Biophysics and Biophysical Chemistry, Johns Hopkins University School of Medicine, Baltimore, MD 21205, USA. [2]Department of Chemistry, Ben-Gurion University of the Negev, Beer Sheva 8410501, Israel. [3]Schulich Faculty of Chemistry, Technion-Israel Institute of Technology, Haifa 3200008, Israel.
*Corresponding author. E-mail: cwolberg@jhmi.edu

We have determined the crystal structure of the DUB module bound to ubiquitinated nucleosomes at 3.9 Å resolution (table S1). The crystallized complex comprises two DUB module heterotetramers bound to a *Xenopus laevis* nucleosome core particle (NCP) containing two copies of H2B with ubiquitin attached to K120 of H2B (corresponding to K123 of yeast H2B) via a nonhydrolyzable dichloroacetone (DCA) linkage (details in materials and methods). Nucleosomes containing DCA-linked H2B-Ub inhibit DUB module cleavage of ubiquitin-AMC (7-amido-4-methylcoumarin) (fig. S1), indicating that the complex containing the DCA linkage mimics the catalytically competent complex. The DUB module in the crystals contains intact yeast Ubp8, Sgf11, and Sus1 and an N-terminal fragment of Sgf73 (residues 1 to 104) that is sufficient for full DUB module activity on nucleosomes (*15*). Substitution of the Ubp8 active-site cysteine with alanine (C146A) was required to promote binding to nucleosomes containing DCA-linked H2B-Ub (fig. S2). The structure was solved by molecular replacement using high-resolution structures of the DUB module bound to ubiquitin (*9*) [Protein Data Bank (PDB): 3MHS] and the *X. laevis* nucleosome core particle (*16*) (PDB: 3LZ0). We validated the solution by zinc anomalous difference Fourier maps and a composite omit map of Sgf11, and by observing DUB module electron density using molecular replacement phases from a partial model (figs. S3 to S5)

The structure contains one DUB module bound to each face of the nucleosome, distal to the entry and exit sites of the nucleosomal DNA (Fig. 1), with the overall structure of each DUB module essentially identical to that previously reported (*9*, *10*). Each DUB module is docked on the nucleosome in a virtually identical manner, indicating that the observed mode of binding is not governed by crystal contacts. No electron density is seen corresponding to the DCA linkage or for ubiquitin residue G76C. The interaction interface between the DUB module and the nucleosome is about 1000 Å^2, while the surface buried by the conjugated ubiquitin and the catalytic domain of Ubp8 is ~1650 Å^2. The bound ubiquitin makes no apparent contacts with the nucleosome itself.

The DUB module engages the nucleosome almost exclusively through histones H2A and H2B (Fig. 2A). The catalytic lobe of the DUB module, which contains the ubiquitin-specific protease (USP) domain of Ubp8 and the Sgf11 zinc finger, contacts the C-terminal helix of H2B and the conserved acidic patch on H2A/H2B (*17*). The nucleosome acidic patch is contacted by the Sgf11-ZnF (Fig. 2A), which is located near the Ubp8 active site and contains a cluster of arginine residues implicated in DUB module interactions with chromatin (*9*, *10*, *18*). In contrast with proposed models in which the Sgf11 zinc finger contacts nucleosomal DNA (*9*, *18*), the DUB module is oriented with the basic Sgf11-ZnF docked on the H2A/H2B acidic patch (Fig. 2B) with an interface area of 610 Å^2. The Sgf11 arginine residues, R78, R84, and R91 (Fig. 2B), that face the nucleosome acidic patch are conserved in the *Drosophila* and human homologs, dSgf11 and ATXN7L3, respectively. Although the resolution of the structure determination is insufficient to show side-chain density for the arginine side chains, salt-bridge interactions can be modeled between Sgf11 residues R78, R84, and R91 and acidic patch residues H2A-E65, H2B-E107, and H2A-E61, respectively (Fig. 2B). The observed mode of nucleosome interactions, in which an arginine-rich motif interacts with the H2A/H2B acidic patch, has been observed in several complexes containing either a peptide or proteins bound to the nucleosome (*17*, *19*–*22*). Despite this qualitative similarity between the DUB module and the nucleosome interactions mediated by Sir3-BAH (*19*), RCC1 (*21*), and the PRC1 E2-E3 complex (*22*), or by the LANA (*17*) and CENP-C (*20*) peptides, there appear to be no common structural features among these different complexes that specify binding to the acidic patch.

To validate the role of the Sgf11 zinc finger in targeting the DUB module to nucleosomes, we assayed the effects of alanine substitutions at each of the six Sgf11-ZnF arginine residues on deubiquitination of nucleosomes. For these in vitro assays, we used semisynthetic methods to generate H2B-Ub containing a native isopeptide linkage (fig. S8). Substitutions of the three Sgf11 arginines located at the DUB module–nucleosome interface, R78A, R84A, and R91A, markedly reduce the rate at which the DUB module cleaves ubiquitin from H2B in nucleosomes (Fig. 2C). By contrast, Sgf11 substitutions R95A, R98A, and R99A, which are located in a disordered C-terminal tail and are not predicted to be involved in nucleosome binding (Fig. 2B), do not have a substantial effect on DUB module activity. The deleterious effect of the Sgf11 arginine substitutions specifically affects targeting to the nucleosome, as none of the Sgf11 mutations tested has a substantial effect on cleavage of K48-linked diubiquitin, a nonspecific DUB module substrate that is cleaved at roughly $^1/_{10}$ the rate of H2B-Ub (Fig. 2D). Our results are consistent with previous studies showing that substitutions

Downloaded from on February 11, 2016

of Sgf11-ZnF residues R84 and R91 disrupt global H2B deubiquitination in vivo (*10*, *18*). Moreover, yeast bearing mutations in Sgf11 residues R84, R91, or the double R84/R91 mutant display growth defects when combined with *gcn5* deletions (*10*), further consistent with the importance of these residues to DUB module activity.

To test the importance of the H2A/H2B acidic patch to the ability of the SAGA DUB module to deubiquitinate nucleosomal H2B, we assayed DUB module activity on ubiquitinated nucleosomes containing a mutation in the acidic patch. Deubiquitination of H2B in nucleosomes containing the mutant, H2A-E65R, is decreased by a factor of ~100 as compared to deubiquitination of H2B in nucleosomes containing wild-type H2A (Fig. 2E). The importance of the acidic patch is also consistent with a recent report that mutations in the H2A acidic patch give rise to defects in H2B ubiquitination downstream of ubiquitin conjugation (*23*).

The C-terminal helix of H2B, which contains the ubiquitinated residue, K120 (corresponding to K123 in yeast H2B), lies in a depression centered at the Ubp8 active site (Fig. 3A). The close approach of Ubp8 to the C-terminal H2B helix and calculated interface area of 376 Å^2 makes it likely that there are several intermolecular contacts along this interface. In particular, Ubp8 residue Y233 projects toward the C-terminal helix of H2B, with electron density corresponding to that of the tyrosine phenyl ring visible in all four copies of the interface in the crystallographic asymmetric unit (fig. S6D). Model building suggests that H2B residues H106 and S109 in the C-terminal helix of H2B could potentially form van der Waals or hydrogen-bonding interactions with Y233 (Fig. 3A). The remainder of the DUB module is positioned too far from the nucleosome to mediate any contacts, with the exception of the "fingers region" of the Ubp8 ubiquitin-binding pocket, which projects toward the nucleosomal DNA (Fig. 3B). Although no direct contacts can be observed due to

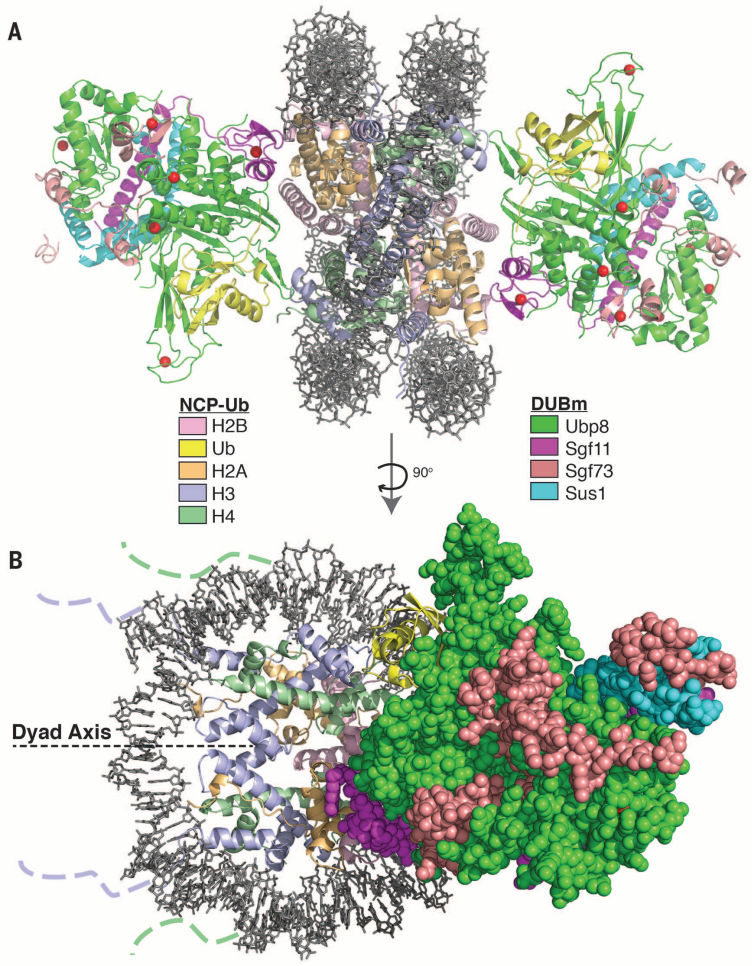

Fig. 1. Overview of the SAGA DUB module bound to the monoubiquitinated nucleosome core particle (NCP-Ub). (**A**) Two DUB modules bind to each NCP-Ub. The catalytic Ubp8 USP domain and the Sgf11 zinc finger contact the substrate. (**B**) View of the complex perpendicular to (A). The nucleosome dyad axis is indicated. Dotted lines indicate where the N-terminal tails of histone H3 and H4 protrude from the DNA gyres.

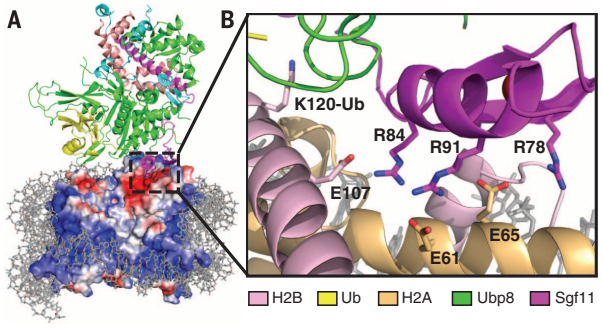

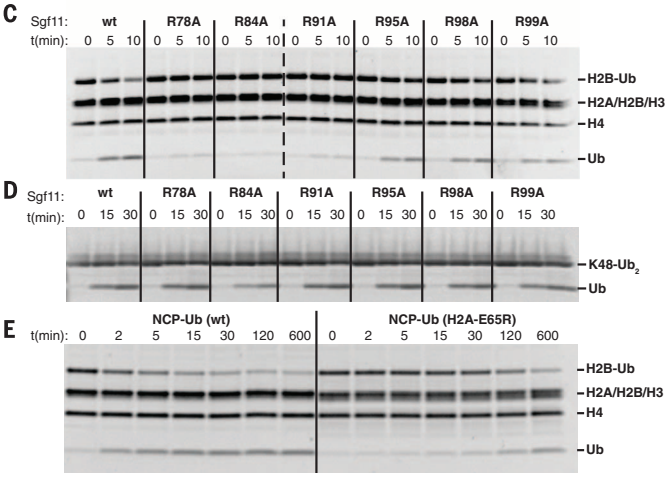

Fig. 2. The DUB module binds the acidic patch of the H2A/H2B heterodimer using the Sgf11 ZnF. (**A**) View of interface between the DUB module and nucleosome showing the electrostatic surface potential of the histone octamer (red, negative; blue, positive). Dashed box indicates region shown in (B). (**B**) Modeled contacts between Sgf11 residues R78, R84, and R91 and acidic patch residues H2A-E65, H2B-E107, and H2A-E61. The ubiquitinated lysine, H2B-K120, is indicated. (**C**) Effect of Sgf11 ZnF mutations on deubiquitination of nucleosomal H2B (NCP-Ub). Monoubiquitinated nucleosomes (2 μM) were incubated with 200 nM wild-type or mutant DUB module for the indicated time. (**D**) Effect of DUB module mutations shown in (C) on cleavage of 2 μM K48-linked diubiquitin (K48-Ub$_2$). (**E**) Effect of acidic patch mutation, H2A-E65R, on deubiquitination of nucleosomal H2B by the DUB module. Conditions as in (C).

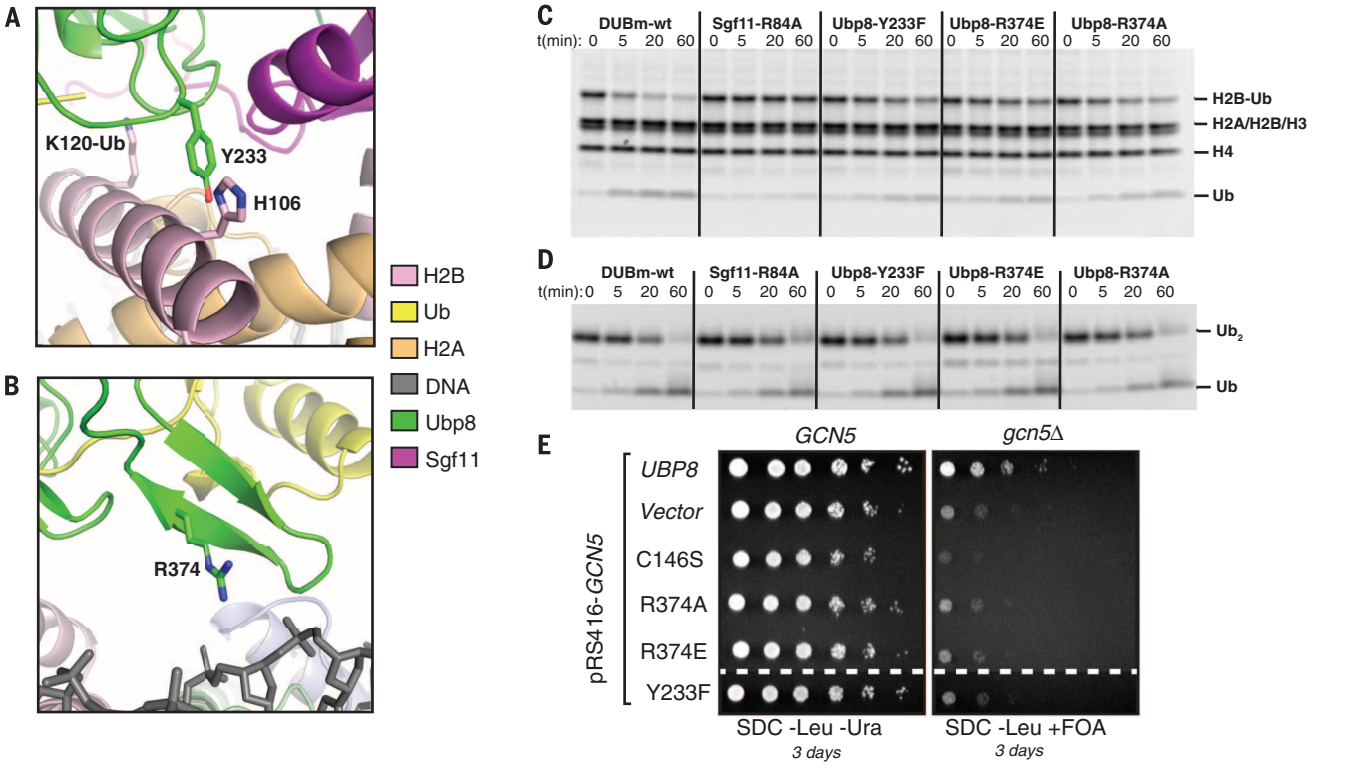

Fig. 3. Contribution of Ubp8 residues to DUB module activity on nucleosomes. (**A**) Ubp8-Y233, which is in a position to form a potential interaction with H2B-H106. (**B**) Modeling showing a potential contact between Ubp8 residue R374 and nucleosomal DNA. (**C**) Activity assay as in Fig. 2C showing effect of Ubp8 mutations Y233F, R374E, and R374A on DUB module activity on H2B-Ub in nucleosomes. Mutant Sgf11-R84A is shown for comparison. (**D**) Activity of DUB module mutants shown in (C) on cleavage of 2 μM K48-linked diubiquitin (Ub_2). (**E**) Synthetic growth assay for effect of Ubp8 mutations in combination with deletion of Gcn5.

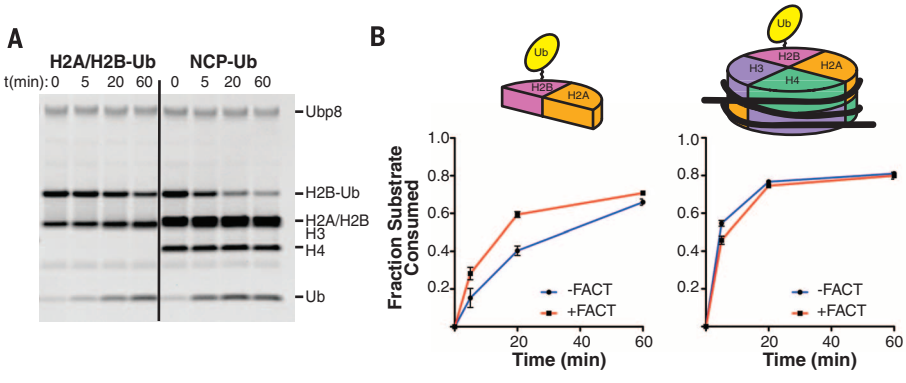

Fig. 4. Activity of the DUB module on monoubiquitinated nucleosomes versus H2A/H2B-Ub in the presence and absence of FACT. (**A**) Time course showing cleavage of H2B-Ub by the DUB module (200 nM) in H2A/H2B dimers (H2A/H2B-Ub, 2 μM) or nucleosomes containing H2B-Ub (NCP-Ub, 1 μM). (**B**) Time course comparing deubiquitination of H2A/H2B-Ub (left) and NCP-Ub (right) in the presence and absence of the FACT complex. Reactions were performed in triplicate; fraction of H2B-Ub consumed was determined by quantitating bands on gels shown in fig. S9).

resolution limits, model building suggests that Ubp8 residue R374 could form electrostatic contacts with the sugar-phosphate backbone of the nucleosomal DNA between bases −32 and −33 (Fig. 3B). Both Y233 and R374 are conserved in fly and human homologs of Ubp8. Mutations Y233F and R374E or R374A in Ubp8 give rise to defects in module activity on nucleosomal H2B-Ub, but not K48-linked diubiquitin (Fig. 3, C and D), suggesting that these residues mediate nucleosome contacts. The effects of the Ubp8 mutations are, however, not as severe as the effects of Sgf11-Znf substitutions in the basic patch (R78, R84, and R91), indicating that Sgf11 contacts with the nucleosome have a greater contribution to substrate specificity. To test the effect of the Ubp8 mutations in yeast, we utilized an assay that was previously used to show that mutations in Sgf11 arginine patch residues give rise to synthetic growth defects (*10*). All three Ubp8 mutations show growth defects comparable to those of a Ubp8 catalytic mutation when combined with a *gcn5* deletion, consistent with their proposed role in Ubp8 activity (Fig. 3E).

In genes regulated by yeast SAGA, FACT binds to H2A/H2B and facilitates nucleosome disassembly and reassembly (*24*), which is required to allow RNA polymerase to transcribe efficiently through chromatin. Recruitment of the FACT complex, Spt16/Pob3/Nhp6 (*25*), is enhanced by H2B monoubiquitination (*6*), although it is not known whether ubiquitin is cleaved from H2B that is still bound to FACT. Because the DUB module almost exclusively contacts H2A/H2B, we tested whether H2A/H2B-Ub alone is a substrate for the DUB module. As shown in Fig. 4A, the DUB module efficiently cleaves ubiquitin from H2A/H2B-Ub heterodimers, albeit about a factor of 5 to 10 more slowly than nucleosomes under the same conditions. We next asked whether FACT binding to the H2A/H2B-Ub heterodimer interferes with DUB module access to H2B-Ub. Structures of the FACT Spt16 subunit (*26*) and Spt16-C peptide bound to an H2A/H2B heterodimer (*27*) indicate that Spt16 does not overlap the DUB module docking surface (fig. S9), although these studies leave open the question of whether the full Spt16/Pob3/Nhp6 FACT complex could interfere with DUB module binding. We preincubated H2A/H2B-Ub heterodimers with

FACT and found that the DUB module could cleave ubiquitin from H2B (Fig. 4B and fig. S10). The rate of H2A/H2B-Ub deubiquitination was somewhat higher in the presence of FACT and is comparable to the rate at which the DUB module deubiquitinates nucleosomes (Fig. 4B). FACT has no effect on the relative rate at which ubiquitin is cleaved from nucleosomes (Fig. 4B), thus ruling out a direct effect of FACT on intrinsic DUB module activity. Our results indicate that the SAGA DUB module can remove ubiquitin from either intact or disassembled nucleosomes and is therefore capable of acting at multiple points as RNA polymerase transcribes through a chromatin template.

Our study provides a framework for understanding global interactions between the SAGA complex and nucleosomes. In addition to the DUB module, SAGA also contains a ~180-kDa subcomplex called the histone acetyltransferase (HAT) module comprising Gcn5, Ada2, Ada3, and Sgf29 (*28*), which acetylates histone H3 N-terminal tails (*29*). The DUB module is located distal to the DNA entry and exit points, where the H3 tails targeted by the HAT module protrude, thus leaving much of the H3/H4 surface exposed and available for interactions with the HAT module or with other SAGA subunits (Fig. 1B). A recent cryo–electron microscopy study of SAGA shows the DUB and HAT modules adjacent to one another, where they could simultaneously engage the same nucleosome (*30*). The Sgf73 SCA7 domain (residues 209 to 280), a nonspecific DNA binding domain that is not present in the fragment used in our crystallographic study, is located between the DUB and HAT modules, where the SCA7 domain could potentially help to position a nucleosome. However, we note that the reported positioning of an unmodified nucleosome relative to the DUB module in intact SAGA (*30*) does not agree with our structure. Given the large contribution of the ubiquitin modification itself to the total interface between ubiquitinated nucleosomes and the DUB module, docking of the DUB module in a manner that mimics the catalytically competent complex is likely predicated on the presence of ubiquitinated H2B.

The structure of the yeast SAGA DUB module bound to ubiquitinated nucleosomes provides a basis for understanding how the human SAGA DUB module engages its H2B-Ub substrate in a chromatin context. The human DUB module comprises USP22, ATXN7L3, ATXN7, and ENY2, homologs of yeast Ubp8, Sgf11, Sgf73, and Sus1, respectively (*31*). The key residues implicated here in yeast DUB module function, including a three-arginine cluster on Sgf11 and residues Y233 and R374 in Ubp8, are conserved in ATXN7 and USP22, respectively. Our structure also accounts for the recent report that H2B deubiquitination by the SAGA DUB module is regulated in both humans and yeast by a newly discovered histone modification, phosphorylation of H2A-Y57/58 (human/yeast) (*32*). This H2A residue lies at the DUB module–nucleosome interface in our structure, where it could readily interfere with the observed docking of the DUB module on H2A/H2B (fig. S12). Further studies will be needed to interrogate the mechanistic details of how H2A–Y57/58 phosphorylation influences DUB module activity.

REFERENCES AND NOTES

1. J. Bonnet, D. Devys, L. Tora, *Drug Discov. Today. Technol.* **12**, e19–e27 (2014).
2. G. Fuchs, M. Oren, *Biochim. Biophys. Acta* **1839**, 694–701 (2014).
3. A. Wood *et al.*, *Mol. Cell* **11**, 267–274 (2003).
4. Z. W. Sun, C. D. Allis, *Nature* **418**, 104–108 (2002).
5. R. K. McGinty, J. Kim, C. Chatterjee, R. G. Roeder, T. W. Muir, *Nature* **453**, 812–816 (2008).
6. A. B. Fleming, C. F. Kao, C. Hillyer, M. Pikaart, M. A. Osley, *Mol. Cell* **31**, 57–66 (2008).
7. R. Pavri *et al.*, *Cell* **125**, 703–717 (2006).
8. K. W. Henry *et al.*, *Genes Dev.* **17**, 2648–2663 (2003).
9. N. L. Samara *et al.*, *Science* **328**, 1025–1029 (2010).
10. A. Köhler, E. Zimmerman, M. Schneider, E. Hurt, N. Zheng, *Cell* **141**, 606–617 (2010).
11. Y. Han, J. Luo, J. Ranish, S. Hahn, *EMBO J.* **33**, 2534–2546 (2014).
12. G. Spedale, H. T. Timmers, W. W. Pijnappel, *Genes Dev.* **26**, 527–541 (2012).
13. N. L. Samara, A. E. Ringel, C. Wolberger, *Structure* **20**, 1414–1424 (2012).
14. M. Yan, C. Wolberger, *J. Mol. Biol.* **427**, 1765–1778 (2015).
15. A. Köhler, M. Schneider, G. G. Cabal, U. Nehrbass, E. Hurt, *Nat. Cell Biol.* **10**, 707–715 (2008).
16. D. Vasudevan, E. Y. Chua, C. A. Davey, *J. Mol. Biol.* **403**, 1–10 (2010).
17. A. J. Barbera *et al.*, *Science* **311**, 856–861 (2006).
18. C. Koehler *et al.*, *J. Biol. Chem.* **289**, 8989–8999 (2014).
19. K. J. Armache, J. D. Garlick, D. Canzio, G. J. Narlikar, R. E. Kingston, *Science* **334**, 977–982 (2011).
20. H. Kato *et al.*, *Science* **340**, 1110–1113 (2013).
21. R. D. Makde, J. R. England, H. P. Yennawar, S. Tan, *Nature* **467**, 562–566 (2010).
22. R. K. McGinty, R. C. Henrici, S. Tan, *Nature* **514**, 591–596 (2014).
23. C. E. Cucinotta, A. N. Young, K. M. Klucevsek, K. M. Arndt, *PLOS Genet.* **11**, e1005420 (2015).
24. R. Belotserkovskaya *et al.*, *Science* **301**, 1090–1093 (2003).
25. T. Formosa *et al.*, *EMBO J.* **20**, 3506–3517 (2001).
26. M. Hondele *et al.*, *Nature* **499**, 111–114 (2013).
27. D. J. Kemble, L. L. McCullough, F. G. Whitby, T. Formosa, C. P. Hill, *Mol. Cell* **60**, 294–306 (2015).
28. K. K. Lee *et al.*, *Mol. Syst. Biol.* **7**, 503 (2011).
29. R. Balasubramanian, M. G. Pray-Grant, W. Selleck, P. A. Grant, S. Tan, *J. Biol. Chem.* **277**, 7989–7995 (2002).
30. A. Durand, J. Bonnet, M. Fournier, V. Chavant, P. Schultz, *Structure* **22**, 1553–1559 (2014).
31. X. Y. Zhang *et al.*, *Mol. Cell* **29**, 102–111 (2008).
32. H. Basnet *et al.*, *Nature* **516**, 267–271 (2014).

ACKNOWLEDGMENTS

We thank T. Formosa for the generous gift of purified FACT and S. Tan for the plasmid, pST55-16x601. We thank X. Zhang for assistance with protein purification, P. Lombardi for assistance with data collection, and D. Leahy for helpful discussions. Supported by grant GM-095822 from the National Institute of General Medical Sciences (C.W.) and by a Ruth L. Kirschstein National Research Service Award (M.M.). A.B. is a Neubauer Professor and a Taub Foundation Fellow. GM/CA @ APS has been funded by the National Cancer Institute (Y1-CO-1020) and the National Institute of General Medical Sciences (Y1-GM-1104). Use of the Advanced Photon Source was supported by the U.S. Department of Energy, Basic Energy Sciences, Office of Science, under contract no. DE-AC02-06CH11357. Coordinates and data have been deposited in the Protein Data Bank with accession code 4ZUX. Plasmid pST55-16xNCP601 expressing the Widom 601 DNA fragment was obtained from S. Tan under a material transfer agreement with Pennsylvania State University.

SUPPLEMENTARY MATERIALS

www.sciencemag.org/content/351/6274/725/suppl/DC1
Materials and Methods
Figs. S1 to S12
Table S1
References (*33*–*48*)

29 May 2015; accepted 15 December 2015
10.1126/science.aac5681

Downloaded from on February 11, 2016

METABOLISM

mTORC1 induces purine synthesis through control of the mitochondrial tetrahydrofolate cycle

Issam Ben-Sahra,[1]* Gerta Hoxhaj,[1]* Stéphane J. H. Ricoult,[1] John M. Asara,[2] Brendan D. Manning[1]†

In response to growth signals, mechanistic target of rapamycin complex 1 (mTORC1) stimulates anabolic processes underlying cell growth. We found that mTORC1 increases metabolic flux through the de novo purine synthesis pathway in various mouse and human cells, thereby influencing the nucleotide pool available for nucleic acid synthesis. mTORC1 had transcriptional effects on multiple enzymes contributing to purine synthesis, with expression of the mitochondrial tetrahydrofolate (mTHF) cycle enzyme methylenetetrahydrofolate dehydrogenase 2 (MTHFD2) being closely associated with mTORC1 signaling in both normal and cancer cells. *MTHFD2* expression and purine synthesis were stimulated by activating transcription factor 4 (ATF4), which was activated by mTORC1 independent of its canonical induction downstream of eukaryotic initiation factor 2α eIF2α phosphorylation. Thus, mTORC1 stimulates the mTHF cycle, which contributes one-carbon units to enhance production of purine nucleotides in response to growth signals.

The mechanistic target of rapamycin complex 1 (mTORC1) kinase integrates diverse growth signals to control nutrient-consuming biosynthetic processes, such as protein and lipid synthesis (*1*). mTORC1 also acutely stimulates the de novo synthesis of pyrimidine nucleotides through a posttranslational mechanism leading to increased intracellular pools of pyrimidines available for RNA and DNA synthesis (*2*, *3*). Whether mTORC1 also influences

the synthesis of purine nucleotides is unknown. Purines are enzymatically assembled on a 5-phosphoribosyl pyrophosphate (PRPP) molecule derived from the pentose phosphate pathway, with carbon and nitrogen moieties donated by nonessential amino acids and one-carbon formyl units from the tetrahydrofolate (THF) cycle (Fig. 1A).

To determine whether mTORC1 signaling affects de novo purine synthesis, we used targeted liquid chromatography–tandem mass spectrometry (LC-MS/MS) to measure relative flux of stable isotope-labeled glutamine (amide-^{15}N), which is incorporated into the purine ring at two positions (Fig. 1A). mTORC1 activation in response to both genetic [*tuberous sclerosis complex 2* (*Tsc2*) null mouse embryo fibroblasts (MEFs)] and physiologic (insulin treatment of wild-type MEFs) stimuli resulted in increased amounts of doubly labeled ^{15}N-purine intermediates, and this labeling was attenuated in cells treated for 12 to 16 hours with the mTORC1 inhibitor rapamycin (Fig. 1, B and D, and fig. S1, A to E). Unlike de novo pyrimidine synthesis, measured in the same metabolite extracts as the intermediate ^{15}N-carbamoyl-aspartate (Fig. 1, C and E, and fig. S1C) (*2*, *3*), a shorter 1-hour stimulation with

[1]Department of Genetics and Complex Diseases, Harvard T. H. Chan School of Public Health, Boston, MA 02115, USA. [2]Division of Signal Transduction, Beth Israel Deaconess Medical Center and Department of Medicine, Harvard Medical School, Boston, MA 02115, USA.
*These authors contributed equally to this work. †Corresponding author. E-mail: bmanning@hsph.harvard.edu

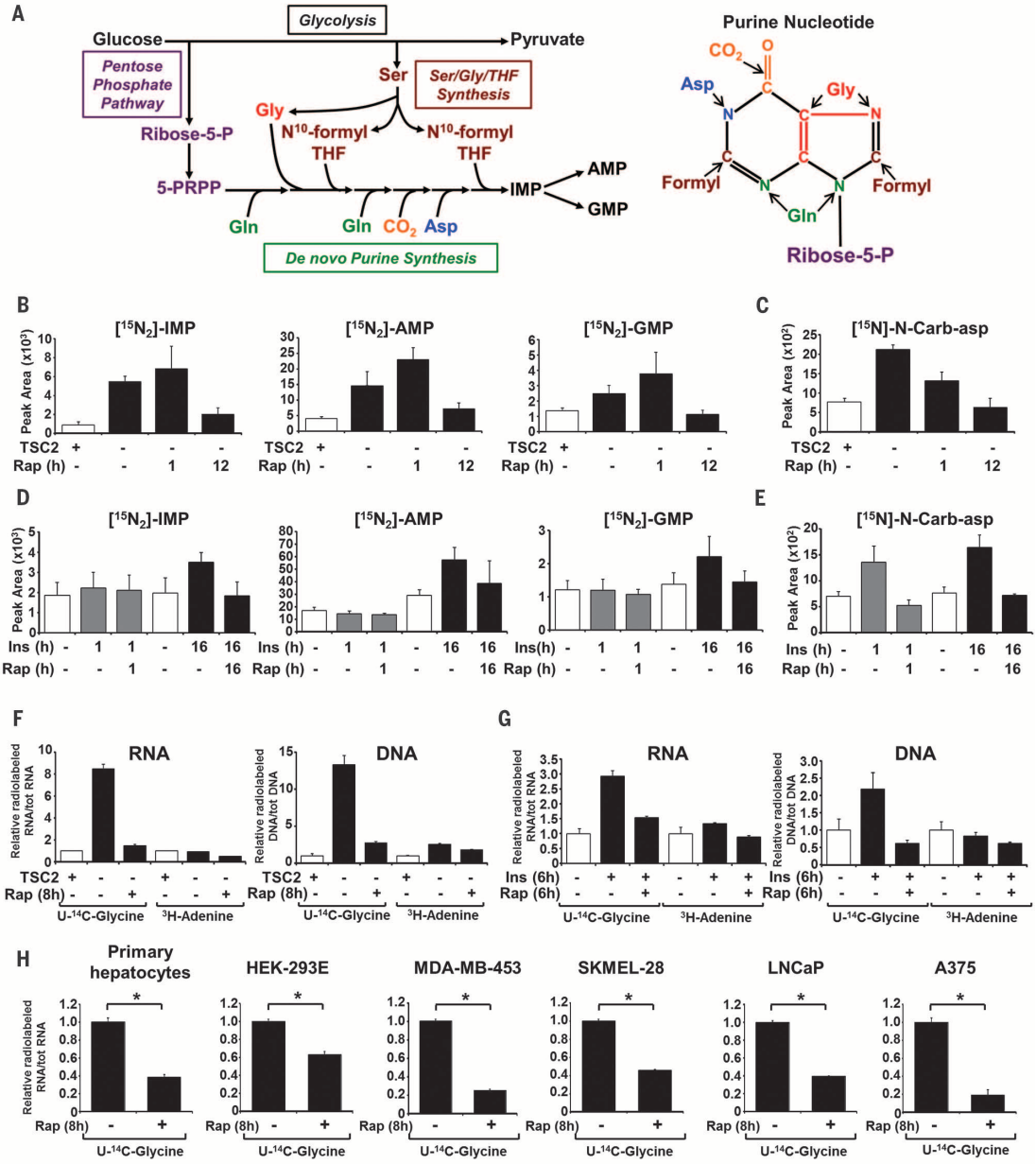

Fig. 1. mTORC1 stimulates de novo purine synthesis. (**A**) Schematic of the de novo purine synthesis pathway. (**B** and **C**) Normalized peak areas of ^{15}N-labeled intermediates of purine (B) and pyrimidine (C) synthesis, measured by targeted LC-MS/MS, from serum-deprived *Tsc2*$^{+/+}$ and *Tsc2*$^{-/-}$ MEFs treated with vehicle or rapamycin (20 nM) for 1 hour or 12 hours and labeled (20 min) with ^{15}N-glutamine. (**D** and **E**) Metabolite abundance from wild-type MEFs treated as in (B) and (C) but stimulated with insulin (500 nM) for 1 hour or 16 hours. (**F** and **G**) Relative incorporation of radiolabel from ^{14}C-glycine or ^{3}H-adenine into RNA and DNA from serum-deprived *Tsc2*$^{+/+}$ and *Tsc2*$^{-/-}$ MEFs treated with vehicle or rapamycin (8 hours, 20 nM) (F) or wild-type MEFs stimulated with insulin (6 hours, 100 nM) with or without rapamycin. (**H**) The given cells were labeled as in (F). [(B) to (H)] Data are presented as mean ± SD of biological triplicates and are representative of at least two independent experiments. *$P < 0.05$ by two-tailed Student's t test.

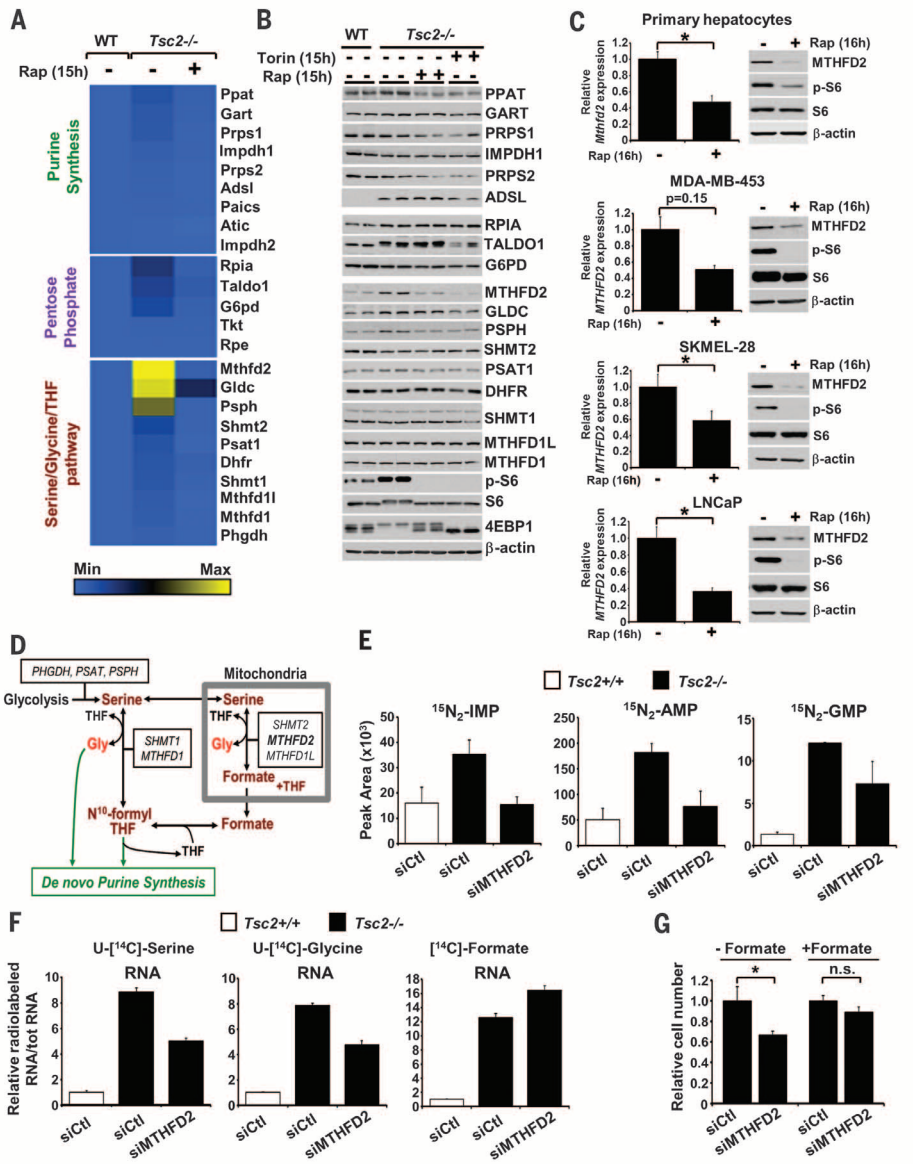

Fig. 2. MTHFD2 is induced downstream of mTORC1 and is required for de novo purine synthesis. (**A**) Heat map of relative gene expression in serum-deprived MEFs treated 15 hours with vehicle or rapamycin (20 nM). Transcripts listed from highest to lowest fold increase in *Tsc2*$^{-/-}$ relative to *Tsc2*$^{+/+}$ MEFs for each category. (**B**) Immunoblots from cells treated as in (A), but also with Torin 1 (250 nM) treatment. Biological duplicates shown. (**C**) MTHFD2 transcript (graphs) and protein (immunoblots) abundance in the given cell lines treated with vehicle or rapamycin (20 nM, 16 hours). (**D**) Schematic of serine synthesis, cytosolic and mitochondrial THF pathways, and their relation to de novo purine synthesis. (**E**) Normalized peak areas of ^{15}N-labeled purine intermediates, measured by targeted LC-MS/MS, from *Tsc2*$^{+/+}$ and *Tsc2*$^{-/-}$ MEFs 48 hours after transfection with *Mthfd2* siRNAs or nontargeting controls (siCtl) and labeled (20 min) with ^{15}N-glutamine. (**F**) Relative incorporation of radiolabel from ^{14}C-serine, ^{14}C-glycine, or ^{14}C-formate (8-hour labeling) into RNA from *Tsc2*$^{+/+}$ and *Tsc2*$^{-/-}$ MEFs treated as in (E). (**G**) Relative cell number 96 hours after transfecting *Tsc2*$^{-/-}$ MEFs as in (E), with growth in low (1%) serum with or without formate (1 mM) for final 60 hours. [(C), (E), (F), and (G)] Data are graphed as mean ± SD of biological triplicates and are representative of at least two independent experiments. *P < 0.05 by two-tailed Student's t test.

insulin or treatment with rapamycin failed to respectively increase or decrease purine flux (Fig. 1, B and D, and fig. S1, B and D). Similar results were obtained when flux from ^{13}C-glycine into purine intermediates was measured (fig. S1F). mTORC1 activation through either loss of *Tsc2* or stimulation of cells with insulin increased flux through de novo purine synthesis into nucleic acids, as measured by ^{14}C-glycine incorporation into RNA and DNA, without pronounced effects on the incorporation of an exogenously provided purine base (^{3}H-adenine) (Fig. 1, F and G, and fig. S1, G to J). Likewise, rapamycin decreased ^{14}C-glycine flux into RNA in primary mouse hepatocytes and a panel of human cell lines (Fig. 1H).

The delayed timing of the respective inhibitory and stimulatory effects of rapamycin and insulin on purine synthesis, relative to that of pyrimidine synthesis (*2*, *3*), suggested that mTORC1 might regulate this pathway through transcriptional mechanisms. Transcripts for specific enzymes within the purine pathway or essential supporting pathways, including the pentose phosphate pathway, serine synthesis, and the THF cycle (fig. S2A), were increased in *Tsc2*-deficient cells and sensitive to rapamycin treatment (Fig. 2A and fig. S2, B to D). Among these genes, *methylenetetrahydrofolate dehydrogenase 2* (*Mthfd2*), encoding an enzyme in the mTHF cycle, showed the greatest mTORC1-dependent induction. Of those genes altered by mTORC1 signaling, *Mthfd2* was among the few that also showed corresponding changes in protein abundance, which were sensitive to both rapamycin and the mTOR kinase inhibitor Torin 1 (Fig. 2B). MTHFD2 was reduced in cells treated with rapamycin for 8 hours (fig. S3A), which was also sufficient to reduce de novo purine synthesis in these cells (Fig. 1F).

Expression of MTHFD2 was broadly regulated by mTORC1 signaling in distinct settings. Insulin increased MTHFD2 mRNA and protein in a rapamycin-sensitive manner in wild-type MEFs (fig. S3, B and C), and these were also decreased by rapamycin in primary mouse hepatocytes and various human cancer cell lines (Fig. 2C and fig. S3D). MTHFD2 is the most highly overexpressed metabolic enzyme in human cancers (*4*). Our data suggest that mTORC1, which is frequently activated in cancer (*5*), might contribute to increased MTHFD2 expression in tumors. In 859 human breast cancer samples (*6*), elevated mTORC1 signaling, as scored by the abundance of phospho-S6, was associated with increased expression of *MTHFD2* and other mTHF cycle genes and, to a lesser extent, enzymes of the serine synthesis pathway. mTORC1 activation did not correlate with expression of cytosolic THF cycle genes (fig. S3, E to G).

The cytosolic and mitochondrial THF cycles produce one-carbon formyl groups for various cellular processes, including de novo purine synthesis (Fig. 2D and fig. S2A) (*7*–*11*). To determine whether the mTORC1-mediated induction of

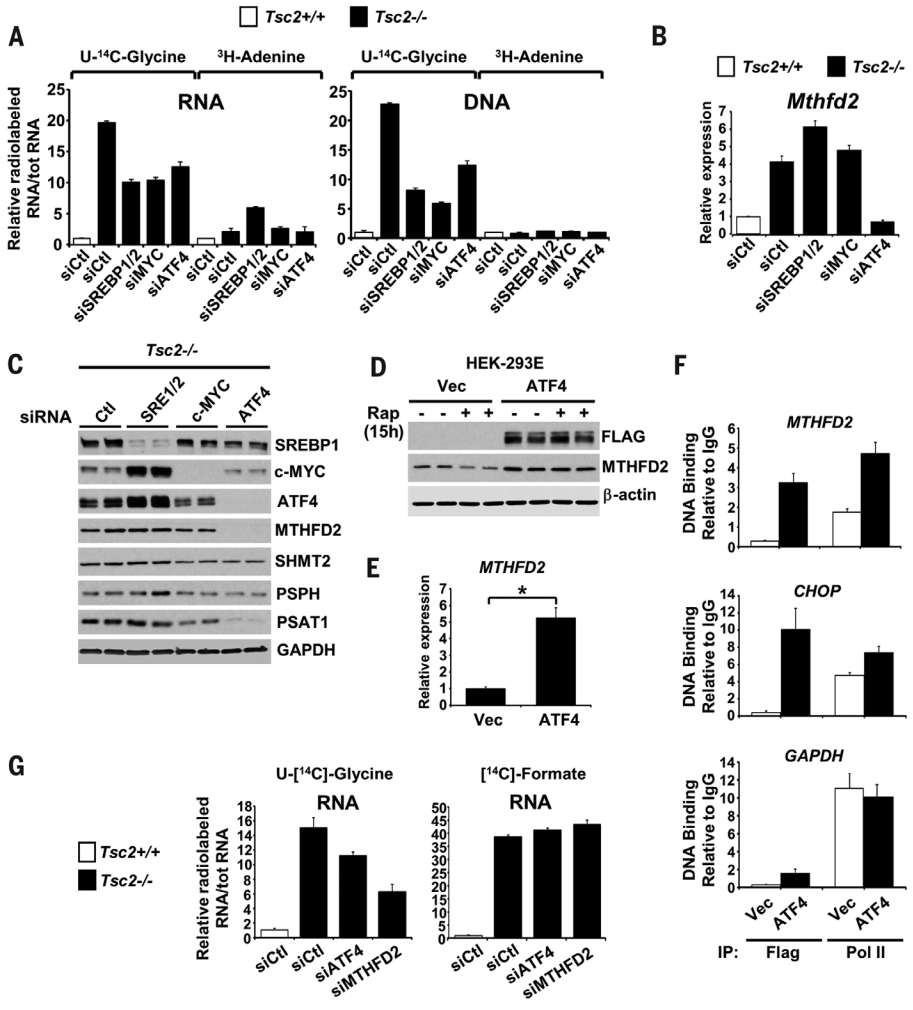

Fig. 3. ATF4 is required for mTORC1 to induce MTHFD2 expression and purine synthesis. (**A**) Relative incorporation of radiolabel from ^{14}C-glycine or ^{3}H-adenine (8-hour labeling) into RNA and DNA from *Tsc2*$^{+/+}$ and *Tsc2*$^{-/-}$ MEFs transfected with the indicated siRNAs is shown relative to that from *Tsc2*$^{+/+}$ MEFs with control siRNAs. (**B**) Relative *Mthfd2* transcript amounts from cells transfected as in (A). (**C**) Immunoblots of proteins in *Tsc2*$^{-/-}$ MEFs transfected as in (A). (**D**) Immunoblots from HEK293E cells expressing empty vector (Vec) or Flag-ATF4 (ATF4) treated, where indicated, with rapamycin (15 hours, 20 nM). [(C) and (D)] Biological duplicates shown. (**E**) *MTHFD2* transcript abundance from cells transfected as in (D). *P < 0.05 by two-tailed Student's t test. (**F**) Cells transfected as in (D) were subjected to ChIP with control immunoglobulin G, antibodies to Flag, or antibodies to Pol II. Bound promoter regions for the given genes were quantified and shown normalized to control IgG. (**G**) Relative incorporation of radiolabel from ^{14}C-glycine or ^{14}C-formate (8-hour labeling) into RNA from *Tsc2*$^{+/+}$ and *Tsc2*$^{-/-}$ MEFs transfected with the indicated siRNAs is shown as in (A). [(A), (B), (E), (F), and (G)] Data are mean ± SD of biological triplicates and are representative of at least two independent experiments.

MTHFD2 contributes to purine synthesis, we measured the effects of small interfering RNA (siRNA)–mediated depletion of MTHFD2 on flux from ^{15}N-glutamine into purine intermediates. Indeed, MTHFD2 depletion lowered flux through de novo purine synthesis without affecting mTORC1 signaling (Fig. 2E and fig. S3, H and I). Formate produced by the mTHF cycle can exit the mitochondria and be converted to the one-carbon donor N^{10}-formyl THF in the cytosol (Fig. 2D and fig. S2A). *Tsc2*-null cells with activated mTORC1 displayed enhanced incorporation into RNA of radiolabeled carbon from multiple substrates specific for purine synthesis, including ^{14}C-serine, ^{14}C-glycine, and ^{14}C-formate. Depletion of MTHFD2 decreased the incorporation from ^{14}C-serine and ^{14}C-glycine but did not influence incorporation of ^{14}C-formate (Fig. 2F and fig. S4A). These data suggest that MTHFD2 is required for the mTORC1-induced increase in purine synthesis because it increases formate production, with exogenous formate bypassing the need for this enzyme. This is further supported by the fact that MTHFD2 depletion consistently slowed proliferation in *Tsc2*$^{-/-}$ MEFs, without substantial effects on cell size, and exogenous formate attenuated this effect (Fig. 2I and fig. S4, B and C). MTHFD2 depletion also blocked ^{14}C-glycine incorporation into RNA in five human cell lines, and, similar to mTORC1 depletion with Raptor siRNAs, loss of MTHFD2 slowed proliferation of these cells (fig. S4, D and E).

We also measured effects of candidate transcription factors downstream of mTORC1 (*12*–*15*) on incorporation of ^{14}C-glycine into RNA and DNA. Of the six transcription factors tested, depletion of the sterol regulatory element binding proteins (SREBP1 and 2), c-Myc, or activating transcription factor 4 (ATF4) specifically attenuated the increase in de novo purine synthesis in *Tsc2*-deficient cells, without decreasing incorporation of ^{3}H-adenine (Fig. 3A and fig. S5A). Of these three transcription factors, only depletion of ATF4 decreased MTHFD2 transcripts and protein in *Tsc2*-deficient cells (Fig. 3, B and C) and abolished MTHFD2 protein in wild-type MEFs stimulated with insulin and in human embryonic kidney 293E (HEK293E) cells (fig. S5, B and C). ATF4 depletion also decreased mRNA for another mTHF gene (*Shmt2*), as well as genes of the serine synthesis pathway (*Psat1* and *Psph*), with lesser effects on their protein products (Fig. 3C and fig. S5D) (*16*, *17*). Consistent with the role of these enzymes in de novo purine synthesis, ATF4 depletion blocked the mTORC1-induced increase in flux from ^{15}N-glutamine into purine intermediates (fig. S5E).

Overexpression of an ATF4 cDNA lacking its 5′-untranslated region increased the abundance of MTHFD2 mRNA and protein and rendered its expression resistant to rapamycin (Fig. 3, D and E), without effects on the cytosolic isoform, MTHFD1 (fig. S5F). Alignment of the human, mouse, and rat *MTHFD2* promoters revealed a highly conserved, consensus DNA-binding motif for ATF4 (fig. S5G). Chromatin immunoprecipitation (ChIP) assays demonstrated that ATF4 bound to the *MTHFD2* promoter, and ATF4 expression increased Pol II binding to this promoter (Fig. 3F). As controls, ATF4 bound the promoter of its established target *CHOP* but not *GAPDH*. Like loss of MTHFD2, depletion of ATF4 decreased flux from ^{14}C-glycine into RNA but failed to block incorporation of ^{14}C-formate (Fig. 3G and fig. S5H). Thus, MTHFD2 is a transcriptional target of ATF4, and ATF4 promotes de novo purine synthesis, at least in part, through its regulation of formate production by the mTHF cycle.

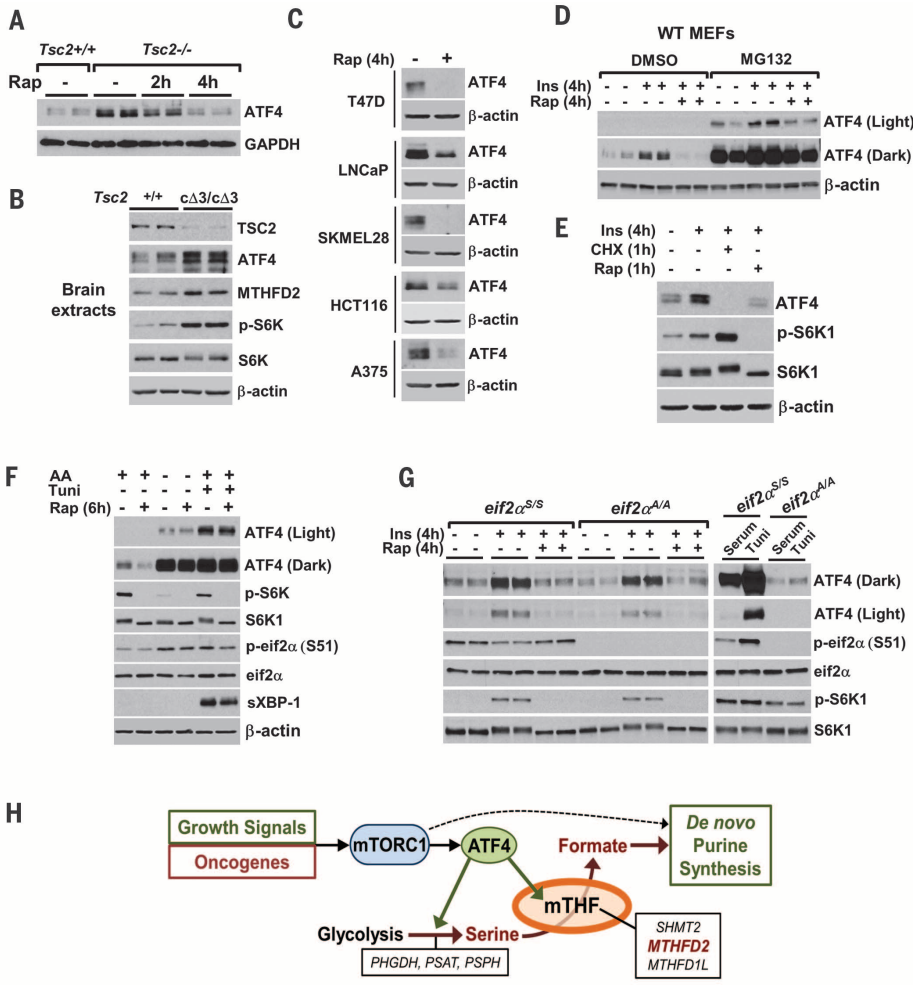

Fig. 4. mTORC1 activates ATF4 independent of cellular stress responses. (**A**) ATF4 abundance in MEFs deprived of serum (15 hours) and treated with rapamycin (20 nM). (**B**) Immunoblots of brain lysates from mice with neuron-specific deletion of *Tsc2* exon 3 (cΔ3/cΔ3) compared with wild-type. (**C**) Amounts of ATF4 in cancer cell lines treated 4 hours with rapamycin (20 nM). (**D**) Amounts of ATF4 in MEFs deprived of serum (15 hours), treated with vehicle or MG132 (2 μM), with or without rapamycin (20 nM), for 30 min before insulin stimulation (4 hours). (**E**) Immunoblots of proteins in MEFs treated with insulin (4 hours, 500 nM) and, for the final hour, cycloheximide (10 μM) or rapamycin (20 nM). (**F**) Immunoblots of proteins from MEFs grown in dialyzed serum and deprived of amino acids (6 hours) or treated with tunicamycin (6 hours, 2 μg/ml) with or without rapamycin (20 nM). (**G**) Immunoblots of proteins from eIF2α S/S or A/A MEFs deprived of serum (16 hours), treated with rapamycin (30 min, 20 nM), then stimulated with insulin (4 hours, 500 nM). (Right) Cells grown in serum were treated with tunicamycin (4 hours, 2 μg/ml). [(A), (B), (D), and (G)] Biological duplicates are shown. (**H**) Model of findings.

ATF4 DNA-binding elements are overrepresented in the promoters of mTORC1-regulated genes (*12*), which suggests that mTORC1 might activate ATF4. *Tsc2*-deficient cells had increased ATF4 that was lowered by 2 to 4 hours of rapamycin treatment (Fig. 4A). Loss of TSC2 function in mouse neurons, through conditional deletion of exon 3 (*18*), activated mTORC1 signaling and increased both ATF4 and its target MTHFD2 in the brain (Fig. 4B). Treatment of a panel of cancer cell lines, primary mouse hepatocytes, or HEK293E cells with rapamycin for 4 hours or less decreased ATF4 (Fig. 4C and fig. S6, A and B). The shorter-term effects of mTORC1 inhibition with rapamycin or activation with insulin did not correspond with changes in ATF4 transcripts (fig. S6, B and C), but prolonged stimulation or inhibition of mTORC1 caused transcriptional changes (fig. S6D) (*16*). Treatment of cells with the proteasome inhibitor MG132 increased ATF4 but did not affect its regulation by mTORC1 (Fig. 4D). Therefore, the primary mechanism of regulation of ATF4 by mTORC1 is neither through transcription nor stability, nor does it appear to influence nuclear shuttling of ATF4 (fig. S6E). The insulin-stimulated increase in ATF4 was blocked in cells upon inhibition of translation with cycloheximide (Fig. 4E) but was unaffected by inhibition of transcription with actinomycin D (fig. S6F). Thus, mTORC1 appears to increase ATF4 abundance by promoting its translation.

The translation of ATF4 is well established to be regulated downstream of eukaryotic initiation factor 2α (eIF2α) phosphorylation on Ser^{51} in response to cellular stresses, including amino acid deprivation and endoplasmic reticulum (ER) stress (*19*–*21*). Unlike growth factor–induced ATF4, the up-regulation of ATF4 upon amino acid starvation or exposure to the ER stress–inducing agent tunicamycin was largely resistant to rapamycin (Fig. 4F). The induction of ATF4 by tunicamycin was abolished in a $Ser^{51}Ala$ knock-in mutant of eIF2α (A/A) (*21*), but the insulin-stimulated, rapamycin-sensitive increase in ATF4 was similar between these cells and their wild-type (S/S) counterparts (Fig. 4G). These data reveal a regulatory input from mTORC1 to ATF4 that is independent of its established mechanism of regulation by cellular stress.

This study adds purine synthesis to the list of anabolic processes induced by mTORC1 in both normal and cancer cells (*1*). In response to growth signals, mTORC1 activates ATF4, which stimulates expression of MTHFD2 and other enzymes of the serine synthesis and mTHF cycle, thereby increasing production of formyl units required for de novo purine synthesis (Fig. 4H).

REFERENCES AND NOTES

1. C. C. Dibble, B. D. Manning, *Nat. Cell Biol.* **15**, 555–564 (2013).
2. I. Ben-Sahra, J. J. Howell, J. M. Asara, B. D. Manning, *Science* **339**, 1323–1328 (2013).
3. A. M. Robitaille *et al.*, *Science* **339**, 1320–1323 (2013).
4. R. Nilsson *et al.*, *Nat. Commun.* **5**, 3128 (2014).
5. S. Menon, B. D. Manning, *Oncogene* **27** (suppl. 2), S43–S51 (2008).
6. Cancer Genome Atlas Network, *Nature* **490**, 61–70 (2012).
7. J. Fan *et al.*, *Nature* **510**, 298–302 (2014).
8. C. F. Labuschagne, N. J. van den Broek, G. M. Mackay, K. H. Vousden, O. D. Maddocks, *Cell Rep.* **7**, 1248–1258 (2014).
9. M. Mehrmohamadi, X. Liu, A. A. Shestov, J. W. Locasale, *Cell Rep.* **9**, 1507–1519 (2014).
10. C. A. Lewis *et al.*, *Mol. Cell* **55**, 253–263 (2014).
11. J. W. Locasale, *Nat. Rev. Cancer* **13**, 572–583 (2013).
12. K. Düvel *et al.*, *Mol. Cell* **39**, 171–183 (2010).
13. Y. Zhang *et al.*, *Nature* **513**, 440–443 (2014).
14. A. Csibi *et al.*, *Curr. Biol.* **24**, 2274–2280 (2014).
15. C. C. Hudson *et al.*, *Mol. Cell. Biol.* **22**, 7004–7014 (2002).
16. C. M. Adams, *J. Biol. Chem.* **282**, 16744–16753 (2007).
17. J. Ye *et al.*, *Proc. Natl. Acad. Sci. U.S.A.* **109**, 6904–6909 (2012).
18. E. Yuan *et al.*, *Hum. Mol. Genet.* **21**, 4286–4300 (2012).
19. H. P. Harding *et al.*, *Mol. Cell* **6**, 1099–1108 (2000).

20. H. P. Harding *et al.*, *Mol. Cell* **11**, 619–633 (2003).
21. D. Scheuner *et al.*, *Mol. Cell* **7**, 1165–1176 (2001).

ACKNOWLEDGMENTS

We thank D. J. Kwiatkowski and R. J. Kaufman for materials and M. Yuan, S. Breitkopf, J. J. Howell, M. Turner, and Y. Zhang for technical assistance. This research was supported by grants from the Bettencourt Foundation and LAM Foundation (I.B.-S.), TS Alliance (G.H.), NSF fellowship DGE-1144152 (S.J.H.R.), and NIH grants K99-CA194192 (I.B.-S.), P01-CA120964 (J.M.A. and B.D.M.), P30-CA006516 (J.M.A.), and R01-CA181390 and R35-CA197459 (B.D.M.). I.B.-S. and G.H. conceived, performed, and analyzed all experiments and prepared the manuscript. S.J.H.R performed the Cancer Genome Atlas analysis. J.M.A. performed LC-MS/MS experiments. B.D.M. directed research, reviewed all data, and prepared the manuscript. All authors reviewed the manuscript and declare no competing financial interests.

SUPPLEMENTARY MATERIALS

www.sciencemag.org/content/351/6274/728/suppl/DC1
Materials and Methods
Figs. S1 to S6
Tables S1 and 2
References (*22*, *23*)

17 July 2015; accepted 11 December 2015
10.1126/science.aad0489

BIOCHEMISTRY

Spatial colocalization and functional link of purinosomes with mitochondria

Jarrod B. French,[1]*† Sara A. Jones,[2]†‡ Huayun Deng,[3] Anthony M. Pedley,[4] Doory Kim,[2,6] Chung Yu Chan,[5] Haibei Hu,[3]§ Raymond J. Pugh,[4] Hong Zhao,[4] Youxin Zhang,[2] Tony Jun Huang,[5] Ye Fang,[3]* Xiaowei Zhuang,[2,6,7]* Stephen J. Benkovic[4]*

Purine biosynthetic enzymes organize into dynamic cellular bodies called purinosomes. Little is known about the spatiotemporal control of these structures. Using super-resolution microscopy, we demonstrated that purinosomes colocalized with mitochondria, and these results were supported by isolation of purinosome enzymes with mitochondria. Moreover, the number of purinosome-containing cells responded to dysregulation of mitochondrial function and metabolism. To explore the role of intracellular signaling, we performed a kinome screen using a label-free assay and found that mechanistic target of rapamycin (mTOR) influenced purinosome assembly. mTOR inhibition reduced purinosome-mitochondria colocalization and suppressed purinosome formation stimulated by mitochondria dysregulation. Collectively, our data suggest an mTOR-mediated link between purinosomes and mitochondria, and a general means by which mTOR regulates nucleotide metabolism by spatiotemporal control over protein association.

Purine levels in mammalian cells are maintained by the coordinated action of complementary salvage and de novo biosynthetic pathways. Whereas the salvage pathway maintains purine nucleotide levels under normal physiological conditions, the de novo pathway is up-regulated during growth (*1*, *2*) and altered in neoplastic cells (*3*, *4*). Purinosomes are mesoscale assemblies formed to protect unstable intermediates and increase metabolic flux through the de novo pathway (*5*–*9*). These structures are dynamic, form reversibly in response to purine depletion, and act to increase de novo purine biosynthesis (*5*, *6*, *10*). Their formation is cell cycle dependent and can be regulated by G protein–coupled receptor (GPCR) agonists and casein kinase 2 (*11*–*14*). An increased number of purinosome-containing cells correlates positively with the degree of purine salvage deficiency in Lesch-Nyhan disease (*15*). Cellular conditions resulting in disruption of purinosome formation led to enhanced sensitivity to cancer chemotherapeutics (*16*). An analogous cellular phenotype was also recently reported for a multifunctional protein involved in pyrimidine biosynthesis (*17*). These structures are examples of an increasing number of reported higher-order organizations involving metabolic proteins (*7*, *18*, *19*).

Considering that de novo purine biosynthesis not only provides the nucleotide precursors necessary for mitochondrial adenosine 5′-triphosphate (ATP) production but also conversely demands ATP for its operation, we hypothesized that a synergistic relationship between purinosomes and mitochondria might exist. This synergy would be even more critical in cells that preferentially use oxidative phosphorylation for ATP production, such as several cervical cancers, breast carcinoma, hepatoma, pancreatic cancer, and glioma cell lines (*20*, *21*). The relationship would also supply one-carbon units generated by the mitochondrial conversion of serine to formate for incorporation into the purine ring during de novo biosynthesis. In this work, we investigated the physical and functional relationship between purinosome and mitochondria using super-resolution imaging, a dynamic mass redistribution assay, and other biochemical measures.

Conventional fluorescence microscopy images initially suggested spatial proximity between purinosomes and mitochondria, but the high density of the mitochondrial network precluded clear demonstration and quantitative characterization of the colocalization between these two structures at diffraction-limited image resolution (fig. S1). To further investigate the spatial distribution of purinosomes, we used three-dimensional stochastic optical reconstruction microscopy (3D STORM), a super-resolution fluorescence imaging method (*22*–*24*), to image HeLa cells under conditions that promote the formation of purinosomes. Purinosomes were imaged via transient transfection of photoactivatable fluorescent protein (mEos2) (*25*) tagged formylglycinamidine ribonucleotide synthase (FGAMS or PFAS), a core purinosome component (*5*, *26*). Given the residual dimerization tendency of mEos2, we also tagged FGAMS to recently developed monomeric photoactivatable fluorescent protein, mMaple3 (*27*). The number and size distributions of purinosomes were independent of the tagging method (fig. S2).

To investigate purinosome-mitochondria colocalization, we induced purinosome formation by purine starvation, fixed the cells, and immunostained them for a mitochondrial outer membrane translocase (TOM20) using a photoswitchable fluorescent dye (Alexa Fluor 647). Two-color 3D STORM images of cells that exhibited purinosomes revealed spatial colocalization between purinosomes and mitochondria (Fig. 1). Under the conditions tested, a substantially larger fraction of purinosomes were colocalized with mitochondria than would be expected if the purinosomes were randomly distributed throughout the cytoplasm (Fig. 1G and fig. S3).

To provide further support for the potential physical interactions between purinosomes and mitochondria, we treated cells cultured in purine-depleted conditions with chemical cross-linkers, isolated the mitochondria, and compared the proteins present in these mitochondrial extracts

[1]Department of Biochemistry and Cell Biology, Department of Chemistry, Stony Brook University, Stony Brook, NY 11794, USA. [2]Department of Chemistry and Chemical Biology, Harvard University, Cambridge, MA 02138, USA. [3]Biochemical Technologies, Science and Technology Division, Corning Incorporated, Corning, NY 14831, USA. [4]Department of Chemistry, The Pennsylvania State University, University Park, PA 16802, USA. [5]Department of Engineering Science and Mechanics, The Pennsylvania State University, University Park, PA 16802, USA. [6]Howard Hughes Medical Institute, Harvard University, Cambridge, MA 02138, USA. [7]Department of Physics, Harvard University, Cambridge, MA 02138, USA.
***Corresponding author. E-mail: jarrod.french@stonybrook.edu (J.B.F.); fangy2@corning.com (Y.F.); zhuang@chemistry.harvard.edu (X.Z.); sjb1@psu.edu (S.J.B.)** †These authors contributed equally to this work. ‡Present address: The Broad Institute of MIT and Harvard, Cambridge, MA 02142, USA. §Present address: Medical Laboratory Science, Jefferson College of Health Science, Roanoke, VA 24013, USA.

Downloaded from on February 11, 2016

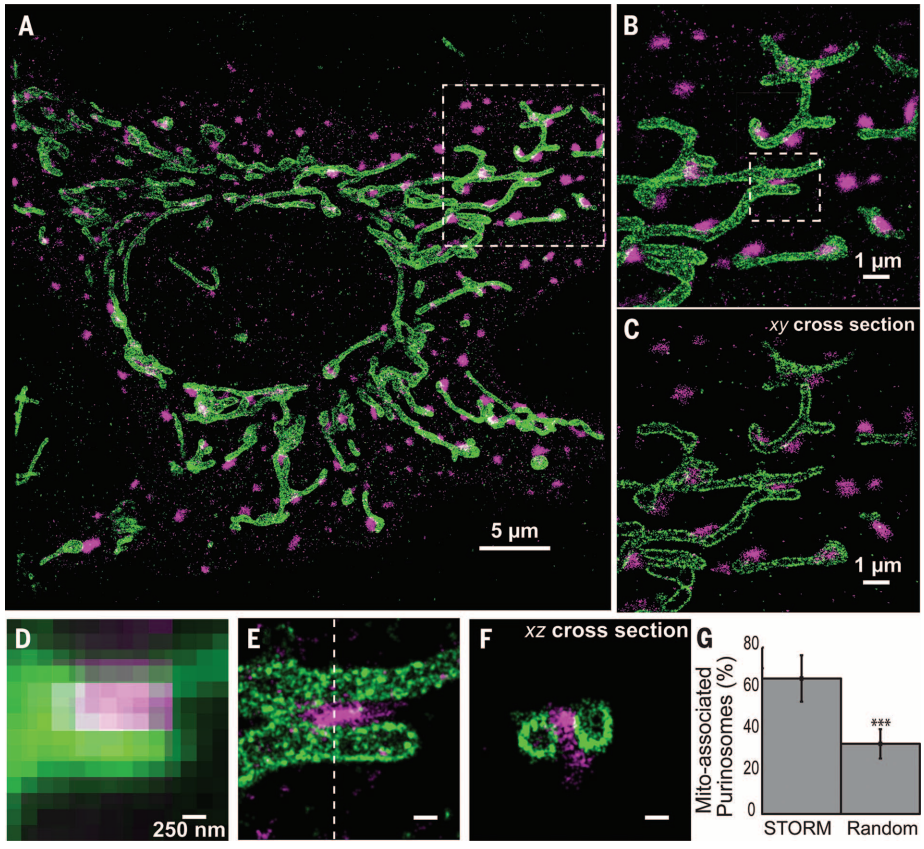

Fig. 1. Super-resolution imaging of purinosomes and mitochondria. (**A**) Two-dimensional projection of a 3D STORM image showing purinosomes labeled with mEos2 fused to a purinosome core protein FGAMS (magenta) and mitochondria immunolabeled against outer membrane protein TOM20 (green) in a HeLa cell grown under purine-depleted conditions. (**B**) Enlargement of the boxed region in (A) showing the close proximity between the two structures. (**C**) A 100-nm-thick *xy* cross section of the region in (B). (**D** and **E**) Comparison of the conventional fluorescence image (D) and corresponding 2D projection STORM image (E) of the boxed region in (B). (**F**) *xz* cross section along the dashed line in (E) showing a purinosome and two neighboring mitochondria. (**G**) The percentage of purinosomes (colocalized with mitochondria observed by STORM (65.1 ± 11.5%, mean ± SD) is significantly higher than the expected value for a randomized purinosome distribution (33.7 ± 7.3%). N = 26 images, Student's t test, $^{***}P << 0.001$. Scale bars (E and F): 250 nm.

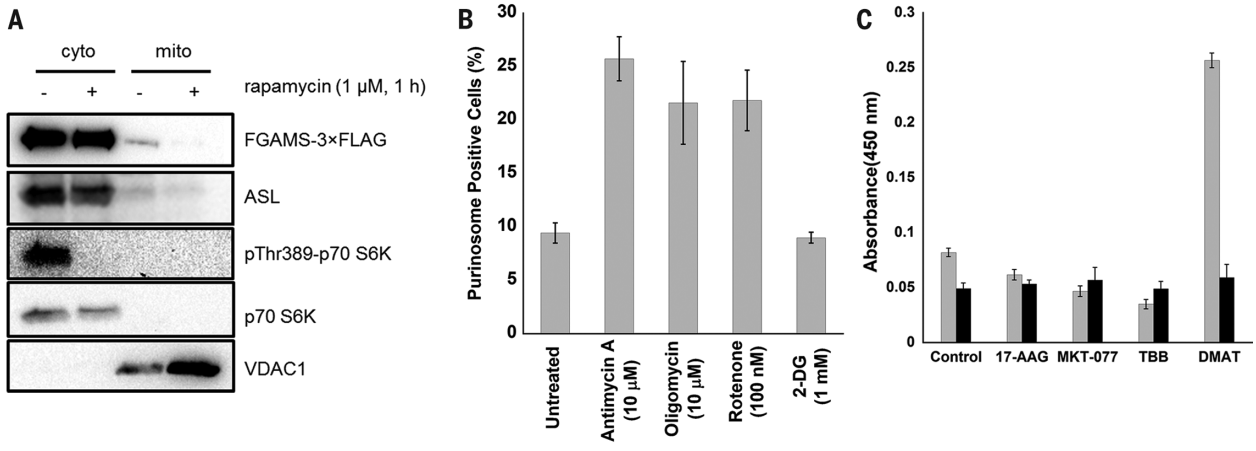

Fig. 2. Physical and functional links between purinosomes and mitochondria. (**A**) Western blot of purified mitochondria showing that purinosome proteins FGAMS and ASL co-isolate with mitochondria in a rapamycin-dependent manner. Mitochondria were isolated from HeLa cells grown under purine-depleted conditions that transiently expressed FGAMS-3×FLAG after treatment with 1 μM rapamycin (+) or vehicle control (-) for 1 hour. Inhibition of mTOR was verified by observing a decrease in the phosphorylated form (pT389) of the mTOR target S6 kinase (p70-S6K). VDAC1 was used as a mitochondria loading control, and p70-S6K served as a cytoplasmic loading control. (**B**) The percentage of cells with visible purinosomes (determined from at least 100 total cells) as a function of modulators of mitochondrial metabolism and glycolysis at their specified concentrations for 1 hour. Values reflect mean ± SD, N = 3 independent samples. (**C**) Intracellular malate (gray) and lactate (black) levels were determined by colorimetric assay after various drug treatments for 1 hour (2 hours for MKT-077). Values reflect mean ± SD, N = 3 independent samples.

to cytosolic fractions. Four different cross-linkers of varying length and reactivity were employed to minimize method bias, and the proteins that copurified with the mitochondria were identified by mass spectrometry (table S1). In addition to mitochondrial proteins such as ATP synthase, voltage-dependent anion channel, and malate dehydrogenase, one of the 174 proteins identified was adenylosuccinate lyase (ASL or ADSL), a known purinosome protein. ASL catalyzes the eighth step in de novo purine biosynthesis and was observed using three out of the four cross-linkers (table S1). To provide further evidence for ASL colocalization with mitochondria, we purified mitochondria from cells under purinosome-forming

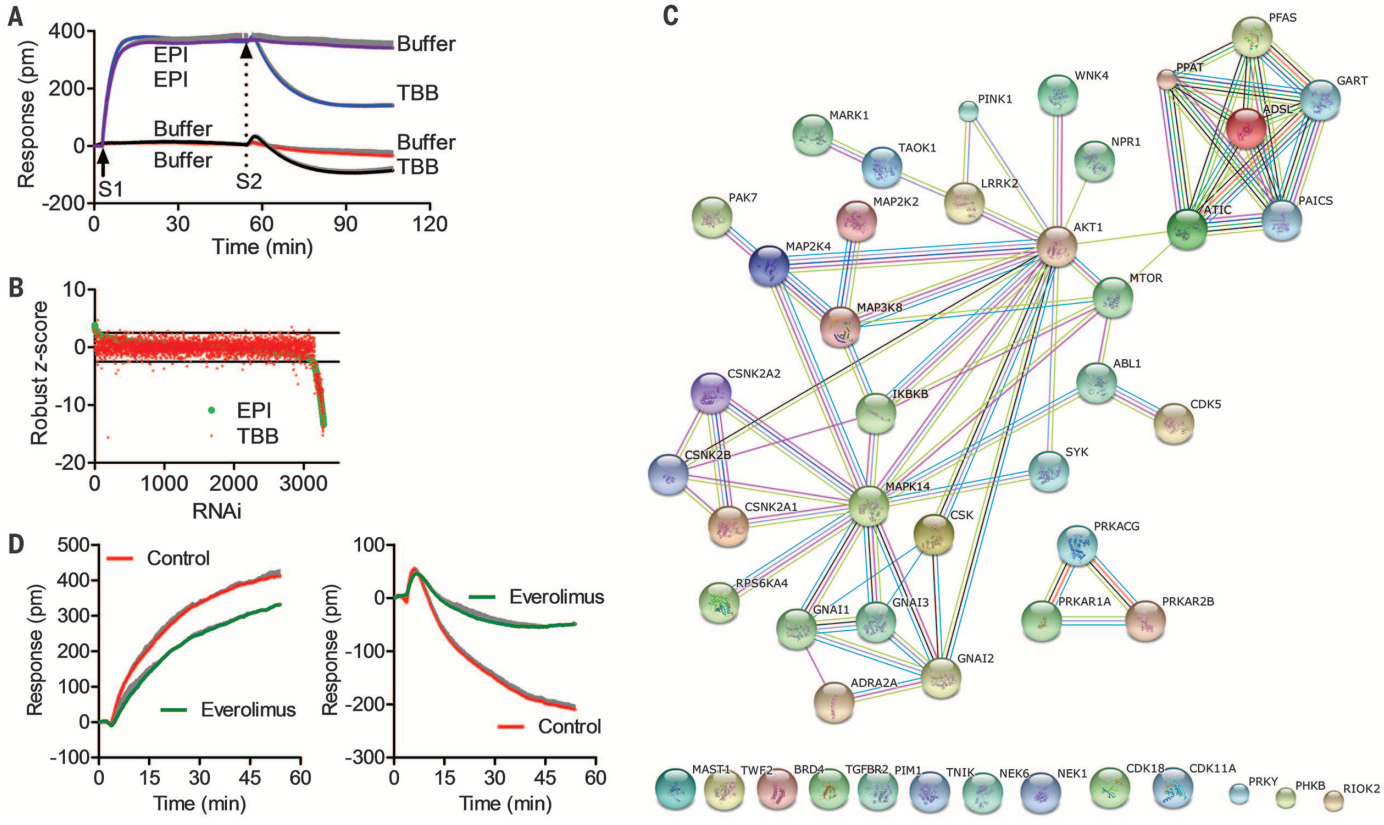

Fig. 3. Human kinome screen identified kinases involved in α_{2A}-adrenergic receptor (α_{2A}-AR) activation-mediated purinosome formation. (**A**) Characteristic DMR of HeLa cells in response to sequential stimulation steps (S1 and S2). Red line: buffer (S1)–buffer (S2); black line: buffer–TBB; purple line: EPI–buffer; blue line: EPI–TBB. The DMR of assay buffer stimulation was used as the negative control. Buffer by itself triggered little DMR and did not alter DMR induced by 100 nM epinephrine (EPI). EPI (100 nM) triggered a positive DMR. Conversely, TBB led to a negative DMR in the buffer-pretreated cells, but a much greater negative DMR in EPI-pretreated cells. (**B**) The robust *z* score of EPI-induced DMR (green dots) or TBB-induced DMR (red dots) as a function of shRNA clones. Robust *z* scores (a *z* score not adversely affected by outliers) were calculated using [(experimental data – median)/median absolute deviation (MAD)], where the normalization set the median to 0 and the MAD to 1. (**C**) Network analysis of the α_{2A}-AR activation-mediated purinosome formation. This analysis combines all hits common to the EPI and TBB DMR responses identified with the current kinome screen with known signaling components of endogenous α_{2A}-AR in HeLa cells, casein kinase 2 (CSNK2B, CSNK2A1, CSNK2A2), and six enzymes (PPAT, GART, PFAS, PAICS, ADSL, ATIC) involved in purine biosynthesis. Hits were selected when at least two shRNA clones for a kinase within the library gave a robust *z* score of ≥3 or ≤−3 (table S2). The network was generated with STRING 9.1. Connecting lines are color coded by the type of evidence used to build the network (details in http://string-db.org/). Unconnected hits are listed at the bottom. (**D**) (Left) The real-time DMR of EPI in the absence (red) or presence of everolimus (green). (Right) The real-time DMR of TBB after EPI prestimulation in the absence (red) or presence of everolimus (green). The dose was 16 μM, 100 nM, or 20 μM for everolimus, EPI, or TBB, respectively. For (A) and (D), data represent mean + SD, $N = 4$ (two independent measurements, each in duplicate). The standard deviation is shown in gray.

conditions without chemical cross-linking, and purinosome enzymes that copurified with mitochondria were detected by Western blot. In addition to ASL, FGAMS, a core protein of the purinosome structure, also coprecipitated with isolated mitochondria (Fig. 2A). Although these data demonstrate a physical link between purinosomes and mitochondria, further experiments are required to characterize the molecular details of this interaction and identify any structural intermediaries.

To investigate the functional relationship of purinosomes with mitochondria, we first examined the effect of mitochondrial poisons on purinosome content of cells. Inhibition of electron transport (using antimycin A or rotenone) or oxidative phosphorylation (using oligomycin) increased the number of purinosome-positive cells cultured in purine-rich conditions by more than twofold (Fig. 2B). Inhibition of glycolysis (using 2-deoxyglucose, 2-DG), which also lowers cellular ATP concentrations (*28*), had no effect on purinosome levels (Fig. 2B). The latter result, combined with previous observations of the effect of exogenous ATP treatments (*14*), suggests that although mitochondrial dysregulation induced a stimulation of purinosome formation in cells, the purinosome assembly is not governed by ATP concentration. Next, we examined the effect of purinosome levels on mitochondrial metabolism. As an approximate measure of glycolytic (cytosolic) and oxidative phosphorylation (mitochondrial) activities, we assayed cellular lactate and malate concentrations, respectively (*29*, *30*). Compounds known to disrupt or inhibit purinosome formation (17-AAG, MKT-077, and TBB) (*11*, *16*) led to decreases in malate levels, whereas an increase in purinosome content induced by DMAT (*11*) significantly increased malate production (Fig. 2C). Lactate levels were not changed by any of the purinosome effectors. These results indicate that there is also a functional link between purinosomes and mitochondria.

Previously, we reported that the assembly of purinosomes was stimulated by agonist binding to the α_{2A}-adenergic receptor and subsequent activation of the $G\alpha_i$-mediated signaling pathway (*14*). To identify the intracellular signaling pathway employed in the control of the relationship between purinosomes and mitochondria, we conducted a short hairpin RNA (shRNA) screen of the human kinome using a two-step dynamic mass redistribution (DMR) assay (Fig. 3A). DMR is a label-free method that uses a resonant waveguide grating biosensor system to

monitor, in real time, refractive-index alterations resulting from stimulus-induced biomass changes near the surface of a sensor (figs. S4 and S5) (*14*, *31*). Epinephrine (EPI) is known to induce purinosome assembly, which contributed to a DMR signal increase; TBB is known to cause purinosome disassembly, which contributed to a DMR signal decrease (*14*). Here we used the EPI-induced DMR signal as a purinosome assembly indicator and the EPI-stimulated TBB response as a purinosome disassembly indicator to identify kinases that influence purinosomes. Analyses of the robust *z* score (*32*) for each shRNA treatment (Fig. 3, A and B; fig. S6; and table S2) and Gene Ontology (GO) enrichment (table S3) suggest that some of the identified kinases are indeed associated with regulation of purine nucleotide metabolism. Using the STRING9.1 database that provides known and predicted protein-protein associations (*33*), we generated networks for the identified kinases that connect them to known components of endogenous α_{2A}-receptor signaling and purinosome assembly, including casein kinase 2 and the six enzymes of the de novo purine biosynthetic pathway (Fig. 3C and figs. S7 and S8). This analysis identifies a putative kinase network involved in directly translating chemical signals into a purinosome response.

Among the kinases identified in this screen were several known to be master regulators of cellular metabolism. Interestingly, one of these kinases was the mechanistic target of rapamycin (mTOR). mTOR, which actively associates with mitochondria-associated endoplasmic reticulum membranes and modulates mitochondrial physiology, is also involved in regulating nucleotide metabolism (*17*, *30*, *34*, *35*). Its role in modulating purine biosynthesis, however, is still unclear (*36*).

We examined the effect of mTOR inhibition on purinosome formation using the described DMR assay. Inhibition of mTOR with everolimus alone did not trigger a DMR response (fig. S9), but partially inhibited the EPI-induced DMR signal in a dose-dependent manner (Fig. 3D and fig. S9). The EPI-induced DMR signal contains contributions from the $G_{\alpha s}$ and $G_{\alpha i}$ pathways, the latter of which is related to purinosome formation (*6*, *14*). Moreover, mTOR inhibition also suppressed the EPI-potentiated TBB-induced DMR signal (Fig. 3D and fig. S9). Taken together, these results suggest a model wherein the inhibition of mTOR impairs α_{2A} receptor activation–stimulated purinosome formation.

To test whether mTOR plays a role in mediating the link between mitochondria and purinosomes, we monitored the observed stimulation of the cellular purinosome level in response to mitochondrial dysregulation. Although a large increase in the percentage of cells containing purinosomes was observed when mitochondrial function was disrupted by antimycin A, oligomycin, or rotenone, this response was abrogated by treatment with the mTOR inhibitor rapamycin (Fig. 4A), similar to the response observed with everolimus treatment of EPI-prestimulated cells (Fig. 3D). Rapamycin treatment alone had no effect on purinosome levels. Notably, the observations were made without purine deprivation or chemical stimulation of purinosome levels, where such an effect would be difficult to detect. We then examined the colocalization between mitochondria and purinosomes, under conditions of purine depletion, in the presence of rapamycin using two-color STORM. Indeed, fractional colocalization between purinosomes and mitochondria decreased in a dose-dependent manner with increasing concentration of rapamycin (Fig. 4B), whereas both the number and size of purinosomes and the cellular distributions of mitochondria were unchanged up to concentrations of 100 nM or higher (fig. S10). Finally, to further show that mTOR plays a role in mediating a physical link between purinosomes and mitochondria, we probed for the presence of FGAMS and ASL in isolated mitochondria from cells treated with rapamycin (Fig. 2A). Although these purinosome markers were observed in the mitochondrial fraction in the absence of rapamycin, they were either not observed or observed at a substantially reduced level in rapamycin-treated cells. Taken together, these data suggest that mTOR plays a role in the link between purinosomes and mitochondria.

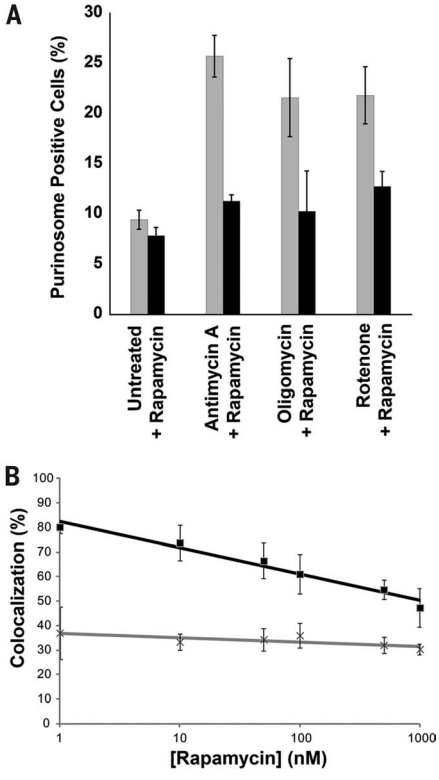

Fig. 4. mTOR affects colocalization and functional links between purinosomes and mitochondria. (**A**) The percentage of purinosome-containing cells (determined from at least 100 cells) as a function of mitochondrial metabolism modulators in the absence (gray) and presence (black) of 100 nM rapamycin. Values reflect the mean ± SD, $N = 3$ independent samples. (**B**) The percentage of purinosomes colocalized with mitochondria (black squares) in STORM images of HeLa cells grown under purine-depleted conditions as a function of increasing rapamycin concentration (10 to 1000 nM, 1 hour). The results after randomization of the purinosome distribution are shown as gray crosses. The colocalization percentage is represented as the mean ± SD, $N = 5$ images per condition.

Two recent reports detailed the mTOR-mediated stimulation of pyrimidine synthesis (*17*, *34*). The mechanism of control exerted by mTOR on pyrimidine metabolism—the change in oligomerization and localization of the enzyme CAD—mirrors the observed effects reported here. Pyrimidine biosynthesis also uses a mitochondrial enzyme, dihydroorotate dehydrogenase, further evidence for the relationship between nucleotide metabolism and the mitochondria. mTOR nucleates into two distinct multiprotein complexes (mTORC1 and mTORC2) and is known to regulate protein associations to control other cellular processes, such as autophagy (*37*–*39*).

The maintenance of nucleotide pools and the rapid response to changing levels of these critical building blocks are vital cellular processes. Management of metabolite levels in a dynamic microenvironment necessitates highly regulated posttranslational control over metabolic flux. This study suggests a spatial mechanism of control. The mTOR-mediated link between purinosomes and mitochondria creates a functional synergy and highlights the interdependence between mitochondrial function and nucleotide metabolism, which could provide a controllable response to changes in metabolic needs. This type of regulation is only beginning to be understood but is likely to emerge as a common mechanism by which cells exploit spatial and temporal control of enzymes and enzyme complexes to increase metabolic efficiency, protect unstable intermediates, and minimize off-target effects.

REFERENCES AND NOTES

1. T. Yamaoka *et al.*, *J. Biol. Chem.* **272**, 17719–17725 (1997).
2. T. Yamaoka *et al.*, *J. Biol. Chem.* **276**, 21285–21291 (2001).
3. L. Antonioli, C. Blandizzi, P. Pacher, G. Haskó, *Nat. Rev. Cancer* **13**, 842–857 (2013).
4. Y. Natsumeda, N. Prajda, J. P. Donohue, J. L. Glover, G. Weber, *Cancer Res.* **44**, 2475–2479 (1984).
5. S. An, R. Kumar, E. D. Sheets, S. J. Benkovic, *Science* **320**, 103–106 (2008).

6. H. Zhao, J. B. French, Y. Fang, S. J. Benkovic, *Chem. Commun. (Camb.)* **49**, 4444–4452 (2013).
7. P. C. Havugimana *et al.*, *Cell* **150**, 1068–1081 (2012).
8. F. J. Schendel, Y. S. Cheng, J. D. Otvos, S. Wehrli, J. Stubbe, *Biochemistry* **27**, 2614–2623 (1988).
9. Q. C. Zhang *et al.*, *Nature* **490**, 556–560 (2012).
10. H. Zhao *et al.*, *J. Biol. Chem.* **290**, 6705–6713 (2015).
11. S. An, M. Kyoung, J. J. Allen, K. M. Shokat, S. J. Benkovic, *J. Biol. Chem.* **285**, 11093–11099 (2010).
12. C. Y. Chan *et al.*, *Proc. Natl. Acad. Sci. U.S.A.* **112**, 1368–1373 (2015).
13. Y. Fang, J. French, H. Zhao, S. Benkovic, *Biotechnol. Genet. Eng. Rev.* **29**, 31–48 (2013).
14. F. Verrier *et al.*, *Nat. Chem. Biol.* **7**, 909–915 (2011).
15. R. Fu *et al.*, *Mol. Genet. Metab.* **114**, 55–61 (2015).
16. J. B. French *et al.*, *Proc. Natl. Acad. Sci. U.S.A.* **110**, 2528–2533 (2013).
17. A. M. Robitaille *et al.*, *Science* **339**, 1320–1323 (2013).
18. F. M. Meyer *et al.*, *Metab. Eng.* **13**, 18–27 (2011).
19. P. D. Straight, M. A. Fischbach, C. T. Walsh, D. Z. Rudner, R. Kolter, *Proc. Natl. Acad. Sci. U.S.A.* **104**, 305–310 (2007).
20. C. Jose, N. Bellance, R. Rossignol, *Biochim. Biophys. Acta* **1807**, 552–561 (2011).
21. L. J. Reitzer, B. M. Wice, D. Kennell, *J. Biol. Chem.* **254**, 2669–2676 (1979).
22. B. Huang, S. A. Jones, B. Brandenburg, X. Zhuang, *Nat. Methods* **5**, 1047–1052 (2008).
23. B. Huang, W. Wang, M. Bates, X. Zhuang, *Science* **319**, 810–813 (2008).
24. M. J. Rust, M. Bates, X. Zhuang, *Nat. Methods* **3**, 793–796 (2006).
25. S. A. McKinney, C. S. Murphy, K. L. Hazelwood, M. W. Davidson, L. L. Looger, *Nat. Methods* **6**, 131–133 (2009).
26. Y. Deng *et al.*, *J. Biol. Chem.* **287**, 36201–36207 (2012).
27. S. Wang, J. R. Moffitt, G. T. Dempsey, X. S. Xie, X. Zhuang, *Proc. Natl. Acad. Sci. U.S.A.* **111**, 8452–8457 (2014).
28. H. Pelicano, D. S. Martin, R. H. Xu, P. Huang, *Oncogene* **25**, 4633–4646 (2006).
29. N. Masson, P. J. Ratcliffe, *Cancer Metab.* **2**, 3 (2014).
30. A. Ramanathan, S. L. Schreiber, *Proc. Natl. Acad. Sci. U.S.A.* **106**, 22229–22232 (2009).
31. Y. Fang, *Front. Pharmacol.* **5**, 52 (2014).
32. A. Birmingham *et al.*, *Nat. Methods* **6**, 569–575 (2009).
33. A. Franceschini *et al.*, *Nucleic Acids Res.* **41** (D1), D808–D815 (2013).
34. I. Ben-Sahra, J. J. Howell, J. M. Asara, B. D. Manning, *Science* **339**, 1323–1328 (2013).
35. K. Düvel *et al.*, *Mol. Cell* **39**, 171–183 (2010).
36. M. Shimobayashi, M. N. Hall, *Nat. Rev. Mol. Cell Biol.* **15**, 155–162 (2014).
37. I. G. Ganley *et al.*, *J. Biol. Chem.* **284**, 12297–12305 (2009).
38. C. H. Jung *et al.*, *Mol. Biol. Cell* **20**, 1992–2003 (2009).
39. M. Laplante, D. M. Sabatini, *J. Cell Sci.* **122**, 3589–3594 (2009).

ACKNOWLEDGMENTS

We thank T. Laremore at the Proteomics and Mass Spectrometry Core Facility of the Huck Institutes of the Life Sciences at The Pennsylvania State University for assistance with data collection and analyses. The Orbitrap mass spectrometer was funded by a grant from the Pennsylvania Department of Health Tobacco Settlement Funds. J.B.F. acknowledges the Canadian Institutes of Health Research for fellowship support. This work was funded by the National Institutes of Health grants NIH GM024129 (S.J.B.) and 1R33EB019785-01 (T.J.H. and S.J.B.) as well as the Howard Hughes Medical Institute (X.Z.). J.B.F., S.A.J., Y.F., X.Z., and S.J.B. designed the experiments; J.B.F., S.A.J., H.D., H.H., A.M.P., C.Y.C., D.K., R.J.P., H.Z., and Y.Z. performed the experiments and analyzed the data; J.B.F., S.A.J., A.M.P., R.J.P., and Y.F. prepared the manuscript; J.B.F., Y.F., X.Z., and S.J.B. directed the research; all authors have reviewed and edited the manuscript. The authors declare that they have no competing interests. Additional data reported in this manuscript are available in the supplementary materials.

SUPPLEMENTARY MATERIALS

www.sciencemag.org/content/351/6274/733/suppl/DC1
Materials and Methods
Figs. S1 to S10
Tables S1 to S3

19 May 2015; accepted 23 December 2015
10.1126/science.aac6054

HUMAN GENOMICS

The phenotypic legacy of admixture between modern humans and Neandertals

Corinne N. Simonti,[1] Benjamin Vernot,[2] Lisa Bastarache,[3] Erwin Bottinger,[4] David S. Carrell,[5] Rex L. Chisholm,[6] David R. Crosslin,[2,5] Scott J. Hebbring,[7] Gail P. Jarvik,[2,5] Iftikhar J. Kullo,[8] Rongling Li,[9] Jyotishman Pathak,[10]* Marylyn D. Ritchie,[11,12] Dan M. Roden,[1,3,13,14] Shefali S. Verma,[11] Gerard Tromp,[15,16] Jeffrey D. Prato,[3] William S. Bush,[17] Joshua M. Akey,[2]† Joshua C. Denny,[1,3,13]† John A. Capra[1,3,18,19]‡

Many modern human genomes retain DNA inherited from interbreeding with archaic hominins, such as Neandertals, yet the influence of this admixture on human traits is largely unknown. We analyzed the contribution of common Neandertal variants to over 1000 electronic health record (EHR)–derived phenotypes in ~28,000 adults of European ancestry. We discovered and replicated associations of Neandertal alleles with neurological, psychiatric, immunological, and dermatological phenotypes. Neandertal alleles together explained a significant fraction of the variation in risk for depression and skin lesions resulting from sun exposure (actinic keratosis), and individual Neandertal alleles were significantly associated with specific human phenotypes, including hypercoagulation and tobacco use. Our results establish that archaic admixture influences disease risk in modern humans, provide hypotheses about the effects of hundreds of Neandertal haplotypes, and demonstrate the utility of EHR data in evolutionary analyses.

As anatomically modern human (AMH) groups left Africa and began to spread across Europe and Asia ~60,000 years ago, they encountered other archaic hominins. The fossil record suggests that AMHs and several archaic hominins overlapped in space and time (*1*), and genomic analyses of modern and ancient humans and of extinct Neandertals and Denisovans have revealed interbreeding between these groups (*2*, *3*). As a result, the genomes of modern Eurasians contain a small fraction (~1.5 to 4%) of DNA inherited from interbreeding with Neandertals around 50,000 years ago (*4*–*6*).

The patterns of surviving Neandertal DNA across modern Eurasian genomes indicate that introgressed Neandertal DNA experienced strong selective pressures. Surviving Neandertal lineages are significantly depleted in several genomic regions, such as on the X chromosome and the q arm of chromosome 7, suggesting that there are deleterious consequences of Neandertal DNA at many loci (*5*, *6*). However, some Neandertal alleles are found at higher than expected frequencies and thus may have provided an evolutionary advantage to AMH populations (*5*–*7*). Consistent with this hypothesis, Neandertals are believed to have lived out of Africa long enough to adapt to the climatic, dietary, and pathogenic landscapes found at higher latitudes.

Indeed, isolated introgressed loci have been identified with potential roles in human adaptation (*7*, *8*). Furthermore, recent studies of genomic regions enriched in Neandertal alleles have suggested potential effects on skin and hair phenotypes, lipid metabolism, depression, and other traits (*5*, *6*, *9*). However, whether introgressed Neandertal alleles have a significant functional effect on these traits in human populations has

[1]Vanderbilt Genetics Institute, Vanderbilt University, Nashville, TN, USA. [2]Department of Genome Sciences, University of Washington, Seattle, WA, USA. [3]Department of Biomedical Informatics, Vanderbilt University, Nashville, TN, USA. [4]Mount Sinai School of Medicine, New York, NY, USA. [5]Department of Medicine (Medical Genetics), University of Washington Medical Center, Seattle, WA, USA. [6]Center for Genetic Medicine, Feinberg School of Medicine, Northwestern University, Chicago, IL, USA. [7]Center for Human Genetics, Marshfield Clinic, Marshfield, WI, USA. [8]Division of Cardiovascular Diseases, Mayo Clinic, Rochester, MN, USA. [9]Division of Genomic Medicine, National Human Genome Research Institute, National Institutes of Health, Bethesda, MD, USA. [10]Division of Health Sciences Research, Mayo Clinic, Rochester, MN, USA. [11]Department of Biochemistry and Molecular Biology, The Pennsylvania State University, University Park, PA, USA. [12]Biomedical and Translational Informatics, Geisinger Health System, Danville, PA, USA. [13]Department of Medicine, Vanderbilt University, Nashville, TN, USA. [14]Department of Pharmacology, Vanderbilt University, Nashville, TN, USA. [15]Weis Center for Research, Geisinger Health System, Danville, PA, USA. [16]Division of Molecular Biology and Human Genetics, Department of Biomedical Sciences, Faculty of Health Science, Stellenbosch University, Tygerberg, South Africa. [17]Department of Epidemiology and Biostatistics, Case Western Reserve University, Cleveland, OH, USA. [18]Department of Biological Sciences, Vanderbilt University, Nashville, TN, USA. [19]Center for Quantitative Sciences, Vanderbilt University, Nashville, TN, USA.
*Department of Healthcare Policy and Research, Weill Cornell Medical College, New York, NY, USA. †These authors contributed equally to this work. ‡**Corresponding author. E-mail: tony.capra@vanderbilt.edu**

Downloaded from on February 11, 2016

not been established, because of the difficulty of confidently identifying Neandertal-derived DNA and the expense of performing tests for trait association between individuals with and without Neandertal ancestry at specific sites.

We addressed these challenges by integrating the phenotype data present in electronic health records (EHRs) with high-resolution maps of Neandertal haplotypes across individual human genomes (Fig. 1A). We performed a large-scale assessment of the functional effects of DNA inherited from Neandertals on health-related traits in modern populations of European ancestry. In particular, we analyzed genotype and phenotype data from the Electronic Medical Records and Genomics (eMERGE) Network, a consortium that unites EHR systems linked to patient genetic data from nine sites across the United States (*10*). EHRs contain quantitative and qualitative data on individuals' traits; however, algorithms are required to derive consistent phenotypes appropriate for use in genetic association testing from these records. For the majority of our analyses, we used a set of 1689 hierarchically related phenotypes (including 1087 leaf phenotypes) defined from the use of International Classification of Diseases (ICD-9) billing codes in the EHRs (*11*). We analyzed a set of 28,416 adults of European ancestry from across the eMERGE sites who had been genotyped on genome-wide arrays and had sufficient EHR data to define phenotypes. These individuals naturally fell into separate discovery and replication cohorts on the basis of their inclusion in the eMERGE Network Phase 1 (E1; N = 13,686 individuals) or Phase 2 (E2; N = 14,730 individuals) data releases (*12*).

To identify Neandertal alleles in the genotyping data available from eMERGE, we used a recent genome-wide map of ~6000 Neandertal haplotypes inferred by computing the S* statistic (*13*) and refining putative introgressed haplotypes by comparing sequenced individuals from the 1000 Genomes (1KG) Project (*14*) with the Altai Neandertal genome (*3*, *6*). We defined ~135,000 high-confidence "Neandertal single-nucleotide polymorphisms (SNPs)" among the introgressed haplotypes by filtering out SNPs whose frequency significantly differed from the overall Neandertal haplotype frequency and removing haplotypes with fewer than four likely Neandertal-derived SNPs (*11*). This filtering was necessary to remove variants unlikely to derive from Neandertal admixture.

Neandertal variants have been hypothesized to influence many phenotypes in AMHs, including lipid metabolism, immunity, depression, digestion, hair, and skin, on the basis of the enrichment of Neandertal variants in regions of the genome relevant to these traits (*3*, *5*, *6*, *9*). Accordingly, we first tested these hypotheses using genome-wide complex trait analysis (GCTA) to estimate the phenotypic risk explained by

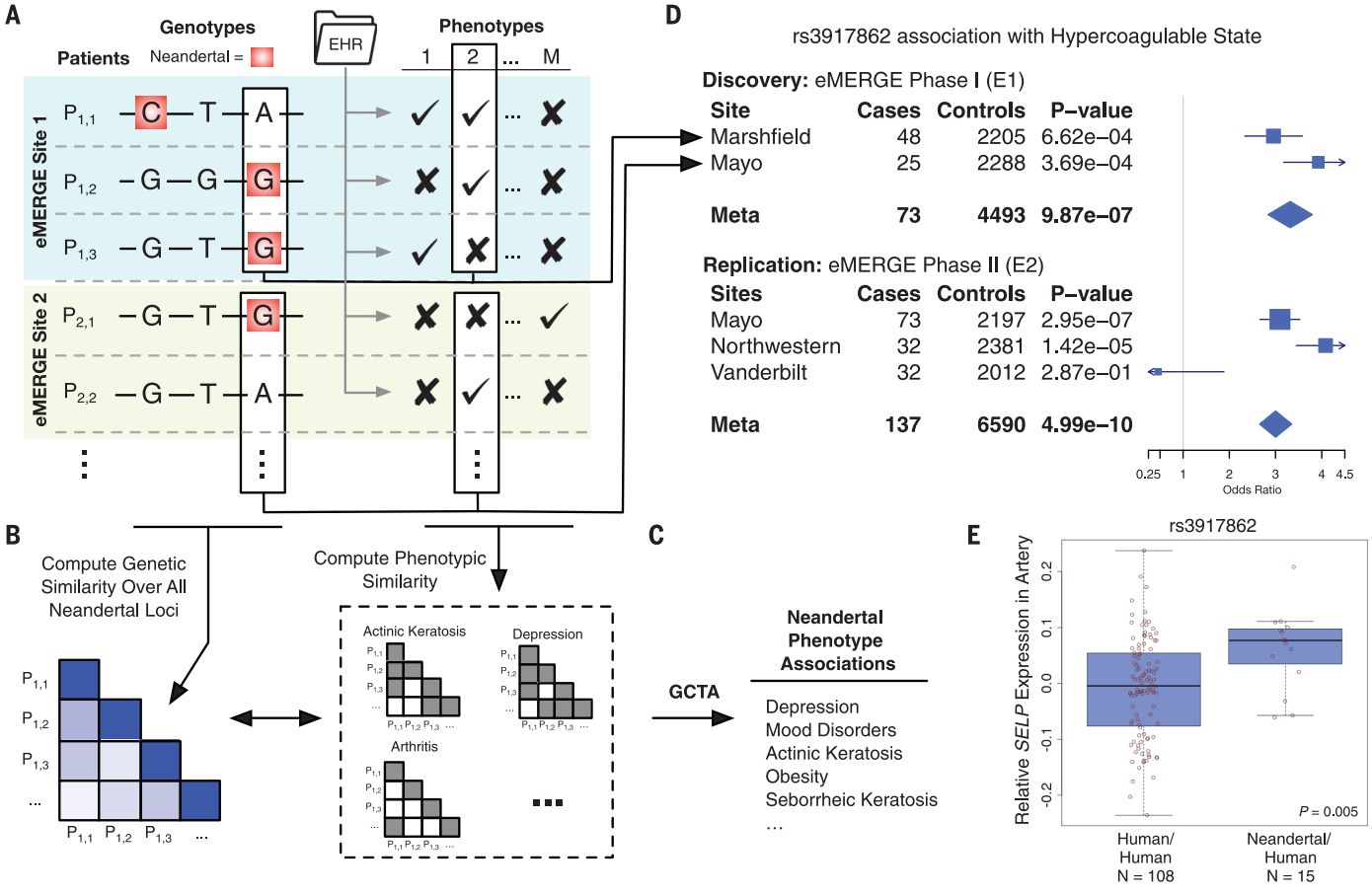

Fig. 1. Analysis of EHRs reveals clinical effects of Neandertal alleles in modern humans. (**A**) Thousands of Neandertal alleles were identified in ~28,000 individuals of European ancestry across the eMERGE Network. We derived phenotypes for each individual from data in their EHRs. (**B**) To test Neandertal alleles in aggregate for phenotype associations, we computed the genetic similarity of all pairs of individuals over 1495 genotyped Neandertal loci and their phenotypic similarity over 46 EHR-derived traits. (**C**) We estimated the overall variance in risk explained by Neandertal alleles using mixed linear models in GCTA (*15*) and found that Neandertal alleles explain significant variance in several traits (Table 1). (**D**) To test individual Neandertal alleles for trait associations, we performed a discovery meta-analysis across eMERGE E1 sites with sufficient data. We then ran a replication meta-analysis over the independent eMERGE E2 cohort. This approach identified and replicated several associations (Table 2). The example forest plot illustrates the association of Neandertal SNP rs3917862 with hypercoagulable state in each site with >=20 cases for the separate discovery and replication analyses. (**E**) rs3917862 is located in an intron of P-selectin (*SELP*), a gene that mediates leukocyte action at injuries in the early stages of inflammation. The Neandertal allele is significantly associated (linear regression, P = 0.005) with increased expression of *SELP* in tibial artery data from GTEx.

1495 genotyped common (minor allele frequency > 1%) Neandertal SNPs for a set of 46 high-prevalence phenotypes from the hypothesized categories, using age, sex, and eMERGE site as covariates (Fig. 1, B and C) (*15*). Neandertal SNPs explained a significant [likelihood ratio test; false discovery rate (FDR) < 0.05 over all phenotype tests] percent of the risk in three traits in the E1 discovery cohort (Table 1): depression (2.03%, $P = 0.0036$), myocardial infarction (1.39%, $P = 0.0026$), and corns and callosities (1.26%, $P = 0.01$). Neandertal SNPs also explained a nominally significant ($P < 0.1$) percent of risk for nine additional traits, including actinic and seborrheic keratosis, coronary atherosclerosis, and obesity (Table 1).

Of the 12 nominally significant associations, 8 were replicated in the independent E2 data set, including actinic keratosis ($P = 0.0059$), mood disorders ($P = 0.018$), depression ($P = 0.020$), obesity ($P = 0.030$), and seborrheic keratosis ($P = 0.045$) at $P < 0.1$ (Table 1; likelihood ratio test). We also tested whether the percent of phenotypic variance explained by Neandertal SNPs remained significant in the context of non-Neandertal SNPs by including an additional genetic relationship matrix (GRM) computed from non-Neandertal SNPs across the rest of the human genome in the mixed linear model (*11*). Depression ($P = 0.031$), mood disorders ($P = 0.029$), and actinic keratosis ($P = 0.036$) were replicated with these stricter criteria in the independent E2 cohort.

These analyses establish the influence of Neandertal SNPs in concert on the variance in these traits. We estimated individual effects for each SNP by the best linear unbiased predictions (BLUPs); this indicated that a similar number of Neandertal SNPs increased and decreased risk for each associated phenotype (table S1) (*11*). To gain insight into the loci driving these associations, we analyzed the genomic distribution of the 10% of SNPs with the highest and lowest BLUPs for actinic keratosis and depression. We found enrichment (FDR < 0.05; hypergeometric test) for many functional annotations: most notably, keratinocyte differentiation and several immune functions for actinic keratosis and regions involved in neurological diseases, cell migration, and circadian clock genes for depression (fig. S1 and table S2) (*11*).

The significant replicated association of Neandertal SNPs with mood disorders, in particular depression, is intriguing because Neandertal alleles are enriched near genes associated with long-term depression (*5*), and human-Neandertal DNA and methylation differences have been hypothesized to influence neurological and psychiatric phenotypes (*16*, *17*). Depression risk in modern human populations is influenced by sunlight exposure (*18*), which differs between high and low latitudes, and we found enrichment of circadian clock genes near the Neandertal alleles that contribute most to this association (*11*). The replicated nominal association of Neandertal SNPs with actinic keratosis (precancerous scaly skin lesions) further links introgressed alleles in AMHs to a phenotype directly related to sun exposure. It also suggests that the signatures of adaptive introgression and strong enrichment of Neandertal alleles near genes associated with keratin filament formation (*5*) and keratinocytes (*6*) reflect the influence of Neandertal alleles on a modern human phenotype. However, further genetic analyses are necessary to resolve the differences in the strength of this association between E1 and E2. These results establish the impact of Neandertal DNA on diseases in AMHs that involve traits potentially influenced by environmental differences experienced by non-African populations.

GCTA quantifies the overall influence of Neandertal SNPs together on traits in AMHs. To identify individual Neandertal loci associated with AMH phenotypes and potentially discover additional biological systems influenced by Neandertal admixture, we performed a phenome-wide association study (PheWAS) of these 1495 Neandertal SNPs with 1152 EHR-derived phenotypes with at least 20 cases in at least one site (Fig. 1D). PheWAS allows for large-scale characterization of the effects of variants of interest (*19*). We carried out two meta-analyses across the eMERGE Network sites: one over the discovery cohort and one over the replication cohort. We focus on the meta-analyses here (Table 2 and table S3), but a pooled analysis using the eMERGE site as a covariate produced largely consistent results (table S4).

Four Neandertal SNP–phenotype associations passed a locus-wise Bonferroni corrected significance threshold ($P = 3.3 \times 10^{-5}$) in the E1 meta-analysis and were replicated ($P < 0.05$) with the same direction of effect in the independent E2 meta-analysis (Table 2). The strongest signal was a Neandertal SNP (rs3917862, 6.5% European (EUR) 1KG frequency) in an intron of P-selectin

Table 1. Neandertal alleles explain risk for human clinical traits. The eight traits for which Neandertal alleles explained a nominally significant proportion of variance in risk in both the E1 discovery and E2 replication analyses are listed (GCTA, $P < 0.1$). The depression association remained significant after controlling the false discovery rate at 5%. The Neandertal associations with actinic keratosis, mood disorders, and depression were also maintained in a two-GRM model that considered the risk explained by non-Neandertal variants. Phenotypes are sorted by their E2 *P* value.

Phenotype	Discovery (E1)		Replication (E2)		Replication (E2; two-GRM)	
	Risk explained	*P*	Risk explained	*P*	Risk explained	*P*
Actinic keratosis	0.64%	0.066	3.37%	0.0059	2.49%	0.036
Mood disorders	1.11%	0.0091	0.75%	0.018	0.68%	0.029
Depression	2.03%	0.0023	1.15%	0.020	1.06%	0.031
Obesity	0.59%	0.048	1.23%	0.030	0.39%	0.27
Seborrheic keratosis	0.77%	0.038	0.61%	0.045	0.41%	0.13
Overweight	0.60%	0.037	0.53%	0.052	0.23%	0.24
Acute upper respiratory infections	0.70%	0.043	0.56%	0.062	0.34%	0.18
Coronary atherosclerosis	0.68%	0.04	0.42%	0.098	0.34%	0.15

Table 2. Individual Neandertal SNPs with significant replicating phenotype associations. Four locus-wise Bonferroni significant Neandertal SNP–phenotype associations replicated (with a fixed effect $P < 0.05$ and consistent direction of effect). Nominally significant replicating results can be found in table S3 and in the PheWAS Catalog (https://phewas.mc.vanderbilt.edu/neanderthal). Chr, chromosome.

Phenotype	Chr:position (hg19)	SNP	Flanking gene(s)	Discovery		Replication	
				Odds ratio	*P*	Odds ratio	*P*
Hypercoagulable state	1:169593113	rs3917862	*SELP*	3.32	9.9×10^{-7}	3.00	5.0×10^{-10}
Protein-calorie malnutrition	1:234099819	rs12049593	*SLC35F3*	1.77	2.0×10^{-6}	1.63	5.5×10^{-5}
Symptoms involving urinary system	11:3867350	rs11030043	*RHOG*, *STIM1*	1.76	7.4×10^{-6}	1.65	4.3×10^{-2}
Tobacco use disorder	3:10962315	rs901033	*SLC6A11*	2.19	1.7×10^{-5}	1.75	7.9×10^{-4}

(*SELP*) that was significantly associated with hypercoagulable state in both E1 and E2 (Table 2; Fig. 1D). This haplotype contains several genes directly involved in blood coagulation and inflammation, most notably *SELP*, which encodes a cell adhesion protein expressed on the surface of endothelial cells and platelets that recruits leukocytes to injuries during inflammation. The gene encoding factor V (*F5*), a coagulation cofactor associated with several coagulation defects, is located ~37 kilobases downstream. The Neandertal haplotype overlaps histone modifications suggestive of gene-regulatory activity in blood cells and vein epithelial cells (fig. S2). Using data from the Genotype-Tissue Expression (GTEx) Project (*20*), we found indications that the Neandertal allele at rs3917862 significantly increased the expression of *SELP* ($P = 0.005$) and *F5* ($P = 0.05$) in arteries (Fig. 1E and fig. S2). The association may be influenced by the *F5* Leiden (F5L) mutation associated with hypercoagulable state; however, the Neandertal allele appears to have an additional influence on risk (*11*). The Neandertal SNP is in low linkage disequilibrium (LD) with F5L ($r^2 = 0.07$, $D' = 0.42$), and increases risk for venous thromboembolism, beyond the risk associated with F5L (*21*). Furthermore, manual review of the EHRs for 16 hypercoagulable state cases revealed a diverse set of causes, and only 4 out of the 11 individuals tested for F5L had the mutation. Due to the direct interaction of coagulation factors with pathogens, these genes have been common targets of positive selection across vertebrate evolution, and *F5* has experienced positive selection in primates (*22*). Thus, it is possible that this Neandertal haplotype and the associated hypercoagulability provided an advantage in early AMHs outside of Africa.

The second replicating association was a SNP (rs12049593, 5.0% EUR frequency) in an intron of *SLC35F3*, a putative thiamine transporter, which associates with protein-calorie malnutrition. Thiamine is crucial to carbohydrate metabolism for all cells, particularly those with increased energy requirements (*23*). Variants in high LD with this SNP ($r^2 > 0.8$, $D' = 1$) are found in regions bearing enhancer histone marks in the gastrointestinal (GI) tract, brain, and other tissues. Decreased expression of this transporter in the brain or GI tract could exacerbate malnutrition or its symptoms. It is possible that new dietary pressures may have caused changes in carbohydrate metabolism to be beneficial in early human migrants out of Africa; indeed, there is evidence suggesting that Neandertal introgression probably influenced lipid catabolism in Europeans (*9*). More recently, the reduction of thiamine present in foods from the grain-refining process, as well as an increased intake of simple carbohydrates, make this a potentially harmful allele, because it could reduce thiamine availability although modern diets increase demand.

Another Neandertal SNP (rs11030043, 9.0% EUR frequency) is upstream of *stromal interaction molecule 1* (*STIM1*) and is associated with a phenotype encompassing incontinence, bladder pain, and urinary tract disorders (fig. S4A). *STIM1* is a ubiquitously expressed gene involved in intracellular calcium signaling. Variants in high LD with the Neandertal SNP are found in regions bearing enhancer histone marks and DNase I hypersensitive sites in the brain. Because of this, we examined whether this SNP was associated with gene expression levels in brain tissues in GTEx. The Neandertal allele is associated with significantly decreased expression of *STIM1* in the caudate basal ganglia ($P = 0.02$; fig. S4B), a region of the brain connected to bladder dysfunction, particularly in those with neurological conditions such as Parkinson's (*24*).

The last replicated association was between rs901033 (0.5% EUR frequency) and tobacco use disorder. This SNP is in an intron of *SLC6A11*, a solute carrier family neurotransmitter transporter that is responsible for reuptake of the neurotransmitter γ-aminobutyric acid (GABA). Nicotine addiction disrupts GABAergic signaling in the brain and reduces expression of *SLC6A11* (*25*). This is the second Neandertal SNP to be associated with smoking risk (*5*).

To test whether Neandertal SNPs were enriched for association with specific classes of phenotypes, we compared the distribution of replicating phenotype associations for a set of 1056 LD-pruned ($r^2 < 0.5$) Neandertal SNPs (table S5) with the associations found in five allele frequency matched non-Neandertal SNP sets (consisting of a total of 5280 SNPs) at a relaxed PheWAS discovery threshold ($P < 0.001$) (*11*). Overall, the Neandertal SNPs appear to influence significantly different classes of phenotypes (chi-squared test, $P = 0.017$; Fig. 2). In particular, Neandertal SNPs were consistently associated with more neurological and psychiatric phenotypes and fewer digestive phenotypes (Fig. 2) (*11*).

Given the enrichment for associations with psychiatric and neurological phenotypes, we tested whether Neandertal SNPs were significantly associated with changes in gene expression in previous expression quantitative trait loci (eQTL) analyses of the cerebellum and temporal cortex. Twenty-nine Neandertal SNPs were significant brain *cis*-eQTL in the cerebellum or temporal cortex (FDR < 0.05) (*11*). This represents significant enrichment for brain eQTL among Neandertal SNPs as compared to the non-Neandertal control SNPs (one-tailed binomial test; $P = 1.68 \times 10^{-4}$ for the cerebellum and $P = 3.49 \times 10^{-5}$ for the temporal cortex) (*11*). Taken together, the influence of Neandertal SNPs on depression risk (Table 1), the association of individual Neandertal SNPs with diseases with a neurological basis (Table 2), the enrichment for nominal associations with psychiatric and neurological phenotypes (Fig. 2), and the enrichment for

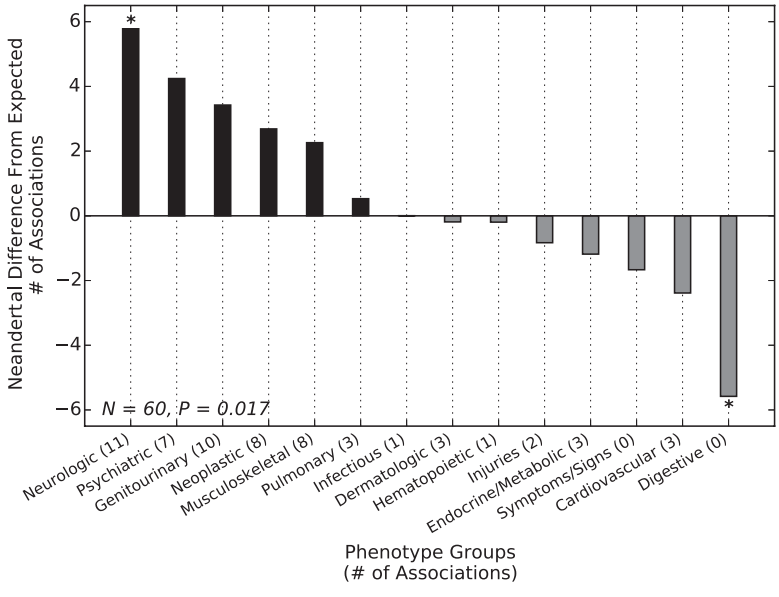

Fig. 2. Neandertal SNPs associate with different phenotypes than matched non-Neandertal SNPs. Each bar gives the difference between the number of replicated Neandertal SNP associations with a phenotype group (at a relaxed discovery threshold of $P < 0.001$) and the number expected from a PheWAS over five sets of non-Neandertal sites matched to the allele frequency of tested Neandertal SNPs. The phenotype distributions were significantly different (chi-squared test, $P = 0.017$), with more Neandertal SNPs associated with neurological and psychiatric phenotypes than expected and fewer digestive phenotypes. The enrichment and depletion were consistent across all five matched non-Neandertal sets (* indicates $P < 0.05$ for all five comparisons; binomial test) (*11*).

brain eQTL in Neandertal SNPs suggest that Neandertal introgression influenced AMH brain phenotypes.

Our approach establishes a new method for understanding the phenotypic legacy of admixture between AMHs and archaic hominins. Using a large clinical cohort, we discovered functional associations between Neandertal alleles and AMH traits, influencing the skin, the immune system, depression, addiction, and metabolism. Furthermore, several lines of evidence suggest enrichment for associations between Neandertal alleles and neurological and psychiatric phenotypes, as well as the importance of differences in sun exposure between high and low latitudes. It is possible that some Neandertal alleles provided a benefit in early AMH populations as they moved out of Africa, but have become detrimental in modern Western environments.

EHR data, paired with DNA sequencing, hold promise for characterizing the phenotypic impact of regions identified through evolutionary analyses. However, there are currently limitations to this approach. It is difficult to extract nonclinical phenotypes from EHRs, and we were not able to analyze all Neandertal haplotypes due to the limited coverage of the available genotyping data. Nonetheless, as EHRs are increasingly linked to whole-genome sequence data and more sophisticated methods are developed for extracting phenotypes from the rich data stored in EHRs, we anticipate further insights into the functional effects of archaic introgression.

REFERENCES AND NOTES

1. T. Higham *et al.*, *Nature* **512**, 306–309 (2014).
2. R. E. Green *et al.*, *Science* **328**, 710–722 (2010).
3. K. Prüfer *et al.*, *Nature* **505**, 43–49 (2014).
4. J. D. Wall *et al.*, *Genetics* **194**, 199–209 (2013).
5. S. Sankararaman *et al.*, *Nature* **507**, 354–357 (2014).
6. B. Vernot, J. M. Akey, *Science* **343**, 1017–1021 (2014).
7. L. Abi-Rached *et al.*, *Science* **334**, 89–94 (2011).
8. E. Huerta-Sánchez *et al.*, *Nature* **512**, 194–197 (2014).
9. E. E. Khrameeva *et al.*, *Nat. Commun.* **5**, 3584 (2014).
10. A. N. Kho *et al.*, *Sci. Transl. Med.* **3**, 79re1 (2011).
11. L. F. Schroeder, E. Robilotti, L. R. Peterson, N. Banaei, D. W. Dowdy, *J. Clin. Microbiol.* **52**, 489–496 (2014).
12. O. Gottesman *et al.*, *Genet. Med.* **15**, 761–771 (2013).
13. V. Plagnol, J. D. Wall, *PLOS Genet.* **2**, e105 (2006).
14. G. R. Abecasis *et al.*, *Nature* **491**, 56–65 (2012).
15. J. Yang, S. H. Lee, M. E. Goddard, P. M. Visscher, *Am. J. Hum. Genet.* **88**, 76–82 (2011).
16. D. Gokhman *et al.*, *Science* **344**, 523–527 (2014).
17. N. Oksenberg, L. Stevison, J. D. Wall, N. Ahituv, *PLOS Genet.* **9**, e1003221 (2013).
18. R. N. Golden *et al.*, *Am. J. Psychiatry* **162**, 656–662 (2005).
19. J. C. Denny *et al.*, *Nat. Biotechnol.* **31**, 1102–1110 (2013).
20. The GTEx Consortium, *Science* **348**, 648–660 (2015).
21. J. A. Heit *et al.*, *J. Thromb. Haemost.* **10**, 1521–1531 (2012).
22. P. M. Rallapalli, C. A. Orengo, R. A. Studer, S. J. Perkins, *Mol. Biol. Evol.* **31**, 3040–3056 (2014).
23. P. R. Martin, C. K. Singleton, S. Hiller-Sturmhöfel, *Alcohol Res. Health* **27**, 134–142 (2003).
24. J. H. Pazo, J. E. Belforte, *Cell. Mol. Neurobiol.* **22**, 645–654 (2002).
25. C. Pickering, V. Bergenheim, H. B. Schiöth, M. Ericson, *Prog. Neuropsychopharmacol. Biol. Psychiatry* **32**, 1521–1526 (2008).

ACKNOWLEDGMENTS

The data reported in this paper are available in the supplementary materials and in the Neandertal PheWAS Catalog (https://phewas.mc.vanderbilt.edu/neanderthal). The raw genotype and phenotype data used in this study are subject to the data use and availability requirements of the eMERGE network outlined at https://emerge.mc.vanderbilt.edu/collaborate. We thank A. Fish, J. Hall, D. Mortlock, D. Samuels, M. Sivley, and P. Wu for helpful discussions. C.N.S. was supported by NIH grant 5T32EY021453 to Vanderbilt University and a pilot project award from the Vanderbilt Center for Quantitative Sciences. The eMERGE Network was initiated and funded by the National Human Genome Research Institute through the following grants: U01HG004438 to Johns Hopkins University; U01HG004610 and U01HG008657 to Group Health Cooperative and University of Washington, Seattle; U01HG004608 and 1K22LM011938 to the Marshfield Clinic; U01HG006389 to the Essentia Institute of Rural Health; U01HG04599 and U01HG006379 to the Mayo Clinic; U01HG004609 and U01HG006388 to Northwestern University; U01HG04603 and U01HG006378 to Vanderbilt University; U01HG006385 to the Coordinating Center of the eMERGE Network; U01HG006382 to the Geisinger Clinic; and U01HG006380 to the Mount Sinai School of Medicine. J.M.A. is a paid consultant for Glenview Capital and provides advice on next-generation sequencing technologies. PheWAS method development was supported by grant R01LM010685. J.M.A. was supported in part by NIH grant R01GM110068. S.J.H was supported in part by NIH grant 1R01GM114128. The authors report no conflicts of interest.

SUPPLEMENTARY MATERIALS

www.sciencemag.org/content/351/6274/737/suppl/DC1
Materials and Methods
Supplementary Text
Figs. S1 to S4
Tables S1 to S5
References (*26*–*51*)

10 August 2015; accepted 8 January 2016
10.1126/science.aad2149

Science
AAAS

The phenotypic legacy of admixture between modern humans and Neandertals

Corinne N. Simonti *et al.*

Science **351**, 737 (2016);
DOI: 10.1126/science.aad2149

This copy is for your personal, non-commercial use only.

If you wish to distribute this article to others, you can order high-quality copies for your colleagues, clients, or customers by clicking here.

Permission to republish or repurpose articles or portions of articles can be obtained by following the guidelines here.

The following resources related to this article are available online at www.sciencemag.org (this information is current as of February 11, 2016):

Updated information and services, including high-resolution figures, can be found in the online version of this article at:
/content/351/6274/737.full.html

Supporting Online Material can be found at:
/content/suppl/2016/02/10/351.6274.737.DC1.html

This article **cites 46 articles**, 15 of which can be accessed free:
/content/351/6274/737.full.html#ref-list-1

This article appears in the following **subject collections:**
Evolution
/cgi/collection/evolution

Downloaded from on February 11, 2016

Science (print ISSN 0036-8075; online ISSN 1095-9203) is published weekly, except the last week in December, by the American Association for the Advancement of Science, 1200 New York Avenue NW, Washington, DC 20005. Copyright 2016 by the American Association for the Advancement of Science; all rights reserved. The title *Science* is a registered trademark of AAAS.

- **Peptidoglycan Metabolism**
  (*Waldemar Vollmer* / Yves Brun / Jonathan Dworkin / Elizabeth Sockett / Kevin Young)
- **Stress Responses and Signaling**
  (*Carol Gross* / Samuel Miller / Karina Xavier)
- **Protein Transport and Secretion**
  (*Maria Sandkvist* / Melanie Blokesh / Jean Francois Collet / Jorge Galan / Kelly Hughes)
- **Bacterial Interactions with Hosts and Surfaces**
  (*Caroline Harwood* / Ivo Boneca / Karine Gibbs / Nina Salama / Wendy Thomas)

Bacterial Cell Surfaces
Assembly and Function of Bacterial Surfaces from the Molecular to Intercellular Scales
Jun 25-26, 2016
Chairs: Thomas Bartlett & Tatyana A. Sysoeva

Barriers of the CNS

Key Interfaces Between the Nervous System and the Rest of the Body in Health and Disease
Jun 19-24, 2016
Colby-Sawyer College, New London, NH
Chair: Robert G. Thorne
Vice Chair: Britta Engelhardt

- **Keynote Session: New Perspectives on the CNS Barriers**
  (*Robert Thorne* / Fiona Doetsch / Costantino Iadecola)
- **Transport, Signaling, and Junctions at the CNS Barriers and Beyond**
  (*Martha O'Donnell, Lester Drewes* / Geoffrey Chang / Tetsuya Terasaki / Nathalie Strazielle / Erin Schuetz / Sabina Hrabetova)
- **Late-Breaking Topics**
  (*Stefan Liebner, Xavier Decleves* / Chenghua Gu / Jonathan Kipnis / Martin Lauritzen / Roosmarijn Vandenbroucke / Holly Johnson)
- **CNS Barrier Function in Stroke, Brain Trauma, and Epilepsy**
  (*Zena Vexler, Richard Daneman* / David Antonetti / Gregory Bix / Richard Keep / Jerome Badaut / Bjoern Bauer / Patricia Dickson)
- **CNS Barrier Function in Neurodegenerative Disease, Brain Cancer, and Drug Abuse**
  (*Elizabeth De Lange, Jeffrey Iliff* / Anika Hartz / Helga De Vries / Richard Egleton / William Elmquist)
- **Immunology of the CNS Barriers and Related Systems**
  (*Britta Engelhardt, Lydia Sorokin* / Michal Schwartz / Zsuzsanna Fabry / Roxana Carare / Erlend Nagelhus / Jorge Alvarez)
- **Novel Approaches: Imaging and Model Systems**
  (*Michael Taylor, Ethan Lippmann* / Christian Klambt / Maria Deli / Daniela Virgintino / Angela Gelli)
- **CNS Drug Delivery and Distribution: New Concepts**
  (*Danica Stanimirovic, Eric Shusta* / Margareta Hammarlund-Udenaes / Frederic Calon / Reina Bendayan / Joseph Nicolazzo)
- **Keynote Session: Evolving Perspectives in CNS Barriers Science: Anticipating the Next Ten Years in Academic and Industrial Partnerships**
  (*Joan N. Abbott, Francesca Bosetti* / Rita Balice-Gordon / Saileta Prabhu / Anne Christiansen)

Barriers of the CNS
Involvement of the CNS Barriers in Health, Drug Discovery, and Disease
Jun 18-19, 2016
Chairs: Roosmarijn Vandenbroucke & Holly L. Johnson

Bioanalytical Sensors

From Atoms to Organisms: Bioanalytical Sensors Elucidating Physicochemical Properties of Multiscale Systems
Jun 26 - Jul 1, 2016
Salve Regina University, Newport, RI
Chairs: Elizabeth Hall & Andre A. Adams
Vice Chairs: Robin L. McCarley & Duncan Graham

- **Keynote Session: The Future for Engineered and Wearable Biology in Bioanalytical Sensors**
  (*Elizabeth Hall* / James Ajioko / John Rogers)
- **Synthetic Biology: Analytical Challenges**
  (*James Ajioko* / Sylvia Daunert / Maarten Merkx / Kevin Plaxco)
- **Nanotechnology: From Material to Sensing**
  (*Kevin Plaxco* / Donglei (Emma) Fan / Xiaolei Zuo / Sabine Szunerits)
- **Microanalytical: Spectroscopy and Spectrometry**
  (*Susan Lunte* / Jin-Ming Lin / Pawel Urban / Karen Faulds)
- **In Vitro and In Vivo Sensing and Imaging**
  (*Robin McCarley* / Gabi Kaminski-Schierle / Thomas Meade / Elizabeth Hillman)
- **Microsystems: Molecular or Cellular?**
  (*Duncan Graham* / Thomas Burg / Antje Baeumner / Pallavi Dhagat / Petra Dittrich)
- **New Analytical Detection Platforms**
  (*Gillian Greenway* / Daniel Citterio / Cullen Buie / Jenny Emneus)
- **Materials and Wearables: Is This the Future?**
  (*Antje Baeumner* / Margaret Frey / Sridhar Iyengar)
- **Young Investigator Presentations**
  (*Andre Adams*)

Bioanalytical Sensors
From Atoms to Organisms: Elucidating Physicochemical Properties of Multiscale Systems
Jun 25-26, 2016
Chairs: Josephine C. Cunningham & Quinn A. Best

New for 2016:

The GRC "Power Hour"

The GRC Power Hour is an informal gathering for all meeting participants. It is designed to help address the challenges women face in science and support the professional growth of women in our communities by providing an open forum for discussion and mentoring.

Look for Power Hours and the names of their respective organizers throughout these program listings.

Biocatalysis

Creative Science and Processes for Biocatalysis
Jul 10-15, 2016
University of New England, Biddeford, ME
Chairs: John M. Woodley & Gjalt W. Huisman
Vice Chairs: David B. Berkowitz & Juergen Eck

- **Keynote Session: From Fundamentals to Applications**
  (*Matthew Truppo* / Donald Hilvert / Greg Stephanopoulos)
- **New Enzymes, New Chemistry**
  (*Joelle Pelletier* / Frank Hollmann / Gerrit Poelarends / Jared Lewis / Marko Mihovilovic)
- **Industrial Processes**
  (*Gerrit Poelarends* / Andreas Vogel / Trevor Hallam / Douglas Fuerst)
- **Enzyme Cascades and Systems Biocatalysis**
  (*Claudia Schmidt-Dannert* / Dorte Rother / Jenny Andexer / Wolf-Dieter Fessner / Sabine Flitsch)
- **Whole-Cell Biocatalysis**
  (*Bernhard Hauer* / Douglas Kell / Zhanglin Lin / Bettina Nestl)
- **Process Science**
  (*Andreas Bommarius* / Gabi Sadowski / Ryan Woodyer / Zheyong Yu)
- **New Materials and Applications**
  (*David Berkowitz* / Nicholas Agard / Birgit Kosjek / Everett Stone)
- **Biocatalytic Retrosynthesis**
  (*Nicholas Turner* / Brian Bachmann / Lucia Gardossi / Silvia Osuna)
- **Selected Poster Presentations**
  (*Juergen Eck*)

Biocatalysis
Combining Science and Engineering for Innovation in Biocatalysis
Jul 9-10, 2016
Chairs: Catarina Seita & Michael J. Fink

Biogenic Hydrocarbons & the Atmosphere

Diversity of Sources, Sinks, and Impacts of Atmospheric Organics
Jun 26 - Jul 1, 2016
PGA Catalunya Business and Convention Centre, Girona, Spain
Chairs: Todd N. Rosenstiel & Thomas Karl
Vice Chairs: Nadine Unger & Riikka Rinnan

- **Keynote Session: Key Perspectives on Biogenics and the Atmosphere**
  (*Thomas Sharkey* / Josep Penuelas)
- **Biogenics: Biochemistry, Cells, and Leaves**
  (*Joerg-Peter Schnitzler* / Manuel Rodriguez-Concepcion / Christiane Werner / Pawel Misztal)
- **Biogenics: Dynamics and Processing Within Canopies**
  (*Silvano Fares* / Kenji Matsui / Valerie Gros)
- **Biogenics: Ecosystem Fluxes and Global Interactions**
  (*Christine Wiedinmyer* / Glenn Wolfe / Tsung Fay Fu / Louisa Emmons)
- **Biogenics and Aerosols at the Soil-Vegetation-Atmosphere Interface**
  (*Astrid Kiendler-Scharr* / Richard Splivallo / Mathias Soergel)
- **Young Investigator Presentations**
  (*Riikka Rinnan, Nadine Unger*)
- **Biogenics: Examining the Atmosphere-Water Interface**
  (*Jonathan Williams* / Barbara Noziere)
- **Novel Sources, Interactions, and Transformations of Atmospheric Organics**
  (*Frank Keutsch* / Kelley Barsanti / Armin Hansel / Saewung Kim)
- **Biogenics: Synthesis, Summary, and Future Directions**
  (*Alex Guenther* / Meehye Lee / Allen Goldstein)

Bioinspired Materials

Materials and Biology from Many Perspectives
Jun 5-10, 2016
Les Diablerets Conference Center, Les Diablerets, Switzerland
Chair: Timothy J. Deming
Vice Chair: Zhibin N. Guan

- **Mechanics of Biological Materials**
  (*Timothy Deming* / Thomas Scheibel / Stanislav Gorb)
- **Biointerfaces and Applications**
  (*Zhibin Guan* / Hagan Bayley / Gerard Wong / Cecilia Leal / Niels Holten-Andersen)
- **Bioinspired Devices**
  (*Holger Frauenrath* / Seung-Wuk Lee / Jennifer Cha / Silvia Vignolini)
- **Engineered Materials for Medicine**
  (*Bradley Olsen* / William Murphy / Darrell Irvine / Julie Champion / Sarah Heilshorn)
- **Peptide Mimetics**
  (*Niels Holten-Andersen* / Jan van Hest / Matthew Tirrell)

Downloaded from on February 11, 2016

Gordon Research Conferences

frontiers of science

2016 "Session II" Meetings will be held between May 14 and August 26 in New England in the United States, and internationally in Italy, Spain, Switzerland and Hong Kong, China. A list of preliminary programs appears on the following 29 pages. For detailed programs, fees, site/travel information and online application, visit our web site at **www.grc.org**.

Look for a new element on GRC programs - our "Power Hour" focuses on issues women face in science. It's a dynamic session open to all conferees. GRC is once again at the frontiers of changing science.

- Susan L. Hamilton, 2016 GRC Board of Trustees Chair

Image: *This Structured Illumination Microscopy (SIM) image depicts a HeLa cell. The cell's golgi (orange) is well polarized on one side of the nucleus (grey), both of which are surrounded by a mitochondrial network (magenta) and are framed by actin stress fibers (blue).* Courtesy of Aidan Fenix and Dylan Burnette (Vanderbilt University). Submitted by Lindsey Seldin & Sergio Simoes, Chairs, Cell Polarity Signaling GRS.

2016 "Session II" Preliminary Programs

The list of meetings, session topics and speakers begins below. Discussion leaders are noted in italics.

*Note: **Gordon Research Seminars (GRS)** are listed below their associated Gordon Research Conference. GRSs are 2-day meetings that precede an associated GRC, designed for graduate students, post-docs, and other young scientists to present and exchange new data and cutting-edge ideas. Seed funding for new Gordon Research Seminars is provided by the Kenan Institute for Engineering, Technology & Science at North Carolina State University and Merck & Co., Inc.*

Advanced Health Informatics

NEW!

The Use of Big Data in Health Related Research
Jul 17-22, 2016
The Chinese University of Hong Kong, Hong Kong, China
Chairs: Benjamin Wah & Nitish Thakor
Vice Chairs: Yuan-Ting Zhang & Ratko Magjarevic

- **Keynote Session: Grand Challenges in Health Informatics**
  (*Benjamin Wah, Nitish Thakor* / Roderic Pettigrew)
- **Medical Informatics**
  (*Shankhar Krishnan* / Mark Musen / Stephen Wong / Lucila Ohno-Machado)
- **Cardiovascular Health Informatics**
  (*Raimond Winslow* / Peter Hunter / Natalia Trayanova)
- **Neuro-Informatics**
  (*Nitish Thakor* / Bin He / Michael Miller / Philip Yu)
- **Big Data Analytics**
  (*Christian Roux* / May Dongmei Wang / Suchi Saria)
- **Wearable Sensing Informatics**
  (*Yuan-Ting Zhang* / Guang-Zhong Yang / Shuming Nie / Ni Zhao)
- **Data Mining and Knowledge Discovery**
  (*Eric Chang* / Rossa Chiu / Timothy Dye)
- **Imaging Informatics**
  (*Andrew Laine* / Lihong Wang / Xiaochuan Pan / Aydogan Ozcan)
- **Healthcare Engineering and Informatics**
  (*Ratko Magjarevic* / Nigel Lovell / Mark Braunstein)

Advanced Materials for Sustainable Infrastructure Development

The Science and Technology of Sustainable Concrete
Jul 31 - Aug 5, 2016
The Hong Kong University of Science and Technology, Hong Kong, China
Chairs: Christopher Leung & David A. Lange
Vice Chairs: Changwen Miao & Pedro Castro Borges

- **Nanoscopic Behavior and Modeling**
  (*Kimberly Kurtis* / Zongjin Li / Jason Weiss)
- **Microstructure Characterization and Multi-Scale Modeling of Concrete**
  (*Eric Landis* / Karen Scrivener / Adnan Ibrahimbegovic)
- **Application of Nanotechnologies in Cementitious Materials**
  (*Paramita Mondal* / Surendra Shah / Maria Kosta-Gdoutos)
- **Alternative Cementitious Materials**
  (*Jannie van Deventer* / Jose Ivan Escalante Garcia / Manu Santhanam / Tongbo Sui)
- **Novel Techniques for Concrete Testing**
  (*Nemkumar Banthia* / Masayasu Ohtsu / Tyler Ley)
- **High Performance Concrete**
  (*Hans Reinhardt* / Paulo Helene / Kamal Khayat / Victor Li)
- **Green Approaches for Concrete Design**
  (*Jianzhuang Xiao* / Chi-sun Poon / Claire White)
- **Functional Concrete**
  (*Konstantin Kovler* / Erik Schlangen / Pedro Garces Terradillos / Min-Hong Zhang)
- **Concrete Design for Durability Under Severe Environment**
  (*Mark Alexander* / Carmen Andrade Perdrix / R. Doug Hooton)

Auditory System

The Plastic and Dynamic Auditory System
Jul 10-15, 2016
Bates College, Lewiston, ME
Chair: Stephen G. Lomber
Vice Chair: Jeffrey Holt

- **Keynote Session: Hearing Across the Auditory System**
  (*Lisa Goodrich* / Barbara Canlon / Donata Oertel / Rhodri Cusack)
- **The Developing Auditory System**
  (*Ed Rubel* / Bechara Kachar / Ronna Hertzano / Dwight Bergles / Deda Gillespie / Merri Rosen)
- **Hair Cells: Turning Motion into Signal**
  (*Barbara Canlon* / Corne Kros / Ruth Anne Eatock / Jutta Engel)
- **Influence of Up, Down and Lateral Connections**
  (*Paul Manis* / Matthew Xu-Friedman / Brett Schofield / Adrian Rees / Stephen David / Jason Middleton)
- **Plasticity in Auditory Cortical Networks**
  (*Chris Petkov* / Andrea Hasenstaub / Daniel Polley / Robert Zatorre)
- **Deafness and Hearing Loss**
  (*Alex Meredith* / Jung-Bum Shin / Marlies Knipper / Andy Forge / Andrej Kral / Dan Sanes)
- **Using Sound to Navigate the World**
  (*Gary Paige* / Tom Yin / John Ratcliffe / Lore Thaler)
- **Biological and Electrical Hearing Restoration**
  (*Andrej Kral* / Brandon Cox / Philine Wangemann / James Fallon / Karen Gordon / Ruth Litovsky)
- **Social and Cognitive Aspects of Hearing**
  (*Robert Zatorre* / Robert Froemke / Yale Cohen / Chris Petkov)
- **Power Hour**
  (*Ruth Anne Eatock*)

GRS **Auditory System**
Auditory and Vestibular Systems: Periphery to Perception
Jul 9-10, 2016
Chair: Catherine Weisz

Bacterial Cell Surfaces

Assembly and Function of Bacterial Surfaces from the Molecular to Intercellular Scales
Jun 26 - Jul 1, 2016
Mount Snow, West Dover, VT
Chairs: Zemer Gitai & Mariana G. Pinho
Vice Chairs: Carol Gross & Waldemar Vollmer

- **Bacterial Communities and Motility**
  (*George O'Toole* / Judith Armitage / Lotte Sogaard-Andersen / Ned Wingreen)
- **Cell Division and Morphogenesis**
  (*Rut Carballido-Lopez* / Christophe Grangeasse / Christine Jacobs-Wagner / German Rivas Caballero / Jan Lowe)
- **Antibiotics - What Works and What's Missing**
  (*Hans-Georg Sahl* / Heike Brotz-Oesterhelt / Steven Projan / Terry Roemer)
- **Membrane Dynamics**
  (*Stephen Trent* / Julie Biteen / Kerwyn Huang / Daniel Kahne / Dan Wall)
- **Surface Polymers**
  (*Lori Burrows* / Sonja-Verena Albers / Katharina Ribbeck / Olaf Schneewind)

- **Bioinspired Synthetic Polymers**
  (*Julie Champion* / Jean Francois Lutz / Kazunori Kataoka / Tanja Weil)
- **Bioinspired Assemblies**
  (*Jennifer Cha* / Daniel Hammer / Holger Frauenrath / Bradley Olsen)
- **Adaptive Design of Materials**
  (*Sarah Heilshorn* / Yi Lu / Sijbren Otto / Christoph Weder)
- **Mineralized/Hybrid Materials**
  (*Cecilia Leal* / Peter Fratzl / LaShanda Korley)

Bioinspired Materials
Translating Biological Mechanisms into Functional Materials
Jun 4-5, 2016
Chairs: Abigail S. Knight & Karla-Luise Herpoldt

Biointerface Science

Active, Adaptive, and Responsive Biointerfaces
Jun 12-17, 2016
Les Diablerets Conference Center, Les Diablerets, Switzerland
Chair: Atul N. Parikh
Vice Chair: Hagan P. Bayley

- **Keynote Session: Active, Adaptive, and Dynamic Biointerfaces**
  (*C. Jeffrey Brinker* / Stephen Mann / Petra Schwille)
- **Smart and Responsive Biointerfaces and Biosensors**
  (*Bengt Kasemo* / Marta Bally / Daniel Fletcher / Dimitrios Stamou)
- **Chemistry of Interfaces**
  (*Atul Parikh* / Paul Cremer / Samuel Stupp)
- **Characterization of Interfaces: New Advances**
  (*Milan Mrksich* / Luke Lee / Daniel Mueller / Sara Sandin)
- **Origins of Life and Synthetic Cell**
  (*Kathryn Whitehead* / Lee Cronin / Dek Woolfson)
- **Cellular and Intercellular Interfaces**
  (*Jay Groves* / Satyajit Mayor / Viola Vogel / Jeanne Stachowiak)
- **Interfaces in Cellular Colonies and Microbial Communities**
  (*Hagan Bayley* / Staffan Kjelleberg / Gerard Wong)
- **Late-Breaking Topics**
  (*Paul Cremer*)
- **Perspectives: What Constitutes Biointerface Science**
  (*Stephen Mann* / Hagan Bayley / Milan Mrksich / Bengt Kasemo)

Biointerface Science
Building Interdisciplinary Bridges Towards Expanding the Frontiers of Biological Science
Jun 11-12, 2016
Chairs: Hudson Pace & Elisa D'Arcangelo

Biomineralization

Interactions Between Organic and Inorganic Materials Across Time and Length Scales
Aug 14-19, 2016
PGA Catalunya Business and Convention Centre, Girona, Spain
Chair: Nico A.J.M. Sommerdijk
Vice Chair: Derk Joester

- **Matrix-Mineral Interactions in Bone**
  (*Steve Weiner* / Melinda Duer / Nadine Nassif)
- **Cellular and Genetic Control of Mineralization**
  (*Nils Kroeger* / Damien Faivre / Michio Suzuki)
- **Pathological Mineralization**
  (*Catherine Shanahan* / Elaine Worcester / Wilhelm Jahnen-Dechent)
- **In Vitro and In Vivo Models of Biomineralization**
  (*Lia Addadi* / Elia Beniash / Marc McKee / Eli Sone)
- **Biomineralization in Sponges and Corals**
  (*Sylvie Tambutte* / Jaap Kaandorp)
- **Mechanisms of Mineral Nucleation and Growth**
  (*Jim De Yoreo* / Patricia Dove / Mark Rodger / Julian Gale)
- **Structure and Function in Biominerals**
  (*Paul Hansma* / Paul Zaslansky / David Kisailus)
- **Bioinspired Crystallization**
  (*Fiona Meldrum* / Peter Davies / Ruikang Tang / Hiroaki Imai)
- **Keynote Session: Biomimetic Materials**
  (*Nico Sommerdijk* / Joanna Aizenberg)

Biomineralization
Exploring Mechanisms Behind Biomineral Formation and Function
Aug 13-14, 2016
Chairs: Betty Hoac, Anat Akiva & Michael L. Whittaker

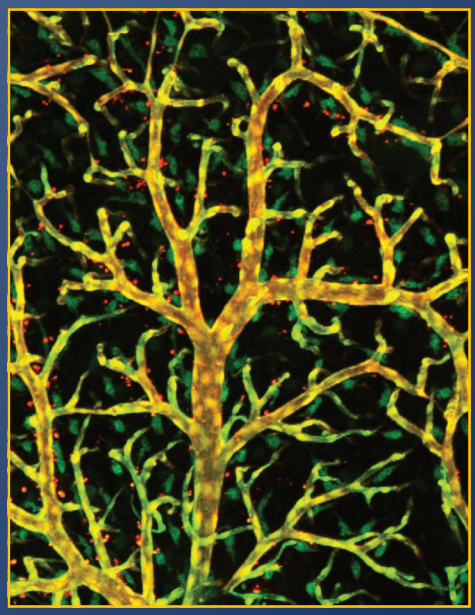

Confocal imaging of the adult zebrafish brain vasculature. All blood vessels are labeled with green fluorescence and vessels with blood-brain barrier properties are labeled with red fluorescence. Courtesy of Michael R. Taylor (University of Wisconsin-Madison). Submitted by Robert Thorne, Chair, Barriers of the CNS GRC.

Bioorganic Chemistry

Chemical Approaches for Unraveling Biology
Jun 5-10, 2016
Proctor Academy, Andover, NH
Chairs: Carole A. Bewley & Douglas S. Johnson
Vice Chairs: Paramjit S. Arora & Frank W. Kotch

- **Keynote Session: Diversity of Chemistry in Nature**
  (*Michael Burkart* / Michael Fischbach / Amy Wright / Craig Townsend)
- **Applications of Bioorthogonal Chemistry**
  (*Kabirul Islam* / Joseph Fox / Kate Carroll / Thomas Sakmar)
- **Illuminating Biology with Imaging**
  (*Timothy Dore* / Alice Ting / Luke Lavis / Marcel Bruchez)
- **Bio-Inspired Synthesis**
  (*Daniel Appella* / Jennifer Cochran / Eric Schmidt / Helma Wennemers / Michael Jewett)
- **Glycans in Health and Biology**
  (*Lara Mahal* / David Vocadlo / Pauline Rudd / James Paulson)
- **Chemoproteomics in Therapeutic Applications**
  (*Brent Martin* / Daniel Nomura / Markus Schirle / Stephan Sieber)
- **Drug Discovery and Therapeutics**
  (*David Rabuka* / Adam Johnson / Markus Bantscheff / David Gray)
- **Approaches to Tame Intractable Targets**
  (*Emily Derbyshire* / Yueming Li / Robert Garbaccio / Gabriela Chiosis)
- **Advances in Chemical Biology**
  (*Douglas Johnson* / Paola Castaldi / John Pezacki / Alanna Schepartz)

Cardiac Regulatory Mechanisms

Atoms to Omics – New Approaches to Understand and Treat Cardiac Disease
Jun 5-10, 2016
Colby-Sawyer College, New London, NH
Chairs: Bjorn C. Knollmann & Barbara Casadei
Vice Chairs: Brian O'Rourke & Thomas Eschenhagen

- **Cardiac Repair and Regeneration**
  (*Mark Sussman, Charles Hong* / Charles Murry / Kai Wollert / Wolfram Zimmerman / Tromondae Feaster)
- **Mitochondrial Function, Redox Signaling and Calcium Handling**
  (*Asa Gustafsson, Elizabeth Murphy* / Christoph Maack / Natalia Shirokova / Jennifer Kwong / Moshi Song / Francesco Cosentino / Michael Murphy)
- **Cardiac Ageing and Rejuvenation**
  (*Steven Houser, Martin Morad* / Michael Ristow / Richard Lee / Satchidananda Panda)
- **Regulation of Myofilament Function in Health and Disease**
  (*John Solaro, Jill Tardiff* / David Warshaw / Sakthivel Sadayappan / Jolanda Van Der Velden / Aldrin Gomes / Dan Beard / Sabine Huke / Benjamin Prosser)
- **Cell to Cell Cross-Talk in the Heart**
  (*Burns Blaxall, Karin Sipido* / Matthias Nahrendorf / Stefan Engelhardt / Marco Mongiello / Charalambos Antoniades)
- **Molecular Mechanism of Atrial Fibrillation**
  (*Dobromir Dobrev* / Pepe Jalife / Sander Verheule / Larissa Fabritz / Maura Greiser / Xander Wehrens)
- **Calcium Signaling and EC Coupling**
  (*Wayne Chen, Alicia Mattiazzi* / Filip Van Petegem / David Eisner / Ye Chen-Izu / Gil Bub)
- **Molecular Signaling in Myocardial Remodeling**
  (*Lucie Carrier, Jeffery Molkentin* / Paula Da Costa-Martins / Thomas Braun / Jennifer Davis / Sarah Franklin / Denise Hilfiker-Kleiner / Roger Hajjar)
- **Keynote Session: Harnessing Big Data for Basic Discovery**
  (*Walter Koch* / Patrick Ellinor / Dan Roden / Christine Seidman)

Cardiac Regulatory Mechanisms
Innovative Answers to Classic Cardiac Questions
Jun 4-5, 2016
Chairs: Jerry Curran & Ronald J. Vagnozzi

Carotenoids

Carotenoid Biosynthesis, Functions, and Application to Human Health
May 22-27, 2016
Renaissance Tuscany Il Ciocco, Lucca (Barga), Italy
Chair: Johannes Von Lintig
Vice Chair: Giovanni Giuliano

- **Pathway Engineering**
  (*Norihiko Misawa* / Paul Christou / Paul Fraser / Ralf Welsch)
- **Carotenoid Biosynthesis**
  (*Barry Pogson* / Dean Dellapenna / Li Li / Manuel Rodriguez-Concepcion)
- **Carotenoids in Health and Disease**
  (*Helmut Sies* / Elizabeth Johnson / George Lietz / Sherry Tanumihardjo)
- **Apocarotenoid Synthesis and Functions**
  (*Salim Al-Babili* / Harro Bouwmeester / Earl Harrison / Maria Jesus-Rodrigo / Philip Kiser)
- **Carotenoids and Disease Prevention**
  (*William Blaner* / Nancy Moran / Yoav Sharoni)
- **Photosynthesis and Plastids**
  (*Krishna Niyogi* / Roberto Bassi / Ralph Bock / Cheryl Kerfeld / Diana Kirilovsky)
- **Apocarotenoid Metabolism**
  (*Loredana Quadro* / Gianfranco Diretto / Alexander Moise / Xiang-Dong Wang)
- **Carotenoids in Vision**
  (*John Landrum* / Darwin Babino / Paul Bernstein / Joseph Corbo / John Nolan)
- **Regulation of the Carotenoid Biosynthetic Pathway**
  (*Joseph Hirschberg* / James Giovannoni / Eleanore Wurtzel)

The GRS allows for significant interaction between early career investigators, and is an experience that is not easily duplicated elsewhere.

- Heather Ford, Chair, 2015 Interior of the Earth GRS

- **Power Hour**
  (*Eleanore Wurtzel, Loredana Quadro*)

GRS Carotenoids
Carotenoid Biosynthesis, Functions, and Application to Human Health
May 21-22, 2016
Chairs: Darwin Babino & Maria Sulli

Catalysis
Catalysis - From Theory to Commercialization
Jun 12-17, 2016
Colby-Sawyer College, New London, NH
Chair: Christopher L. Marshall
Vice Chair: Fabio H. Ribeiro

- **Paraffin Upgrading**
  (*Rajamani Gounder* / Thomas Degnan / Lars Grabow)
- **Organometallic Routes to Heterogeneous Catalysts**
  (*Dongxia Liu* / Alex Katz / Susannah Scott / Adam Hock)
- **Watching Working Catalysts**
  (*Rebecca Fushimi* / Pratibha Gai / Simon Bare)
- **Model Catalyst Systems**
  (*Yu Lei* / Hans-Joachim Freund / Jeff Greeley / Jochen Lauterbach)
- **New Catalysts for Biomass Feedstocks**
  (*Jason Hicks* / Carsten Sievers / Yong Wang)
- **Elucidating Catalytic Mechanisms**
  (*Eranda Nikolla* / Ya-Huei (Cathy) Chin / Cynthia Friend / Suljo Linic)
- **Non-Traditional Catalyst Supports**
  (*Bin Liu* / Yuriy Roman-Leshkov / Laura Gagliardi)
- **New Materials for Catalysis**
  (*Feng Gao* / David Barton / Xiaofan Yang / Axel Gross)
- **Keynote Session: Surface Chemistry of Catalytic Systems**
  (*Fabio Ribeiro* / Charles Campbell)

Cell Biology of the Neuron
The Mechanisms Underlying Development, Function, and Pathological Malfunctions in Neurons
Jun 26 - Jul 1, 2016
Waterville Valley, Waterville Valley, NH
Chairs: Thomas L. Schwarz & Claudia Bagni
Vice Chairs: Erika L.F. Holzbaur & Matthijs Verhage

- **Keynote Session: Mechanisms of Intracellular Membrane Traffic**
  (*Claudia Bagni* / Pietro De Camilli)
- **Trans-Synaptic Transfer in Development and Disease**
  (*Ryohei Yasuda* / Holly Cline / Larry Benowitz / Vivian Budnik)
- **Protein and RNA Trafficking in Dendrites and Axons**
  (*Erika Holzbaur* / Casper Hoogenraad / Erin Schuman / Kelsey Martin / Gary Banker / Kozo Kaibuchi)
- **Assembly and Plasticity of Postsynaptic Structures**
  (*Yishi Jin* / Yimin Zou / Daniel Choquet / Eunjoon Kim / Peter Scheiffele)
- **Assembly of Presynaptic Structures**
  (*Timothy Ryan* / Kang Shen / Daniel Colon-Ramos / Pico Caroni / Matthew Pecot)
- **Cell Signalling and Cell Growth in Neurons**
  (*Susumu Tomita* / Dorothy Schafer / Michelle Monje / Freda Miller / Rosalind Segal)
- **Function and Plasticity of the Synaptic Vesicle Cycle**
  (*Matthijs Verhage* / Graeme Davis / Nils Brose / Ricardo Dolmetsch / Patrik Verstrecken)
- **Cell Biology of Neuronal Degeneration and Regeneration**
  (*Erik Jorgensen* / Aaron Diantonio / Marc Freeman / Alison Lloyd / Frank Bradke / Valeria Cavalli)
- **Keynote Session: Protein Aggregation and Neuropathology**
  (*Thomas Schwarz* / Susan Lindquist)

GRS Cell Biology of the Neuron
The Life of a Neuron: Mechanistic Insights into Neural Development, Function, Regeneration and Disease
Jun 25-26, 2016
Chairs: Shan Meltzer & Natasha Khatri

Cell Death
New Concepts in Cell Death Research: From Basic Mechanisms to Clinical Opportunities
Jul 3-8, 2016
PGA Catalunya Business and Convention Centre, Girona, Spain
Chair: Henning Walczak
Vice Chair: Marion Macfarlane

- **Keynote Session: Perspectives on Cell Death and Survival**
  (*Henning Walczak* / Eric Baehrecke / Douglas Green)
- **Cell Signalling, Survival and Death**
  (*Marion Macfarlane* / Vishva Dixit / Seamus Martin / Hao Wu / Domagoj Vucic)
- **Mitochondria and Cell Death in Cancer**
  (*Richard Youle* / Joseph Opferman / Andreas Villunger / Ana Garcia-Saez)
- **Mitochondria and Cell Death in Neurodegeneration and Autoimmunity**
  (*Douglas Green* / Richard Youle / J. Marie Hardwick / Atan Gross / Nika Danial)
- **Cell Death Networks and Clearance**
  (*John Abrams* / Shigekazu Nagata / Inna Lavrik / Will Wood)
- **Cell Survival and Death in Cancer**
  (*Andreas Strasser* / Scott Lowe / Junying Yuan / Guy Salvesen)
- **Non-Canonical Death Pathways and Model Organisms**
  (*Eric Baehrecke* / Christine Watson / John Abrams / Marcus Peter)
- **Programmed Necrosis and Inflammation**
  (*Guy Salvesen* / Francis Chan / Kim Newton / John Silke / Peter Vandenabeele)
- **Translating Cell Death Discoveries Towards the Clinic**
  (*J. Marie Hardwick* / Anthony Letai / Pascal Meier / Andreas Strasser / Sandra Zinkel)

Cell Polarity Signaling
Cell Polarity in Development, Division, and Disease
Jun 12-17, 2016
Mount Snow, West Dover, VT
Chair: Ian G. Macara
Vice Chair: Ulrich Tepass

- **Keynote Session: Cell Polarization Mechanisms**
  (*Ian Macara* / Daniel St. Johnston)
- **Cell Polarity in Unicellular Organisms**
  (*Anne Spang* / Daniel Lew / Urs Jenal / Sophie Martin)
- **Polarity in Development: Stem Cells**
  (*Jeremy Nance* / Elaine Fuchs / Ken Prehoda)
- **Polarity in Development: Epithelia**
  (*Elizabeth Knust* / Greg Longmore / Bob Varelas / Fernando Martin-Belmonte / Michel Bagnat)
- **Epithelial Mechanobiology - Extrusion and Strain**
  (*Alpha Yap* / Jody Rosenblatt / Ulrich Tepass)
- **Polarity in Disease: Cancer**
  (*Luke McCaffrey* / Andrea McClatchy / Andrew Ewald / Joseph Kissil)
- **Polarity in Disease: PCD, Wound Healing, Immune Response**
  (*William Bement* / Gillian Griffiths / Paul Martin)
- **Mitotic Spindle Orientation Mechanisms**
  (*Terry Lechler* / Matthew Gibson / Jessica Feldman / Patrick Laprise)
- **Planar Polarity and Tissue Morphogenesis**
  (*Helen McNeill* / Danelle Davenport / Sergei Sokol)
- **Power Hour**
  (*Jody Rosenblatt*)

GRS Cell Polarity Signaling
Cell Polarity in Development and Disease
Jun 11-12, 2016
Chairs: Sergio Simoes & Lindsey Seldin

Cellular & Molecular Fungal Biology
Dynamic Interactions Across Scales from Single Molecules to Fungal Communities
Jun 19-24, 2016
Holderness School, Holderness, NH
Chairs: Amy S. Gladfelter & Natalia N. Requena
Vice Chairs: Antonis Rokas & Alistair J.P. Brown

- **Cell Dynamics**
  (*Meritxell Riquelme* / Maria Harrison / Michael Feldbrugge / Marko Kaksonen / Steve Osmani)
- **Environmental Sensing**
  (*Louise Glass* / Jennifer Hurley / Alexander Idnurm / Leah Cowen / Robert Cramer / Michael Brunner / Antonio Di Pietro)
- **Fungal Communities**
  (*Deborah Hogan* / Paola Bonfante / Michelle Momany / Clarissa Nobile / Thomas Richards)
- **Fungal Evolution and Genome Dynamics**
  (*Jason Stajich* / Liedewij Laan / Bruce McDonald / Anna Selmecki / Sophien Kamoun / Hanna Johannesson / Jonathan Jones)
- **Late-Breaking Topics**
  (*Alistair Brown, Antonis Rokas*)
- **Physics and Mathematical Modeling of Fungi**
  (*Peter Philippsen* / Susanne Rafelski / Marcus Roper / Nick Money / Christian Hong / Alexandra Brand / Roger R. Lew)
- **Fungi Responding to Stress**
  (*Judy Bermann* / Sabine Fillinger / Axel Brakhage / Katherine Borkovich / Alfredo Herrera-Estrella)
- **Host Interactions: Fungi Interacting with Plants**
  (*Barbara Valent* / Nicholas Talbot / Alga Zuccaro / Barry Scott / Elodie Gaulin / Francois Lutzoni / Regine Kahmann)
- **Host Interactions: Fungi Interacting with Animals**
  (*Geraldine Butler* / Matthias Brock / Kirsten Nielsen / Emily Troemel / Anita Sil)

Centromere Biology
Structural and Functional Dynamics of the Centromere in Mitosis and Meiosis
Jul 24-29, 2016
Mount Snow, West Dover, VT
Chair: Beth A. Sullivan
Vice Chair: Aaron F. Straight

- **Keynote Session: Centromere Basics: Composition, Architecture, and Function**
  (*Rachel O'Neill* / Sue Biggins / Gary Karpen)
- **Biophysical and Structural Properties of Centromeres**
  (*Daniel Foltz* / Ben Black / Ajit Joglekar / Kerry Bloom / Charles Asbury)
- **Meiotic Specialization of Centromeres**
  (*Michael Lampson* / Scott Hawley / Julie Cooper / Arshad Desai)
- **Centromeres: Drivers and Shapers of Genomes**
  (*Kerry Bloom* / Michael Lampson / Harmit Malik / Kelly Dawe)

- **Genomics and Sequence-Dependent Centromere Function**
  (*Munira Basrai* / Karen Miga / Michael Freitag / Steven Henikoff)
- **Centromeres Throughout the Cell Cycle**
  (*Sylvia Erhardt* / Barbara Mellone / Daniel Foltz / Patrick Heun)
- **Centromere Epigenetics**
  (*Steven Friedman* / James Birchler / William Earnshaw / Jiming Jiang / Tatsuo Fukagawa)
- **RNAs in Centromere and Kinetochore Function**
  (*Shannon McNulty* / Robin Allshire / Sylvia Erhardt / Rachel O'Neill)
- **Centromeres and Genome Stability**
  (*Arshad Desai* / Yamini Dalal / Don Cleveland)
- **Power Hour**
  (*Rachel O'Neill*)

Centromere Biology
Building a Bridge from Centromeres to Spindle Microtubules
Jul 23-24, 2016
Chairs: Steven Friedman & Shannon L. McNulty

Ceramics, Solid State Studies in
Creating Functionality of Advanced Ceramics by Innovative Materials Processing
Jul 31 - Aug 5, 2016
Mount Holyoke College, South Hadley, MA
Chair: Michael J. Hoffmann
Vice Chair: Jian Luo

- **Bioinspired Ceramics**
  (*Marina Pascucci* / Anna Tamperini / Gerold Schneider)
- **Designing Microstructures for Functional Applications**
  (*Shen Dillon* / Yet-Ming Chiang / Gary Messing / Barbara Malic)
- **Ceramics with Controlled Porosity**
  (*Ivar Reimanis* / Norbert Willenbacher / Rajendra Bordia)
- **New Paradigms for Grain Boundaries and Interfaces**
  (*Gregory Rohrer* / Martin Harmer / Suk-Joong Kang / Veena Tikare)
- **New Insights in Characterizing Grain Boundaries and Interfaces**
  (*Wayne Kaplan* / Klaus van Benthem / Bilge Yildiz)
- **Advanced Manufacturing Technologies**
  (*John Blendell* / John Halloran / Alexander Michaelis / Brian Derby)
- **Recent Advances in Sintering Technologies**
  (*Eugene Olevsky* / Olivier Gullion / Hermann Riedel)
- **Designing Microstructures for Structural Applications**
  (*Martha Mecartney* / Helen Chan / Tatsuki Ohji / Frank Zok)
- **Keynote Session: XRD Tomography - A Key to Obtain Better Materials**
  (*Edwin Garcia* / Carl Krill)

Ceramics, Solid State Studies in
Ceramics at the Microscale: State-of-the-Art in Processing, Properties and Microstructure
Jul 30-31, 2016
Chairs: William J. Bowman & Marc Dumerac

Chemotactic Cytokines
From Molecular Mechanisms of Chemokine Biology and Pathophysiology to Progress and Challenges in the Development of Therapeutics
May 29 - Jun 3, 2016
PGA Catalunya Business and Convention Centre, Girona, Spain
Chair: Tracy M. Handel
Vice Chair: Reinhold J. Forster

- **Keynote Session: Visualizing Cancer Invasion**
  (*Tracy Handel* / Peter Friedl)
- **Atypical Receptors and Atypical Interactions in Chemokine Function and in Disease**
  (*Massimo Locati* / Marcus Thelen / Antal Rot / Ralf Stumm / Kathleen Caron)
- **Chemokines in Immunity, Host Defense and Inflammation**
  (*Sergio Lira* / Gerry Graham / Heather Hickman / Federica Sallusto)
- **Therapeutic Targeting of Chemokine Receptors**
  (*Philip Murphy* / Amanda Proudfoot / Thomas Schall / John Westwick / Ola Winqvist)
- **Mechanisms of Cell Migration and Gradient Sensing**
  (*Ronen Alon* / Michael Sixt / Tim Lammermann / Sussan Nourshargh)
- **Chemokines, Inflammation and Cancer**
  (*Barrett Rollins* / Jeffrey Pollard / Andrew Luster / Ann Richmond)
- **Control of Cell Function by Chemokines in the Microenvironment**
  (*Ann Richmond* / Shannon Turley / Barrett Rollins / Paul Frenette)
- **Novel Mechanisms for Regulating Chemokine Function**
  (*Mario Mellado* / Eleanor Fish / Richard Ransohoff / Matthew Albert / Martine Smit)
- **Mechanisms of Immune System Development and Homeostasis**
  (*Federica Sallusto* / Reina Mebius / Ellen Robey / Reinhold Forster)

Chemotactic Cytokines
Emerging Concepts in Chemokine Biology
May 28-29, 2016
Chairs: Maud Deruaz & Douglas P. Dyer

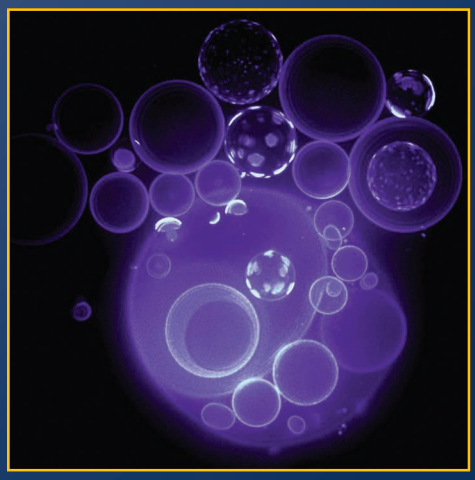

Oscillatory dynamics of giant vesicular compartments under osmotic stress. This reveals a novel autonomous capability of lipid vesicles, in which an external osmotic perturbation is managed by a coordinated and cyclical sequence of physical mechanisms allowing vesicles to sense (by domain formation) and regulate (by solute efflux) their local environment in a negative feedback loop. Courtesy of Atul N. Parikh, Kamila Oglecka, Rachel Kraut and Bo Liedberg. Submitted by Atul N. Parikh, Chair, Biointerface Science GRC.

Chromatin Structure & Function
Regulating and Re-Engineering Chromatin: Control of Genome Function
May 22-27, 2016
Les Diablerets Conference Center, Les Diablerets, Switzerland
Chair: Wendy Bickmore
Vice Chair: Karolin Luger

- **From Nucleosomes to Chromosomes, Single Molecules to Single Cells**
  (*Peter Becker* / Geeta Narlikar / Guohong Li / Maria-Elena Torres-Padilla / William Greenleaf)
- **The Many Faces of the Nucleosome**
  (*Genevieve Almouzni* / Carl Wu / Frank Pugh / Yawen Bai)
- **Engineering Chromatin**
  (*Song Tan* / Tom Muir / Jerry Crabtree / Jurg Muller / Qiang Wu)
- **Establishing Chromatin States**
  (*Anja Groth* / Rob Klose / Craig Peterson / Susan Gasser / Petra Hajkova)
- **Chromatin Complexes**
  (*Carl Wu* / Juri Rappsilber / Asifa Akhtar / Song Tan / Tatsuya Hirano)
- **Chromosome Folding, Topography and Domains**
  (*Edith Heard* / Nick Gilbert / Shiv Grewal / Ana Pombo / Job Dekker)
- **Propagating and Re-Programming Chromatin Landscapes**
  (*Shiv Grewal* / Robin Allshire / Anja Groth / Genevieve Almouzni / Abdenour Soufi)
- **Regulation and Cross-Talk Between Chromatin States**
  (*Geeta Narlikar* / Hiten Madhani / Bing Zhu / Peter Becker / Ben Black)
- **RNA and Chromatin**
  (*Susan Gasser* / Edith Heard / Mitch Guttman / Danny Reinberg)

Colloidal Semiconductor Nanocrystals
Nanocrystal Physics and Chemistry Enabling Applications
Jul 31 - Aug 5, 2016
Mount Snow, West Dover, VT
Chair: Delia J. Milliron
Vice Chairs: Daniel R. Gamelin & Zeger Hens

- **Doping and Plasmonics**
  (*David Norris* / Uwe Korteshagen / Alex Govorov)
- **Optoelectronics**
  (*Cherie Kagan* / Neil Greenham / Sandra Rosenthal)
- **Integration, Assembly, and Electronic Transport**
  (*Matt Law* / Maria Loi / Tobias Hanrath)
- **Carrier Dynamics**
  (*Jillian Dempsey* / Marco Califano / Efrat Lifshitz / Matthew Pelton / David Watson)
- **Synthesis and Surface Chemistry**
  (*Susan Kauzlarich* / Stephanie Brock / Richard Brutchey / Javier Vela-Becerra / Benoit Dubertret)
- **Biological Applications**
  (*Brett Helms* / Molly Stevens / Xiaohu Gao)
- **Photochemistry**
  (*Andrew Greytak* / Jochen Feldmann / Emily Weiss)
- **Pnictides and Halides**
  (*Remi Beaulac* / Jillian Buriak / Brandi Cossairt / Maksym Kovalenko / Paul O'Brien)
- **Photonics and Excitons**
  (*William Tisdale* / Richard Loomis / Iwan Moreels / Daniel Vanmaekelbergh / Philippe Guyot-Sionnest)

Colloidal Semiconductor Nanocrystals
New Semiconductor Nanocrystal Materials and Advances in Nano Characterization Techniques
Jul 30-31, 2016
Chairs: Robert W. Johns & Charles Barrows

Computational Chemistry
Theory and Simulation Across Scales in Molecular Science
Jul 24-29, 2016
PGA Catalunya Business and Convention Centre, Girona, Spain
Chair: Adrian J. Mulholland
Vice Chair: Angela Wilson

- **Keynote Session: Frontiers in Computational Molecular Science**
  (*Kenneth Merz* / Todd Martinez / Sharon Glotzer)
- **Quantum Chemistry**
  (*Julia Rice* / Garnet Chan / Alexandre Tkachenko)
- **Catalysis and Reactivity**
  (*Jan Jensen* / Fahmi Himo / Qiang Cui)
- **Chemical Reactions and Dynamics**
  (*Jeremy Harvey* / Johan Aqvist / Ignacio Tunon)
- **Simulation Across Scales**
  (*Vicente Moliner* / Peter Bolhuis / David Wales)

- **Free Energy Methods and Enhanced Sampling** (*William Swope* / Frank Noe / Gerhard Hummer)
- **Biomolecular Simulation and Drug Development** (*Woody Sherman* / Alessio Lodola / Zoe Cournia / Modesto Orozco)
- **Simulations: Pushing the Boundaries** (*Syma Khalid* / Rebecca Wade / Ross Walker)
- **Mechanisms and Modelling** (*Maria Ramos* / Massimo Noro / Sharon Hammes-Schiffer / Adrian Roitberg)

GRS **Computational Chemistry**
Bridging Computation and Experiment at All Scales
Jul 23-24, 2016
Chair: Nicholas Leioatts

Conductivity & Magnetism in Molecular Materials

Molecular Materials: Frontiers in Functional Design
Aug 14-19, 2016
Mount Holyoke College, South Hadley, MA
Chairs: Stuart Brown & Stephen Hill
Vice Chairs: Kazushi Kanoda & Corine Mathoniere

- **Optical Switching** (*Daniel Talham* / Rodolphe Clerac / Mark Meisel)
- **Competing Interactions and Frustration** (*Benjamin Powell* / Reizo Kato / Senthil Todadri)
- **Molecular Nanomagnets** (*Muralee Murugesu* / Jeffrey Long)
- **Molecular Spin Qubits** (*Jonathan Friedman* / Danna Freedman / Stefano Carretta / Arzhang Ardavan)
- **Theory and Modeling** (*Hitoshi Seo* / Vladimir Dobrosavljevic / Roser Valenti)
- **Organic Superconductivity** (*Shinya Uji* / Joachim Wosnitza / Hiroshi Yamamoto / Vesna Mitrovic)
- **Ultrafast Phenomena and Spectroscopy** (*Martin Dressel* / Daniele Nicoletti / Eric Collet)
- **Single Molecule Devices** (*Enrique Del Barco* / Roberta Sessoli / Sebastian Loth)
- **Coupled Conductivity and Magnetism** (*Richard Oakley* / Eugenio Coronado)

GRS **Conductivity & Magnetism in Molecular Materials**
Molecular Materials: Fundamentals and Emerging Functionality
Aug 13-14, 2016
Chairs: Stephen M. Winter & Liya Khadeeva

Correlated Electron Systems

New Kinds of Electronic Order in Quantum Materials
Jun 26 - Jul 1, 2016
Mount Holyoke College, South Hadley, MA
Chairs: Peter Abbamonte & Joel E. Moore
Vice Chairs: Piers Coleman & Nigel Hussey

- **Synergies of Spin-Orbit Coupling and Electronic Repulsion** (*Leon Balents* / Hidenori Takagi)
- **Excitations of Frustrated Magnets** (*Senthil Todadri* / J.C. Seamus Davis / Gregory MacDougall / Stephen Nagler)
- **Strange Metals and Insulators in Heavy-Fermion Compounds** (*Meigan Aronson* / Colin Broholm)
- **Interaction Effects in 2D Chalcogenides** (*Vidya Madhavan* / Jennifer Hoffman)
- **Interaction Effects in Bulk Chalcogenides** (*Kai Rossnagel* / Minhyea Lee / Jasper Van Wezel / Anshul Kogar)
- **Charge Order Versus Superconductivity in Copper Oxides** (*Erica Carlson* / Riccardo Comin / Eugene Demler / Louis Taillefer)
- **New Theoretical Methods for Strong Correlations** (*Jan Zaanen* / Garnet Chan / Shinsei Ryu)
- **Topological Four-Letter Words: FQHE, QSHE and QAHE** (*Mansour Shayegan* / David Goldhaber-Gordon / Pablo Jarillo-Herrero)
- **Late-Breaking Topics** (*Peter Abbamonte* / James Analytis)
- **Power Hour** (*Vidya Madhavan*)

GRS **Correlated Electron Systems**
Developments at the Frontier of Quantum Many-Electron Physics
Jun 25-26, 2016
Chairs: Cassandra R. Hunt & Sid Parameswaran

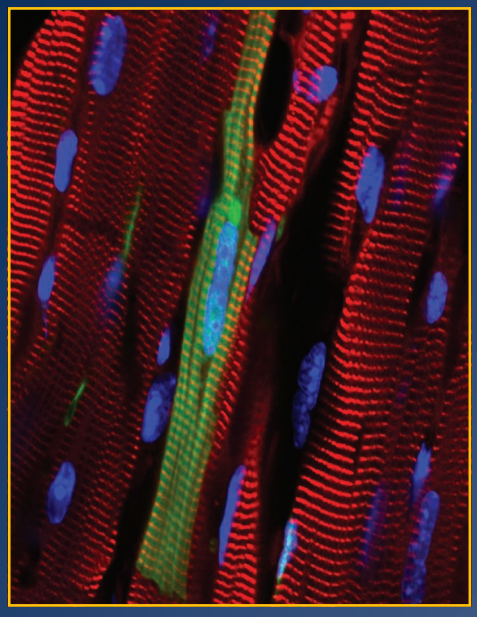

Understanding the cellular and molecular programs underlying cardiac homeostasis is essential for developing new avenues to repair or regenerate the heart after injury. Genetic lineage tracing models in the mouse reveal the relative contribution of endogenous progenitor cell-derived cardiomyocytes (green, GFP+) to the overall myocardium (red, α-actinin+). Courtesy of Ronald J. Vagnozzi and Jeffery D. Molkentin (Cincinnati Children's Hospital Medical Center). Submitted by Ronald J. Vagnozzi & Jerry Curran, Chairs, Cardiac Regulatory Mechanisms GRS.

Corrosion - Aqueous

Corrosion Under Control? From Mechanisms to Sustainable Applications
Jul 10-15, 2016
Colby-Sawyer College, New London, NH
Chair: Sannakaisa Virtanen
Vice Chair: Nick Birbilis

- **Dissolution Mechanisms in Experiment and Theory** (*Alison Davenport* / Jerry Frankel / Mira Todorova)
- **Passivity and Oxide Films** (*Jamie Noel* / Philippe Marcus / Paul Natishan / Hiroki Habazaki)
- **Localized Corrosion Mechanisms** (*Shinji Fujimoto* / Robert Kelly / Scott Lillard)
- **Advanced Techniques and Approaches** (*Hugh Isaacs* / Mary Ryan / Arjan Mol / Achim Hassel)
- **Advances in Corrosion Protection Principles** (*Rudy Buchheit* / Herman Terryn / Christopher Taylor)
- **Corrosion of Metallic Biomaterials** (*Douglas Hansen* / Ingrid Milosev / Sachiko Hiromoto / Yolanda Hedberg)
- **Corrosion of Advanced Materials** (*Matthew Asmussen, Lisa Rossrucker* / Annett Gebert)
- **Corrosion and Protection in Engineering Applications** (*Ronald Latanision* / Joseph Kish / David Shoesmith / Srdjan Nesic)
- **Past and Future Developments in Experiment and Modeling of Corrosion: From Mechanisms to Sustainable Applications** (*Nick Birbilis* / David Williams / John Scully)

GRS **Corrosion - Aqueous**
Multidisciplinary Approaches to Solving Global Corrosion Issues
Jul 9-10, 2016
Chairs: Matthew Asmussen & Lisa Rossrucker

Crystal Engineering

Advancing the Design of Crystals
Jun 26 - Jul 1, 2016
Stoweflake Conference Center, Stowe, VT
Chair: Adam Matzger
Vice Chair: Len R. Macgillivray

- **Crystal Growth** (*William Jones* / Lara Estroff / Bart Kahr)
- **Engineering Guest Interactions in Coordination Polymers** (*Xianhui Bu* / Makoto Fujita / Myoung Soo Lah)
- **Assembly** (*Radu Custelcean* / Tomislav Friscic / Linda Shimizu)
- **Crystal Engineering of Magnetic Interactions** (*Jing Li* / Kim Dunbar / Kathryn Preuss)
- **Structure Prediction** (*Gregory Beran* / Sally Price / Mark Tuckerman)
- **Cocrystal Engineering** (*Vilmali Lopez-Mejias* / Christer Aakeroy / Andrew Bond / Ashwini Nangia)
- **Coordination Polymer Function** (*Nathaniel Rosi* / Mircea Dinca / Dirk De Vos / Pingyun Feng)
- **Ionic Liquids as Crystallization Media** (*Jeremy Feldblyum* / Russell Morris / Anja Mudring / Robin Rogers)
- **Applied Crystallization** (*Robin Rogers* / Susan Reutzel-Edens / Reginald Tan / Narayan Variankaval)

GRS **Crystal Engineering**
Functional Cocrystals
Jun 25-26, 2016
Chairs: Rajesh Goud Nagula & Jonathan C. Bennion

Cyclic Nucleotide Phosphodiesterases

Mechanisms of PDE Nano-Domain Control and Impacts on Disease
Jun 12-17, 2016
PGA Catalunya Business and Convention Centre, Girona, Spain
Chairs: Rodolphe P. Fischmeister & David Kass
Vice Chairs: George S. Baillie & Christopher Schmidt

- **Non-Canonical Cyclic Nucleotides and Protein Regulators** (*David Kass* / Thomas Brand / Roland Seifert)
- **Imaging Cyclic Nucleotide/Effector Kinase Nano-Domains** (*Choel Kim* / Manuela Zaccolo / Viacheslav Nikolaev / Jin Zhang)
- **New Insights into the Control of Cyclic AMP** (*William Catterall* / Carmen Dessauer / John Scott / Chen Yan / Scott Soderling / Joseph Beavo)
- **PDE Regulatory Interactions with Receptors and Kinases** (*Emilio Hirsch* / Yang Xiang / Gregoire Vandecasteele / Yassine Sassi / Alessandra Ghigo)

- **Role of PDE1 and PDE2 in Cardiac, Pulmonary, and Neurological Diseases**
  (*Claire Lugnier* / Lawrence Wennogle / Ali El-Armouche / Ying Xu / Adrian Hobbs)
- **PDE3 and PDE4: Vascular Disease and Inflammation**
  (*Veronique Leblais* / Sylvia Bahring / Vincent Manganiello / Jian-Dong Li / Donald Maurice)
- **Regulation of PDE4 Signaling and PDE5-Inhibition for Duchene Muscular Dystrophy**
  (*Susan Taylor* / Marco Conti / George Baillie / Miles Houslay / Ronald Victor)
- **Neurological Role for PDEs: Therapeutic Implications**
  (*Eva Degerman* / Nikolai Artemyev / Ana Perez-Castillo / Cornelia Dorner-Ciossek / Michael Russwurm)
- **PDEs and the Central Nervous System**
  (*Christopher Schmidt* / Liliana Castro / Nick Brandon / Michy Kelly)

Cyclic Nucleotide Phosphodiesterases
New Layers of Complexity in Cyclic Nucleotide Phosphodiesterase Signaling
Jun 11-12, 2016
Chairs: Alessandra Ghigo & Sarah N. Rampersad

Defects in Semiconductors

Fundamental Research on Defects: Enabling Technological Advances in Semiconductor-Based Devices
Aug 14-19, 2016
Colby-Sawyer College, New London, NH
Chair: Martin Brandt
Vice Chair: Mary Ellen Zvanut

- **Photovoltaics: Stability of Si- and Perovskite-Based Solar Cells**
  (*Shengbai Zhang* / Giso Hahn / Jeanette Lindroos / Aron Walsh)
- **Alternatives to the NV Center in Diamond**
  (*Jeffrey McCallum* / Adam Gali / Helena Knowles)
- **Other Wide-Gap Semiconductors Have Useful Color Centers as Well**
  (*Vladimir Dyakonov* / Gregory Fuchs / Jurgen von Bardeleben)
- **Quantum Properties of Dopants in Silicon**
  (*Uwe Gerstmann* / Neil Curson / Stephanie Simmons)
- **The Role of Defects in Photocatalysis and Novel 2D Materials**
  (*Ian Sharp* / Luca Bertoluzzi / Hannu-Pekka Komsa / Kevin Sivula)
- **Luminescence in Group-III Nitrides**
  (*Evan Glaser* / Yasumi Fujiwara / Joy McNamara)
- **Oxides: Vacancies and Hydrogen**
  (*Michael Stavola* / Eduard Lavrov / Jan Stehr)
- **The Theory of Defects in and on Oxides**
  (*Chris Van De Walle* / Lars Bjaalie / Peter Broqvist)
- **Advances in Defect Spectroscopy**
  (*Kohei Itoh* / Roger Lichti / John Morton)

Defects in Semiconductors
Identifying, Understanding, and Using Defects in Semiconductors
Aug 13-14, 2016
Chairs: Mark T. Durniak & Natalie Segercrantz

Diffraction Methods in Structural Biology

Probing the Structure and Dynamics of Macromolecules
Jul 17-22, 2016
Bates College, Lewiston, ME
Chair: Edward Snell
Vice Chair: Arwen R. Pearson

- **Keynote Session: Structure and Dynamics**
  (*Elspeth Garman* / Carrie Wilmot / Joseph Ferrara)
- **New Instruments and Opportunities**
  (*Sean McSweeny* / Armin Wagner / Matthew Bowler / Marjolein Thunnissen)
- **Improving Maps and Models**
  (*Airlie McCoy* / Elspeth Garman / Frank Von Delft / James Fraser)
- **Structural Biology Requires Multiple Methods**
  (*Nozomi Ando* / Allison Edwards / Neil Ranson / Saikrishnan Kayarat)
- **Dynamically Resolved Methods**
  (*Carrie Wilmot* / Thomas Barends / Henrike Muller-Werkmeister / Gergely Katona / Petra Fromme)
- **Hybridization of Synchrotron and XFEL Approaches**
  (*Aina Cohen* / Elizabeth Baxter / Manfred Burghammer / Helen Ginn / Thomas White)
- **Developments in Diffraction Methods**
  (*Arwen Pearson* / Isabel Uson / Kartik Ayyer / Andrea Thorne)
- **Selected Poster Presentations: New Cool Methods and Hot New Structures**
  (*James Fraser*)
- **Structural and Dynamical Information Beyond Bragg**
  (*James Holton* / Michael Wall / Robert Rambo / Nozomi Ando)

Diffraction Methods in Structural Biology
Protein Function in Time and Space: Insights from Diffraction Experiments
Jul 16-17, 2016
Chairs: Henrike M. Mueller-Werkmeister & Bradley J. Hintze

Conferees enjoy a mountain hike at Sunday River in Maine.

DNA Topoisomerases in Biology & Medicine

The Interplay of DNA Topoisomerases and DNA Topology in Biology - Emerging Technologies, Dynamics of Enzyme Function and Opportunities in Drug Discovery
Aug 7-12, 2016
Sunday River, Newry, ME
Chair: Mary-Ann Bjornsti
Vice Chair: Yves G. Pommier

- **Keynote Session: The Biological Impact of DNA Topology: What Have We Learned?**
  (*Stewart Shuman* / James Berger / Karl Drlica)
- **Single Molecule Analyses of DNA Topoisomerizations**
  (*Dagmar Klostermeier* / Stephen Kowalczykowski / John Marko)
- **DNA Topology and Biological Processes**
  (*Lynn Zechiedrich* / Andrzej Stasiak / Michelle Wang)
- **Bacterial Topoisomerases as Drug Targets: Opportunities and Challenges**
  (*Yuk-Ching Tse-Dinh* / Anthony Maxwell / Charles Dorman)
- **Topoisomerases: Structure, Protein Interactions and Enzyme Mechanism**
  (*Keir Neuman* / Ram Madabhushi / Claudine Mayer)
- **Topoisomerases and Genomic Stability**
  (*Mary-Ann Bjornsti* / Srinivasan Yegnasubramanian / Joaquim Roca / Hannah Klein)
- **DNA Topoisomerase-Induced DNA Damage and Repair**
  (*Scott Kaufmann* / Wojciech Niedzwiedz / Scott Keeney)
- **DNA Topoisomerases in Cancer Therapy: Discovery and Development**
  (*Yves Pommier* / Susan Blaney / Daniel Santi / Neil Osheroff)
- **Cellular Responses to Topoisomerase-Targeted Therapies**
  (*John Nitiss* / Susan Jinks-Robertson / Peter McKinnon)

DNA Topoisomerases in Biology & Medicine
New Roles, New Drugs, and New Interactions for DNA Topoisomerases
Aug 6-7, 2016
Chairs: Natassja G. Bush & Selma M. Cuya

Drug Carriers in Medicine & Biology

Understanding Physiological Barriers to Inform Drug Carrier Design
Aug 7-12, 2016
Waterville Valley, Waterville Valley, NH
Chairs: Paula T. Hammond & Jan E. Schnitzer
Vice Chairs: Jeffrey A. Hubbell & Muthiah Manoharan

- **Big Perspectives of Drug Delivery: Cell Biology, Physiology and Engineering Perspectives**
  (*Paula Hammond* / Harold Dvorak / Justin Hanes)
- **Barriers and Carriers for Delivery Across Epithelial and Extracellular Barriers**
  (*Rebecca Carrier, David Grainger* / Claus-Michael Lehr / Samir Mitragotri / Theresa Reineke / Kanjiro Miyata)
- **Targets and Carriers to Overcome Endothelial Barriers**
  (*Jan Schnitzer* / Fitz-Roy Curry / Silvia Muro / Vladimir Muzykantov)
- **Barriers and Carriers in Cancer: Treating Solid Tumors**
  (*Leaf Huang, Nicole Steinmetz* / Angela Belcher / Pete Choyke / Gregory Lanza / Martina Stenzel)
- **Overcoming Delivery Barriers to the Brain/BBB**
  (*Harold Dvorak* / Jennifer Cochran / Per-Ola Freskgard / Danica Stanimirovic)
- **Challenges and Frontiers for Nanomedicine and Nanodelivery**
  (*Christopher Alabi, Alexander Kabanov* / Doo Sung Lee / Bogdan Olenyuk / Suzie Pun / Maria Vicent)
- **Late-Breaking Topics / Young Investigator Presentations**
  (*Jeffrey Hubbell, Muthiah Manoharan*)
- **Barriers and Carriers for Infectious Disease and Vaccines: Targeting the Immune System**
  (*Cory Berkland, Darrell Irvine* / Mark Prausnitz / Peter Seeberger / Matthias Stephan / Liangfang Zhang)
- **Translational Approaches to RNA Delivery**
  (*Martin Latterich* / Debra Auguste / Judy Lieberman / Anil Sood)

Drug Carriers in Medicine & Biology
Leveraging Drug Carrier Design and Mechanistic Insight of Nanoparticle Therapeutics to Optimize Clinical Efficacy
Aug 6-7, 2016
Chairs: Ramsey N. Majzoub & Santiago Correa

Drug Metabolism

The Precision Medicine Revolution: New Frontiers for Scientists in Drug Metabolism, Transport and Pharmacokinetics
Jul 10-15, 2016
Holderness School, Holderness, NH
Chair: Kim L.R. Brouwer
Vice Chair: Donavon J. McConn

- **Keynote Session: New Frontiers for DMPK in Precision Medicine**
  (*Kim Brouwer* / Allan Rettie)
- **Advances in Precision Medicine: Endogenous Biomarkers**
  (*John Wagner* / Shashi Amur / Rima Kaddurah-Daouk / Frank Sistare)

Gordon conferences are different from other scientific conferences because these conferences strike a perfect balance between science and social – learn and have fun with the brightest in the field!

- Charuni Gunaratne, Chair, 2015 Neuroethology: Behavior, Evolution & Neurobiology GRS

- **Clinical and Real World Applications of Precision Medicine**
  (*Michael Zientek* / Joshua Denny / Rebecca Blanchard)
- **Orphan P450s: Discovery of Function and Relevance to Applications in Medicine**
  (*F. Peter Guengerich* / Edward Kelly / Michal Siller / John Stegeman)
- **Targeted Covalent Inhibitors – Risks, Benefits, and Promise for Precision Medicine**
  (*Thomas Baillie* / Deqiang Niu / John Kath)
- **Transporters: To Precision and Beyond**
  (*Sonia de Morais* / Allan Wolkoff / Bo Feng / Alex Galetin / Kathleen Giacomini)
- **Young Investigator Presentations**
  (*Henry Strobel*)
- **New Frontiers for Predicting Renal Toxicity and Clearance, and Applications in Precision Medicine**
  (*Deanna Kroetz* / Vishal Vaidya / Adrian Ray / Benjamin Freedman)
- **Precision Medicine Applications and Opportunities: Case Studies**
  (*Bob Powell* / Richard Peck / Norman Stockbridge)

Drug Resistance

Experiences with Antimicrobials and Anticancer Agents, as Well as Herbicides and Pesticides
Jun 12-17, 2016
University of New England, Biddeford, ME
Chairs: Manuel A. Navia & Pradipsinh K. Rathod
Vice Chairs: Jean Patel & Jared A. Silverman

- **Keynote Session: Threats and Responses**
  (*Jean Patel* / Dennis Dixon / Rick Fairhurst)
- **Understanding Resistance**
  (*Amy Anderson* / Robert Douglas Sammons / Erica Ollmann Saphire / Ashley Vaughan)
- **Paths to Stable Resistance Traits**
  (*Manuel Navia* / Marc Ouellette / David Skurnik)
- **Avoiding Resistance**
  (*Michael Cynamon* / Martin Burke / Robert Bonomo / Ethan Settembre)
- **Advancing Tools and Methods**
  (*Celia Schiffer* / Harren Jhoti / Sriram Subramaniam)
- **Exploiting Existing Resistance**
  (*Juswinder Singh* / Skirmantas Kriaucionis / Margaret Riley)
- **Targeting Host Processes**
  (*Mariano Garcia-Blanco* / Michael Starnbach / Alexis Kaushansky)
- **Generalizable Strategies: Combinations, Multi-Targeting, or Privileged Targets**
  (*Pradipsinh Rathod* / Didier Leroy / Ronald Farquhar / Gautan Dantas)
- **Keynote Session: Connecting Paths to Patients**
  (*Jared Silverman* / Keith Jerome / Wendy Sanhai)

Drug Safety

Improving Drug Safety: From Innovation in the Lab to Application in the Clinic
Jun 26 - Jul 1, 2016
Stonehill College, Easton, MA
Chair: Thomas Schroeter
Vice Chair: James L. Stevens

- **Keynote Session: Network Pharmacology and Toxicology**
  (*Thomas Schroeter* / Ravi Iyengar)
- **Computational Toxicology and Systems Biology**
  (*Jeffrey Sutherland* / Brian Shoichet / Russell Thomas / Weida Tong)
- **Stem Cells and Tissue Engineering – Advances, Opportunities, Limitations**
  (*Myrtle Davis* / Peter Kuhn / Joseph Wu)
- **Applications of Microphysiologic Systems to Drug Safety Assessment**
  (*Rachelle Prantil-Baun* / Anthony Bahinski / Jonathan Himmelfarb / John Wikswo)
- **Drug Safety of Large Molecules: Translational Safety**
  (*Joy Cavagnaro* / Helen Haggerty / Shawn Heidel)
- **Modeling Clinical Drug Toxicity**
  (*Vikram Sinha* / Donald Mager / Paul Watkins)
- **Translational Safety and Patient Tailoring**
  (*Donna Mendrick* / Elizabeth Phillips / David Strauss)
- **Pharmacovigilance and Leveraging Big Data to Detect Safety Signals**
  (*Michael von Forstner* / Andrew Bate / Olaf Klungel / Nicholas Tatonetti)
- **Keynote Session: Pharmacogenomics in Drug Safety Assessment**
  (*James Stevens* / Munir Sir Pirmohamed)

GRS Drug Safety
Drug Safety Assessment in the 21st Century: From In Silico and Tissue Chips to Patient Tailoring
Jun 25-26, 2016
Chairs: Peter Loskill & Rowena R. Sison-Young

Electron Donor-Acceptor Interactions

Fundamentals of Electron- and Energy-Transfer Processes in Materials and Biology
Aug 7-12, 2016
Salve Regina University, Newport, RI
Chairs: Natia L. Frank & Dirk M. Guldi
Vice Chairs: David N. Beratan & Elena Galoppini

- **Charge Transfer in Organic Networks**
  (*Elena Galoppini* / Bo Albinson / Trisha Andrew / Thomas Bein)
- **Photoinduced Charge and Energy Transfer Processes in Biology**
  (*Oliver Wenger* / James Barber / Bern Kohler / Frederick Lewis / Luisa Torsi / Valentine Vullev)
- **Theory in Charge and Energy Transfer Processes**
  (*Thomas Whitesides* / Gemma Solomon / Alexandra Olaya-Castro)
- **Charge Transport Across Interfaces and Through Single Molecules**
  (*Gerald Meyer* / Tetsuro Majima / Paul Mulvaney / Colin Nuckolls / Sylwia Ptasinska / Robert Schlogl)
- **Charge and Energy Transfer in Inorganic Materials**
  (*Paula Diaconescu* / Ana De Bettencourt-Dias / Wonwoo Nam / Sven Rao)
- **Solar Cells / Singlet Fission / Multiple Exciton Generation**
  (*Leif Hammarstrom* / Juan Bisquert / Hiroshi Imahori / Richard Schaller / Natalie Stingelin-Stutzmann / Xiaoyang Zhu)
- **Charge Transfer for Chemical Fuels and Catalysis**
  (*Ksenija Glusac* / Heinz Frei / Tianquan Lian / Erwin Reisner)
- **Charge Transfer Processes in Carbon-Based Materials and Spin Effects**
  (*James McCusker* / Francis D'Souza / Sandrine Heutz / Yasuhiro Kobori / Michael Therien / Malcolm Forbes)
- **Keynote Session: Light Harvesting for Energy Applications**
  (*Felix Castellano* / Ana Moore)

GRS Electron Donor-Acceptor Interactions
New Frontiers in Energy Harvesting and Storage from Biological Systems to Nanostructured Materials
Aug 6-7, 2016
Chairs: Aiko Kurimoto & Christoph Schierl

Electronic Processes in Organic Materials

The Intersection of Organic and Hybrid Materials for Electronics and Optoelectronics
Jun 5-10, 2016
Renaissance Tuscany Il Ciocco, Lucca (Barga), Italy
Chairs: David S. Ginger & Natalie Stingelin-Stutzmann
Vice Chairs: Antoine Kahn & Anna Koehler

- **Spin Transport**
  (*Sandrine Heutz* / Henning Sirringhaus / Christoph Boehme)
- **Charge Separation and Transport: Theory**
  (*Amy Scott* / Alessandro Troisi / Alberto Salleo / Carlos Silva)
- **Organic Bioelectronics**
  (*Ana Claudia Arias* / Roisin Owens / Gianluca Farinola)
- **Hybrid Perovskites: Transport and Photophysics**
  (*Tsutomu Miyasaka* / Henry Snaith / Paul Meredith / Annamaria Petrozza)
- **Charge Separation and Transport: Photophysics**
  (*Eric Bittner* / Sergei Tretiak / Natalie Banerji)
- **New Organic Electronic Materials**
  (*Christine Luscombe* / Antonio Facchetti / He (Henry) Ye / Wenping Hu)
- **2D Materials**
  (*Kees Hummelen* / Xiadong Xu / Hua Zhang)
- **Device Physics**
  (*Peter Ho* / Koen Vandewal / Naomi Ginsberg / Luis Campos)
- **Interfaces**
  (*Sarah Burke* / Aram Amassian / Seth Marder / Xiaoyang Zhu)

GRS Electronic Processes in Organic Materials
Exploring Processes and New Directions in Organic and Hybrid Materials
Jun 4-5, 2016
Chairs: Kyra N. Schwarz & Timothy S. Gehan

Endothelial Cell Phenotypes in Health & Disease

New Insights into Endothelial Cell Phenotypes: Formation, Pathogenesis and Regeneration
Jul 17-22, 2016
PGA Catalunya Business and Convention Centre, Girona, Spain
Chair: Victoria L. Bautch
Vice Chair: Ralf H. Adams

- **Keynote Session: Specific Functions of Endothelial Cells**
  (*Victoria Bautch* / Laura Niklason / Ralf Adams)
- **Endothelial Origins and Multi-Potentiality**
  (*Susan Quaggin* / Mervin Yoder / Christiana Ruhrberg / Kristy Red-Horse / Karen Hirschi)
- **Organ-Specific Phenotypes**
  (*S. Ananth Karumanchi* / Richard Daneman / Steven George / Mark Kahn)
- **Lymphatics: Heterogeneous Origins and Functions**
  (*Karen Hirschi* / Kari Alitalo / Taija Makinen / Tatiana Petrova / Susan Quaggin)
- **Vessel Phenotypes in Disease**
  (*Asrar Malik* / Roger Kamm / Eugene Butcher / Noo Li Jeon / William Muller)
- **Vasculature as a Stem Cell Niche**
  (*Jan Kitajewski* / Karina Yaniv / Sharon Gerecht / Shahin Rafii / Eli Keshet)
- **Vessels and Regenerative Medicine**
  (*Timothy Hla* / Shulamit Levenberg / Christopher Chen / Christopher Hughes)
- **EC Heterogeneity: Signaling and Mechanotransduction**
  (*Christopher Hughes* / Weilan Ye / Eleni Tzima / Hanjoong Jo / Timothy Hla)

- **Keynote Session: Neurovascular Interactions in Translation**
  (*Ralf Adams* / Elisabetta Dejana / Chenghua Gu)

GRS Endothelial Cell Phenotypes in Health & Disease
Balancing Endothelial Stability and Activation: Development, Disease, and Repairing Damage
Jul 16-17, 2016
Chairs: Erich Kushner & Kevin Mouillesseaux

Energetic Materials

Expanding the Limits of Our Understanding of Energetic Materials Behavior
Jun 5-10, 2016
Stoweflake Conference Center, Stowe, VT
Chair: Nick Glumac
Vice Chair: Betsy M. Rice

- **The State of Energetic Materials Research**
  (*Mario Fajardo* / Thomas Russell)
- **Experimental Developments: Fundamental Studies**
  (*Dana Dattelbaum* / Jennifer Gottfried / Dana Dattelbaum)
- **Synthesis of Novel Energetic Materials**
  (*Nirupam Trivedi* / Karl Christe / Rebecca Wilson / Michael Zdilla)
- **Computations and Modeling of Energetic Materials**
  (*Maija Kukla* / Ryan Austin / Santanu Chaudhuri / Suresh Menon / Alejandro Strachen)
- **Extreme Phenomena in Energetic Materials**
  (*Blaine Asay* / Ronald Brown / Doug Tasker / Steven Todd)
- **Theoretical, Modeling, and Computational Research**
  (*DeCarlos Taylor* / Anguang Hu / Thomas Sewell)
- **Energetic and Reactive Materials Systems**
  (*Naresh Thadani* / Virginia Manner / Timothy Weihs / Michael Zachariah)
- **Experiments: Macroscale and Systems-Level**
  (*Fan Zhang* / David Frost / Kevin McNesby)
- **Reactive Energetic Materials**
  (*Steven Son* / Ed Dreizin / Alex Mukasyan / Lori Groven / Kyle Sullivan)

GRS Energetic Materials
Molecular to Macroscale Mechanisms in Energetic Materials Performance
Jun 4-5, 2016
Chairs: Katie E. Brown & Hayleigh J. Lloyd

Environmental Endocrine Disruptors

The Next Generation of Endocrine Disruption: Emerging Contaminants, Tools and Research Approaches for Assessing Multigenerational Effects
Jun 19-24, 2016
Sunday River, Newry, ME
Chair: Heather B. Patisaul
Vice Chairs: Daniel Zalko & Jerrold J. Heindel

- **Keynote Session: Our Stolen Future? Reflections on the Past, Present and Future of EDC Research**
  (*Heather Patisaul* / Jerrold Heindel / Melissa Perry)
- **Evidence for and Mechanisms of Transgenerational Inheritance of EDC Effects**
  (*Vasantha Padmanabhan* / Piroska Szabo / Jodi Flaws / Claudine Junien)
- **EDC Impacts on the Global Community**
  (*Joe Braun* / Leo Transande / David Aylor / Frank von Hippel)
- **Neural and Behavioral Impacts**
  (*Andrea Gore* / Deborah Kurrasch / Valerie Hu / Joe Braun)
- **Late-Breaking Topics**
  (*Heather Patisaul*)
- **Endocrine Disruption of Cellular Energy Balance and Metabolism**
  (*Vasantha Padmanabhan, Daniel Zalko* / Robert Sargis / Andrea Baccarelli / Fabian Jourdan / Paloma Alonso-Magdalena)
- **Assessing the Risks: New Directions in EDC Assessment and Public Policy**
  (*Carol Kwiatkowski, David Dix* / Russell Thomas / Douglas Bell / Tracey Woodruff)
- **Surveying the Landscape: Emerging EDCs**
  (*Jerrold Heindel* / Susan Nagel / Kim Anderson / Heather Stapleton)
- **Keynote Session: Our Reclaimed Future? Precedents and Priorities**
  (*Ann Petersen* / Frederica Perera / Sheldon Krimsky)
- **Power Hour**
  (*Heather Stapleton*)

GRS Environmental Endocrine Disruptors
Evaluating Effects of EDCs in the Era of Genes, Genetics, and Genomics: How Will Molecular Data Inform and Transform Our Understanding of Endocrine Disruption in Clinical, Conservation, and Evolutionary Biology?
Jun 18-19, 2016
Chair: Ann M. Petersen

Mouse embryos at mid-gestation. Left: wild-type embryo showing vascularized yolk sac. Right: Hoip-deficient embryo showing absence of yolk sac vascularization. Courtesy of Nieves Peltzer (UCL Cancer Institute). Submitted by Henning Walczak, Chair, Cell Death GRC.

Environmental Sciences: Water

Opportunities for Aquatic Sciences to Impact a Changing World
Jun 26 - Jul 1, 2016
Holderness School, Holderness, NH
Chair: Allison MacKay
Vice Chair: William A. Arnold

- **Water 2050: The Future of Water Technology and Treatment**
  (*Daniel Yeh* / H.V.M. (Bert) Hamelers / Kartik Chandran)
- **Systems Thinking**
  (*Susan Powers* / Miriam Diamond / Ferdi Hellweger / Meagan Mauter)
- **Water, Carbon and Climate**
  (*Christine Foreman* / Rose Cory / Jemma Wadham)
- **Water Pollution and Treatment in Developing Countries**
  (*Jenna Davis* / Jerker Fick / Daniele Lantagne / Monroe Weber-Shirk)
- **Our Stolen Present: Pollution and Health**
  (*Kurt Pennell* / Margaret Karagas / Leonardo Trasande)
- **New Views on Legacy Problems**
  (*Lynn Katz* / Christopher Higgins / Craig Just / Daniel Giammar)
- **Food, Water and Contaminants**
  (*Michelle Hladik* / Jason White / Laura McConnell)
- **Environmental Molecular Science**
  (*Charles Wong* / Thomas Hofstetter / Desiree Plata / Timothy LaPara)
- **Swimming in Chemicals (and Water)**
  (*Allison MacKay* / Andreas Fath)
- **Power Hour**
  (*Linda Weavers*)

GRS Environmental Sciences: Water
From Molecular Processes to Water Management Practices: Translational Environmental Science
Jun 25-26, 2016
Chairs: Gordon J. Getzinger & Will C. Jolin

Enzymes, Coenzymes & Metabolic Pathways

Advances in Enzymology from Determining Enzyme Function to the Interplay of Large Enzyme Systems
Jul 24-29, 2016
Waterville Valley, Waterville Valley, NH
Chairs: Adrian T. Keatinge-Clay & Audrey L. Lamb
Vice Chairs: Graham R. Moran & Andrea Mattevi

- **Unusual Natural Product Enzymology**
  (*Squire Booker* / Gregory Challis / David Christianson / Bradley Moore)
- **Enzyme Inhibition**
  (*Lynn Abell* / Benjamin Cravatt / Dennis Murphy / Alan Rendina)
- **Metalloenzymes**
  (*Joshua Finkelstein* / Amie Boal / Pinghua Liu / Hideaki Ogata)
- **Large Complexes**
  (*Martin St. Maurice* / Timm Maier / Shelley Minteer / Liang Tong / Lorenzo Finci)
- **Assembly Lines**
  (*Barbara Gerratana* / Andrew Gulick / Joern Piel / Sheryl Tsai)
- **Determining Enzyme Function**
  (*Elham Behshad* / Valerie De Crecy-Lagard / Graham Moran / Reuben Peters / Elizabeth Sattely)
- **Biocatalysis**
  (*Thomas Meek* / Robert Dicosimo / Jon Stewart / Kevin Walker)
- **Unusual Coenzymes**
  (*Tadhg Begley* / Paul Fitzpatrick / Hung-Wen Liu / Robert White)
- **Keynote Session: Learning from Naturally Gifted Enzymes**
  (*Karen Allen* / Debra Dunaway-Mariano / Dale Poulter)

GRS Enzymes, Coenzymes & Metabolic Pathways
Enzymology in the 21st Century: New Concepts, Methods, and Systems
Jul 23-24, 2016
Chair: Zhen Wang

Extracellular Vesicles

NEW!

Biologic Effects and Therapeutic Potential of Extracellular Vesicles
Aug 21-26, 2016
Sunday River, Newry, ME
Chair: Peter Quesenberry
Vice Chair: Giovanni Camussi

- **Keynote Session: Extracellular Vesicle Isolation and Vesicle Characterization (Proteins, RNA Species, Lipids)**
  (*Richard Simpson* / Randy Schekman / Edwin van der Pol)
- **Extracellular RNA**
  (*David Wong* / Esther Nolte-'t Hoen / Nobuyoshi Kosaka / Raghu Kalluri)
- **Extracellular Vesicle Biogenesis, Vesicle Cargo Loading and Targeting RNA**
  (*Stephen Gould* / Graca Raposo / Pascale Zimmermann)

- **Extracellular Vesicles in Tissue Injury and Tissue Repair** (*Willem Stoorvogel* / Stefania Bruno / Duncan Stewart / Jason Aliotta / Bernd Giebel)
- **The Role of Extracellular Vesicles in Inflammation** (*Philip Askenase* / Paul Robbins / Edit Buzas)
- **Non-Mammalian and Plant Extracellular Vesicles** (*Meta Kuehn* / Huang-Ge Zhang / Laura De La Canal / Amy Buck)
- **Extracellular Vesicles and Thrombosis** (*Benjamin Brenner* / Mary Collier / Nigel Mackman / Romaric Lacroix)
- **Extracellular Vesicles in Neurobiology** (*Andrew Hill* / Fred Hochberg / Richard Kraig / Michael Chopp / Claudia Verderio / Randolph Corteling)
- **Extracellular Vesicles in Cancer** (*David Lyden* / Clotilde Thery / Peter Kurre / Johan Skog)

Fibroblast Growth Factors in Development & Disease

FGF Signalling: From Molecular Understanding to Therapeutic Targeting
Jun 5-10, 2016
The Chinese University of Hong Kong, Hong Kong, China
Chairs: Richard Grose & Anne-Karina Perl
Vice Chair: Marja Hurley

- **Keynote Session: Mechanistic Basis of Pathological FGFR Signal Transduction** (*Richard Grose* / John Ladbury / Philippe Soriano)
- **FGFR Signaling** (*Sabine Werner* / Chiara Francavilla / Alvaro Ingles-Prieto / Moosa Mohammadi / Tatjana Piotrowski / Dina Ron)
- **Endocrine FGFs / FGFs and Matrix Interactions** (*Matthew Hoffmann* / Dave Fernig / Beate Lanske / Yang Li)
- **Developmental Models** (*Saverio Bellusci* / Denise Al Alam / Suzanne Mansour / David Ornitz / Xin Zhang)
- **Development and Disease** (*Anne-Karina Perl* / Rashmi Bansal / Saverio Bellusci / Mohammad Hajihosseini / Matthew Hoffmann)
- **Regeneration and Repair** (*Xiaokun Li* / Lin Chen / Regina Irschick / Luigi Maddaluno / Bradley Olwin / Jeremy Turnbull)
- **Genetic Diseases** (*Marja Hurley* / Vincent Harley / Laurence Legeai-Mallet / Amy Merrill-Brugger)
- **Cancer** (*Abbie Fearon* / Tomoko Betsuyaku / Paolo Dotto / Pamela Pollock / Fen Wang)
- **Novel Therapeutics and Clinical Trials** (*Michael Seckl* / Simon Cook / Chao Jiang / Elaine Kilgour)

GRS Fibroblast Growth Factors in Development & Disease
FGF Signalling: From Molecular Understanding to Therapeutic Targeting
Jun 4-5, 2016
Chairs: Abbie E. Fearon & Luigi Maddaluno

Flow & Transport in Permeable Media

Bridging the Gap Between Scales and Processes for Strongly Coupled Systems
Jul 31 - Aug 5, 2016
PGA Catalunya Business and Convention Centre, Girona, Spain
Chair: Rainer Helmig
Vice Chair: Ruben Juanes

- **The Future of CCS, Energy Storage, and Fracking from a European and American Perspective** (*Michael Celia* / Terry Engelder / Philip Ringrose)
- **Theory and Models: What Is Necessary and Available?** (*Steffen Berg* / Tanguy Le Borgne / Vahid Niasar / Holger Steeb)
- **Capillarity, Wetting and Flow: Basic Physical Understanding and Implications for Porous Media** (*Ruben Juanes* / Joanna Aizenberg / Martin Brinkmann)
- **Coupled Flow Dynamics** (*Patrick Jenny* / Thijs Defraeye / Nima Shokri / Kathleen Smits)
- **Subsurface Characterization and Flow Modeling** (*Martin Blunt* / Veerle Cnudde / Insa Neuweiler)
- **Life in Porous Media** (*Dorthe Wildenschild* / Luis Cardoso / Pietro de Anna / Alfio Quarteroni)
- **Subsurface Energy Storage** (*Hamdi Tchelepi* / Jens Birkholzer / Sebastian Geiger)
- **Porous Media and Society** (*Dani Or* / Praveen Kumar / Holly Michael / Frank Reith)
- **Numerical Models for Fractured-Porous Media Systems** (*Inga Berre* / Luca Formaggia / Jan Nordbotten)
- **Power Hour** (*Gabriele Seitz, Beatrix Becker*)

GRS Flow & Transport in Permeable Media
The Impact of Interfaces in Permeable Media
Jul 30-31, 2016
Chairs: Maria T. Elenius & Amir Raoof

The sensitivity of a primary explosive to electrostatic discharge is demonstrated in a small-scale safety test. Courtesy of Daniel Preston (Los Alamos National Laboratory). Submitted by Katie E. Brown & Hayleigh J. Lloyd, Chairs, Energetic Materials GRS.

Forensic Analysis of Human DNA

NEW!

Advancing Fundamental Technologies from the Crime Lab to the Crime Scene
Jun 19-24, 2016
Waterville Valley, Waterville Valley, NH
Chairs: James P. Landers & Joan M. Bienvenue
Vice Chairs: Robin Cotton & Steven Lee

- **Forensic DNA Analysis: Challenges and Triumphs** (*Timothy McMahon* / Turi King / Neils Morling)
- **Analysis of DNA Mixtures** (*Margaret Ewing* / Michael Coble / Catherine Grgicak / Joel Sutton)
- **Single Nucleotide Polymorphisms for Phenotyping** (*Katherine Gettings* / Danielle Podini / Mark Shriver)
- **Nucleic Acid Interrogation for Body Fluid Identification** (*Rick Tontarski* / Jack Ballantyne / Sally Harbison / Titia Sijen)
- **Contextual Bias** (*Itiel Dror* / Cecelia Crouse / William Thompson)
- **Trace DNA Analysis** (*Minh Nyugen* / Todd Bille / Mechthild Prinz / R.A.H. van Oorschot)
- **DNA Typing for Familial Linkage** (*Bruce Budowle* / Charles Brenner / Thomas Parsons)
- **Next Generation Technology for Rapid, Comprehensive DNA Analysis** (*Bruce McCord* / Marie Allen / Peter de Knijff / Peter Vallone)
- **Bioinformatics and Probabilistic Genotyping** (*Charlotte Word* / John Buckleton / Craig O'Connor)

Fragile X and Autism-Related Disorders

New Insights into Disease Mechanisms Leading to Improved Therapeutics for Neurodevelopmental Disorders
Jun 5-10, 2016
Mount Snow, West Dover, VT
Chair: Michael R. Tranfaglia
Vice Chair: Peter Kind

- **Keynote Session: Translating Neuroscience into Therapeutics** (*Peter Kind* / Kimberly Huber)
- **The Molecular Genetics of ASDs and Targets of FMRP** (*Joel Richter* / David Nelson / Jennifer Darnell / Herve Moine / Stephen Warren)
- **Postsynaptic Phenotypes: Signaling Pathways and Protein Translation** (*Eric Klann* / Joseph Buxbaum / Nahum Sonenberg)
- **Other Disease Mechanisms: Presynaptic Phenotypes and Channelopathies** (*David Nelson* / Vitaly Klyachko / Leonard Kaczmarek)
- **Other Disease Mechanisms: Glial and Extracellular Phenotypes** (*Laura Mamounas* / Iryna Ethell / Claudia Bagni / Laurie Doering)
- **Circuits and Development** (*Kimberly Huber* / Sumantra Chattarji / Anis Contractor / Carlos Portera-Cailliau)
- **Clinical Trials** (*Tiina Urv* / Mustafa Sahin / Elizabeth Berry-Kravis)
- **Imaging, Clinical Assessments, and Outcome Measures** (*Elizabeth Berry-Kravis* / John Sweeney / Allan Reiss / Joseph Piven)
- **Future Directions: Emerging Therapeutic Technologies** (*Jennifer Darnell* / Gary Bassell)

GRS Fragile X and Autism-Related Disorders
Fragile X and ASDs: Unlocking Complex Disorders with Basic Research
Jun 4-5, 2016
Chairs: Kirsty J. Sawicka & Sally Till

Fuel Cells

The Next Generation of Durable, High-Performance Components and Fuel Cells, Including Modeling, Diagnostics, and Materials Development Advancements
Aug 7-12, 2016
Stonehill College, Easton, MA
Chairs: Adam Z. Weber & Plamen Atanassov
Vice Chairs: Kunal Karan & Deborah J. Jones

- **Hydrogen and Its Electrochemical Applications** (*Mark Mathias* / Shanna Knights / Joeseph Cargnelli)
- **Ion-Conducting Membranes and Understanding** (*Klaus-Dieter Kreuer* / Michael Yandrasits / Michael Hibbs / Gregory Voth)
- **Durability and Transport in Cells and MEAs** (*Rod Borup* / Sylvie Escribano / Marc Secanell)
- **Young Investigator Presentations** (*Andrew Herring* / Paul Shearing / Svitlana Pylypenko / Tatyana Reshetenko / Ifan Stephens)
- **Alternate Fuel Cells** (*Scott Calabrese Barton* / Shelley Minteer / Enrico Traversa)
- **MEA and Catalyst Layer Analysis** (*Deborah Myers* / Laure Guetaz / Atsushi Ohma / Kourosh Malek)
- **Ionomer Diagnostics and Durability** (*James Waldecker* / Steven Holdcroft / Ahmet Kusoglu)
- **Novel Catalysts and Catalyst Related Phenomena** (*Radenka Maric* / Karl Mayrhofer / Vojislav Stamenkovic / Andreas Friedrich)
- **Keynote Session: Lessons Learned from Deployment and Analysis of Fuel-Cell Technologies** (*Plamen Atanassov, Adam Weber* / Kenneth Nealson / Hirohisa Tanaka)

GRS Fuel Cells
From Fundamentals to Practical Applications of Fuel Cells
Aug 6-7, 2016
Chairs: Ashley M. Maes & Michael R. Gerhardt

Genomic Instability

DNA Packaging, Replication, and Repair
Jul 24-29, 2016
The Hong Kong University of Science and Technology, Hong Kong, China
Chairs: Robert S. Weiss & Junjie Chen
Vice Chairs: Anja Groth & Anindya Dutta

- **Telomere Replication and Integrity**
  (*Lee Zou* / Roger Greenberg / Jan Karlseder / Roger Reddel)
- **Chromosome Cohesion, Condensation, and Segregation**
  (*Kyungjae Myung* / Lars Jansen / Camilla Sjogren / Yoshinori Watanabe / Karen Wing Yee Yuen)
- **DSB Repair and Recombination**
  (*Tanya Paull* / Patrick Sung / K. Muniyappa / Gaelle Legube)
- **Replication Fork Challenges: Coiling, Collapse and Coalition**
  (*Patrick Sung* / Anindya Dutta / Marco Foiani / Thanos Halazonetis / Jesper Svejstrup)
- **Replication of Normal and Damaged DNA Templates**
  (*Thanos Halazonetis* / Hiroyuki Araki / Bik Tye / Deog Su Hwang)
- **Chromatin Dynamics and (Epi)Genome Maintenance**
  (*Roger Greenberg* / Anja Groth / Titia Sixma / Guoliang Xu / Kui Ming Chan)
- **DNA Repair in Development and Aging**
  (*Jan Karlseder* / Vera Gorbunova / Peter McKinnon / Zhongjun Zhou)
- **DNA Damage Signaling**
  (*Titia Sixma* / Tanya Paull / Michael Huen / Lee Zou)
- **DNA Repair as a Therapeutic Target**
  (*Michael Huen* / Eric Lightcap / Xiaochun Yu / Kyungjae Myung)
- **Power Hour**
  (*Bik Tye*)

GFS Genomic Instability
Molecular Interplay of Chromatin Organization, Replication and Repair
Jul 23-24, 2016
Chairs: Darshil Patel & Mrinal Srivastava

Granular Matter

Particulate Systems in Science and Technology
Jul 24-29, 2016
Stonehill College, Easton, MA
Chairs: Douglas J. Durian & Matthias Schroeter
Vice Chairs: Devaraj Van Der Meer & Aparna Baskaran

- **Shape Design and Packings**
  (*Arshad Kudrolli* / Sharon Glotzer / Heinrich Jaeger)
- **Impact and Locomotion**
  (*Hiroaki Katsuragi* / Robert Behringer / Xiang Cheng)
- **Mixing, Segregation, and Fluidization**
  (*Kimberly Hill* / Christine Hrenya / Rich Lueptow)
- **Foams, Emulsions, and Non-Frictional Grains**
  (*Reinhard Hohler* / Jasna Brujic / Wiebke Drenckhan / Eric Weeks)
- **Nonlocality, Aging, and Creep**
  (*Ken Kamrin* / Eric Clement / David Henann)
- **Submerged Grains and Suspensions**
  (*Jeffrey Morris* / Philippe Claudin / Alexandre Valance / Luis Pugnaloni)
- **Grains in Space and Microgravity**
  (*Kirsten Harth* / Meiying Hou / Gerhard Wurm)
- **Grain-Scale Theory**
  (*Bulbul Chakraborty* / Hernan Makse / Antoinette Tordesillas)
- **Shear-Flows and Avalanches**
  (*Karen Daniels* / Remi Dreyfus / Lydie Staron)

GFS Granular Matter
Particulate Systems in Science and Technology
Jul 23-24, 2016
Chairs: Kirsten Harth & Carlos F. Orellana

Green Chemistry

Commercial Successes and Remaining Challenges After a Twenty Year Investment in Green Chemistry Principles
Jul 31 - Aug 5, 2016
Stoweflake Conference Center, Stowe, VT
Chairs: William J. Kruper & Elsje (Alessandra) Quadrelli
Vice Chairs: Bala Subramaniam & Anna Simpson

- **Keynote Session: 20 Years of Green Chemistry: What's Next?**
  (*Elsje (Alessandra) Quadrelli* / Paul Anastas / John Warner)
- **Industrial Chemical Manufacturing from Basic to Specialty Chemicals**
  (*Emilio Bunel* / Mario Nappa / David Rosell / Fabrisio Cavani)
- **Trends in Pharma, Agrochemical Production and Toxicology**
  (*John Gavenonis* / Shannon Stahl / Gregory Whiteker)
- **Renewable Resources and Expansion of Feedstocks**
  (*Patrick Smith* / Marc Jacquin / John Hansen)
- **Renewable Energies, Energy Storage, and Photochemistry**
  (*Peter Nickias* / William Tumas / Roy Gordon / Vincent Arturo)
- **Green Engineering and Processing**
  (*Oliver Kappe* / Jennifer Kan / Karen Frost / Raghunath Chaudhari)
- **Polymers, Advanced Materials and Nanodevices**
  (*Hari Reddy* / Arthur Ragauskas / Emmett Crawford / Marcella Bonchio)
- **Catalysis**
  (*William Kruper* / Karen Goldberg / Walter Leitner / Bruce Lipschutz)
- **Life Cycle Analysis, Predictive Computation and Analytics**
  (*Mark Harmer* / Philippe Sautet)

GFS Green Chemistry
The Relevance of Green Chemical Mechanisms in Academia and Industry
Jul 30-31, 2016
Chair: Giuliana Rubulotta

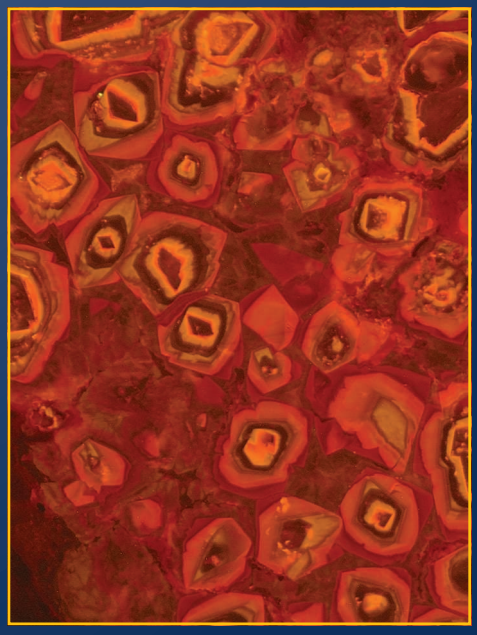

Microscopy cathodoluminescence image of a rock sample collected along the great North Anatolian Fault in Turkey. Here, calcite crystals have grown in cavities and fractures, which indicate a formation process that involves circulations of fluids originated from depth through the seismic fault. Courtesy of Maor Kaduri, Jean-Pierre Gratier, Cécile Lasserre, François Renard (ISTerre, University Grenoble Alpes & CNRS, PGP, University of Oslo), and Ziyadin Çakir (Istanbul Technical University). Funding by ITN FlowTrans (7th European Framework Program, n°316889). Submitted by François Renard, Chair, Rock Deformation GRC.

Geochemistry of Mineral Deposits

From Deep Earth to Surface: Metals for Society
Jun 19-24, 2016
Les Diablerets Conference Center, Les Diablerets, Switzerland
Chairs: Robert P. Moritz & Francois Robert
Vice Chair: David Cooke

- **Mineral Systems – Contrasting Perspectives**
  (*Larry Meinert* / Jeremy Richards / Anthony Harris)
- **Efficiency of Ore-Forming Processes**
  (*Jean Cline* / Andreas Audetat / Adam Simon / John Dilles / Nigel Cook)
- **Surface Processes and Ore Deposits**
  (*Richard Herrington* / Martin Reich / Paulo Vasconcelos)
- **Magmatic-Related Ore-Forming Systems**
  (*Massimo Chiaradia* / Luca Caricchi / Andrew Tomkins / Jess Robertson / Celestine Mercer)
- **Ore-Forming Systems in Sedimentary Environments**
  (*Sarah Gleeson* / Shaun Barker / Ross Large)
- **Belt- to District-Scale Fertility Indicators, and Ore Deposit Vectoring**
  (*Richard Tosdal* / Paul Agnew / Kurt Kyser / Peter Winterburn)
- **Geometallurgy: Improving Metal Extraction**
  (*Julie Hunt* / Karin Olson Hoal / Regina Baumgartner)
- **Microbes, Organic Matter and the Formation of Ore Deposits**
  (*Poul Emsbo* / Geoffrey Gadd / Gordon Southam / Sean Crowe)
- **Outlook: Creative Research for the Needs of Industry and Society**
  (*Stephen Enders* / Eric Jensen / Richard Chuchula)

Hemostasis

Research at the Interface of Hemostasis and Human Disease
Jul 24-29, 2016
Stoweflake Conference Center, Stowe, VT
Chairs: James H. Morrissey & Jorge A. DiPaola
Vice Chair: Alisa S. Wolberg

- **Clotting Factors and Platelets – Beyond Hemostasis**
  (*Robert Montgomery* / Shaun Jackson / Eric Mullins / Bernhard Nieswandt)
- **Inflammation and Hemostasis**
  (*Kathleen Brummel-Ziedins* / Alireza Rezaie / Keith McCrae / Edward Conway / Matthew Rondina)
- **Megakaryocytes, Platelets and Cancer**
  (*Edward Plow* / Tatiana Byzova / Herve Falet / Myriam Labelle)
- **Factor VIII and Von Willebrand Factor: Redefining the Relationship**
  (*Paula Tracy* / Andrew Yee / X. Long Zheng / Peter Lenting / Karl Desch / Paul Monahan)
- **Platelets and Clotting Factors in Normal Hemostasis**
  (*Peter Newman* / Wolfgang Bergmeier / Rodney Camire / Jordan Shavit)
- **Megakaryocytes, Platelets and the Bone Marrow Niche**
  (*Steven McKenzie* / Paul Bray / Karin Hoffmeister / Benjamin Kile / Joe Italiano / Alessandra Balduini)
- **Late-Breaking Topics**
  (*Alisa Wolberg*)
- **Hemostasis and the Interface with the Vessel Wall**
  (*Skip Brass* / Keith Neeves / Renhao Li / Satya Kunapuli / Wilbur Lam / Matthew Auton)
- **Keynote Session: New Therapies and Targets**
  (*Kenneth Mann* / Denisa Wagner / J Evan Sadler)
- **Power Hour**
  (*Alisa Wolberg*)

Many of the advances we have seen in the past 10 years have been originally discussed or conceived at the Gordon Research Conferences.

- Joseph Rogers, Chair, 2015 Assisted Circulation GRC

Hemostasis
Coagulation, Platelet Biology, and Inflammation
Jul 23-24, 2016
Chairs: Leila Noetzli & Carleigh F. Hebbard

Heterocyclic Compounds

New Reactions, Innovation and Creative Design in the Synthesis and Applications of Heterocyclic Compounds
Jun 19-24, 2016
Salve Regina University, Newport, RI
Chair: Scott C. Sutton
Vice Chair: Daniel Romo

- **New Methods for the Synthesis of Heterocyclic Compounds**
  (*Mark Behnke* / Gojko Lalic / Andrei Yudin)
- **Catalysis in Heterocyclic Chemistry**
  (*Catharine Larsen* / Mary Watson / Sherry Chemler / Chad Eichman / Guangbin Dong)
- **Synthesis of Heterocyclic Natural Products**
  (*Simon Bailey* / Regan Thomson / Thomas Maimone / Neil Garg)
- **Route Optimization of Biologically Active Heterocyles**
  (*Daniel Fandrick* / Sebastien Caille / Lakshmaiah Gingipalli / Louis-Charles Campeau)
- **Insights into the Biosynthesis of Heterocyclic Natural Products**
  (*Jason Herr* / Sarah O'Connor / Eric Schmidt / Craig Williams)
- **New Strategies to Construct Heterocyclic Compounds**
  (*Cynthia Shafer* / Ian Baxendale / Dipannita Kalyani / William Chain / Daniel Little)
- **Design and Synthesis of Biologically Active Heterocyclic Compounds**
  (*Eric Voight* / Peter Dragovich / David Hennings / Prabhakar Jadhav / Youla Tsantrizos)
- **Heterocyles as Tools Impacting the Study of Human Disease**
  (*Jennifer Roizen* / Susan Meschwitz / Andrei Kutateladze)
- **Keynote Session: Perspectives on Heterocyclic Chemistry**
  (*Qiu Wang* / Erick Carreira / John Hartwig)

High Pressure, Research at

Emergent Properties at High Material Densities
Jul 17-22, 2016
Holderness School, Holderness, NH
Chair: Shanti Deemyad
Vice Chair: Jon H. Eggert

- **New Methods in High Pressure Science and Technology**
  (*Stanley Tozer* / Stanislav Sinogeikin / Raffaella Torchio)
- **Biology and Organic Chemistry**
  (*Roland Winter* / Paul McMillan / Aude Picard)
- **Chemistry and Compounds**
  (*Choong-Shik Yoo* / John Badding / Yaming Ma)
- **Earth, Planetary and Mineral Science**
  (*Kei Hirose* / Jennifer Jackson / Renata Wentzcovitch)
- **Condensed Matter Physics at Extreme Conditions**
  (*Katsuya Shimizu* / Gabor Csathy / Mikhail Eremets / Liling Sun)
- **Material Science Under Pressure**
  (*Guoyin Shen* / Rajeev Ahuja / Anatoly Tsvyashchenko / Naira- Maria Balzaretti)
- **Light Elements, Carbon and Below**
  (*Paul Loubeyre* / David Ceperley / Isaac Silvera / Bartomeu Monserrat)
- **Melting Under Pressure**
  (*Reinhard Boehler* / Frederic Datchi / Malcolm McMahon / Wendy Mao)
- **Keynote Session: Future Directions and the Frontiers of Science and Technology at Extreme Conditions**
  (*Jon Eggert* / Gilbert Collins)
- **Power Hour**
  (*Julia Contreras-Garcia, Miriam Pena Alvarez*)

High Pressure, Research at
Exploring the Diversity of Phenomena Within the High Pressure Landscape over a Wide Range of Timescales
Jul 16-17, 2016
Chairs: Richard G. Kraus & Amalia Fernandez Panella

Host-Parasite Interactions, Biology of

Molecular and Translational Advances in Parasitic Diseases
Jun 12-17, 2016
Salve Regina University, Newport, RI
Chairs: Kasturi Haldar & Malcolm J. McConville
Vice Chairs: Meg Phillips & Luisa M. Figueiredo

- **Pharma Partnerships in Parasitic Diseases**
  (*Margaret Phillips* / Jeremy Burrows / Thierry Diagana)
- **Advancing New Therapies to Block Disease and Transmission**
  (*Kasturi Haldar* / Margaret Phillips / Ogobara Doumbo / Ian Gilbert / Elizabeth Winzeler)
- **Genomic/Genetic Regulation and Manipulation**
  (*David Sibley* / Boris Striepen / David Fidock / James Collins)
- **Emerging Drug Resistance**
  (*Jeremy Burrows* / Kasturi Haldar / Arjen Dondorp / Leann Tilley / Abdoulaye Djimde)
- **Sensing and Signaling in Parasitism**
  (*Matthias Marti* / Martin Olivier / Kenneth Stuart / Alok Bhattacharya)
- **Biochemistry and Metabolism**
  (*Malcolm McConville* / Daniel Goldberg / Michael Barrett / Domique Soldati / Audrey Odom)
- **Immunity and Persistence**
  (*Maria Mota* / Nisha Garg / Michael Hsieh / Dan Neafsey)
- **Parasite Development, Differentiation and Transmission**
  (*Steve Beverly* / Flaminia Catteruccia / Oliver Billker / Nina Papavasiliou / David Sacks)
- **New Targets in Host Entry and Remodeling**
  (*John Boothroyd* / Manoj Duraisingh / Stefan Kappe / Luisa Figueiredo)

Host-Parasite Interactions, Biology of
Molecular-Genetic Studies to Control Parasitic Diseases
Jun 11-12, 2016
Chairs: Alassane Mbengue & Eleanor Saunders

Human Single Nucleotide Polymorphisms & Disease

Understanding the Mechanisms of Variant Effects in the Era of Genome Sequencing
Jun 12-17, 2016
Mount Holyoke College, South Hadley, MA
Chairs: Anna R. Panchenko & Sean D. Mooney
Vice Chairs: Rita Casadio & Rachel Karchin

- **Keynote Session: Characterizing the Common Patterns of Genetic Variation**
  (*Joel Bader* / Michael Lynch / Kari Stefansson)
- **Assessing the Effects of Variations on Protein Biophysical Characteristics**
  (*Nir Ben-Tal* / Olivier Lichtarge / Marianne Rooman / Daniel Bolon)
- **Mutations, Protein Interaction Networks and Pathways**
  (*Ozlem Keskin* / Ruth Nussinov / Bruce Aronow)
- **Characterizing Variants in Cancer**
  (*Cristina Marino-Buslje* / Zemin Zhang / Yue Xiong)
- **Computational Prediction of Phenotypic Effects of Disease Mutations**
  (*Predrag Radivojac* / Mauno Vihinen / Yana Bromberg)
- **SNVs and Copy Number Variations in Complex Diseases**
  (*Bonnie Berger* / Igor Rogozin / Lilia Iakoucheva)
- **Variants Causing Rare Diseases**
  (*Charles Sanders* / Michael Brudno / Steven Brenner)
- **Precision Medicine in Practice**
  (*Nicholas Tatonetti* / Yves Pommier / Emil Alexov)
- **Variants and Pharmacogenomics**
  (*Yves Pommier* / Bissan Al-Lazikani / Deanna Kroetz)
- **Power Hour**
  (*Yana Bromberg, Lilia Iakoucheva*)

Hybrid Electronic & Photonic Materials and Phenomena

Fundamentals of Organic and Inorganic Semiconductors and Their Integration in Hybrid Electronic and Photonic Devices
Jun 19-24, 2016
The Hong Kong University of Science and Technology, Hong Kong, China
Chairs: Tobin J. Marks & Henry Yan
Vice Chairs: Deqing Zhang & Licheng Sun

- **Perovskite Solar Cells**
  (*Hin-Lap Yip* / Michael Graetzel / Sang Il Seok)
- **Interface Engineering and Phenomena**
  (*Xugang Guo* / Hongzhen Chen / Alex Jen / Emily Weiss)
- **Fundamentals of Organic Semiconductors**
  (*Dahui Zhao* / Iain McCouloch / Luping Yu)
- **Inorganic Semiconductors**
  (*Lei Fang* / Hideya Kumomi / David Mitzi / Wei Chen)
- **Hybrid Electronic Devices**
  (*Rongrong Hu* / Antonio Facchetti / Paras Prasad)
- **Nano and 2D Materials**
  (*Charles Y.-C. Lee* / Mercouri Kanatzidis / Lijun Wan / Phoebe Huei Shuan Tan)
- **Theoretical Aspects of Hybrid Devices**
  (*Ni Zhao* / James Durrant / Can Li)
- **Device Physics**
  (*Feng Yan* / Thuc-Quyen Nguyen / Franky So / Jinsong Huang)
- **Selected Poster Presentations / Late-Breaking Topics**
  (*Jiannong Wang*)

Image Science

Image Science in Sequence: From Detection to Decision
Jun 5-10, 2016
Stonehill College, Easton, MA
Chair: Richard G. Paxman
Vice Chair: Michael Insana

- **Decision Making in Image Science**
  (*Kyle Myers* / Polina Golland / Miles Wernick)
- **Multi-Mode/Multi-Wave Imaging**
  (*Meredith Kupinski* / Rebecca Fahrig / Matthew O'Donnell / Mathias Fink)
- **Novel Acquisition**
  (*Joseph Mait* / Harrison Barrett / Eric Fossum)
- **Imaging at the Physical Limits**
  (*James Fienup* / Lihong Wang / Ibrahim Cisse / Henry Chapman)
- **Use of Object Models and Priors**
  (*Craig Abbey* / David Donoho / Joseph Webster Stayman)
- **Computational Imaging**
  (*Laura Waller* / Oliver Cossairt / Peyman Milanfar / Michael Gehm)

- **Dynamic Imaging**
  (*James Duncan* / Yoram Bresler / Mathews Jacob)
- **Imaging Through Complex Media**
  (*Thomas Bifano* / Eva Sevick-Muraca / Ori Katz / Jerome Mertz)
- **Emerging Imaging Modalities**
  (*Ravindra Athale* / Dimitri Mawet / Bahaa E.A. Saleh)
- **Power Hour**
  (*Kyle Myers*)

Immunochemistry & Immunobiology

Immunity in Homeostasis, Disease and Therapy
Jun 19-24, 2016
Renaissance Tuscany Il Ciocco, Lucca (Barga), Italy
Chair: Yasmine Belkaid
Vice Chair: Federica Sallusto

- **Keynote Session: Innate Sensors**
  (*Caetano Reis e Sousa* / Max Cooper / Hamida Hammad / Bana Jabri)
- **Myeloid Cell Development and Gene Regulation**
  (*Miriam Merad* / Edward Pearce / Ken Murphy / Gioacchino Natoli)
- **Transcriptional and Post-Transcriptional Regulation of Lymphocytes**
  (*Donna Farber* / Vigo Heissmeyer / John O'Shea / Sasha Rudensky)
- **Immune Networks**
  (*Ronald Gemain* / Facundo Batista / Philippe Bousso / Carola Vinuesa)
- **Primary and Memory Responses**
  (*Sebastian Amigorena* / Federica Sallusto / Dirk Busch / Mike Dustin)
- **Host-Microbe Interactions**
  (*Akiko Iwasaki* / Kenya Honda / Eric Pamer / Eran Elinav)
- **Interventions and Monitoring in Vaccination**
  (*Michel Nussenzweig* / Mark Davis / Peter Kwong / Antonio Lanzavecchia)
- **Cytokines and Tissue Responses**
  (*Fiona Powrie* / David Artis / Burkhard Becher)
- **Microenvironment and Immunotherapy in Cancer and Chronic Infections**
  (*Shannon Turley* / John Wherry / Dietmar Zehn)

Immunochemistry & Immunobiology
Technologies and Discoveries Advancing the Frontiers of Immunology
Jun 18-19, 2016
Chairs: Robert Kimmerling & Gregory L. Szeto

In Vivo Magnetic Resonance

MRI Inside-Out and Outside-In: Innovative Technologies, Unmet Needs and New Opportunities
Jul 17-22, 2016
Proctor Academy, Andover, NH
Chair: Jurgen K. Hennig
Vice Chair: Daniel K. Sodickson

- **Keynote Session: MR Microscopy: Technologies and Applications**
  (*Axel Haase* / Stephen Blackband / Jan Korvink)
- **Future Technologies: Coils and More**
  (*Oliver Speck* / Jason Stockmann / Graham Wiggins / John Pauly)
- **Clinical Challenges and Opportunities**
  (*Elna-Marie Larsson* / Dieter Enzmann / Marion Smits)
- **Future Technologies: Magnets and Systems**
  (*Joel Garbow, Lawrence Wald* / Mark Bird / Panu Vesanen)
- **Hyperpolarization Somewhat Different**
  (*Kevin Brindle* / Jim Kempf / Leif Schroeder)
- **Imaging and Genetics**
  (*Cornelius Faber* / Viviana Gradinaru / Brigitte Kieffer / Jin Hyung Lee)
- **Quantitative MRI**
  (*Scott Beeman* / Jeffrey Evelhoch / Dan Ma)
- **Future Technologies: New Concepts for Data Acquisition**
  (*Oliver Wieben* / Kai Tobias Block / Zhi-Pei Liang / Kawin Setsompop)
- **MRI Beyond the Trodden Path**
  (*Joseph Hajnal* / Christine Chung / Petra Huppi)
- **Power Hour**
  (*Cornelia (Corree) Laule, Penny Gowland*)

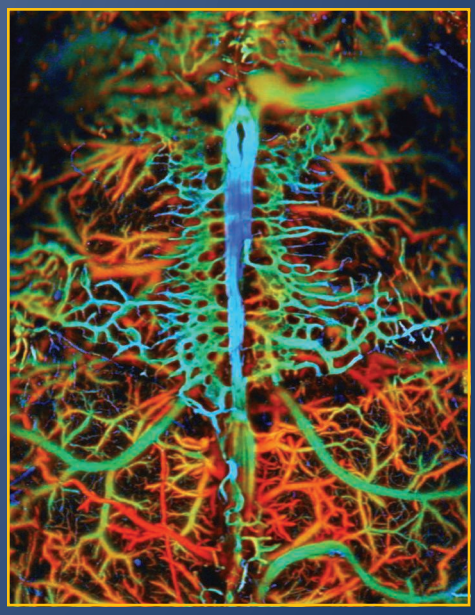

Functional vascular brain image: A representative oxygen saturation (sO_2) map in a whole mouse brain in vivo, acquired by fast functional photoacoustic microscopy (PAM) through an intact skull, using hemoglobin as the endogenous contrast. The sO_2 is color-encoded from blue (low oxygenation) to red (high oxygenation). Courtesy of Junjie Yao and Lihong V. Wang (Washington University in St. Louis). Submitted by Richard G. Paxman, Chair, Image Science GRC.

Industrial Ecology

Opportunities for the Critical Decade – Decoupling Well-Being from Environmental Pressures and Impacts
Jun 19-24, 2016
Stoweflake Conference Center, Stowe, VT
Chair: Heinz Schandl
Vice Chair: Stefanie Hellweg

- **The Science of Industrial Ecology and Its Contribution to Decoupling Economic Activity from Environmental Impact**
  (*Thomas Graedel* / Mark Swilling / Helga Weisz)
- **Creating Environmentally Sustainable Value Chains for Products and Services**
  (*Ester Van Der Voet* / Sangwon Suh / Shelie Miller / Sabrina Spatari)
- **Improving the Analytical Capacity to Analyze the Growing Complexity of Global Supply Chains of Energy and Materials**
  (*Stefan Pauliuk* / Anke Schaffartzik / Jan Heemann-Minx)
- **Tailoring the Science of Industrial Ecology to the Needs of the Urban Planning and Design Process**
  (*Anthony Capon* / Anu Ramaswami / Jessica Seddon / Clinton Andrews)
- **New Methods to Analyze the Natural Resource Demand of Cities**
  (*Tim Baynes* / Hiroki Tanikawa / John Fernandez)
- **Guiding Sustainable Consumption and Production in Developed and Developing Countries**
  (*Anthony Chiu* / James West / Arnulf Grubler / Faye Duchin)
- **Improving Industrial Systems - The Contribution of Industrial Ecology to Innovation in the Business Sector**
  (*Lewis Akenji* / Marian Chertow / Sarah Sim)
- **How to Conceptualize a Sociologically Informed Industrial Ecology**
  (*Vered Blass* / Andrew Jorgenson / Henrikke Baumann / Joshua Newell)
- **A Green and Circular Economy - The Impact of Industrial Ecology as a Science for Policy**
  (*Reid Lifset* / Simon Corbell / Shi Lei)

Industrial Ecology
Transparency and Interdisciplinary Collaboration on Popular Approaches to the Environmental Crisis in a Critical Decade
Jun 18-19, 2016
Chairs: Dominik Wiedenhofer & Heidi von Korff

Inorganic Chemistry

Bridging Core Discoveries and Applications in Inorganic Chemistry
Jun 19-24, 2016
University of New England, Biddeford, ME
Chair: Francois P. Gabbai
Vice Chair: Stosh A. Kozimor

- **Keynote Session: Frontiers in Inorganic Chemistry Research**
  (*Francois Gabbai* / Jacqueline Barton / Morris Bullock / Jeffrey Long)
- **Solid State Materials**
  (*Amy Prieto* / Sabarjit Banerjee / Claudia Felser / Hemamala Karunadasa)
- **Inorganic Chemistry in Biological Systems**
  (*Victoria DeRose* / Rebecca Abergel / Christopher Chang / Elizabeth Nolan)
- **Catalysis**
  (*Dawn Mason* / Paul Chirik / Donald Darensbourg / Alexander Radosevich)
- **Main Group Chemistry**
  (*Rory Waterman* / Todd Hudnall / Dwight Seferos / Jose Goicoechea)
- **Coordination Chemistry**
  (*Paula Diaconescu* / John Berry / David Harris / Jillian Dempsey)
- **When Inorganic Chemistry Gets Physical**
  (*Alfred Sattelberger* / Danna Freedman / James McCusker)
- **Inorganic Chemistry at the Nanoscale**
  (*Keith Watson* / Brandi Cossairt / Javier Vela-Becerra)
- **Novel Bonding Modes and Structures in Inorganic Chemistry**
  (*Stosh Kozimor* / Guy Bertrand / Theodor Agapie / George Stanley)

Inorganic Chemistry
Across the Periodic Table: Chemistry Advancing Technology and Energy Development
Jun 18-19, 2016
Chairs: Anna Marie Christianson & Luis De Jesus

Intermediate Filaments

Breaking Barriers in Intermediate Filament Biology: From Structure to Mechanisms and Targets in Human Diseases
Jun 12-17, 2016
Stoweflake Conference Center, Stowe, VT
Chair: Karen M. Ridge
Vice Chair: Milos Pekny

- **New Insights into Intermediate Filaments as Integral Regulators in Health and Disease**
  (*Karen Ridge* / Bishr Omary / Robert Goldman)
- **Mechanosensing and Regulating the Cell Microenvironment**
  (*Paul Janmey* / Gaudenz Danuser / Dennis Discher / Jan Lammerding)
- **Metabolic Regulation and Mitochondria**
  (*Alexander Minin* / Diana Toivola / John Eriksson / Vladimir Gelfand)
- **Cellular Organization, Adhesion, and Migration**
  (*Thomas Magin* / Kathleen Green / Gerhard Wiche)
- **Complexity, Integration, and Regulation of Signaling Networks**
  (*Natasha Snider* / Cecilia Sahlgren / Pierre Coulombe)
- **Cardiac and Muscular Control and Diseases**
  (*Howard Worman* / Gisele Bonne / Yassemi Capetanaki)
- **Aging and Age-Related Diseases**
  (*Yosef Gruenbaum* / Masaki Inagaki / Yixian Zheng)

- **Intersection of Cell Stress and Disease**
  (*Birgit Lane* / Roland Foisner / Ronald Liem)
- **Causes and Consequences in Neurodegeneration**
  (*Harish Pant* / Elly Hol / Jean-Pierre Julien / Milos Pekny)
- **Power Hour**
  (*Natasha Snider*)

Intermediate Filaments
Breaking Barriers in Intermediate Filament Biology: From Structure to Mechanisms and Targets in Human Diseases
Jun 11-12, 2016
Chairs: Iris Lähdeniemi & Noam Zuela

Intrinsically Disordered Proteins

Disordered Proteins: From Mechanisms to Therapeutic Opportunities
Jun 26 - Jul 1, 2016
Les Diablerets Conference Center, Les Diablerets, Switzerland
Chairs: Richard W. Kriwacki & Monika Fuxreiter
Vice Chairs: Vincent J. Hilser & Sonia Longhi

- **Keynote Session: Emerging Themes; Disorder in Cellular Organization and as a Therapeutic Target**
  (*Sonia Longhi* / Madan Babu / Wolfgang Peti)
- **Exploring the Diversity of IDP Cellular Functions**
  (*Keith Dunker* / John Bushweller / Martha Cyert / Mark Hochstrasser / James Hurley)
- **Protein Disorder Within Assemblies and Machines**
  (*Benjamin Schuler* / Bernd Bukau / Steven Hahn / Markus Zweckstetter)
- **Mechanisms of Interactions Involving Disorder**
  (*Peter Tompa* / Charalampos "Babis" Kaladimos / Rachel Klevit / Louis Renault / Katherine Stott)
- **The Diverse Biology of Disordered Proteins**
  (*Madan Babu* / Norman Davey / Lila Gierasch / Anthony Hyman)
- **Roles of IDPs in Membrane-Less Organelles; Form and Function**
  (*Rohit Pappu* / Julie Forman-Kay / Steve McKnight / Ivan De Curtis / J. Paul Taylor / Geraldine Seydoux)
- **Ensemble Representations of IDPs; Methods and Links with Function**
  (*Martin Blackledge* / Toshio Ando / Perdita Barran / Robert Konrat / Claudio Luchinat)
- **Therapeutic Strategies Involving IDPs**
  (*Wolfgang Peti* / Kurt Deshayes / Jonathan Moore / Steven Finkbeiner)
- **Disorder in Protein Aggregation and Inheritance; Future Directions of IDP Research**
  (*Vincent Hilser* / Gary Daughdrill / Eckhart Mandelkow)

Intrinsically Disordered Proteins
Function Through Disorder: Intrinsically Disordered Proteins in Biology and Medicine
Jun 25-26, 2016
Chairs: Rebecca B. Berlow & Ofrah Faust

Ion Channels

Molecular Basis for Electrical Signaling in the Nervous System and Beyond
Jul 10-15, 2016
Mount Holyoke College, South Hadley, MA
Chair: Emily R. Liman
Vice Chair: Chris A. Ahern

- **Keynote Session: New Directions in Ion Channel Research**
  (*David Clapham* / David Julius / Christopher Miller)
- **Thermosensing Through Ion Channels**
  (*Magdalene Moran* / Baron Chanda / Rachelle Gaudet / Ramon Latorre / Jie Zheng)
- **Structure of Ion Channels**
  (*Brad Rothberg* / Daniel Minor / Donald Gill / Bailong Xiao)
- **Mechanosensory Ion Channels**
  (*Miriam Goodman* / Sviatoslav Bagriantsev / Jorg Grandl / Craig Montell / Tibor Rohacs)
- **Modulation of Ion Channels**
  (*Ann Rittenbouse* / Bruce Bean / Sharona Gordon / Diomedes Logothetis)
- **Ion Channels in Concert**
  (*Bertil Hille* / Andrea Meredith / Mark Nelson / Diane Papazian / Mark Shapiro)
- **Assembly and Trafficking of Ion Channels**
  (*Carol Deutsch* / Colin Nichols / Gail Robertson / Paul Slesinger)
- **Engineering Ion Channels**
  (*Francisco Bezanilla* / Ehud Isacoff / William Kobertz / Richard Kramer / Andrew Plested)
- **New Ion Channels / New Functions for Ion Channels**
  (*Chris Ahern* / Kevin Foskett / Richard Tsien)

Ion Channels
Exploring the Molecular Basis of Cellular Excitability
Jul 9-10, 2016
Chair: David K. Jones
Associate Chair: Anna L. Carbone

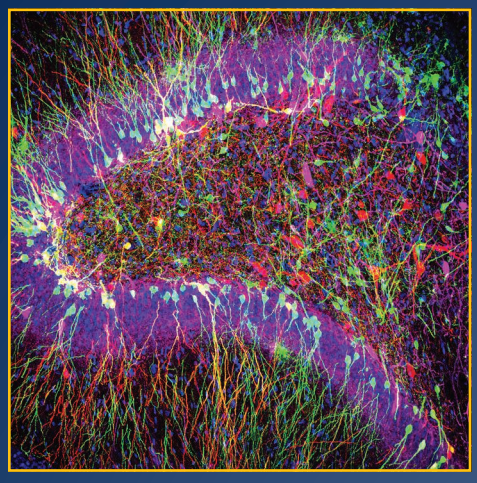

Rabies virus labeled monosynaptic inputs onto birth-dated, adult-born neurons in the epileptic rat dentate gyrus. Red is rabies-mCherry, retrovirus-birthdated neurons labeled with GFP (green), interneurons labeled with parvalbumin (magenta) and Hoechst nuclear stain (blue). Courtesy of Jack Parent and Xixi Du (University of Michigan). Submitted by Steve C. Danzer & Heinz W. Beck, Chairs, Mechanisms of Epilepsy & Neuronal Synchronization GRC.

Ionic Liquids

Ionic Liquids for Future Technologies
Aug 14-19, 2016
Sunday River, Newry, ME
Chair: Anja V. Mudring
Vice Chair: Jim Davis

- **Keynote Session: Ionic Liquids - Where Do We Stand and Where Do We Go?**
  (*Gerd Meyer* / Charles Hussey / Robin Rogers)
- **Ionic Liquids, Polymers and Where the Two Meet**
  (*Matthew Reichert, Scott Shaw* / Paul Trulove / Joshua Sangoro / Timothy Long)
- **Ionic Liquids as Nano-Ordered Solvents for Materials Design**
  (*Arsalan Mirjafari* / Andreas Taubert / Laurent Douce)
- **Structure-Property Relationships in Ionic Liquids and Their Implication for Materials Synthesis and Properties**
  (*Suojiang Zhang* / Barbara Kirchner / Agilio Padua / John Holbrey)
- **Elucidating Structure and Interactions in Ionic Liquids**
  (*Annegret Stark* / Andrea Mele / Alessandro Triolo)
- **Ionic Liquids and Interfaces**
  (*Roland Kalb* / Peter Licence / Rob Atkin / Edward Castner)
- **Energy-Related Applications of Ionic Liquids**
  (*Gabriela Gurau* / Jerry Boatz / Jenny Pringle)
- **Inorganic Chemistry's Contribution to Ionic Liquids**
  (*Mihkel Koel* / Andreas Bundt / Patricia Hunt / Jared Anderson)
- **Ionic Liquids for Future Sustainable Technologies**
  (*Mara Freire* / Roberto Rinaldi / Anders Riisager)

Ionic Liquids
Ionic Liquids for Future Technologies
Aug 13-14, 2016
Chairs: Juan Araque & Kevin Clark

Lasers in Medicine & Biology

Optical Innovations Solving Challenges in the Life Sciences
Jul 10-15, 2016
Mount Snow, West Dover, VT
Chairs: Brett E. Bouma & Paola Taroni
Vice Chairs: Anita Mahadevan-Jansen & Paul M.W. French

- **Keynote Session: Quantum Mechanics in Biology and Imaging**
  (*Warwick Bowen* / Ronald Walsworth / Leonid Krivitsky / Theodore Goodson)
- **Neurophotonics**
  (*Daniel Cote* / Thomas Blanpied / Yves De Koninck / Kwanghun Chung / Karin Wardell)
- **On the Cusp of Translation**
  (*Rebecca Richards-Kortum* / Stephen Boppart / Dvir Yelin / Daniel Cote)
- **Functional Measurements in Ophthalmology**
  (*Austin Roorda* / Shy Shoham / Jennifer Hunter / Alfredo Dubra)
- **Advances in Optical Spectroscopy**
  (*Bruce Tromberg* / Antonio Pifferi / Elizabeth Hillman / Christine Hendon)
- **Propagation and Imaging Through Turbidity**
  (*Maciej Wojtkowski* / Hui Cao / Wonsik Choi / Alwin Kienle / Monika Ritsch-Marte)
- **Multi-Scale Imaging**
  (*Melissa Skala* / Benjamin Vakoc / Kristen Maitland / Vasilis Ntziachristoz)
- **Elastography and Micro-Biomechanics**
  (*David Sampson* / Seemantini Nadkarni / Giuliano Scarcelli / Amy Oldenburg)
- **Keynote Session: Looking Outside the Box: What Can We Learn from Advances in Other Optical Fields?**
  (*Johannes De Boer* / David Sampson)

Lipoprotein Metabolism

Lipid and Lipoprotein Metabolism in Chronic Disease Pathogenesis and Treatment
Jun 12-17, 2016
Waterville Valley, Waterville Valley, NH
Chair: John S. Parks
Vice Chairs: Alan Remaley & Cheryl Wellington

- **Keynote Session: Fatty Liver Disease: A Tale of Two Genes**
  (*Russell Debose-Boyd* / Helen Hobbs)
- **Lipoproteins and the Vascular Wall**
  (*Cheryl Wellington* / Yury Miller / Arnold von Eckardstein / Kathryn Moore / Miranda Van Eck / Berislav Zlokovic)
- **Lipid Transport and Catabolism**
  (*Rosalind Coleman* / Stephen Young / Rudolf Zechner / Ira Goldberg)
- ***In Vivo* Physiology of Lipid Metabolism**
  (*Ira Goldberg* / Timothy Osborne / Karen Reue / Sudha Biddinger / Rebecca Haeusler)
- **Liver and Intestinal Lipid/Lipoprotein Metabolism**
  (*Dawn Brasaemle* / M. Mahmood Hussain / Rosalind Coleman / Paul Dawson / Khosrow Adeli)
- **HDL Metabolism**
  (*Daniel Rader* / Daisy Sahoo / Nancy Webb / Frank Sacks)
- **Genetics of Lipid/Lipoprotein Metabolism**
  (*Karen Reue* / Ruth McPherson / Kiran Musunuru / Ruth Frikke-Schmidt / Daniel Rader)

- **Intracellular Lipid Metabolism**
  (*Timothy Osborne* / Russell Debose-Boyd / Robert Farese / Dawn Brasaemle / Gad Asher / Daniel Ory)
- **Therapeutics for Cardiovascular and Neurodegenerative Diseases**
  (*Alan Remaley* / Daniel Michaelson / Douglas Johns / Kelly Bales / Thomas Beyer)

Lipoprotein Metabolism
Recent Advances in Lipoprotein Physiology and Related Disease
Jun 11-12, 2016
Chairs: Scott M. Gordon & Marjolein A. van den Boogert

Lysosomes & Endocytosis

Molecular Mechanisms and Functions of Endosomal and Lysosomal Pathways
Jun 12-17, 2016
Proctor Academy, Andover, NH
Chair: Roberto Weigert
Vice Chair: Lois S. Weisman

- **Endocytic Machinery at the Plasma Membrane**
  (*Sandra Schmid, Mark Von Zastrow* / Volker Haucke / Ludger Johannes / Margaret Robinson)
- **Endosomal Sorting and Recycling**
  (*Elizabeth Conibear, Scott Emr* / Peter Cullen / Julie Donaldson / Erik Jorgensen / Julie Magarian Blander / Julie Brill)
- **Exploiting the Endocytic Machinery During Host-Pathogen Interactions**
  (*Sergio Grinstein, Fabienne Paumet* / Nihal Altan-Bonnet / Mark Marsh / Nels Elde / Gillian Griffiths)
- **Dysregulation of Endosomal and Lysosomal Trafficking During Cancer and Other Pathologies**
  (*Alexander Sorkin, JoAnn Trejo* / Philippe Chavrier / Victor Faundez / Rosalind Segal / Alissa Weaver)
- **Metabolism and Related Diseases**
  (*Frances Brodsky, Timothy McGraw* / Andrea Ballabio / Amira Klip / Jennifer Lippincott-Schwartz / Bao-Liang Song)
- **Mechanisms of Lysosomal Degradation and Autophagy**
  (*Olivia Majer, Christian Ungermann* / Markus Babst / Vojo Deretic / Haoxing Xu / Richard Youle)
- **Late-Breaking Topics**
  (*Tom Kirchhausen, Lois Weisman* / Toyoshi Fujimoto)
- **Lysosomes, and Lysosome-Related Organelles**
  (*Robert Piper* / Norma Andrews / Juan Bonifacino / Michael Marks / Graca Raposo)
- **Keynote Session: Organization and Function of the Endosomal System: From Cells to Tissues**
  (*Roberto Weigert* / Marino Zerial)

Lysosomes & Endocytosis
Moving Endosomes from Basic Principles to Development and Disease
Jun 11-12, 2016
Chairs: Colin D.H. Ratcliffe & Olivia Majer

Mammalian Reproduction

Regulatory Processes Modulating Mammalian Reproduction
Aug 21-26, 2016
Waterville Valley, Waterville Valley, NH
Chairs: Anne Croy & Amander T. Clark
Vice Chairs: Humphrey H. Yao & Jon Oatley

- **Environmental Impacts upon Reproduction and Offspring Health**
  (*Patricia Hunt* / Tracey Woodruff / Jodi Flaws / Douglas Kwon)
- **Genetic Regulation of Reproductive Outcomes**
  (*Margaret (Peggy) Petroff* / Kjersti Aagaard / Alex Bortvin / Monika Ward)
- **Editing the Genes of Gametes and Embryos**
  (*Francesco Demayo* / John Schimenti / F. Kent Hamra / Randall Prather)
- **Epigenetic Regulation in Reproduction**
  (*John McCarrey* / Marisa Bartolomei / Myriam Hemberger / Sue Hammoud)
- **Stem Cells in Reproduction**
  (*Wei Yan* / Jan Brosens / Brian Hermann / Mitinori Saitou)
- **Bioengineering and Reproductive Health**
  (*Kyle Orwig* / Daniela Ulrich / Mats Brannstrom / Joanna Burdette)
- **Reproductive Transcription and Signaling Pathways**
  (*Diana Laird* / Blanche Capel / Haibin Wang / Aleksandar Rajkovic)
- **Continuing Challenges to Human Reproductive Health**
  (*Xiujun Fan* / Jacquetta Trasler / Michal Neeman / Andrew Sharkey)
- **Keynote Session: Milestones in Reproductive Biology**
  (*Jon Oatley, Humphrey Yao* / Mitch Eddy / Marilyn Renfree)
- **Power Hour**
  (*Margaret (Peggy) Petroff*)

Conferees take a break from their soccer game to pose for a group photo at sunny Stonehill College.

Mammary Gland Biology

The Mammary Gland in Normal Development and Progression to Cancer
May 29 - Jun 3, 2016
Renaissance Tuscany Il Ciocco, Lucca (Barga), Italy
Chair: Geoffrey J. Lindeman
Vice Chairs: Heide L. Ford & Michael T. Lewis

- **Keynote Session: The Mammary Gland Genome in Development and Cancer**
  (*Geoffrey Lindeman* / Charles Perou)
- **Making a Mammary Gland - Stem Cells and Development**
  (*Silvia Fre* / Geoffrey Wahl / Jane Visvader / Lindsay Hinck / Renee Van Amerongen)
- **Regulators of Functional Maturation and Regression in the Mammary Gland**
  (*Kay-Uwe Wagner* / Christine Watson / Christina Scheel)
- **Hormonal Cues and Connections: Clues for Treatment and Prevention**
  (*Cathrin Brisken* / Wayne Tilley / Robert Clarke / Steffi Oesterreich)
- **BRCA1 and Beyond – Two Decades On**
  (*Matthew Smalley* / Jos Jonkers / Josef Penninger)
- **Normal Development Gone Awry - Mouse Mammary Tumor Models**
  (*Michael Lewis* / Mohamed Bentires-Alj / Christopher Ormandy / Barry Gusterson)
- **Mammary Tumor Heterogeneity, Dormancy and Metastasis**
  (*Maria Vivanco* / Paolo Di Fiore / Peter Eirew)
- **Growth and Inhibitory Signals – Epithelial and Stromal Cues**
  (*Heide Ford* / Marja Mikkola / Martin Eilers / Mary Helen Barcellos-Hoff)
- **Keynote Session: Modeling Mammary Gland Development and Cancer**
  (*Nancy Hynes* / Lothar Hennighausen)

Mammary Gland Biology
Building Your Route Between Mammary Gland Development and Cancer
May 28-29, 2016
Chairs: Kara Britt & Bruno Mafra Simoes

Marine Microbes

The Evolution, Nature and Function of Microbial Interactions
Jun 19-24, 2016
PGA Catalunya Business and Convention Centre, Girona, Spain
Chair: Catherine Legrand
Vice Chair: Kay Bidle

- **Microbial Activities and Interactions in Natural Communities and Ecosystem Foodwebs**
  (*Pep Gasol* / Ilana Berman-Frank / Morten Iversen)
- **Linking Microbial Diversity and Function to Ecology and Biogeochemistry**
  (*Jed Fuhrman* / Pierre Galand / Adina Howe / Shinichi Sunagawa)
- **Evolution of Microbial Interactions and Function**
  (*Corina Brussaard* / Assaf Vardi / Debbie Lindell)
- **Environmental Shaping of Functional Traits and Community Structure**
  (*Eva Lindstrom* / Laura Gomez-Consarnau / Otto Cordero / Zoe Finkel)
- **Interactive Pressures on Microbial Genome Structure**
  (*Jakob Pernthaler* / Angus Buckling / Richard Lenski)
- **Host-Associated Microbiome Communities**
  (*Melissa Garren* / Jillian Petersen / Russell Hill / Jesse Zaneveld)
- **Infochemicals and Cell Signaling as Drivers of Microbial Interactions**
  (*Julia Kubanek* / Benjamin Van Mooy / Einat Segev Ben-Yair / Sebastian Fraune)
- **Incorporating Microbes into Biogeochemical and Climate Models**
  (*Kay Bidle* / Stephanie Dutkiewicz / Colin Brownlee)
- **Microbes, Well-Being and Sustainability**
  (*Carlos Pedros-Alio* / Jessica Green / Suzanne Lee)

Marine Microbes
Microbe Coexistence and Coevolution in a Changing Ocean
Jun 18-19, 2016
Chairs: Javier Del Campo & Bryndan P. Durham

Mechanisms of Epilepsy & Neuronal Synchronization

Aberrant Circuits to Impaired Function in Epilepsy
Aug 21-26, 2016
PGA Catalunya Business and Convention Centre, Girona, Spain
Chairs: Steve C. Danzer & Heinz W. Beck
Vice Chairs: Christophe Bernard & Amy Brooks-Kayal

- **Keynote Session: Network Function in the Normal and Diseased Brain**
  (*Heinz Beck, Steve Danzer* / Yehezkel Ben-Ari / Hannah Monyer)
- **Network Dysfunction in Genetic Epilepsies**
  (*Jeffrey Noebels* / Dirk Isbrandt / Michael Wong / Holger Lerche / Ype Elgersma / Christina Gross)
- **Regulation and Mis-Regulation of Neuronal Circuit Development**
  (*Kevin Staley* / Thomas Südhof / Albert Becker / Jack Parent)
- **Regulation of Neuronal Circuits by Astrocytes**
  (*Karen Wilcox* / Christian Henneberger / Nicola Allen / Catherine Christian)
- **GABAergic Circuit Function and Neuronal Oscillations**
  (*Douglas Coulter* / Scott Baraban / Rosa Cossart / Laura Colgin)
- **Normal Circuit Function in Cognition**
  (*Ivan Soltesz* / Carol Barnes / Anton Sirota / Florian Mormann / Ueli Rutishauser)
- **Pathological Circuit Function in Epilepsy**
  (*Viji Santhakumar* / Valerie Crepel / Peyman Golshani / Liset Menendez de la Prida)
- **Circuit Dysfunction in Epilepsy Comorbidities**
  (*Sheryl Haut* / Lennart Mucke / Jamie Maguire / Aynara Wulsin / Tallie Z. Baram / Laura Cancedda)

Gordon Conferences are different from other scientific conferences because they are intense, inclusive, cutting edge, and engaging.

- Jacqueline Fletcher, Chair, 2015 Chemical & Biological Terrorism Defense GRC

- **Using Circuit-Level Insights to Repair and Manipulate the Epileptic Brain**
  (*Istvan Mody* / Esther Krook-Magnuson / Loren Looger / Jeanne Paz)
- **Power Hour**
  (*Candi LaSarge*)

Mechanisms of Epilepsy & Neuronal Synchronization
Dynamic Epilepsy Circuits and Their Modulation
Aug 20-21, 2016
Chairs: Omar J. Ahmed & Laura A. Ewell

Medicinal Chemistry

Innovations in Small Molecule Drug Discovery in Oncology, Neglected Diseases, Immunology, Parkinson's Disease, Fibrosis, First Disclosure Clinical Candidates, and New Drug Discovery Technologies
Aug 7-12, 2016
Colby-Sawyer College, New London, NH
Chair: Bradley Tait
Vice Chair: Matthew Marx

- **Small Molecule Anti-Fibrotics**
  (*Jehrod Brenneman* / Sabine Hadida / Tom Heightman / Lara Kallander)
- **Neglected Tropical Diseases**
  (*Cindy Parrish* / Christopher Cooper / Valentina Molteni / Isabel Castellote Alvaro / Stacie Canan)
- **Enabling New Technologies in Medicinal Chemistry**
  (*Matthew Bourbeau* / Ian Churcher / Jeffrey Dodge / Woody Sherman)
- **Approaches to the Treatment of Parkinson's Disease**
  (*Michael Ellis* / Marco Baptista / Jorg Holenz / Yeon-Hee Lim)
- **Advances in Lead Generation**
  (*Jorg Holenz* / Erin Dimauro / Franz Von Nussbaum / Katherine Lee)
- **Exciting Advances Toward New Treatments for Autoimmune Disorders**
  (*Dustin Mergott* / Michelle Machacek / Steve Staben / Atli Thorarensen / Peter Toogood)
- **Oncology Drug Discovery**
  (*Eugene Chekler* / Bayard Huck / Kurt Pike / Kurt Deshayes)
- **Late Breaking Topics: Disclosures of Clinical Candidates**
  (*Brock Shireman* / Grace Chuang / Gregory Notte / David Weinstein)
- **Keynote Session: Embracing and Anticipating Change in a Dynamic Industry – View from One Medicinal Chemist**
  (*Bradley Tait* / Kazumi Shiosaki)

Medicinal Chemistry
Understanding Key Concepts for Lead Optimization
Aug 6-7, 2016
Chair: Michael P. Pollastri

Meiosis

Molecular Mechanisms, Regulation and Integration of the Meiotic Program
Jun 26 - Jul 1, 2016
Colby-Sawyer College, New London, NH
Chair: Neil Hunter
Vice Chair: Monica P. Colaiacovo

- **The Synaptonemal Complex: Formation, Structure, and Function**
  (*Michael Lichten* / Scott Hawley / Monica Colaiacovo / Abby Dernburg)
- **Homologous Recombination: Mechanisms, Integration and Regulation**
  (*Eva Hoffmann* / Raphael Mercier / Douglas Bishop / Jeff Sekelsky / Francesca Cole / Michael Lichten / Jeremy Wang / Nancy Hollingsworth)
- **Meiotic Errors: Mechanisms and Clinical Implications**
  (*Matthew Neale* / Eva Hoffmann / Tomoya Kitajima / Katja Wassmann)
- **Chromosome Segregation: Kinetochores, Cohesion, Chiasmata and Spindles**
  (*Gloria Brar* / Yoshinori Watanabe / Adele Marston / Julie Cooper)
- **Epigenetics, Germ Cells and Gametes**
  (*Joanne Engebrecht* / Paula Cohen / Satoshi Namekawa / Gloria Brar / Alex Bortvin)
- **Checkpoints and Regulation of Meiotic Progression**
  (*Adele Marston* / Joanne Engebrecht / Kevin Corbett / Matthew Neale)
- **Homologous Recombination: When, Where and How Many**
  (*Roberto Pezza* / Gerald Smith / Bernard De Massy / Anne Villeneuve / Scott Keeney / Barbara Meyer / Gregory Copenhaver)
- **Meiotic Chromosome Morphogenesis: Cohesins, Axes and Homolog Pairing**
  (*Kevin Corbett* / Akira Shinohara / Denise Zickler / Roberto Pezza / Andreas Hochwagen / Nancy Kleckner / Verena Jantsch)
- **Evolution of Meiosis: Conservation and Diversity of Programs, Structures and Mechanisms**
  (*Andreas Hochwagen* / R. Daniel Camerini-Otero / Monique Zetka / Amy Macqueen)
- **Power Hour**
  (*Amy MacQueen, Julie Cooper*)

Meiosis
Mechanisms of Sexual Reproduction Through Meiosis
Jun 25-26, 2016
Chairs: Talia L. Hatkevich & Mercedes R. Gyuricza

Membrane Transport Proteins

Membrane Transporters: Translating Molecules to Medicine
Jun 12-17, 2016
Renaissance Tuscany Il Ciocco, Lucca (Barga), Italy
Chair: Rajini Rao
Vice Chair: Harald H. Sitte

- **Molecules in Motion: Transporter Dynamics, Single Molecules and Movies**
  (*Poul Nissen* / Lucy Forrest / Hassane Mchaourab / Emad Tajkhorshid / Poul Nissen)
- **Big Data: Virtual Mining, Genomes and Phenomes**
  (*Matthias Hediger* / Debora Marks / Jean-Louis Reymond / Giulio Superti-Furga)
- **Transport in 3D: From Stem Cells to Organoids**
  (*Daniel Fuster* / Mark Donowitz / Sofia Lizarraga / Stine Pedersen)
- **Unconventional Transporters: Flipping Lipids, Porting Peptides and More**
  (*Lydia Aguilar-Bryan* / Raimund Dutzler / Christiane Albrecht / Robert Tampe)
- **Bench to Bedside: Perspectives from Pharma and Academia**
  (*Min Li* / Gavin Kilpatrick / Claire Steppan)
- **Neurochemistry and Neurotransmitter Transporters**
  (*Harald Sitte* / Gaia Novarino / Randy Blakely / Aurelio Galli / Ulrik Gether / Manju Kurian)
- **TRP Channels in Health and Disease**
  (*Haoxing Xu* / Emily Liman / Dimitra Gkika / Haoxing Xu)
- **Transporter Trafficking, Organellar and Vesicular Transport**
  (*Joseph Mindell* / Robert Edwards / Michael Freissmuth / Luis Galietta / Joseph Mindell)
- **Structural Insight into Disease**
  (*Rajini Rao* / Dax Fu / Joseph Bryan / Kathy Sweadner / Alexander M. Cruickshank Lecture: Nieng Yan)
- **Power Hour**
  (*Christiane Albrecht*)

Membrane Transport Proteins
Membrane Transporters in Health and Disease
Jun 11-12, 2016
Chairs: Thomas Steinkellner & Hari Prasad

Membranes: Materials & Processes

Debates and Controversies in the Field of Membranes
Jul 31 - Aug 5, 2016
Colby-Sawyer College, New London, NH
Chairs: Jamie Hestekin, Nancy K. Lape & Jeffrey R. McCutcheon
Vice Chairs: Mary L. Lind & Manish Kumar

- **Keynote Session: Membrane Materials and Processes**
  (*Kerri Hickenbottom* / Andrew Livingston)
- **Membranes for Water Treatment**
  (*William Phillip* / Meagan Mauter / Baoxia Mi / Hyung Gyu Park)
- **Modeling Membrane Transport**
  (*Sylvie Neyertz* / Rich Lueptow / David Sholl)
- **Gas Separation Membranes**
  (*J.R. Johnson* / Andre Beyer / Ryan Lively / Ho Bum Park)
- **Inorganic Membranes**
  (*Jerry Lin* / Kang Li / Arian Nijmeijer)
- **The Business of Membranes**
  (*Mary Lind* / Hans Wijmans / Robert McGinnis)
- **Biological, Biomimetic, and Biomedical Applications**
  (*Andrew Zydney* / Claus Helix-Nielsen / Bruce Hinds)
- **Advanced Membrane Materials**
  (*David Jassby* / Nieck Benes / Brian Benicewicz / Ulrich Wiesner)
- **Keynote Session: Membrane Controversies and Perspectives**
  (*Manish Kumar* / Richard Baker / Isabel Escobar / Scott Husson / David Ladner / John Pellegrino)

Membranes: Materials & Processes
Membrane Engineering at the Edge of Innovation and Global Advances
Jul 30-31, 2016
Chairs: Patrick Saboe & Kerri L. Hickenbottom

Metallocofactors

Inorganic Components of Nature that Drive Metabolism
Jun 12-17, 2016
Stonehill College, Easton, MA
Chair: Jonas C. Peters
Vice Chair: Sean J. Elliott

- **Keynote Session: Metallocofactors that Feed and Fuel Our Planet**
  (*Harry Gray* / Jian-Ren Shen / Brian Hoffman)
- **Photosynthetic Cofactors in Biology**
  (*R. David Britt* / Junko Yano / Wolfgang Lubitz / Erwin Reisner / Daniel Nocera)
- **Modeling the Structure and Function of Photosynthetic Cofactors**
  (*Theodore Betley* / Theodor Agapie / Chunxi Zhang / Per E. Siegbahn)

- **Nitrogenase Enzymes**
  (*Douglas Rees* / Thomas Spatzal / Serena Debeer / Stephen Cramer)
- **Modeling the Structure and Function of Nitrogenase Cofactors**
  (*Connie Lu* / Frank Neese / Leslie Murray / Patrick Holland)
- **Assembly, Structure, and Function of FeS-Cofactors**
  (*Joan Broderick* / Deborah Perlstein / Sheila David / Amie Boal)
- **Fe and Ni Cofactors that Interact with O_2, H_2, and CO_2**
  (*Fraser Armstrong* / Robert Hausinger / Juan Fontecilla-Camps / Michael Green)
- ***De Novo* Cofactor Design and Characterization**
  (*Yi Lu* / Akif Tezcan / Thomas Ward / Giovanna Ghirlanda)
- **Keynote Session: The Latest on Radical SAM Enzymes**
  (*Squire Booker* / Catherine Drennan / Markus Ribbe)

Metals in Medicine

The Interplay of Creative Chemistry and Cellular Processes in Metals in Medicine
Jun 26 - Jul 1, 2016
Proctor Academy, Andover, NH
Chairs: Katherine J. Franz & Nils Metzler-Nolte
Vice Chairs: Seth M. Cohen & Kenneth Kam-Wing Lo

- **Keynote Session: Metal-Based Drugs and Cellular Redox Biochemistry**
  (*Katherine Franz, Nils Metzler-Nolte* / Thomas O'Halloran / Ruma Banerjee)
- **Harnessing Metal Trafficking Pathways for Antimicrobial Drug Development**
  (*Elizabeth Nolan* / Celia Goulding / Jeffrey Henderson / Amanda Oglesby-Sherrouse / Timothy Wencewicz)
- **Targeting Cancer and Infection with Photodynamic Compounds**
  (*Edith (Phoebe) Glazer* / Adah Almutairi / Gilles Gasser / Sherri McFarland)
- **Emerging Analytical Methods (or, What Happens to My Metallodrug *In Vivo*?)**
  (*Angela Casini* / Fabio Arnesano / Lydia Finney / Christian Hartinger)
- **Inorganic Chemistry and Cellular Redox Regulation**
  (*Peter Sadler* / Alexander M. Cruickshank Lecture: Christopher J. Chang / Milos Filipovic / Elisa Tomat)
- **Creative Approaches in Imaging Agent Design**
  (*Matthew Allen* / Jens Hasserodt / Elizabeth New / Clotilde Policar / Thomas Meade)
- **Compound to Clinic: Not Lost in Translation**
  (*Seth Cohen* / Chris Orvig / Des Richardson / Amir Nashat)
- **Late-Breaking Topics**
  (*Kenneth Kam-Wing Lo*)
- **Neurodegeneration: Biology, Pathology, Chemistry and Collaboration**
  (*Paul Donnelly* / Peter Crouch / Anthony R. White / Blaine Roberts)

Microbial Stress Response

Sensing, Adaptation and Evolution in Microbes that Experience Stress
Jul 17-22, 2016
Mount Holyoke College, South Hadley, MA
Chairs: Eduardo A. Groisman & Dianne K. Newman
Vice Chairs: Petra A. Levin & William W. Navarre

- **Keynote Session: From Physiology to Stress**
  (*Eduardo Groisman, Dianne Newman* / Susan Gottesman / Moselio Schaechter)
- **Variations in Bacterial Adaptive Responses**
  (*Amy Cheng Vollmer* / Mark Buttner / Urs Jenal / Nicholas Shikuma / Nicola Stanley-Wall)
- **A Diversity in Bacterial Stress Responses**
  (*Joan Slonczewski* / Arash Komeili / Alexander Petroff / Paula Welander)
- **Stress Response: From Structure to Group Behavior**
  (*Kelly Hughes* / Patricia Casino / Karine Gibbs / Christine Jacobs-Wagner / Karina Xavier)
- **Signaling Cytoplasmic and Extracytoplasmic Stress**
  (*Carol Gross* / Michael Gilmore / Jade Wang / James Williamson)
- **Genetic and Phenotypic Resistance to Antimicrobial Agents**
  (*Amy Gehring* / Martin Ackermann / Dan Andersson / Nathalie Balaban / Sophie Helaine)
- **Coping with Oxidative Stress**
  (*Monica Chander* / Frederic Barras / Ursula Jakob / Graham Walker)
- **An Applied View of Bacterial Physiology**
  (*Chris Kaiser* / John Helmann / Jennifer Leeds / Richard Roberts)
- **Post-Transcriptional Response to Stress**
  (*Mark Goulian* / Jason Crawford / Michael Ibba / Gisela Storz)

GRS Microbial Stress Response
Detecting and Exploring Microbial Behavior and Physiology
Jul 16-17, 2016
Chairs: Julia L. Willett & Philip R. Bennallack

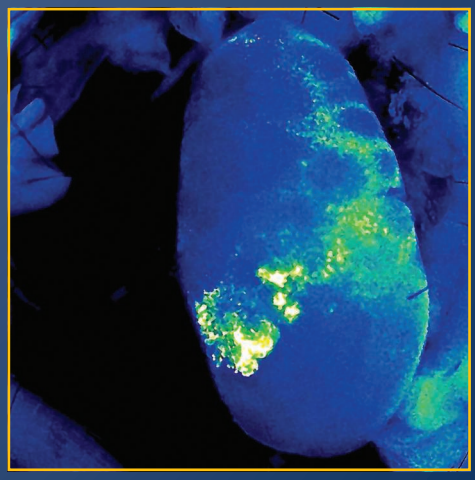

Visualization of lymph node colonization by the bubonic plague pathogen, Yersinia pestis. Yersinia pestis (expressing GFP; green) travels from the skin into draining lymph nodes (DAPI stain; blue) shortly after inoculation. Inflamed lymph nodes with high bacterial burdens are a hallmark of bubonic plague. Courtesy of Virginia L. Miller and Rodrigo Gonzalez. Submitted by Virginia L. Miller, Chair, Microbial Toxins & Pathogenicity GRC.

Microbial Toxins & Pathogenicity

Bacterial Pathogens: From Basics to Encounters with the Host Cell
Jul 10-15, 2016
Waterville Valley, Waterville Valley, NH
Chair: Virginia L. Miller
Vice Chair: Andrew Camilli

- **Keynote Session: Microbial Toxins and Pathogenicity**
  (*Andy Camille* / Pascale Cossart)
- **Toxins - Action, Targeting and Structure**
  (*Joseph Barbieri* / Neal Alto / Jimmy Ballard / Jorge Galan / Borden Lacy / Wayne Lencer)
- **Regulation of Virulence**
  (*Peggy Cotter* / Melanie Blokesch / Theresa Koehler / Victoria Stone)
- **Pathogenesis**
  (*Beth McCormick* / Michael Bachman / Joanne Engel / Sarah Fortune / Arturo Zychlinsky / Joan Mesas)
- **Pathogen Evolution**
  (*William Goldman* / Nels Elde / Wyndham Lathem / Kim Seed)
- **Basics of Bacterial Pathogens**
  (*Heran Darwin* / Miriam Braunstein / Andrew Darwin / Michael Federle / Nina Salama / Vincent Lee)
- **Close Encounters with the Host Cell**
  (*Mary O'Riordan* / Alison Criss / Barbara Kazmierczak / Raphael Valdivia)
- **Innate Immune Responses and Pathogenesis**
  (*Manuela Raffatellu* / Ken Cadwell / Jorge Henao-Mejia / Jyothi Rengarajan / Sunny Shin / David Underhill)
- **Keynote Session: Perspectives on the Future of Host-Pathogen Interaction Research**
  (*Karen Ottemann* / Eric Skaar)
- **Power Hour**
  (*Heran Darwin*)

GRS Microbial Toxins & Pathogenicity
Defining Pathogenesis and the Host-Microbe Dynamic
Jul 9-10, 2016
Chairs: Aaron T. Whiteley & Cara Mozola Forsberg

Mitochondria & Chloroplasts

Evolution, Biogenesis and Quality Control of Organelles of Endosymbiotic Origin
Jun 19-24, 2016
Mount Snow, West Dover, VT
Chair: Klaas J. Van Wijk
Vice Chair: Johannes M. Herrmann

- **Organelle Evolution and Diversification**
  (*John Archibald* / Ross Waller / Sven Gould / Geoffrey McFadden)
- **Organelle DNA and RNA**
  (*Maureen Hanson* / Ian Small / Dmitry Terniakov / Toshiharu Shikanai / Aleksandra Trifunovic)
- **Protein Synthesis in Organelles**
  (*Francis-Andre Wollman* / Alexey Amunts / Alice Barkan / Zofia Chrzanowska-Lighto / David Meinke)
- **Sorting of Organellar Proteins**
  (*Doron Rapoport* / Masato Nakai / Jonathan Weissman / Danja Schunemann / Carla Koehler / Toshiya Endo)
- **Assembly of Organellar Protein Complexes and Their Cofactors**
  (*Dennis Winge* / Peter Rehling / Sabeeha Merchant / Ulrich Brandt / Eva-Mari Aro)
- **Organellar Signaling**
  (*Eric Shoubridge* / Barry Pogson / Cole Haynes / James Whelan / Agnieszka Chacinska)
- **Large Scale Organelle Biology**
  (*Paul Jarvis* / Vamsi Mootha / Sacha Baginsky / Mike Ryan / A. Harvey Millar)
- **Organelle Proteostasis**
  (*Thomas Langer* / Chris Meisinger / Elzbieta Glaser / Bertrand Friguet / Kentaro Inoue)
- **Organelle Autophagy, Aging and Senescence**
  (*Roberta Gottlieb* / Luca Scorrano / Gad Galli / Richard Youle / Marisa Otegui)

GRS Mitochondria & Chloroplasts
Endosymbiotic Organelles: Biogenesis, Homeostasis and Integration
Jun 18-19, 2016
Chairs: Elden E. Rowland & Katja Hansen

Molecular & Cellular Neurobiology

Novel Approaches and New Advancement in Neural Development, Plasticity, and Diseases
Jun 12-17, 2016
The Hong Kong University of Science and Technology, Hong Kong, China
Chair: Yi E. Sun
Vice Chair: John J. Ngai

- **Neural Stem Cells and Neural Lineage Development**
  (*John Ngai* / Simon Hippenmeyer)
- **Wiring of the Nervous System: Axon Guidance and Dendritic Development**
  (*Wen-Cheng Xiong* / Rachel Wong / Xiang Yu / Yuh-Nung Jan)
- **Synapse Formation and Synaptic Plasticity**
  (*Rafael Fernandez-Chacon* / Pascal Kaeser / Lily Jan / Thomas Sudhof)
- **Circuits-Based Behavioral Study**
  (*Yuh-Nung Jan* / Jun Ding / Qiufu Ma / Yi Zuo / Nirao Shah)
- **Epigenetics and Behavioral Plasticity**
  (*Lin Mei* / Azad Bonni)

- **Disease Modeling from Yeast to Non-Human Primate**
  (*Louis Reichardt* / Aaron Gitler / Zilong Qiu)
- **Application of Stem Cells in Disease Modeling and Neural Repair**
  (*Yi Sun* / Gong Chen / Zhiping Pang)
- **New Advancements in Understanding Neurodegeneration and Repair**
  (*Aaron Gitler* / Keqiang Ye / Yimin Zou / Nancy Ip)
- **Connectome, Brain Imaging, and Single Cell Transcriptome Analyses**
  (*Nirao Shah* / Hongwei Dong)

Molecular & Cellular Neurobiology
Disruptive New Technologies in Studying Neural Development, Plasticity, and Diseases
Jun 11-12, 2016
Chairs: Hao Wu & Michael Hart

Molecular Basis of Microbial One-Carbon Metabolism

Exploring, Understanding and Applying the Diversity of One-Carbon Metabolism
Jul 31 - Aug 5, 2016
Waterville Valley, Waterville Valley, NH
Chair: Stephane Vuilleumier
Vice Chair: Victoria J. Orphan

- **Structure and Mechanisms in C1 Enzymes**
  (*Steve Ragsdale* / Rolf Thauer / John Peters / Catherine Drennan)
- **Microbial C1 Metabolism in the Environment**
  (*Harold Drake* / Michael Wagner / Marina Kalyuzhnaya / Xiuzhu Dong / Anne-Marie Delort)
- **The Human C1 Microbiome**
  (*Michael Rother* / Ruth Schmitz-Streit / Emily Balskus)
- **New C1 Pathways and Organisms**
  (*Mike Jetten* / Julia Vorholt / Ivan Berg / Thomas Hanson)
- **C1 Microbiology of Climate Change**
  (*Lisa Stein* / Antje Boetius / Paul Bodelier / Patricia Yager)
- **Applications of Microbial C1 Metabolism**
  (*Colin Murrell* / Mike Manefield / Michael Koepke / Markus Buchhaupt)
- **Specialized Microbial C1 Metabolism**
  (*Joseph Krzycki* / Huub Op Den Camp / Yin Chen / Gary King)
- **Engineering New C1 Metabolisms**
  (*F. Robert Tabita* / Cheryl Kerfeld / Tobias Erb)
- **Microbial C1 Metabolism in Associations**
  (*Yasuyoshi Sakai* / Ludmila Chistoserdova / Yahai Lu / Andreas Brune)
- **Power Hour**
  (*Lisa Stein*)

Molecular Basis of Microbial One-Carbon Metabolism
From Enzyme Mechanisms to Multispecies Interactions: Understanding Biological One-Carbon Conversions to Address Future Challenges
Jul 30-31, 2016
Chairs: Dipti D. Nayak & Kai Schuchmann

Molecular Interactions & Dynamics

Energy Transfer and Dynamics of Chemical Reactions Involving Isolated Molecules, Clusters, Interfaces, Solutions, Materials, and Biological Systems
Jul 10-15, 2016
Stonehill College, Easton, MA
Chairs: Gilbert M. Nathanson & Spiridoula Matsika
Vice Chair: Richard A. Loomis

- **Reactions in the Atmosphere: Energy and Climate**
  (*Scott Kable* / Marsha Lester / Benny Gerber / Nicholas Shuman)
- **Intermolecular Interactions and Dynamics**
  (*Timothy Zwier* / Xueming Yang / Joel Bowman / Sotiris Xantheas / Heather Lewandowski)
- **Dynamics of Biological Systems**
  (*Jan Verlet* / Christine Peter / Christopher Cheatum / Sharon Hammes-Schiffer)
- **Interactions and Dynamics in Materials**
  (*Valeria Kleiman* / Alan Aspuru-Guzik / Tamar Seideman / Scott Reid / Irene Burghardt)
- **Dynamics and Reactions in Solutions and in Clusters**
  (*Valeria Molinero* / Andrew Orr-Ewing / Stephen Bradforth / Hanna Reisler)
- **Interfacial Dynamics and Reactions**
  (*David Nesbitt* / Ilan Benjamin / Francesco Paesani / Julia Stahler / Alec Wodtke)
- **Unraveling the Dynamics of Catalytic Reactions**
  (*Bruce Kay* / Tanja Cuk / Etienne Garand / Thomas Miller)
- **Photochemistry and Nonadiabatic Dynamics**
  (*David Yarkony* / David Osborn / Laurie Butler / Albert Stolow / Laura Gagliardi)
- **Paradigms of Molecular Interactions and Dynamics**
  (*Anne McCoy* / Leticia Gonzalez / Stephen Leone / Richard Zare)
- **Power Hour**
  (*Hanna Reisler, Anne McCoy*)

Molecular Interactions & Dynamics
New Experimental and Theoretical Techniques for Understanding Energy Transfer and Dynamics of Chemical Reactions
Jul 9-10, 2016
Chairs: Olga Gorlova & Mark Shapero

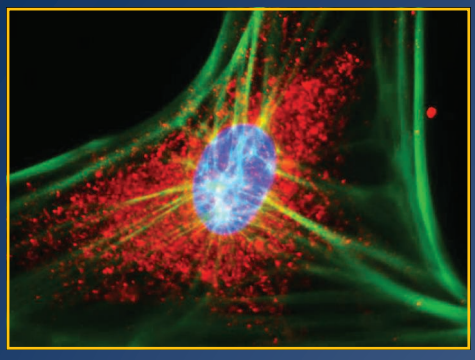

Peri-nuclear calmodulin immunofluorescent staining (red) in a mesenchymal stem cell plated on a stiff substrate. Co-staining of actin cytoskeleton (green) and nucleus (blue). Submitted by Robert L. Mauck, Chair, Musculoskeletal Biology & Bioengineering GRC.

Molecular Structure Elucidation

NEW!

Technologies in Defining Molecular Structure and Function
Aug 14-19, 2016
Mount Snow, West Dover, VT
Chairs: Nelu Grinberg & Nina C. Gonnella
Vice Chairs: Yong Liu & Zheng Ouyang

- **Keynote Session: Biomolecular Processes**
  (*Gary Martin* / Thomas Steitz)
- **Protein Structure**
  (*Shyam Vyas* / Irina Gutsche / Timothy Keiderling / Prasad Polavarapu)
- **Protein Dynamics**
  (*Sonia Rodriguez* / Peter Wright / Mei Hong / Dorothee Kern)
- **Computational Chemistry in Structural Elucidation**
  (*Roy Helmy* / Lyndon Emsley / Gaetano Montelione / Kendall Houk)
- **Advances in Crystallography**
  (*Gaetano Montelione* / Makoto Fujita / Ian Wilson)
- **Mass Spectrometry in Biological/Biomarker Characterization**
  (*Sue Pan* / Graham Cooks / Julia Laskin / John Engen)
- **Separation Sciences**
  (*Wes Schafer* / Bezhan Chankvetadze / Attila Felinger / Eli Grushka)
- **Pharmaceutical Applications**
  (*Dorothee Kern* / Michael Kress / Gary Martin / Mark Strohmeier)
- **Microscale Structural Analysis**
  (*Roger Kautz* / Marcel Jaspars / Aaron Lewis)

Multiferroic & Magnetoelectric Materials

Multiferroics: From Fundamentals to Novel Functionalities and Applications
Aug 7-12, 2016
Bates College, Lewiston, ME
Chair: Bernd Lorenz
Vice Chair: Thomas Palstra

- **Theory and Models**
  (*Silvia Picozzi* / Nicola Spaldin / Daniel Khomskii / Philippe Ghosez)
- **New Multiferroic and Magnetoelectric Materials**
  (*Kee-Hoon Kim* / Yoshinori Tokura / Craig Fennie / Konstantin Zvezdin / Martha Greenblatt)
- **Thin Films and Heterostructures**
  (*John Prater* / Ramamoorthy Ramesh / Sebastiaan Van Dijken / Yayoi Takamura)
- **Multiferroic Domains, Domain Walls, and Interfaces**
  (*Weida Wu* / Manfred Fiebig / Sang-Wook Cheong / Ingrid Mertig / Manuel Bibes)
- **Novel Control of Multiferroics by Pressure and Strain**
  (*Vivien Zapf* / Tsuyoshi Kimura / Taka-Hisa Arima / Feng Ye)
- **Magnetoelectricity and Topological Orders**
  (*Masahita Mochizuki* / Maxim Mostovoy / Avadh Saxena / Shinichiro Seki / Alois Loidl)
- **Near Room Temperature Multiferroics and Novel Interactions**
  (*Tanusri Saha-Dasgupta* / Je-Geun Park / Marisa Medarde / Paul C. Chu)
- **Spectroscopy and Scattering, Symmetry**
  (*Randy Fishman* / Janice Musfeldt / Jens Kreisel / Laurent Chapon / Jeffrey Lynn)
- **Devices and Applications**
  (*Peter Finkel* / Ram Katiyar / Nian Sun)
- **Power Hour**
  (*Janice Musfeldt*)

Multiphoton Processes

Attoseconds, Ultrafast Strong Field Processes, and Intense Fields
Jun 19-24, 2016
Proctor Academy, Andover, NH
Chair: Johan Mauritsson
Vice Chair: Itzik Ben-Itzhak

- **Keynote Session: Multiphoton Science**
  (*Johan Mauritsson* / Anne L'Huillier)
- **Molecular Dynamics in Strong Fields**
  (*Caterina Vozzi* / Hans Jakob Worner / Albert Stolow / Daniel Strasser)
- **Superintense Laser Fields**
  (*Itzik Ben-Itzhak* / Barry Walker / Julia Mikhailova)
- **High-Harmonic Spectroscopy**
  (*Mette Gaarde* / Olga Smirnova / Richard Taieb / Nirit Dudovich)
- **Controlling Light and Matter**
  (*Marcos Dantus* / Timm Bredtmann / Christian Ott)
- **Ultrafast Imaging**
  (*Marc Vrakking* / Louis Dimauro / Margaret Murnane / Fernando Martin Garcia)
- **New Laser Sources**
  (*Dimitrios Charalambidis* / Jens Biegert / Katsumi Midorikawa)
- **Attosecond Dynamics**
  (*Stefan Haessler* / Anthony Starace / Reinhard Kienberger / Brett Esry)
- **Multiphoton FEL Science**
  (*Philip Bucksbaum* / Robert Moshammer / Giuseppe Sansone / Rebecca Boll)

Multiscale Plant Vascular Biology

NEW!

Identifying Interdisciplinary Opportunities for a New Era of Plant Vascular Biology
Jun 26 - Jul 1, 2016
Sunday River, Newry, ME
Chairs: William T. Pockman & Juliana S. Medeiros
Vice Chair: Barbara Lachenbruch

- **Keynote Session: Multiscale Plant Vascular Biology** (*N. Michele Holbrook* / William Adams)
- **Modeling Physical Processes in Vascular Systems** (*John Sperry* / Uwe Hacke / Steven Jansen / Xavier Noblin)
- **Genetic and Environmental Controls on Vascular Development and Function** (*Rachel Spicer* / Kaisa Nieminen)
- **Phloem Ecophysiology** (*Sanna Sevanto* / Brendan Choat / Susanne Hoffmann-Benning / Michael Clearwater)
- **Modeling and Quantification of Vascular Networks** (*Jonathan Wilson* / Andrew McElrone)
- **Vascular Biology in Ecological Patterns and Processes** (*Tim Brodribb* / Richard Dick / Jordi Martinez-Vilalta / Lawren Sack)
- **Trait-Based Approaches in Comparative Vascular Biology** (*Jeannine Cavender-Bares* / Jens Kattge / Benjamin Blonder)
- **Plant Vascular Processes in Ecosystem and Earth System Models** (*Brent Helliker* / Gaby Katul / Ying Fan Reinfelder / Alexandra Konings)
- **Evolution of Plant Vascular Systems** (*Jarmila Pittermann* / Franco Biondi / Nick Rowe)

Muscle & Molecular Motors

Motor Mechanisms from Single Molecules to Cellular Function
Jul 17-22, 2016
Mount Snow, West Dover, VT
Chair: Kathleen M. Trybus
Vice Chair: Samara L. Reck-Peterson

- **Keynote Session: From Motor Structure to Cellular Function** (*Samara Reck-Peterson* / Andrew Carter / Anna Akhmanova)
- **Seeing Is Believing: Structure Informs Mechanism** (*Trina Schroer* / Andres Leschziner / Anne Houdusse / Donald Winkelmann / Trina Schroer)
- **How Cytoskeletal Elements Generate Force and Motion** (*William Hancock* / Lee Sweeney / Michael Ostap / William Hancock)
- **Dynamics of Actin and Microtubules** (*Enrique De La Cruz* / David Kovar / Sabine Petry / Luke Rice / Enrique De La Cruz)
- **Motors Functioning in Organized Assemblies** (*Daniela Nicastro* / Tarun Kapoor / Ryoma Ohi / Dilson Rassier / Daniela Nicastro)
- **Building Complexity to Understand Cytoskeletal Function** (*Simon Bullock* / Mohan Balasubramanian / Nikta Fakhri / Simon Bullock)
- **Tuning and Regulating Motor-Track Interactions** (*Kristen Verhey* / Jonathan Howard / Antonina Roll-Mecak / Kristen Verhey)
- **Motors Functioning in the Cellular Environment** (*Matthew Tyska* / Lukas Kapitein / Magdalena Bezanilla / Guangshuo Ou / Matthew Tyska)
- **Malfunctioning Motors and Disease** (*Leslie Leinwand* / James Stull / Jonathan Bird / Leslie Leinwand)

Musculoskeletal Biology & Bioengineering

Stepping Across Disciplines to Spur Innovation in Musculoskeletal Biology and Bioengineering
Aug 7-12, 2016
Proctor Academy, Andover, NH
Chair: Robert L. Mauck
Vice Chair: Peter Johnson

- **Keynote Session: Cross-Disciplinary Innovations in Musculoskeletal Biology and Bioengineering** (*Robert Mauck, Peter Johnson* / Helen Blau / Farshid Guilak)
- **Growth and Development** (*Ronen Schweitzer* / Jenna Galloway / Gabrielle Kardon / Yingzi Yang / Elazar Zelzer)
- **Multi-Scale Tissue Structure and Function** (*Dawn Elliott* / Alan Grodzinsky / Karl Kadler / Silvia Salinas Blemker)
- **Endogenous Stem Cells and Their Microenvironment** (*Johnny Huard* / Benjamin Alman / Christopher Evans / Bruno Peault)
- **Molecular Tools to Manipulate the Cellular Program** (*Matthew Warman* / April Craft / Charles Gersbach)
- **Materials to Construct the Microenvironment** (*Jason Burdick* / Stephanie Bryant / Andres Garcia / David Kaplan / Daniel Kelly)
- **Multi-Scale Mechanobiology in Health and Disease** (*Tamara Alliston* / Boris Hinz / Jan Lammerding / Viola Vogel)
- **Models Systems to Study MSK Injury, Repair, and Regeneration** (*Chunfeng Zhao* / Hani Awad / Thomas Clemens / Kurt Hankenson / Fergal O'Brien)
- **Confounders of Regeneration: Aging, Inflammation, Fibrosis, and Other Factors** (*Nadeen Chahine* / James Iatridis / Beth Winkelstein / Martin Lotz)

GRS Musculoskeletal Biology & Bioengineering
Moving Forward in Musculoskeletal Biology and Bioengineering: New Approaches from Diverse Disciplines
Aug 6-7, 2016
Chairs: Megan L. Killian & Anne M. Gingery

Conferees enjoying an afternoon of kayaking at the Norton Reservoir near Stonehill College.

Mutagenesis

Mechanisms of Mutagenesis and Genome Alterations
Jun 5-10, 2016
PGA Catalunya Business and Convention Centre, Girona, Spain
Chair: Simon Boulton
Vice Chair: Karlene Cimprich

- **Keynote Session: Focus on Cancer and Aging** (*Simon Boulton* / Ketan Patel / Ian Hickson)
- **Genome Instability Driven by Transcription/ Replication Collisions** (*Sue Jinks-Robertson* / Andres Aguilera / Jesper Svejstrup / Andre Nussemzweig / Philippe Pasero)
- **Replication Stress, Aging and Cancer** (*Thomas Kunkel* / Eric Brown / Oskar Fernandez-Capetillo / Mark O'Connor)
- **DNA Repair and Mutagenesis** (*Robert Lahue* / Josef Jiricny / Samuel Wilson / Susan Rosenberg / Reuben Harris)
- **Error-Prone DNA Replication and Repair** (*Roger Woodgate* / Anna Malkova / Richard Wood / Orlando Scharer)
- **Aging and Cancer-Associated DNA Repair Processes** (*Wei Yang* / Sylvie Doublie / Scott Williams / Keith Caldecott)
- **Complex Genome Alterations** (*Ian Hickson* / Martin Hetzer / Jacqueline Jacobs / Agnel Sfeir)
- **DNA Secondary Structures and Repair** (*Nancy Maizels* / Julian Sale / Catherine Freudenreich / Christopher Pearson / Daniel Jarosz)
- **Mutational Signatures in Aging and Cancer** (*Karlene Cimprich* / Ben Lehner / Steve Jackson / Charles Swanton)

GRS Mutagenesis
Mechanisms of Mutagenesis and Genome Alterations
Jun 4-5, 2016
Chair: Aishwarya Prakash

Myelin

Myelin – Rethinking Functions, Revealing Mechanisms, Developing Medicines
May 15-20, 2016
Renaissance Tuscany Il Ciocco, Lucca (Barga), Italy
Chairs: Charles ffrench-Constant & Robin Franklin
Vice Chairs: Patrizia Casaccia & David H. Rowitch

- **Keynote Session: Making and Imaging Myelin** (*Akiko Nishiyama, Ueli Suter* / Thomas Misgeld / Carla Taveggia / Tara De Silva / Bruce Appel / Ashwin Woodhoo)
- **Myelin Mechanics - Physical Forces and Oligodendrocyte Biology** (*Babette Fuss, James Salzer* / Kevin Chalut / Jonah Chan / Anna Jagielska)
- **Maintaining Myelin - Building the Internode and Sustaining the Axon** (*Peter Brophy, Kaylene Young* / Ben Emery / Sharyl Fyffe-Maricich / Ori Peles)
- **Myelin and the Axon** (*David Attwell, Julia Edgar* / Eva-Maria Kramer-Albers / Michael Sereda / Kenneth Smith)
- **Myelin and the Mind - Adaptive Myelination and Neural Plasticity** (*Ragnhildur Karadottir, William Richardson* / Douglas Fields / Benedikt Grothe / Erin Gibson)
- **Myelin Pathology** (*Marianna Bugiani, Klaus-Armin Nave* / Tanja Kuhlmann / Viviane Tabar / Marius Wernig)
- **Mending Myelin** (*Vittorio Gallo, Paul Tesar* / Mark Kotter / Patrick Kuery / Alison Lloyd / Veronique Miron)
- **Monitoring Myelin** (*Dwight Bergles, Leda Dimou* / Jaime Grutzendler / Heidi Johansen-Berg / Daniel Reich / Bruno Stankoff)
- **Myelin Medicines** (*Catherine Lubetzki, Wee Yong* / Ari Green / Luke Lairson / Aurora Pujol)
- **Power Hour** (*Kelly Monk, Jacqueline Trotter*)

GRS Myelin
Unravelling Myelin: New Insights into Generation and Regeneration
May 14-15, 2016
Chairs: Abbe H. Crawford & Ethan G. Hughes

Gordon Conferences are different from other scientific conferences because they facilitate the detailed discussion of potentially groundbreaking science and technology.

- Gordon Tatlock, Chair, 2015 High Temperature Corrosion GRC

Nasopharyngeal Carcinoma

NEW!

Global Lessons on Cancer Pathogenesis from Insights into a Geographically Restricted Tumor of the Nasopharynx
Jun 26 - Jul 1, 2016
The Hong Kong University of Science and Technology, Hong Kong, China
Chairs: Maria Lung & Lawrence Young
Vice Chairs: George S. Tsao & Jaap Middeldorp

- **Cancer: Viruses and Signaling**
  (*Joseph Pagano* / Harald Zur Hausen / Hans Clevers)
- **Cancer Genomics**
  (*Yu Sun Chang* / Andrew Futreal / Yi Xin Zeng / Kwok Wai Lo)
- **Lessons from an Epithelial Cancer**
  (*Nancy Raab-Traub* / Elaine Fuchs / Mu Sheng Zeng)
- **EBV Genetics and Biology**
  (*Lori Frappier* / Henri-Jacques Delecluse / Richard Longnecker / George Tsao)
- **Risk Factors and Cancer**
  (*Eric Stanbridge* / Frederick Alt / Allan Hildesheim)
- **NPC Diagnostic Biomarkers**
  (*Pierre Busson* / Dennis Lo / Jaap Middeldorp / Honglin Chen / Wei Dai)
- **Challenges for Primary Treatment of NPC**
  (*Anne Lee* / Brian O'Sullivan / Roger Ngan / Jun Ma)
- **Innovative Therapies for NPC**
  (*Rajiv Khanna* / Cliona Rooney / Brigette Ma / William Wei)
- **Future Prospects for NPC**
  (*Fei-Fei Liu* / Alan Rickinson / Qyuhn Le)
- **Power Hour**
  (*Fei-Fei Liu, Anne Lee*)

Natural Products & Bioactive Compounds

Exploring the Therapeutic Potential of Natural Products and Biologically Active Compounds Through Chemical and Biological Technologies
Jul 31 - Aug 5, 2016
Proctor Academy, Andover, NH
Chair: Richard E. Taylor
Vice Chair: Steven J. Wittenberger

- **Synthesis Enabled Biological Studies**
  (*Joanne Harvey* / Emmanuel Theodorakis / Corinna Schindler / Armen Zakarian)
- **Technology Driven Chemical Synthesis**
  (*Mark Goldsmith* / Timothy Jamison / Alexander Godfrey / Peter Seeberger / Ian Davies)
- **Antibiotic Discovery**
  (*Marcy Balunas* / Christian Melander / Elizabeth Nolan / Daniel Marquess)
- **Drug Discovery Efforts from Academia**
  (*Leslie Aldrich* / Stephen Frye / Denise Barrault / Hendrik Luesch / John MacMillan)
- **Chemistry of the Human Microbiome**
  (*Sean Davies* / Emily Balskus / Michael Fischbach / Pieter Dorrestein)
- **Strategies and Tactics for Chemical Synthesis**
  (*Joshua Pierce* / Paul Floreancig / Patrick Harran / Rendy Kartika / Toshiaki Sunazuka)
- **Biosynthesis-Inspired Technologies**
  (*Wendy Kelly* / Michelle Chang / Michael Burkart / Adrian Keatinge-Clay)
- **Drug Discovery Platforms for Cancer and Rare Diseases**
  (*Michelle Garnsey* / Andres Francesch / Roger Linington / Qiu Wang / Mark O'Neil-Johnson)
- **Keynote Session: State-of-the-Art Chemistry and Biology**
  (*Jon Rainier* / Gabriela Chiosis / Thomas Hoye / Stephen Moss)
- **Power Hour**
  (*Michelle Garnsey*)

Neural Development

Nervous System Assembly, Plasticity, and Disease
Jul 31 - Aug 5, 2016
Salve Regina University, Newport, RI
Chair: Marc R. Freeman
Vice Chair: Rosalind A. Segal

- **Patterning the Nervous System**
  (*Claude Desplan* / Jeremy Dasen / Nancy Ip / Jeremy Reiter / Paola Bovolenta / Gordon Fishell)
- **Generating Diversity in Neural Cell Fate and Function**
  (*Liqun Luo* / Claude Desplan / Corey Harwell / Fiona Doetsch / Chris Doe)
- **Stem Cells in Circuit Assembly and Repair**
  (*Fiona Doetsch* / Yukiko Gotoh / Soo-Kyung Lee / Pierre Vanderhaeghen)
- **Wiring Neural Circuits**
  (*Kelly Monk* / Samuel Pfaff / Cagla Eroglu / David Ginty / Alex Kolodkin)
- **Neuron-Glia Interactions During Development**
  (*Cagla Eroglu* / Kelly Monk / William Talbot / Shai Shaham / Michelle Monje / Jan Pielage)
- **Establishing and Maintaining Functional Circuits**
  (*Dorothy Schafer* / Larry Zipursky / Luisa Cochella / Dwight Bergles / Nils Brose)
- **Neurite Polarity, Outgrowth, and Survival**
  (*Corey Harwell* / Frank Bradke / Marc Tessier-Lavigne / Freda Miller / Claudia Bagni / Daniel Colon-Ramos)
- **Neurodevelopmental Disorders and Pruning**
  (*Alex Kolodkin* / Oren Schuldiner / Angelique Bordey / Dorothy Schafer / Marc Hammarlund)
- **Keynote Session: Molecular Control of Connectivity**
  (*Marc Freeman, Rosalind Segal* / Liqun Luo / Ben Barres)
- **Power Hour**
  (*Rosalind Segal*)

GRS Neural Development
The Molecular Basis of Nervous System Assembly, Plasticity, and Disease
Jul 30-31, 2016
Chairs: Elena V. Abarinov & Jan H. Lui

Neurobiology of Brain Disorders

Changes in Normal Functions of the Nervous System Leading to Neurodegeneration
Aug 7-12, 2016
PGA Catalunya Business and Convention Centre, Girona, Spain
Chairs: Luciano D'Adamio & Bart De Strooper
Vice Chairs: David M. Holtzman & Cheryl Wellington

- **Keynote Session: ApoE Function in Neurons / Targeting ApoE4 for the Prevention of Alzheimer's Disease**
  (*Luciano D'Adamio* / John O'Keefe / Thomas Sudhof)
- **Genetic and Epigenetic Factors in Neurodegeneration**
  (*Bart Destrooper* / Alison Goate / John Hardy / Li-Huei Tsai / Stephen Cohen)
- **Seeding and Spreading of Proteopathic Seeds**
  (*John Trojanowski* / Virginia Lee / Lary Walker / Karen Ashe)
- **Synaptic Plasticity in Health and Disease**
  (*Pablo Castillo* / Ottavio Arancio / Jie Shen / Inna Slutsky)
- **Inflammation, Immunity and Neurodegeneration**
  (*David Holtzman* / Christian Haass / Morgan Sheng / Hui Zheng)
- **Mitochondrial and Metabolic Dysfunction**
  (*Jie Shen* / Giovanni Manfredi / Vanessa Morais / Amantha Thathiah)
- **Selected Poster Presentations**
  (*Karen Ashe* / Joachim Herz)
- **Biomarkers and Therapeutics**
  (*Li-Huei Tsai* / Leonard Petrucelli / Don Cleveland / Karen Duff / Lennart Mucke)
- **Protein Homeostasis**
  (*Cheryl Wellington* / Ana Maria Cuervo / Patrik Verstreken / Michael Lee / Li Gan)

GRS Neurobiology of Brain Disorders
Neurodegenerative Disease: New Directions in Synaptic Dysfunction and Cell Biology
Aug 6-7, 2016
Chairs: Courtney E. Lane-Donovan & Lorena Saelices Gomez

Neurobiology of Cognition

Neural Circuits for Perception, Memory, Thought and Consciousness
Jul 24-29, 2016
Sunday River, Newry, ME
Chair: Tatiana Pasternak
Vice Chair: David Leopold

- **Keynote Session: Brain Mechanisms of Cognition: Clinical Perspective**
  (*Robert Desimone* / Antonio Damasio)
- **Cognitive Influences in Early Vision**
  (*Tony Movshon* / W. Martin Usrey / Anna Roe / Bruce Cumming / Alexander Maier / Adam Kohn / Pieter Roelfsema)
- **Multisensory Integration**
  (*Dora Angelaki* / Greg DeAngelis / Laden Shams / Uta Noppeny / David Burr)
- **Neurobiology of Social Interaction**
  (*Michael Platt* / Larry Young / Katalin Gothard / Asif Ghazanfar / Jean-Rene Duhamel / Uri Hasson / Amanda Woodward)
- **Categories and Origins of Concepts**
  (*Nancy Kanwisher* / Jessica Cantlon / Marge Livingstone / Brad Mahon / Marlene Behrmann)
- **Working Memory: Storage and Access**
  (*Albert Compte* / Rob Hampton / Tim Buschman / Kia Nobre / Brad Postle / John Serences / Robert Knight)
- **Functional Specialization in Prefrontal Cortex**
  (*Earl Miller* / Carlos Brody / Matthew Chafee / Elisabeth Murray / Matthew Rushworth)
- **Representation of Space and Time**
  (*James Knierim* / Charan Ranganath / Liora Las / Howard Eichenbaum / Ila Fiete / Jennifer Groh / Elizabeth Buffalo)
- **Decoding Consciousness**
  (*Christof Koch* / Melanie Boly / Emery Brown / Adrian Owen / Giulio Tononi)

GRS Neurobiology of Cognition
Neural Circuits for Perception, Memory, Thought and Consciousness
Jul 23-24, 2016
Chairs: Brian Russ & Sarah R. Heilbronner

Noble Metal Nanoparticles

From Crystal Form to Active Functions in Physics, Chemistry and Biology
Jun 19-24, 2016
Mount Holyoke College, South Hadley, MA
Chair: Catherine J. Murphy
Vice Chair: Stephan Link

- **Keynote Session: Mesoscale Assembly and Hierarchical Properties**
  (*So-Jung Park* / Nicholas Kotov / Christopher Murray)
- **Crystal Structure, Growth, and Clusters**
  (*Cecilia Noguez* / Emilie Ringe / Yu Huang / Thomas Buergi / Flavio Maran)
- **Spectroscopy, Sensing, and Imaging**
  (*Renee Frontiera* / Katherine Willets / Julie Biteen / Kenneth Knappenberger)
- **Active Plasmonics**
  (*Jeremy Baumberg* / Laura Na Liu / David Masiello / Renaud Bachelot / George Thomas)

- **Electrochemistry and Catalysis**
  (*Donna Chen* / Shi-Gang Sun / Bo Zhang / Manos Mavrikakis)
- **Multimetallics**
  (*Sara Skrabalak* / Raymond Schaak / Elena Shevchenko / Chia-Kuang Tsung)
- **Biomedical Applications and Implications**
  (*Niveen Khachab* / Srikanth Sigamaneni / Chad Mirkin / Warren Chan)
- **Electronic Applications**
  (*Jennifer Dionne* / Harry Atwater / Cherie Kagan / Benjamin Wiley)
- **Late-Breaking Topics / Plasmonic Mapping in Nanostructures**
  (*Stephan Link* / Paul Mulvaney)
- **Power Hour**
  (*Julie Biteen, Emilie Ringe*)

Noble Metal Nanoparticles
From Crystal Form to Active Functions in Physics, Chemistry and Biology
Jun 18-19, 2016
Chairs: Lisa V. Brown & Amanda M. Goodman

Notch Signaling in Development, Regeneration & Disease

Notch Signaling: Phenotypes to Molecular Mechanisms
Jul 31 - Aug 5, 2016
Bates College, Lewiston, ME
Chairs: Stephen Blacklow & Warren Pear
Vice Chairs: Sarah J. Bray & Christian Siebel

- **Keynote Session: From Function to Structure**
  (*Stephen Blacklow, Warren Pear* / Juergen Knoblich / K. Christopher Garcia)
- **Mechanistic Aspects of Notch Signaling**
  (*Christian Siebel* / Sarah Bray / Francois Schweisguth / Penny Handford / Carl Blobel / Robert Haltiwanger / Michael Elowitz)
- **Notch and Stem Cells**
  (*Ivan Maillard* / Thomas Rando / Linda Samuelson / Judith Kimble)
- **Notch and Development**
  (*Ryoichiro Kageyama* / Ellen Rotherberg / Kim Dale / Achim Gossler / Oliver Pourquie / Jayaraj Rajagopal / Ralf Adams)
- **Notch and Cell Fate Choice**
  (*Irwin Bernstein* / Luisa Iruela-Arispe / Anna Bigas / David Traver)
- **Notch, Transcription, and Epigenetics**
  (*Sarah Bray* / Jon Aster / Tilman Borgreffe / Rhett Kovall / Adolfo Ferrando / Raphael Kopan)
- **Late-Breaking Topics**
  (*Jon Aster*)
- **Notch, Cancer, and Therapeutics**
  (*Lucio Miele* / Philip Jones / Freddy Radtke / Barbara Bedogni / Tian-Li Wang / Gavin Thurston / Timothy Hoey)
- **Modulators of Signaling**
  (*Pamela Stanley* / Susan Cole / Christy Fryer / Iannis Aifantis)

Notch Signaling in Development, Regeneration & Disease
Notch Signaling During Development, Adult Stage Tissue Maintenance, and Disease
Jul 30-31, 2016
Chairs: Mustafa Turkoz & Rolake Alabi

NOX Family NADPH Oxidases

NOX Molecular Insights Leading to Translation
Jun 5-10, 2016
Waterville Valley, Waterville Valley, NH
Chair: Francisco R.M. Laurindo
Vice Chair: Ulla Knaus

- **Keynote Session: Thinking Outside of the BOX in NOX Signaling and Homeostasis**
  (*Robert Clark* / Michael Marletta / Ursula Jakob)
- **NOX Activation: From Protein Structure to Subunit Assembly**
  (*Edgar Pick* / Paul Karplus / Laura Baciou / Nicolas Demaurex / Anny Slama-Schwok)
- **NOXes and Microbial Sensing**
  (*Albert Van Der Vliet* / Andrew Neish / Venizelos Papayannopoulos)
- **Metabolic and Inflammatory Mechanisms in NOX-Related Pathophysiology**
  (*Marie Jose Stasia* / Ajay Shah / Michelle Block / Simone Di Giovanni / Jaehyung (Gus) Cho)
- **Mechanobiology and NOXes**
  (*Kathy Griendling* / Hanjoong Jo / Eleni Tzima)
- **Novel Modes of NOX Regulation**
  (*Miklos Geiszt* / Wenjun Ouyang / Poul Sorensen / Sharon Campbell / Roberto Sitia)
- **NOX Genetics and Epigenetics**
  (*Mary Dinauer* / Victor Thannickal / Francis Miller / Beth Kozel)
- **NOXes in the Pathogenesis and Progression of Cancer**
  (*Corinne Dupuy* / Isabel Fabregat / Katrin Schroder / Thomas Leto)
- **NOX Inhibitors: Perspectives and Critical Analysis**
  (*David Lambeth* / Balaraman Kalyanaraman / Philippe Wiesel / Per Wikstrom)

NOX Family NADPH Oxidases
NOX Biology: From Mechanistic Insights Toward Functional Understanding
Jun 4-5, 2016
Chairs: Adam A. Nabeebaccus & Leonardo Y. Tanaka

Ocean Biogeochemistry

NEW!

The Biologically-Driven Ocean Carbon Pumps
Jun 12-17, 2016
The Chinese University of Hong Kong, Hong Kong, China
Chairs: Nianzhi Jiao & Eileen E. Hofmann
Vice Chairs: Louis Legendre & Sylvia Sander

- **The Ocean Carbon Pumps: From Ancient to Future Oceans**
  (*Susana Agusti* / Andy Ridgwell / Fortunat Joos)
- **The Biological Carbon Pump**
  (*Chuanlun Zhang* / Sarah Giering / Stephanie Henson / Susanne Neuer)
- **The Carbonate Pump**
  (*Dieter Wolf-Gladrow* / Marion Gehlen / Richard Zeebe)
- **The Microbial Carbon Pump and the Roles of Microbes**
  (*Farooq Azam* / Ronald Benner / Gerhard Herndl / Richard Rivkin)
- **Iron and Other Trace Metals: Roles in Carbon Pumps**
  (*Philip Boyd* / Chris German / Cecile Guieu)
- **Silicon, Nitrogen and Phosphorus: Roles in Carbon Pumps**
  (*Christiane Lancelot* / Richard Dugdale / Paul Treguer / Tron Frede Thingstad)
- **Methane and Sulfur: Roles in Carbon Pumps**
  (*Chao Li* / Fengping Wang / Maurice Levasseur)
- **Interactions Among the Three Ocean Carbon Pumps**
  (*Xiqiu Han* / Eun Young Kwon / Uta Passow / Carol Robinson)
- **The Ocean Carbon Pumps and Society**
  (*Rachel Gjelsvik Tiller* / Areti Kontogianni / Qingchen Chao)

Ocean Global Change Biology

Classifying Biotic Responses to a Rapidly Changing Ocean: From Genes to Ecosystems
Jul 17-22, 2016
Waterville Valley, Waterville Valley, NH
Chair: Philip Boyd
Vice Chair: Gretchen E. Hofmann

- **Advances in Ocean Global Change Biology Research**
  (*David Hutchins* / Andrew Barton / Thorsten Reusch / Jean-Pierre Gattuso)
- **Multi-Stressors in the Coastal Ocean**
  (*Gretchen Hofmann* / Frank Melzner / Francis Chan / Madeleine van Oppen)
- **Lessons in Studying Multi-Stressors from Other Disciplines: Ecotoxicology, Paleoceanography and Freshwater Research**
  (*Denise Breitburg* / David Costantini / Craig Williamson / David Secor)
- **The Quest for Unifying Concepts in Ocean Global Change Studies: Energetics, Biophysics and Trait-Based Research**
  (*Brian Helmuth* / Inna Sokolova / Mark Denny / Becca Kordas)
- **Adaptation, Microevolution, and Evolutionary Rescue**
  (*Sinead Collins* / Andrew Hendry / Josianne Lachapelle / Gabriel Yvon-Durocher)
- **Multi-Stressors Across Foodwebs: Effects of Differential Vulnerability and the Role of Species Interactions**
  (*Cathy Pfister* / Sophie McCoy / Sean Connell)
- **The Importance of Experimental Design in Ocean Global Change Studies**
  (*Jean-Pierre Gattuso* / Christopher Cornwall / Ulf Riebesell / Jonathan Havenhand)
- **Modeling of Multiple Stressors – From Physiology to Biogeochemistry**
  (*Scott Doney* / Kevin Flynn / Kenneth Denman / Charles Stock)
- **Communicating Multi-Stressor Issues to Policymakers and Managers**
  (*Philip Williamson* / Lucia Fanning / Skyli McAfee / Libby Jewett)

Ocean Global Change Biology
Understanding the Biological Consequences of Global Ocean Change: Insights from Environmental History
Jul 16-17, 2016
Chairs: Emily B. Rivest & Christopher E. Cornwall

Optogenetic Approaches to Understanding Neural Circuits & Behavior

NEW!

Integrating Optical Control with Diverse Experimental Measures and Readouts
Jul 17-22, 2016
Sunday River, Newry, ME
Chair: Karl Deisseroth
Vice Chair: Kay M. Tye

- **Understanding Behaviors Relevant to Psychiatric Disease**
  (*Robert Malenka* / Vikaas Sohal / Melissa Warden)
- **Large-Scale Dynamics of Neural Activity *In Vivo***
  (*Mark Schnitzer* / Edward Boyden / Ilana Witten / Rafael Yuste)
- **Manipulation of Circuits to Promote Reward and Aversion**
  (*Patricia Janak* / Gero Meisenbock / Naoshige Uchida)
- **Experience-Dependent Synaptic Plasticity and Neuromodulation**
  (*George Augustine* / Michael Bruchas / Thomas Kash / Christian Luscher)
- **Memory Engram Manipulation**
  (*Susumu Tonegawa* / Sheena Josselyn / Alcino Silva)
- **Understanding the Neural Circuitry of Sleep and Arousal**
  (*Viviana Gradinaru* / Yang Dan / Luis De Lecea)

- **Sensorimotor Systems and Neurodegenerative Disease**
  (*Christopher Moore* / Anatol Kreitzer / Bernardo Sabatini / Karel Svoboda)
- **Circuits Involved in Feeding and Consummatory Behavior**
  (*Lex Kravitz* / Scott Sternson / Garret Stuber)
- **Circuits Mediating Social Behavior**
  (*Feng Zhang* / David Anderson / Ofer Yizhar)

Organic Geochemistry

Advancing Technology in Organic Geochemistry to Address Society's Challenges
Jul 24-29, 2016
Holderness School, Holderness, NH
Chair: Ann Pearson
Vice Chair: Lloyd R. Snowdon

- **Past Climates, Analogues for Future Change**
  (*Sarah Feakins* / Philip Meyers / Isla Castaneda / Daniel Stoddart)
- **Old Stuff Doing Good: Soils and Recalcitrant Organic Matter**
  (*Nagissa Mahmoudi* / Thomas Bianchi / Janet Rethemeyer / Myrna Simpson / Caroline Masiello)
- **High Tech Analytical Tools Come of Age**
  (*Clifford Walters* / Marcel Kuypers / Bruno Schuler / Richard Camilli)
- **The Hot and Cold of Organic-Inorganic Interactions**
  (*Svenja Erdmann* / Paul Greenwood / Renzo Silva / Jill McDermott / Hilairy Hartnett)
- **Advances in Modeling**
  (*Lloyd Snowdon* / Chris Cornford / Maowen Li / Jessica Tierney)
- **Microbial Interactions and Processes**
  (*Roger Summons* / Sabine Lengger / Yuki Weber / Roland Hatzenpichler / Shuhei Ono)
- **The Future of Unconventionals**
  (*Kenneth Peters* / Eric Michael / Dariusz Strapoc)
- **The Anthropocene**
  (*Christopher Reddy* / Blandine Courel / Tom Ryerson / Elsie Sunderland / Mark Yunker)
- **Late-Breaking Topics**
  (*Ryan Pereira*)

Organic Geochemistry
Advancing Technology in Organic Geochemistry to Address Society's Challenges
Jul 23-24, 2016
Chair: Ryan A. Pereira

Organic Reactions & Processes

Emerging Concepts and Technologies for Organic Processes
Jul 17-22, 2016
Stonehill College, Easton, MA
Chairs: Neal G. Anderson & Vy Dong
Vice Chairs: Silas Cook & Travis P. Remarchuk

- **From Flask to Reactor: Strategies and Tactics for Scale-Up**
  (*Neal Anderson* / Michael Bech Sommer / Ryan Shenvi / David Waller)
- **Strategies for Preparing Complex Molecules**
  (*Scott Sieburth* / Andre Beauchemin / Kevin Brown / Kami Hull / Johan Wennerberg)
- **Precious or Non-Precious Metals: Organometallic Reagents Using or Avoiding Transition Metals, Precious Metals, and Rare Earth Elements**
  (*Vladimir Gevorgyan* / Olafs Daugulis / David MacMillan / Donald Watson)
- **Enlightening Tools: Photoredox Catalysis and Other "One-Electron" Chemistry**
  (*Pamela Tadross* / Robert Knowles / Melanie Sanford / Jenny Yang / Tehshik Yoon)
- **Going with or Against the Flow: Guidelines and Applications for Continuous-Flow Operations**
  (*Vy Dong* / Klavs Jensen / Martin Johnson / Thomas Razler)
- **Inspired by Nature: Biomimetic Syntheses, Biocatalysis, and Applications of "Large Molecules"**
  (*Dominique Hebrault* / David Entwistle / Jared Lewis / Robert Linhardt / Thomas Maimone)
- **Approaches for Innovative Medicines**
  (*Daniele Leonori* / Nicole Goodwin / Veronique Gouverneur / Kris Jones)
- **Advances in Catalysis**
  (*Silas Cook* / Brenda Burke / Jean-Philip Lumb / Matthew Meyer)
- **Keynote Session: The Mystery of Organic Chemistry: Exploiting Surprises, Molecular Machines, and Legerdemain**
  (*Travis Remarchuk* / David A. Leigh / Nicola Pohl)
- **Power Hour**
  (*Pamela Tadross*)

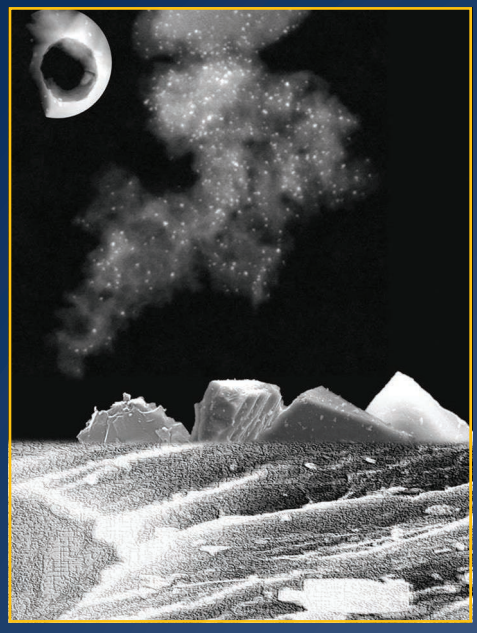

This image looking like a lunar landscape was created combining different TEM, STEM and SEM images of nanomaterials (carbon supports and Pt based catalyst on carbon). This artistic composition of scientific images is meant as a tribute to the nanocatalysts, masterpieces of material science. Courtesy of Giuliana Rubulotta and Matilde Solmi. Submitted by Giuliana Rubulotta, Chair, Green Chemistry GRS.

Organometallic Chemistry

Discovery and Applications at the Intersection of Inorganic, Organic, and Catalysis Chemistry
Jul 10-15, 2016
Salve Regina University, Newport, RI
Chair: Clark R. Landis
Vice Chair: John C. Gordon

- **Small Molecule Activation**
  (*John Gordon* / Sven Schneider / Karen Goldberg)
- **Organometallics and Organic Synthesis**
  (*Patrick Holland* / Guosheng Liu / Guy Lloyd-Jones)
- **Main Group Organometallics**
  (*Mitch Smith* / R. Tom Baker / Christopher Cummins / Gregory Robinson)
- **Catalysis and Commodities**
  (*Matthew Christianson* / Ruth Figueroa / Roy Periana)
- **Ligand Design**
  (*Nilay Hazari* / Jorg Eppinger / Alexander Miller)
- **Chemistry of Early Metals and the F-Block**
  (*John Gordon* / Aaron Odom)
- **Materials and Organometallics**
  (*Lisa McElwee-White* / Anne McNeil / Patrick Brant / Jonathan Owen)
- **Reaction Mechanisms**
  (*Seth Brown* / Eric Clot / Christophe Coperet / John Berry)
- **Keynote Session: How Organometallic Chemistry Serves Society**
  (*Seth Brown* / Richard Schrock / Robert Crabtree)

Organometallic Chemistry
Frontiers and Challenges in Organometallic Synthesis and Catalysis
Jul 9-10, 2016
Chairs: Alex E. Carpenter & Ekaterina V. Vinogradova

Oscillations & Dynamic Instabilities in Chemical Systems

Chemical Self-Organization Far from Equilibrium
Jul 17-22, 2016
Stoweflake Conference Center, Stowe, VT
Chair: Annette F. Taylor
Vice Chair: Istvan Z. Kiss

- **Electrochemical and Nanoscale Instabilities**
  (*Tomohiko Yamaguchi* / Hamilton Varela / Zuzanna Siwy)
- **Biological Oscillators**
  (*Stanislav Shvartsman* / Marcus Hauser / Carl Johnson)
- **Reaction Network Design**
  (*Igor Schreiber* / John Tyson / Wilhelm Huck)
- **Self-Propelled Motion and Active Matter**
  (*Jonathan Howse* / Cecile Cottin-Bizonne / Samuel Sanchez / Satoshi Nakata)
- **Spatial Organisation in Heterogeneous Media**
  (*Istvan Lagzi* / Irving Epstein / Oliver Steinbock)
- **Self-Replicating Chemical Systems**
  (*Mark Tinsley* / Gonen Ashkenasy / Sijbren Otto)
- **Programming Dynamic Behavior in Materials**
  (*Istvan Szalai* / John Pojman / Andreas Walther)
- **Reactive Flow Systems**
  (*Anne De Wit* / Julyan Cartwright / Tanguy Le Borgne / Agota Toth)
- **Active Particles and Molecules on the Micro- and Nano-Scales**
  (*Kenneth Showalter* / Raymond Kapral / Ayusman Sen)

Oscillations & Dynamic Instabilities in Chemical Systems
Chemical Self-Organization Far from Equilibrium
Jul 16-17, 2016
Chair: Marcello A. Budroni

Personalized Medicine

NEW!

Realizing Personalized Medicine Through Integrative Medicine, Science and Technology
Jul 10-15, 2016
The Hong Kong University of Science and Technology, Hong Kong, China
Chairs: Chih-Ming Ho & Edward McCabe
Vice Chairs: Yen Yun & Edward J. Benz

- **Genotypic Precision Medicine and Phenotypic Personalized Medicine**
  (*Bill Gahl* / Bruce Gelb / Wee Joo Chng)
- **Personalized/Precision Medicine and Enabling Technologies**
  (*Megan Frisk* / Steven Rosen / Dean Ho / Ali Zarrinpar / Geoffrey Ginsburg)
- **Personalized Pediatric Medicine**
  (*Katherine Janeway* / Dennis Lo / Charles Roberts)
- **Intersection of Engineering and Medicine**
  (*Hsing Jien Kung* / Stephen Quake / Garry Nolan / Pasi Janne)
- **Individualized Medicine for Cancers**
  (*Edison Liu* / Xianting Ding / Vincent H.S. Chang / Arjan Griffioen / Patrycja Nowak-Sliwinska)
- **Genomics and Molecular Targets**
  (*Garry Cutting* / Pan-Chyr Yang / C. Thomas Caskey)
- **Personalized Therapies for Blood Disorders**
  (*Kaixian Chen* / Andrew Feldman / Karl Tsim / Yi-Kuen Lee)

- **Personalized Immunotherapy**
  (*Patrick Tan* / Yusuke Nakumura / Lieping Chen)
- **The Future of Personalized/Precision Medicine**
  (*Yiwu He* / Edward Kai-Hua Chow)

Phosphorylation & G-Protein Mediated Signaling Networks

New Druggable Targets Underlying Structural and Spatial Aspects of Signaling in Metabolic, Inflammatory, and Other Stress-Related Disease Pathways
Jun 5-10, 2016
University of New England, Biddeford, ME
Chair: Carmen W. Dessauer
Vice Chair: Anton Bennett

- **Keynote Session: G Proteins, Kinases, and Phosphatases - Druggable Targets**
  (*Anton Bennett* / Gary Johnson / Tracy Handel / Nicholas Tonks)
- **Spatial and Temporal Dynamics of Cellular Signaling**
  (*Eileen Kennedy* / Viacheslav Nikolaev / Jin Zhang / Narasimhan Gautam / John Scott)
- **Lipid Modifications and Signaling**
  (*Maurine Linder* / Jonathan Backer / Ilya Levental / Carol Williams)
- **Structural Organization of Cellular Signaling**
  (*Stephen Sprang* / Anne-Claude Gingras / Roger Sunahara / John Tesmer)
- **New Twists on Cyclic Nucleotide Signaling**
  (*Carmen Dessauer* / Mark Von Zastrow / Xiaodong Cheng / Rebecca Berdeaux)
- **Signaling Networks in Nutrient Sensing and Metabolism**
  (*Rebecca Berdeaux* / Anton Bennett / Kun-Liang Guan / Stefan Offermanns / Tony Tiganis / Melanie Cobb)
- **Regulation of G Protein Networks**
  (*Kendall Blumer* / Kirill Martemyanov / John Hepler)
- **Signaling Networks in Times of Stress**
  (*Melanie Cobb* / Silvio Gutkind / Venetia Zachariou / Henrik Dohlman / Jing Liu)
- **Signaling Networks in Cardiac Stress and Disease**
  (*Natalia Riobo* / Maria Kontaridis / Alan Smrcka / Joan Heller Brown)

GRS **Phosphorylation & G-Protein Mediated Signaling Networks**
Emerging Advances in Signaling Downstream of GPCRs and Kinases from Basic Mechanisms to Human Disease
Jun 4-5, 2016
Chairs: Tanya Baldwin & Randi Fitzgibbon

Photonuclear Reactions

New Trends in Probing Quark-Gluon Dynamics
Aug 7-12, 2016
Holderness School, Holderness, NH
Chair: Alberto Accardi
Vice Chairs: Julie Roche & Barbara Pasquini

- **Photonuclear Physics on the Spotlight**
  (*Kawtar Hafidi* / Geoffrey Greene / Daniel Tapia Takaki / Kenneth Hicks)
- **Hadron Spectrum and QCD**
  (*Matthew Shepherd* / Raul Briceno / Gernot Eichmann / Lothar Tiator / Marco Battaglieri / Justin Stevens)
- **Nucleon Spin Structure**
  (*Sebastian Kuhn* / Zein-Eddine Meziani / Fabienne Kunne / Renee Fatemi / Wally Melnitchouk)
- **Long Range Hadron Structure**
  (*Valentina Vegna* / Miha Mihovilovic / Gilberto Colangelo / Jan Friedrich / Cristina Collicott / Keith Griffioen / Elena Long)
- **Standard Model and New Physics with Photon-Induced and Electroweak Processes**
  (*Susan Gardner* / Krishna Kumar / Vincenzo Cirigliano)
- **Parton Structure of Nucleons and Nuclei**
  (*Alessandro Bacchetta* / Ted Rogers / Kalyan Allada / Nicole D'Hose / Christine Aidala)
- **New Results in QCD Theory**
  (*Jianwei Qiu* / Bowen Xiao / Duff Neill / Pavel Nadolsky)
- **Few and Many Nucleon Systems**
  (*Sonia Bacca* / Kent Paschke / Alessandro Lovato)
- **Hadronic and Nuclear Physics at Future Facilities**
  (*Frank Ewald Maas* / Abhay Deshpande)

Physics Research & Education

Relativity and Gravitation: Contemporary Research and Teaching of Einstein's Physics
Jun 5-10, 2016
Salve Regina University, Newport, RI
Chairs: Duncan Brown & Dean A. Zollman
Vice Chairs: Nancy Ruzycki & Dawn C. Meredith

- **Contemporary Research and Teaching in Relativity**
  (*Shane Larson* / Nergis Mavalvala / Thomas Moore)
- **Gravitational Wave Physics and Astronomy**
  (*Sarah Caudill* / Matthew Evans / Vicky Kalogera / Peter Saulson)
- **Cosmology, Relativity, and Gravity in Introductory Physics**
  (*Dawn Meredith* / Kim Coble / Edward Prather)
- **Undergraduate Research and Teaching in Relativity**
  (*Geoffrey Lovelace* / Thomas Baumgarte / Jocelyn Read / Rachel Scherr)
- **Physics Education Research on Teaching Relativity**
  (*Dean Zollman* / Mark Haugan / Eleanor Sayre)
- **General Relativity in the Undergraduate Curriculum**
  (*Nancy Ruzycki* / Elisha Huggins / Richard Price / Tevian Dray)
- **Relativity: A Historical Perspective**
  (*Chiara Mingarelli* / Beverly Berger)
- **Frontiers in Relativity and Cosmology**
  (*Chanda Prescod-Weinstein* / Mark Trodden / Abhay Ashtekar / Manuela Campanelli)
- **Relativity in Informal Education**
  (*Duncan Brown* / Lynn Cominsky)

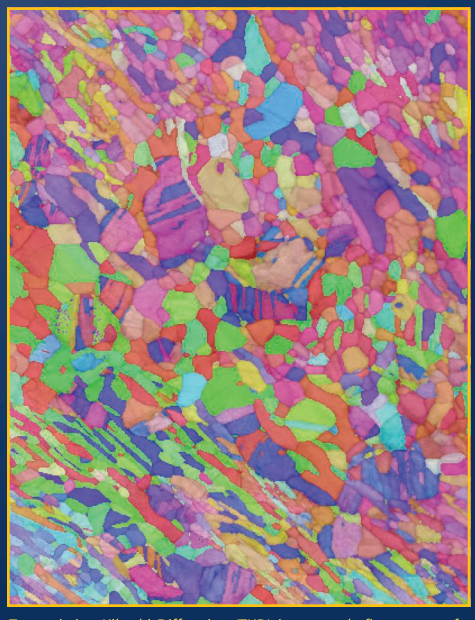

Transmission Kikuchi Diffraction (TKD) inverse pole figure map of a high strength duplex steel containing austenite and ferrite. Image size: 6.2 microns x 8 microns. Courtesy of Mehdi Eizadjou, Andrew Breen, Alec Day, Patrick Trimby, and Simon Ringer (University of Sydney). Submitted by Simon Ringer & Z.P. Lu, Vice Chairs, and Jian Lu & Christopher Schuh, Chairs, Structural Nanomaterials GRC.

Plant & Microbial Cytoskeleton

The Mechanics of Building Cells in Plants and Microbes
Aug 14-19, 2016
Proctor Academy, Andover, NH
Chair: Magdalena Bezanilla
Vice Chair: David R. Kovar

- **Keynote Session: The Cytoskeleton Across Kingdoms**
  (*Magdalena Bezanilla* / Kathy Gould / Chris Staiger / Arash Komeili)
- **Cytoskeletal Dynamics**
  (*Harold Erickson* / Erin Goley / Bruce Goode / Ram Dixit / Brad Nolen)
- **Chromosome Segregation During Cell Division**
  (*Sabine Muller* / Trisha Davis / Melissa Gardner / Daniel Van Damme)
- **Cellular Compartmentalization**
  (*Katherine Osteryoung* / Scott Dawson / David Drubin / Benjamin (Buzz) Baum)
- **Selected Poster Presentations**
  (*David Kovar*)
- **Cellular Morphogenesis**
  (*Daniel Szymanski* / Ethan Garner / Amy Gladfelter / David Ehrhardt / Fred Chang)
- **Cell Polarity**
  (*Daniel Lew* / Susan Dutcher / Ying Fu)
- **The Mechanics of Cell Division**
  (*Thomas Pollard* / Carolyn Rasmussen / Silvia Bulgheresi / Harold Erickson)
- **Membrane Trafficking**
  (*Anja Geitmann* / Georgia Drakakaki / Geoffrey Wasteneys / Kathryn Ayscough)

Plant Molecular Biology

How Plants Sense, Process, Integrate and Store Information
Jun 12-17, 2016
Holderness School, Holderness, NH
Chair: Mary Lou Guerinot
Vice Chair: Gloria M. Coruzzi

- **Keynote Session: Chemical Genomics**
  (*Sean Cutler* / Natasha Raihkel)
- **Abiotic Factors**
  (*Erin Connolly* / Joanne Chory / Christian Fankhauser / Ullas Pedmale)
- **Hormones**
  (*Joanne Chory* / Sean Cutler / Mark Estelle / Gregory Vert)
- **Plant Microbes**
  (*Mary Lou Guerinot* / Cara Haney / Giles Oldroyd)
- **Regulation of Plant Development**
  (*Elena Monte* / Andrea Eveland / Miltos Tsiantis)
- **Signaling and Regulation**
  (*Mathew Lewsey* / Pamela Green / Julia Bailey-Serres / David Nelson)
- **Natural Variation**
  (*Robert Schmitz* / Rob McClung / Thomas Mitchell-Olds)
- **Crop Models**
  (*Steven Briggs* / Thomas Brutnell / Michael Purugganan)
- **Systems Biology and Networks**
  (*Gloria Coruzzi* / Elena Monte / Ross Sozzani)

GRS **Plant Molecular Biology**
Revealing New Insights into Plant Biology Through Novel Techniques and Analyses
Jun 11-12, 2016
Chairs: Garo Akmakjian & Joseph Swift

Plasma Processing Science

Plasmas with Complex Interactions - Exploiting the Non-Equilibrium
Jul 24-29, 2016
Proctor Academy, Andover, NH
Chair: Achim Von Keudell
Vice Chair: Peter Bruggeman

- **Novel Diagnostic Concepts**
  (*Edward Barnat* / Keiichiro Urabe / Sukesh Roy)

The Gordon Research Conferences have cultivated an atmosphere that promotes networking and career development that is extremely unique and invaluable.

- Matthew J. Sikora, Chair, 2015 Hormone-Dependent Cancers GRS

- **Plasma-Astro Chemistry**
  (*Nigel Mason* / Eric Herbst / Harold Linnartz / Isabel Tanarro)
- **Transferring the Non-Equilibrium from Plasmas to Solids**
  (*Gottlieb Oehrlein* / Franz Bronold / Geun Young Yeom)
- **Plasmas for Soft Ionization**
  (*Hendrik Kersten* / Robert Cody / Gary Hieftje)
- **Plasma Driven Liquid Chemistry**
  (*Bill Graham* / Dragana Maric / Selma Medevodic Thagard / Ryo Ono)
- **Multi-Scale Modeling and Simulation**
  (*Luis Alves* / Jean Pierre Boeuf / Yasunori Tanaka / Laxminarayan Raja)
- **Bridging High and Low Temperature Plasma Research**
  (*Gerard Van Rooij* / Matteo Zuin / Yevgeny Raitses)
- **Interfacing Plasma with Living Matter**
  (*Jean-Michel Pouvesle* / Vandana Miller / Steffen Emmert)
- **Plasmas at Extreme Temporal and Spatial Scales**
  (*Juergen Kolb* / J. Gary Eden / Svetlana Starikovskaia)

Plasma Processing Science
New Challenges of Plasma Science and Cutting Edge Plasma Applications
Jul 23-24, 2016
Chairs: Natalie Chernets & Matteo Gherardi

Plasmonics & Nanophotonics

From Plasmonic Fundamentals to Nanooptical Applications
Jul 10-15, 2016
Sunday River, Newry, ME
Chair: Harald W. Giessen
Vice Chair: Peter Nordlander

- **Hybrid and Active Plasmonics, Nanooptics, and Metasurfaces**
  (*Harry Atwater* / Andrea Alu / Mark Brongersma / Yuri Kivshar / Arseniy Kuznetsov / Nikolay Zheludev)
- **Nonlinear and Ultrafast Optics and Plasmonics**
  (*Jacob Khurgin* / Martin Aeschlimann / Christoph Lienau / Markus Raschke / Thomas Zentgraf)
- **Plasmon-Induced Chemistry**
  (*Laura Na Liu* / James Hutchinson / Naomi Halas / Tim Lian / Christy Landes)
- **Low-Energy Photonics and Plasmonics**
  (*Lukas Novotny* / Rainer Hillenbrand / Annmarie Pucci)
- **2D and Van-der-Waals Solids**
  (*Albert Polman* / Javier Garcia De Abajo / Frank Koppens / Alejandro Manjavacas)
- **Hybrid Photonics and Light-Matter Interaction**
  (*Romain Quidant* / Maiken Mikkelsen / Arno Rauschenbeutel / Paivi Torma)
- **Novel Concepts, Devices, and Applications**
  (*Alexandra Boltasseva* / Juerg Leuthold / Hans Lochbihler / Yurii Vlasov / Joel Yang / Uriel Levy)
- **Late-Breaking Topics: Latest Developments in Plasmonics and Nanophotonics**
  (*Nader Engheta* / Phillip Christopher / Jennifer Dionne)
- **Outlook onto Plasmonics and Nanophotonics: Where Do We Go from Here?**
  (*Benjamin Gallinet* / Vladimir Shalaev)
- **Power Hour**
  (*Maiken Mikkelsen, Jennifer Dionne*)

Plasmonics & Nanophotonics
Towards Plasmonic Applications and Novel Nanooptical Concepts
Jul 9-10, 2016
Chair: Nikolai Strohfeldt

Polymer Physics

Emerging Topics in the Behavior of Neat and Hybrid Polymer Materials
Jul 24-29, 2016
Mount Holyoke College, South Hadley, MA
Chair: Richard A. Register
Vice Chair: Amalie L. Frischknecht

- **Crystallization and Crystalline Polymers**
  (*Gregory Rutledge* / Scott Milner / Christopher Li)
- **Polymer-Polymer Phase Behavior**
  (*Chinedum Osuji* / Bradley Olsen / Monica Olvera De La Cruz / Mark Matsen)
- **Structured Polymer Conductors**
  (*Christopher Soles* / Timothy Lodge / Enrique Gomez)
- **Block Copolymer Thin Films**
  (*Thomas Epps* / Paul Nealey / Gila Stein / Christopher Ellison)
- **Segmental, Chain, and Ion Dynamics**
  (*Rodney Priestley* / Spiros Anastasiadis / Ralph Colby)
- **Young Investigator Presentations: Future Directions in Polymer Physics**
  (*Yueh-Lin Loo, Andrew Spakowitz* / Lisa Hall / David Simmons / Zahra Fakhraai / Bryan Boudouris / Megan Robertson / Carlos Lopez-Barron)
- **Confined Polymers**
  (*Ophelia Tsui* / Sindee Simon / Peter Green)
- **Nanocomposites**
  (*Jeffrey Meth* / Arthi Jayaraman / Ting Xu / Sanat Kumar)
- **Ionomers**
  (*Karen Winey* / Amalie Frischknecht / Moon Jeong Park)
- **Power Hour**
  (*Amalie Frischknecht*)

Polymer Physics
Building and Leveraging a Nanoscopic Understanding of Polymer Physics
Jul 23-24, 2016
Chair: Adam B. Burns

Post-Transcriptional Gene Regulation

RNA: From Single Molecule to Transcriptome
Jul 10-15, 2016
Stoweflake Conference Center, Stowe, VT
Chairs: Peter Sarnow & Chris Burge
Vice Chairs: Tracy L. Johnson & Brenton Graveley

- **Keynote Session: Post-Transcriptional Processes in Transcription and RNA Stability**
  (*Gideon Dreyfuss* / Phillip Sharp / Torben Jensen / Tracy Johnson)
- **Single Molecules, Structures and Mechanisms**
  (*Joan Steitz* / Joseph Puglisi / Rebecca Voorhees)
- **RNA Localization and Transport**
  (*Robert Singer* / Kelsey Martin / Eric Lecuyer)
- **Regulation of Translation**
  (*Joseph Puglisi* / Susan Ackerman / Nicholas Ingolia / Jon Lorsch / Maria Barna)
- **RNA Modification, Decay and Silencing**
  (*Lynne Maquat* / Brenda Bass / Hiten Madhani)
- **Virus-Host Interactions**
  (*Joan Steitz* / Sara Cherry / Eva Gottwein)
- **Processing and Function of Coding and Noncoding RNAs**
  (*Gideon Dreyfuss* / John Rinn / Jeremy Wilusz / Sandra Wolin)
- **RNA in Disease**
  (*Sara Cherry* / Maurice Swanson / John Carulli / Frank Bennett / Eliezer Calo / Mark Kay / Adam Pavlicek)
- **Global Analysis of Post-Transcriptional Gene Regulation**
  (*Brenton Graveley* / Benjamin Blencowe / Nikolaus Rajewsky / Brenton Graveley)

Post-Transcriptional Gene Regulation
Discoveries for the Future of RNA Biology
Jul 9-10, 2016
Chairs: Melanie A. Preston & Aimee L. Jalkanen

Protein Processing, Trafficking & Secretion

Secretory and Endocytic Pathways in Health and Disease
Jul 24-29, 2016
Colby-Sawyer College, New London, NH
Chair: Paul H. Taghert
Vice Chair: Klaudia Brix

- **Keynote Session: Next-Gen Protein Processing**
  (*Iris Lindberg* / Peter Arvan / Robert Day / Bertrand Cariou)
- **Generation of the Endolysosomal Pathway**
  (*Richard Mains* / Robert Fuller / Phyllis Hanson / Adam Linstedt / Avital Rodal)
- **New Views on Peptide Processing and Release**
  (*Kelly Ten Hagen* / Robert Edwards / Seung Kim / Jonathan Sweedler / Tamas Horvath)
- **Regulated Intramembrane Proteolysis**
  (*Nabil Seidah* / Regina Fluhrer / Joanne Lemieux / Michael Glickman)
- **Inter-Organelle Communication**
  (*Kristi Wharton* / Loydie Jerome-Majewska / Rajini Rao / Gary Thomas)
- **Molecular Takes on Dense Core Vesicles**
  (*Alan Attie* / Heather Brohier / Betty Eipper / Erik Jorgensen / Michele Solimena)
- **Processing Enzymes in the Secretory and Endocytic Pathways**
  (*Lloyd Fricker* / John Creemers / Klaudia Brix / Galia Blum)
- **Feeding into Autophagosomes and Lysosomes**
  (*Indira Mysorekar* / Ana Maria Cuervo / Jason Mills / Sharon Tooze / Roberto Zoncu)
- **To Image Trafficking and Exocytosis**
  (*Ronald Holz* / Edwin Chapman / Edwin Levitan / Matthijs Verhage / Patrik Verstraken)
- **Power Hour**
  (*Betty Eipper, Avital Rodal*)

Protein Processing, Trafficking & Secretion
At the Cutting Edge of Understanding Protein Fates in Health and Diseases
Jul 23-24, 2016
Chairs: Frederic Couture & Anna M. Jansen

Proteoglycans

The Proteoglycan Arc - From Molecular Mechanisms to Therapeutic Exploitation
Jul 10-15, 2016
Proctor Academy, Andover, NH
Chairs: Jeremy E. Turnbull & Sarah M. Knox
Vice Chair: Anthony J. Day

- **Late-Breaking Topics**
  (*Lena Kjellen, Thomas Neill* / Randy Schekman / Jeffrey Esko / Laura Kiessling)
- **Technology Advances and State-of-the-Art Methods for Proteoglycan Research**
  (*Robert Linhardt, Matthew Nugent* / Geert-Jan Boons / Linda Hsieh-Wilson)
- **Proteoglycans: Partners in Cell Signaling and Trafficking**
  (*Lianchun Wang, Pascale Zimmermann* / Mattias Belting / Andrew Chisholm / Yingjie Shen / Tatjana Piotrowski)
- **Development and Stem Cells**
  (*Natasza Kurpios, Yu Yamaguchi* / Larisa Haupt / Molly Shoichet / Roger Pocock)

- **Ageing and Chronic Diseases**
  (*Eri Hirasawa-Arikawa, Addolorata Pisconti* / Dulce Papy-Garcia / Saul Villeda / Maurizio Pacifici)
- **Bioengineering and Regenerative Medicine**
  (*Catherine Merry, John Whitelock* / Karen Christman / Glenn Prestwich / Valerie Weaver / Alyssa Panitch)
- **Musculoskeletal Biology and Disease**
  (*Andrea Vortkamp, Marian Young* / Brendan Lee / Nancy Schwartz)
- **Cancer and Infectious Diseases**
  (*Joanna Phillips, Ralph Sanderson* / Ulf Lindahl / Alan Rapraeger)
- **Cardiovascular Disease and Inflammatory Processes**
  (*Carol Dela Motte, Jin-Ping Li* / Paul Bollyky / Jens Fischer / Pyong Woo Park / Liliana Schaefer)

Proteoglycans
Proteoglycans as Functional Regulators of Development and Disease
Jul 9-10, 2016
Chair: Tabea Dierker

Proteolytic Enzymes & Their Inhibitors

Exploring and Exploiting Proteases in Development and Disease
Jun 26 - Jul 1, 2016
Renaissance Tuscany Il Ciocco, Lucca (Barga), Italy
Chair: Johanna A. Joyce
Vice Chair: Matthew S. Bogyo

- **Stem Cells and Development**
  (*Margarete M.S. Heck* / Rama Khokha / James Whisstock)
- **Advances in Analyzing Protease Activity and Function**
  (*Irit Sagi* / Ulrich Auf Dem Keller / Matthew Bogyo / Marcin Drag / James Wells)
- **Proteases in Neural Development and Neurodegeneration**
  (*Klaudia Brix* / Michael Ehrmann / Isabel Farinas / Bart De Strooper)
- **Cell Signaling**
  (*James McKerrow, Jan Potempa* / Carl Blobel / Nigel Bunnett / Matthew Freeman / Christopher Overall)
- **Therapeutic Targeting of Proteases**
  (*Galia Blum, Christopher Scott* / Irit Sagi / Vicki Plaks)
- **Cancer**
  (*Christoph Peters* / Matthew Albert / Klaudia Brix / Thomas Reinheckel / Oliver Schilling)
- **Structural Insights into Cell Biology of Proteases**
  (*Sheena McGowan* / Tania Baker / Tim Clausen / Sinisa Urban)
- **New Strategies for Protease Inhibition**
  (*Matthew Bogyo, Edwin Madison* / Paula Da Fonseca / Bob Lazarus / Celia Schiffer)
- **Intracellular Proteolysis in Cell Fate Decisions**
  (*Rob Pike, Boris Turk* / Marius Lemberg / Guy Salvesen)

Proteolytic Enzymes & Their Inhibitors
Understanding the Role of Proteolysis in Homeostasis and Disease
Jun 25-26, 2016
Chairs: Anthony J. O'Donoghue & Leila Akkari

Quantum Science

Quantum Entanglement, New States of Matter, and Correlated Dynamics
Jul 31 - Aug 5, 2016
Stonehill College, Easton, MA
Chairs: Jun Ye & Frank Verstraete
Vice Chairs: Ana Maria Rey & Andrew Houck

- **Quantum Information and Condensed Matter**
  (*Norbert Schuch* / Matthew P. Fisher / Charles Marcus)
- **Many-Body Entanglement and Dynamics, Decoherence, Thermalization/Localization**
  (*Eugene Demler* / Ehud Altman / Markus Greiner / Christian Gross)
- **Novel Quantum Systems, Such as Long-Range Interactions, Spin-Orbit Coupling**
  (*Antoine Browaeys* / John Bollinger / Francesca Ferlaino / Deborah Jin)
- **Quantum Computation Algorithm, Error Corrections**
  (*Barbara Terhal* / Rainer Blatt / Barbara Terhal)
- **Computational Architecture, Entanglement/ Computation Through Dissipation**
  (*Ignacio Cirac* / Yiheng Lin / Robert Schoelkopf)
- **Quantum Information and Entanglement in High Energy and General Relativity**
  (*Philipp Hauke* / Igor Pikovski / Philipp Hauke)
- **Quantum Metrology, Sensing, and Other Areas (Chemistry/Biology)**
  (*Vladan Vuletic* / Mark Kasevich / David Reitze)
- **Strongly Interacting Photons, Cavity QED with Real and Artificial Atoms**
  (*Konrad Lehnert* / Jeff Kimble / Konrad Lehnert)
- **Hybrid Systems, Quantum Networks/Communication**
  (*Eugene Polzik* / Ronald Hanson / Alexander M. Cruickshank Lecture: Mikhail Lukin / Oskar Painter)

Quantum Science
Quantum Simulation, Entanglement and Dynamics of Condensed Matter Systems and Field Theories
Jul 30-31, 2016
Chairs: Jutho Haegeman & Jacob Covey

Rare Cells in Circulation

Circulating Tumor Cells and Other Tumor Products in the Circulation
Aug 7-12, 2016
Mount Holyoke College, South Hadley, MA
Chairs: Andrew D. Rhim & Howard I. Scher
Vice Chairs: Shannon Stott & Stefanie Jeffrey

- **Keynote Session: The State of Liquid Biopsies**
  (*Anirban Maitra* / Caroline Dive / Shana Kelley / Vikram Bajaj)
- **Clinical Testing and Applications: Considerations for Implementation**
  (*Klaus Pantel* / Howard Scher / Lisa McShane / Klaus Pantel)
- **Intellectual Property, Regulatory Approval, and Statistical Considerations**
  (*Peter Kuhn* / Elizabeth Mansfield / Richard Marshall)
- **Exosomes and Microvesicles in Cancer**
  (*Brian Kirby* / Ben Stanger / Raghu Kalluri / Dolores Di Vizio / Xandra Breakefield)
- **Circulating Tumor Cells**
  (*Shannon Stott* / Daniel Haber / Ryan Dittamore / Christopher Love / Amir Goldkorn)
- **Circulating Tumor DNA and Heterogeneity**
  (*Luis Diaz* / Nicholas Turner / Robert Corcoran / Scott Lowe / Nicholas Navin / Luis Diaz)
- **Opportunities in and Biology of Early Dissemination and Metastasis**
  (*Ben Stanger* / Andrew Rhim / Anirban Maitra / Shiladitya Sengupta / Christoph Klein / Dino DiCarlo)
- **Clinical Applications: Guiding Treatment**
  (*Gerhardt Attard* / Peter Kuhn / Sean Morrison / Andy Minn)
- **Clinical Applications: Response and Relapse**
  (*Stefanie Jeffrey* / Gerhardt Attard / Jeannie Tie / Keith Flaherty)

Rock Deformation

From Slow to Fast Rock Deformation and Back
Aug 21-26, 2016
Proctor Academy, Andover, NH
Chair: François Renard
Vice Chair: Julia Morgan

- **Architecture and Behavior of Faults and Shear Zones**
  (*Christie Rowe* / Chris Scholz / John Platt)
- **Dynamics of Rock-Rock Interfaces: Forces and Friction**
  (*Diane Moore* / Ikuo Katayama / Andre Niemeijer / Anja Røyne)
- **Geoengineering and Induced Rock Deformation**
  (*William Ellsworth* / Gunter Siddiqi / Shemin Ge)
- **Slow and Fast Earthquakes**
  (*Chris Marone* / John Platt / Brett Carpenter / Heidi Houston)
- **Pore Fluid and Rock Deformation**
  (*Bjørn Jamtveit* / Wenlu Zhu / Yves Guglielmi)
- **Plasticity of Grains and Ductile Rheology**
  (*Philip Skemer* / Patrick Cordier / Lars Hansen / Pamela Burnley)
- **Evolving Microstructures and Effect on Rheology**
  (*Georg Dresen* / Maurine Montagnat / Andrew Cross)
- **Coupling Scales in Modelling Rock Deformation**
  (*Nadia Lapusta* / David Bercovici / Marine Denolle / Liran Goren)
- **Young Investigator Presentations**
  (*Michele Cooke*)
- **Power Hour**
  (*Julia Morgan*)

Rock Deformation
From the Lab to the Field – Combining Observation, Theory and Modelling to Understand Rock Deformation Processes
Aug 20-21, 2016
Chairs: Elizabeth H. Madden & Suzanne Hangx

Salt & Water Stress in Plants

Moving from Mechanism to Crop Yield Stability
May 29 - Jun 3, 2016
Les Diablerets Conference Center, Les Diablerets, Switzerland
Chairs: Julia Bailey-Serres & Erwin Grill
Vice Chairs: Melvin J. Oliver & Jill Farrant

- **Keynote Session: Climate Change and Food Security**
  (*Eduardo Blumwald* / Michael Nuccio / Markus Reichstein / Chiara Tonelli)
- **Stress and Development**
  (*Christa Testerlink* / Marie Barberon / Malcolm Bennett / Jose Dinneny / Neelima Sinha)
- **Natural Variation of Stress Resistance**
  (*Paul Verslues* / Maheshi Dassanayake / Thomas Juenger / Yusuka Uga)
- **Signaling**
  (*Teun Munnik* / Zhen-Ming Pei / Barry Pogson / Ari Sadanandom / Zhizhong Gong)
- **Gas Exchange and Photosynthesis**
  (*Michael Blatt* / Jaume Flexas / Julie Gray / Julian Schroeder)
- **Response Networks: Gene to Metabolite**
  (*Pierdomenico Perata* / Rashmi Sasidharan / Kazuko Yamaguchi-Shinozaki / Wolf Frommer / Diana Santelia)
- **Yield Stability**
  (*Francois Tardieu* / Jill Cairns / Mark Tester)
- **From Gene to Field – Single and Pyramided Genetic Determinants**
  (*Andy Pereira* / Tobias Kretzschmar / Stuart Roy / Chris-Carolin Schoen)
- **Engineering for Water Efficiency and Stress Tolerance**
  (*Kazuo Shinozaki* / Sean Cutler / Dirk Inze / Pedro Rodriguez)

Salt & Water Stress in Plants
New Discoveries in Plant Salt and Water Stress: From Phenotype to Mechanism
May 28-29, 2016
Chairs: Magdalena M. Julkowska & Aaron B. Stephan

Scientific Methods in Cultural Heritage Research

Probing Hierarchically Complex Historical Materials and Their Modes of Characterization and Alteration
Jul 31 - Aug 5, 2016
Sunday River, Newry, ME
Chairs: Jennifer Mass & Tim Wess
Vice Chairs: C. Richard Johnson & Robert Van Langh

- **Forensic Science and Cultural Heritage Science – Cross-Disciplinary Problem Solving**
  (*John Lombardi* / Maurice Aalders / Greg Smith)
- **Biofilms and Biodeteriorated Systems – Characterization Challenges Across Disciplines**
  (*John Moreau* / Caroline Kyi / Benjamin Ortega / Francesca Cappitelli)
- **The Fossil Record and Finds from Anaerobic and Arid Environments: New Preservation Problems and Analytical Tools**
  (*Nicholas Edwards* / Michael Toth / Uwe Bergmann)
- **The Preservation Challenges of Protein-Based Materials: Characterization and Quantification of Degradation**
  (*Michael Buckley* / Loic Bertrand / Matthew Collins / Colin Smith)
- **Technological Challenges of the Inaccessible: On-Site Cultural Heritage Investigations and Buried Stratigraphies**
  (*John Delaney* / Koen Janssens / Warren Warren)
- **Failure Mechanisms in Cultural Heritage Objects**
  (*Katrien Keune* / Austin Nevin / Antje Postthast / Shelley Svoboda / Kristin Wustholz)
- **Cultural Heritage in Crisis – Scientific and Conservation Interventions to Preserve the Present for the Future**
  (*Yvonne Shashoua* / Cory Rogge / John Delaney)
- **First Nations' Art and Artists' Materials: Preserving Meaning, Appearance, and Function**
  (*Nancy Odegaard* / Carole Dignard / Rachel Popelka-Filcoff)
- **Innovative Surface Sensitive Probes and New Sampling Methods in Cultural Heritage Research (Including Handheld Device Data Acquisition for Monitoring Cultural Heritage)**
  (*Thomas Beebe* / Bartosz Dajnowski / Graham Davis / Claire Gervais / David Mills / Marcello Picollo)

GRS Scientific Methods in Cultural Heritage Research
Cross-Disciplinary Connections in Conservation Science and Technical Art History
Jul 30-31, 2016
Chairs: Tana E. Villafana & Alyssa Hull

Signal Transduction by Engineered Extracellular Matrices

Integration of Systems Biology with Tissue Engineering for Development of Molecular and Regenerative Therapies
Jun 26 - Jul 1, 2016
University of New England, Biddeford, ME
Chair: Linda G. Griffith
Vice Chair: Sarah C. Heilshorn

- **Keynote Session: Frontiers in Integration of Matrix and Systems Biology in Understanding and Control of Stem Cell Differentiation**
  (*Linda Griffith* / Fiona Watt / David Schaffer)
- **Analysis and Control of Early Stem Cell Fate Decisions**
  (*David Schaffer* / Todd McDevitt / Matthias Lutolf / Madeline Lancaster / Randolph Ashton)
- **Matrix Cues Regulating Morphogenesis and Regeneration**
  (*Manu Platt* / Brendan Harley / Penney Gilbert / Celeste Nelson)
- **The Other Extracellular Matrix: Understanding and Engineering Mucosal Barriers**
  (*Sarah Heilshorn* / Andrea Cerutti / Katharina Ribbeck / Rebecca Carrier / Thaddeus Stappenbeck)
- **Dynamic Multiscale Matrices for Engineering 3D Tissue Function**
  (*Elliot Chaikof* / Jean Schwartzbauer / Jason Burdick / Kamil Goduda)
- **Systems Biology Approaches to Signaling in Morphogenesis, Homeostasis, and Remodeling**
  (*Fiona Watt* / Kevin Janes / Stanislav Shvartsman / Claus Jorgensen / Katja Schenke-Layland)
- **Engineering Microenvironments to Probe and Control Immune Responses**
  (*Daniel Hammer* / Bjorn Millard / Princess Imoukhuede)
- **Cells and Matrix on the Move**
  (*Brendan Harley* / Daniel Hammer / Ulrik Nielsen / Manu Platt)
- **Translation to Drug Development and the Clinic**
  (*Rebecca Carrier* / Elliot Chaikof / Keith Isaacson)

GRS Signal Transduction by Engineered Extracellular Matrices
Intersection of Extracellular Matrix and Clinical Pathology to Inform Tissue Engineering for Development of Molecular and Regenerative Therapies
Jun 25-26, 2016
Chairs: Christi D. Cook & Chris Madl

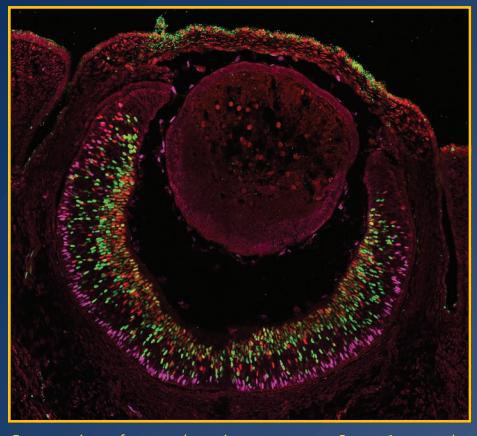

Cross-section of an embryonic mouse eye. Onecut1-expressing retinal progenitor cells (green) can produce Blimp1+ photoreceptors (purple) and Brn3+ ganglion cells (red). Courtesy of Tatiana Eliseeva and Joseph Brzezinski (University of Colorado Denver). Submitted by Nadean Brown, Chair, Visual System Development GRC.

Signaling by Adhesion Receptors

Adhesion: The Cellular Basis of Tissue Homeostasis and Dysfunction
Jun 19-24, 2016
Bates College, Lewiston, ME
Chair: Alpha S. Yap
Vice Chair: Christopher S. Chen

- **Keynote Session: Perspectives in Adhesion and Homeostasis**
  (*Alpha Yap* / Ian Macara / Valerie Horsley / Jody Rosenblatt)
- **New Mechanisms in Cell Adhesion**
  (*Christopher Chen* / William Weis / Clare Waterman / Nicholas Brown)
- **Myosin and Adhesion: Its Roles as Force Generator and Scaffold**
  (*Clare Waterman* / Stephan Grill / Margaret Gardel / John Hammer)
- **Advances in Adhesion Signaling**
  (*Tony Koleske* / Jay Groves / Ann Miller / Hisataka Sabe)
- **Inside-Out Integrin Signaling**
  (*Nicholas Brown* / David Calderwood / Martin Humphries)
- **Adhesion and Tissue Homeostasis**
  (*Erin Cram* / Jay Humphrey / John Wallingford / Anna Huttenlocher / Hilary Ashe)
- **New Approaches to Integrate Across Biological Scales**
  (*Martin Schwartz* / Celeste Nelson / Virgile Viasnoff / Christopher Chen)
- **Disease: Adhesion and Its Discontents**
  (*Jody Rosenblatt* / Peter Friedl / Martin Schwartz / Valerie Weaver)
- **Systems Approaches to Quantitative Analysis**
  (*Brenton Hoffman* / Alexander Mogilner / Xavier Trepat)

GRS Signaling by Adhesion Receptors
Outside-In and Inside-Out: Adhesion Signaling from Cells to Systems
Jun 18-19, 2016
Chairs: Madeleine J. Oudin & Nisha Mohd Rafiq

Single Molecule Approaches to Biology

Single-Molecule Microscopy: Life at a Higher Resolution
Jul 3-8, 2016
The Chinese University of Hong Kong, Hong Kong, China
Chairs: David Rueda & Toshio Yanagida
Vice Chairs: Julie Biteen & Antoine Van Oijen

- **Keynote Session: Imaging Biology from Single Molecules to Single Cells**
  (*David Rueda* / Taekjip Ha / Xiaowei Zhuang)
- **Nucleic Acids Enzymes**
  (*Antoine Van Oijen* / Eric Greene / Gijs Wuite / Sungchul Hohng / Chirlmin Joo)
- **Transactions on Chromatin**
  (*Jan Liphardt* / Melike Lakadamyali / Michael Stone)
- **Gene Expression and Processing**
  (*Achillefs Kapanidis* / Michelle Wang / Jeff Gelles / Maria Carmo-Fonseca / Daniel Larson / Aaron Hoskins)
- **Folding and Function**
  (*William Eaton* / Benjamin Schuler / Sergi Garcia-Manyes / Michael Woodside / David Lilley)
- **Super-Resolution Imaging and Emerging Technologies**
  (*Julie Biteen* / Peng Yin / Takeharu Nagai / Jonas Korlach / Hiroyuki Noji / Joerg Bewersdorf)
- **Neuronal Biophysics**
  (*Yasushi Okada* / Antonie Triller / Roland Brandt)
- **Mechanobiology**
  (*Thomas Perkins* / Hermann Gaub / Yale Goldman / Arne Gennerich / Takayuki Uchihashi / Alexander Dunn)
- **Cell Signaling**
  (*Mariko Okada* / Masahiro Ueda / Takahiro Fujiwara)

GRS Single Molecule Approaches to Biology
Single-Molecule Microscopy: Life at a Higher Resolution
Jul 2-3, 2016
Chair: Kathy R. Chaurasiya

Solar Energy Conversion

NEW!

Materials, Physics and Devices for Solar Electricity and Energy Storage
Jul 17-22, 2016
The Hong Kong University of Science and Technology, Hong Kong, China
Chairs: Edward Sargent & Wei Huang
Vice Chairs: Ali Javey & Jia Zhu

- **Theory and Mechanism**
  (*Guozhong Cao* / Eli Yablonovitch / Marin Soljacic)
- **Polymers and Small Molecules**
  (*Linda Wu* / Vivian Yam / Angus Yip / Mark Thompson)
- **Perovskite Solar Cells**
  (*Shihe Yang* / Dapeng Yu / Sang Il Seok / Yang Yang)
- **Silicon and III-V Materials**
  (*Rao Tatavarti* / Yi Cui / Harry Atwater / Frank Dimroth)
- **Novel Solar Materials**
  (*Feng Yan* / Jiang Tang / Curtis Berlinguette / Zhijun Ning)
- **Carrier Dynamics**
  (*Tao Deng* / Anders Hagfeldt / Guichuan Xing)
- **Solar Thermal and Hot Carriers**
  (*Elisa Ranieri* / Peter Bermel / David Norris)
- **Solar Fuels**
  (*Dunwei Wang* / Can Li / Song Jin)

- **Fuel and Catalysis**
  (*Zhiyong Tang* / Matthew Kanan / Peidong Yang)

Solid State Chemistry

Strategies for Materials Discovery: Progress Toward Tomorrow's Materials
Jul 17-22, 2016
Colby-Sawyer College, New London, NH
Chair: Hans-Conrad zur Loye
Vice Chair: Patrick M. Woodward

- **Theory on the Path to New Materials**
  (*Richard Dronskowski* / Alex Zunger / Kristin Persson)
- **Energy Materials of Tomorrow**
  (*Tyrel McQueen* / Athena Sefat / Kirill Kovnir / Efrain Rodriguez / Hemamala Karunadasa)
- **New Functional Materials for the Future**
  (*Amy Prieto* / Jean Marie Tarascon / Mercouri Kanatzidis)
- **Advances in Intermetallics**
  (*Svilen Bobev* / Arthur Mar / Daniel Fredrickson / Julia Chan)
- **Putting Pressure on Synthesis**
  (*Kwang-Hwa Lii* / Joseph Kolis / Eva Zurek)
- **Directed Assembly and Crystal Growth**
  (*Bettina Lotsch* / Qichun Zhang / Fiona Meldrum / Brent Melot / Mircea Dinca)
- **Chemistry of Mixed Anion Structures**
  (*Patrick Woodward* / Kenneth Poeppelmeier / Alain Demorgues)
- **Advances in Transition Metal Oxides**
  (*Amparo Fuertes* / Steven Suib / Hiroshi Kageyama / Juan Nino / Abbie McLaughlin)
- **Crystals and Their Applications**
  (*Hans-Conrad zur Loye* / Kevin Stevens / Susan Kauzlarich)
- **Power Hour**
  (*Susan Kauzlarich, Julia Chan*)

GFS **Solid State Chemistry**
Strategies for Materials Discovery: New Functional Materials and Their Applications
Jul 16-17, 2016
Chairs: Allison M. Latshaw & Joya Cooley

Stereochemistry

21st Century Stereochemistry: Synthesis, Structure, Function, and Properties
Jul 24-29, 2016
Salve Regina University, Newport, RI
Chairs: Scott E. Denmark & John A. Ragan
Vice Chairs: Gregory C. Fu & Cameron J. Cowden

- **Frontiers of Stereochemistry: Synthesis and Mechanism**
  (*Gregory Fu* / Donna Blackmond / David Macmillan)
- **Stereoselective Organocatalysis**
  (*Noah Burns* / Benjamin List / Babak Borhan / Helma Wennemers / Dean Toste)
- **Biosynthesis and Biocatalysis**
  (*Rajesh Kumar* / Geert-Jan Boons / Nicholas Turner / David Cane)
- **Stereoselective Synthesis in Industry**
  (*Francis Gosselin* / Carl Busacca / Francisco Gonzales-Bobes / Laurie Schenkel / Robert Scott)
- **Physical Methods of Stereochemistry**
  (*Alexander Radosevich* / Joel Hawkins / Leo Joyce / Dean Tantillo)
- **Higher Order Stereochemistry: Beyond the Molecule**
  (*Brett Fors* / Egbert Meijer / Lia Addadi / Karen Wooley / Fraser Stoddart)
- **Stereoselective Synthesis**
  (*Thomas Maimone* / Robert Knowles / Jennifer Schomaker / Varinder Aggarwal)
- **Stereoselective Organometallic Catalysis**
  (*David Sarlah* / Peter Zhang / Jin-Quan Yu / John Hartwig)
- **Keynote Session: Structure and Function**
  (*Cameron Cowden* / Amir Hoveyda / Dieter Seebach)

Structural Nanomaterials

Interfacial and Surface Effects on Structural Nanomaterial Properties
Jul 10-15, 2016
The Chinese University of Hong Kong, Hong Kong, China
Chairs: Jian Lu & Christopher Schuh
Vice Chairs: Z. P. Lu & Simon Ringer

- **Keynote Session: Nanostructure in High Entropy Alloys**
  (*Simon Ringer* / T. Nieh / Z. P. Lu)
- **Nanoparticle and Nanoprecipitate Reinforcements**
  (*Jeff De Hosson* / Sybrand Van Der Zwaag / Chain Tsuan Liu / Allison Beese / Julie Schoenung)
- **Contact and Wear in Nanomaterials**
  (*Yip-Wah Chung* / Ruth Schwaiger / Izabela Szlufarska / Blythe Clark)
- **Frontiers in Nanostructure Stability and Instability: Glasses and Nanocrystalline Materials**
  (*Herbert Gleiter* / Scott Mao / Lei Lu / Timothy Rupert)
- **Frontiers in Nanostructure Stability and Instability: Films and Laminates**
  (*Long-Qing Chen* / Irene Beyerlein / Andrea Hodge / Zi-Kui Liu)
- **Bio-Nanomechanics**
  (*Siu-Wai Chan* / David Kisailus / Quan Li / Xinrui Niu)
- **Nanomechanical Effects on Functional Properties**
  (*Yi Li* / Daniel Gianola / Jianmin Qu)
- **Advanced Experimental Nanomechanics: Bulk Materials**
  (*Xiaoxu Huang* / Ze Zhang / Luchang Qin / Jun Lou)
- **Advanced Experimental Nanomechanics: Nanomaterials**
  (*Qing Ping Sun* / Keyu Li / Erica Lilleodden)

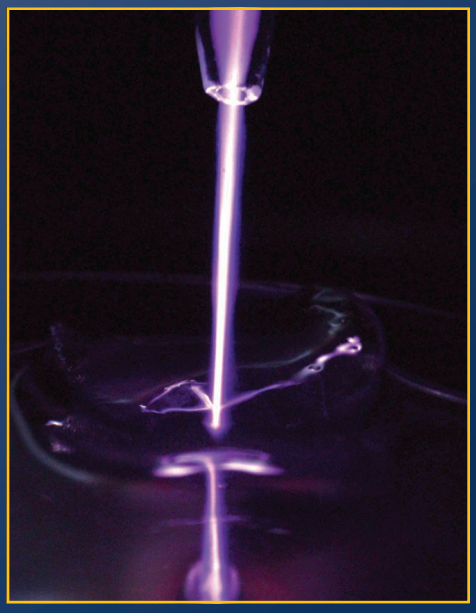

A jet of plasma, the 4th state of matter, propagating in air (gas) and impinging on ice (solid) suspended in water (liquid). Plasma science is a key enabling technology for many applications. Courtesy of Augusto Stancampiano, Emanuele Simoncelli, Vittorio Colombo, and Matteo Gherardi (Alma Mater Studiorum - Università di Bologna). Submitted by Matteo Gherardi & Natalie Chernets, Chairs, Plasma Processing Science GRS.

Synaptic Transmission

From Nanostructures to Microcircuits in Health and Disease
Aug 14-19, 2016
Waterville Valley, Waterville Valley, NH
Chair: Ege Kavalali
Vice Chair: Kristen M. Harris

- **Keynote Session: Synaptic Transmission: From Nanostructures to Microcircuits**
  (*Ege Kavalali* / Cornelia Bargmann / Alexander M. Cruickshank Lecture: Xiaowei Zhuang)
- **Presynaptic Structure and Mechanisms**
  (*Erwin Neher* / Yishi Jin / Vladan Lucic / David Zenisek / Lu-Yang Wang)
- **Presynaptic Plasticity**
  (*Richard Tsien* / Alain Marty / Katalin Toth / David Sulzer)
- **Postsynaptic Structure and Mechanisms**
  (*Robert Malenka* / Thomas Blanpied / Pablo Castillo / Lu Chen / Kimberly Huber)
- **Postsynaptic Plasticity**
  (*Julie Kauer* / Inna Slutsky / Gina Turrigiano / Marina Wolf)
- **Synaptic Circuits**
  (*Martha Constantine-Paton* / Haruhiko Bito / Li-Huei Tsai / Richard Tsien / Min Zhuo)
- **Synaptic Circuits and Plasticity**
  (*Kristen Harris* / Julie Kauer / Indira Raman / Thomas Sudhof)
- **Synapse Development**
  (*Erik Jorgensen* / Vivian Budnik / Chinfei Chen / Cagla Eroglu / Karen Zito / Martha Constantine-Paton)
- **Synapse Evolution**
  (*Thomas Sudhof* / Erik Jorgensen / Kenneth Kosik / Leonid Moroz)

GFS **Synaptic Transmission**
From SNAREs to Small Networks - New Insights into Synaptic Transmission
Aug 13-14, 2016
Chair: James A. Daniel

Tetrapyrroles, Chemistry & Biology of

Biology of Heme, Chlorophyll, Porphyrins, Chlorins and Bilins - The Pigments of Life
Jul 17-22, 2016
Salve Regina University, Newport, RI
Chair: John Phillips
Vice Chair: Iqbal Hamza

- **Chlorophyll, Light Harvesting Systems and Tetrapyrroles that Produce Energy**
  (*Neil Hunter* / Daniel Canniffe / Gongfang Hu)
- **The Chemistry of Tetrapyrroles**
  (*Kara Bren* / Ekaterina Pletneva / Xiao-an Zhang / Ricardo Louro)
- **Linear Tetrapyrroles in Biology**
  (*J. Clark Lagarias* / Jeff Tabor / Beronda Montgomery)
- **The Next 50 Years of Chlorophyll**
  (*Samuel Beale* / Robert Blankenship / Donald Bryant / Robert Willows)
- **The Synthesis, Biology and Use of Cobalamine**
  (*Ruma Banerjee* / Martin Warren / Markos Koutmos)
- **Heme Biosynthesis in Disease**
  (*Robert Desnick* / Amy Simon / Marcelo Bozza / Julia Kardon)
- **The Pathobiology of Heme: Tetrapyrroles and Host Microbe Interactions**
  (*Miguel Soares* / Solomon Ofori-Acquah / Malay Haldar)
- **Synthesis and Optimal Use of Vitamin B12**
  (*Michiko Taga* / Olivier Berteau / Montserrat Elias-Arnanz / Wyatt Yue)
- **The Diseases of Heme and Porphyrin Biosynthesis**
  (*Sylvia Bottomley* / Michael Marletta / Jean-Charles Deybach)

Thin Film & Small Scale Mechanical Behavior

Scientific Insights from Small-Scale Mechanical Behavior: From Nano-Materials to Nano-Mediated Bulk Response
Jul 24-29, 2016
Bates College, Lewiston, ME
Chair: Erica T. Lilleodden
Vice Chair: Andrew J. Bushby

- **Advances in Indentation Testing**
  (*Megan Cordill* / Erik Herbert / Jodie Bradby)
- **Advances in *In Situ* Microscopy**
  (*Gerhard Dehm* / Marc Legros / Steven Van Petegem / Geoff Campbell)

I volunteered to chair a GRC because I attended GRCs for a number of years and benefited greatly from these meetings, and I wanted to contribute back to both GRC and my community.

- Jerzy Klosin, Chair, 2015 Organometallic Chemistry GRC

- **Size Effects in Collective Dislocation Plasticity**
  (*Daniel Gianola* / Jerome Weiss / Karin Dahmen / Stefan Sandfeld)
- **Mechanics of Thin Films**
  (*Graham Cross* / Joseph Paulsen / Paul McEuen)
- **Shear Transformations and Deformation Twinning**
  (*Jon Molina-Aldareguia* / Jafaar El-Awady / Irene Beyerlein / Dierk Raabe)
- **Micromechanics of Fracture and Failure at Interfaces**
  (*Robert Cook* / Igor Zlotnikov / Erik Bitzek / Robert Ritchie)
- **Scaling Up: "Small" for the Sake of "Big"**
  (*Kevin Hemker* / Paul Shade / Tresa Pollock)
- **Advances in the Micromechanics of Functional Materials**
  (*Nancy Sottos* / Katia Bertoldi)
- **Keynote Session: Micromechanics for Evolutionary Insight into Dinosaurs**
  (*Erica Lilleodden* / Greg Erickson)

Thin Film & Small Scale Mechanical Behavior
New Insights into Understanding the Limits of Small
Jul 23-24, 2016
Chairs: Julian E.C. Sabisch & Paula O. Guglielmi

Thiol-Based Redox Regulation & Signaling

Thiols in Biology and Medicine: Innovations Driving Disease Prevention, Therapeutics and Quality of Life
Aug 7-12, 2016
Stoweflake Conference Center, Stowe, VT
Chair: Cristina M. Furdui
Vice Chair: Tobias Dick

- **Keynote Session: A Sulfur-Centered World: From Primordial Chemistry to Human Biology**
  (*Tobias Dick, Cristina Furdui* / Ruma Banerjee / Michel Toledano)
- **Emerging Chemical, Omics and Computational Tools for Redox Biologists**
  (*Vsevolod Belousov, Christopher Chang* / Dean Jones / Harry Ischiropoulos / Melissa Kemp / Eranthie Weerapana / Milos Filipovic / Hadley Sikes)
- **Essential Function of H_2S and Other S-Containing Biomolecules in Human Health and Biology**
  (*Vadim Gladyshev, Ming Xian* / James Mitchell / Ed Schmidt / Beatriz Alvarez)
- **Exploiting Redox Effects in Modern Therapeutics**
  (*Kate Carroll, Arne Holmgren* / David Boothman / Brion Murray / Daret St. Clair / Martin Bergo)
- **Redox Regulation of Cellular Communication**
  (*Thomas Michel, Sue Goo Rhee* / Agnieszka Chacinska / Michael Ristow / Patricia Zambryski)
- **Case Studies in Redox Control of Signaling, Metabolism and Epigenetics**
  (*Elena Hidalgo, Leslie Poole* / Jose Antonio Barcena / Myra Conway / Ana Denicola / Malcolm Jackson)
- **Signaling Mediated by Reactive Oxygen, Nitrogen and Sulfur Species**
  (*Roberto Sitia, Christine Winterbourn* / Takaaki Akaike / Kwang-Hyun Cho / Elizabeth Veal / Gary Loake)
- **Redox Research at the Interface of Environment, Aging and Cancer**
  (*Ursula Jakob, W. Todd Lowther* / Anna Rubartelli / Mary Helen Barcellos-Hoff / Rafael De Cabo / David Gius)
- **Thiols and Antioxidant Defense in Bacteria and Plants**
  (*Luise Krauth-Siegel, Andreas Meyer* / Joris Messens / Aaron Wright)
- **Power Hour**
  (*Melissa Kemp, Kate Carroll*)

Thiol-Based Redox Regulation & Signaling
Redox Biology in Diseases of Aging: Fundamental Mechanisms and Therapeutic Potential
Aug 6-7, 2016
Chairs: Edward T. Chouchani & Jade T. Mims

Three Dimensional Electron Microscopy

Advancing and Reshaping Structural Biology with Electron Cryo-Microscopy
Jun 19-24, 2016
The Chinese University of Hong Kong, Hong Kong, China
Chair: Yifan Cheng
Vice Chair: John Briggs

- **Keynote Session: Reshaping Structural Biology with Cryo-EM**
  (*Yifan Cheng* / Stephen Harrison / Richard Henderson)
- **Methodologies that Drive the Field Forward**
  (*Keiichi Namba* / David Agard / Joachim Frank / Sjors Scheres)
- **Validation of Cryo-EM Structures, from Maps to Atomic Models**
  (*John Rubinstein* / Irina Serysheva / Jiawei Wang)
- **Structures that Are Beyond the Reach of X-Ray Crystallography**
  (*Thomas Walz* / Yigong Shi / Eva Nogales / Huilin Li)
- **Selected Poster Presentations: Recent Advances in Cryo-EM**
  (*Robert Glaeser*)
- **Structures in the Cellular Context**
  (*Karen Davies* / John Briggs / Elizabeth Villa)
- **Strategies for Improving Cryo-EM Sample Preparation and Quality**
  (*Lori Passmore* / Bridget Carragher)
- **Emerging New Cryo-EM Technologies**
  (*Peijun Zhang* / Radostin Danev / Tamir Gonen / Yoshinori Fujiyoshi)
- **Selected Poster Presentations: Recent Advances in the Application of Cryo-EM Methodology**
  (*Sharon Wolf*)
- **Power Hour**
  (*Eva Nogales, Bridget Carragher*)

Tissue Niches & Resident Stem Cells in Adult Epithelia

NEW!

Regulation of Tissue Homeostasis by Signaling in the Stem Cell Niche
Aug 7-12, 2016
The Hong Kong University of Science and Technology, Hong Kong, China
Chairs: Tudorita Doina Tumbar & Rongwen Xi
Vice Chairs: Carla Kim & Jane E. Visvader

- **Keynote Session: Signaling Unity Within Epithelial Stem Cell Diversity**
  (*Allan Spradling* / Hans Clevers / Roeland Nusse)
- **Epidermal Stem Cells and Their Skin Niches**
  (*Fiona Watt* / Howard Chang / Pritinder Kaur / Valerie Horsley / Fiona Watt)
- **Reconstructing the Eye from Epithelial Stem Cells**
  (*Michele De Luca* / David Schwartz / Michele De Luca)
- **Hair Follicle Stem Cells**
  (*George Cotsarelis* / Xing Dai / Sung-Jan Lin / Ting Chen / George Cotsarelis)
- **Lung Stem Cells**
  (*Brigid Hogan, Carla Kim* / Jayaraj Rajagopal / Barry Stripp / Brigid Hogan)
- **Gastrointestinal Stem Cells**
  (*Bruce Edgar* / Tony Ip / Heinrich Jasper / Nick Barker / Bruce Edgar)
- **Stem Cells of Transitional Zones**
  (*Alexander Nikitin* / Frank McKeon / Geraldine Guasch / Alexander Nikitin)
- **Mammary, Prostate, and Ovarian Stem Cells**
  (*Michael Shen, Jane Visvader* / Li Xin / Arial Zeng / Michael Shen / Allan Spradling)
- **Epithelial Stem Cells of Oral and Craniofacial Complex**
  (*Ophir Klein* / Catherine Ovitt / Yang Chai / Ophir Klein)

Transglutaminases in Human Disease Processes

Understanding the Varied Pathological Roles of a Multifunctional Enzyme Family
Jul 10-15, 2016
PGA Catalunya Business and Convention Centre, Girona, Spain
Chair: Timothy Johnson
Vice Chair: Mari T. Kaartinen

- **Keynote Session: Transglutaminases: Multifaceted Enzymes with Multiple Roles in Disease Processes**
  (*Timothy Johnson* / Mauro Piacentini / Kapil Mehta / Benjamin Drukarch)
- **Modulators, Structures and Substrates of Transglutaminases**
  (*Jeffrey Keillor* / Christopher Clouthier / Muriel Maurer / Candace Kerr / Laszlo Fesus / Brad Palanski)
- **The Function of Transglutaminases in Cardiovascular Disease**
  (*Dan Berkowitz* / Erik Bakker / Maria Nurminskaya / Lakshmi Santhanam)
- **Transglutaminases in Tissue Remodeling, Fibrosis and Scarring**
  (*Patricia Sime* / Martin Griffin / Elisabetta Verderio / David Abraham / Barry Fanburg / Timothy Johnson)
- **Do Transglutaminases Play a Role in Immunology and Rheumatology?**
  (*Riccardo Ientile* / Zsuzsa Szondy / Daniela Caccamo / Patrick Schloss)
- **What Role Do Transglutaminases Play in Neurological Disease?**
  (*Anne-Marie Van Dam* / Scott Brady / Katsuhiko Mikoshiba / Micha Wilhelmus / M. Maral Mouradian / Daniel Aeschlimann)
- **Celiac Disease, Gastroenterology and Transglutaminases**
  (*Katri Lindfors* / Ludvig Sollid / Aaron Lerner / Renato Monteiro)
- **Transglutaminases in Oncology**
  (*Daniela Matei* / Richard Eckert / Salvatore Condello / Wenguo Jiang)
- **The Contribution of Transglutaminases to Connective Tissue Disorders**
  (*Mari Kaartinen* / Matthew Flick / Huifang Sun / Martine Charbonneau)

Tribology

Scientific Advancements for Critical Applications in Friction, Lubrication, and Wear
Jun 26 - Jul 1, 2016
Bates College, Lewiston, ME
Chair: Robert W. Carpick
Vice Chair: Ashlie Martini

- **Tribology Controversies: Shear Flow, and Rough Contact**
  (*Juliette Cayer-Barrioz* / Mark Robbins / Martin Mueser)
- **Tribology from Geo to Nano: Rate, State, and Scale Dependence**
  (*Izabela Szlufarska* / Emily Brodsky / Nadia Lapusta / Maarten De Boer)
- **Tribology of Metals**
  (*Andrew Jackson* / Srinivasan Chandrasekar / Nicolas Argibay / Michael Chandross)

- **Triboelectricity**
  (*Roland Bennewitz* / Thomas Reddyhoff / Zhong-Lin Wang)
- **Soft Materials: Rheology Meets Tribology**
  (*Rosa Espinoza-Marzal* / Jacob Israelacvhili / W. Gregory Sawyer / Janet Wong)
- **Next Generation Lubricants**
  (*Susan Perkins* / Rob Atkin / Jun Qu / Olga Shenderova)
- **Ultralow Friction: Materials and Mechanisms**
  (*Lars Pastewka* / Quanshui Zheng / Vladan Vuletic / Diana Berman)
- **Tribology in Material Modification: From Nanomanufacturing to Machining**
  (*Dalia Yablon* / Armin Knoll / Lars Pastewka)
- **Keynote Session: Friction and Seismology**
  (*Ashlie Martini* / James Rice)

Tribology
Multi-Scale Challenges in Tribology: Implications for Fundamental Research and Industrial Applications
Jun 25-26, 2016
Chairs: Xin Liu & Emily E. Hoffman

Two Dimensional Electronics Beyond Graphene

NEW!

Exploring and Utilizing Electronic Properties of 2D Systems
Jun 5-10, 2016
Mount Holyoke College, South Hadley, MA
Chairs: David Tomanek & Janice L. Musfeldt
Vice Chairs: Philip Kim & James Hone

- **Unique Electronic and Thermal Transport in 2D Systems**
  (*Jeanie Lau* / Michael Fuhrer / Li Shi)
- **Synthesis of Layered and 2D Materials**
  (*Pulickel Ajayan* / David Mandrus / Ji-Woong Park / Scott Warren)
- **Characterization of 2D Materials**
  (*Marcos Pimenta* / Janina Maultzsch / Luis Balicas)
- **Theory and Modeling of 2D Materials**
  (*Gotthard Seifert* / Steven Louie / Thomas Heine / Di Xiao)
- **Optoelectronics and Photonics with 2D Materials**
  (*Tony Heinz* / Fengnian Xia / Feng Wang)
- **Manipulation and Passivation of 2D Materials**
  (*Paul McEuen* / Yoshihiro Iwasa / Zhixian Zhou / Cory Dean)
- **Spintronics and Valleytronics with 2D Materials**
  (*Roland Kawakami* / Scott Crooker / Kin Fai Mak)
- **Electronic Devices Based on 2D Systems**
  (*Peide Ye* / P. Jarillo-Herrero / Deji Akinwande / Kaustav Banerjee)
- **Complex Phenomena in 2D Materials**
  (*Sang-Wook Cheong* / Abhay Pasupathy / Han-Woong Yeom)
- **Power Hour**
  (*Janice Musfeldt*)

Unifying Ecology Across Scales

Linking the Levels from Physiological to Ecosystem Ecology
Jul 24-29, 2016
University of New England, Biddeford, ME
Chair: Richard M. Sibly
Vice Chair: Mary I. O'Connor

- **Making Links Between Physiological, Behavioral, Population, Community and Ecosystems Ecology**
  (*Mary O'Connor* / James Brown / Roger Nisbet)
- **Metabolic Traits and Biotic Interactions**
  (*Gabriel Yvon-Durocher* / Mark Bradford / Thomas Bell / Anita Narwani / Mridul Thomas / Elisa Schaum)
- **Linking Ecological, Evolutionary and Ecosystem Dynamics**
  (*Samraat Pawar* / Gabriel Yvon-Durocher / Michael Follows)
- **Linking the Levels Using Individual Based Models (IBMs)**
  (*Roger Nisbet* / Volker Grimm / Steve Railsback / Richard Sibly / Elske van der Vaart)
- **New Insights from Individual Based Models**
  (*Volker Grimm* / Jaclyn Matthes)
- **Biological Allometry - Organismal Form, Function, and Evolution**
  (*Van Savage* / Brian Enquist / Chris Doughty / Cyrille Violle / Lisa Bentley)
- **Biological Allometry - Constraints on Ecosystem Functioning and Biological Diversity**
  (*Brian Enquist* / Van Savage)
- **Stoichiometry in Ecological Interactions and Evolutionary Dynamics**
  (*Angelica Gonzalez* / Michelle Evans-White / Kathleen Treseder / Caroline Turner / Arianne Cease / Krista Capps / Jim Heffernan)
- **Stoichiometry from Ecosystems to Molecules**
  (*Richard Sibly* / Michael Lomas / Mary O'Connor)
- **Power Hour**
  (*Mary O'Connor, Angelica Gonzalez*)

Unifying Ecology Across Scales
Linking the Levels from Physiological to Ecosystem Ecology: Identifying Challenges and Opportunities
Jul 23-24, 2016
Chairs: Jessica R. Corman & Jessica R. Coyle

Conferees are excited to board a ferry to Boston for an afternoon exploring the city.

Vibrational Spectroscopy

Vibrational Structures and Dynamics
Jul 17-22, 2016
University of New England, Biddeford, ME
Chairs: Elsa C.Y. Yan & Victor S. Batista
Vice Chairs: Andrew Orr-Ewing & Nien-Hui Ge

- **Vibrational Dynamics in Isolated Molecules and Clusters**
  (*Mark Johnson* / Gary Douberly / Etienne Garand)
- **Vibrational Structures and Dynamics at Interfaces**
  (*Dennis Hore* / Alex Benderskii / Mischa Bonn / Eric Tyrode / Eric Borguet)
- **Energy and Materials: Simulations and Experiments**
  (*Carlos Silva* / Munira Khalil / Francesco Paesani)
- **Ultrafast Vibrational Dynamics and Energy Transfer**
  (*Fleming Crim, Arthur Utz* / Jahan Dawlaty / Philipp Kukura / Erik Nibbering / Julia Weinstein)
- **Theory and Computation of Vibrational Structures and Dynamics**
  (*Ned Sibert* / Marie-Pierre Gaigeot / Shaul Mukamel)
- **Vibrational Structures and Dynamics of Biomacromolecules**
  (*Judy Kim, Lauren Webb* / Bridgette Barry / Chris Cheatum / Chong Fang / Susan Quinn)
- **Chiral Vibrational Structures and Dynamics**
  (*Hongfei Wang* / Yunjie Xu / Wei Zhuang)
- **Energy and Materials: Vibrational Dynamics**
  (*Tim Lian, David Moore* / John Asbury / Art Bragg / Tamar Seideman / Jaime Stearns)
- **Gas Phase and Atmospheric Vibrational Dynamics**
  (*Franz Geiger* / Marsha Lester / Tim Zwier)

Vibrational Spectroscopy
Molecular Vibrations as Spectroscopic Probes of Chemical Dynamics
Jul 16-17, 2016
Chairs: Adam Dunkelberger & Brett M. Marsh

Visual System Development

Circuits, Evolution and Disease in Visual System Development
Aug 7-12, 2016
Mount Snow, West Dover, VT
Chair: Nadean Brown
Vice Chair: Graeme Mardon

- **Keynote Session: Frontiers in Visual System Development and Disease**
  (*Nadean Brown, Graeme Mardon* / Patricia D'Amore / Carla Shatz)
- **Model Organism Genetics in Visual System Development**
  (*Ruth Ashery-Padan* / Hugo Bellen / Jessica Triesman / Joseph Brzezinski / Brian Link)
- **Regenerating Vision**
  (*Valerie Wallace* / Daniel Goldman / Katia Del Rio-Tsonis / Ryan Thummel)
- **Stem Cells to Organs**
  (*Jane Sowden* / Valeria Canto-Soler / Anna La Torre / Guillermo Oliver / Jane Sowden)
- **Circuitry, Synapses and Biologic Clocks**
  (*Claude Desplan* / Sujata Rao / Steven Altshuler / Iris Selecker)
- **Ocular Disease Mechanisms**
  (*Shiming Chen* / Brian Brooks / Rui Chen / Brian Perkins)
- **Non-Neural Cells and Tissues**
  (*Ales Cvekl* / Melinda Duncan / Marek Mlodzik / Sabine Fuhrmann)
- **Conserved Mechanisms of Gene Regulation**
  (*Zbynek Kozmik* / Xin Zhang / Monica Vetter / Nicholas Baker / Joseph Corbo)
- **Evolutionary Changes to the Visual System**
  (*Dan-Eric Nilsson* / William Jeffreys / Megan Porter / Dan-Eric Nilsson)
- **Power Hour**
  (*Sabine Fuhrmann, Tiffany Cook*)

Visual System Development
Fundamental Mechanisms Underlying Health and Disease in Visual System Development
Aug 6-7, 2016
Chair: Mark A. Charlton-Perkins

Water & Aqueous Solutions

Fundamental Properties and Real Applications of Water: A Ubiquitous and Enigmatic Substance
Jul 31 - Aug 5, 2016
Holderness School, Holderness, NH
Chair: Nancy E. Levinger
Vice Chair: Alenka Luzar

- **Water Properties from Fundamental Studies**
  (*Francesco Paesani* / Michael Duncan / Sortiris Xantheas)
- **How Water Drives Biology**
  (*Sihyun Ham* / Bertil Halle / Martina Havenith / Joan-Emma Shea / Steven Corcelli)
- **Extreme Environments**
  (*Nancy Levinger* / Livia Bove / Fabio Sterpone)
- **Water in the Environment**
  (*Cari Dutcher* / Valeria Molinero / Margaret Tolbert)
- **How Biology Drives Water**
  (*Damien Laage* / Gregory Voth)
- **Touching Water: Surfaces and Interfaces**
  (*Heather Allen* / Franz Geiger / Amber Krummel / James Skinner / M. Scott Shell)
- **The Love-Hate Relationship of Water with Charges**
  (*Revati Kumar* / Pavel Jungwirth / Minhaeng Cho)
- **Nucleation and Ice**
  (*Dor Ben-Amotz* / Mary Jane Shultz / Sapna Sarupria)
- **From Water Molecules to Water Issues in the Real World**
  (*Veronica Vaida* / Peter Rossky / Maureen McCarthy)

Water & Aqueous Solutions
Studying Water Properties at Multiple Time and Length Scales
Jul 30-31, 2016
Chairs: Jana Hladilkova & Sebastian Busch

What if you could...

- use up to **44% less plastic** for your nucleic acid purification*
- **recycle ALL** of your packaging and plastics
- AND, still recover the same **highly pure DNA**?

Now, you can.

NEW ENGLAND BioLabs® Inc.

It's time for change.

Introducing Monarch™ Nucleic Acid Purification Kits

It's time to transform your DNA purification experience. NEB's Monarch Nucleic Acid Purification Kits are optimized for maximum performance and minimal environmental impact. With an innovative column design, buffer retention is prevented, eliminating risk of carryover contamination and enabling elution in smaller volumes. The result – highly pure DNA for your downstream applications.

Make the change and migrate to Monarch today.

Optimized design of Monarch Miniprep Columns

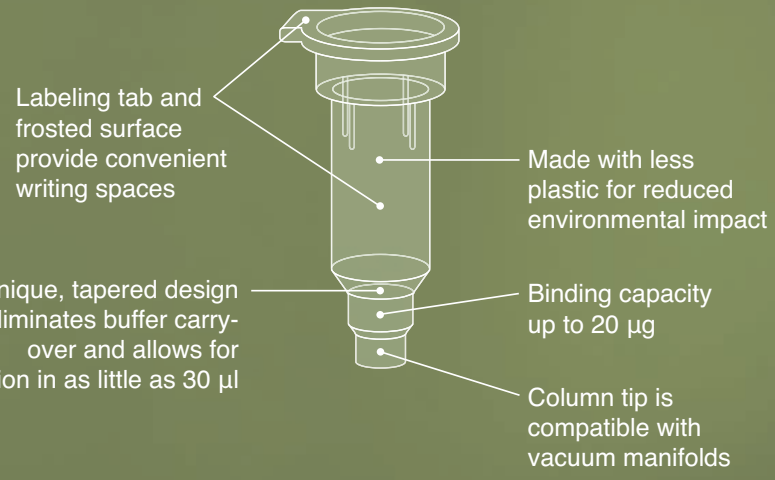

Request your free sample at **NEBMonarch.com**

NEW ENGLAND BIOLABS® and NEB® are registered trademarks of New England Biolabs, Inc.
MONARCH™ is a trademark of New England Biolabs, Inc.
*Visit NEBMonarchPackaging.com for details.

Let your work flow.

Introducing MiniSeq. Our simplest, most affordable sequencing solution yet.

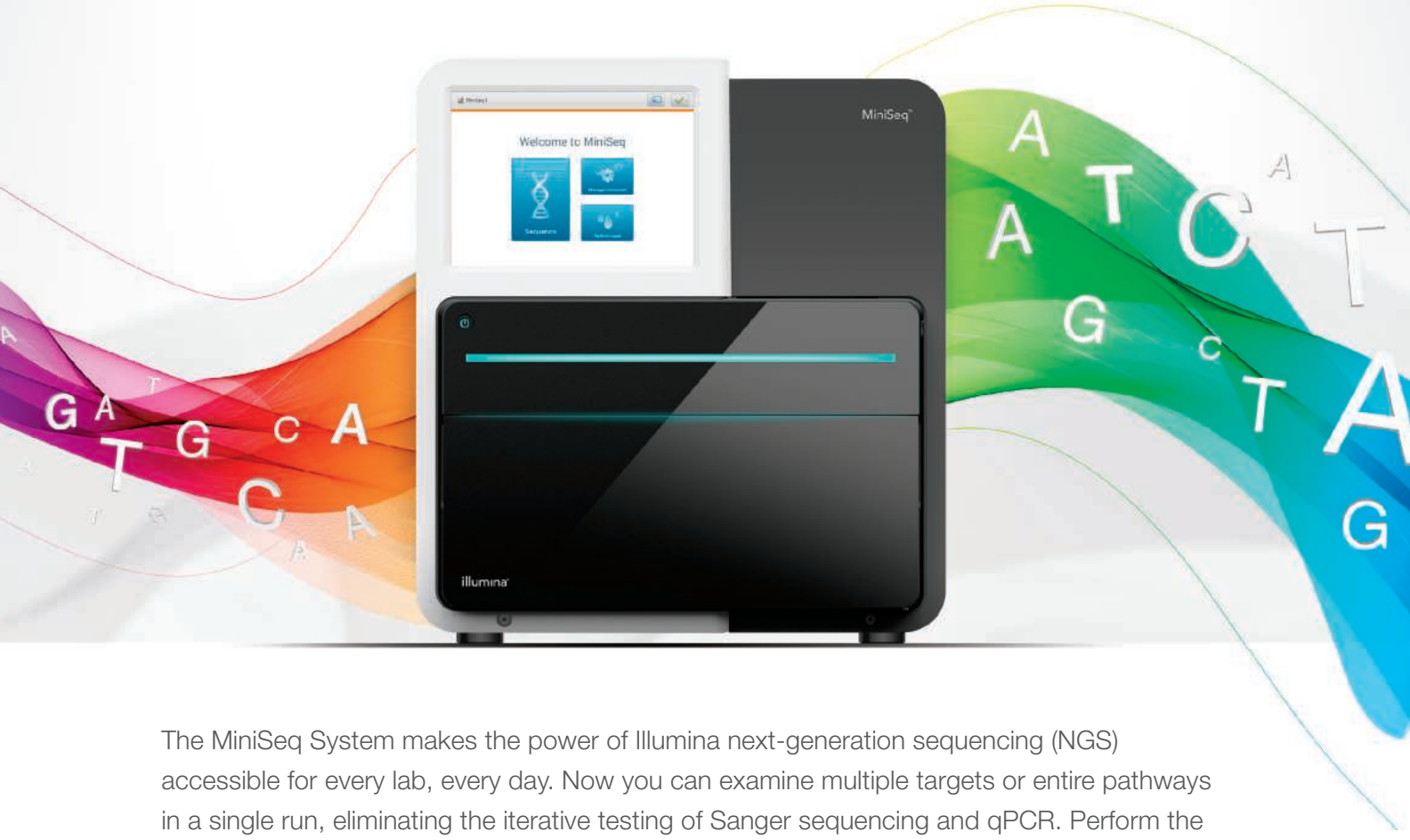

The MiniSeq System makes the power of Illumina next-generation sequencing (NGS) accessible for every lab, every day. Now you can examine multiple targets or entire pathways in a single run, eliminating the iterative testing of Sanger sequencing and qPCR. Perform the most popular NGS applications in your own lab with this walk-away, library-to-results solution.

Explore NGS that fits your bench and your budget.

www.illumina.com/miniseq

For Research Use Only. Not for use in diagnostic procedures.

©2016 Illumina, Inc. All rights reserved.

illumina®

2016 (32nd) Japan Prize Laureates

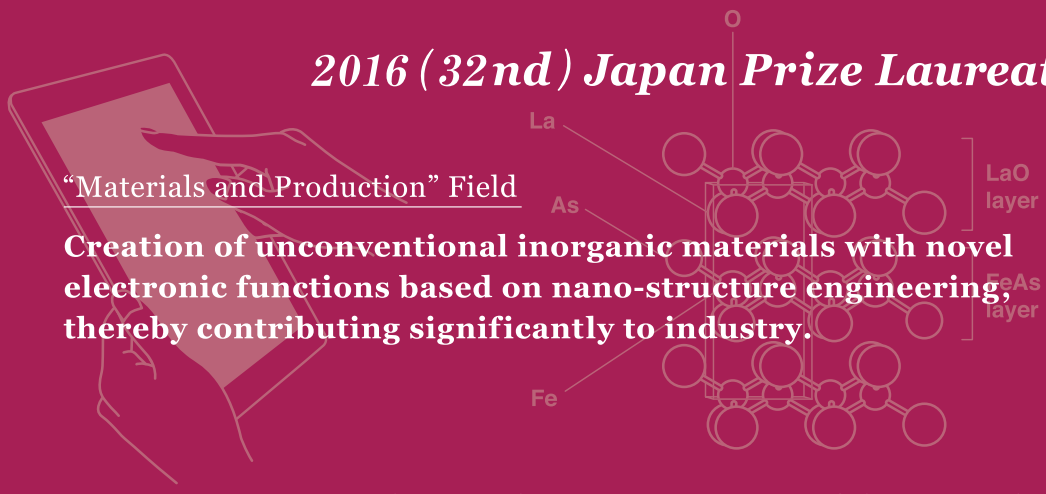

"Materials and Production" Field

Creation of unconventional inorganic materials with novel electronic functions based on nano-structure engineering, thereby contributing significantly to industry.

Dr. Hideo Hosono, Japan

How they have contributed to the peace and prosperity of mankind through science and technology?

Dr. Steven D. Tanksley, USA

"Biological Production and Biological Environment" Field

Contribution to modern crop breeding through research on development of molecular genetic analysis, thereby contributing profoundly to the stable production of food crops in the world.

Japan prize selection criteria

The Japan Prize is awarded to scientists and engineers from around the world who are recognized as having achieved original and dramatic accomplishments that greatly enhance the progress of science and technology, thereby contributing to the peace and prosperity of mankind.

JAPAN PRIZE

▶ Visit for details on the Japan Prize and its laureates
www.japanprize.jp

JAPAN PRIZE

eppendorf & Science

PRIZE FOR NEURO BIOLOGY

2015 Winner
Shigeki Watanabe, Ph.D.
Johns Hopkins University
For research on synaptic vesicle endocytosis

Application Deadline
June 15, 2016

Call for Entries

Eppendorf & Science Prize for Neurobiology
The annual Eppendorf & Science Prize for Neurobiology is an international award which honors young scientists for their outstanding contributions to neurobiological research based on methods of molecular and cell biology. The winner and finalists are selected by a committee of independent scientists, chaired by Science's Senior Editor, Dr. Peter Stern. Researchers who are not older than 35 years are invited to apply.

You could be next to win this prize and to receive
> Prize money of US$25,000
> Publication of your work in Science
> Full support to attend the Prize Ceremony held in conjunction with the Annual Meeting of the Society for Neuroscience in the USA
> An invitation to visit Eppendorf in Hamburg, Germany

It's easy to apply!
Learn more about the Prize and its past winners at:

www.eppendorf.com/prize

eppendorf Science AAAS

AAAS® and Science® are registered trademarks of the American Association for the Advancement of Science, USA. Eppendorf® and the Eppendorf logo are registered trademarks of Eppendorf AG, Germany. U.S. Design Patents are listed on www.eppendorf.com/ip. All rights reserved, including graphics and images. Copyright © 2016 by Eppendorf AG. Kurstin Roe Photography.

Cambridge Healthtech Institute's 23rd International

Molecular Med TRI-CON 2016

March 6 - 11, 2016 | Moscone North Convention Center | San Francisco, CA

With 400+ Presentations and Panel Discussions Covering:

- DIAGNOSTICS
- CANCER
- GENOMICS
- INFORMATICS

EXHIBIT HALL IS ALMOST SOLD-OUT!

To secure your sponsorship or exhibit package, contact:

Companies A-K
Jon Stroup
Senior Manager,
Business Development
781-972-5483
jstroup@healthtech.com

Companies L-Z
Joseph Vacca
Associate Director,
Business Development
781-972-5431
jvacca@healthtech.com

REGISTER EARLY FOR MAXIMUM SAVINGS!

Mention Keycode **L35** when registering.

TriConference.com

LIFE SCIENCE TECHNOLOGIES
GENOMICS

Hard-core sequencing

For many molecular biologists, a specimen that is too degraded for easy DNA sequencing is a minor annoyance, but samples isolated from rare sources present unique obstacles. As sequencing technology steadily improves, such irremediably difficult samples have gradually begun yielding usable sequences.

See the full story on page 772.

Upcoming Features
Tissue Analysis—March 4
General Lab Equipment—April 29
Microscopy—May 13

Produced by the *Science*/AAAS Custom Publishing Office

AAAS *Travels*

Discover Spitsbergen & the Arctic!

TO THE EDGE OF THE ARCTIC ICE

August 27–September 8, 2016
on board M/V *Plancius*

An outstanding itinerary for polar bears, glaciers and the geology of Spitsbergen, and an excellent opportunity to learn about climate change in the Arctic. See polar bears, ringed and bearded seals, walrus, feeding baleen whales, and spectacular glaciers. Also see bird rookeries, historic encampments, sky blue glaciers, carved icebergs, scenic ice falls & waterfalls—an Arctic paradise! From $5,795 + air.

For a detailed brochure, call (800) 252-4910
All prices are per person twin share + air

BETCHART EXPEDITIONS INC.
17050 Montebello Rd, Cupertino, CA 95014
Email: AAASInfo@betchartexpeditions.com
www.betchartexpeditions.com

Museum specimen of *Dryococelus australis*

Hard-core sequencing

For many molecular biologists, a specimen that is too degraded for easy DNA sequencing is a minor annoyance. They simply prepare another, better sample from the abundant source material they have on hand in cultured cells, laboratory animals, or a freezer full of tissues. But what if the only available specimen is an arsenic-preserved pelt from 150 years ago, a pile of mummified dung found in a cave, or a single formalin-fixed pathology slide? As sequencing technology steadily improves, such irremediably difficult samples have gradually begun yielding usable sequences. **By Alan Dove**

The goals of these hard-core sequencing projects range from studying climate change, to classifying—or even resurrecting—extinct species, to improving cancer diagnosis. Nonetheless, they share many of the same challenges, as stored DNA breaks down into progressively smaller fragments over time. Moreover, standard preservatives or compounds in the environment chemically modify the nucleic acids, thereby making modern sequencing techniques produce vast quantities of often cryptic data. Despite those barriers, scientists and equipment makers are pushing sequencing techniques steadily forward, often with surprising results.

Not dead yet

In 2001, a team of scientists visiting Ball's Pyramid, an isolated rock spire off Lord Howe Island in the Tasman Sea, discovered the world's rarest invertebrate: an apparent relict population of two dozen Lord Howe Island stick insects (*Dryococelus australis*). Once abundant on their nearby namesake island, the insects went extinct there shortly after the introduction of rats in 1918. The population on Ball's Pyramid looks like the same species, but to be sure, researchers want to compare its DNA to that of museum specimens collected over a century ago.

For Alexander Mikheyev, assistant professor in the ecology and evolution unit at the **Okinawa Institute of Science and Technology** in Okinawa, Japan, it's a familiar problem. "Nothing I work with is really preserved well, but there's some bad and some really bad," says Mikheyev, who specializes in sequencing preserved insects. The *D. australis* samples he hopes to analyze have been stored dried on pins in museum drawers.

Old specimens' DNA is typically fragmented into small pieces. "This is where next-gen[eration sequencing] technology comes to help us, because it's actually good at sequencing small pieces and lots of them," says Mikheyev. A trickier problem is that old DNA, especially in samples preserved with alcohol or other fixatives, tends to become chemically derivatized, changing both the backbone structure and apparent base sequence. After a simple DNA preparation, researchers use polymerase chain reaction (PCR) to amplify a library of all the fragments in the sample. The PCR process often substitutes incorrect bases for ones that have been chemically derivatized. "Once you have prepared your library, you also have to make sure that when you analyze it you're not introducing a lot of biases as a consequence of these postmortem information content changes," Mikheyev adds.

The internal quality controls built into sequencing systems don't help with these types of artifacts. "The sequencer confidently substitutes [bases] and tells you with great certainty the wrong answer," says Mikheyev.

Investigators typically control for such biases by comparing their sequence reads to known sequences from the same or a closely related species. "In insects this could be a huge problem, because insects are highly polymorphic genetically," says Mikheyev. With the high background level of polymorphism, postmortem changes in the DNA can make sequences from long-dead animals hard to align with those of freshly sampled ones. Sequencing multiple specimens to establish population-level statistics can help reduce those errors. For *D. australis*, a successful captive breeding program means that at least the Ball's Pyramid population will be relatively easy to sample.

With a badly degraded sample, researchers may also need to apply extremely rigorous statistical filters, discarding the overwhelming majority of the raw data from the sequencer in order to generate an accurate final sequence. Patience and flexibility also help. "For a lot of these methods, there really are no established protocols," says Mikheyev, adding that "every sample is going to have its own challenges."

Besides having degraded DNA, preserved museum specimens are often irreplaceable. "We were able to analyze one specimen collected by Alfred Russel Wallace in 1860 in Raja Ampat during his travel through the 'Malay Archipelago,'" says Guillaume Besnard, a researcher at the **Laboratory of Evolution and Biological Diversity** at the Université Paul Sabatier in Toulouse, France. To conserve

PHOTO: Y. N. SU, AUSTRALIAN NATIONAL INSECT COLLECTION, COMMONWEALTH SCIENTIFIC AND INDUSTRIAL RESEARCH ORGANISATION

Upcoming Features
Tissue Analysis—March 4 ■ *General Lab Equipment—April 29* ■ *Microscopy—May 13*

Featured Participants

Aarhus University Hospital
www.en.auh.dk

Cancer Research UK Cambridge Institute
www.cruk.cam.ac.uk

Illumina
www.illumina.com

Laboratory of Evolution and Biological Diversity, Université Paul Sabatier
www.edb.ups-tlse.fr/Laboratory-Evolution-and?lang=en

McMaster University
www.mcmaster.ca

New England BioLabs
www.neb.com

Okinawa Institute of Science and Technology
www.oist.jp

Thermo Fisher Scientific
www.thermofisher.com

the famous naturalist's specimen, a southern crowned pigeon (*Goura scheepmakeri*), Besnard and his colleagues snipped a tiny piece of dried flesh from the bird's toe pad. They chose this region because it has a large number of cells and because the bird's feet hadn't been treated with arsenic, leaving the DNA there in better shape than on the rest of the preserved carcass.

In their studies on phylogenetics and biogeography, Besnard and his colleagues have also sequenced DNA from preserved plants in herbaria. "For plants, usually we choose one leaf as green as possible," says Besnard, but he adds that seeds are also good sources for DNA. In all cases, he says, "I recommend choosing the best samples that are as young as possible, collected and preserved in good conditions."

After identifying a suitable sample and designing a general strategy, Besnard says researchers should test their plan on easily replaced specimens. That will allow them to refine their techniques and ensure that they only have to dip into the valuable specimen once. "Depending on the research questions, it may also be important to define the appropriate strategy to use, either whole-genome sequencing or just targeting some genomic regions with a gene baiting approach," says Besnard. In gene-baiting, scientists use targeted PCR primers to amplify specific genes during the library preparation step, rather than amplifying all of the DNA fragments in the sample.

Focusing on specific genes or regions is an especially good strategy for taxonomy projects, where variation in a few genes is often sufficient to place an organism on a phylogenetic tree. "We generally focus on abundant genomic regions such as organellar DNA, and when sequencing depth is sufficiently high, it's relatively easy to assemble high-quality sequences," says Besnard. Sequencing nuclear genomes requires sequencing the DNA library many times over, increasing the "depth" of sequence reads at each base. This procedure amplifies both the valid and invalid data, though, so researchers have to apply more stringent filters to their results.

Rare samples also need to be analyzed in a clean environment to minimize contamination. Even so, investigators should expect to spend some time scrubbing bacterial and fungal sequences out of their data. Sequencing-equipment vendors can help researchers choose appropriate bioinformatics algorithms for all of these analyses.

Data dumps

Ironically, some of the best DNA sources for extinct species and ancient humans are specimens nobody has tried to preserve. Dried feces from caves and pit toilets have proven especially fruitful. In a dry environment, the Maillard reaction—the same chemical process that browns a steak—causes feces to develop a protective outer shell. The resulting paleofeces can survive for centuries, encapsulating a mixed pool of DNA that includes cells from the animal that produced it, as well as a sampling of the animal's diet.

Hendrik Poinar, professor of physical anthropology at **McMaster University** in Hamilton, Ontario, was one of the first researchers to dig into this trove of data. Since the late 1990s, Poinar and his colleagues have analyzed everything from ancient human to extinct ground sloth samples. Besides paleofeces, the team has also successfully sequenced DNA from animal carcasses found in Arctic permafrost, including woolly mammoths.

Poinar says that "the technology has changed dramatically" since he started, adding that "everything for the copying and the sequencing of those molecules has grown at an exponential rate, so we're doing things now that I couldn't envision we could do even [a few] years ago." Despite the progress in sequencing technology, however, Poinar says he's frustrated that the tools for preparing the samples have hardly changed. "I think the access to samples in both deeper time and from more complicated remains is still a limiting factor because of these rather rudimentary extraction techniques," he says. Standard laboratory DNA isolation methods, such as sonication, ribonuclease (RNase) treatment, and ethanol precipitation may reduce the available pool of DNA enough to prevent recovering usable sequences from the oldest samples.

Investigators studying paleofeces and other unpreserved samples also face thoroughly degraded DNA. Indeed, some of the breakdown products occur often enough to be useful internal controls. Poinar's team has cataloged specific degradation artifacts that can distinguish ancient from modern DNA. "We use that as a way to say, 'This is real to the sample, and is not a modern contaminant coming in,'" says Poinar.

Scientists who sequence ancient or preserved specimens seem to favor the **Illumina** next-generation platform to perform the sequencing itself, though **Thermo Fisher Scientific's** IonTorrent offers similar capabilities. Poinar says the choice is largely a matter of convenience: "The platforms themselves are not going to make any difference as far as I can tell; the difference will be the repair of the molecules that come from your extracts, and then the library prep that's done." continued>

"I recommend choosing the best samples that are as young as possible, collected and preserved in good conditions."
— Guillaume Besnard

For researchers just starting to explore ancient samples, Poinar echoes Mikheyev's advice to be flexible. "Play around a bit; I think the biggest issue that people have is they're just using standardized methods for extraction of samples, and I don't think that's very successful," says Poinar.

Pathological fixations

Although a pile of dung from a cave poses serious analytical challenges, it's probably not the most difficult specimen researchers are sequencing now. Instead, one of the most challenging types of samples is also the kind biomedical researchers are most likely to find interesting: formalin-fixed, paraffin-embedded (FFPE) tissue.

Pathologists and histologists have been fixing tissues with formalin for more than a century, and FFPE sections are a mainstay of clinical pathology labs. The technique is simple and robust. Unfortunately, this robustness promotes a casual attitude toward fixation. "In some cases the sample may have been fixed for several days or over the weekend; in other cases it may be just overnight, so there's a big difference between the samples," says Jakob Hedegaard , a postdoctoral fellow in the Department of Molecular Medicine at **Aarhus University Hospital** in Aarhus, Denmark who has worked extensively with FFPE samples.

Varying the fixation time has little or no effect on a tissue's morphology, but it plays havoc at the molecular level. Over time, formalin crosslinks proteins in the cells, and fragments and derivatizes both DNA and RNA. Without knowing how long the chemical insult lasted, researchers have a hard time predicting the quality of the DNA they'll recover.

As with other degraded DNA specimens, derivatized bases pose the biggest challenge. The standard library amplification step in most sequencing protocols substitutes erroneous bases for the ones that have been modified, yielding high-quality but incorrect sequences. Investigators then have to filter the raw data to separate real polymorphisms from artifacts. "Fixation-introduced variants tend to be randomly distributed all over the place, so if you sequence very deep, then you should be able to see the true variants and exclude the noise," says Hedegaard, adding that "in general the data are much more noisy when the DNA is of FFPE origin."

Scientists analyzing FFPE tissues usually work with more samples than those studying rare or unusual specimens. For a project on tumor genetics, for example, a team may need to sequence hundreds or thousands of FFPE tissue slices from different patients to find statistically meaningful variations. Even as sequencing costs decline, such high-throughput efforts require pooling the DNA samples.

Hedegaard and his colleagues typically attach specific tags to the DNA from each tissue sample before pooling them, allowing them to sequence numerous specimens in each sequencing run. They then use the tag sequences to separate individual samples from the raw data.

Some molecular biologists may have enough clout to coax pathologists into mending their poorly controlled ways. "The main thing we've been working on over the last 6 to 18 months is to look at how we might improve getting sequenceable samples, and it does seem to be that controlling those fixation steps is going to have a marked impact," says James Hadfield, director of the genomics core for the **Cancer Research UK Cambridge Institute** at the University of Cambridge in Cambridge, United Kingdom.

Hadfield and his colleagues are doing large-scale genomic analyses of different tumor types, as part of the massive Genomics England project to sequence 100,000 British genomes. But even with the leverage of a big, well-supported project, changing old habits is hard. Hadfield says packaging the change as a general quality-control improvement may help: "In our research institute, our histopathology core is very carefully controlled in the time of fixation, [and] being controlled in any scientific or diagnostic process means that things are more robust."

For researchers whose pathology collaborators remain intransigent or those working on historical specimens, equipment and reagent makers may be able to help. Illumina offers a range of microarrays and other tools designed to optimize results from badly degraded FFPE samples, and **New England BioLabs** sells the NEBNext FFPE DNA repair mix, for example.

Hadfield and others are also trying to develop and promote DNA-friendly fixatives that pathologists could use in lieu of formalin. Although that work has produced promising results, Hadfield emphasizes that getting clinical labs to switch from well-tested methods remains a major challenge.

Scientists with very focused projects may also have the option of avoiding genome-level sequencing entirely. Hadfield echoes Besnard's suggestion to amplify and sequence specific genes rather than whole genomes, if that will answer the research question.

Regardless of the types of samples they're sequencing or the strategies they're using, those working with difficult DNA samples agree that the field calls for a strong dose of skepticism. As Mikheyev says, "Always question your data and prove to yourself using some kind of orthogonal method that the data are telling you what you think they're telling you."

Alan Dove is a science writer and editor based in Massachusetts.

DOI: 10.1126/science.opms.p1600102

PHOTO: © ROMAN SAKHNO/SHUTTERSTOCK.COM

Sequencing System

A new nucleic acid sequencing platform, the Sequel System, provides higher throughput, more scalability, a reduced footprint, and lower sequencing project costs compared to the PacBio RS II System, while maintaining the existing benefits of single molecule, real-time (SMRT) technology. The core of the Sequel System is the capacity of its redesigned SMRT Cells, which contain 1 million zero-mode waveguides (ZMWs) at launch, compared to 150,000 ZMWs in the PacBio RS II. Active individual polymerases are immobilized within the ZMWs, providing windows to observe and record DNA sequencing in real time. The system is designed for projects such as rapid and cost-effective generation of high-quality, whole-genome de novo assemblies. The system can also generate data for full-length transcriptomes and targeted transcripts using the company's Iso-Seq protocol. The Sequel System's increased throughput should also facilitate applications of SMRT technology in metagenomics and targeted gene applications for which interrogation of larger numbers of individual DNA molecules is important.

Pacific Biosciences
For info: 650-521-8000
www.pacb.com

DNA Analysis System

The DNAscan 6C Rapid DNA Analysis System increases short tandem repeat (STR) chemistry options with its High DNA Content Flexplex BioChipSet Cassette. The six-dye Flexplex chemistry generates STR profiles containing 27 loci, and as a result is compatible with major DNA databases globally. The new Flexplex assay coamplifies 23 autosomal STR loci, three Y-STR loci, and amelogenin for advanced sample discrimination. Flexplex chemistry offers global compatibility by spanning the extended European Standard Set, the expanded U.S. Combined DNA Index System (CODIS) core loci, and other commonly used region-specific loci. Fully automated, the DNAscan 6C Rapid DNA Analysis System performs sample-in to results-out processing with integrated expert system software, providing high-quality STR profiles for up to five samples in less than 90 minutes. The High DNA Content Flexplex BioChipSet Cassette offers the following features: expanded STR locus set, global compatibility, all-in-one consumable, room temperature storage, closed system for contamination control, and radio frequency identification (RFID) tags for sample tracking.

GE Healthcare Life Sciences
For info: 800-526-3593
www.gelifesciences.com/dnascan

Reference Standards

Cell-free DNA (cfDNA) HDx Reference Standards support the development and optimization of cfDNA assays, which are emerging as an important tool for noninvasive liquid biopsies. cfDNA Reference Standards enable researchers to demonstrate the performance of their cfDNA assays by providing a reproducible, consistent, and reliable source of reference material for their development and evaluation. Created from engineered cell lines, cfDNA Reference Standards are available in both singleplex and multiplex format with cancer-relevant mutations. These reference standards consist of human genomic DNA fragmented to 160 base pairs, representative of plasma-derived cfDNA, and are provided as a set of precisely defined allelic frequencies from as low as 0.1%. A matched wild type is included. These highly characterized standards are able to feed directly into any cfDNA workflow from whole-genome, whole-exome, or amplicon-based next-generation sequencing (NGS) to quantitative polymerase chain reaction (qPCR) and droplet digital PCR (ddPCR) platforms.

Horizon Discovery
For info: 844-655-7800
www.horizondiscovery.com

Transfection Reagent

DNA-In CRISPR is an innovative transfection reagent that simplifies and accelerates genome editing using large plasmids and difficult-to-transfect cells for life science researchers generating disease models. Using this approach, researchers can easily generate disease-relevant isogenic models to determine the impact of correcting or introducing disease-relevant mutations on cellular phenotypes in a tissue-appropriate context. However, problems have remained with certain cell types that are more resistant to transfection and with larger plasmids. DNA-In CRISPR has been specially formulated to enable highly efficient transfection of large plasmids [containing CRISPR-associated protein 9 (Cas9), guide RNAs, and reporter cassettes], particularly when using hard-to-transfect cell types. The reagent is fully chemically defined and animal component-free, leading to increased reliability and low cell toxicity. This makes it ideally suited for many applications, including use in preclinical investigations, giving researchers a regulatory head start in their hunt for new therapeutics.

AMS Biotechnology
For info: +44-1235-828200
www.amsbio.com

Genome Editing System

A new approach to clustered regularly interspaced short palindromic repeats (CRISPR), the innovative Alt-R CRISPR-Cas9 System, is based on the naturally occurring *S. pyogenes* CRISPR RNA system. The Alt-R CRISPR-Cas9 System greatly improves genome editing potency, thanks to research-optimized crRNAs (CRISPR RNAs) and transactivating crRNAs (tracrRNAs). Along with improved potency and safety, the system saves time by providing easy, ready-to-use RNA reagents that also reduce cell toxicity by avoiding activation of cellular innate immune responses. Using a two-part crRNA:tracrRNA complex to direct CRISPR-associated protein 9 (Cas9) cleavage, both the crRNA and tracrRNAs can be shortened to 36 and 67 nucleotides, respectively. Doing so increases the on-target potency of the reaction compared with other approaches. Shortening these RNAs enables Integrated DNA Technologies to manufacture the components as high-quality, synthetic RNA oligonucleotides that elicit less toxicity and innate immune response activation in cells. Researchers can also benefit from a safe, fast, and easy protocol with no viral particle preparation, in vitro transcription, or purification steps.

Integrated DNA Technologies
For info: 800-328-2661
www.idtdna.com

Electronically submit your new product description or product literature information! Go to www.sciencemag.org/products/newproducts.dtl for more information.

Newly offered instrumentation, apparatus, and laboratory materials of interest to researchers in all disciplines in academic, industrial, and governmental organizations are featured in this space. Emphasis is given to purpose, chief characteristics, and availability of products and materials. Endorsement by *Science* or AAAS of any products or materials mentioned is not implied. Additional information may be obtained from the manufacturer or supplier.

AAAS 2017 ANNUAL MEETING

FEBRUARY 16-20 • BOSTON

SERVING SOCIETY THROUGH

SCIENCE POLICY

To make decisions, societies rely on knowledge and multiple perspectives. Policies both within and outside science should be informed by the best available evidence. Science alone cannot translate knowledge into viable policy options; other factors include societal norms and cultural values.

One aspect of science policy is advancing the practice of science: How do we continually improve scientific methods, mechanisms, and outputs to increase the value of science to society?

Another aspect of science policy is providing the best available scientific evidence to policymakers, community leaders, and citizens. How can we most effectively provide scientific evidence that informs policy? What are the roles for scientists as individuals and for the scientific enterprise as a whole in the policy landscape? What emerging and established areas of science are essential to future policy decisions?

Call for Session Proposals

Session proposals for the 2017 AAAS Annual Meeting are now being solicited. To submit a proposal, visit **aaas.org/meetings**.
The deadline for submission is **April 22, 2016**.

aaas.org/meetings

SPEND LESS TIME DESIGNING AND MORE TIME DISCOVERING

Tools for Gene Expression

We know how important it is to improve your experimental reproducibility. That's why we've developed innovative reagents to knockdown expression of your gene of interest and quantify the resulting expression levels.

Our products provide accurate and efficient Gene Expression Measurement and Modulation. Explore the benefits of:

- KiCqStart® qPCR ReadyMixes™ and pre-designed primer pairs and arrays
- MISSION® esiRNA and esiFlex
- X-tremeGENE™ transfection reagents

To learn more, visit
sigma-aldrich.com/geneexpression

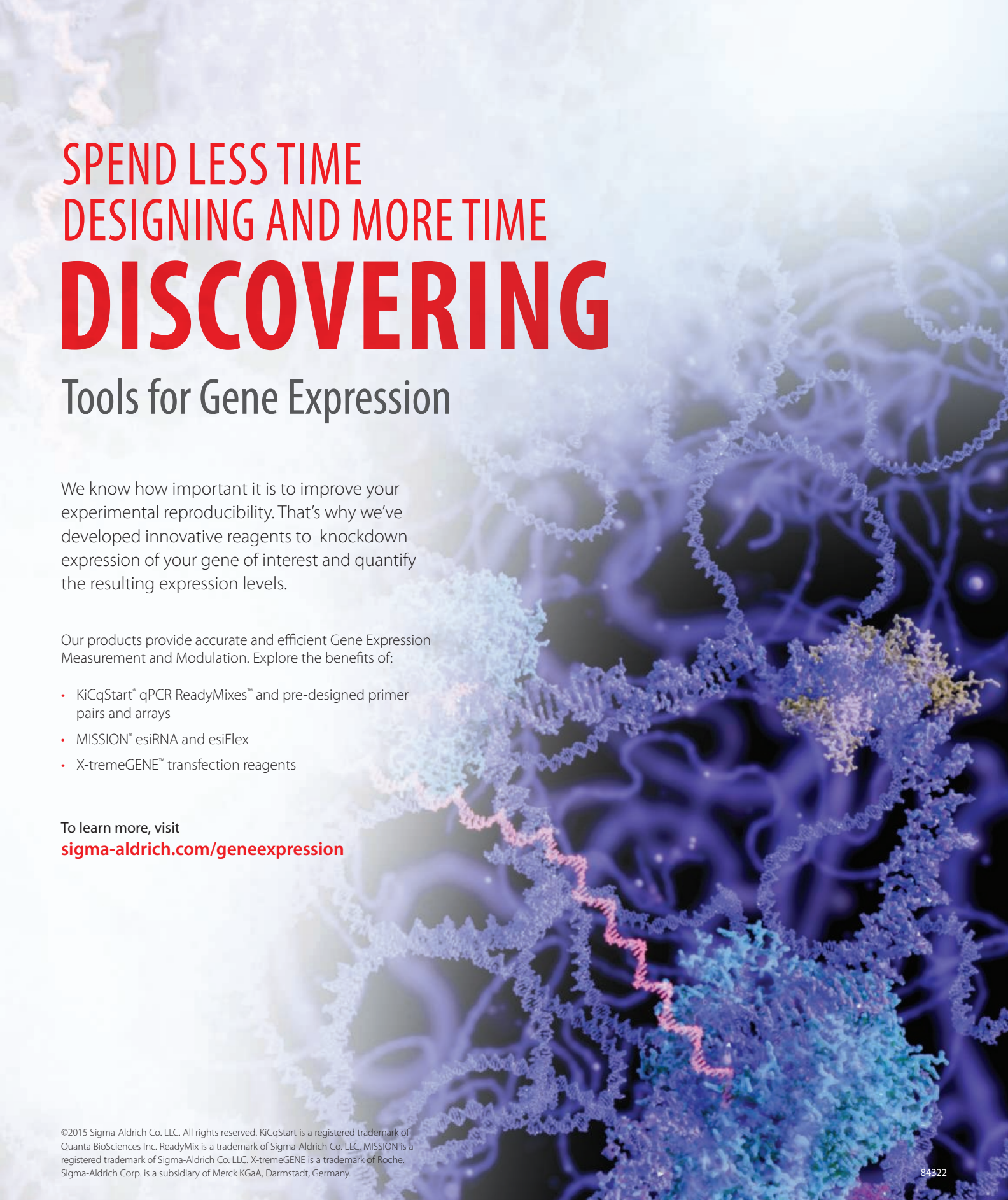

©2015 Sigma-Aldrich Co. LLC. All rights reserved. KiCqStart is a registered trademark of Quanta BioSciences Inc. ReadyMix is a trademark of Sigma-Aldrich Co. LLC. MISSION is a registered trademark of Sigma-Aldrich Co. LLC. X-tremeGENE is a trademark of Roche. Sigma-Aldrich Corp. is a subsidiary of Merck KGaA, Darmstadt, Germany.

84322

SIGMA-ALDRICH®

Science Careers Advertising

For full advertising details, go to ScienceCareers.org and click For Employers, or call one of our representatives.

Tracy Holmes
Worldwide Associate Director
Science Careers
Phone: +44 (0) 1223 326525

THE AMERICAS

E-mail: advertise@sciencecareers.org

Fax: +1 (202) 289 6742

Tina Burks
Phone: +1 (202) 326 6577

Nancy Toema
Phone: +1 (202) 326 6578

Online Job Posting Questions
Phone: +1 (202) 312 6375

EUROPE / INDIA / AUSTRALIA / NEW ZEALAND / REST OF WORLD

E-mail: ads@science-int.co.uk

Fax: +44 (0) 1223 326532

Sarah Lelarge
Phone: +44 (0) 1223 326527

Kelly Grace
Phone: +44 (0) 1223 326528

Online Job Posting Questions
Phone: +44 (0) 1223 326528

JAPAN

Katsuyoshi Fukamizu (Tokyo)
E-mail: kfukamizu@aaas.org
Phone: +81 3 3219 5777

Hiroyuki Mashiki (Kyoto)
E-mail: hmashiki@aaas.org
Phone: +81 75 823 1109

CHINA / KOREA / SINGAPORE / TAIWAN / THAILAND

Ruolei Wu
Phone: +86 186 0082 9345
E-mail: rwu@aaas.org

All ads submitted for publication must comply with applicable U.S. and non-U.S. laws. *Science* reserves the right to refuse any advertisement at its sole discretion for any reason, including without limitation for offensive language or inappropriate content, and all advertising is subject to publisher approval. *Science* encourages our readers to alert us to any ads that they feel may be discriminatory or offensive.

ScienceCareers
FROM THE JOURNAL SCIENCE AAAS

ScienceCareers.org

Postdoctoral Fellowships in Anticancer Drug Discovery at the University of Illinois at Urbana-Champaign

The Carl R. Wose Institute for Genomic Biology at the University of Illinois at Urbana-Champaign offers a number of fellowships for truly exceptional young scholars who have completed their Ph.D. within the last several years, and who are looking for a stimulating and supportive interdisciplinary environment to carry out independent and collaborative research in the field of anticancer drug discovery. IGB Fellows will typically spend two or more years conducting research in one of the IGB themes. A personalized mentoring plan will be developed for each Fellow. Annual salary is $50,000, in addition to a $7,500 allowance.

Anticancer Discovery from Pets to People

We seek an individual with a background in medicinal chemistry, chemical biology, cancer research, comparative genomics, veterinary oncology, or a related discipline to conduct research on the discovery of novel anticancer compounds. The Fellow will lead interactions between medicinal chemists, computational biologists, and veterinary oncologists. They will conduct independent research while working with Principal Investigators in this new IGB theme (http://go.illinois.edu/ACPP). The ideal candidate will strengthen a multidisciplinary team working to drive advances in the field of anticancer discovery through leveraging companion animals with cancer as a means to identify novel anticancer compounds and novel biological targets. The theme takes a precision medicine-based approach to anticancer drug discovery, and evaluates novel compounds in pets with cancer as a compassionate means to treat these veterinary patients and as a prelude to human clinical trials.

Applicants should submit a CV, a research summary, and the names of three recommenders who can write letters on their behalf. This information should be sent to Professor Paul J. Hergenrother (Theme Leader), hergenro@illinois.edu in advance of the March 12, 2016 closing date.

The University of Illinois is an Affirmative Action/Equal Opportunity Employer. The Carl R. Woese Institute for Genomic Biology is a pioneer in advancing life sciences research with program areas in systems biology, cellular and metabolic engineering, and genome technology. Visit www.igb.illinois.edu for additional information.

Stony Brook Medicine

Tenure-Track Faculty Position in Immunology of Infection

The Department of Molecular Genetics and Microbiology in the School of Medicine at Stony Brook University invites applications for a tenure-track faculty position at the level of Assistant Professor. Applicants must hold a Ph.D. or MD degree (or equivalent), and at least three years of postdoctoral experience. Ideal candidates will be those with research interests in the subject area of molecular/cellular immunology as it relates to infection. The successful candidate will establish a vigorous extramural research program that complements existing areas of expertise within the Department, participate in the Department's educational mission of graduate and medical school teaching, and perform University and Departmental service.

The Department (**http://www.mgm.stonybrook.edu/index.shtml**) and the adjacent Center for Infectious Diseases (**http:www.stonybrook.edu/ commcms/cid/**) provide a highly interactive scientific community. The position offers competitive start up support and salary, quality research space, and a dynamic intellectual environment. Stony Brook University maintains state-of-the-art core facilities that provide support in a number of areas including microscopy and animal imaging, flow cytometry and cell sorting, genomics, transcriptomics, proteomics, bioinformatics, animal maintenance, and BSL-3 containment, including animal BSL-3 containment.

Application Procedure: To ensure full consideration, applications should be received by March 31, 2016. The review of applications will continue on a rolling basis until the position is filled. Those interested in this position should submit a State employment application, cover letter, resume/CV, a three page summary of accomplishments and future research interests, and the names and addresses of three references (**electronic submission in one PDF document at web address below is highly preferred**) to: Dr. Carol Carter, Chair, Search Committee, Department of Molecular Genetics and Microbiology, Life Sciences Building, Room 130, Stony Brook University, Stony Brook, NY 11794-5222. Competitive applicants will be asked to have letters of recommendation sent to search committee.

For a full position description, or to apply online, visit:
www.stonybrook.edu/jobs (**Ref. # F-9602-16-02**).

Equal Opportunity Employer, females, minorities, disabled, veterans

UCF

We're seeking the **best new minds** to decode the **science of life.**

The University of Central Florida's Faculty Cluster Initiative fosters the development of talented, interdisciplinary teams focused on solving today's toughest scientific and societal challenges through teaching and research. ***We're hiring new faculty members in the area of genomics and bioinformatics to advance UCF's unique areas of excellence and global impact.***

ucf.edu/research/genomics

UCF is an equal opportunity/affirmative action employer.

PRIZES

The 2016 Tinker-Muse Prize for Science and Policy in Antarctica

The "Tinker-Muse Prize for Science and Policy in Antarctica" is a USD $100,000 unrestricted award presented to an individual in the fields of Antarctic science and/or policy who has demonstrated potential for sustained and significant contributions that will enhance the understanding and/or preservation of Antarctica. The Prize is inspired by Martha T. Muse's passion for Antarctica and is a legacy of the International Polar Year 2007-2008.

The prize-winner can be from any country and work in any field of Antarctic science and/or policy. The goal is to provide recognition of the important work being done by the individual and to call attention to the significance of understanding Antarctica in a time of change. A website with further details, including the process of nomination, closing date and selection of the Prize recipients, is available at **www.museprize.org**.

The Prize is awarded by the Tinker Foundation and administered by the Scientific Committee on Antarctic Research (SCAR).

TFI TINKER FOUNDATION INCORPORATED

Nominations open until 11 May 2016

SCAR

Trinity College Dublin
Coláiste na Tríonóide, Baile Átha Cliath
The University of Dublin

RECRUITMENT

Trinity College Dublin Invites applications for the following positions:

- **Professor of Psychology (Chair Established 1968)**
- **Thomas Mitchell Professor of Cognitive Neuroscience (Chair Established 2006)**

Salary: €106,516 - €136,276 € per annum

Closing date: 24/03/2016

For further information please visit:
http://jobs.tcd.ie

Trinity College Dublin, The University of Dublin **www.tcd.ie**

UNIVERSITY OF CAMBRIDGE

www.pdn.cam.ac.uk

THE BP PROFESSORSHIP OF CHEMISTRY (1702)

The Board of Electors to the BP Professorship of Chemistry (1702) invite applications for this Professorship from persons whose work falls within the general field of organic chemistry to take up appointment on 1 January 2018 or as soon as possible thereafter.

Candidates will have an outstanding research record of international stature in organic chemistry and the vision, leadership, experience and enthusiasm to build on current strengths in maintaining and developing a leading research presence. They will hold a PhD or equivalent postgraduate qualification.

Standard professorial duties include teaching and research, examining, supervision and administration. The Professor will be based in Cambridge. A competitive salary will be offered.

Further information is available at: www.admin.cam.ac.uk/offices/academic/secretary/professorships/ or contact the Academic Secretary, University Offices, The Old Schools, Cambridge, CB2 1TT, (email: ibise@admin.cam.ac.uk)

Applications, consisting of a letter of application, a statement of current and future research plans, a curriculum vitae and a publications list, along with details of three referees should be made online no later than 24 March 2016.

Informal enquiries about this position may be directed to Professor John Pyle, Head of the Department (tel: +44 (0)1223 336343, email: chemhod@hermes.cam.ac.uk), or to Professor Chris Hunter, (tel: +44 (0)1223 336710, email: herchelsmith.orgchem@ch.cam.ac.uk)

The University values diversity and is committed to equality of opportunity.

The University has a responsibility to ensure that all employees are eligible to live and work in the UK.

THE GEORGE WASHINGTON UNIVERSITY

WASHINGTON, DC

Medical Educator, Pharmacology/Physiology

The Department of Pharmacology and Physiology at The George Washington University School of Medicine and Health Sciences invites applications for full-time teaching faculty positions at the rank of Assistant or Associate Professor (non-tenure track). The successful applicants will teach primarily to medical and health science students in team-taught Physiology/Pharmacology courses and will serve as course director for one or more courses.

Basic qualifications: A Ph.D. in physiology, pharmacology, or related discipline and/or an M.D. Strong teaching credentials, as evidenced by experience and teaching evaluations in relevant courses, and the potential to develop an appropriate scholarly research program.

To Apply: Please complete an online faculty application at **http://www.gwu.jobs/postings/32362** and submit a complete curriculum vitae, cover letter, statement describing relevant teaching experience (including results of student evaluations), and the names of three individuals who can provide reference letters. Review of applications will begin **March 12, 2016**, and will continue until the positions are filled. Only complete applications will be considered. Employment offers are contingent on the satisfactory outcome of a standard background screening.

The George Washington University and the George Washington University Medical Faculty Associates are an Equal Employment Opportunity/Affirmative Action Employer that does not unlawfully discriminate in any of its programs or activities on the basis of race, color, religion, sex, national origin, age, disability, veteran status, sexual orientation, gender identity or expression, or on any other basis prohibited by applicable law.

THE OHIO STATE UNIVERSITY

COLUMBUS, OHIO

Assistant Professor of Phytobacteriology

The Department of Plant Pathology in The College of Food, Agricultural and Environmental Sciences (CFAES) at The Ohio State University (OSU), The Ohio Agricultural Research and Development Center (OARDC) seeks applicants for a tenure-track faculty position at the Assistant Professor level in phytobacteriology with an emphasis in phytobiomes analysis and interactions among plants and microbes.

Preferred Qualifications:
Ph.D. in plant pathology, microbial ecology, plant molecular biology, or related field. Post-doctoral research experience in phytobacteriology and/or phytobiome analysis is preferred.

Applications:
For a complete position description and application instructions, please visit **www.jobsatosu.com** and search by job opening number **415016.**
For questions regarding the application and processes please send e-mail to: taylor.1886@osu.edu

Review of complete applications will begin on March 1, and will continue until a suitable candidate is found.

The Ohio State University is an equal opportunity employer. All qualified applicants will receive consideration for employment without regard to race, color, religion, sex, sexual orientation or gender identity, national origin, disability status, or protected veteran status.

Download the Science Careers Job App

SEARCH JOBS ON THE GO!

apps.sciencemag.org

PRIZES

KFAS
مؤسسة الكويت للتقدم العلمي
Kuwait Foundation for the Advancement of Sciences

KUWAIT PRIZE 2016
Invitation for Nominations

In fulfillment of the objectives of the Kuwait Foundation for the Advancement of Sciences (KFAS) in supporting scientific research and encouraging Arab scholars and researchers, KFAS has dedicated Prizes in the fields of Sciences, Arts and Literature, Economic and Social Sciences as per its annual programs. The prizes are designed to recognize intellectual achievements that contribute to scientific advancement and raise the standard of academic dialogue in various fields.

The topics for the **Kuwait Prize 2016** in the four fields are as follows:

1. **Basic Sciences** - Physics
2. **Applied Sciences** - Food and Agriculture
3. **Economics & Social Sciences** - Banking and Finance
4. **Arts and Literature** - Studies in the Fine and Performing Arts and Music

For each of the above-mentioned fields, the foundation awards an annual Prize of a cash sum of K.D. **40,000** (Forty Thousand Kuwaiti Dinars), a Gold medal, a KFAS shield and a certificate of recognition to one or more of the citizens of Kuwait and the other Arab countries. The topics of the fields are subject to change annually.

Conditions and requirements:

1. The applicant must be from an Arab nationality and have a proof of Arabic origin either an Arabic birth certificate or a valid Arabic passport. A copy of an Arabic birth certificate or an Arabic Passport should be attached along with the submitted application.
2. The work submitted should be innovative, significant in the announced field, and published during the past twenty years. Submitted work may include papers published or accepted for publication in refereed journals, and books with ISSN number (authored, translated, edited, and chapter in a book). MA or PhD theses shall not be evaluated as part of the Applicant's scientific work.
3. KFAS will consider nominations from universities, academic and research institutions, scientific centres, past recipients of the prizes and peers of the nominees.
4. KFAS will accept self-nominations. To support self-nominations, applicants should provide a list of five references: four academics/researchers and one scientific organization. KFAS will seek out support letters from three of these references.
5. KFAS decisions concerning the prizes are final and objections are not accepted.
6. Applicants must fill in the prize application form and send it along with the submitted work electronically. The application form is obtained from KFAS website **www.kfas.org**. The Application should be submitted in English for Basic Sciences and Applied Sciences Fields.
7. The Application form along with the comprehensive scientific achievements completed in the past twenty years should be sent in PDF format, either via USB memory stick addressed to: Kuwait Foundation for the Advancement of Sciences-AL shark, Ahmed Al-Jaber St., or through the cloud storage services sites such as (google drive – dropbox – OneDrive) via Prizes email: **prize@kfas.org.kw**
8. **Required documents must be sent no later than 31/3/2016**

For more information and inquiries please, contact the Prizes Office on the following: Tel: (+965) 22270465 / Fax: 22270462 or
E-Mail: **prize@kfas.org.kw**

UNIVERSITY OF CALIFORNIA
UC RIVERSIDE

Cluster Hire: Spatial Analysis Center Director

The University of California at Riverside (UCR) is embarking on a major new hiring initiative that will add 300 tenure-track positions in 33 cross-disciplinary areas selected through a peer-reviewed competition (clusterhiring.ucr.edu). Over the next three years, we will hire multiple faculty members in each area and invest in research infrastructure to support their work. This initiative will build critical mass in vital and emerging fields of scholarship, foster truly cross-disciplinary work and further diversify the faculty at one of America's most diverse research universities. We encourage applications from scholars committed to excellence and seeking to help redefine the research university for the next generation.

We seek a Founding Director, at the Associate or Full Professor rank, for a new Spatial Analysis Center at University of California Riverside (UCR). The Director will provide vision and leadership for coordinated efforts with center faculty spanning engineering, science, and humanities, policy, and education colleges. While the expertise of the center Director may emphasize applications in spatial science from any discipline or the management of spatial information, experience leading interdisciplinary research teams is valued. A Ph.D. and a record of excellence and leadership in spatial research is required. Through the creation of the Spatial Analysis Center we will bring together a critical mass of researchers at UCR who will enable coordinated advances in how dynamic spatial databases are built, how people interact with spatial data of immense complexity, and how new spatial analysis systems are used for understanding dynamics and feedbacks in the built and natural environment. Additional new faculty hired following the Director will join an existing research community that is developing cutting-edge spatial technologies and applying these tools to university-wide interdisciplinary challenges in fields spanning global climate and biodiversity, autonomous vehicles, cultural heritage, demographic changes, and big-data. The new center is part of a substantial recent investment by UCR in high performance computing and Data Science, which provides an exciting environment for advancing spatial analysis throughout the university. As part of a university-wide center, the Director will have an appropriate academic departmental home but the center will report to the Vice Chancellor for Research.

Depending upon the department of appointment, the position may include an appointment in the Agricultural Experiment Station, which includes the responsibility to conduct research and outreach relevant to the mission of the California Agricultural Experiment Station (http://cnas.ucr.edu/about/aes/).

Applications must include a curriculum vitae, cover letter, statements of research and teaching interests, a leadership statement for the center, statement of contributions to diversity, and full contact information for three to five references. All application materials must be submitted through AP Recruit at: **https://aprecruit.ucr.edu/apply/JPF00526**. Review of applications will begin **March 15, 2016** and will continue until the position is filled with an anticipated start date of June 30, 2016. Salary is commensurate with education and experience. For more information about the position, contact **Darrel Jenerette** (**darrel.jenerette@ucr.edu**), Search Chair, Department of Botany and Plant Sciences, University of California Riverside.

The University of California is an Equal Opportunity/Affirmative Action Employer with a strong institutional commitment to the achievement of excellence and diversity among its faculty and staff. All qualified applicants will receive consideration for employment without regard to race, color, religion, sex, sexual orientation, gender identity, national origin, age, disability, protected veteran status, or any other characteristic protected by law.

UCR is a world-class research university with an exceptionally diverse undergraduate student body. Its mission is explicitly linked to providing routes to educational success for underrepresented and first-generation college students. A commitment to this mission is a preferred qualification. Advancement through the faculty ranks at the University of California is through a series of structured, merit-based evaluations, occurring every 2-3 years, each of which includes substantial peer input.

Science Careers online @sciencecareers.org

ScienceCareers online @sciencecareers.org

AAAS

ADVANCING SCIENCE, SERVING SOCIETY

Science Translational Medicine and AAAS seek a talented immunologist to join our editorial team in Washington DC

This position is designed for a talented immunologist with broad interests, a lively curiosity, excellent communication skills and experience with cutting-edge immunology research in one or more biomedical or clinical fields.

The **tasks include**, but are not limited to:

- Manage the evaluation, review, and editing of submitted manuscripts in the field of immunology including vaccines, infectious disease, allergy, immunotherapy
- Show leadership in the further development of immunology as a key field contributing to the success of Science Translational Medicine
- Judge the scientific value of research and select reviewers for submitted manuscripts;
- Discuss and make recommendations regarding manuscripts and reviews with other staff, advisors, authors;
- Write summaries of research results for publication;
- Guide authors on manuscript revisions and edit the manuscripts for scientific content and style before and after revisions;
- Follow the manuscript through the production process to ensure material is published in a timely manner;
- Commission and edit timely Review articles on a broad range of topics
- Foster relationships and communication with the scientific community through meetings and professional contacts;
- Represent Science Translational Medicine at scientific meetings nationally and internationally.

The **minimum qualifications** to be competitive and considered for the position are:

- Extensive university or college-level training leading to a Ph.D. in at least one biomedical or clinical research field
- 3 to 5 years post PhD experience, including postdoctoral research experience and multiple publications;
- Ability to work constructively as a member of a tight-knit team;
- Experience with cutting-edge research in immunology;
- Comprehensive knowledge of scientific research methods in order to discuss technical issues with authors;
- Exceptional written, communication, and listening skills in order to communicate with authors and reviewers in evaluating, editing and modifying manuscripts.
- Prior scientific editorial experience is not essential but is an advantage.

Please visit our job information website **http://www.aaas.org/page/employment-aaas** to get more information, and to apply to AAAS online.

AAAS is an EO Employer. All qualified applicants will receive consideration for employment without regard to race, color, religion, sexual orientation, gender identity, national origin, age, disability, veteran status, or other protected category. AAAS uses E-Verify to confirm the employment eligibility of all newly hired employees.

AAAS

ADVANCING SCIENCE, SERVING SOCIETY

AAAS's new journal *Science Immunology* is seeking an **energetic and insightful immunologist to join our editorial team** in Washington DC in the launch of this latest member of the Science family of journals.

This position is designed for an immunologist with broad interests, a lively curiosity, excellent communication skills and experience with cutting-edge immunology research, preferably in one or more systems. This position reports to the Editor, Science Immunology.

Responsibilities include, but are not limited to:

- With the Editor, Chief Scientific Editors, and the Advisory Board, contribute to refining the scope and mission of Science Immunology.
- Manage the evaluation, review, and editing of submitted manuscripts in all areas of immunology.
- Judge the scientific value of research and select reviewers for submitted manuscripts;
- Discuss and make recommendations regarding manuscripts and reviews with other staff, advisors, authors;
- Write summaries of research results for publication;
- Guide authors on manuscript revisions and edit the manuscripts for scientific content and style before and after revisions;
- Follow the manuscript through the production process to ensure material is published in a timely manner;
- Commission and edit timely Review articles on a broad range of topics
- Foster relationships and communication with the scientific community through meetings and professional contacts;
- Represent Science Immunology at scientific meetings nationally and internationally.

The **minimum qualifications** to be competitive and considered for the position are:

- Mastery of a professional field typically acquired through completion of a doctoral degree in at least one biomedical or clinical research field;
- 1 to 5 years post PhD experience, including postdoctoral research experience and multiple publications;
- Ability to work constructively as a member of a tight-knit team;
- Experience with cutting-edge research in immunology;
- Comprehensive knowledge of scientific research methods in order to discuss technical issues with authors;
- Exceptional written, communication, and listening skills in order to communicate with authors and reviewers in evaluating, editing and modifying manuscripts.
- Prior scientific editorial experience is not essential but is an advantage.

Please visit our job information website **http://www.aaas.org/page/employment-aaas** to get more information, and to apply to AAAS online.

AAAS is an EO Employer. All qualified applicants will receive consideration for employment without regard to race, color, religion, sexual orientation, gender identity, national origin, age, disability, veteran status, or other protected category. AAAS uses E-Verify to confirm the employment eligibility of all newly hired employees.

Yale SCHOOL OF MEDICINE

Department of Neuroscience
New Haven, CT
http://medicine.yale.edu/neuroscience/index.aspx

Staff Scientist/Engineer in Optical Microscopy at Yale University

We are looking to hire a Staff Scientist/Engineer with expertise in optics and optical microscopy to develop, set up and maintain custom-built light microscopes and other optics-based instruments in the recently expanded Department of Neuroscience at Yale University School of Medicine (New Haven, Connecticut, USA).

An initial goal will be to establish, refine and maintain custom-built light sheet microscopes. The applicant will also have the opportunity to influence and participate in the development of other optical approaches in neuroscience. The individual will have access to the resources of, and be embedded in, the intellectual environment of a very strong, collaborative and growing imaging community at the Yale School of Medicine, which includes labs that develop and use advanced optical techniques for the manipulation and recording of neuronal activity.

The applicant should have a PhD degree (preferably in the area of physical sciences or engineering). A minimum of 3 years of experience in the development, setup and use of optical instrumentation is preferred. Strong motivation to develop and advance methodology, as well as willingness to perform collaborative scientific work is expected. Experience with the development of optical instruments as well as programming expertise (especially Labview, MatLab or python) are required.

Please send one PDF file with a cover letter and curriculum vitae, and arrange for submission of 3 letters of recommendation. All application materials should be sent **electronically** to **Pietro De Camilli** at the following e-mail address: **neuro.search@yale.edu**. Applications will be reviewed as they are received, but full consideration will be given to applications received by **March 30, 2016**.

Yale is an Affirmative Action Equal Opportunity Employer. Yale values diversity among its students, faculty, and staff. Women, persons with disabilities, protected veterans, and underrepresented minorities are encouraged to apply.

Director, Minnesota Institute on the Biology of Aging and Metabolism

University of Minnesota Medical School

As a component of the medical discovery team initiative at the University of Minnesota Medical School, exceptional scientists are invited to apply for a tenured faculty position at the full professor level as the founding director of the Minnesota Institute for the Biology of Aging and Metabolism (iBAM). This State of Minnesota funded initiative is designed to develop centers of excellence in targeted areas relevant to the mission of the Medical School and University. The successful candidate is expected to maintain their active and vibrant research program in the biology of aging, to develop the Institute and its research themes, to recruit new investigators to the Institute and to work with the leadership of the Medical School and University to develop philanthropy around healthspan research. Preference will be given to scientists focusing on the molecular and cellular basis of aging and is expected to complement existing strength in genome stability, energy metabolism and proteostasis.

Applicants must apply online at: **http://www1.umn.edu/ohr/employment/**. Click on the appropriate tab under **"Search & Apply for Openings"**, enter **307216** into the **"Keywords"** field, then click the "Search" tab. Applicants should attach a cover letter, curriculum vitae, a description of their research program and a list of 3 potential references. Minimum qualifications include an M.D. or Ph.D. degree (or equivalent) and a track record of academic leadership and experience in leading interdisciplinary teams of scientists. Review of applications will begin immediately and continue until the position is filled. More information concerning the medical discovery team initiative and this position can be found at http://www.med.umn.edu/research/medical-discovery-teams.

The University of Minnesota provides equal access to and opportunity in its programs, facilities, and employment without regard to race, color, creed, religion, national origin, gender, age, marital status, disability, public assistance status, veteran status, sexual orientation, gender identity, or gender expression. The University supports the work-life balance of its faculty and especially encourages applications from women and members of under-represented groups.

PRIZES

The 2016 (32nd) International Prize for Biology

Calling for Nominations

This year's research field:

Biology of Biodiversity

Please access at: **http://www.jsps.go.jp/english/e-biol**

Deadline: April 22, 2016

- The International Prize for Biology was established in 1985 to commemorate the 60-year reign of Emperor Showa and his longtime devotion to biological research.
- The Prize is awarded each year to an individual who has made an outstanding contribution to the advancement of basic research in a field of biology.
- The Prize shall consist of a medal and a prize of 10-million yen.

Recent Years Prize Winners

2015
Dr. Yoshinori Ohsumi
(Cell Biology)

2014
Prof. Sir Peter Crane FRS
(Systematic Biology and Taxonomy)

2013
Dr. Joseph Felsenstein
(Biology of Evolution)

JSPS

Director of Research at Masonic Medical Research Laboratory

The Masonic Medical Research Laboratory (MMRL) seeks an exceptional scientist as Director of Research. The next Director is expected to further MMRL's reputation as an internationally recognized leader in the field of cardiovascular research. MMRL, located in Utica, NY, is an independent, non-profit research institute with a long history of groundbreaking cardiovascular research that focuses on the study of mechanisms of cardiac arrhythmias. Unique opportunities are present for collaboration with a preeminent local nano-technology center, hospitals, and higher education centers.

MMRL research focuses on cardiac pathophysiology and arrhythmia research to study molecular, cellular, and computational cardiac myocyte electrophysiological functions and derangements in a variety of disease states; to develop the next generation of future gene diagnostic technologies; and to advance models of drug/phenotype interaction to study safety and efficacy of treating disorders of the cardiac impulse generation and conduction system.

A selected candidate must have an exceptional track record of high impact publications, a history of consistent external funding, and strong reputation in his/her field.

The Director must be capable of managing a complex organization with diverse participants (research staff, students, Board of Directors, Advisory Board Members, administrators, donors, public, etc.). The next Director will also be expected to develop his/her own vision for advancing the scope of research.

Please apply with CV to **hr_services@mmrl.edu**.

MMRL is committed to fostering a diverse and inclusive academic global community; as an EEO/AA employer, MMRL considers applicants for employment without regard to, and does not discriminate on the basis of, gender, race, protected veteran status, disability, or any other legally protected status.

ScienceCareers online @sciencecareers.org

By **Andrew Scott**

Science in the shadows

One morning in 1979, while cycling toward the University of Cambridge laboratory where I was in the second year of my chemistry Ph.D. program, I noticed the vendors setting up their stalls in the market square. "Every damn day," I thought as I rolled quietly past. "They do the same thing every damn day." A wave of gloom swept through me. How could anyone get up each morning to do the same thing every day? Science was one of my passions, but the setbacks of research were beginning to grind me down, and I was realizing that actually doing science was not for me. By the time I reached the lab that day, I knew that I needed to do something different with my life than chase the "regular" job in academia or industry that I was being encouraged to prepare for.

My other passion was writing, so the way forward seemed clear: I should become a science writer. As I continued my Ph.D. studies, I began to pitch short articles to a popular science magazine. The rejections I initially received stung as much as the frustrations and failures of scientific research, but I persisted. I pondered some tough advice from a couple of helpful editors, and eventually I began to regularly see my words in print. When I graduated, I decided I wanted to become a writer. I was on my way to a career that brought me little more glory than research would have—but far more satisfaction.

"The way forward seemed clear: I should become a science writer."

Few fledgling freelance science writers can survive by writing alone. I certainly couldn't. Teaching seemed an obvious source of additional income, and I was soon explaining basic science to youngsters at a small local college. Although the resources at my disposal were a far cry from what I had been used to in my research training, I came to enjoy the interaction with the students, and I soon became a regular member of the part-time teaching team. Teaching for part of the week and writing the rest of the time kept me intellectually stimulated, and I enjoyed the variety. I also found that teaching kept me aware of the difficulties many encounter in understanding science, which helped me when writing for a general audience. But while most of my former university colleagues seemed to be prospering financially, I was just scraping by.

I had the naive impression that if I could write a book, I would make some money, so I was overjoyed when an editor who had read a magazine article I had written about viruses invited me to expand it into a book for the general public. After a year of effort, my book was published and received excellent reviews, which supported my belief that I was on my way to riches. This prospect was further reinforced when I wandered into a large London bookshop and was astonished to discover more than 20 copies of my book. I was told that it was a recommended text at the University of London.

Despite the excitement I felt, reality kicked in when I realized that—even with great reviews, academic recommendations, and eventual translations into many languages—I was never going to earn enough from writing as a freelancer to live by that alone. I have now published nine science books, including two textbooks for major academic publishers in the United States, but I remain a hybrid writer-lecturer. I have not achieved the level of sales success that I had hoped for, but I have found a way to remain involved in science. I also hugely enjoy self-publishing my fiction, even though the readers of this work are relatively few.

It now occurs to me that in some ways, my life in science writing has been very similar to the lives of many science graduates who stay in research. Our driving force is a passion for what we do, but in the same way that my books are falling out of date and out of print, most research papers soon sink into the swamps of the rarely cited and the never applied. Most of us, whatever path we choose through science, must be ready to be content with a life in the shadows rather than in the limelight. But such a life, I have found, can still be fun and fulfilling. ■

Andrew Scott is a freelance science writer and part-time lecturer in Scotland. Send your story to SciCareerEditor@aaas.org.

ILLUSTRATION: ROBERT NEUBECKER

Downloaded from on February 11, 2016

Published by AAAS